IARC MONOGRAPHS

# SOME NANOMATERIALS AND SOME FIBRES

VOLUME 111

IARC MONOGRAPHS
ON THE EVALUATION
OF CARCINOGENIC RISKS
TO HUMANS

SOME NANOMATERIALS AND SOME FIBRES

VOLUME 111

IARC MONOGRAPHS

Corrigenda to the IARC Monographs are published online at http://monographs.iarc.fr/ENG/Publications/corrigenda.php
To report an error, please contact: editimo@iarc.fr

Co-funded by the European Union

CONTENTS

NOTE TO THE READER

The term 'carcinogenic risk' in the *IARC Monographs* series is taken to mean that an agent is capable of causing cancer. The *Monographs* evaluate cancer hazards, despite the historical presence of the word 'risks' in the title.

Inclusion of an agent in the *Monographs* does not imply that it is a carcinogen, only that the published data have been examined. Equally, the fact that an agent has not yet been evaluated in a *Monograph* does not mean that it is not carcinogenic. Similarly, identification of cancer sites with *sufficient evidence* or *limited evidence* in humans should not be viewed as precluding the possibility that an agent may cause cancer at other sites.

The evaluations of carcinogenic risk are made by international working groups of independent scientists and are qualitative in nature. No recommendation is given for regulation or legislation.

Anyone who is aware of published data that may alter the evaluation of the carcinogenic risk of an agent to humans is encouraged to make this information available to the Section of IARC Monographs, International Agency for Research on Cancer, 150 cours Albert Thomas, 69372 Lyon Cedex 08, France, in order that the agent may be considered for re-evaluation by a future Working Group.

Although every effort is made to prepare the *Monographs* as accurately as possible, mistakes may occur. Readers are requested to communicate any errors to the Section of IARC Monographs, so that corrections can be reported in future volumes.

LIST OF PARTICIPANTS

Members [1]

Thomas F. Bateson (Co-Subgroup Chair, Exposure Data)

Effects Identification and Characterization Group
United States Environmental Protection Agency
Washington, DC
USA

Merete Drevvatne Bugge

National Institute of Occupational Health
Oslo
Norway

Pietro Comba (Subgroup Chair, Cancer in Humans)

Department of Environment and Primary Prevention
National Institute of Health (ISS)
Rome
Italy

Maximilien Debia

School of Public Health
University of Montreal
Montreal, Quebec
Canada

Chantal Dion

Research and Expertise Division
Institut de recherche Robert-Sauvé en santé
et en sécurité du travail (IRSST)
Montreal, Quebec
Canada

Bice Fubini (Co-Subgroup Chair, Mechanistic
and Other Relevant Data)

Department of Chemistry
University of Turin
Turin
Italy

Irina Guseva Canu

Département santé travail
Institut de veille sanitaire
Saint-Maurice
France

Marie-Claude Jaurand

Institut national de la santé et de la
recherche médicale (INSERM)
Paris
France

Agnes B. Kane (Overall Chair)

Department of Pathology & Laboratory
Medicine
Brown University
Providence, RI
USA

Norihiro Kobayashi

National Institute of Health Sciences
Tokyo
Japan

Eileen D. Kuempel (Co-Subgroup Chair,
Mechanistic and Other Relevant Data)

Nanotechnology Research Center
National Institute for Occupational Safety
and Health
Cincinnati, OH
USA

Daniel L. Morgan (Subgroup Chair, Cancer in
Animals)

National Toxicology Program
National Institute of Environmental Health
Sciences
Research Triangle Park, NC
USA

Yasuo Morimoto

Department of Occupational Pneumology
University of Occupational and
Environmental Health
Kitakyushu City
Japan

Peter Møller

Department of Public Health
University of Copenhagen
Copenhagen
Denmark

Kent E. Pinkerton

Center for Health and the Environment
University of California
Davis, CA
USA

Linda Sargent

National Institute for Occupational Safety
and Health
Morgantown, WV
USA

Kai Savolainen

> Nanosafety Research Centre
> Finnish Institute of Occupational Health
> Helsinki
> Finland

Leslie Stayner

> School of Public Health
> University of Illinois at Chicago
> Chicago, IL
> USA

Hiroyuki Tsuda

> Nanotoxicology Project Laboratory
> Nagoya City University
> Nagoya
> Japan

Roel Vermeulen

> Division of Environmental Epidemiology
> Institute for Risk Assessment Sciences
> University of Utrecht
> Utrecht
> The Netherlands

Il Je Yu (Co-Subgroup Chair, Exposure Data)

> Fusion Technology Laboratory
> Hoseo University
> Asan
> Republic of Korea

Representatives

Amira Ben Amara [2]

> National Agency of Sanitary and
> Environmental Control of Products
> (ANCSEP)
> Tunis
> Tunisia

Hamadi Dekhil [unable to attend] [3]

> National Agency of Sanitary and
> Environmental Control of Products
> (ANCSEP)
> Tunis
> Tunisia

Marie-Estelle Gouze [4]

> French Agency for Food, Environment, and
> Occupational Health Safety (ANSES)
> Maisons-Alfort
> France

Nathalie Thieriet [5]

> French Agency for Food, Environment, and
> Occupational Health Safety (ANSES)
> Maisons-Alfort
> France

---

[2] Amira Ben Amara attended as a Representative of the National Agency of Sanitary and Environmental Control of Products (ANCSEP), Tunisia.

[3] Hamadi Dekhil attended as a Representative of the National Agency of Sanitary and Environmental Control of Products (ANCSEP), Tunisia.

[4] Marie-Estelle Gouze attended as a Representative of French Agency for Food, Environment, and Occupational Health Safety (ANSES), France.

[5] Nathalie Thieriet attended as a Representative of French Agency for Food, Environment, and Occupational Health Safety (ANSES), France.

Observers [6]

Judy Choi [unable to attend] [7]

BiPRO GmbH
Munich
Germany

Nicole Falette [8]

Department of Cancer and the Environment
Centre Léon Bérard
Lyon
France

Solveig Føreland [9]

Department of Occupational Medicine
Trondheim
Norway

Tom Holthe [unable to attend] [10]

Trondheim
Norway

Anke Joas [unable to attend] [11]

BiPRO GmbH
Munich
Germany

Julie Muller-Bondue [12]

Nanocyl SA
Sambreville
Belgium

IARC/WHO Secretariat

Lamia Benbrahim-Tallaa (*Rapporteur, Mechanistic and Other Relevant Data*)
Véronique Bouvard (*Rapporteur, Exposure Data*)
Rafael Carel (Visiting Scientist)
Fatiha El Ghissassi (*Rapporteur, Mechanistic and Other Relevant Data*)
Yann Grosse (*Responsible Officer, and Rapporteur, Cancer in Experimental Animals*)
Neela Guha (*Rapporteur, Cancer in Humans*)
Kathryn Guyton (*Rapporteur, Mechanistic and Other Relevant Data*)
Béatrice Lauby-Secretan
Dana Loomis (*Rapporteur, Cancer in Humans*)
Heidi Mattock (*Scientific Editor*)
Marco Martuzzi (*WHO European Centre for Environment and Health, Germany*)

---

[6] Each Observer agreed to respect the Guidelines for Observers at *IARC Monographs* meetings. Observers did not serve as Meeting Chair or Subgroup Chair, draft any part of a *Monograph*, or participate in the evaluations. They also agreed not to contact participants before the meeting, not to lobby them at any time, not to send them written materials, and not to offer them meals or other favours. IARC asked and reminded Working Group Members to report any contact or attempt to influence that they may have encountered, either before or during the meeting.

[7] Observer for BiPRO GmbH, Germany. Judy Choi is employed by BiPRO GmbH, which receives funding from the Silicon Carbide Manufacturers Association (SiCMa) for regulatory consulting services.

[8] Observer for the Centre Léon Bérard.

[9] Observer for Silicon Carbide Manufacturers Association (SiCMa), Luxembourg. Solveig Føreland's partner is production manager at Washington Mills AS, Norway, a company manufacturing silicon carbide grains and powders.

[10] Observer for Silicon Carbide Manufacturers Association (SiCMa), Luxembourg. Tom Holthe is Medical Advisor for Washington Mills AS, Norway and the Silicon Carbide Manufacturers Association (SiCMa).

[11] Observer for BiPRO GmbH, Germany. Anke Joas is employed by BiPRO GmbH, which receives funding from the Silicon Carbide Manufacturers Association (SiCMa) for regulatory consulting services.

[12] Observer for Nanocyl SA, Belgium. Julie Muller is employed as a toxicologist by Nanocyl SA, Belgium, a company manufacturing carbon nanotubes.

Chiara Scoccianti
Kurt Straif (*Head of Programme*)

Administrative Assistance

Sandrine Egraz
Michel Javin
Brigitte Kajo
Annick Leroux
Helene Lorenzen-Augros

Production Team

Natacha Blavoyer
Elisabeth Elbers
Solène Quennehen

Post-Meeting Assistance

Jane Mitchell (*Technical Editor*)

PREAMBLE

The Preamble to the *IARC Monographs* describes the objective and scope of the programme, the scientific principles and procedures used in developing a Monograph, the types of evidence considered and the scientific criteria that guide the evaluations. The Preamble should be consulted when reading a Monograph or list of evaluations.

A. GENERAL PRINCIPLES AND PROCEDURES

1. Background

Soon after IARC was established in 1965, it received frequent requests for advice on the carcinogenic risk of chemicals, including requests for lists of known and suspected human carcinogens. It was clear that it would not be a simple task to summarize adequately the complexity of the information that was available, and IARC began to consider means of obtaining international expert opinion on this topic. In 1970, the IARC Advisory Committee on Environmental Carcinogenesis recommended '… that a compendium on carcinogenic chemicals be prepared by experts. The biological activity and evaluation of practical importance to public health should be referenced and documented.' The IARC Governing Council adopted a resolution concerning the role of IARC in providing government authorities with expert, independent, scientific opinion on environmental carcinogenesis. As one means to that end, the Governing Council recommended that IARC should prepare monographs on the evaluation of carcinogenic risk of chemicals to man, which became the initial title of the series.

In the succeeding years, the scope of the programme broadened as *Monographs* were developed for groups of related chemicals, complex mixtures, occupational exposures, physical and biological agents and lifestyle factors. In 1988, the phrase 'of chemicals' was dropped from the title, which assumed its present form, *IARC Monographs on the Evaluation of Carcinogenic Risks to Humans*.

Through the *Monographs* programme, IARC seeks to identify the causes of human cancer. This is the first step in cancer prevention, which is needed as much today as when IARC was established. The global burden of cancer is high and continues to increase: the annual number of new cases was estimated at 10.1 million in 2000 and is expected to reach 15 million by 2020 (Stewart & Kleihues, 2003). With current trends in demographics and exposure, the cancer burden has been shifting from high-resource countries to low- and medium-resource countries. As a result of *Monographs* evaluations, national health agencies have been able, on scientific grounds, to take measures to reduce human exposure to carcinogens in the workplace and in the environment.

The criteria established in 1971 to evaluate carcinogenic risks to humans were adopted by the Working Groups whose deliberations resulted in the first 16 volumes of the *Monographs* series. Those criteria were subsequently updated by further ad hoc Advisory Groups ([IARC, 1977](), [1978](), [1979](), [1982](), [1983](), [1987](), [1988](), [1991]; [Vainio et al., 1992](); [IARC, 2005](), [2006]()).

The Preamble is primarily a statement of scientific principles, rather than a specification of working procedures. The procedures through which a Working Group implements these principles are not specified in detail. They usually involve operations that have been established as being effective during previous *Monograph* meetings but remain, predominantly, the prerogative of each individual Working Group.

2.   Objective and scope

The objective of the programme is to prepare, with the help of international Working Groups of experts, and to publish in the form of *Monographs*, critical reviews and evaluations of evidence on the carcinogenicity of a wide range of human exposures. The *Monographs* represent the first step in carcinogen risk assessment, which involves examination of all relevant information to assess the strength of the available evidence that an agent could alter the age-specific incidence of cancer in humans. The *Monographs* may also indicate where additional research efforts are needed, specifically when data immediately relevant to an evaluation are not available.

In this Preamble, the term 'agent' refers to any entity or circumstance that is subject to evaluation in a *Monograph*. As the scope of the programme has broadened, categories of agents now include specific chemicals, groups of related chemicals, complex mixtures, occupational or environmental exposures, cultural or behavioural practices, biological organisms and physical agents. This list of categories may expand as causation of, and susceptibility to, malignant disease become more fully understood.

A cancer 'hazard' is an agent that is capable of causing cancer under some circumstances, while a cancer 'risk' is an estimate of the carcinogenic effects expected from exposure to a cancer hazard. The *Monographs* are an exercise in evaluating cancer hazards, despite the historical presence of the word 'risks' in the title. The distinction between hazard and risk is important, and the *Monographs* identify cancer hazards even when risks are very low at current exposure levels, because new uses or unforeseen exposures could engender risks that are significantly higher.

In the *Monographs*, an agent is termed 'carcinogenic' if it is capable of increasing the incidence of malignant neoplasms, reducing their latency, or increasing their severity or multiplicity. The induction of benign neoplasms may in some circumstances (see Part B, Section 3a) contribute to the judgement that the agent is carcinogenic. The terms 'neoplasm' and 'tumour' are used interchangeably.

The Preamble continues the previous usage of the phrase 'strength of evidence' as a matter of historical continuity, although it should be understood that *Monographs* evaluations consider studies that support a finding of a cancer hazard as well as studies that do not.

Some epidemiological and experimental studies indicate that different agents may act at different stages in the carcinogenic process, and several different mechanisms may be involved. The aim of the *Monographs* has been, from their inception, to evaluate evidence of carcinogenicity at any stage in the carcinogenesis process, independently of the underlying mechanisms. Information on mechanisms may, however, be used in making the overall evaluation ([IARC, 1991](); [Vainio et al., 1992](); [IARC, 2005](), [2006](); see also Part B, Sections 4 and 6). As mechanisms of carcinogenesis are elucidated, IARC convenes international scientific conferences to determine whether a broad-based consensus has emerged

on how specific mechanistic data can be used in an evaluation of human carcinogenicity. The results of such conferences are reported in IARC Scientific Publications, which, as long as they still reflect the current state of scientific knowledge, may guide subsequent Working Groups.

Although the *Monographs* have emphasized hazard identification, important issues may also involve dose–response assessment. In many cases, the same epidemiological and experimental studies used to evaluate a cancer hazard can also be used to estimate a dose–response relationship. A *Monograph* may undertake to estimate dose–response relationships within the range of the available epidemiological data, or it may compare the dose–response information from experimental and epidemiological studies. In some cases, a subsequent publication may be prepared by a separate Working Group with expertise in quantitative dose–response assessment.

The *Monographs* are used by national and international authorities to make risk assessments, formulate decisions concerning preventive measures, provide effective cancer control programmes and decide among alternative options for public health decisions. The evaluations of IARC Working Groups are scientific, qualitative judgements on the evidence for or against carcinogenicity provided by the available data. These evaluations represent only one part of the body of information on which public health decisions may be based. Public health options vary from one situation to another and from country to country and relate to many factors, including different socioeconomic and national priorities. Therefore, no recommendation is given with regard to regulation or legislation, which are the responsibility of individual governments or other international organizations.

3. Selection of agents for review

Agents are selected for review on the basis of two main criteria: (a) there is evidence of human exposure and (b) there is some evidence or suspicion of carcinogenicity. Mixed exposures may occur in occupational and environmental settings and as a result of individual and cultural habits (such as tobacco smoking and dietary practices). Chemical analogues and compounds with biological or physical characteristics similar to those of suspected carcinogens may also be considered, even in the absence of data on a possible carcinogenic effect in humans or experimental animals.

The scientific literature is surveyed for published data relevant to an assessment of carcinogenicity. Ad hoc Advisory Groups convened by IARC in 1984, 1989, 1991, 1993, 1998 and 2003 made recommendations as to which agents should be evaluated in the *Monographs* series. Recent recommendations are available on the *Monographs* programme web site (http:// monographs.iarc.fr). IARC may schedule other agents for review as it becomes aware of new scientific information or as national health agencies identify an urgent public health need related to cancer.

As significant new data become available on an agent for which a *Monograph* exists, a re-evaluation may be made at a subsequent meeting, and a new *Monograph* published. In some cases it may be appropriate to review only the data published since a prior evaluation. This can be useful for updating a database, reviewing new data to resolve a previously open question or identifying new tumour sites associated with a carcinogenic agent. Major changes in an evaluation (e.g. a new classification in Group 1 or a determination that a mechanism does not operate in humans, see Part B, Section 6) are more appropriately addressed by a full review.

4.   Data for the *Monographs*

Each *Monograph* reviews all pertinent epidemiological studies and cancer bioassays in experimental animals. Those judged inadequate or irrelevant to the evaluation may be cited but not summarized. If a group of similar studies is not reviewed, the reasons are indicated.

Mechanistic and other relevant data are also reviewed. A *Monograph* does not necessarily cite all the mechanistic literature concerning the agent being evaluated (see Part B, Section 4). Only those data considered by the Working Group to be relevant to making the evaluation are included.

With regard to epidemiological studies, cancer bioassays, and mechanistic and other relevant data, only reports that have been published or accepted for publication in the openly available scientific literature are reviewed. The same publication requirement applies to studies originating from IARC, including meta-analyses or pooled analyses commissioned by IARC in advance of a meeting (see Part B, Section 2c). Data from government agency reports that are publicly available are also considered. Exceptionally, doctoral theses and other material that are in their final form and publicly available may be reviewed.

Exposure data and other information on an agent under consideration are also reviewed. In the sections on chemical and physical properties, on analysis, on production and use and on occurrence, published and unpublished sources of information may be considered.

Inclusion of a study does not imply acceptance of the adequacy of the study design or of the analysis and interpretation of the results, and limitations are clearly outlined in square brackets at the end of each study description (see Part B). The reasons for not giving further consideration to an individual study also are indicated in the square brackets.

5.   Meeting participants

Five categories of participant can be present at *Monograph* meetings.

(a)   The Working Group

The Working Group is responsible for the critical reviews and evaluations that are developed during the meeting. The tasks of Working Group Members are: (i) to ascertain that all appropriate data have been collected; (ii) to select the data relevant for the evaluation on the basis of scientific merit; (iii) to prepare accurate summaries of the data to enable the reader to follow the reasoning of the Working Group; (iv) to evaluate the results of epidemiological and experimental studies on cancer; (v) to evaluate data relevant to the understanding of mechanisms of carcinogenesis; and (vi) to make an overall evaluation of the carcinogenicity of the exposure to humans. Working Group Members generally have published significant research related to the carcinogenicity of the agents being reviewed, and IARC uses literature searches to identify most experts. Working Group Members are selected on the basis of (a) knowledge and experience and (b) absence of real or apparent conflicts of interests. Consideration is also given to demographic diversity and balance of scientific findings and views.

(b)   Invited Specialists

Invited Specialists are experts who also have critical knowledge and experience but have a real or apparent conflict of interests. These experts are invited when necessary to assist in the Working Group by contributing their unique knowledge and experience during subgroup and plenary discussions. They may also contribute text on non-influential issues in the section on exposure, such as a general description of data on production and use (see Part B, Section 1). Invited Specialists do not serve as meeting chair

or subgroup chair, draft text that pertains to the description or interpretation of cancer data, or participate in the evaluations.

(c)   Representatives of national and international health agencies

Representatives of national and international health agencies often attend meetings because their agencies sponsor the programme or are interested in the subject of a meeting. Representatives do not serve as meeting chair or subgroup chair, draft any part of a *Monograph,* or participate in the evaluations.

(d)   Observers with relevant scientific credentials

Observers with relevant scientific credentials may be admitted to a meeting by IARC in limited numbers. Attention will be given to achieving a balance of Observers from constituencies with differing perspectives. They are invited to observe the meeting and should not attempt to influence it. Observers do not serve as meeting chair or subgroup chair, draft any part of a *Monograph*, or participate in the evaluations. At the meeting, the meeting chair and subgroup chairs may grant Observers an opportunity to speak, generally after they have observed a discussion. Observers agree to respect the Guidelines for Observers at *IARC Monographs* meetings (available at http://monographs.iarc.fr).

(e)   The IARC Secretariat

The IARC Secretariat consists of scientists who are designated by IARC and who have relevant expertise. They serve as rapporteurs and participate in all discussions. When requested by the meeting chair or subgroup chair, they may also draft text or prepare tables and analyses. Before an invitation is extended, each potential participant, including the IARC Secretariat, completes the WHO Declaration of Interests

to report financial interests, employment and consulting, and individual and institutional research support related to the subject of the meeting. IARC assesses these interests to determine whether there is a conflict that warrants some limitation on participation. The declarations are updated and reviewed again at the opening of the meeting. Interests related to the subject of the meeting are disclosed to the meeting participants and in the published volume (Cogliano et al., 2004).

The names and principal affiliations of participants are available on the *Monographs* programme web site (http://monographs.iarc.fr) approximately two months before each meeting. It is not acceptable for Observers or third parties to contact other participants before a meeting or to lobby them at any time. Meeting participants are asked to report all such contacts to IARC (Cogliano et al., 2005).

All participants are listed, with their principal affiliations, at the beginning of each volume. Each participant who is a Member of a Working Group serves as an individual scientist and not as a representative of any organization, government or industry.

6.   Working procedures

A separate Working Group is responsible for developing each volume of *Monographs*. A volume contains one or more *Monographs*, which can cover either a single agent or several related agents. Approximately one year in advance of the meeting of a Working Group, the agents to be reviewed are announced on the *Monographs* programme web site (http://monographs.iarc.fr) and participants are selected by IARC staff in consultation with other experts. Subsequently, relevant biological and epidemiological data are collected by IARC from recognized sources of information on carcinogenesis, including data storage and retrieval systems such as PubMed. Meeting participants who are asked to prepare

preliminary working papers for specific sections are expected to supplement the IARC literature searches with their own searches.

Industrial associations, labour unions and other knowledgeable organizations may be asked to provide input to the sections on production and use, although this involvement is not required as a general rule. Information on production and trade is obtained from governmental, trade and market research publications and, in some cases, by direct contact with industries. Separate production data on some agents may not be available for a variety of reasons (e.g. not collected or made public in all producing countries, production is small). Information on uses may be obtained from published sources but is often complemented by direct contact with manufacturers. Efforts are made to supplement this information with data from other national and international sources.

Six months before the meeting, the material obtained is sent to meeting participants to prepare preliminary working papers. The working papers are compiled by IARC staff and sent, before the meeting, to Working Group Members and Invited Specialists for review.

The Working Group meets at IARC for seven to eight days to discuss and finalize the texts and to formulate the evaluations. The objectives of the meeting are peer review and consensus. During the first few days, four subgroups (covering exposure data, cancer in humans, cancer in experimental animals, and mechanistic and other relevant data) review the working papers, develop a joint subgroup draft and write summaries. Care is taken to ensure that each study summary is written or reviewed by someone not associated with the study being considered. During the last few days, the Working Group meets in plenary session to review the subgroup drafts and develop the evaluations. As a result, the entire volume is the joint product of the Working Group, and there are no individually authored sections.

IARC Working Groups strive to achieve a consensus evaluation. Consensus reflects broad agreement among Working Group Members, but not necessarily unanimity. The chair may elect to poll Working Group Members to determine the diversity of scientific opinion on issues where consensus is not readily apparent.

After the meeting, the master copy is verified by consulting the original literature, edited and prepared for publication. The aim is to publish the volume within six months of the Working Group meeting. A summary of the outcome is available on the *Monographs* programme web site soon after the meeting.

B.   SCIENTIFIC REVIEW AND EVALUATION

The available studies are summarized by the Working Group, with particular regard to the qualitative aspects discussed below. In general, numerical findings are indicated as they appear in the original report; units are converted when necessary for easier comparison. The Working Group may conduct additional analyses of the published data and use them in their assessment of the evidence; the results of such supplementary analyses are given in square brackets. When an important aspect of a study that directly impinges on its interpretation should be brought to the attention of the reader, a Working Group comment is given in square brackets.

The scope of the *IARC Monographs* programme has expanded beyond chemicals to include complex mixtures, occupational exposures, physical and biological agents, lifestyle factors and other potentially carcinogenic exposures. Over time, the structure of a *Monograph* has evolved to include the following sections:

Exposure data
Studies of cancer in humans

Studies of cancer in experimental animals

Mechanistic and other relevant data

Summary

Evaluation and rationale

In addition, a section of General Remarks at the front of the volume discusses the reasons the agents were scheduled for evaluation and some key issues the Working Group encountered during the meeting.

This part of the Preamble discusses the types of evidence considered and summarized in each section of a *Monograph*, followed by the scientific criteria that guide the evaluations.

1. Exposure data

Each *Monograph* includes general information on the agent: this information may vary substantially between agents and must be adapted accordingly. Also included is information on production and use (when appropriate), methods of analysis and detection, occurrence, and sources and routes of human occupational and environmental exposures. Depending on the agent, regulations and guidelines for use may be presented.

(a) General information on the agent

For chemical agents, sections on chemical and physical data are included: the Chemical Abstracts Service Registry Number, the latest primary name and the IUPAC systematic name are recorded; other synonyms are given, but the list is not necessarily comprehensive. Information on chemical and physical properties that are relevant to identification, occurrence and biological activity is included. A description of technical products of chemicals includes trade names, relevant specifications and available information on composition and impurities. Some of the trade names given may be those of mixtures in which the agent being evaluated is only one of the ingredients.

For biological agents, taxonomy, structure and biology are described, and the degree of variability is indicated. Mode of replication, life cycle, target cells, persistence, latency, host response and clinical disease other than cancer are also presented.

For physical agents that are forms of radiation, energy and range of the radiation are included. For foreign bodies, fibres and respirable particles, size range and relative dimensions are indicated.

For agents such as mixtures, drugs or lifestyle factors, a description of the agent, including its composition, is given.

Whenever appropriate, other information, such as historical perspectives or the description of an industry or habit, may be included.

(b) Analysis and detection

An overview of methods of analysis and detection of the agent is presented, including their sensitivity, specificity and reproducibility. Methods widely used for regulatory purposes are emphasized. Methods for monitoring human exposure are also given. No critical evaluation or recommendation of any method is meant or implied.

(c) Production and use

The dates of first synthesis and of first commercial production of a chemical, mixture or other agent are provided when available; for agents that do not occur naturally, this information may allow a reasonable estimate to be made of the date before which no human exposure to the agent could have occurred. The dates of first reported occurrence of an exposure are also provided when available. In addition, methods of synthesis used in past and present commercial production and different methods of production,

which may give rise to different impurities, are described.

The countries where companies report production of the agent, and the number of companies in each country, are identified. Available data on production, international trade and uses are obtained for representative regions. It should not, however, be inferred that those areas or nations are necessarily the sole or major sources or users of the agent. Some identified uses may not be current or major applications, and the coverage is not necessarily comprehensive. In the case of drugs, mention of their therapeutic uses does not necessarily represent current practice nor does it imply judgement as to their therapeutic efficacy.

(d)   Occurrence and exposure

Information on the occurrence of an agent in the environment is obtained from data derived from the monitoring and surveillance of levels in occupational environments, air, water, soil, plants, foods and animal and human tissues. When available, data on the generation, persistence and bioaccumulation of the agent are also included. Such data may be available from national databases.

Data that indicate the extent of past and present human exposure, the sources of exposure, the people most likely to be exposed and the factors that contribute to the exposure are reported. Information is presented on the range of human exposure, including occupational and environmental exposures. This includes relevant findings from both developed and developing countries. Some of these data are not distributed widely and may be available from government reports and other sources. In the case of mixtures, industries, occupations or processes, information is given about all agents known to be present. For processes, industries and occupations, a historical description is also given, noting variations in chemical composition, physical properties and levels of occupational exposure

with date and place. For biological agents, the epidemiology of infection is described.

(e)   Regulations and guidelines

Statements concerning regulations and guidelines (e.g. occupational exposure limits, maximal levels permitted in foods and water, pesticide registrations) are included, but they may not reflect the most recent situation, since such limits are continuously reviewed and modified. The absence of information on regulatory status for a country should not be taken to imply that that country does not have regulations with regard to the exposure. For biological agents, legislation and control, including vaccination and therapy, are described.

2.   Studies of cancer in humans

This section includes all pertinent epidemiological studies (see Part A, Section 4). Studies of biomarkers are included when they are relevant to an evaluation of carcinogenicity to humans.

(a)   Types of study considered

Several types of epidemiological study contribute to the assessment of carcinogenicity in humans — cohort studies, case–control studies, correlation (or ecological) studies and intervention studies. Rarely, results from randomized trials may be available. Case reports and case series of cancer in humans may also be reviewed.

Cohort and case–control studies relate individual exposures under study to the occurrence of cancer in individuals and provide an estimate of effect (such as relative risk) as the main measure of association. Intervention studies may provide strong evidence for making causal inferences, as exemplified by cessation of smoking and the subsequent decrease in risk for lung cancer.

In correlation studies, the units of investigation are usually whole populations (e.g. in

particular geographical areas or at particular times), and cancer frequency is related to a summary measure of the exposure of the population to the agent under study. In correlation studies, individual exposure is not documented, which renders this kind of study more prone to confounding. In some circumstances, however, correlation studies may be more informative than analytical study designs (see, for example, the *Monograph* on arsenic in drinking-water; IARC, 2004).

In some instances, case reports and case series have provided important information about the carcinogenicity of an agent. These types of study generally arise from a suspicion, based on clinical experience, that the concurrence of two events — that is, a particular exposure and occurrence of a cancer — has happened rather more frequently than would be expected by chance. Case reports and case series usually lack complete ascertainment of cases in any population, definition or enumeration of the population at risk and estimation of the expected number of cases in the absence of exposure.

The uncertainties that surround the interpretation of case reports, case series and correlation studies make them inadequate, except in rare instances, to form the sole basis for inferring a causal relationship. When taken together with case–control and cohort studies, however, these types of study may add materially to the judgement that a causal relationship exists.

Epidemiological studies of benign neoplasms, presumed preneoplastic lesions and other end-points thought to be relevant to cancer are also reviewed. They may, in some instances, strengthen inferences drawn from studies of cancer itself.

(b) Quality of studies considered

It is necessary to take into account the possible roles of bias, confounding and chance in the interpretation of epidemiological studies.

Bias is the effect of factors in study design or execution that lead erroneously to a stronger or weaker association than in fact exists between an agent and disease. Confounding is a form of bias that occurs when the relationship with disease is made to appear stronger or weaker than it truly is as a result of an association between the apparent causal factor and another factor that is associated with either an increase or decrease in the incidence of the disease. The role of chance is related to biological variability and the influence of sample size on the precision of estimates of effect.

In evaluating the extent to which these factors have been minimized in an individual study, consideration is given to several aspects of design and analysis as described in the report of the study. For example, when suspicion of carcinogenicity arises largely from a single small study, careful consideration is given when interpreting subsequent studies that included these data in an enlarged population. Most of these considerations apply equally to case–control, cohort and correlation studies. Lack of clarity of any of these aspects in the reporting of a study can decrease its credibility and the weight given to it in the final evaluation of the exposure.

First, the study population, disease (or diseases) and exposure should have been well defined by the authors. Cases of disease in the study population should have been identified in a way that was independent of the exposure of interest, and exposure should have been assessed in a way that was not related to disease status.

Second, the authors should have taken into account — in the study design and analysis — other variables that can influence the risk of disease and may have been related to the exposure of interest. Potential confounding by such variables should have been dealt with either in the design of the study, such as by matching, or in the analysis, by statistical adjustment. In cohort studies, comparisons with local rates of disease may or may not be more appropriate than

those with national rates. Internal comparisons of frequency of disease among individuals at different levels of exposure are also desirable in cohort studies, since they minimize the potential for confounding related to the difference in risk factors between an external reference group and the study population.

Third, the authors should have reported the basic data on which the conclusions are founded, even if sophisticated statistical analyses were employed. At the very least, they should have given the numbers of exposed and unexposed cases and controls in a case–control study and the numbers of cases observed and expected in a cohort study. Further tabulations by time since exposure began and other temporal factors are also important. In a cohort study, data on all cancer sites and all causes of death should have been given, to reveal the possibility of reporting bias. In a case–control study, the effects of investigated factors other than the exposure of interest should have been reported.

Finally, the statistical methods used to obtain estimates of relative risk, absolute rates of cancer, confidence intervals and significance tests, and to adjust for confounding should have been clearly stated by the authors. These methods have been reviewed for case–control studies (Breslow & Day, 1980) and for cohort studies (Breslow & Day, 1987).

(c)   Meta-analyses and pooled analyses

Independent epidemiological studies of the same agent may lead to results that are difficult to interpret. Combined analyses of data from multiple studies are a means of resolving this ambiguity, and well conducted analyses can be considered. There are two types of combined analysis. The first involves combining summary statistics such as relative risks from individual studies (meta-analysis) and the second involves a pooled analysis of the raw data from the individual studies (pooled analysis) (Greenland, 1998).

The advantages of combined analyses are increased precision due to increased sample size and the opportunity to explore potential confounders, interactions and modifying effects that may explain heterogeneity among studies in more detail. A disadvantage of combined analyses is the possible lack of compatibility of data from various studies due to differences in subject recruitment, procedures of data collection, methods of measurement and effects of unmeasured co-variates that may differ among studies. Despite these limitations, well conducted combined analyses may provide a firmer basis than individual studies for drawing conclusions about the potential carcinogenicity of agents.

IARC may commission a meta-analysis or pooled analysis that is pertinent to a particular *Monograph* (see Part A, Section 4). Additionally, as a means of gaining insight from the results of multiple individual studies, ad hoc calculations that combine data from different studies may be conducted by the Working Group during the course of a *Monograph* meeting. The results of such original calculations, which would be specified in the text by presentation in square brackets, might involve updates of previously conducted analyses that incorporate the results of more recent studies or de-novo analyses. Irrespective of the source of data for the meta-analyses and pooled analyses, it is important that the same criteria for data quality be applied as those that would be applied to individual studies and to ensure also that sources of heterogeneity between studies be taken into account.

(d)   Temporal effects

Detailed analyses of both relative and absolute risks in relation to temporal variables, such as age at first exposure, time since first exposure, duration of exposure, cumulative exposure, peak exposure (when appropriate) and

time since cessation of exposure, are reviewed and summarized when available. Analyses of temporal relationships may be useful in making causal inferences. In addition, such analyses may suggest whether a carcinogen acts early or late in the process of carcinogenesis, although, at best, they allow only indirect inferences about mechanisms of carcinogenesis.

(e)   Use of biomarkers in epidemiological studies

Biomarkers indicate molecular, cellular or other biological changes and are increasingly used in epidemiological studies for various purposes (IARC, 1991; Vainio et al., 1992; Toniolo et al., 1997; Vineis et al., 1999; Buffler et al., 2004). These may include evidence of exposure, of early effects, of cellular, tissue or organism responses, of individual susceptibility or host responses, and inference of a mechanism (see Part B, Section 4b). This is a rapidly evolving field that encompasses developments in genomics, epigenomics and other emerging technologies.

Molecular epidemiological data that identify associations between genetic polymorphisms and interindividual differences in susceptibility to the agent(s) being evaluated may contribute to the identification of carcinogenic hazards to humans. If the polymorphism has been demonstrated experimentally to modify the functional activity of the gene product in a manner that is consistent with increased susceptibility, these data may be useful in making causal inferences. Similarly, molecular epidemiological studies that measure cell functions, enzymes or metabolites that are thought to be the basis of susceptibility may provide evidence that reinforces biological plausibility. It should be noted, however, that when data on genetic susceptibility originate from multiple comparisons that arise from subgroup analyses, this can generate false-positive results and inconsistencies across studies, and such data therefore require careful evaluation. If the

known phenotype of a genetic polymorphism can explain the carcinogenic mechanism of the agent being evaluated, data on this phenotype may be useful in making causal inferences.

(f)   Criteria for causality

After the quality of individual epidemiological studies of cancer has been summarized and assessed, a judgement is made concerning the strength of evidence that the agent in question is carcinogenic to humans. In making its judgement, the Working Group considers several criteria for causality (Hill, 1965). A strong association (e.g. a large relative risk) is more likely to indicate causality than a weak association, although it is recognized that estimates of effect of small magnitude do not imply lack of causality and may be important if the disease or exposure is common. Associations that are replicated in several studies of the same design or that use different epidemiological approaches or under different circumstances of exposure are more likely to represent a causal relationship than isolated observations from single studies. If there are inconsistent results among investigations, possible reasons are sought (such as differences in exposure), and results of studies that are judged to be of high quality are given more weight than those of studies that are judged to be methodologically less sound.

If the risk increases with the exposure, this is considered to be a strong indication of causality, although the absence of a graded response is not necessarily evidence against a causal relationship. The demonstration of a decline in risk after cessation of or reduction in exposure in individuals or in whole populations also supports a causal interpretation of the findings.

Several scenarios may increase confidence in a causal relationship. On the one hand, an agent may be specific in causing tumours at one site or of one morphological type. On the other, carcinogenicity may be evident through the causation of

multiple tumour types. Temporality, precision of estimates of effect, biological plausibility and coherence of the overall database are considered. Data on biomarkers may be employed in an assessment of the biological plausibility of epidemiological observations.

Although rarely available, results from randomized trials that show different rates of cancer among exposed and unexposed individuals provide particularly strong evidence for causality.

When several epidemiological studies show little or no indication of an association between an exposure and cancer, a judgement may be made that, in the aggregate, they show evidence of lack of carcinogenicity. Such a judgement requires first that the studies meet, to a sufficient degree, the standards of design and analysis described above. Specifically, the possibility that bias, confounding or misclassification of exposure or outcome could explain the observed results should be considered and excluded with reasonable certainty. In addition, all studies that are judged to be methodologically sound should (a) be consistent with an estimate of effect of unity for any observed level of exposure, (b) when considered together, provide a pooled estimate of relative risk that is at or near to unity, and (c) have a narrow confidence interval, due to sufficient population size. Moreover, no individual study nor the pooled results of all the studies should show any consistent tendency that the relative risk of cancer increases with increasing level of exposure. It is important to note that evidence of lack of carcinogenicity obtained from several epidemiological studies can apply only to the type(s) of cancer studied, to the dose levels reported, and to the intervals between first exposure and disease onset observed in these studies. Experience with human cancer indicates that the period from first exposure to the development of clinical cancer is sometimes longer than 20 years; latent periods substantially shorter than 30 years cannot provide evidence for lack of carcinogenicity.

3. Studies of cancer in experimental animals

All known human carcinogens that have been studied adequately for carcinogenicity in experimental animals have produced positive results in one or more animal species (Wilbourn et al., 1986; Tomatis et al., 1989). For several agents (e.g. aflatoxins, diethylstilbestrol, solar radiation, vinyl chloride), carcinogenicity in experimental animals was established or highly suspected before epidemiological studies confirmed their carcinogenicity in humans (Vainio et al., 1995). Although this association cannot establish that all agents that cause cancer in experimental animals also cause cancer in humans, it is biologically plausible that agents for which there is *sufficient evidence of carcinogenicity* in experimental animals (see Part B, Section 6b) also present a carcinogenic hazard to humans. Accordingly, in the absence of additional scientific information, these agents are considered to pose a carcinogenic hazard to humans. Examples of additional scientific information are data that demonstrate that a given agent causes cancer in animals through a species-specific mechanism that does not operate in humans or data that demonstrate that the mechanism in experimental animals also operates in humans (see Part B, Section 6).

Consideration is given to all available long-term studies of cancer in experimental animals with the agent under review (see Part A, Section 4). In all experimental settings, the nature and extent of impurities or contaminants present in the agent being evaluated are given when available. Animal species, strain (including genetic background where applicable), sex, numbers per group, age at start of treatment, route of exposure, dose levels, duration of exposure, survival and information on tumours (incidence, latency, severity or multiplicity of neoplasms or preneoplastic lesions) are reported. Those studies in experimental animals that are judged to be irrelevant to the evaluation or judged to be inadequate

(e.g. too short a duration, too few animals, poor survival; see below) may be omitted. Guidelines for conducting long-term carcinogenicity experiments have been published (e.g. OECD, 2002).

Other studies considered may include: experiments in which the agent was administered in the presence of factors that modify carcinogenic effects (e.g. initiation–promotion studies, co-carcinogenicity studies and studies in genetically modified animals); studies in which the end-point was not cancer but a defined precancerous lesion; experiments on the carcinogenicity of known metabolites and derivatives; and studies of cancer in non-laboratory animals (e.g. livestock and companion animals) exposed to the agent.

For studies of mixtures, consideration is given to the possibility that changes in the physicochemical properties of the individual substances may occur during collection, storage, extraction, concentration and delivery. Another consideration is that chemical and toxicological interactions of components in a mixture may alter dose–response relationships. The relevance to human exposure of the test mixture administered in the animal experiment is also assessed. This may involve consideration of the following aspects of the mixture tested: (i) physical and chemical characteristics, (ii) identified constituents that may indicate the presence of a class of substances and (iii) the results of genetic toxicity and related tests.

The relevance of results obtained with an agent that is analogous (e.g. similar in structure or of a similar virus genus) to that being evaluated is also considered. Such results may provide biological and mechanistic information that is relevant to the understanding of the process of carcinogenesis in humans and may strengthen the biological plausibility that the agent being evaluated is carcinogenic to humans (see Part B, Section 2f).

(a)   Qualitative aspects

An assessment of carcinogenicity involves several considerations of qualitative importance, including (i) the experimental conditions under which the test was performed, including route, schedule and duration of exposure, species, strain (including genetic background where applicable), sex, age and duration of follow-up; (ii) the consistency of the results, for example, across species and target organ(s); (iii) the spectrum of neoplastic response, from preneoplastic lesions and benign tumours to malignant neoplasms; and (iv) the possible role of modifying factors.

Considerations of importance in the interpretation and evaluation of a particular study include: (i) how clearly the agent was defined and, in the case of mixtures, how adequately the sample characterization was reported; (ii) whether the dose was monitored adequately, particularly in inhalation experiments; (iii) whether the doses, duration of treatment and route of exposure were appropriate; (iv) whether the survival of treated animals was similar to that of controls; (v) whether there were adequate numbers of animals per group; (vi) whether both male and female animals were used; (vii) whether animals were allocated randomly to groups; (viii) whether the duration of observation was adequate; and (ix) whether the data were reported and analysed adequately.

When benign tumours (a) occur together with and originate from the same cell type as malignant tumours in an organ or tissue in a particular study and (b) appear to represent a stage in the progression to malignancy, they are usually combined in the assessment of tumour incidence (Huff et al., 1989). The occurrence of lesions presumed to be preneoplastic may in certain instances aid in assessing the biological plausibility of any neoplastic response observed. If an agent induces only benign neoplasms that appear to be end-points that do not readily undergo transition to malignancy, the agent

should nevertheless be suspected of being carcinogenic and requires further investigation.

(b) Quantitative aspects

The probability that tumours will occur may depend on the species, sex, strain, genetic background and age of the animal, and on the dose, route, timing and duration of the exposure. Evidence of an increased incidence of neoplasms with increasing levels of exposure strengthens the inference of a causal association between the exposure and the development of neoplasms.

The form of the dose–response relationship can vary widely, depending on the particular agent under study and the target organ. Mechanisms such as induction of DNA damage or inhibition of repair, altered cell division and cell death rates and changes in intercellular communication are important determinants of dose–response relationships for some carcinogens. Since many chemicals require metabolic activation before being converted to their reactive intermediates, both metabolic and toxicokinetic aspects are important in determining the dose–response pattern. Saturation of steps such as absorption, activation, inactivation and elimination may produce nonlinearity in the dose–response relationship (Hoel et al., 1983; Gart et al., 1986), as could saturation of processes such as DNA repair. The dose–response relationship can also be affected by differences in survival among the treatment groups.

(c) Statistical analyses

Factors considered include the adequacy of the information given for each treatment group: (i) number of animals studied and number examined histologically, (ii) number of animals with a given tumour type and (iii) length of survival. The statistical methods used should be clearly stated and should be the generally accepted techniques refined for this purpose (Peto et al., 1980;

Gart et al., 1986; Portier & Bailer, 1989; Bieler & Williams, 1993). The choice of the most appropriate statistical method requires consideration of whether or not there are differences in survival among the treatment groups; for example, reduced survival because of non-tumour-related mortality can preclude the occurrence of tumours later in life. When detailed information on survival is not available, comparisons of the proportions of tumour-bearing animals among the effective number of animals (alive at the time the first tumour was discovered) can be useful when significant differences in survival occur before tumours appear. The lethality of the tumour also requires consideration: for rapidly fatal tumours, the time of death provides an indication of the time of tumour onset and can be assessed using life-table methods; non-fatal or incidental tumours that do not affect survival can be assessed using methods such as the Mantel-Haenzel test for changes in tumour prevalence. Because tumour lethality is often difficult to determine, methods such as the Poly-K test that do not require such information can also be used. When results are available on the number and size of tumours seen in experimental animals (e.g. papillomas on mouse skin, liver tumours observed through nuclear magnetic resonance tomography), other more complicated statistical procedures may be needed (Sherman et al., 1994; Dunson et al., 2003).

Formal statistical methods have been developed to incorporate historical control data into the analysis of data from a given experiment. These methods assign an appropriate weight to historical and concurrent controls on the basis of the extent of between-study and within-study variability: less weight is given to historical controls when they show a high degree of variability, and greater weight when they show little variability. It is generally not appropriate to discount a tumour response that is significantly increased compared with concurrent controls by arguing that it falls within the range of historical controls, particularly

when historical controls show high between-study variability and are, thus, of little relevance to the current experiment. In analysing results for uncommon tumours, however, the analysis may be improved by considering historical control data, particularly when between-study variability is low. Historical controls should be selected to resemble the concurrent controls as closely as possible with respect to species, gender and strain, as well as other factors such as basal diet and general laboratory environment, which may affect tumour-response rates in control animals (Haseman et al., 1984; Fung et al., 1996; Greim et al., 2003).

Although meta-analyses and combined analyses are conducted less frequently for animal experiments than for epidemiological studies due to differences in animal strains, they can be useful aids in interpreting animal data when the experimental protocols are sufficiently similar.

4. Mechanistic and other relevant data

Mechanistic and other relevant data may provide evidence of carcinogenicity and also help in assessing the relevance and importance of findings of cancer in animals and in humans. The nature of the mechanistic and other relevant data depends on the biological activity of the agent being considered. The Working Group considers representative studies to give a concise description of the relevant data and issues that they consider to be important; thus, not every available study is cited. Relevant topics may include toxicokinetics, mechanisms of carcinogenesis, susceptible individuals, populations and life-stages, other relevant data and other adverse effects. When data on biomarkers are informative about the mechanisms of carcinogenesis, they are included in this section.

These topics are not mutually exclusive; thus, the same studies may be discussed in more than one subsection. For example, a mutation in a gene that codes for an enzyme that metabolizes the agent under study could be discussed in the subsections on toxicokinetics, mechanisms and individual susceptibility if it also exists as an inherited polymorphism.

(a)   Toxicokinetic data

Toxicokinetics refers to the absorption, distribution, metabolism and elimination of agents in humans, experimental animals and, where relevant, cellular systems. Examples of kinetic factors that may affect dose–response relationships include uptake, deposition, biopersistence and half-life in tissues, protein binding, metabolic activation and detoxification. Studies that indicate the metabolic fate of the agent in humans and in experimental animals are summarized briefly, and comparisons of data from humans and animals are made when possible. Comparative information on the relationship between exposure and the dose that reaches the target site may be important for the extrapolation of hazards between species and in clarifying the role of in-vitro findings.

(b)   Data on mechanisms of carcinogenesis

To provide focus, the Working Group attempts to identify the possible mechanisms by which the agent may increase the risk of cancer. For each possible mechanism, a representative selection of key data from humans and experimental systems is summarized. Attention is given to gaps in the data and to data that suggests that more than one mechanism may be operating. The relevance of the mechanism to humans is discussed, in particular, when mechanistic data are derived from experimental model systems. Changes in the affected organs, tissues or cells can be divided into three non-exclusive levels as described below.

(i) Changes in physiology

Physiological changes refer to exposure-related modifications to the physiology and/or response of cells, tissues and organs. Examples of potentially adverse physiological changes include mitogenesis, compensatory cell division, escape from apoptosis and/or senescence, presence of inflammation, hyperplasia, metaplasia and/or preneoplasia, angiogenesis, alterations in cellular adhesion, changes in steroidal hormones and changes in immune surveillance.

(ii) Functional changes at the cellular level

Functional changes refer to exposure-related alterations in the signalling pathways used by cells to manage critical processes that are related to increased risk for cancer. Examples of functional changes include modified activities of enzymes involved in the metabolism of xenobiotics, alterations in the expression of key genes that regulate DNA repair, alterations in cyclin-dependent kinases that govern cell cycle progression, changes in the patterns of post-translational modifications of proteins, changes in regulatory factors that alter apoptotic rates, changes in the secretion of factors related to the stimulation of DNA replication and transcription and changes in gap–junction-mediated intercellular communication.

(iii) Changes at the molecular level

Molecular changes refer to exposure-related changes in key cellular structures at the molecular level, including, in particular, genotoxicity. Examples of molecular changes include formation of DNA adducts and DNA strand breaks, mutations in genes, chromosomal aberrations, aneuploidy and changes in DNA methylation patterns. Greater emphasis is given to irreversible effects.

The use of mechanistic data in the identification of a carcinogenic hazard is specific to the mechanism being addressed and is not readily described for every possible level and mechanism discussed above.

Genotoxicity data are discussed here to illustrate the key issues involved in the evaluation of mechanistic data.

Tests for genetic and related effects are described in view of the relevance of gene mutation and chromosomal aberration/aneuploidy to carcinogenesis (Vainio et al., 1992; McGregor et al., 1999). The adequacy of the reporting of sample characterization is considered and, when necessary, commented upon; with regard to complex mixtures, such comments are similar to those described for animal carcinogenicity tests. The available data are interpreted critically according to the end-points detected, which may include DNA damage, gene mutation, sister chromatid exchange, micronucleus formation, chromosomal aberrations and aneuploidy. The concentrations employed are given, and mention is made of whether the use of an exogenous metabolic system in vitro affected the test result. These data are listed in tabular form by phylogenetic classification.

Positive results in tests using prokaryotes, lower eukaryotes, insects, plants and cultured mammalian cells suggest that genetic and related effects could occur in mammals. Results from such tests may also give information on the types of genetic effect produced and on the involvement of metabolic activation. Some end-points described are clearly genetic in nature (e.g. gene mutations), while others are associated with genetic effects (e.g. unscheduled DNA synthesis). In-vitro tests for tumour promotion, cell transformation and gap–junction intercellular communication may be sensitive to changes that are not necessarily the result of genetic alterations but that may have specific relevance to the process of carcinogenesis. Critical appraisals of these tests have been published (Montesano et al., 1986; McGregor et al., 1999).

Genetic or other activity manifest in humans and experimental mammals is regarded to be of

greater relevance than that in other organisms. The demonstration that an agent can induce gene and chromosomal mutations in mammals in vivo indicates that it may have carcinogenic activity. Negative results in tests for mutagenicity in selected tissues from animals treated in vivo provide less weight, partly because they do not exclude the possibility of an effect in tissues other than those examined. Moreover, negative results in short-term tests with genetic end-points cannot be considered to provide evidence that rules out the carcinogenicity of agents that act through other mechanisms (e.g. receptor-mediated effects, cellular toxicity with regenerative cell division, peroxisome proliferation) (Vainio et al., 1992). Factors that may give misleading results in short-term tests have been discussed in detail elsewhere (Montesano et al., 1986; McGregor et al., 1999).

When there is evidence that an agent acts by a specific mechanism that does not involve genotoxicity (e.g. hormonal dysregulation, immune suppression, and formation of calculi and other deposits that cause chronic irritation), that evidence is presented and reviewed critically in the context of rigorous criteria for the operation of that mechanism in carcinogenesis (e.g. Capen et al., 1999).

For biological agents such as viruses, bacteria and parasites, other data relevant to carcinogenicity may include descriptions of the pathology of infection, integration and expression of viruses, and genetic alterations seen in human tumours. Other observations that might comprise cellular and tissue responses to infection, immune response and the presence of tumour markers are also considered.

For physical agents that are forms of radiation, other data relevant to carcinogenicity may include descriptions of damaging effects at the physiological, cellular and molecular level, as for chemical agents, and descriptions of how these effects occur. 'Physical agents' may also be considered to comprise foreign bodies, such as surgical implants of various kinds, and poorly soluble fibres, dusts and particles of various sizes, the pathogenic effects of which are a result of their physical presence in tissues or body cavities. Other relevant data for such materials may include characterization of cellular, tissue and physiological reactions to these materials and descriptions of pathological conditions other than neoplasia with which they may be associated.

(c) Other data relevant to mechanisms

A description is provided of any structure–activity relationships that may be relevant to an evaluation of the carcinogenicity of an agent, the toxicological implications of the physical and chemical properties, and any other data relevant to the evaluation that are not included elsewhere.

High-output data, such as those derived from gene expression microarrays, and high-throughput data, such as those that result from testing hundreds of agents for a single end-point, pose a unique problem for the use of mechanistic data in the evaluation of a carcinogenic hazard. In the case of high-output data, there is the possibility to overinterpret changes in individual end-points (e.g. changes in expression in one gene) without considering the consistency of that finding in the broader context of the other end-points (e.g. other genes with linked transcriptional control). High-output data can be used in assessing mechanisms, but all end-points measured in a single experiment need to be considered in the proper context. For high-throughput data, where the number of observations far exceeds the number of end-points measured, their utility for identifying common mechanisms across multiple agents is enhanced. These data can be used to identify mechanisms that not only seem plausible, but also have a consistent pattern of carcinogenic response across entire classes of related compounds.

(d) Susceptibility data

Individuals, populations and life-stages may have greater or lesser susceptibility to an agent, based on toxicokinetics, mechanisms of carcinogenesis and other factors. Examples of host and genetic factors that affect individual susceptibility include sex, genetic polymorphisms of genes involved in the metabolism of the agent under evaluation, differences in metabolic capacity due to life-stage or the presence of disease, differences in DNA repair capacity, competition for or alteration of metabolic capacity by medications or other chemical exposures, pre-existing hormonal imbalance that is exacerbated by a chemical exposure, a suppressed immune system, periods of higher-than-usual tissue growth or regeneration and genetic polymorphisms that lead to differences in behaviour (e.g. addiction). Such data can substantially increase the strength of the evidence from epidemiological data and enhance the linkage of in-vivo and in-vitro laboratory studies to humans.

(e) Data on other adverse effects

Data on acute, subchronic and chronic adverse effects relevant to the cancer evaluation are summarized. Adverse effects that confirm distribution and biological effects at the sites of tumour development, or alterations in physiology that could lead to tumour development, are emphasized. Effects on reproduction, embryonic and fetal survival and development are summarized briefly. The adequacy of epidemiological studies of reproductive outcome and genetic and related effects in humans is judged by the same criteria as those applied to epidemiological studies of cancer, but fewer details are given.

5. Summary

This section is a summary of data presented in the preceding sections. Summaries can be found on the *Monographs* programme web site (http://monographs.iarc.fr).

(a) Exposure data

Data are summarized, as appropriate, on the basis of elements such as production, use, occurrence and exposure levels in the workplace and environment and measurements in human tissues and body fluids. Quantitative data and time trends are given to compare exposures in different occupations and environmental settings. Exposure to biological agents is described in terms of transmission, prevalence and persistence of infection.

(b) Cancer in humans

Results of epidemiological studies pertinent to an assessment of human carcinogenicity are summarized. When relevant, case reports and correlation studies are also summarized. The target organ(s) or tissue(s) in which an increase in cancer was observed is identified. Dose–response and other quantitative data may be summarized when available.

(c) Cancer in experimental animals

Data relevant to an evaluation of carcinogenicity in animals are summarized. For each animal species, study design and route of administration, it is stated whether an increased incidence, reduced latency, or increased severity or multiplicity of neoplasms or preneoplastic lesions were observed, and the tumour sites are indicated. If the agent produced tumours after prenatal exposure or in single-dose experiments, this is also mentioned. Negative findings, inverse relationships, dose–response and other quantitative data are also summarized.

(d) Mechanistic and other relevant data

Data relevant to the toxicokinetics (absorption, distribution, metabolism, elimination) and the possible mechanism(s) of carcinogenesis (e.g. genetic toxicity, epigenetic effects) are summarized. In addition, information on susceptible individuals, populations and life-stages is summarized. This section also reports on other toxic effects, including reproductive and developmental effects, as well as additional relevant data that are considered to be important.

6.   Evaluation and rationale

Evaluations of the strength of the evidence for carcinogenicity arising from human and experimental animal data are made, using standard terms. The strength of the mechanistic evidence is also characterized.

It is recognized that the criteria for these evaluations, described below, cannot encompass all of the factors that may be relevant to an evaluation of carcinogenicity. In considering all of the relevant scientific data, the Working Group may assign the agent to a higher or lower category than a strict interpretation of these criteria would indicate.

These categories refer only to the strength of the evidence that an exposure is carcinogenic and not to the extent of its carcinogenic activity (potency). A classification may change as new information becomes available.

An evaluation of the degree of evidence is limited to the materials tested, as defined physically, chemically or biologically. When the agents evaluated are considered by the Working Group to be sufficiently closely related, they may be grouped together for the purpose of a single evaluation of the degree of evidence.

(a)   Carcinogenicity in humans

The evidence relevant to carcinogenicity from studies in humans is classified into one of the following categories:

Sufficient evidence of carcinogenicity:
The Working Group considers that a causal relationship has been established between exposure to the agent and human cancer. That is, a positive relationship has been observed between the exposure and cancer in studies in which chance, bias and confounding could be ruled out with reasonable confidence. A statement that there is *sufficient evidence* is followed by a separate sentence that identifies the target organ(s) or tissue(s) where an increased risk of cancer was observed in humans. Identification of a specific target organ or tissue does not preclude the possibility that the agent may cause cancer at other sites.

Limited evidence of carcinogenicity:
A positive association has been observed between exposure to the agent and cancer for which a causal interpretation is considered by the Working Group to be credible, but chance, bias or confounding could not be ruled out with reasonable confidence.

Inadequate evidence of carcinogenicity:
The available studies are of insufficient quality, consistency or statistical power to permit a conclusion regarding the presence or absence of a causal association between exposure and cancer, or no data on cancer in humans are available.

Evidence suggesting lack of carcinogenicity:
There are several adequate studies covering the full range of levels of exposure that humans are known to encounter, which are mutually consistent in not showing a positive association between exposure to the agent and any studied cancer at any observed level of exposure. The results from these studies alone or combined should have narrow confidence intervals with an upper limit close to the null value (e.g. a relative

risk of 1.0). Bias and confounding should be ruled out with reasonable confidence, and the studies should have an adequate length of follow-up. A conclusion of *evidence suggesting lack of carcinogenicity* is inevitably limited to the cancer sites, conditions and levels of exposure, and length of observation covered by the available studies. In addition, the possibility of a very small risk at the levels of exposure studied can never be excluded.

In some instances, the above categories may be used to classify the degree of evidence related to carcinogenicity in specific organs or tissues.

When the available epidemiological studies pertain to a mixture, process, occupation or industry, the Working Group seeks to identify the specific agent considered most likely to be responsible for any excess risk. The evaluation is focused as narrowly as the available data on exposure and other aspects permit.

(b)   Carcinogenicity in experimental animals

Carcinogenicity in experimental animals can be evaluated using conventional bioassays, bioassays that employ genetically modified animals, and other in-vivo bioassays that focus on one or more of the critical stages of carcinogenesis. In the absence of data from conventional long-term bioassays or from assays with neoplasia as the end-point, consistently positive results in several models that address several stages in the multistage process of carcinogenesis should be considered in evaluating the degree of evidence of carcinogenicity in experimental animals.

The evidence relevant to carcinogenicity in experimental animals is classified into one of the following categories:

Sufficient evidence of carcinogenicity:

The Working Group considers that a causal relationship has been established between the agent and an increased incidence of malignant neoplasms or of an appropriate combination of benign and malignant neoplasms in (a) two or more species of animals or (b) two or more independent studies in one species carried out at different times or in different laboratories or under different protocols. An increased incidence of tumours in both sexes of a single species in a well conducted study, ideally conducted under Good Laboratory Practices, can also provide *sufficient evidence.*

A single study in one species and sex might be considered to provide *sufficient evidence of carcinogenicity* when malignant neoplasms occur to an unusual degree with regard to incidence, site, type of tumour or age at onset, or when there are strong findings of tumours at multiple sites.

Limited evidence of carcinogenicity:

The data suggest a carcinogenic effect but are limited for making a definitive evaluation because, e.g. (a) the evidence of carcinogenicity is restricted to a single experiment; (b) there are unresolved questions regarding the adequacy of the design, conduct or interpretation of the studies; (c) the agent increases the incidence only of benign neoplasms or lesions of uncertain neoplastic potential; or (d) the evidence of carcinogenicity is restricted to studies that demonstrate only promoting activity in a narrow range of tissues or organs.

Inadequate evidence of carcinogenicity:

The studies cannot be interpreted as showing either the presence or absence of a carcinogenic effect because of major qualitative or quantitative limitations, or no data on cancer in experimental animals are available.

Evidence suggesting lack of carcinogenicity:

Adequate studies involving at least two species are available which show that, within the limits of the tests used, the agent is not carcinogenic. A conclusion of *evidence suggesting lack of carcinogenicity* is inevitably limited to the species, tumour sites, age at exposure, and conditions and levels of exposure studied.

(c)   Mechanistic and other relevant data

Mechanistic and other evidence judged to be relevant to an evaluation of carcinogenicity and of sufficient importance to affect the overall evaluation is highlighted. This may include data on preneoplastic lesions, tumour pathology, genetic and related effects, structure–activity relationships, metabolism and toxicokinetics, physico-chemical parameters and analogous biological agents.

The strength of the evidence that any carcinogenic effect observed is due to a particular mechanism is evaluated, using terms such as 'weak', 'moderate' or 'strong'. The Working Group then assesses whether that particular mechanism is likely to be operative in humans. The strongest indications that a particular mechanism operates in humans derive from data on humans or biological specimens obtained from exposed humans. The data may be considered to be especially relevant if they show that the agent in question has caused changes in exposed humans that are on the causal pathway to carcinogenesis. Such data may, however, never become available, because it is at least conceivable that certain compounds may be kept from human use solely on the basis of evidence of their toxicity and/or carcinogenicity in experimental systems.

The conclusion that a mechanism operates in experimental animals is strengthened by findings of consistent results in different experimental systems, by the demonstration of biological plausibility and by coherence of the overall database. Strong support can be obtained from studies that challenge the hypothesized mechanism experimentally, by demonstrating that the suppression of key mechanistic processes leads to the suppression of tumour development. The Working Group considers whether multiple mechanisms might contribute to tumour development, whether different mechanisms might operate in different dose ranges, whether separate mechanisms might operate in humans and experimental animals and whether a unique mechanism might operate in a susceptible group. The possible contribution of alternative mechanisms must be considered before concluding that tumours observed in experimental animals are not relevant to humans. An uneven level of experimental support for different mechanisms may reflect that disproportionate resources have been focused on investigating a favoured mechanism.

For complex exposures, including occupational and industrial exposures, the chemical composition and the potential contribution of carcinogens known to be present are considered by the Working Group in its overall evaluation of human carcinogenicity. The Working Group also determines the extent to which the materials tested in experimental systems are related to those to which humans are exposed.

(d)   Overall evaluation

Finally, the body of evidence is considered as a whole, to reach an overall evaluation of the carcinogenicity of the agent to humans.

An evaluation may be made for a group of agents that have been evaluated by the Working Group. In addition, when supporting data indicate that other related agents, for which there is no direct evidence of their capacity to induce cancer in humans or in animals, may also be carcinogenic, a statement describing the rationale for this conclusion is added to the evaluation narrative; an additional evaluation may be made for this broader group of agents if the strength of the evidence warrants it.

The agent is described according to the wording of one of the following categories, and the designated group is given. The categorization of an agent is a matter of scientific judgement that reflects the strength of the evidence derived from studies in humans and in experimental animals and from mechanistic and other relevant data.

Group 1: The agent is carcinogenic to humans.

This category is used when there is *sufficient evidence of carcinogenicity* in humans. Exceptionally, an agent may be placed in this category when evidence of carcinogenicity in humans is less than *sufficient* but there is *sufficient evidence of carcinogenicity* in experimental animals and strong evidence in exposed humans that the agent acts through a relevant mechanism of carcinogenicity.

Group 2.

This category includes agents for which, at one extreme, the degree of evidence of carcinogenicity in humans is almost *sufficient*, as well as those for which, at the other extreme, there are no human data but for which there is evidence of carcinogenicity in experimental animals. Agents are assigned to either Group 2A (*probably carcinogenic to humans*) or Group 2B (*possibly carcinogenic to humans*) on the basis of epidemiological and experimental evidence of carcinogenicity and mechanistic and other relevant data. The terms *probably carcinogenic* and *possibly carcinogenic* have no quantitative significance and are used simply as descriptors of different levels of evidence of human carcinogenicity, with *probably carcinogenic* signifying a higher level of evidence than *possibly carcinogenic*.

Group 2A: The agent is probably carcinogenic to humans.

This category is used when there is *limited evidence of carcinogenicity* in humans and *sufficient evidence of carcinogenicity* in experimental animals. In some cases, an agent may be classified in this category when there is *inadequate evidence of carcinogenicity* in humans and *sufficient evidence of carcinogenicity* in experimental animals and strong evidence that the carcinogenesis is mediated by a mechanism that also operates in humans. Exceptionally, an agent may

be classified in this category solely on the basis of *limited evidence of carcinogenicity* in humans. An agent may be assigned to this category if it clearly belongs, based on mechanistic considerations, to a class of agents for which one or more members have been classified in Group 1 or Group 2A.

Group 2B: The agent is possibly carcinogenic to humans.

This category is used for agents for which there is *limited evidence of carcinogenicity* in humans and less than *sufficient evidence of carcinogenicity* in experimental animals. It may also be used when there is *inadequate evidence of carcinogenicity* in humans but there is *sufficient evidence of carcinogenicity* in experimental animals. In some instances, an agent for which there is *inadequate evidence of carcinogenicity* in humans and less than *sufficient evidence of carcinogenicity* in experimental animals together with supporting evidence from mechanistic and other relevant data may be placed in this group. An agent may be classified in this category solely on the basis of strong evidence from mechanistic and other relevant data.

Group 3: The agent is not classifiable as to its carcinogenicity to humans.

This category is used most commonly for agents for which the evidence of carcinogenicity is *inadequate* in humans and *inadequate* or *limited* in experimental animals.

Exceptionally, agents for which the evidence of carcinogenicity is *inadequate* in humans but *sufficient* in experimental animals may be placed in this category when there is strong evidence that the mechanism of carcinogenicity in experimental animals does not operate in humans.

Agents that do not fall into any other group are also placed in this category.

An evaluation in Group 3 is not a determination of non-carcinogenicity or overall safety. It often means that further research is needed,

especially when exposures are widespread or the cancer data are consistent with differing interpretations.

Group 4: The agent is probably not carcinogenic to humans.

This category is used for agents for which there is *evidence suggesting lack of carcinogenicity* in humans and in experimental animals. In some instances, agents for which there is *inadequate evidence of carcinogenicity* in humans but *evidence suggesting lack of carcinogenicity* in experimental animals, consistently and strongly supported by a broad range of mechanistic and other relevant data, may be classified in this group.

(e)   Rationale

The reasoning that the Working Group used to reach its evaluation is presented and discussed. This section integrates the major findings from studies of cancer in humans, studies of cancer in experimental animals, and mechanistic and other relevant data. It includes concise statements of the principal line(s) of argument that emerged, the conclusions of the Working Group on the strength of the evidence for each group of studies, citations to indicate which studies were pivotal to these conclusions, and an explanation of the reasoning of the Working Group in weighing data and making evaluations. When there are significant differences of scientific interpretation among Working Group Members, a brief summary of the alternative interpretations is provided, together with their scientific rationale and an indication of the relative degree of support for each alternative.

References

Bieler GS, Williams RL (1993). Ratio estimates, the delta method, and quantal response tests for increased carcinogenicity. *Biometrics*, 49:793–801. doi:10.2307/2532200 PMID:8241374

Breslow NE, Day NE (1980). Statistical methods in cancer research. Volume I - The analysis of case-control studies. *IARC Sci Publ*, 32:5–338. PMID:7216345

Breslow NE, Day NE (1987). Statistical methods in cancer research. Volume II–The design and analysis of cohort studies. *IARC Sci Publ*, 82:1–406. PMID:3329634

Buffler P, Rice J, Baan R et al. (2004). Workshop on mechanisms of carcinogenesis: contributions of molecular epidemiology. Lyon, 14–17 November 2001. Workshop report. *IARC Sci Publ*, 157:1–27. PMID:15055286

Capen CC, Dybing E, Rice JM, Wilbourn JD (1999). Species differences in thyroid, kidney and urinary bladder carcinogenesis. Proceedings of a consensus conference. Lyon, France, 3–7 November 1997. *IARC Sci Publ*, 147:1–225. PMID:10627184

Cogliano V, Baan R, Straif K et al. (2005). Transparency in IARC Monographs. *Lancet Oncol*, 6:747. doi:10.1016/S1470-2045(05)70380-6

Cogliano VJ, Baan RA, Straif K et al. (2004). The science and practice of carcinogen identification and evaluation. *Environ Health Perspect*, 112:1269–1274. doi:10.1289/ehp.6950 PMID:15345338

Dunson DB, Chen Z, Harry J (2003). A Bayesian approach for joint modeling of cluster size and subunit-specific outcomes. *Biometrics*, 59:521–530. doi:10.1111/1541-0420.00062 PMID:14601753

Fung KY, Krewski D, Smythe RT (1996). A comparison of tests for trend with historical controls in carcinogen bioassay. *Can J Stat*, 24:431–454. doi:10.2307/3315326

Gart JJ, Krewski D, Lee PN et al. (1986). Statistical methods in cancer research. Volume III–The design and analysis of long-term animal experiments. *IARC Sci Publ*, 79:1–219. PMID:3301661

Greenland S (1998). Meta-analysis. In: Rothman KJ, Greenland S, editors. Modern epidemiology. Philadelphia: Lippincott Williams & Wilkins, pp. 643–673.

Greim H, Gelbke H-P, Reuter U et al. (2003). Evaluation of historical control data in carcinogenicity studies. *Hum Exp Toxicol*, 22:541–549. doi:10.1191/0960327103ht394oa PMID:14655720

Haseman JK, Huff J, Boorman GA (1984). Use of historical control data in carcinogenicity studies in rodents. *Toxicol Pathol*, 12:126–135. doi:10.1177/019262338401200203 PMID:11478313

Hill AB (1965). The environment and disease: Association or causation? *Proc R Soc Med*, 58:295–300. PMID:14283879

Hoel DG, Kaplan NL, Anderson MW (1983). Implication of nonlinear kinetics on risk estimation in carcinogenesis. *Science*, 219:1032–1037. doi:10.1126/science.6823565 PMID:6823565

Huff JE, Eustis SL, Haseman JK (1989). Occurrence and relevance of chemically induced benign neoplasms in long-term carcinogenicity studies. *Cancer Metastasis Rev*, 8:1–22. doi:10.1007/BF00047055 PMID:2667783

IARC (1977). IARC Monographs Programme on the Evaluation of the Carcinogenic Risk of Chemicals to Humans. Preamble (IARC Intern Tech Rep No. 77/002).

IARC (1978). Chemicals with sufficient evidence of carcinogenicity in experimental animals – IARC Monographs Volumes 1–17 (IARC Intern Tech Rep No. 78/003).

IARC (1979). Criteria to select chemicals for IARC Monographs (IARC Intern Tech Rep No. 79/003).

IARC (1982). Chemicals, industrial processes and industries associated with cancer in humans (IARC Monographs, volumes 1 to 29). *IARC Monogr Eval Carcinog Risk Chem Hum Suppl*, 4:1–292.

IARC (1983). Approaches to classifying chemical carcinogens according to mechanism of action (IARC Intern Tech Rep No. 83/001).

IARC (1987). Overall evaluations of carcinogenicity: an updating of IARC Monographs volumes 1 to 42. *IARC Monogr Eval Carcinog Risks Hum Suppl*, 7:1–440. PMID:3482203

IARC (1988). Report of an IARC Working Group to Review the Approaches and Processes Used to Evaluate the Carcinogenicity of Mixtures and Groups of Chemicals (IARC Intern Tech Rep No. 88/002).

IARC (1991). A consensus report of an IARC Monographs Working Group on the Use of Mechanisms of Carcinogenesis in Risk Identification (IARC Intern Tech Rep No. 91/002).

IARC (2004). Some drinking-water disinfectants and contaminants, including arsenic. *IARC Monogr Eval Carcinog Risks Hum*, 84:1–477. PMID:15645577

IARC (2005). Report of the Advisory Group to Recommend Updates to the Preamble to the IARC Monographs (IARC Intern Rep No. 05/001).

IARC (2006). Report of the Advisory Group to Review the Amended Preamble to the IARC Monographs (IARC Intern Rep No. 06/001).

McGregor DB, Rice JM, Venitt S (1999). The use of short- and medium-term tests for carcinogens and data on genetic effects in carcinogenic hazard evaluation. Consensus report. *IARC Sci Publ*, 146:1–18. PMID:10353381

Montesano R, Bartsch H, Vainio H et al., editors (1986). Long-term and short-term assays for carcinogenesis—a critical appraisal. *IARC Sci Publ*, 83:1–564. PMID:3623675

OECD (2002). Guidance notes for analysis and evaluation of chronic toxicity and carcinogenicity studies (Series on Testing and Assessment No. 35), Paris: OECD.

Peto R, Pike MC, Day NE et al. (1980). Guidelines for simple, sensitive significance tests for carcinogenic effects in long-term animal experiments. *IARC Monogr Eval Carcinog Risk Chem Hum Suppl*, 2:Suppl: 311–426. PMID:6935185

Portier CJ, Bailer AJ (1989). Testing for increased carcinogenicity using a survival-adjusted quantal response test. *Fundam Appl Toxicol*, 12:731–737. doi:10.1016/0272-0590(89)90004-3 PMID:2744275

Sherman CD, Portier CJ, Kopp-Schneider A (1994). Multistage models of carcinogenesis: an approximation for the size and number distribution of late-stage clones. *Risk Anal*, 14:1039–1048. doi:10.1111/j.1539-6924.1994.tb00074.x PMID:7846311

Stewart BW, Kleihues P, editors (2003). World cancer report, Lyon: IARC.

Tomatis L, Aitio A, Wilbourn J, Shuker L (1989). Human carcinogens so far identified. *Jpn J Cancer Res*, 80:795–807. doi:10.1111/j.1349-7006.1989.tb01717.x PMID:2513295

Toniolo P, Boffetta P, Shuker DEG et al. (1997). Proceedings of the workshop on application of biomarkers to cancer epidemiology. Lyon, France, 20–23 February 1996. *IARC Sci Publ*, 142:1–318. PMID:9410826

Vainio H, Magee P, McGregor D, McMichael A (1992). Mechanisms of carcinogenesis in risk identification. IARC Working Group Meeting. Lyon, 11–18 June 1991. *IARC Sci Publ*, 116:1–608. PMID:1428077

Vainio H, Wilbourn JD, Sasco AJ et al. (1995). [Identification of human carcinogenic risks in IARC monographs] *Bull Cancer*, 82:339–348. PMID:7626841

Vineis P, Malats N, Lang M et al., editors (1999). Metabolic polymorphisms and susceptibility to cancer. *IARC Sci Publ*, 148:1–510. PMID:10493243

Wilbourn J, Haroun L, Heseltine E et al. (1986). Response of experimental animals to human carcinogens: an analysis based upon the IARC Monographs programme. *Carcinogenesis*, 7:1853–1863. doi:10.1093/carcin/7.11.1853 PMID:3769134

GENERAL REMARKS

This one-hundred-and-eleventh volume of the *IARC Monographs* contains evaluations of the carcinogenic hazard to humans of fluoro-edenite fibrous amphibole, silicon carbide fibres and whiskers, and carbon nanotubes. None of these agents had been evaluated previously by the Working Group. A summary of the findings of this volume appears in *The Lancet Oncology* (Grosse et al., 2014).

The relevant route of exposure for studies of carcinogenicity with fibres or carbon nanotubes in experimental animals is inhalation, since humans are most likely to be exposed to fibres or carbon nanotubes by this route. Exposure by inhalation to fibres or carbon nanotubes involves distribution, deposition, and clearance from the lung, and potential translocation of fibres to the pleura. However, in most of the studies of carcinogenicity in experimental animals reviewed in the present volume, fibres or carbon nanotubes were administered by intraperitoneal or intrapleural injection of a bolus of fibres or carbon nanotubes directly to the mesothelium, resulting in a high dose. These non-physiological routes of exposure can induce mesothelioma with a relatively short latency, and have been used historically as sensitive methods for the evaluation of carcinogenicity caused by fibres. For the agents evaluated in the present volume, several of the latter types of studies were judged inadequate due to the use of insufficient numbers of animals, the short study duration, or the lack of concurrent controls. However, the Working Group gave some consideration to studies of sufficient duration that included adequate numbers of animals, but lacked concurrent controls, because mesothelioma is a rare spontaneous tumour.

The assessment of the numerous mechanistic studies on carbon nanotubes revealed variability in the physicochemical properties of the carbon nanotubes tested, the toxicological end-points assessed, and the experimental procedures adopted. In addition, data on end-points related to chronic toxicity were lacking for many types of carbon nanotube. As a result, the Working Group considered the overall mechanistic data to be uninformative regarding the carcinogenicity of specific types of carbon nanotube (see also Kuempel et al., 2017).

References

Grosse Y, Loomis D, Guyton KZ, Lauby-Secretan B, El Ghissassi F, Bouvard V, et al.; International Agency for Research on Cancer Monograph Working Group(2014). Carcinogenicity of fluoro-edenite, silicon carbide fibres and whiskers, and carbon nanotubes. *Lancet Oncol*, 15(13):1427–8. doi:10.1016/S1470-2045(14)71109-X PMID:25499275

Kuempel ED, Jaurand MC, Møller P, Morimoto Y, Kobayashi N, Pinkerton KE, et al. (2017). Evaluating the mechanistic evidence and key data gaps in assessing the potential carcinogenicity of carbon nanotubes and nanofibers in humans. *Crit Rev Toxicol*, 47(1):1–58. doi: 10.1080/10408444.2016.1206061 PMID:27537422

CARBON NANOTUBES

1. Exposure Data

The Working Group limited the scope of this *Monograph* on carbon nanotubes (CNT) to engineered/manufactured CNT, on the basis of three issues.

The Working Group recognized that co-exposure to CNT and carbon nanofibres (CNF) could arise, because CNF may be generated as impurities during the synthesis of CNT. However, CNT and CNF are usually produced separately. Of 11 studies in the workplace, only one reported the use of both CNT and CNF at one secondary manufacturing facility that produced composite materials.

The Working Group did not consider the use of CNT that are specifically designed for medical purposes, for which human exposures have not yet been described.

While the existence of naturally and incidentally occurring CNT has been acknowledged, the physico-chemical properties and biological reactivity of CNT in the general atmosphere are unknown.

1.1 Chemical and physical properties

1.1.1 Nomenclature and general description

Although single-walled (SWCNT) and multiwalled (MWCNT) CNT were discovered in 1991 (Iijima, 1991), only one Chemical Abstracts Service number, 308068-56-6, has been given to reference CNT to date; however, this number is not representative of all CNT because of great variations in the size and other characteristics of the tubes. In addition, with regard to nomenclature, CNT and CNF are often discussed together.

Table 1.1 gives the most common definitions of CNT and other parameters related to nanomaterials. According to the International Organization for Standardization (ISO), CNT are defined as "nanotubes composed of carbon. CNT usually consist of curved graphene layers, including single-wall CNT and multiwall CNT" and CNF are defined as "nanofibres composed of carbon." A nanofibre is described as a "nano-object with two similar external dimensions in the nanoscale and the third dimension significantly larger. A nanofibre can be flexible or rigid. The two similar external dimensions are considered to differ in size by less than three times and the significantly larger external dimension is considered to differ from the other two by more than three times. The largest external dimension is not necessarily in nanoscale" (ISO, 2008).

As a working definition for this *Monograph*, to counteract any potential confusion between the ISO definitions, we used the following differentiation between CNT and CNF proposed by Kim et al. (2013): "The geometry of CNF is different from the CNT containing an entire hollow core, because they can be visualized as regularly stacked truncated conical and planar layers along the filament length" (see Fig. 1.1).

Table 1.1 Definitions relevant to nanomaterials and carbon nanotubes

Term	Definition	Reference
Agglomerate	Collection of weakly bound particles or aggregates or mixtures of the two, in which the resulting external surface area is similar to the sum of the surface areas of the individual components Note 1: The forces holding an agglomerate together are weak, for example, van der Waals forces, or simple physical entanglement Note 2: Agglomerates are also termed secondary particles, and particles from the original source are termed primary particles	ISO (2008)
Aggregate	Particle comprising strongly bonded or fused particles, in which the resulting external surface area may be significantly smaller than the sum of calculated surface areas of the individual components Note 1: The forces holding an aggregate together are strong, for example, covalent bonds, or those resulting from sintering or complex physical entanglement Note 2: Aggregates are also termed secondary particles and particles from the original source are termed primary particles	ISO (2008)
CNF	Nanofibre composed of carbon	ISO (2010b)
Carbon nanohorn	Short and irregular shaped CNT with a nanocone apex Note: In general, hundreds of carbon nanohorns constitute an aggregate nanoparticle	ISO (2010b)
Carbon nanopeapod	Linear array of fullerenes enclosed in a CNT Note: This is an example of a composite nanofibre	ISO (2010b)
Carbon nanoribbon	Nanoribbon composed of carbon Note: Carbon nanoribbons are often in the form of multiple layers of graphene. In the case of a single graphene layer, the term "graphene ribbon" is used	ISO (2010b)
CNT	Nanotube composed of carbon Note: CNT are generally comprised of curved graphene layers, including single-walled (SWCNT) and multiwalled (MWCNT)	ISO (2010b)
Chiral vector of SWCNT	Vector notation used to describe the helical structure of a SWCNT	ISO (2010b)
Coating	Non-covalent surface modification Note: Coating includes Pluronic F108, Tween-80, or polyethylene glycol phospholipid	Ali-Boucetta & Kostarelos (2013)
Cup stack CNT	CNT composed of stacked truncated graphene nanocones Note: These are completely different from SWCNT or MWCNT in structure. The open top and bottom edges of truncated graphene nanocones appear on the inner and outer surfaces of the nanotube, respectively	ISO (2010b)
Doping	Physical alteration of the surface of CNT with ions or molecules using weak forces such as van der Waals	ISO (2010b)
Double-walled carbon nanotube (DWCNT)	MWCNT composed of only two nested, concentric SWCNT Note: Although this is a type of MWCNT, its properties are rather closer to SWCNT	ISO (2010b)
Engineered nanomaterial	Nanomaterial designed for a specific purpose or function	ISO (2010a)
Fullerene	Molecule composed solely of an even number of carbon atoms, which form a closed cage-like fused-ring polycyclic system with 12 five-membered rings and the remainder as six-membered rings	ISO (2010b)

Table 1.1   (continued)

Term	Definition	Reference
Functionalization	Covalent modification of CNT Note: Covalent functional groups include hydroxyl, ammonium, glucosamine, taurine, diethylenetriaminepentaacetic acid, and 2-(4-isothiocyanatobenzyl)-1,4,7,10-tetraazacyclodecane	Singh et al. (2006), Lacerda et al. (2008a, b), Ali-Boucetta & Kostarelos (2013)
Graphene	Single layer of carbon atoms with each atom bound to three neighbours in a honeycomb structure Note: This is an important building block of many carbon nano-objects	ISO (2010b)
Graphite	Allotropic form of elemental carbon comprised of graphene layers stacked in parallel to each other in a three-dimensional, crystalline, long-range order Note 1: Adapted from the definition in the IUPAC *Compendium of Chemical Terminology* Note 2: Two allotropic forms exist with different stacking arrangements: hexagonal and rhombohedral	ISO (2010b), IUPAC (2014)
Graphite nanofibre	Carbon nanofibre composed of multilayered graphene structures Note: Graphene layers can have any orientation with respect to the fibre axis without long-range order	ISO (2010b)
Incidental nanomaterial	Nanomaterial generated as an unintentional by-product of a process Note: The process includes manufacturing, biotechnological, or other processes	ISO (2010a)
Manufactured nanomaterial	Nanomaterial intentionally produced for commercial purposes with specific properties or composition	ISO (2010a)
MWCNT	CNT composed of nested, concentric or near-concentric graphene sheets with interlayer distances similar to those of graphite Note: The structure is normally considered to be many SWCNT nesting within each other, and would be cylindrical for small diameters but tends to have a polygonal cross-section as the diameter increases	ISO (2010b)
Nanocone	Cone-shaped nanofibre or nanoparticle	ISO (2010b)
Nanofibre	Nano-object with two similar external dimensions in the nanoscale and the third dimension significantly larger Note 1: A nanofibre can be flexible or rigid Note 2: The two similar external dimensions are considered to differ in size by less than threefold and the significantly larger external dimension is considered to differ from the other two by more than threefold Note 3: The largest external dimension is not necessarily in the nanoscale	ISO (2008)
Nanomaterial	Material with any external dimension in the nanoscale or having an internal structure or surface structure in the nanoscale Note: This generic term is inclusive of nano-objects and nanostructured material	ISO (2010a)

Table 1.1 Definitions relevant to nanomaterials and carbon nanotubes (continued)

Term	Definition	Reference
	Definition of the Commission of the European Union: Point 1. "Nanomaterial" means a natural, incidental or manufactured material containing particles, in an unbound state or as an aggregate or as an agglomerate and where, for 50% or more of the particles in the number size distribution, one or more external dimensions is in the size range 1 nm–100 nm. (In specific cases and where warranted by concerns for the environment, health, safety, or competitiveness the number size distribution threshold of 50% may be replaced by a threshold between 1 and 50%) Point 2. By derogation from point 1, fullerenes, graphene flakes and single wall carbon nanotubes with one or more external dimensions below 1 nm should be considered as nanomaterials Point 3. A material should be considered as falling under the definition in point 1 where the specific surface area by volume of the material is greater than 60 m^2/cm^3. However, a material which, based on its number size distribution, is a nanomaterial should be considered as complying with the definition in point 1 even if the material has a specific surface area lower than 60 m^2/m^3	EU Commission (2011)
Nano-object	Material with one, two or three external dimensions in the nanoscale Note: Generic term for all discrete nanoscale objects	ISO (2008)
Nano-onion	Spherical nanoparticle with concentric multiple shell structure	ISO (2010b)
Nanoparticle	Nano-object with all three external dimensions in the nanoscale Note: If the lengths of the longest to the shortest axes of the nano-object differ significantly (typically by more than threefold), the terms nanorod or nanoplate are intended to be used instead of the term nanoparticle	ISO (2008)
Nanoplate	Nano-object with one external dimension in the nanoscale and the two other external dimensions significantly larger Note 1: The smallest external dimension is the thickness of the nanoplate Note 2: The two significantly larger dimensions are considered to differ from the nanoscale dimension by more than threefold Note 3: The larger external dimensions are not necessarily in the nanoscale	ISO (2008)
Nanoribbon	Nanoplate with one of its two larger dimensions in the nanoscale and the other significantly larger	ISO (2010b)
Nanorod	Solid nanofibre	ISO (2010b)
Nanoscale	Size range of approximately 1–100 nm	ISO (2008)
Nanotube	Hollow nanofibre	ISO (2010b)
Pristine	As-produced, as manufactured primarily	
SWCNT	CNT comprised of a single cylindrical graphene layer Note: The structure can be visualized as a graphene sheet rolled into a cylindrical honeycomb structure	ISO (2010b)

CNF, carbon nanofibre; CNT, carbon nanotube; MWCNT, multiwalled carbon nanotube; SWCNT, single-walled carbon nanotube
Compiled by the Working Group

Fig. 1.1 Schematic comparison of various types of fibrous carbon by diameter on a log scale

Carbon nanotube   Carbon nanofibre   Carbon fibre

1 10^1 10^2 10^3 10^4

Diameter (nm)
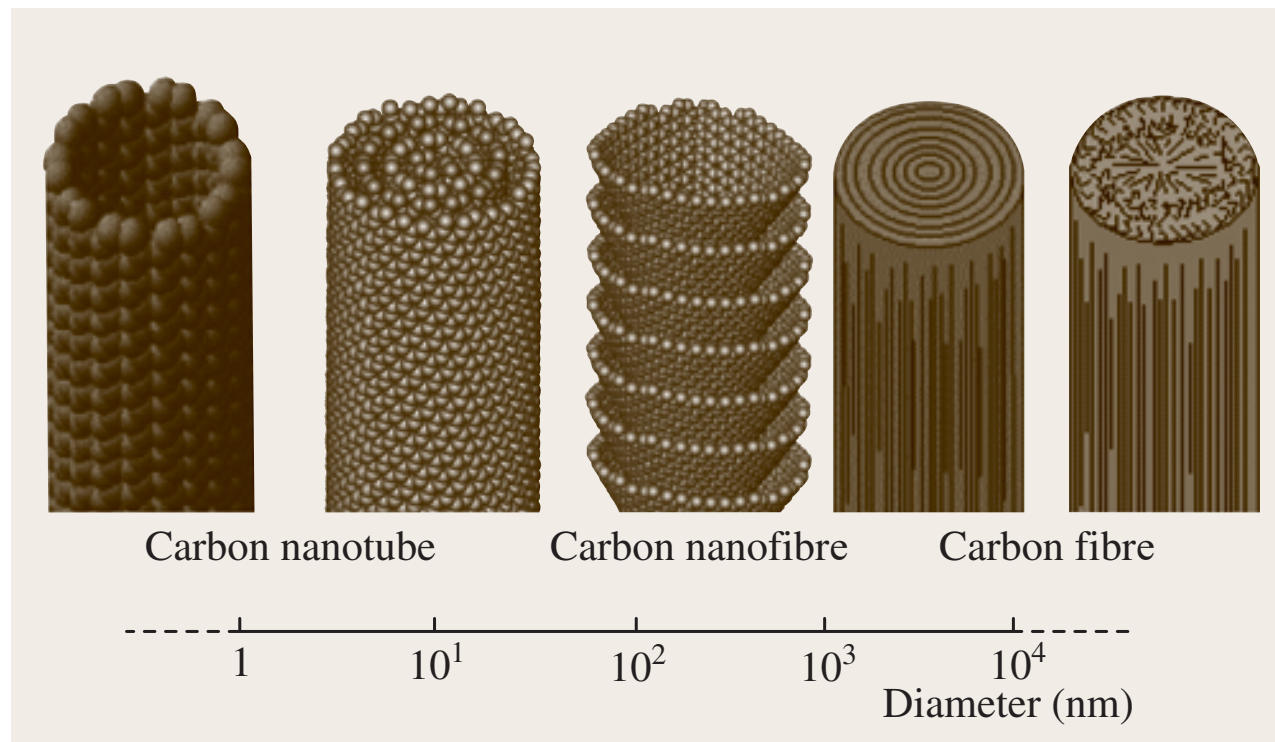
From Kim et al. (2013), with permission from Springer

While CNF may be produced as impurities during the synthesis of CNT (see Section 1.2), CNF are not the subject of this review.

CNT comprise a graphene sheet rolled into a cylinder which can, in some cases, be extremely long, occasionally reaching several hundreds of micrometres in length. In each of the carbon sheets, one carbon atom is bonded to three others in one place, and gives rise to hexagonal rings similar to those found in aromatic hydrocarbons. CNT may consist of a single graphene cylinder (SWCNT) or of many graphene cylinders inside one another in concentric layers kept together by van der Waals forces (MWCNT). The larger MWCNT can contain hundreds of concentric layers separated by a distance of 0.34 nm (Popov, 2004). The length of a C–C bond in a graphene sheet of SWCNT is 0.142 nm (Wildoer et al., 1998).

CNT have generally been categorized into two groups: SWCNT and MWCNT. However, double-walled CNT (DWCNT) have also frequently been listed as a separate class. Depending on the production process, the physical and chemical characteristics (e.g. diameter and length) of CNT vary greatly (Table 1.2).

SWCNT do not normally exist as individual tubes (Lam et al., 2006). Due to the van der Waals forces, they are wont to form agglomerates or aggregates leading to the construction of microscopic bundles or ropes which can reach 5–50 nm in diameter (Maynard et al., 2007). These bundles tend to agglomerate loosely into small clumps. MWCNT are multiple graphene layers that surround one another and also tend to form bundles, but the van der Waals forces are usually weaker than those of SWCNT and MWCNT are therefore more likely to exist as single fibres (Lam et al., 2006).

Table 1.2 Characteristic size and specific surface areas (surface area per mass) of carbon nanotubes

Material	Particle size: diameter (nm) × length (µm)	Specific surface area (m²/g)	Process	Reported purity (%)	Manufacturer	Reference
SWCNT	1–2 × 0.5–2	343	CVD	> 90[a]	Cheap Tubes Inc., Brattleborough, VT, USA	Bello et al. (2009a)
SWCNT	1–2 × 5–30	510	CVD	> 99[a]	Cheap Tubes Inc., Brattleborough, VT, USA	Bello et al. (2009a)
SWCNT	0.8–1.2 × 0.1–1	508	HiPCO	> 85–95[a]	Carbon Nanotechnologies, Houston, TX, USA	Shvedova et al. (2008)
SWCNT	0.9–1.7 × < 1	731	NR	NR	Thomas Swan, Consett, United Kingdom	Jacobsen et al. (2008)
SWCNT	1–4 × 0.5–2	1040	HiPCO	> 85–95[a]	Carbon Nanotechnologies, Houston, TX, USA	Witasp et al. (2009)
SWCNT	12 × 0.32 (bundle in air)	1064	CVD	NR	National Institute of Advanced Industrial Science and Technology, Japan	Morimoto et al. (2012a)
SWCNT	1.3–3.5	1700	CVD	50[a]	SES Research, Houston, TX, USA	Hamilton et al. (2007)
MWCNT	110–170 × 5–9	12.8	CVD	> 90[b]	Sigma Aldrich, St Louis, MO, USA	Park et al. (2009)
MWCNT (Mitsui–7)	49 × 3.9	26	CVD	99[a]	Mitsui & Co., Ltd, Tokyo, Japan	Porter et al. (2010), Mercer et al. (2011)
MWCNT	63 × 1.1 (in air)	69	CVD	NR	Nikkiso Co., Ltd, Tokyo, Japan	Morimoto et al. (2012b)
MWCNT	10–20 × 5–15	100	CVD	> 95[a]	Shenzhen Nanotech, Port, Shenzhen, China	Mitchell et al. (2007)
MWCNT	11 × 1.1	130	CVD	75	SES Research, Houston, TX, USA	Hamilton et al. (2007)
MWCNT (NC 7000)	5–15 × 0.1–10	250–300	CVD	> 90[a]	Nanocyl S.A., Sambreville, Belgium	Ma-Hock et al. (2009)
MWCNT (Baytubes)	10–15 × 0.2–1	257	CVD	> 95[a]; 1% cobalt	Bayer Material Science, Leverkusen, Germany	Ellinger-Ziegelbauer & Pauluhn (2009), Pauluhn (2010a)
MWCNT	50 × 10	280	CVD	> 95[a]	Shenzhen Nanotech, Port, Shenzhen, China	Li et al. (2007a)
MWCNT	20–40 × 0.5–5	300	CVD	80	Nanolab, Inc., USA	Sato et al. (2005)
MWCNT	20–40 × 5–30	380	CVD	> 99	Nanotech Port, Shenzhen, China	Ye et al. (2009)
MWCNT	10–20 × 0.5–2	140.6	CVD	> 96	Cheap Tubes Inc., Brattleborough, VT, USA	Hamilton et al. (2013a)
MWCNT	10–20 × 10–30	204.9	CVD	> 95	Cheap Tubes Inc., Brattleborough, VT, USA	Hamilton et al. (2013a)
MWCNT	30–50 × 0.5–2	217.3	CVD	> 98	Cheap Tubes Inc., Brattleborough, VT, USA	Hamilton et al. (2013a)

[a] Purity reported in the producer's product catalogue
[b] Carbon content, based on Ono–Ogasawara & Myojo (2013)
CNT, carbon nanotubes; CVD, chemical vapour deposition; HiPCO, high-pressure carbon monoxide process; MWCNT, multiwalled carbon nanotubes; NR, not reported; SWCNT, single-walled carbon nanotubes
Compiled by the Working Group

Fig. 1.2 Possible components of a mixture of a sample of pristine carbon nanotubes (unpurified carbon nanotubes)
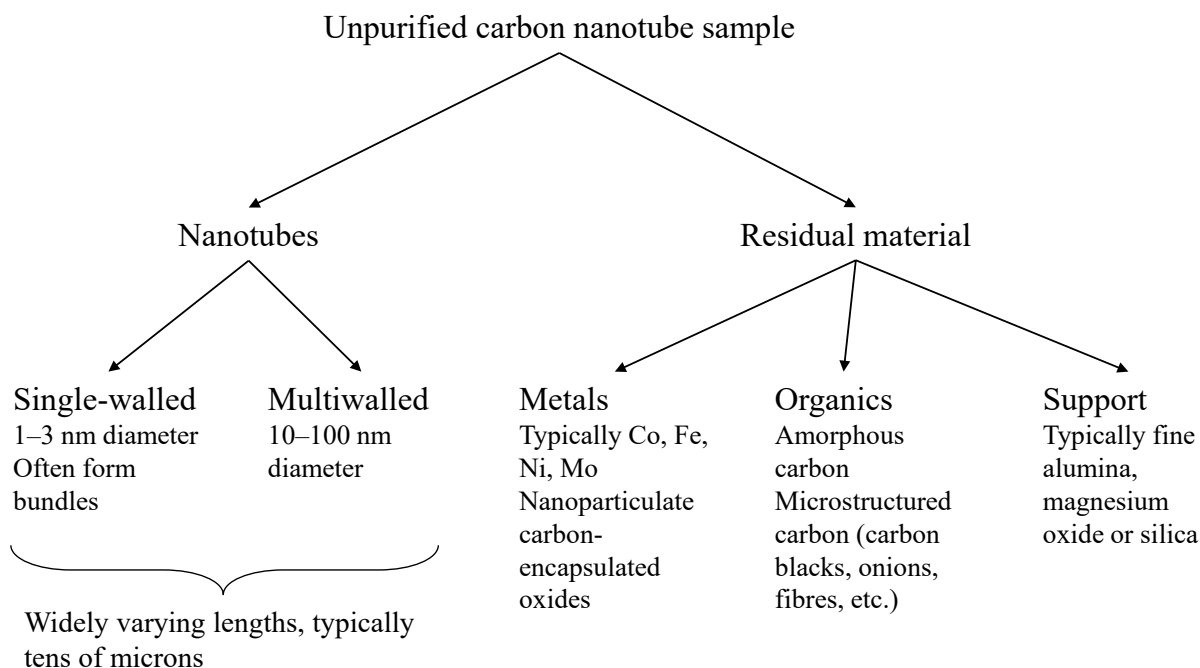
From Donaldson et al. (2006) by permission of Oxford University Press

1.1.2 Chemical properties

(a) Elemental composition

Pure CNT consist of only one or several hexagonal graphene sheets of carbon atoms rolled into tubes and are considered to be rather non-reactive; for example, SWCNT have to be heated up to 500 °C to become oxidized and burned in the air (Zhang et al., 2002).

(b) Impurities

Because the synthesis of CNT frequently requires the presence of catalytic metals in the manufacturing process, CNT contain several residual impurities in addition to SWCNT and MWCNT, the concentrations of which may be relatively high in industrial-grade CNT (Donaldson et al., 2006; Fig. 1.2).

CNT samples have various levels of purity and those of several market materials are reported in Table 1.2. In the pristine [as-produced] samples, residual materials include metals (i.e. iron and molybdenum), support substances (i.e. alumina and silica) and organics (i.e. carbon blacks and fibres). Metal catalysts are frequently used in the manufacture of SWCNT, the most common of which are iron, nickel, cobalt, and molybdenum (Donaldson et al., 2006). Hence, pristine SWCNT usually contain higher concentrations of trace metals (Kitiyanan et al., 2000) than MWCNT. Support materials, including fine alumina, magnesium oxide, or silica, are often included to support the catalyst or the region of growth of the tubes (Donaldson et al., 2006).

Residual organic materials can be divided into two categories: organic molecules and various forms – amorphous or micro-structured – of bulk carbon, such as soot particles, fullerenes, and graphene sheets (Donaldson et al., 2006). The levels and types of impurity depend on the production process. In general, gas-phase processes such as chemical vapour deposition (CVD) tend

to produce CNT with fewer impurities and are also suitable for large-scale production. The purity of commercial CNT preparations may vary considerably (50–99.9%), but post-production purification processes can be used to remove the remaining impurities and unwanted defects of graphene sheets. These involve harsh procedures such as mechanical handling and the use of strong acids and tend to shorten the CNT (Lam et al., 2006; Alexander, 2007).

1.1.3 Physical properties

CNT preparations vary greatly in terms of diameter, length, atomic structure, surface chemistry, and defects (e.g. catalysts such as iron). Other important physical properties include mechanical, electrical, optical, and thermal characteristics and also the agglomeration and aggregation state, bulk density, and the specific surface area.

(a) Thickness

The thickness of CNT mainly depends on the number of graphene layers contained and the chirality of the tubes. In general, the outer diameter of SWCNT is 1–3 nm (Jorio et al., 2001) and that of MWCNT is 10–200 nm (Hou et al., 2003). Changes in the diameter depend on the synthetic process, in which the diameter of the catalytic metal plays an important role, especially in the case of SWCNT.

(b) Length

The length of typical CNT is a few micrometres, but this can vary between only a few hundred nanometres and several tens of micrometres. Tubes of 50 μm in length are common and some are occasionally several hundreds of micrometres long. Variations in the length of the tubes are a rule rather than an exception in CNT preparations (Lam et al., 2006).

(c) Atomic structure

The atomic structure of CNT is described in terms of tube chirality, which is determined by the orientation of the graphene sheet when the tube is synthesized. Two common conformations include the so-called armchair and zig-zag conformations, which generally occur in a mixture of different conformations (Fig. 1.2; Thostenson et al., 2001). The chiral axis, defined as the orientation of the axis of the carbon hexagon relative to the axis of the CNT, also has an effect on the diameter of the nanotube because the inter-atomic spacing of the carbon atoms is fixed as mentioned above (0.142 nm) (Wildoer et al., 1998; Hedmer et al., 2013). In MWCNT, the adjacent graphene layers have different chiralities. Chirality also influences the optical and electrical properties of the CNT. Although graphene is a semi-metal, CNT can be either metallic or semi-conducting depending on the chiral angle. Chirality does not, however, modify the mechanical properties of CNT. Importantly, because SWCNT are frequently a mixture of single-walled tubes with different lengths and different chiralities, the existence of an aerosol, for example, consisting of SWCNT with only one type of chirality is not a viable assumption (Thostenson et al., 2001).

(d) Defects

During the synthesis of CNT, certain types of defect may occur, one example of which is the collapse of the tube that may arise from "bamboo-like" closures in the tube that can be detected by transmission electron microscopy (TEM) (Saito & Zettl, 2008). Such geometrical and typographical defects may be technologically important because they may dramatically alter the electrical properties of the CNT (Ishigami et al., 2004; Saito & Zettl, 2008). For example, the pentagon–heptagon pair (5–7 pair), one of the simple and elegant topological defects (Ishigami et al., 2004), can be used to connect metallic and

semi-conducting tubes enabling the formation of semiconductor–semiconductor, semiconductor–metal, and metal–metal interfaces (Bernholc et al., 1997). For the above reasons, nanoscale devices comprised only of carbon can be produced. CNT are usually non-reactive, although defects in the structure, including missing carbon atoms, could increase their reactivity (Bernholc et al., 1997).

(e) Surface-to-mass ratio or specific surface area

Because of their small size and structure, each of the CNT exhibits extremely high surface-to-mass ratios, also referred to as the specific surface area. The specific surface area depends on the diameter, number of concentric graphene layers, and degree of bundling. The specific surface area of SWCNT is usually 1300 m^2/g, but the corresponding value for bundles of SWCNT is often six times lower (about 300 m^2/g) (Ye et al., 1999).

(f) Bulk density

The bulk density of CNT is quite low and varies according to the production process. For example, a comparison of the powder resulting from laser ablation with that produced by the high-pressure carbon monoxide (HiPCO) process showed that the latter resulted in a bulk density as low as 1 mg/cm^3, whereas the bulk density of the MWCNT Baytubes was as great as 120–170 mg/cm^3. For example, the bulk density of pure graphite and graphene powder are 2200 and 200–600 mg/cm^3, respectively (Chung et al., 1982; Stankovich et al., 2007).

(g) Physical strength

The physical strength of CNT is one their remarkable advantages. In terms of tensile strength and elastic modulus, CNT are the strongest and stiffest material to have been discovered to date, with an estimated tensile strength of 200 GPa (Cheung et al., 2010), and SWCNT can be 10 times stronger than high-strength stainless steel (Walters et al., 1999; Yu et al., 2000). Closely packed CNT ropes have shown tensile strength in excess of 45 GPa, more than 20 times higher than that of typical high-strength steel (2 GPa) (Walters et al., 1999; Thostenson et al., 2005). With a tensile modulus of more than 1 TPa, CNT can also be 20% stiffer than diamonds (Thostenson et al., 2005). The remarkable strength of the CNT is due to the covalent bonds (sp^2 hybridization) formed between the individual carbon atoms. High strength is thought to be a purely axial property of CNT because, in the radial direction, they are rather soft and can be deformed by van der Waals interactions between adjacent CNT (Ruoff et al., 1993). CNT are very flexible and can be bent more than 110° without damage (Iijima et al., 1996).

(h) Electrical properties

CNT can act as either semiconductors or conductors depending on their chirality (Bernholc et al., 1997), to which the electrical properties of the tubes are directly proportional; in the case of thin SWCNT, curvature is also a factor (Lu & Chen, 2005). In theory, metallic CNT can carry an electric current density of 4×10^9 A/cm^2, which exceeds that of copper by a factor of 1000 (Thostenson et al., 2005; Cheung et al., 2010). CNT have numerous potential applications in electric components and devices, and SWCNT with different electrical properties can be joined to make a diode (Chico et al., 1996). Furthermore, because CNT can be modified by deformation and stretching, they could, for example, be applied in sensors (Mahar et al., 2007).

(i) Thermal and optical properties

CNT also have remarkable optical and thermal properties. SWCNT readily absorb near infrared light (800–1600 nm) (Cheung et al., 2010) which covers the wavelength range that passes through biological tissues without remarkable scattering, absorption, heating, or damaging the

tissue. Hence, the optical properties of SWCNT can be used in photo-thermal therapy (Kam et al., 2005; Chakravarty et al., 2008; Xiao et al., 2009). CNT also exhibit remarkable thermal conductivity. SWCNT have thermal conductivities as high as 6000 W/(m.K) at room temperature, at which the corresponding value for diamonds is 3320 W/(m.K). SWCNT are also stable at temperatures as high as 2800 °C in a vacuum and 750 °C in air (Thostenson et al., 2005). These thermal properties could probably be used in the future in highly conducting components of integrated nanoscale circuits, such as transistors, and in thermal management (Sinha et al., 2005; Pop et al., 2006).

(j) Dustiness

Dustiness corresponds to the propensity of a material to generate airborne dust during its handling (Evans et al., 2013) and, depending on the dustiness of the CNT/CNF material, the exposure of workers could vary significantly. A simulated workplace study of scooping/weighing/adding and cleaning/sweeping powders by Brouwer et al. (2006) found that dustiness was a major determinant of the exposure of workers and accounted for approximately 70% of variability in exposure. Evans et al. (2013) tested the dustiness of different materials including SWCNT, MWCNT, and CNF. Both the total and respirable dustiness of the dispersed powders spanned two orders of magnitude (0.3–37.9% and 0.1–31.8%, respectively). For many powders, significant respirable dustiness was observed, suggesting that workplace procedures may result in inhaled airborne dust, a large fraction of which may be capable of reaching the deep lung of a worker, and respirable dustiness accounted for approximately one-third of the total dustiness of most powders studied. The dustiest material examined was SWCNT manufactured by the HiPCO process, with 37.9 ± 3.4% total dustiness and 31.8 ± 3.3% respirable dustiness, which is of particular concern because of the high respirable fraction (Evans et al., 2013).

1.1.4 Other properties

Prototype or unchanged pristine preparations of all forms of CNT are extremely resistant to wetting and are exceedingly difficult to disperse or dissolve in aqueous solutions or organic media due to their high hydrophobicity and tendency to aggregate (Kostarelos et al., 2009). Hence, the use of CNT in composites is a challenge (Sinnott, 2002; Hirsch & Vostronowsky, 2005).

Functionalization of CNT is a post-production process used to attach chemical groups to modify properties and handling and can be physical (non-covalent) and chemical (covalent). Attachments can occur outside or inside the tubes and can be used to increase the dispersibility of the tubes in surfactants or aqueous solutions because pristine CNT have a high tendency to interact in a hydrophobic manner and form aggregates or make nanoscale biosensors (Thostenson et al., 2001; Hirsch & Vostronowsky, 2005; Alexander, 2007; Kostarelos et al., 2009). The functionalization can be divided into two categories: a direct attachment of functional groups to the graphitic surface; and the use of the nanotube-bound carboxylic acids (Sun et al., 2002). The ability to disperse CNT into water can be improved dramatically by their functionalization, which can also enhance their mechanical and electrical properties (Kostarelos et al., 2009). An alternative process to the functionalization of CNT – doping – has frequently been used in the nano-fabrication sector.

Doping is the physical alteration of the surface of CNT with ions or molecules using weak forces such as van der Waals. For example, DWCNT cables with iodine doping were shown to outperform copper and aluminium cables with regard to specific electrical conductivity as well as tensile strength (Zhao et al., 2011).

1.2 Sampling and analytical methods

The recommended physico-chemical characterization of nanomaterials includes the particle size and size distribution, aggregation/agglomeration state in relevant media, shape, surface area, composition, surface chemistry and solubility/dispersibility (ISO TR/13014, 2012). Selected methods of sampling and analysis in various matrices are given in Table 1.3 and are discussed below.

1.2.1 Bulk samples

Several international standards are currently available to characterize CNT in powder form or liquid suspension (see also Table 1.3). Other methods that are not internationally standardized can be found in ISO (2012a).

Bulk samples of CNT are invariably analysed using scanning electron microscopy (SEM), TEM, near infrared photoluminescence spectroscopy, thermogravimetric analysis, and Raman spectroscopy. TEM has better resolution than SEM and allows electron diffraction with the use of an energy dispersive X-ray analyser to evaluate the morphology and aspect ratio, including the length and diameter of the tube structure. However, TEM generally needs more complicated and time-consuming sample preparation than SEM. Dynamic light scattering has been used to measure the hydrodynamic size of CNT in liquid media (Kim et al., 2011). In addition, the components of CNT can be analysed chemically by inductive coupled plasma-mass spectrometry, which is capable of detecting metals and many non-metals. Raman spectroscopy has been used to measure the diameter and crystallinity of CNT. Thermogravimetric analysis is commonly used to determine certain material characteristics that exhibit either a mass loss or gain due to decomposition, oxidation, or loss of volatile compounds (such as moisture) and to determine the mass

composition of CNT. Brunauer–Emmett–Teller analysis has been used to evaluate the surface area of CNT in powder form.

1.2.2 Air samples

No consensus has currently been reached on the best sampling method for characterizing exposure to CNT. Qualitative assessments comparing particle concentrations at the emission source with background particle concentrations are frequently used to identify emission sources of nanomaterials and implement measures for the mitigation of exposure (Tsai et al., 2009; Lee et al., 2010; Methner et al., 2010; Birch et al., 2011). Various approaches can be applied to characterize exposure in an environment, and the monitoring devices generally used for nanoparticles or CNT have been described by Yu et al. (2014).

(a) Direct reading instruments

Direct reading instruments, such as the condensation particle counter and the optical particle counter, are non-specific devices that can be used to measure the particle number concentration directly (including CNT and their aggregates and agglomerates) (Johnson et al., 2010; Lee et al., 2010; Dahm et al., 2011, 2012). The number concentration, mass concentration, surface area concentration, and size distribution can be measured using a differential mobility analysing system and an electrical low-pressure impactor. These instruments do not give the CNT concentration, but give the airborne particle number concentration.

(b) Filter sampling

Area and personal filter-based samples are usually collected on appropriate filters for the measurement of mass concentration, electron microscopy combined with an energy dispersive X-ray analyser are used to estimate CNT morphology and count (Han et al., 2008).

Table 1.3 Selected methods of sampling and analysis of carbon nanotubes in various matrices

Sample matrix	Sample preparation	Assay method	Detection limit	Reference
Bulk	TEM-grid	TEM-EDX		Birch et al. (2011), ISO (2012b)
	SEM-stub	SEM-EDX		Birch et al. (2011), ISO (2011a)
	Suspension in water, sodium dodecyl sulfate, sodium dodecylbenzene sulfonate, or sodium cholate	NIR		ISO (2010c)
		TGA		ISO (2011b)
		GC-MS		ISO (2010d)
	Powder	BET		Birch et al. (2011)
	Nitric acid/perchloric acid (4:1)	ICP-AES		NIOSH 7300 (NIOSH, 2003c)
Air	Direct-reading instruments	SMPS	4.2 nm < dm < 100 nm	Maynard et al. (2004)
			69.8 nm < dm < 777 nm	
			5 nm < dm < 500 nm	Lee et al. (2010)
			14 nm < dm < 630 nm	Han et al. (2008)
		Dust monitor	250 nm < dm < 32 000 nm	Lee et al. (2010)
		DustTrak	10 nm < dm < 10 000 nm	Bello et al. (2010)
		APS	500 nm < dae < 20 000 nm	Maynard et al. (2004), Han et al. (2008), Bello et al. (2010)
		CPC	10 nm < dm < 1000 nm	Bello et al. (2010), Johnson et al. (2010)
			0–10^8 particle/mL	Lee et al. (2010)
		FMPS	5.6 nm < dm < 560 nm	Tsai et al. (2009), Bello et al. (2010)
	Personal and area sampling MCE filters (37 mm, 0.8 µm pore size)	TEM-EDX	0.04–0.5 fibres/mL for a 1000-L air sample	NIOSH 7402 (NIOSH, 1994a), Han et al. (2008), Methner et al. (2010), Johnson et al. (2010), Lee et al. (2010)
	Cascade impactors, carbon-coated nickel grid, silicon monoxide-coated nickel grid, 25 mm MCE filter	TEM-EDX	0.04–0.5 fibres/mL for a 1000-L air sample	NIOSH 7402 (NIOSH, 1994a), Birch et al. (2011)
	Electrostatic precipitator	TEM-EDX	0.04–0.5 fibres/mL for a 1000-L air sample	NIOSH 7402 (NIOSH, 1994a), Birch et al. (2011)
	Personal and area sampling quartz-fibre filter (37 mm) with cyclone	EC/OC	0.3 µg per filter portion	NIOSH 5040 (NIOSH, 1999), Birch et al. (2011), Dahm et al. (2012)
	MOUDI-quartz-fibre filter (47 mm)	EC/OC	0.3 µg per filter portion	NIOSH 5040 (NIOSH, 1999), Birch et al. (2011)
	Personal and area sampling quartz-fibre filter (37 mm), 3:1 nitric/perchloric acid mixture extraction	ICP-AES	Depending on metal	NIOSH 7300 (NIOSH, 2003a), Birch et al. (2011)
	Personal and area sampling MCE filters (37 mm, 0.8 µm pore size)	Gravimetry	0.03 mg per sample	NIOSH 0500 (NIOSH, 1994b), Han et al. (2008), Methner et al. (2010), Lee et al. (2010)

Table 1.3 (continued)

Sample matrix	Sample preparation	Assay method	Detection limit	Reference
Dermal	Cotton gloves	ICP-AES	Depending on metal	NIOSH 7300 (NIOSH, 2003a), Maynard et al. (2004)

APS, aerodynamic particle sizer; BET, Brunauer-Emmett-Teller; CNF, carbon nanofibres; CNT, carbon nanotubes; CPC, condensation particle counter; dae, aerodynamic diameter; dm, mobility diameter; EC/OC, elemental carbon/organic carbon; EDX, energy dispersive X-ray analyser; ELPI, electrical low-pressure impactor; ESP, electrostatic precipitator; FMPS, fast mobility particle sizer; GC-MS, gas chromatograph-mass spectrometry; ICP-AES, inductive coupled plasma-atomic emission spectroscopy; ICP-MS, inductive coupled plasma-mass spectroscopy; MCE, mixed cellulose ester; MOUDI, micro orifice uniform-deposit impactor; NIR, near infrared photoluminescence spectroscopy; PAS, photoelectric aerosol sensor; PBZ, personal breathing zone; SEM, scanning electron microscopy; SMPS, scanning mobility particle sizers; STEM, scanning transmission electron microscopy; TEM, transmission electron microscopy; TGA, thermogravimetric analysis; TP, thermal precipitator; TSP, total suspended particulate; WRASS, wide-range aerosol sampling system
Compiled by the Working Group

Chemical analysis involves the use of inductive coupled plasma-mass spectrometry and atomic absorption spectrometry. These filter-based air samples provide more specific information than direct reading instruments on the target CNT (e.g. size, shape, mass, and composition). Air samples allow an elemental mass analysis to determine the levels of metal (e.g. NIOSH Method 7303; NIOSH, 2003b) or elemental carbon (EC; e.g. NIOSH Method 5040; NIOSH, 1999), depending on the composition of the manufactured nano-materials, plus particle characterization (e.g. size, shape, dimension, and degree of agglomeration) using TEM or SEM based on the measurement techniques specified in NIOSH Methods 7402 (NIOSH, 1994a) and 7404 (NIOSH, 2003c), respectively.

CNT in suspended particles can be measured in ambient particles separately from EC by selecting a specific oxidizing temperature (Chow et al., 1993; Hedmer et al., 2014)

Electrostatic precipitator or cascade impactor grid sampling (Birch et al., 2011) or filter sampling followed by grid mounting have been used to collect CNT structures from the air (Han et al., 2008; Lee et al., 2010). These structures can be identified and counted using SEM or TEM or by combining these with an energy dispersive X-ray analyser to identify their constituents (Han et al., 2008; Lee et al., 2010; Dahm et al., 2012). Chen et al. (2012) published a protocol for counting MWCNT microscopically, geometrically sizing the particles, and collecting size-classified samples to determine the aerodynamic size distribution.

(c) Dermal exposure

To estimate the level of dermal exposure to CNT, cotton gloves are placed over rubber gloves, are removed immediately after handling the nanotubes, and are then sealed in separate plastic bags. The gloves are then analysed for catalyst metals as the surrogate total nanotube product mass. The samples are treated with nitric acid and perchloric acid and analysed using inductive coupled plasma emission spectrometry (NIOSH, 2003a; Maynard et al., 2004).

(d) CNT in consumer products

The process of the release of CNT from consumer products that contain them has been investigated using direct reading instruments to count airborne particle number concentrations, and TEM or SEM to identify whether free CNT or CNT composite structures are released during the life-cycle of such consumer products (Bello et al., 2010).

(e) Limitations

The assessment of exposure to CNT, such as SWCNT and MWCNT, remains a challenge in the field of occupational hygiene, because relatively few studies on CNT sampling have been carried out and the best sampling filters and methods have not yet been established. Most number-counting devices, such as the condensation particle counter and the optical particle counter, do not represent the exact exposure to CNT; measurements using a differential mobility analysing system (or a scanning mobility particle sizer) also do not always provide accurate information due to the arc charge caused by the charged CNT in the dynamic mechanical analysis (Ku et al., 2007). Although several groups have attempted to count the CNT structures using TEM or other microscopic methods (Han et al., 2008; Dahm et al., 2012), no standard methods for CNT counting have yet been established. In addition, determining the mass concentration of CNT based on the measurement of EC remains a challenge due to the technical limitations of current analytical methods. Despite these limitations in assessing the exposure to nanomaterials or CNT, guidelines and reports have been published to guide and harmonize strategies for exposure measurement (OECD, 2009a, b, c, d, 2010; Brouwer et al., 2012).

1.3 Production and use

1.3.1 Production levels

CNT preparations are not homogenous, but contain a diverse mixture of many different types of tube. The number of walls, diameters, lengths, chiral angles, chemical functionalization (i.e. surface modifications), purities, and bulk densities may all vary. In 2005, global production figures for MWCNT and SWCNT were estimated at 294 tons [~299 tonnes] and several hundred kilograms, respectively (Köhler et al., 2008). In 2006, the corresponding amounts were estimated to be ~300 tons [305 tonnes] and 7 tons [7.11 tonnes], respectively (WTEC, 2007). Today, the global production capacity, mainly of MWCNT, is probably much higher. However, an estimation of the production capacities for CNT at the country level is difficult because of the scarcity of governmental reports. The significant uncertainty in the estimation of global production is due to the continuously changing situation caused by new producers coming into the market; however, some data from the Republic of Korea and France are publicly available. For example, according to the nanomaterial inventory of the Ministry of Environment of the Republic of Korea, 3.0 tonnes of CNT were reported in 2009 (NSTC, 2011). In France, the nanomaterial inventory estimated that around 1 tonne of CNT was used by five industries involved in the production of inks, paints and plastics in 2009 (Honnert & Grzebyk, 2014). A public report on the use and production of nanomaterials in France in 2012 stated that several tens of tonnes of nanofibres and nanotubes were produced in 2011, but no precise figures were given regarding CNT (DGCIS, 2012).

The data on global CNT production are also uncertain because the estimates made by the industry vary between 100 and 1000 tonnes annually (Piccinno et al., 2012).

1.3.2 Production methods

Several methods of CNT production have been described (Bhushan, 2004; Fig. 1.3), one of the most commonly used of which involves the use of transition metals in the presence of atomic carbon at a high temperatures and/or pressure (Maynard et al., 2004). Both SWCNT and MWCNT are generally produced by one of the three principal techniques, i.e. CVD, arc discharge, or laser ablation. Depending on the production technique, various levels of impurities, such as metal catalysts, amorphous carbon, soot, graphite, and non-tubular fullerenes, may be present in the final preparation (ENRHES, 2009; Hedmer et al., 2013). Removal of impurities requires the application of chemical purification processes, such as acid reflux, filtration, centrifugation, and repeated washing with solvents or water (ENRHES, 2009).

(a) Chemical vapour deposition

Thermal CVD, also called catalyst CVD, is most widely used in the production of CNT (Kumar & Ando, 2010). Low-temperature CVD (600–900 °C) yields MWCNT, whereas higher temperatures (900–1200 °C) promote SWCNT (Karthikeyan et al., 2009). CVD is based on the decomposition of hydrocarbon vapour in the presence of a metal catalyst. The precursor of CNT is a carbon-containing gas or vapour, such as carbon monoxide (HiPCO process), methane, acetylene, ethylene, benzene, or xylene. This is first heated with a plasma or coil and then allowed to react with the metal catalyst, which can be nickel, cobalt, or iron and acts as a seed for the growth of the tubes (WTEC, 2007; ENRHES, 2009; Singh et al., 2009). Although CNT can be produced in its absence, the use of catalysts is extremely helpful (Lam et al., 2006; Hedmer et al., 2013).

Fig. 1.3 Production process for carbon nanotubes
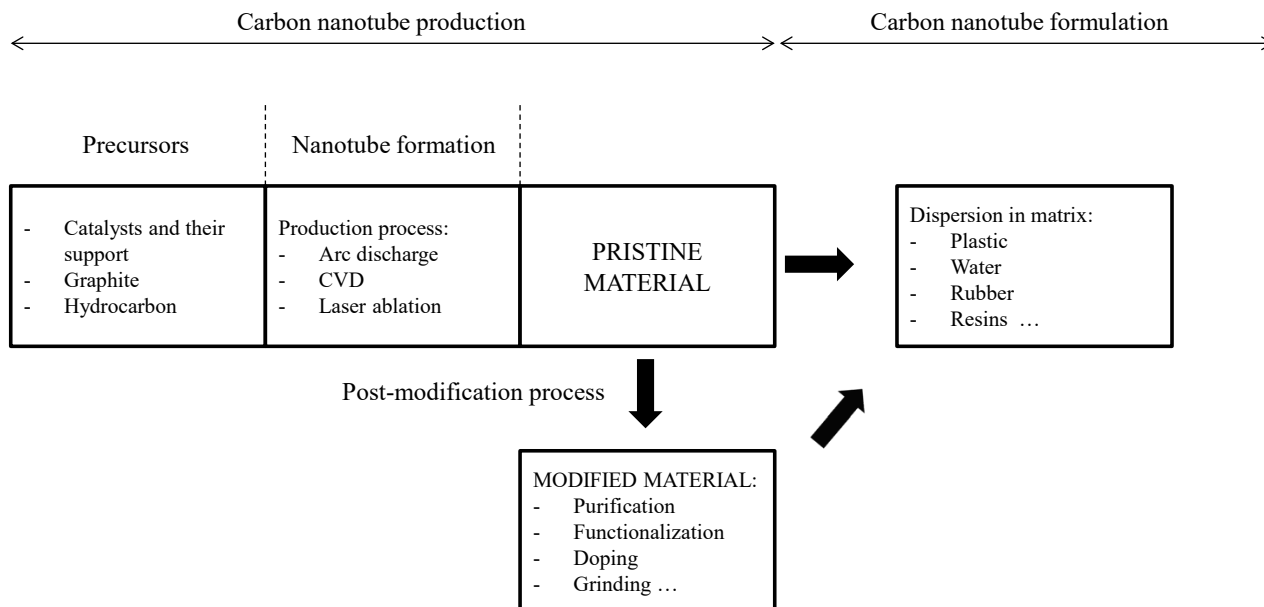
CVD, chemical vapour deposition
Compiled by the Working Group

(b) Arc discharge

Arc discharge was the first technique reported to produce CNT (Iijima, 1991). The method usually included an anode and a cathode made of high-purity graphite. A voltage is applied across these rods until a stable arc is achieved in which the anode is consumed and the cathode is used to grow the tubes. The whole process takes place under a helium atmosphere. To obtain SWCNT, the electrodes are doped with a small amount of catalyst metal particles (Thostenson et al., 2001). This process produces a high yield of CNT but the levels of impurities in the final preparation are also high (Donaldson et al., 2006).

(c) Laser ablation

Laser ablation, similarly to arc discharge, produces MWCNT (Guo et al., 1995a). More recently, this technique has been improved by using catalyst nanoparticles, notably a cobalt and nickel mixture, which also enables the synthesis of SWCNT (Guo et al., 1995b; Rinzler et al., 1998). A graphite target is maintained close to 1200 °C while an inert gas, frequently argon, is bled into the chamber. Thereafter, pulses of high-intensity laser beam are used to vapourize the graphite target and CNT develop on the cooler surfaces of the reactor when the vapourized carbon condenses (Thostenson et al., 2001).

1.3.3 Use

CNT have a wide variety of applications, including their incorporation into fabrics in the textile industry, plastics, rubbers, reinforced structures, composite materials, and household commodities to reduce their weight and improve water- and wear-resistance (Lam et al., 2006). At present, CNT are also found in products made of nanocomposites such as polymers that contain up to 10% CNT by mass, e.g. sports articles such as jogging shoes and sportswear, tennis rackets, ice hockey sticks, bicycles (to strengthen and reduce weight), cycling shoes, golf clubs, skis, car parts, and wind power plants (to strengthen and reduce the weight of energy production wind mill wings)

(Hussain et al., 2006; Köhler et al., 2008; Thomas et al., 2009). Lithium ion batteries used in mobile phones and laptops also contain CNT (Köhler et al., 2008; Zhang et al., 2010). Other uses involve textiles made of fibres of CNT, including polymers with electrical antistatic, thermal conductive, flame retardant, and tear-proof properties (Beyer, 2002; Köhler et al., 2008), and concrete reinforced with CNT (Schneider et al., 2007; Köhler et al., 2008; Wohlleben et al., 2011). CNT can also be used in car tyres to improve their strength (Observatory Nano, 2011). Research and development are still at the prototype stage in many cases, but development will be rapid and increasingly more products containing CNT are entering the market and being used in industrial processes (Beyer, 2002; Aitken et al., 2006; Köhler et al., 2008).

1.4 Occurrence and exposure

1.4.1 Environmental occurrence

Little is known about environmental exposure to CNT mainly because very few quantitative and specific trace analytical methods are available at present (Gottschalk et al., 2013).

Naturally occurring CNT have been found in 10 000-year-old ice core melt water in Greenland (Murr et al., 2004a), in smoke from wood combustion (Murr & Guerrero, 2006), and in a mixture of coal and petroleum (Velasco-Santos et al., 2003).

Sources of natural gas and propane gas, such as domestic (kitchen) stoves, were found to yield aggregates of silica nanocrystals intermixed with CNT and other carbon nanocrystals (Murr et al., 2004b). Murr et al. (2006) reported aggregate concentrations on outdoor sampling grids measured by TEM of about 10^2–10^3 aggregates/m³, while indoor aggregate concentrations in kitchens were found to be more variable, averaging 10^3–10^5 aggregates/m³ above gas burners. According to Murr & Soto (2005), these aggregates contained MWCNT of various sizes and aspect ratios and other concentric, fullerenic polyhedra.

CNT may also enter the environment directly after unintentional release during the manufacture, use, and consumption of goods containing CNT or as waste from sewage-treatment plants, waste-incineration plants, and landfills (Petersen et al., 2011; Nowack et al., 2013; Guseva Canu et al., 2016). Modelling studies dealing with the environmental release of and exposure to nanomaterials have been published and provide estimates of predicted environmental concentrations (Gottschalk et al., 2013). Gottschalk et al. (2009, 2010) modelled concentrations of CNT for Europe, Switzerland, and the USA. The simulated modes (most frequent values) and range of the lower and upper quantiles for 2008 are reported in Table 1.4.

1.4.2 Exposure of the general population

The main exposures of the general population probably result from the abrasion and weathering of consumer products that contain CNT embedded into a matrix. Exposure from medical devices (internal exposure through targeted drug delivery or contrast agents) is also possible. No quantitative data on the exposure of the general population to CNT have been identified. Although exposure from applications in which CNT are matrix-bound is expected to be very low, this may be increased when these consumer products are incinerated (Aschberger et al., 2010). CNT were found in the lung tissues of patients who were exposed to dust and smoke after the collapse of the World Trade Center on 11 September 2001 (Wu et al., 2010). Simulation studies have addressed the exposure of consumers (Bello et al., 2009a, 2010).

Table 1.4 Predicted environmental concentrations of carbon nanotubes for Europe, Switzerland, and the USA in 2008[a]

Environmental compartments	Europe	USA	Switzerland
Air (ng/m³)	0.003 [0.0025–0.007]	0.001 [0.00096–0.003]	0.008 [0.006–0.017]
Soil (Δ ng/kg/year)	1.51 [1.07–3.22]	0.56 [0.43–1.34]	1.92 [1.44–3.83]
Sludge-treated soil (Δ ng/kg per year)	73.6 [52.1–157]	31.4 [23.9–74.6]	Not reported
Surface water (ng/L)	0.004 [0.0035–0.021]	0.001 [0.0006–0.004]	0.003 [0.0028–0.025]
Sediment (Δ ng/kg per year)	241 [215–1321]	46 [40–229]	229 [176–1557]
Sewage-treatment plant effluent (ng/L)	14.8 [11.4–31.5]	8.6 [6.6–18.4]	11.8 [7.6–19.1]
Sewage-treatment plant sludge (mg/kg)	0.062 [0.047–0.129]	0.068 [0.053–0.147]	0.069 [0.051–0.129]

[a] Based on estimations of both public sector expenditure to promote nanotechnology and the worldwide market value for products incorporating nano-sized materials for the period 2001–12, the modelled increase (base year 2008) in concentrations of engineered nanomaterials in sludge-treated soil and sediment was scaled to calculate annual increases of these concentrations for each year within the indicated period. Concentrations are expressed as mode (most frequent value) [lower quantile $Q(0.15)$–upper quantile $Q(0.85)$]. For air, surface water and sewage-treatment plant effluents, the data illustrate the 2008 concentrations of CNT; for soil, sludge-treated soil and sediments, the data illustrate the annual increase in the concentration of engineered nanomaterials (base year 2008).
Adapted with permission from Gottschalk et al. (2009). Copyright (2009) American Chemical Society

1.4.3 Occupational exposure

In occupational settings, exposure of workers to CNT could occur in principle at all phases of the generation and application of the material. Workers are not generally expected to be exposed during the synthesis phase of commercial production, which is performed in a closed reaction chamber; however, exposure is more liable to occur in subsequent phases when the reaction chamber is opened to recover the product, during the extraction and transport of the material produced, or when the system is cleaned. The highest exposures most probably occur when handling the dry powder, for example, during the collection, weighing, blending, transferral to containers and bagging of the material, and the maintenance of machinery. Various downstream applications of CNT may also result in occupational exposure, e.g. when the material containing CNT is machined or drilled, during wear and tear, and during disposal. The use and fabrication of CNT in drug delivery systems and imaging may also potentially give rise to occupational exposure to those who manufacture and administer the products as well as academic research staff (Guseva Canu et al., 2016).

The main routes of exposure in the occupational setting are anticipated to be inhalation and dermal contact. Ingestion may also occur as a consequence of swallowing inhaled material after mucociliary clearance or as a result of hand-to-mouth contact.

(a) General overview

The industrial production and use of CNT material is relatively recent and the size of the workforce in the CNT/CNF sector remains small; therefore, the currently available data on occupational exposure are still limited. Moreover, the available data are extremely heterogeneous due to the high variability of the methods and instruments used for sampling and analysis of exposure and that of the criteria used for interpreting the results.

Little consensus has been reached to date on the exposure metrics that would best correlate with adverse health outcomes (Dahm et al., 2012; Hedmer et al., 2014). For instance, in early studies, gravimetric concentrations were measured for total suspended particles, then for the respirable or alveolar fraction of the aerosol or for particles smaller than 2.5 μm. With the development of real-time aerosol monitoring

instruments, particle number concentration and specific or active surface area measurement results became available but without a common strategy (Guseva Canu et al., 2016). In the context of rapidly changing manufacturing technology, an additional difficulty arises from the diversity of the CNT material, the physical and chemical properties of which influence their potential release and dispersal (Guseva Canu et al., 2016).

Of the 19 studies that were reviewed, eight were simulation studies of exposure (i.e. carried out under well controlled laboratory conditions) and 11 were on-site studies conducted in real occupational settings. While the on-site studies were intended to evaluate the actual exposure of workers to CNT, simulation studies of exposure were performed to assess the release of CNT into the air under experimental or simulated industrial process conditions, often using a particular, well-characterized test material, to estimate the potential exposure of workers without protection. These two sets of data were considered separately.

(b)   Simulation studies of exposure to emissions

(i)   Measurement of particle number concentration

Tsai et al. (2009) characterized particle morphology and aerosol size during the synthesis of SWCNT by CVD (with and without a catalyst) and during the growth of MWCNT in the presence or absence of a substrate. Particle measurements made inside a fume hood during the synthesis of SWCNT were found to be as high as 10^7 particles/cm^3 with an average particle diameter of 50 nm; personal breathing zone (PBZ) samples collected from workers near the fume hood were considerably lower (< 2000 particles/cm^3). The difference between the particle concentrations obtained during SWCNT growth using a catalyst and the control data (no catalyst) was small. Particle measurements made during the synthesis of MWCNT were found to peak at 4×10^6 particles/cm^3 when

measured inside the fume hood; the particle size ranged from 25 to 100 nm when a substrate was used for MWCNT growth and from 20 to 200 nm when no substrate was present. PBZ samples collected from workers near the fume hood during MWCNT synthesis had particle concentrations similar to background. TEM analysis of MWCNT samples indicated the presence of individual particles as small as 20 nm with particle agglomerates as large as 300 nm. Some individual MWCNT were observed, but were often accompanied by clusters of carbon and iron particles. The diameter of the tubes was reported to be about 50 nm.

Bello et al. (2008) reported no increase in total airborne particle concentrations (compared with background) either during the removal of MWCNT from the reactor furnace or during the detachment of MWCNT from the growth substrate (with a razor blade), and no detectable amount of MWCNT, either as individual tubes or as agglomerates, in PBZ samples.

Johnson et al. (2010) investigated the release of airborne carbon-based nanomaterials (CNM) during the transfer and ultrasonic dispersion of MWCNT (diameter, 10–20 nm), fullerenes, and carbon black inside a laboratory fume hood (with the airflow turned off and the sash half open) during the weighing and transferral of dry CNM to beakers filled with reconstituted freshwater with and without natural organic matter that was then sonicated. Particle number concentrations for MWCNT and carbon black during the sonication of water samples were significantly greater than those found during the weighing and transferral of dry CNM. TEM analysis revealed agglomerates of all CNM and agglomerates of MWCNT 300–1000 nm in diameter.

Ogura et al. (2013a) investigated particle release during the grinding of polystyrene-based composites that contained 0 and 5% weight (wt) SWCNT (diameter, 3 nm) synthesized using a water-assisted CVD method. Considerable increases in the number concentration of

nano-sized aerosol particles were observed during the grinding of polystyrene containing CNT and CNT-free polystyrene. Nanoparticles were presumably volatile particles released by the friction heat produced by grinding the composite. In TEM analysis, micron-sized particles with protruding fibres (probably CNT) were observed, whereas free-standing CNT were not observed.

Ji et al. (2013) assessed the release of nanomaterials during the preparation of conductive films by a spray-coating process using MWCNT. During a series of three processes, the number concentration, measured by an optical particle counter, increased from 0 to 290 particles/cm^3, then dropped to 263 particles/cm^3, and increased again to 724 particles/cm^3. Using TEM, bundled CNT, long MWCNT with aggregations of other particles, and particle aggregations without MWCNT were observed.

(ii) Measurement of particle number and/or respirable mass concentrations

Cena & Peters (2011) evaluated the airborne release of CNT during the weighing of bulk CNT and the sanding of epoxy nanocomposite test samples. Particle number concentrations determined during the weighing process differed little from that observed in background samples (process to background ratio [P/B], 1.06), whereas the respirable mass concentration was increased (P/B, 1.79). The geometric mean (GM) respirable mass concentration inside the glove box was reported to be 0.03 μg/m^3 (background GM, 0.02 μg/m^3). During the sanding process (with no local exhaust ventilation, in a fume hood, or in a biological safety cabinet), the PBZ nanoparticle number concentrations were negligible compared with background concentrations (average P/B, 1.04). Particles generated during sanding were reported to be predominantly micron-sized with protruding CNT and differed considerably from those of bulk CNT that tended to remain in large (> 1 μm) tangled agglomerates. Respirable mass concentrations

in the workers' breathing zones were elevated. However, the concentrations were lower when sanding was performed in the biological safety cabinet (GM, 0.2 μg/m^3) than with no local exhaust ventilation (GM, 2.68 μg/m^3; $P < 0.0001$) or inside the fume hood (GM, 21.4 μg/m^3; $P < 0.0001$).

(iii) Measurement of respirable mass concentrations and/or the count of structures containing CNT

Bello et al. (2009b) investigated the release of CNT during the dry and wet cutting of a CNT-alumina composite (CNT diameter, 10–20 nm) using a band saw or rotary cutting wheel. Submicron and respirable fibres were both generated from dry cutting. Reported mean respirable mass concentrations were 2.11 and 8.38 mg/m^3 for area samples and 0.8 and 2.4 mg/m^3 for PBZ samples. TEM analysis found a concentration of 1.6 fibres/cm^3 in area samples and 0.2 fibres/cm^3 in PBZ samples. No data on fibre measurements were reported for the wet cutting of composite materials.

In a subsequent study, Bello et al. (2010) investigated the airborne release of CNT and other nano-sized fibres during the solid-core drilling of two types of advanced CNT-hybrid composite: (1) reinforced plastic hybrid laminates (alumina fibres and CNT); and (2) graphite-epoxy composites (carbon fibres and CNT). Airborne exposure to both alumina fibre and CNT structures were found to range in concentration from 1.0 fibres/cm^3 (alumina composite) to 1.9 fibres/cm^3 (carbon and CNT composite) for PBZ samples; similar concentrations were observed in area samples.

In summary, all but one simulation study of exposure identified either micron-sized particles with protruding CNT or bulk CNT in large tangled agglomerates by TEM analysis, providing evidence for potential exposure. The operations that may lead to exposure to CNT include CVD synthesis and sonication of MWCNT, and the

dry cutting, drilling, grinding, and sanding of composite materials containing CNT.

(c) On-site studies

Eleven on-site studies were carried out in different workplaces, including research and development laboratories, pilot small-scale production facilities, and, more rarely, large-scale primary or secondary manufacturer/user facilities. Most published studies were conducted in Japan, the Republic of Korea, and the USA, and only one study was recently carried out in Sweden. These data have been reviewed in detail (Guseva Canu et al., 2016) and the results are summarized in Table 1.5.

In summary, taken together the available 11 on-site studies provided strong evidence that the exposure of workers to CNT/CNF material may occur, especially at workstations where no exposure control measures are implemented. In almost all situations where detectable amounts of either EC or the EC3 subfraction were found, the presence of CNT material was confirmed by TEM/SEM analyses of PBZ of area air samples. CNT were more frequently found to be attached to the soot or metal catalyst particles, embedded in other impurities or in the form of large entangled agglomerates. Individual CNT were rarely observed by SEM and TEM analysis and no validated protocol is available for counting such different structures, therefore only four studies attempted their quantification in PBZ samples. Nevertheless, different criteria for counting were applied which precluded any statistical treatment of the results. The reported values ranged between 0.003 and 0.01 structures/cm^3 for SWCNT and 0.008 and 193.6 structures/cm^3 for MWCNT, corresponding to the situation described in research and development laboratories compared with industrial settings. The operations yielding the highest release of CNT material/cm^3 included blending, transferral, sieving, pouring, and weighing as well as CNT production in both CVD and arc discharge processes, which encompasses

synthesis, harvesting from the reactor, and subsequent cleaning of the reactor. When the EC mass concentration was considered, values as high as 7.4–10 μg/m^3 and ranging from 0.68 to 38 μg/m^3 were measured in the PBZ samples of workers in MWCNT and SWCNT production. The operations in which the highest levels of EC were found included harvesting of CNT from the reactor, transferral of CNT and loading flasks with CNT, use of a batch mixer, CNT production, and cleaving of deposits. Only six studies measured the EC concentration and a comparison of the results is difficult because of the different EC protocols applied. Consequently, the reported values should be interpreted cautiously.

Erdely et al. (2013) adapted the results from the Dahm et al. (2012) study and those collected at three other facilities producing or using MWCNT in the USA to generate Fig. 1.4. The average EC concentrations in the inhalable size fraction from the eight MWCNT sites were found to have an arithmetic mean of 10.6 μg/m^3 with a standard deviation (SD) of 17.2 (GM, 4.21 μg/m^3; geometric SD [GSD], 4.15). In these eight MWCNT facilities, exposures ranged from non-detectable to 79.6 μg/m^3 and the exposure levels were log normally distributed (Shapiro-Wilk $P = 0.97$).

(d) Conclusion

Uncertainty still exists regarding which exposure metrics should be used as indicators of potential exposure-related health effects. The results from studies using direct reading instruments are not appropriate for quantitative exposure assessment of CNT, because particle number concentration and active surface area are dominated by ultrafine particles, mostly of incidental or outdoor origin, and are not representative of engineered CNT release. The filter-based methods in combination with SEM/TEM analysis appear to be more selective and sensitive for the characterization of exposure to CNT. However, the results of studies that focused on

Table 1.5 Occupational exposure to carbon nanotubes in different work settings

Reference	Workplace, activity	Nanomaterial	Operation/ process	Sample	Total dust mass concentration (µg/m³) [range]	Proxy[a] of CNT/CNF gravimetric concentration (µg/m³)	Evidence of CNT by TEM/SEM	Number of CNT (structures/cm³)	Protective equipment
Japan									
Ogura et al. (2013b)	Pilot-scale manufacture	SWCNT	Synthesis, harvesting, and package/water-assisted CVD	Area	1.6 (respirable)	from < 0.56 to < 2.3 (EC)	No	NM	Enclosure
Takaya et al. (2012)	Polyester textile plant	MWCNT-coated yarn	Weaving a conductive fabric	Personal	92 (all); 66 (respirable)	4.8–35 (EC3')	Yes	NM	No
				Area	NR	5.3 (EC3')	NM	NM	
Republic of Korea									
Han et al. (2008)	A-R&D laboratory	MWCNT produced by CVD	Thermal CVD	Personal	ND	NM	No	ND	No
				Personal	ND	NM	Yes	0.08	Fan installation, cleaning, and rearrangement
				Area	38.8	NM	No	ND	Fan installation, cleaning, and rearrangement
	A-R&D laboratory		Al/CNT ball milling	Personal	ND	NM	No	ND	No
				Personal	NM	NM	Yes	0.018	
	B-R&D laboratory		CNT solution spraying	Personal	193	NM	No	ND	No
				Personal	30.9	NM	Yes	0.008	
	C-R&D laboratory		Blending	Personal	331.7	NM	Yes	193.6	No
				Personal	ND	NM	Yes	0.018	Chiller delocalization and blender enclosure
				Area	434.5	NM	Yes	172.9	No
				Area	209	NM	No	NM	No
				Area	ND	NM	Yes	0.05	Chiller delocalisation and blender enclosure
				Area	ND	NM	No	ND	

Table 1.5 (continued)

Reference	Workplace, activity	Nanomaterial	Operation/process	Sample	Total dust mass concentration (µg/m³) [range]	Proxy[a] of CNT/CNF gravimetric concentration (µg/m³)	Evidence of CNT by TEM/SEM	Number of CNT (structures/cm³)	Protective equipment
Han et al. (2008) (cont.)	B-R&D laboratory		Weighing	Area	113.3	NM	No	ND	No
			Weighing/spraying	Area	36.6	NM	No	ND	No
			Weighing	Area	ND	NM	Yes	1.997	No
Lee et al. (2010)	Industry	A-MWCNT	Catalyst manufacturing, MWCNT manufacturing (Bag cyclone, CVD)	Personal	[21.2–79.5]	NM	No	ND	Fume hood, enclosure, half-mask, skin protective gloves
				Area	[17.7–124.1]	NM	No	ND	
		C-MWCNT	MWCNT manufacturing (CVD), spray and filtration of CNT solution	Personal	[42.2–285.9]	NM	No	ND	Natural ventilation
				Area	[31.1–120.4]	NM	No	ND	
				Area	56	NM	Yes	0.00312	
	Research institute	D-MWCNT	MWCNT application (ultrasonic dispersion, addition of sulfuric acid in fume hood)	Personal	[7.8–145]	NM	No	ND	Fume hood
				Area	[87.7–160.9]	NM	No	ND	
	Research institute	E-MWCNT	MWCNT application, spraying CNT solution, and wafer heating	Personal	[44.2–109.3]	NM	No	ND	Fume hood, enclosed, local exhaust system
				Area	[80.4–127.5]	NM	No	ND	

Table 1.5 Occupational exposure to carbon nanotubes in different work settings (continued)

Reference	Workplace, activity	Nanomaterial	Operation/process	Sample	Total dust mass concentration (µg/m³) [range]	Proxy[a] of CNT/CNF gravimetric concentration (µg/m³)	Evidence of CNT by TEM/SEM	Number of CNT (structures/cm³)	Protective equipment
Lee et al. (2013)	Two printed electronics facilities	CNT and silver nanoparticles	Roll to roll and roll to plate printing using nano-conductive ink	PBZ	[340–2930]	NM	No	NM	Fume hood, LEV
			Manufacture of CNT-nano-thin film solar cells/super capacitor	PBZ	[690–4240]	NM	No	NM	Fume hood, LEV
Sweden									
Hedmer et al. (2014)	Small-scale factory, production and sieving	Unrefined MWCNT produced by arc discharge	Opening reactor and collecting the deposits	Area	< 2100 (respiratory fraction)	140 (EC); 91 (EC3)	No	ND	LEV/half- face respirator, nitrile gloves, and protecting overall
			Cleaving deposits	Area	< 1900	470 (EC); 460 (EC3)	Yes	1.6	None/same as above
			Harvesting MWCNT from deposits	Area	< 1300	< 1.4 (EC); < 1.4 (EC3)	No	ND	
			Sieving, mechanical work-up, pouring, weighing, and packaging	Area	< 430	250 (EC); 240 (EC3)	Yes	11	
			Lathe machining graphite electrode	Area	< 1700	NM	Yes	1.2	
			Reactor clean out Part I	Area	< 2800	NM	No	ND	As above
			Reactor clean out Part II	Area	6800	550 (EC); 190 (EC3)	No	ND	As above
			All operations	PBZ	79–93	7.4 (EC); 6.3 (EC3)	Yes	0.6–2.0	As above

Table 1.5 (continued)

Reference	Workplace, activity	Nanomaterial	Operation/ process	Sample	Total dust mass concentration (µg/m³) [range]	Proxy[a] of CNT/CNF gravimetric concentration (µg/m³)	Evidence of CNT by TEM/SEM	Number of CNT (structures/cm³)	Protective equipment
Hedmer et al. (2014) (cont.)	Small-scale factory, purification of MWCNT	Purified and functionalized MWCNT produced by arc discharge	Purification Part I	Area	< 360	0.05 (EC); 0.05 (EC3)	No	ND	Fume hood/ nitrile gloves, and protecting overall
			Purification Part II	Area	< 320	NM	Yes	0.46	
			Functionalization Part I	Area	< 1700	NM	Yes	1.0	Fume hood/ nitrile gloves, and protecting overall
			Functionalization Part II	Area	< 910	NM	No	ND	
			Grinding	Area	< 620	NM	No	ND	As above
			All operations	PBZ*	< 71 (LOD)	< 0.08 (EC); < 0.08 (EC3)	Yes	0.04–0.1	As above
USA									
Maynard et al. (2004)	R&D laboratory	Unprocessed SWCNT	Laser ablation CNT removal	Personal	NM	[0.70] (Ni)	NM	NM	Clean enclosure
			Pouring CNT generated by HiPCO	Personal	NM	36.29 (Fe)	NM	NM	Clean enclosure
			Opening the chamber, removing CNT, cleaning	Personal	NM	9.86 (Ni)	NM	NM	Clean enclosure
			Enclosure dismantling/ HiPCO	Personal	NM	51.73 (Ni), 52.73 (Fe)	NM	NM	Clean enclosure
Yeganeh et al. (2008)	Primary manufacture	CNT, fullerenes	Synthesis/arc reaction	Area	[50–125] (PM$_{2.5}$)	NM	NM	NM	Fume hood
Methner et al. (2012)	Industry production and handling of SWCNT	SWCNT	Harvesting material from reactor	PBZ	NR	38 (EC)	Yes	NM	General room ventilation, ceiling-mounted supply and exhaust
				Area	NR	15 (EC)	Yes	NM	
			Wet wiping and mopping the room	PBZ	NR	ND (EC)	Yes	NM	
				Area	NR	ND (EC)	No	NM	

59

Table 1.5 Occupational exposure to carbon nanotubes in different work settings (continued)

Reference	Workplace, activity	Nanomaterial	Operation/process	Sample	Total dust mass concentration (µg/m³) [range]	Proxy[a] of CNT/CNF gravimetric concentration (µg/m³)	Evidence of CNT by TEM/SEM	Number of CNT (structures/cm³)	Protective equipment
Methner et al. (2012) (cont.)			Loading flasks with material	PBZ	NR	33 (EC)	Yes	NM	NA
				Area	NR	39 (EC)	Yes	NM	
			Loading trays with material	PBZ	NR	ND (EC)	Yes	NM	
				Area	NR	ND (EC)	Yes	NM	
Dahm et al. (2012)	Primary CNT manufacture (CVD)	MWCNT, DWCNT	Outdoor background	AS	NR	0.33 (EC)	NM	NM	NA
			MWCNT production	AS	NR	0.49[b] (EC)	Yes	0.034	Enclosed process ventilated to roof/nitrile gloves
				ASC	NR	0.78[b] (EC)	NM	NM	
			Harvesting MWCNT	PBZ	NR	2.28[b] (EC)	Yes	0.090	None/nitrile gloves, half-face respirator
				AS	NR	4.62 (EC)	Yes	0.026	
				ASC	NR	PF	NM	NM	
			Harvesting DWCNT	PBZ	NR	5.25[b] (EC)	Yes	0.123	None/nitrile gloves
				AS	NR	ND (EC)	Yes	0.047	
			Harvesting MWCNT (second batch)	PBZ	NR	2.74[b] (EC)	Yes	0.399	None/nuisance dust mask
				AS	NR	3.84[b] (EC)	Yes	0.134	
			Outdoor background	AS	NR	0.76 (EC)	NM	NM	NA
	Primary SWCNT manufacture	SWCNT	SWCNT production, harvesting, and reactor clean out (PBZ-reactor clean out only)	PBZ	NR	3.28[b] (EC)	Yes	0.013	Reactor under vacuum/nitrile gloves, R-95 filtering face piece, and half-face respirator
				AS	NR	1.13 (EC)	Yes	0.012	
				ASC	NR	ND (EC)	NM	NM	
			Outdoor background (day 2)	AS	NR	0.89 (EC)	NM	NM	NA

Table 1.5 (continued)

Reference	Workplace, activity	Nanomaterial	Operation/process	Sample	Total dust mass concentration (µg/m³) [range]	Proxy[a] of CNT/CNF gravimetric concentration (µg/m³)	Evidence of CNT by TEM/SEM	Number of CNT (structures/cm³)	Protective equipment
Dahm et al. (2012) (cont.)			SWCNT production, harvesting, and reactor clean out (day 2)	PBZ AS ASC	NR NR NR	0.68 (EC) 1.02 (EC) 1.88 (EC)	Yes Yes NM	0.003 0.007 NM	Reactor under vacuum/nitrile gloves, R-95 filtering face piece, and half-face respirator
	Primary and secondary MWCNT manufacture	MWCNT	Outdoor background	AS	NR	0.76[b] (EC)	NM	NM	NA
			Production and harvesting of MWCNT	PBZ AS ASC	NR NR NR	1.6 (EC) 0.47[b] (EC) 0.96[b] (EC)	Yes No NM	0.012 ND NM	Custom glove box/laboratory coat, latex gloves, surgical mask, and safety glasses
			Sonication (day 2) (PBZ-sonication, sieving, and spray coating)	PBZ AS	NR NR	1.13[b] (EC) ND (EC)	Yes Yes	0.010 0.002	None/ laboratory coat, latex gloves, and half-face respirator
			Sieving and spray coating (day 2)	AS ASC	NR NR	ND (EC) 0.7[b] (EC)	Yes NM	0.002 NM	Chemical fume hood/ laboratory coat, latex gloves, and half-face respirator
			General office worker	PBZ	NR	0.8 (EC)	Yes	0.001	None/none
	Secondary MWCNT manufacture for semiconductor devices	MWCNT	CNT waste collection and disposal	PBZ	NR	1.06[b] (EC)	Yes	0.214	None/full protective suit with booties, nitrile gloves

Table 1.5 Occupational exposure to carbon nanotubes in different work settings (continued)

Reference	Workplace, activity	Nanomaterial	Operation/process	Sample	Total dust mass concentration (µg/m³) [range]	Proxy[a] of CNT/CNF gravimetric concentration (µg/m³)	Evidence of CNT by TEM/SEM	Number of CNT (structures/cm³)	Protective equipment
Dahm et al. (2012) (cont.)			Weighing	PBZ	NR	ND (EC)	No	ND	Ventilated glove box/full protective suit with booties, nitrile gloves, and full-face respirator
				AS	NR	ND (EC)	No	ND	
			Sonication	PBZ	NR	0.83[b] (EC)	No	ND	Chemical fume hood/full protective suit with booties, gloves, acid smock, and face shield
				AS	NR	ND (EC)	Yes	0.003	
	Secondary MWCNT manufacture/ mixing with different resin formulations	MWCNT	Extrusion, weighing	PBZ	NR	3.19 (EC)	Yes	0.067	Chemical fume hood and glove box/safety glasses, half-face respirator, Tyvek suit/ laboratory coat, and nitrile gloves
			Batch mixer use	PBZ	NR	7.86[b] (EC)	Yes	0.242	
				AS	NR	1.01[b] (EC)	Yes	0.008	
				ASC	NR	1.89[b] (EC)	NM	NM	
			Milling CNT composite	PBZ	NR	ND (EC)	No	ND	HEPA vacuum/ safety glasses, half-face respirator, laboratory coat, and nitrile gloves
				AS	NR	ND (EC)	No	ND	

Table 1.5 (continued)

Reference	Workplace, activity	Nanomaterial	Operation/ process	Sample	Total dust mass concentration (µg/m³) [range]	Proxy[a] of CNT/CNF gravimetric concentration (µg/m³)	Evidence of CNT by TEM/SEM	Number of CNT (structures/cm³)	Protective equipment
Dahm et al. (2012) (cont.)	Secondary MWCNT and CNF manufacture	MWCNT/ CNF	Transferral of nanofibres	PBZ	NR	4.15[b] (EC)	Yes	1.1613	Clean room, custom glove box/latex gloves, half-face respirator, and Tyvek smock
				AS	NR	ND (EC)	Yes	0.295	
			Weighing, mixing, and sonication of CNT and CNF	PBZ	NR	7.54 (EC)	Yes	0.065	
				AS	NR	ND (EC)	Yes	0.003	
				ASC	NR	2.76[b] (EC)	NM	NM	

[a]   The mass of total carbon (TC), total elemental carbon (EC), EC found at the highest oxidation temperature step (900 °C or 920 °C) (EC3 or EC3') or metal catalyser (nickel or iron) was used as the elemental marker for the presence of CNT/CNF

[b]   Results were between the LOD and limit of quantification.

CNF, carbon nanofibres; CNT, carbon nanotubes; CVD, chemical vapour deposition; D, diameter; DWCNT, double-walled carbon nanotubes; Fe, iron; HEPA, high-efficiency particulate air; HiPCO, high-pressure carbon monoxide; LEV, local exhaust ventilation; LOD, limit of detection; µg/m³, micrograms per cubic metre of air; MWCNT, multiwalled carbon nanotubes; NA, not applicable; ND, not detected (analytical limit of detection = 0.6 µg/sample); Ni, nickel; NM, not measured; NR, not reported; PBZ, personal breathing zone; PM$_{2.5}$, particulate matter with particles of aerodynamic diameter < 2.5 µm; R&D, research and development; SEM, scanning electron microscopy; SWCNT, single-walled carbon nanotubes; TEM, transmission electron microscopy

In Han et al. (2008), total particle concentration (µg/m³) and number of MWCNT (tubes/cm³) were measured

In Hedmer et al. (2014), respiratory dust concentration was measured. *The two workers in the purification laboratory only worked there for part of a shift and only occasionally worked there at the same time. Therefore, one sampler was used by both workers

In Maynard et al. (2004), nanotube concentrations were estimated assuming that the combined mass of nickel and iron constitute 30% of the SWCNT material. Measured amounts below the limit of quantification are shown in square brackets. Iron: limit of detection, 0.0643 µg; limit of quantification, 0.212 µg; nickel: limit of detection, 0.0182 µg; limit of quantification, 0.0601 µg

In Dahm et al. (2012), all EC concentrations were media blank corrected. PF, pump fault; AS, area sample (25-mm cassette collected at a fixed position); PBZ (25-mm cassette fixed to lapel of worker); ASC, area sample cyclone (37-mm cassette w/cyclone collected at a fixed position)

Fig. 1.4 Concentrations of inhalable elemental carbon at eight facilities producing multiwalled carbon nanotubes
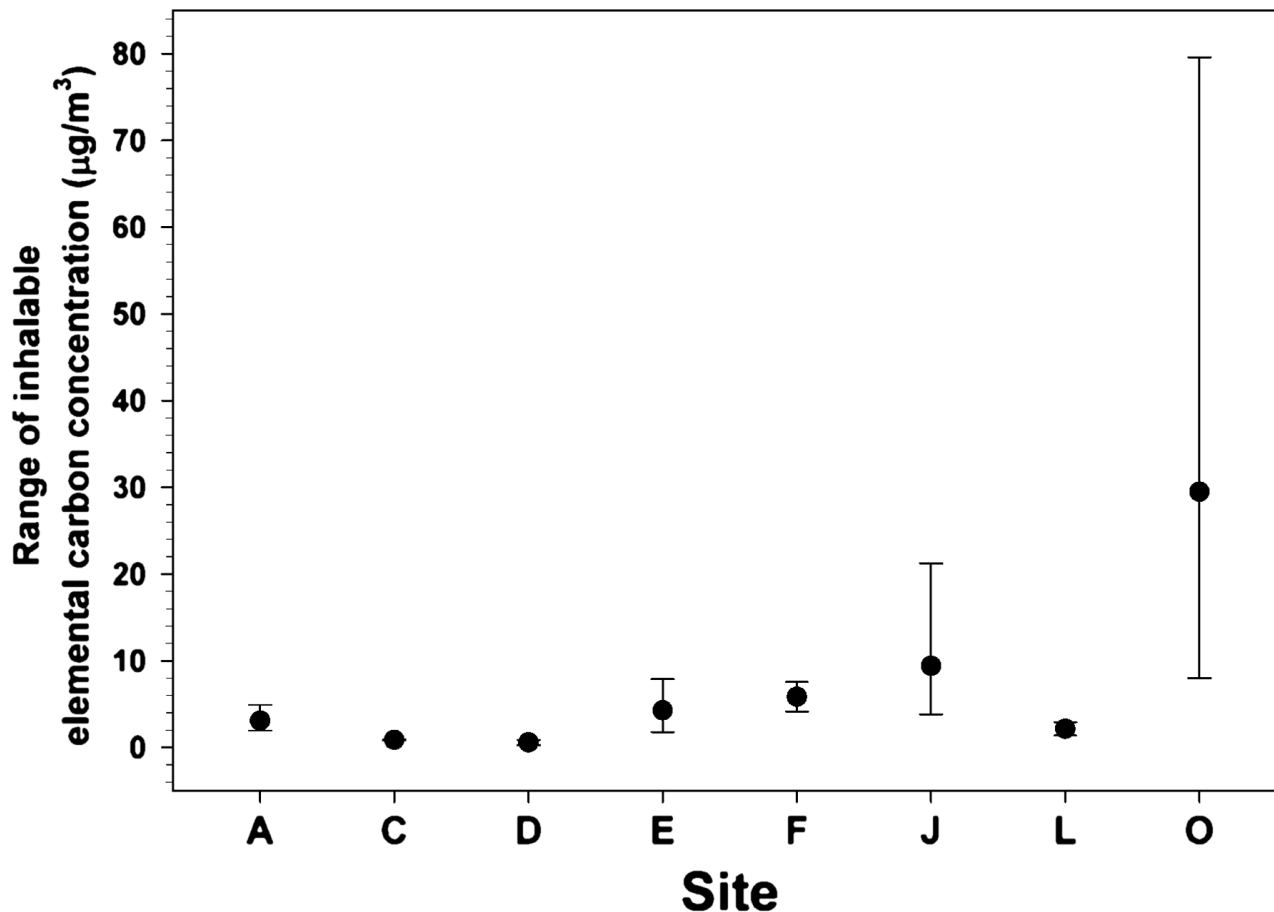
The mean, with error bars representing the upper and lower range, of measured concentrations of elemental carbon (µg/m³) with background correction. The figure was adapted from previously published data: sites A, and C–F, from Dahm et al. (2012); and sites J, L, and O from Dahm et al. (2013) and Erdely et al. (2013)
From Erdely et al. (2013). © Erdely et al.; licensee BioMed Central Ltd 2013

the collection of samples for the chemical-specific mass concentration analyses, such as EC mass concentration and TEM/SEM, were mostly based on original unvalidated methods and cannot be summarized appropriately. Consequently, the current available data do not allow the complete characterization of occupational exposure to CNT and only enable a limited description of some of occupational exposure situations.

1.5 Regulations and guidelines

No legal occupational exposure limit has been set for CNT.

In 2007, the British Standards Institution proposed a workplace exposure limit of 0.01 fibres/mL for fibrous nanomaterials with high aspect ratios (BSI, 2007) and published a "Guide to assessing airborne exposure in occupational settings relevant to nanomaterials" (BSI, 2010). The Dutch Social and Economic Council (2012) recommended an occupational exposure limit (OEL) of 0.01 fibres/cm³ for SWCNT or MWCNT

Table 1.6 Recommended occupational exposure limits for carbon nanotubes

Institution	Concentration	Interpretation	Year
British Standards Institution (WEL)	0.01 fibres/mL	Fibrous nanomaterials with high aspect ratios (> 3:1) and length > 5000 nm	2007
Dutch Social and Economic Council (OEL)	0.01 fibres/cm^3	SWCNT or MWCNT or metal oxide fibres for which asbestos-like effects are not excluded	2012
US NIOSH (REL)	1 μg/m^3 (EC)	8-hour TWA	2013
US OSHA (recommendation)	1 μg/m^3 (EC)	8-hour TWA	2013

EC, elemental carbon; NIOSH, National Institute for Occupational Safety and Health; OEL, occupational exposure limit; OSHA, Occupational Safety and Health Administration; REL, recommended exposure limit; TWA, time-weighted average; WEL, workplace exposure limit
Compiled by the Working Group

or metal oxide fibres for which asbestos-like effects are not excluded (van Broekhuizen et al., 2012).

The United States National Institute for Occupational Safety and Health (NIOSH) has set a recommended exposure limit for CNT and CNF of 1 μg/m^3 as an 8-hour time-weighted average (TWA) of EC for the respirable range fraction (NIOSH, 2013). In 2013, the United States Occupational Safety and Health Administration published a Fact Sheet which recommends that exposure of workers to respirable CNT and CNF should not exceed 1 μg/m^3 as an 8-hour TWA, based on the NIOSH proposed recommended exposure limit (OSHA, 2013).

These recommended values are presented in Table 1.6.

Other OELs have been proposed for CNT ranging from 1 to 50 μg/m^3 (8-hour TWA concentration) (Nanocyl, 2009; Aschberger et al., 2010; Pauluhn, 2010a). Despite the differences in risk assessment methods and assumptions, all of the derived OELs for CNT are low airborne mass concentrations relative to OELs for larger respirable carbon-based particles (NIOSH, 2013).

SWCNT and MWCNT are subject to regulation based on a US Toxic Substance Control Act (premanufacture notice) and Toxic Substance Control Act (significant new use rule) (EPA, 2011, 2014). Thus, a manufacturer or importer should submit a premanufacture notice to the US

Environmental Protection Agency (EPA) 90 days before manufacture or importation. In addition, SWCNT and MWCNT that are manufactured for uses other than those on the premanufacture notice are subject to a significant new use rule. A similar regulation applies to CNT in the Canadian Environment Protection Act (2014).

The Australian National Industrial Chemical Notification and Assessment Scheme (2010) also applies to substances containing 10% or more nanomaterials, including CNT. According to the implementation of the Globally Harmonized Classification and Labelling of Chemicals in Australia under the National Model Work Health and Safety Regulations, the classification of specific target organ toxicity applies to mixtures containing at least 10% SWCNT or MWCNT and the classification of carcinogenicity applies to mixtures containing at least 10% or more SWCNT or MWCNT (Safe Work Australia, 2010).

CNT are the subject of compulsory annual declarations of nanomaterials in France (Journal Officiel, 2012), Belgium (Arrêté Royal, 2014), and Denmark (Danish Environment Protection, 2014).

2. Cancer in Humans

No data were available to the Working Group.

3. Cancer in Experimental Animals

3.1 MWCNT

3.1.1 Mouse

See Table 3.1

(a) Inhalation

In an initiation-promotion study, groups of 60 male B6C3F$_1$ mice (age, 6 weeks) were given a single intraperitoneal injection of vehicle (corn oil) or 10 µg/g body weight (bw) of 3-methylcholanthrene (3-MC) in corn oil to initiate carcinogenesis. One week after the injection, the mice were exposed to filtered air or 5 mg/m^3 of MWCNT-7 (Mitsui-7, Hodogaya Chemical Co.) for 5 hours per day for 15 days and were then observed for 17 months. MWCNT-7 particles ranged from single fibre-like nanotubes to tangled agglomerates with a mass median aerodynamic diameter (MMAD) of 1.59 µm and a GSD of 1.69. The count mode aerodynamic diameter of the MWCNT-7 fibres was 420 nm. Trace metal contamination was 1.32%, and iron was the major metal contaminant (1.06%). Tumour promotion activity was assessed by comparing the 3-MC plus MWCNT-7-exposed group with the 3-MC-exposed groups. The incidence of bronchiolo-alveolar lesions in mice receiving air, 3-MC, MWCNT-7, and 3-MC plus MWCNT-7 was: adenoma or carcinoma (combined) – 13 out of 56, 28 out of 54, 13 out of 49, and 38 out of 42, respectively; adenoma – 6 out of 56, 18 out of 54, 9 out of 49, and 32 out of 42, respectively; and carcinoma –7 out of 56, 12 out of 54, 7 out of 49, and 26 out of 42, respectively. These results showed a significant difference between the 3-MC plus MWCNT-7 and 3-MC groups ($P < 0.0001$),

indicating that MCWNT-7 promoted the induction of benign and malignant lung tumours. The incidence of lung tumours in animals treated with MCWNT-7 (in the absence of initiation with 3-MC) did not differ significantly from that in the filtered-air controls. However, the volume of lung tumours was significantly greater ($P < 0.0001$) in the MWCNT-7-exposed group than in the air-exposed group (Sargent et al., 2014).

(b) Intratracheal instillation

Three groups of three male C57BL/6 mice (age, 6 weeks) were given a single intratracheal instillation of either a 50-µL aliquot of saline or MWCNT CM-95 (Hanwha Nanotech; as-produced; length, 7.71 µm; diameter, 13.5 nm) or acid-treated MWCNT CM-95 (length, 567.4 nm; diameter, 7.5 nm) in 50 µL saline (100 µg MWCNT/mouse) and were killed 6 months after the injection. None of the three mice given saline developed hyperplasia, adenoma, or adenocarcinoma of the lung. Of the three mice given MWCNT (as-produced), two developed peri-bronchial lymphoid hyperplasia, two developed adenomas, and one developed adenocarcinoma of the lung. Of the three mice given acid-treated MWCNT, two developed hyperplasia and one developed adenoma (described by the authors as a "slight" adenoma) of the lung (Yu et al., 2013). [The Working Group noted the short duration of the experiment, the very small number of animals that precluded a statistical assessment of the results, and the low susceptibility of this strain to lung carcinogenesis. The study was judged to be inadequate for an evaluation of carcinogenicity.]

(c) Intraperitoneal injection

Two groups of 19 male p53$^{+/-}$mice (C57BL/6 background; age, 9–11 weeks) received a single intraperitoneal injection of either 1 mL of vehicle (control) or 3 mg (particle count, 1×10^9) of MWCNT-7 (Mitsui; length, 1–19 (median, 2) µm; diameter, 70–170 (median, 90) nm; impurities:

Table 3.1 Studies on carcinogenicity with multiwalled carbon nanotubes in mice

Strain (sex) Duration Reference	Dosing regimen, Animals/group at start	Incidence of tumours	Significance	Comments
B6C3F₁ (M) 17 mo Sargent et al. (2014)	Intraperitoneal injection of 0 or 10 µg/g bw of 3-MC in corn oil once (initiation) Inhalation exposure 0 or 5 mg/m³ of MWCNT-7 (Mitsui-7, Hodogaya, Japan) in air, 5 h/day for 15 days, 1 wk later, then observed for 17 mo (promotion) 60/group	Bronchiolo-alveolar adenoma: Air, 6/56; 3-MC, 18/54; MWCNT-7, 9/49; 3-MC+MWCNT-7, 32/42 Bronchiolo-alveolar carcinoma: Air, 7/56; 3-MC, 12/54; MWCNT-7, 7/49; 3-MC+MWCNT-7, 26/42 Bronchiolo-alveolar adenoma or carcinoma (combined): Air, 13/56; 3-MC, 28/54; MWCNT-7, 13/49; 3-MC+MWCNT-7, 38/42	Air vs MWCNT-7, NS; 3-MC vs 3-MC+MWCNT-7, P < 0.0001, Fisher exact test Air vs MWCNT-7, NS; 3-MC vs 3-MC+MWCNT-7, P < 0.0001, Fisher exact test Air vs MWCNT-7, NS; 3-MC vs 3-MC+MWCNT-7, P < 0.0001, Fisher exact test	Primary particles: MWCNT particles ranged from single fibre-like nanotubes to tangled agglomerates; MMAD, 1.59 µm; GSD, 1.69; count mode aerodynamic diameter, 420 nm; trace metal contamination, 1.32% (iron was the major metal contaminant, 1.06%) The lung tumour volume was significantly greater (P < 0.0001) in the MWCNT-7-exposed groups compared with the air-exposed groups
C57BL/6 (M) 6 mo Yu et al. (2013)	Intratracheal instillation 0 or 100 µg/mouse of as-produced or acid-treated MWCNT in 50 µL of saline once, then killed 6 mo later 3/group	Lung hyperplasia: 0/3, 2/3 (as-produced), 2/3 (acid-treated) Lung adenoma: 0/3, 2/3 (as-produced), 1/3 (acid-treated) Lung adenocarcinoma: 0/3, 1/3 (as-produced), 0/3 (acid-treated)	NA	MWCNT CM-95 (Hanwha Nanotech, Republic of Korea); primary particles: as-produced (length, 7.71 µm; diameter, 13.5 nm); acid-treated (treated with sulfuric:nitric acid (3:1, v/v); length, 567 nm; diameter, 7.5 nm) Small number of animals and short duration of the experiment; the very small number of animals precluded statistical assessment of the results; C57BL/6 mice have a low susceptibility to lung carcinogenesis
p53⁺/⁻ (C57BL/6 background) (M) 180 days Takagi et al. (2008)	Intraperitoneal injection 0 (vehicle control) or 3 mg/mouse (particle count/mouse, 1 × 10⁹) of MWCNT-7 (Mitsui) in 1 mL of 0.5% methyl cellulose + 1.0% Tween 80 once, then observed up to 180 days 19/group	Peritoneal mesothelioma (epithelial type): 0/19, 14/16*	* [P < 0.0001, Fisher's exact test]	Primary particles: length, 1–19 (median, 2) µm; diameter, 70–170 (median, 90) nm; iron, 3500 ppm (0.35%); sulfur, 470 ppm; chlorine, 20 ppm; fluorine, < 5 ppm; bromine, < 40 ppm

Table 3.1   (continued)

Strain (sex) Duration Reference	Dosing regimen, Animals/group at start	Incidence of tumours	Significance	Comments
p53+/- (C57BL/6 background) (M) 365 days Takagi et al. (2012)	Intraperitoneal injection 1 mL of 0 (vehicle control), 3 (particle count, 1×10^6), 30 (particle count, 1×10^7), or 300 (particle count, 1×10^8) μg/ mouse of MWCNT-7 (Mitsui) in 0.5% methyl cellulose + 1.0% Tween 80 once, then observed up to 365 days 20/group	Peritoneal mesothelioma (epithelial type): 0/20, 5/20*, 17/20**, 19/20**	* [$P < 0.05$, Fisher's exact test] ** [$P < 0.0001$, Fisher's exact test]	Primary particles: length, 1–19 (median, 2) μm; diameter, 70–170 (median, 90) nm; iron, 3500 ppm (0.35%); sulfur, 470 ppm; chlorine, 20 ppm; fluorine, < 5 ppm; bromine, < 40 ppm
rasH2 (C57BL/6 background) (M) 26 wk Takanashi et al. (2012)	Subcutaneous injection 550 μL of 0 (control) or 75 mg/kg bw of MWCNT dispersed in saline containing 0.1% Tween 80 in the back, then killed after 26 wk 10/group	No increase in tumour incidence at any site in treated mice	NS	VGCF-S MWCNT (Showa Denko, Japan): mean length, 10 μm; mean diameter, 100 nm

bw, body weight; GSD, geometric standard deviation; M, male; 3-MC, 3-methylcholanthrene; MMAD, mass median aerodynamic diameter; mo, month; MWCNT, multiwalled carbon nanotubes; NA, not applicable; NS, not significant; ppm, parts per million; wk, week

iron, 3500 ppm (0.35%); sulfur, 470 ppm; chlorine, 20 ppm; fluorine, < 5 ppm; and bromine, < 40 ppm) in 1 mL of 0.5% methyl cellulose with 1.0% Tween 80, and were then observed for up to 180 days. The incidence of peritoneal mesothelioma was significantly increased in the MWCNT-7-exposed group (14 out of 16 versus 0 out of 19; [$P < 0.0001$]) (Takagi et al., 2008).

Four groups of 20 male p53$^{+/-}$ mice (C57BL/6 background; age, 9–11 weeks) received a single intraperitoneal injection of 0 (vehicle control), 3, 30, or 300 μg/mouse of MWCNT-7 (Mitsui; length, 1–19 (median, 2) μm; diameter, 70–170 (median, 90) nm; impurities: iron, 3500 ppm (0.35%); sulfur, 470 ppm; chlorine, 20 ppm; fluorine, < 5 ppm; and bromine, < 40 ppm) (particle count: 0, 1×10^6, 1×10^7, or 1×10^8, respectively) in 1 mL of 0.5% methyl cellulose with 1.0% Tween 80, and were then observed for up to 365 days. Survival of the mice in the dosed groups was shorter due to the high incidence of lethal mesothelioma. The incidence of peritoneal mesothelioma (0 out of 20 [control], 5 out of 20, 17 out of 20, and 19 out of 20, respectively) was significantly increased in all treated groups ([$P < 0.05$, $P < 0.0001$, and $P < 0.0001$], respectively) compared with controls (Takagi et al., 2012).

(d)   Subcutaneous injection

Two groups of 10 male rasH2 (human c-Ha-*ras* proto-oncogene) transgenic mice (C57BL/6 background; age, 6 weeks) received a single subcutaneous injection in the back of 550 μL of vehicle or 75 mg/kg bw of MWCNT (VGCF-S; Showa Denko, Japan; mean length, 10 μm; mean diameter, 100 nm) dispersed in 550 μL saline containing 0.1% Tween 80, and were killed after 26 weeks. No significant increase in tumour incidence was observed at any site in the treated mice (Takanashi et al., 2012).

3.1.2 Rat

See Table 3.2

(a)   Intraperitoneal injection/implantation

The carcinogenic potential of two different MWCNT (MWCNT+ and MWCNT–; University of Namur, Belgium) was compared. MWCNT+ had a length and diameter of about 0.7 μm and 11.3 ± 3.9 nm, respectively, and a metal content (%) of: aluminium, 1.97; iron, 0.49; and cobalt, 0.48. MWCNT– had the same length and diameter, but a lower metal content (aluminium, 0.37%; iron, < 0.01%; and cobalt, < 0.01%) and fewer structural defects. Groups of 26 or 50 male Wistar rats (age, 10–13 weeks) received a single intraperitoneal injection of vehicle (control), MWCNT+ (2 mg or 20 mg/rat), MWCNT– (20 mg/rat), or crocidolite (2 mg/rat, positive control) in 2 mL phosphate-buffered saline (PBS) and were then observed for up to 24 months. The incidence of peritoneal mesothelioma was 1 out of 26, 2 out of 50, 0 out of 50, 3 out of 50, and 9 out of 26 ($P < 0.01$, crocidolite-treated group), respectively, and that of peritoneal lipoma, liposarcoma, or angiosarcoma (combined) was 0 out of 26, 1 out of 50, 3 out of 50, 3 out of 50, and 0 out of 26 (no significant difference), respectively (Muller et al., 2009). [The Working Group noted that peritoneal mesotheliomas are rare spontaneous neoplasms in rats. The Working Group also noted that the incidence of peritoneal mesothelioma in the vehicle-control group was unusually high (1 out of 26; 3.8%) and did not exclude the possibility that this tumour originated from the scrotum and spread into the peritoneal cavity.]

Two groups of six male Fischer 344 rats (weighing 400 g) [age and sex unspecified] received an intraperitoneal implant of a gelatin capsule containing either 10 mg/rat of MWCNT (Shenzhen Nanotech; length, 1–2 μm; diameter, 10–30 nm; 95–98% pure) or crystalline zinc oxide as a negative control. The experiment was terminated after 12 months. Mesotheliomas were not found but foreign body granulomatous lesions were observed in MWCNT-exposed rats (Varga

Table 3.2 Studies of carcinogenicity with multiwalled carbon nanotubes in rats

Strain (sex) Duration Reference	Dosing regimen, Animals/group at start	Incidence of tumours	Significance	Comments
Wistar (M) 24 mo Muller et al. (2009)	Intraperitoneal injection 2 mL of 0 (vehicle control), 2 or 20 mg/rat of MWCNT+, 20 mg/rat of MWCNT–, or 2 mg/rat of crocidolite in PBS, then observed up to 24 mo Vehicle, 26 rats; 2 mg MWCNT+, 50 rats; 20 mg MWCNT+, 50 rats; 20 mg MWCNT–, 50 rats; 2 mg crocidolite, 26 rats	Peritoneal mesothelioma: 1/26, 2/50 (2 mg MWCNT+), 0/50 (20 mg MWCNT+), 3/50 (MWCNT–), 9/26* (crocidolite) Peritoneal lipoma, liposarcoma or angiosarcoma (combined): 0/26, 1/50 (2 mg MWCNT+), 3/50 (20 mg MWCNT+), 3/50 (MWCNT–), 0/26 (crocidolite)	*$P < 0.01$, Fisher's exact test NS	MWCNT (University of Namur, Belgium); MWCNT+: length, ~0.7 μm; diameter, 11.3 ± 3.9 nm; metal content (%): aluminium, 1.97; iron, 0.49; cobalt, 0.48 MWCNT–: length, ~0.7 μm; diameter, 11.3 ± 3.9 nm; metal content (%): aluminium, 0.37; iron, < 0.01; cobalt, < 0.01
F344 (NR) 12 mo Varga & Szendi (2010)	Intraperitoneal implantation Gelatin capsule filled with crystalline zinc oxide (negative control) or 10 mg of MWCNT once, then observed for 12 mo 6/group	Mesothelioma: 0/6, 0/6	NS	MWCNT (length, 1–2 μm; diameter, 10–30 nm; 95–98% pure) produced by Shenzhen Nanotech Port Co. Ltd, China. Study duration was short; no vehicle control; small number of animals per group; foreign body granulomatous lesions observed in MWCNT-exposed rats
F344/Brown Norway F$_1$ hybrid (M, F) 350 days or up to 3 yr Nagai et al. (2011, 2013)	Intraperitoneal injection 1 mL of 0, 0.5 or 5 mg/mL of MWCNT in 0.5% BSA in saline, twice within a 1-wk period, then observed for up to 3 yr 6–43 M+F/group	Mesothelioma (M+F) at 350 days: 0/23 (0%), 12/15 (80%; NT50a(–agg*))*, 13/13 (100%; 1 mg/rat NT50a)*, 43/43 (100%; 10 mg/rat NT50a)*, 6/6 (100%; 10 mg/rat NT50b)*, 5/29 (17%; 1 mg/rat NT145)**, 28/30 (93%; 10 mg/rat NT145)*, 0/6 (0%; 10 mg/rat NTtngl) Mesothelioma (M+F) at 3 yr: 0/6 (0%; 10 mg/rat NTtngl)	* [$P < 0.0001$], Fisher's exact test; ** [$P < 0.05$], Fisher's exact test NS	MWCNT [NT50a (MWCNT-7) from Mitsui, others from Showa Denko] NT50a(–agg*): length, 5.29 μm; diameter, 49.95 nm; no aggregation; same number of fibres as in the NT145 suspension NT50a: length, 5.29 μm; diameter, 49.95 nm; high level of aggregation NT50b: length, 4.60 μm; diameter, 52.40 nm; high level of aggregation NT145: length, 4.34 μm; diameter, 143.5 nm; low level of aggregation NTtngl: tangled conformation; diameter, 2–20 nm

Table 3.2 (continued)

Strain (sex) Duration Reference	Dosing regimen, Animals/group at start	Incidence of tumours	Significance	Comments
F344 (M) 52 wk Sakamoto et al. (2009)	Intrascrotal injection 0 (vehicle control) in 2 mL/kg bw or 0.5 mg/mL (3.55 × 10⁸ particles/mg) of MWCNT-7 (Mitsui) in 2% carboxymethyl cellulose (0.24 mg/rat, 1.0 mg/kg bw) once, then observed up to 52 wk Vehicle, 5 rats; MWCNT-7, 7 rats.	Peritoneal mesothelium hyperplasia: 0/5, 7/7* Peritoneal mesothelioma (epithelial and sarcomatoid mixed type): 0/5, 6/7*	*P < 0.05, Fisher's exact test	Primary particles: length, 1–19 (median, 2) μm; diameter, 70–170 (median, 90) nm; iron, 3500 ppm; sulfur, 470 ppm; chlorine, 20 ppm; fluorine, < 5 ppm; bromine, < 40 ppm Small number of animals per group

BSA, bovine serum albumin; F, female; M, male; mo, month; MWCNT, multiwalled carbon nanotubes; NR, not reported; NS, not significant; PBS, phosphate-buffered saline; wk, week; yr, year

& Szendi, 2010). [The Working Group noted the small number of animals, the short duration of the study, that the age and sex of the animals were not reported, and the lack of a vehicle control. The study was judged to be inadequate for an evaluation of carcinogenicity.]

Groups of male and female Fischer 344/ Brown Norway F_1 hybrid rats (age, 6 weeks) received two intraperitoneal injections during a 1-week period of 1 mL of 0.5 or 5 mg/mL of NT50a or NT145 MWCNT, 0.5 mg/mL of NT50a(–agg*) MWCNT, or 5 mg/mL NT50b or NTtngl MWCNT, and were then observed for up to 350 days. Control rats received two injections of the vehicle (0.5% bovine serum albumin in saline) alone. NT50a (MWCNT-7; length, 5.29 μm; diameter, 49.95 nm) was purchased from Mitsui; NT50b (length, 4.60 μm; diameter, 52.40 nm), NT145 (length, 4.34 μm; diameter, 143.5 nm), and NTtngl (diameter, 2–20 nm; tangled conformation, therefore length was not determined) were purchased from Showa Denko. NT50a(–agg*) was obtained from the supernatant after the centrifugation of NT50a at 2200 g for 10 seconds, which was then concentrated to obtain the same fibre count as that of NT145. Aggregation was high in NT50a and NT50b suspensions, low in the NT145 suspension, and very high in the NTtngl suspension; no agglomerates were present in the NT50a(–agg*) suspension. There was a significant increase in the incidence of mesothelioma in all MWCNT-treated groups, except in the NTtngl-treated group. The incidences of mesothelioma at 350 days were 0 out of 23 (control), 12 out of 15 (1 mg NT50a(–agg*)), 13 out of 13 (1 mg NT50a), 43 out of 43 (10 mg NT50a), 6 out of 6 (10 mg NT50b), 5 out of 29 (1 mg NT145), 28 out of 30 (10 mg NT145), and 0 out of 6 (10 mg NTtngl) (Nagai et al., 2011). An additional six rats treated with 10 mg NTtngl were held for up to 3 years after treatment. Granulomas were induced but no mesotheliomas were observed (Nagai et al., 2013). [The Working Group noted the varying

number of animals per group and the small number of animals exposed to MWCNT with a tangled conformation. The authors stated that they found no evidence of mesothelioma induced by MWCNT with a tangled conformation, but the Working Group believed that the demonstration of a negative result requires a study with high statistical power which would not be reached with a sample size of six animals.]

(b) Intrascrotal injection

Two groups of male Fischer 344 rats (age, 12 weeks) received a single intrascrotal injection of vehicle (5 rats, 2 mL/kg bw) or 0.24 mg of 0.5 mg/mL MWCNT-7 (Mitsui; length, 1–19 (median, 2) μm; diameter, 70–170 (median, 90) nm; impurities: iron, 3500 ppm (0.35%); sulfur, 470 ppm; chlorine, 20 ppm; fluorine, < 5 ppm; and bromine, < 40 ppm) (7 rats, 1.0 mg/kg bw) in 2% carboxymethyl cellulose and were then observed for up to 52 weeks. The incidence of peritoneal mesothelial cell hyperplasia in the control and treated group was 0 out of 5 and 7 out of 7 ($P < 0.05$), respectively, and that of peritoneal mesothelioma was 0 out of 5 and 6 out of 7 ($P < 0.05$), respectively (Sakamoto et al., 2009). [The Working Group noted the small numbers of animals per group.]

3.2 SWCNT

See Table 3.3

Rat

(a) Intratracheal instillation

Groups of male Crl: CD (SD) rats (age, 8 weeks) received intratracheal instillations with a type of SWCNT synthesized by the National Institute of Advanced Industrial Science and Technology, Japan (primary particle maximum length, 1200 μm; primary particle diameter, 3.0 nm; metal content: 145 ppm iron, 103 ppm

Table 3.3 Studies of carcinogenicity with single-walled carbon nanotubes in rats

Species, strain (sex) Duration Reference	Dosing regimen, Animals/group at start	Incidence of tumours	Significance	Comments
Rat, Crl: CD (SD) (M) Up to 26 wk Kobayashi et al. (2011)	Experiment 1: Intratracheal instillation 1 mL/kg bw of 0 (vehicle), 0.2, or 2.0 mg/mL of SWCNT in Tween 80 in PBS once, then killed at 24 h, 3 days, 1 wk, 4 wks, or 13 wk Experiment 2: Intratracheal instillation 1 mL/kg bw of 0 (vehicle), 0.04, 0.2, or 1.0 mg/mL of SWCNT in Tween 80 in PBS once, then killed at 3 days, 1 wk, 4 wks, 13 wks, or 26 wk 6/group at each time-point	Lung tumour: None reported in any group	NS	Synthesized by National Institute of Advanced Industrial Science and Technology, Japan; primary particles: maximum length, 1200 μm; diameter, 3.0 ± 1.1 nm; iron, 145 ppm; nickel, 103 ppm; chromium, 34 ppm; manganese, 2 ppm; aluminium, 12 ppm; aggregates: length, 0.32 μm; diameter, 12.0 ± 6.5 nm Short duration of the study
Rat, F344 (NR) 12 mo Varga & Szendi (2010)	Intraperitoneal implantation Gelatin capsule filled with crystalline zinc oxide (negative control) or 10 mg of SWCNT once, then observed for 12 mo 6/group	Mesothelioma 0/6, 0/6	NS	SWCNT (length, 4–15 μm; diameter, < 2 nm; 90% pure) produced by Shenzhen Nanotech Port Co. Ltd, China Short duration of the study; no vehicle control; small number of animals per group; foreign body granulomatous lesions observed in SWCNT-exposed rats

bw, body weight; M, male; mo, month; NR, not reported; NS, not significant; PBS, phosphate-buffered saline; SWCNT, single-walled carbon nanotubes; wk, week

nickel, 34 ppm chromium, 2 ppm manganese, and 12 ppm aluminium; and aggregate length, 0.32 μm; aggregate diameter, 12.0 nm). In a first experiment, the rats were given a single dose of 1 mL/kg bw of a 0 (vehicle)-, 0.2-, or 2.0-mg/mL solution of SWCNT in Tween 80 in PBS (doses corresponding to 0.0, 0.2, or 2.0 mg/kg bw), and six rats per group were killed 24 hours, 3 days, 1 week, 4 weeks, or 13 weeks later. In a second experiment, the rats were given a single dose of 1 mL/kg bw of a 0 (vehicle)-, 0.04-, 0.2-, or 1.0-mg/mL solution of SWCNT in Tween 80 in PBS (doses corresponding to 0.0, 0.4, 0.2, or 1.0 mg/kg bw), and six rats per group were killed 3 days, 1 week, 4 weeks, 13 weeks, or 26 weeks later. No lung tumours were reported in any group (Kobayashi et al., 2011). [The Working Group noted the short duration of the experiments and judged the study to be inadequate for an evaluation of carcinogenicity.]

(b) Intraperitoneal implantation

Two groups of six Fischer 344 rats (weighing 400 g) [age and sex unspecified] received an intraperitoneal implant of a gelatin capsule containing either 10 mg/rat of SWCNT (Shenzhen Nanotech; diameter < 2 nm; length, 4–15 μm; 90% pure) or crystalline zinc oxide as a negative control, and the experiment was terminated after 12 months. Mesotheliomas were not found but foreign body granulomatous lesions were observed in SWCNT-exposed rats (Varga & Szendi, 2010). [The Working Group noted the small number of animals, the short duration of the study, that the age and sex of the animals were not reported, and the lack of a vehicle control. The study was judged to be inadequate for an evaluation of carcinogenicity.]

4. Mechanistic and Other Relevant Data

4.1 Deposition, phagocytosis, translocation, retention, and clearance

4.1.1 Humans

No data were available to the Working Group.

4.1.2 Experimental animals

(a) Deposition

In male Wistar rats exposed by whole-body inhalation for 6 hours per day on 5 days per week to 0.37 mg/m^3 of MWCNT (Nikkiso Co., Ltd; length, 1.1 μm; diameter, 63 nm) dispersed in an aqueous solution of 0.5 mg/mL Triton X-100 and atomized by a nebulizer into the exposure chamber (MWCNT aerosol comprised of approximately 70% of single fibres), lung deposition fractions of 0.18 or 0.2 were estimated from the measured mass of CNT in the lungs 3 days after the end of the 4-week experiment. The retained mass lung burdens were measured by X-ray diffraction or EC analysis at 3 days, 1 month, and 3 months after exposure, and the mass of MWCNT in the lungs 3 days after exposure was 68 and 76 μg/lung, as measured by the two methods, respectively (Oyabu et al., 2011).

A deposition fraction of 5.7% MWCNT was estimated in rats by Pauluhn (2010b) using data on the airborne size distribution (e.g. MMAD, ~3 μm; GSD, ~2) and the Multiple-Path Particle Dosimetry (MPPD) model 2 software (Anjilvel & Asgharian, 1995). NIOSH (2013) provided a comparison of the rat alveolar deposition fraction estimates from Pauluhn (2010b) using two different versions of the MPPD software (v. 2.0 and 2.1) (CIIT & RIVM, 2006; ARA, 2011) and density values of either 1 or 0.2 g/mL. Estimated deposition fractions were 0.046, 0.027, or 0.023

from MPPD 2.0 (density 1 g/mL), MPPD 2.1 (density 1 g/mL), or MPPD 2.1 (density 0.2 g/mL), respectively. The aerodynamic particle size used was 2.74 μm MMAD (GSD, 2.11) [middle of the three measures reported by Pauluhn (2010b)].

A 3-week inhalation study in male C57BL/6J mice exposed to 5 mg/m³ of MWCNT (Mitsui-7 [MWCNT-7]; Hodogaya Chemical Co.) for 5 hours per day for 12 days provided information to estimate the lung deposition fraction (Mercer et al., 2013a). [The Working Group noted that, although a mouse lung deposition fraction was not reported in Mercer et al. (2013a), it can be estimated (as shown below) to provide additional information to and enable comparisons with estimates from other animal studies on the inhalation of CNT. The Working Group also noted that estimation of the deposition fraction from the measured lung burden at the end of inhalation exposure would be underestimated by the amount of CNT that was cleared from the lungs during the exposure period.]

The average lung burden measured 1 day after the end of the 3-week inhalation exposure was 28.1 μg (Mercer et al., 2013a). The estimated deposition fraction can be estimated as:

Deposition fraction = total lung dose (mg)/ exposure (h/d * d * min/h) * L/min * m³/L, or

0.0095 = 28.1/5*(5 * 12 * 60) * 0.165 * (1/1000)

where the total lung dose was measured 1 day (d) after the end of the 12-day inhalation exposure (Mercer et al., 2013a; Table 4.1) and the minute ventilation rate was 0.165 L/min (Shvedova et al., 2008). Shvedova et al. (2008) stated that mouse ventilation rates (including both tidal volumes and breathing rates) can be highly variable depending on how the values were measured. Using the EPA (1988, 2006) minute ventilation rate of 0.037 L/min in mice, the deposition fraction would be 0.042.

Expressed as a percentage, the mouse lung deposition fractions estimated above were approximately 1% or 4% for MWCNT in Mercer et al. (2013a) (using a minute ventilation rate

of either 0.165 or 0.037 L/min, respectively). In comparison, a mouse lung deposition fraction of 0.5% was reported for SWCNT by Shvedova et al. (2008), which was based on a mass mode aerodynamic diameter of 4.2 μm and estimation of the deposition fraction from Raabe et al. (1988) [Shvedova et al. (2008) used the estimated deposition fraction in mice to estimate the deposited lung dose in mice and the worker-equivalent lung dose.] The mass mode aerodynamic diameter of MWCNT was 1.3 μm (Mercer et al., 2013a) and the MMAD was 1.5 μm (GSD, 1.67) (Chen et al., 2012). [This comparison shows reasonably consistent estimated deposition fractions in mice inhaling CNT, given the differences in the measures of aerodynamic diameter and the uncertainty about mouse ventilation rates.]

A study of MWCNT in male Sprague-Dawley rats (age, 9–10 weeks) provided a comparison of the lung responses to exposure to three different forms of MWCNT, including original (O), purified (P), and carboxylic acid-functionalized (F), at similar estimated lung doses by nose-only inhalation or tracheal instillation (Silva et al., 2014). The O-MWCNT contained 4.49% nickel and 0.76% iron residual catalysts; P-MWCNT contained 1.8% nickel and 0.08% iron; while F-MWCNT contained no detectable levels of nickel or iron. The dimensions of these MWCNT were: outer diameter, 20–30 nm; inner diameter, 5–10 nm; and length, 10–30 μm. The MWCNT were aerosolized for inhalation by nebulization. The MMADs (GSD) for O-, P-, and F-MWCNT were 3.7 (2.5), 4.8 (2.9), and 3.3 (3.1) μm, respectively. Doses for tracheal instillation were 0, 10, 50, or 200 μg in a biocompatible dispersion medium. The single (6-hour) inhalation exposure at a concentration of approximately 30 mg/m³ was estimated to result in a deposited lung dose that was similar to or higher than that of the intratracheally administered dose of 200 μg (estimated by assuming an alveolar and tracheobronchial deposition fraction of 0.14 and a ventilation rate of 0.15 L/min: 30 mg/m³ × 0.15 L/min × 6 h × 60

min/h×1m³/1000L×0.14×1000µg/1mg=227µg). [The Working Group noted that the "Inhalation Exposure and Aerosol Characterization" section of the Methods in the publication reported a MWCNT aerosol concentration of 38 µg/L (equal to 38 mg/m³), which would result in a deposition of 287 µg MWCNT.]

(b) Phagocytosis

CNT have been observed in cells using confocal Raman microscopy (Romero et al., 2011) or TEM (Ryman-Rasmussen et al., 2009a). The possible mechanisms by which CNT can enter cells include diffusion or penetration through cell membranes (passive internalization) or endocytosis (active internalization) (Kunzmann et al., 2011; Ye et al., 2013), both of which may depend on the surface properties of the CNT and the activation state of the phagocytic cells. Four types of endocytosis have been reported (Ye et al., 2013): phagocytosis, clathrin-mediated endocytosis, caveolea-mediated endocytosis, and macrophage pinocytosis. The first three types have been studied in relation to CNT. Phagocytosis is the engulfment of foreign materials by macrophages, monocytes, and neutrophils, the primary purpose of which is considered to be the elimination of larger pathogens (bacteria and yeast) or cell debris. Larger CNT structures (e.g. > 400 nm) or agglomerates were recognized by phagocytes, while individual structures evaded phagocytosis (Antonelli et al., 2010; Ali-Boucetta & Kostarelos, 2013). Clathrin-mediated endocytosis involves the internalization of macromolecules by the inward budding of plasma membrane vesicles (with or without receptor- or ligand-specific binding) and many studies have reported the cell uptake of CNT by this mechanism (Ye et al., 2013). Caveolea-mediated endocytosis involves caveolar vesicles that are composed of cholesterol and sphingolipids. A CNT radius of 25 nm was estimated to be associated with a maximal rate of endocytosis (Jin et al., 2009), while a maximum length of 189 nm

of DNA-wrapped SWCNT was effectively endocytosed by various cell lines (Becker et al., 2007).

The mechanisms of cell uptake also depend on the cell type encountered by the CNT (which also depends on the route of exposure). Macrophages in the pulmonary or interstitial regions of the lungs are capable of phagocytosing CNT, although the size and surface properties of CNT influence their ability to be recognized and phagocytosed by these cells. In the liver, Kupffer cells are the primary cellular site where CNT are observed. Functionalizations/modifications to the surface of CNT (e.g. covalently bonded functional groups or non-covalently bonded coatings) can also influence the cell uptake of CNT (Ali-Boucetta & Kostarelos, 2013).

In rats exposed by pharyngeal aspiration, the alveolar macrophage uptake of SWCNT (< 0.23% iron) was low (Shvedova et al., 2005). Morphological analysis showed that only 10% of the alveolar burden of SWCNT was located within the alveolar macrophages (Shvedova et al., 2005), while 90% of the dispersed SWCNT structures were observed to cross alveolar epithelial cells and enter the interstitium (Mercer et al., 2008). MWCNT were recognized more proficiently by alveolar macrophages; approximately 70% of MWCNT in the respiratory airways was taken up by alveolar macrophages, 8% migrated into the alveolar septa, and 22% was observed in granulomatous lesions (Mercer et al., 2010, 2011).

In an additional investigation of rats in a subchronic inhalation study (Ma-Hock et al., 2009), Treumann et al. (2013) examined ultrathin lung tissue sections from two rats by TEM at the end of the 13-week exposure to 2.5 mg/m³ of MWCNT. MWCNT structures were observed in the alveolar macrophages within the cytoplasm and membrane-bound organelles (phagosomes) in the form of "large (> 2 µm) electron-dense clews of intermingled MWCNT" and irregularly shaped structures up to 100 nm in diameter; some MWCNT were observed free in the alveolar lumen. MWCNT were also observed in

Table 4.1 Kinetics of carbon nanotubes in experimental animals

Particle type	Particle dimensions and surface area	Species, strain (age; sex)	Route of exposure; dose/exposure concentration	Duration of study	Results	Comments	Reference
SWCNT (HiPCO purified); < 2 wt% of contaminants	SWCNT: max. area-equivalent diameter, 15.2 μm; dispersed SWCNT: mean diameter, 0.69 μm; max. area-equivalent diameter, 3.7 μm	Mouse, C57BL/6 (24 wk; M)	Pharyngeal aspiration; 10 μg/mouse (SWCNT or dispersed SWCNT)	1 h, 1–7 days, and 1 mo after exposure	Dispersed SWCNT were rapidly (1 day after exposure) incorporated into the alveolar interstitium (and produced increased collagen deposition); less dispersed SWCNT were concentrated near the proximal alveolar region (the main area of granulomatous lesion formation)	SWCNT labelled with gold particles	Mercer et al. (2008)
SWCNT, raw (10% iron) or super purified	Diameter, 0.8–1.2 nm; length, 0.1–1 μm	Rat, Sprague-Dawley (6–8 wk; M)	Intratracheal or intravenous administration; 0.5 mg/animal (~2 μg/g bw)	2 wk after exposure	In intratracheal group, no CNT detected in liver, spleen, or kidneys; in intravenous group, decreased CNR at 6 and 24 h; similar to controls by 2 wk after exposure	CNR of MRI used to detect CNT	Al Faraj et al. (2009)
SWCNT, raw (10% iron)	Diameter, 0.8–1.2 nm; length, 0.1–1 μm	Rat, Sprague-Dawley (6–8 wk; M)	Intratracheal administration; 0, 0.1, 0.5, or 1 mg/animal	1, 7, 30, or 90 days after exposure	Significant CNR detected in lungs after exposure to 0.5 and 1 mg	MRI and TEM used to detect CNT biodistribution (adverse lung effects)	Al Faraj et al. (2010)
SWCNT, three types: pristine (raw and purified) and functionalized (F-)	Pristine (raw and purified) CNT: diameter, 0.8–1.2 nm; length, 0.1–1 μm; F-CNT: diameter, 1–2 nm; length, 0.5–2 μm	Rat, Sprague-Dawley (6–8 wk; M)	Intravenous administration; 0.5 mg/animal	5 h, 1, 2, 7, or 14 days after exposure	Raw SWCNT detected in spleen (up to 7 days), liver (up to 2 days), and kidney (up to 5 h)	MRI, Raman spectroscopy and iron assays used to assess biodistribution; no significant detection of purified or F-CNT due to low iron	Al Faraj et al. (2011)

Table 4.1 Kinetics of carbon nanotubes in experimental animals (continued)

Particle type	Particle dimensions and surface area	Species, strain (age; sex)	Route of exposure; dose/exposure concentration	Duration of study	Results	Comments	Reference
MWCNT	MMAD, ~3 µm; GSD, ~2	Rat, Wistar (2 mo; M)	Inhalation (nose-only); 0.1, 0.4, 1.5, and 6 mg/m³	13 wk (6 h/day, 5 days/wk) inhalation (nose-only); 1 day and 17, 26, and 39 wk after exposure	MWCNT lung burden (as ng cobalt) decreased slowly during the period after exposure, while the LN burden increased after 1.5 and 6 mg/m³; retention $t_{1/2}$ estimates: 151, 350, 318, and 375 days after exposure to 0.1, 0.4, 1.5, and 6 mg/m³, respectively	Cobalt tracer used to measure MWCNT lung and LN burdens	Pauluhn (2010b)
MWCNT-7 (Mitsui)	Median length, 3.86 µm; count mean diameter, 49 ± 13.4 (SD) nm	Mouse, C57BL/6J (7 wk; M)	Pharyngeal aspiration; 10, 20, 40, or 80 µg of MWCNT or vehicle control	1, 7, 28, and 56 days after exposure	MWCNT distribution at d 1 after exposure: 18% in airways; 81% in alveolar region; 0.6% in the subpleura; the density of MWCNT penetrations of subpleural tissue increased 28 and 56 days after exposure		Mercer et al. (2010)
MWCNT-7 (Mitsui)	Median length, 3.86 µm; count mean diameter, 49 ± 13.4 (SD) nm; SA (BET): 26 m²/g	Mouse, C57BL/6J (7 wk; M)	Pharyngeal aspiration; 10, 20, 40, or 80 µg of MWCNT or vehicle control	1, 7, 28, and 56 days after exposure	MWCNT distribution at 56 days after exposure: 68.7% in alveolar macrophages; 7.5% in alveolar tissue; 22% in granulomatous lesions; 1.6% in subpleural tissues; no MWCNT found in the airways at 7, 28, or 56 days after exposure		Mercer et al. (2011)
MWCNT-7 (Mitsui)	NR	Rat, F344 (13 wk; M)	Intratracheal administration; 40 or 160 µg/animal	1, 7, 28, or 91 days after exposure	Translocation to LN (right and left mediastinal and parathymus), which increased with dose and time after exposure; small aggregates of MWCNT-laden nodal macrophages on day 91	CNT observed in LN by TEM	Aiso et al. (2011)

Table 4.1 (continued)

Particle type	Particle dimensions and surface area	Species, strain (age; sex)	Route of exposure; dose/exposure concentration	Duration of study	Results	Comments	Reference
MWCNT, well dispersed	GMD (GSD): 63 nm (1.5); GML (GSD): 1.1 μm (2.7); SA: 69 m²/g	Rat, Wistar (age NR; M)	Inhalation (whole-body); 0.37 mg/m³ (~70% single fibres)	6 h/day, 5 days/ wk for 4 wk; 3 days, 1 mo, and 3 mo after exposure	Dose of MWCNT in lungs 3 days after exposure: 68 ± 10 μg/lung (by X-ray diffraction) or 76 ± 9 μg/lung (by elemental chemical analysis); estimated deposition fractions: 18% or 2%, by respective methods; calculated $t_{1/2}$: 51 or 54 days, respectively (assuming first-order clearance, i.e. the amount cleared is proportional to the amount deposited)	MWCNT in aqueous solution of 0.5 mg/mL Triton X-100 atomized into exposure chambers by a nebulizer; no reduction in the clearance rate (due to overloading of clearance mechanisms) observed at the exposure concentration and duration used in this study; 10 rats per group	Oyabu et al. (2011)
MWCNT-7 (Mitsui)	MMAD, 1.5 μm; GSD, 1.67; mean fibre length, 4.3 μm	Mouse, C57BL/6 (7 wk; M)	Inhalation (whole-body); 5 mg/m³	3 wk (5 h/ day for 12 days); 1, 14, 28, 84, 168, or 336 days after exposure	MWCNT lung burden measured 1 day after exposure: 28.1 μg; at day 336, 65% remained in the lungs; the number of MWCNT structures with multiple fibres decreased from day 1 to day 168, while the single fibre number remained the same		Mercer et al. (2013b)

Table 4.1 Kinetics of carbon nanotubes in experimental animals (continued)

Particle type	Particle dimensions and surface area	Species, strain (age; sex)	Route of exposure; dose/exposure concentration	Duration of study	Results	Comments	Reference
MWCNT-7 (Mitsui)	MMAD, 1.5 μm; GSD, 1.67; mean fibre length, 4.3 μm	Mouse, C57BL/6 (7 wk; M)	Inhalation (whole-body); 5 mg/m³	3 wk (5 h/ day, 4 times per week); 1, 14, 28, 84, 168, or 336 days after exposure	MWCNT observed in liver, kidney, heart, brain, diaphragm, and chest wall as single fibres only; lung burden included 54% agglomerated MWCNT; single fibre lengths were similar in lung and liver/ kidney (7.5 and 8.2 μm, respectively); most of the extrapulmonary MWCNT were in the tracheobronchial LN (1.08% on day 1 and 7.34% after 336 days of exposure)		Mercer et al. (2013a)
MWCNT, carboxyl or hydroxyl functional groups, hydrophilic	Diameter, 30 nm; length, 1–5 μm (80 nm agglom.); SA, NR	Mouse, JcL: ICR (8–12 wk; M)	Intravenous administration (tail vein); 0.25 mg/animal	28 days after exposure	Distinct colour change seen in lungs and liver 1 wk after injection; large number of CNT observed by TEM in lungs, small number in spleen and kidneys; amount of CNT decreased but remained in lungs and liver 4 wk after injection	Qualitative observations of organ dose only	Abe et al. (2012)
MWCNT, ¹⁴C-radiolabelled	Length, 3.9 μm (range, 0.5–12 μm); mean diameter, ~40 nm (range, 10–150 nm); 42 m²/g SA	Mouse, Balb/c (6 wk; F)	Pharyngeal aspiration; 20 μg/animal [10 μg in lungs on day 1 after exposure]	1 day, 7 days, 1, 3, 6, 9, and 12 mo after exposure	CNT decreased in the lungs to approximately 10% of administered dose at 3 mo and longer after exposure; CNT detected in liver and spleen on day 1 after exposure, and increased over time after exposure	Lung dose at day 1 after exposure was only 10 μg (suggesting the remainder was swallowed); CNT increased in the lungs at 9 and 12 mo after exposure	Czarny et al. (2014)

Table 4.1 (continued)

Particle type	Particle dimensions and surface area	Species, strain (age; sex)	Route of exposure; dose/exposure concentration	Duration of study	Results	Comments	Reference
MWCNT-7 (Mitsui)	Diameter, 90.7 nm; length, 5.7 μm; MMAD (GSD), 1.4–1.6 μm (2.3–3.0); SA, 24–28 m²/g	Rat, F344/ DuCrlCrlj (4 wk; M and F)	Inhalation (whole-body); 0, 0.2, 1, and 5 mg/m³	6 h/day, 5 days/wk, 13 wk	Exposure-related increase in MWCNT lung dose at the end of the 13-wk exposure; mean lung dose of MWCNT at end of 13-wk exposure to 0.2, 1, and 5 mg/m³, respectively: 3.23, 21.2, and 120.3 μg/left lung (M); 2.30, 13.7, and 80.3 μg/left lung (F)	MWCNT quantified by a technique that uses a specific polycyclic aromatic hydrocarbon (benzo[g,h,i]perylene) as a marker of MWCNT	Kasai et al. (2015)
MWCNT: original (O-), purified (P-), and carboxylic acid functionalized (F-), (Cheap Tubes, Inc., Brattleboro, VT, USA)	Outer diameter, 20–30 nm; length: 10–30 μm; SA: 182, 168, and 224 m²/g (O-, P-, and F- forms, respectively)	Rat, Sprague-Dawley (9–10 wk; M)	Inhalation (nose-only), ~30 mg/m³; or intratracheal instillation, 0, 10, 50, or 200 μg (in dispersion medium)	1 day or 21 days after exposure	Uptake of MWCNT in alveolar macrophages greater for F-MWCNT than for O- or P-MWCNT; phagocytosed O- and P-MWCNT observed within phagolysosomes initially while F-MWCNT found in the cytosol or penetrating the cell membrane	Six rats/group	Silva et al. (2014)

agglom., agglomerated; BET, Brunauer-Emmett-Teller method; bw, body weight; CNR, contrast-to-noise ratio; CNT, carbon nanotubes; F, female; F-CNT, functionalized CNT; GMD, geometric mean diameter; GML, geometric mean length; GSD, geometric standard deviation; HiPCO, high-pressure carbon monoxide production process; LN, lymph nodes; M, male; MMAD, mass median aerodynamic diameter; mo, month; MRI, magnetic resonance imaging; MWCNT, multiwalled carbon nanotubes; NR, not reported; SA, surface area; $t_{1/2}$, retention half-life; SWCNT, single-walled carbon nanotubes; TEM, transmission electron microscopy; wk, week; wt, weight

focal accumulations of phagocytic cells within the subpleural connective tissue.

In the study by Silva et al. (2014), the physico-chemical properties of MWCNT influenced their uptake, location, and structure within the alveolar macrophages (as observed by TEM and bright-field microscopy). Rats that inhaled F-MWCNT had significantly more alveolar macrophages containing MWCNT structures than rats that inhaled O-MWCNT or P-MWCNT (as observed in the bronchoalveolar lavage fluid [BALF]) on days 1 and 21 after exposure (P-MWCNT were obtained after the treatment of O-MWCNT with nitric acid and ethyldiamine tetra-acetate in acetic acid at pH 4 to remove residual metals and amorphous carbon). On day 1 after exposure, O-MWCNT and P-MWCNT were observed within the phagolysosomes of macrophages, while F-MWCNT were seen in the cytosol and also protruding the cell membrane. On day 21 after exposure, O- and P-MWCNT were no longer compartmentalized but were observed in the cytosol as larger focal agglomerates; the F-MWCNT (obtained by adding the P-MWCNT to a reaction chamber containing nitric acid and sulfuric acid) in the cytosol were smaller, dispersed aggregates. The acidic functional groups brought about by increasing the pH and the resulting increase in hydrophilicity were thought to reduce the toxicity of F-MWCNT by preventing phagolysosome permeability – and the subsequent release of lysosomal contents into the cytosol with the downstream activation of the nucleotide-binding oligomerization domain receptor (NLRP3) inflammasome – after F-MWCNT were taken up by the alveolar macrophages. Thus the uptake of F-MWCNT into macrophages did not appear to cause cell toxicity at the doses and observation time-points in this study (Silva et al., 2014).

(c)   Translocation

Several studies have provided evidence that CNT can translocate from the lungs into the blood circulation. Adult CD-1 mice [sex unspecified] were exposed to untreated SWCNT (synthesized with an iron-cobalt/magnesium oxide catalyst) by nebulization. Acute exposures to a water aerosol containing CNT [concentration and dose unspecified] lasted 15 minutes. CNT structures were observed by Raman spectroscopy in blood samples taken from mice 24 hours after the inhalation of CNT. The quantity was not specified, but exceeded the detection limit of Raman spectroscopy. These CNT were observed as clusters with average diameters of several micrometres (Ingle et al., 2013). [The Working Group noted that smaller CNT clusters, if present, would have been below the detection threshold due to the qualitative nature of the Raman spectroscopy methods, which detect CNT in tissues but cannot provide quantitative dose measures.]

Evidence that CNT could translocate from the lungs of adult male Wistar albino rats (weighing 0.2–0.225 kg) after intratracheal administration of two types of MWCNT at a dose of 0.2, 1, or 5 mg/kg bw was reported by Reddy et al. (2010a). CNT were produced by electric arc (size, 90–150 nm; surface area, 197 mg^2/g; crystallinity, hexagonal) or CVD (size, 60–80 nm; surface area, 252 mg^2/g; crystallinity, cubic) and were dispersed in PBS plus Tween 80 solution then sonicated to prevent agglomeration before administration. Dose-dependent toxicity was observed in the liver and kidney of rats exposed to either type of MWCNT. Light micrographs of the liver tissue 1 day after instillation showed black pigments, but no quantitative data on CNT tissue doses were provided.

Inhaled MWCNT were observed in the subpleural wall and within the subpleural macrophages in groups of 10 male C57BL6 mice after a single 6-hour inhalation exposure

to 1 or 30 mg/m³ of MWCNT (Helix, Inc.; MMAD, 164 or 183 nm, respectively; length, < 100 nm to > 10 μm; diameter, 10–50 nm) (Ryman-Rasmussen et al., 2009a). Carbon black (MMAD, 209 nm) at a concentration of 30 mg/m³ was used as a comparison material. Lung tissues were collected 1 day, 2 weeks, 6 weeks, or 14 weeks after exposure. The calculated deposited doses of CNT were 0.2 or 4 mg/kg at concentrations of 1 or 30 mg/m³ MWCNT, respectively (assuming a 10% deposition of the inhaled dose). The inhaled MWCNT were engulfed by macrophages, which migrated to the subpleural region. TEM images showed CNT within macrophages beneath the pleura. The authors hypothesized that activated macrophages containing MWCNT migrate through the pleural lymphatic drainage and stimulate the recruitment of mononuclear cells in the pleura (consistent with their previous finding (Ryman-Rasmussen et al., 2009b) that monocyte chemokine CCL2 was increased in mice after inhalation of MWCNT). Significant fibrosis (focal subpleural) was observed in mice 2 and 6 weeks after inhalation exposure to 30 mg/m³ of MWCNT, but not in mice exposed to 1 mg/m³ of MWCNT or 30 mg/m³ of carbon black. Aggregates of MWCNT in lung tissues were significantly elevated in mice inhaling 30 mg/m³ of MWCNT (but not carbon black or 1 mg/m³ of MWCNT). No quantitative data on the dose of MWCNT in the lung tissues were reported (Ryman-Rasmussen et al., 2009a).

Translocation to the pleura was observed in a study of male Fischer 344 rats exposed five times to MWCNT (0.5 mL of 500 μg/mL) by intrapulmonary spraying over a 9-day period (Xu et al., 2012). The total mass dose was 1.25 mg/rat. Two types of MWCNT were studied – MWCNT-N (Nikkiso Co., Ltd) and MWCNT-M (Mitsui-7; Mitsui Chemicals, Inc.) – in addition to crocidolite as a control. Pleural cavity lavage was used to examine the presence of MWCNT or crocidolite in the pleural cavity, and SEM was used to confirm the location of the MWCNT or crocidolite fibres in lung tissue sections. Both types of MWCNT and crocidolite fibres were found in the pleural cavity lavage cell pellets, mostly in macrophages. A few fibres were found in the intercellular space or on cell surfaces. In the tissue sections, both MWCNT and crocidolite were observed in the focal granulomatous lesions in alveoli and in alveolar macrophages. The MWCNT or crocidolite fibres were also found in the mediastinal lymph nodes, and a few were observed in liver sinusoid cells, blood vessel wall cells in the brain, renal tubular cells, and spleen sinus and macrophages. A few fibres were observed penetrating directly from the lungs to the pleural cavity through the visceral pleura, but no fibres were seen in the parietal pleura.

Mercer et al. (2013a) investigated the extrapulmonary transport of MWCNT in male C57BL/6 mice after inhalation exposure to 5 mg/m³ of MWCNT (Mitsui-7) for 5 hours per day for 12 days in a 3-week study [the same study as that reported in Mercer et al. (2013b) for disposition in the lungs]. The lung burden of MWCNT on day 1 after exposure was 28.1 μg (47 × 10⁶ MWCNT fibres/μg). Optical sectioning through serial sections of the lung, liver, and kidney was carried out to measure the length of the single MWCNT in those organs on days 1 and 336 after the end of inhalation exposure (Mercer et al., 2013b). The amount of MWCNT in the tracheobronchial lymph nodes was determined as the volume density of MWCNT in the lymph nodes relative to the volume density of MWCNT in the lungs 1 day after exposure. The numbers of MWCNT fibres in the extrapulmonary organs, diaphragm, and chest wall were counted per unit area and converted to number per organ using morphometric methods. Enhanced-darkfield light microscopy imaging of CNT was performed on sections of the exposed lungs to identify CNT that would not otherwise be detected. Most of the MWCNT that translocated from the lungs were found in the tracheobronchial lymph nodes

(1.08% on day 1 and 7.34% on day 336 after exposure, as a percentage of the lung burden on day 1 after exposure). The next highest extrapulmonary tissue burdens of MWCNT were reported in the liver (0.0028% on day 1 and 0.027% on day 336) and kidneys (0.0010% on day 1 and 0.0052% on day 336). Smaller amounts of MWCNT were detected in the heart, brain, chest wall, and diaphragm (with higher amounts at day 336 than at day 1 after exposure in all tissues except the chest wall). In the lungs, 54% of the MWCNT burden was agglomerated, while only singlet MWCNT were observed in the liver, kidney, heart, brain, chest wall, and diaphragm (Mercer et al., 2013a).

In an ex-vivo model, SWCNT (100 µg) were instilled into the airway of isolated perfused rat lung. The isolated perfused rat lung model retains the lung architecture but eliminates the systemic pharmacokinetics. The pulmonary translocation of SWCNT from the airways across the pulmonary barrier was less than 0.05% of the instilled dose after 90 minutes. A pharmacokinetic simulation estimated a cumulative pulmonary translocation from the rat lung of less than 0.15% over 14 days (Matthews et al., 2013).

The length of CNT that translocate from the lungs to the pleura (or were instilled therein in an experimental study) may influence their retention. Longer structures (> 5 µm) were retained in the pleura, while shorter structures were able to drain to the lymph nodes (Poland et al., 2008; Murphy et al., 2011); however, Kim et al. (2014) found a persistent presence in the pleura and lung parenchyma 90 days after subacute (28 days) inhalation exposure to short-length (330.18 ± 1.72 nm) MWCNT. Stomata are outlets in the parietal pleura through which lymphatic drainage occurs (Donaldson et al., 2010; Murphy et al., 2011). The maximum diameter of stomata in mice is 10 µm (Murphy et al., 2011). Using single-photon emission computed tomographic imaging, Murphy et al. (2011) reported that radiolabelled short CNT (length, 0.5–2 µm)

were observed in the cranial mediastinal lymph nodes (two bilateral lymph nodes located lateral to the thymus) within 1 hour of intrapleural injection of 5 µg/mouse, and increased up to the end of observation 24 hours after the injection. Qualitatively, fewer long (length, > 15 µm) than short CNT were observed in the lymph nodes (Murphy et al., 2011).

The translocation of ^{14}C-radiolabelled MWCNT from the lungs to other organs up to 1 year after pharyngeal aspiration of 20 µg CNT (suspended in 50 µL dispersion medium) was investigated in seven groups of 4 female Balb/c mice (age, 6 weeks). After dispersion, the mean length of the CNT was 3.9 µm (range, 500 nm–12 µm) and the mean diameter was approximately 40 nm (range, 10–150 nm). Time-points of examination were 1 and 7 days, and 1, 3, 6, 9, and 12 months after exposure. At 6 months after exposure, the average concentration of MWCNT in the lungs decreased to less than 10% of the administered dose, but increased at the last two time-points (to about 20% at 12 months after exposure). In contrast, the MWCNT concentration in the spleen and liver – which was detectable on day 1 after exposure – increased over time to approximately 0.1–0.2% of the administered dose in the spleen at 6–12 months after exposure and approximately 0.5–1% in the liver at the same time-points, although the liver had about half the mass concentration of MWCNT (µg/g) compared with the spleen (Czarny et al., 2014). [The Working Group noted that the authors reported that only half of the 20-µg dose administered was measured in the lungs on day 1 after exposure, and the initial lung dose was therefore adjusted to 10 µg; the remainder of the lung dose was considered to have probably been swallowed, thus reaching the stomach and gastrointestinal tract.]

A subsequent experiment on oral ingestion through the intra-oesophageal instillation of 50 µg of ^{14}C-MWCNT showed that approximately

95% of the ingested MWCNT dose was measured in the gastrointestinal tract and faeces after 24 hours; no MWCNT were detected (by radioactive signal) after 4 days; and no MWCNT were detected in the spleen or liver tissue sections on 1, 7, and 30 days after gavage with MWCNT. This finding was considered by the authors to support the evidence that translocation of the MWCNT after pharyngeal aspiration occurred through the air–blood barrier (including crossing the epithelial cells of the airways or the alveoli) and not across the intestinal lining (Czarny et al., 2014).

(d)   Retention

Retention refers to the temporal distribution of uncleared particles in the respiratory tract (Lioy et al., 1984). This section focuses on retention in the lungs and lung-associated tissues (i.e. lung parenchyma, pleura, and lung-associated lymph nodes) (see also Section 4.1.2 (c) for data on doses of CNT in extrapulmonary organs). Retention (or biopersistence) in the lungs is higher for inhaled particles that are poorly soluble and poorly cleared from the lungs (e.g. due to size, shape, surface reactivity, and/or to a high dose that exceeds clearance capacity).

The lung burden of MWCNT (Baytubes, a proprietary product; Bayer MaterialScience, Germany) was measured in male Wistar rats 1 day, and 17, 26, and 39 weeks after 13 weeks of inhalation exposure to 0.1, 0.4, 1.5, and 6 mg/m³ for 6 hours per day on 5 days per week. Tissue burdens of MWCNT (in the left lung lobe and in the lung-associated lymph nodes) were estimated from the measurements of residual cobalt tracer (0.115% matrix-bound). The dose deposited in the alveoli was calculated from the following information: concentration of cobalt (ng/L [air]) × minute ventilation rate (0.8 L/min/kg) [male rat control body weights: 231 and 369 g, at the beginning and end, respectively, of the 13-week exposure] × the alveolar deposition fraction (5.7%) × the cobalt fraction (%/100) (see also Section 4.1.2 (a) for more information on the estimated deposition

fraction). The retained MWCNT dose (measured as µg cobalt tracer/lung) in the lungs decreased slowly during the 39-week period after exposure, while the MWCNT in the lung-associated lymph nodes increased after exposure in mice exposed to 1.5 or 6 mg/m³ (Pauluhn, 2010a).

The retention half-times at each concentration were calculated in Pauluhn (2010a) from the equation: dc/dt = a(1–kt) where k is the first-order elimination constant (calculated from the cobalt lung burden data 17, 26, and 39 weeks after exposure [although not reported]). The retention half-time (i.e. time to reduce the retained lung dose by half; also called the elimination half-time [$t_{1/2}$]) was calculated from $t_{1/2}$ = ln(2)/k. The retention $t_{1/2}$ was 151, 350, 318, and 375 days at exposure concentrations of 0.1, 0.4, 1.5, and 6 mg/m³, respectively. [From the retention half-times [$t_{1/2}$], the first-order rate constant k can be estimated as approximately 0.002 d⁻¹ for the three higher concentrations and approximately 0.004 d⁻¹ for the lowest concentration.] Pauluhn (2010a) noted that the levels of cobalt measured in the lungs at the lowest concentration (0.1 mg/m³) were in the range of the limit of quantification, indicating possible imprecision in the $t_{1/2}$ estimate at that concentration. In comparison, the retention $t_{1/2}$ for respirable particles in rats at non-overloading doses was approximately 60 days, indicating that the rat lung clearance rates of MWCNT (Baytubes) were reduced by several fold at all exposure concentrations.

Pauluhn (2010a) estimated the MWCNT particle volume lung dose as 107–325, 466–1413, 1192–3917, and 3961–12 002 nL/g of lung in rats exposed to 0.1, 0.4, 1.5, and 6 mg/m³, respectively (at a density of MWCNT of 0.1–0.3 g/cm³, "corrected for void space volume which is 1.43 times greater than the volume of the MWCNT themselves" (Brown et al., 2005)). In comparison, Pauluhn (2010a) quoted Morrow (1988, 1994), who found no significant difference in retention half-times between the control (unexposed) rats and the rats that had a particle volume lung dose

of 100 nL/g of rat lung, and Oberdörster (1995), who observed a doubling of the retention half-times in rats with a particle volume lung dose of 1400 nL/g of lung. Pauluhn (2010a) interpreted these comparisons as indicating that overloading of lung clearance was "minimal to moderate" in rats at 0.1 and 0.4 mg/m³ of MWCNT while, at 1.5 and 6 mg/m³, clearance may have been completely impaired.

Mercer et al. (2010) reported the distribution of MWCNT-7 (Mitsui & Co.) (diameter, 49 nm; length, 3.9 μm) in the lungs of male C57BL/6J mice exposed by pharyngeal aspiration to 10, 20, 40, and 80 μg of MWCNT or the vehicle. The distribution of MWCNT was determined in fixed lung sections using morphometric methods at 1, 7, 28, and 56 days after exposure. Field-emission SEM was used to detect and count the number of MWCNT fibre penetrations of three biological tissue barriers: the alveolar epithelium (alveolar penetrations), the alveolar epithelium immediately adjacent to the pleura (subpleural tissue), and the visceral pleural surface (intrapleural space). The number of penetrations per lung (into the subpleural tissue and intrapleural space) increased with increasing dose administered. On day 1 after exposure to 80 μg, 18% of the MWCNT was observed in the airways, 81% in the alveolar region, and 0.6% in the subpleural tissue. Within the alveolar region, 62% of the dose was inside alveolar macrophages on day 1 after exposure. MWCNT penetrations were observed most frequently in the alveolar macrophages, followed by alveolar type I epithelial cells, and less frequently in alveolar interstitial cells (typically observed as fibres passing through adjacent epithelial cells). MWCNT inside the cells were not confined to phagolysosomes and were observed to extend from the cell surface through the nuclei and other organelles. Alveolar type II epithelial cells (2% of the normal epithelial surface) were rarely found to be penetrated by MWCNT. In the airways, MWCNT were observed in the mucous layer above airway epithelial cells and in airway macrophages contained in the cilia-mucous lining layer; penetrations by MWCNT in the airways were rare. At the 20-μg dose, a total of 15×10^6 MWCNT penetrations were observed in the 11×10^6 alveolar type I epithelial cells in mouse lungs (Mercer et al., 2010).

The time course of this MWCNT in the intrapleural space showed a decrease from day 1 to day 7 after exposure (Mercer et al., 2010). This is consistent with a mechanism of shorter fibre clearance from the intrapleural space through the stomata (duct in the parietal pleura) to the lymphatic system (Donaldson et al., 2010; Murphy et al., 2011). However, the amount of MWCNT in the intrapleural space increased again at day 28 after exposure and remained elevated at 56 days after exposure. The lung burden of MWCNT may act as a reservoir to replenish MWCNT in the intrapleural space or that even shorter fibres (length, 3.9 μm) could begin to clog the ducts if they reach a sufficient level within the intrapleural space (Mercer et al., 2010).

Mercer et al. (2013b) provided quantitative data on the retention and distribution of MWCNT in the lung and associated tissues of male C57BL/6 mice after a 3-week exposure by inhalation for 5 hours per day for 12 days to 5 mg/m³ of MWCNT (Mitsui-7; mean length, 4.3 μm). The MWCNT lung burden was determined using a method reported by Elder et al. (2005). The lungs were removed after mice were killed on 1, 14, 28, 84, 168, or 336 days after exposure. Lung tissue was processed by digestion (in 25% potassium hydroxide/methanol (w/v)), centrifugation, and re-suspension of the pellet, and measurements of the optical density of the solution were compared with MWCNT standards that were processed in parallel with the lung samples. The mass of MWCNT in the lungs was determined from a standard curve. [Elder et al. (2005) reported that the limit of detection of this assay was 0.1 μg/mL of suspended solution.] Several imaging techniques (light microscopy, field emission SEM, and enhanced-darkfield

microscopy) were used to observe and quantify the distribution of the MWCNT fibres in tissue sections of the lungs. MWCNT were counted in lung tissue sections using an enhanced-darkfield optical system; eight animals were analysed per group and counting was accomplished using an 11 × 11 (121 point) overlay grid pattern to ensure uniform sampling of the section. The number of fibres per MWCNT structure was also determined by enhanced-darkfield microscopy. MWCNT fibres were observed in the alveolar macrophages and alveolar interstitium, and penetrated the visceral pleura (Mercer et al., 2013b). On day 14 and later time-points after exposure, clusters of MWCNT were observed within the ridge of the first alveolar duct bifurcation [which is the primary site of particle deposition after inhalation exposures to particles and fibres, as reported previously by Brody & Roe (1983) and Chang et al. (1988)]. The MWCNT lung burden in mice measured on day 1 after exposure was 28.1 µg (1321 × 10⁹; total fibre number estimate based on 47 million MWCNT fibres/µg [conversion reported in Chen et al. (2012)]) (Mercer et al., 2013b). Of this lung burden, 84% (23.6 µg) was found in the alveolar (pulmonary) region of the lungs and 16% (4.5 µg) in the airways. Similar distributions of MWCNT were observed in two previous studies of MWCNT by Porter et al. (2010, 2013) in mice exposed by pharyngeal aspiration or acute inhalation.

Within the alveolar region, 56% of the MWCNT lung burden was in alveolar macrophages on day 1 after exposure, 7% was in the alveolar airways, and 20% was in the alveolar tissue. These findings indicated a fairly rapid and substantial distribution of inhaled MWCNT to the lung interstitium. By day 1 after exposure, ~1.2% (0.34 µg) of the MWCNT lung burden was observed as single fibres in the pleural compartment (including the subpleural tissue and visceral pleura) (Mercer et al., 2013b).

At 336 days after exposure, 65% of the MWCNT lung burden (28.1 µg) on day 1 after exposure was retained in the lungs (18.2 µg), most of which (96%) was retained in the alveolar region (including 4.8% in subpleural tissue) and 4% (0.73 µg) of which was retained in the airways. The distribution of MWCNT in the lungs shifted from alveolar macrophages (3 times more than in lung tissue on day 1 after exposure) to the alveolar tissue, where the dose increased from 5.8 to 9.5 µg on days 1 and 168 after exposure, respectively. Thus, the alveolar interstitial lung burden increased as the MWCNT in the alveoli were cleared (Mercer et al., 2013b).

The number of larger or agglomerated MWCNT structures (> 4 fibres/MWCNT) decreased over time (from 53 to 25% of the lung burden on days 1 and 168 after exposure, respectively). The number of structures with 2, 3, or 4 fibres also decreased significantly. However, the percentage of single fibres in the MWCNT lung burden did not change significantly from days 1 to 168 after exposure. Thus, the MWCNT structures decreased in size, resulting in a relatively constant number of single MWCNT fibres in the lungs over time (Mercer et al., 2013b).

The mouse lung response on day 1 of this study after exposure to a lung dose of 28.1 µg MWCNT was an increase in the thickness (fibrillar collagen) of the alveolar connective tissue over time, with a 70% increase on day 336 after exposure (Mercer et al., 2013b). The translocation of MWCNT to extrapulmonary organs were described in Mercer et al. (2013a) (see also Section 4.1.2 (c)).

The lung burden of MWCNT (diameter, 90.7 nm; length, 5.7 µm; MMAD (GSD), 1.4–1.6 µm (2.3–3.0)) was measured in male and female Fischer 344 rats after 13 weeks of whole-body inhalation exposure for 6 hours per day on 5 days per week to concentrations of 0, 0.2, 1, and 5 mg/m³. Left lung tissues (0.18–0.36 g) were sampled from five rats in each MWCNT-exposed group. MWCNT was quantified using a technique in which a specific polycyclic aromatic hydrocarbon (benzo[*g,h,i*]perylene) serves as a

marker of these MWCNT. The mass of MWCNT in the lungs of male and female rats increased in relation to the exposure concentration (Table 4.1) and was reported to be 1.4–1.6 times greater in the left lungs of males than in those of females (Kasai et al., 2015). [The Working Group noted that, when the measured MWCNT lung doses are normalized to the average control left lung weight (0.43 g, males; 0.32 g, females), the retained lung doses in males were similar (1.0–1.2 times the lung doses in females).]

In the study by Silva et al. (2014), the physico-chemical properties (metal content, hydrophilicity, and carboxylic acid functionalization) or route of exposure did not significantly influence the retention of MWCNT in the lungs of male Sprague-Dawley rats (as measured in the right caudal lung lobe by programmed thermal analysis). However, the findings suggested that instilled F-MWCNT were retained in the lungs to a greater extent than the same instilled dose of O-MWCNT or P-MWCNT. The retention of instilled F-MWCNT in the lungs was also greater, although not significantly, than the retention of a similar deposited dose of inhaled F-MWCNT (Silva et al., 2014).

(e) Clearance

The mechanisms of clearance depend on the initial site of particle deposition within the respiratory tract and on the physico-chemical properties of the particle (e.g. solubility and functionalization). Soluble particles can dissolve in alveolar lining fluid and then enter the blood or lymph (Dahl et al., 1991; ICRP, 1994; Schlesinger, 1995). Dissolution rates do not vary widely across species, because they are primarily determined by the physico-chemical properties of the material (Dahl et al., 1991). Clearance rates of poorly soluble particles, however, can fluctuate among species due to differences in the macrophage-mediated clearance from the alveolar region and the rates of mucociliary transport in the conducting airways (Snipes, 1989).

Inhaled CNT may be phagocytosed by macrophages and cleared from the lungs by the mucociliary escalator and swallowed (entering the gut). CNT that are not cleared from the lungs by macrophages may enter the epithelial cells that line the alveolar region of the lungs, where their fibres can be retained in the lung interstitium or pass into the lymph or blood circulation (Mercer et al., 2008; Ryman-Rasmussen et al., 2009a; Mercer et al., 2013a, b).

CNT that reach the blood circulation (either by translocation from the lungs or through direct intravenous administration) may be excreted from the body through either the renal (urine) or biliary pathway. Many SWCNT or MWCNT exceed the particle size threshold for renal excretion, particularly if agglomerated (Liu et al., 2008a), and thus accumulate in the liver where they undergo biliary excretion (Cherukuri et al., 2006). The type of surface functionalization can also strongly influence the biodistribution and elimination pathways (see also Section 4.1.2 (g)).

In a study of male Wistar rats that inhaled 0.37 mg/m^3 of MWCNT for 6 hours per day on 5 days per week for 4 weeks, lung clearance was reported to be proportional to the amount in the lungs. The retention half-time ($t_{1/2}$), defined as the time for the retained dose to be reduced by half, was estimated to be 51 or 54 days (based on the lung dose measured by X-ray diffraction or EC analysis, respectively) (Oyabu et al., 2011). [These retention half-time estimates are consistent with normal rat clearance rates reported in other studies, indicating that no reduction in the clearance rate (due to overloading of clearance mechanisms) occurred at the concentration and duration of exposure used in this study.]

In a study of the intratracheal instillation of 10 or 100 µg/mouse of pristine [as-produced] (mean length, 7.5 nm; mean diameter, 13.5 nm) or acid-treated (mean length, 400 nm; mean diameter, 15 µm) MWCNT in male C57BL/6 mice, both types of MWCNT were seen in the lymphatic system in the mediastinal lymph nodes. The

acid-treated MWCNT (that contained fewer metal contaminants and were more hydrophilic) induced less severe acute lung inflammation than the pristine MWCNT (Kim et al., 2010). [No quantitative data on the dose were provided.]

No significant lung clearance was observed from day 1 to day 21 after intratracheal administration of O-, P-, or F-MWCNT to male Sprague-Dawley rats. MWCNT structures were observed inside the alveolar macrophages and polymorphonuclear leukocytes in BALF and in the airway cilia, suggesting some, but insignificant, MWCNT clearance (Silva et al. 2014).

(f) Biodegradation

The size, structure (wall number), and functionalization of CNT may influence their distribution in the body and their ability to pass into cells through cell membranes (Bianco et al., 2011). Much of the literature on the kinetics of CNT is motivated by the potential use of CNT as targeted medical delivery systems to specific tissues for therapeutic purposes (Ali-Boucetta & Kostarelos, 2013). SWCNT functionalized with polyethylene glycol (PEG) were more hydrophilic, had greater dispersibility in aqueous media than unfunctionalized SWCNT, and were excreted through biliary and renal pathways (Bhirde et al., 2010).

(i) In vitro and ex vivo

Pulmonary eosinophils from humans (in vitro) and mice (activated ex vivo) were shown to degrade SWCNT through an enzyme (eosinophil peroxidase, EPO) that is exocytosed when cells are activated (e.g. by the presence of CNT) and is one of the major oxidant-generating enzymes in the human lung. The EPO-catalysed oxidative biodegradation was assessed by TEM, ultraviolet-visible-near-infrared absorption spectroscopy, and Raman spectroscopy and was found to occur extracellularly (Andón et al., 2013).

Another study by Kagan et al. (2010) showed that polymorphonuclear leukocyte (neutrophil)

myeloperoxidase (MPO) also catalysed the biodegradation of SWCNT, although the SWCNT in this study were pre-opsonized with immunoglobulins to increase the internalization efficiency by neutrophils. The difference in the mechanisms of degradation of the two cell types is due to neutrophils using MPO to kill bacteria inside the phagolysosome, while eosinophils use secreted EPO to kill larger extracellular organisms, such as parasites.

(ii) In vivo

The role of neutrophils or eosinophils in the biodegradation of CNT in vivo is unclear. In the lungs, CNT that are not cleared by alveolar macrophages may translocate into the lung interstitium and stimulate the development of fibrosis or translocate to distant sites and elicit systemic inflammatory and/or immunological responses (Mercer et al., 2008; Ryman-Rasmussen et al., 2009a).

Shvedova et al. (2012a) demonstrated the role of MPO, an abundant enzyme in inflammatory cells such as polymorphonuclear leukocytes (or neutrophils), in the clearance and retention of CNT in the lungs of mice by comparing the clearance of SWCNT in wild-type and MPO-deficient (knockout) C57Bl/6 mice given 40 µg/mouse by pharyngeal aspiration. The MPO-mediated biodegradation of SWCNT occurs through the oxidative modification or "cutting" of the SWCNT (resulting in oxidative defects in CNT that are detectable by Raman spectroscopy). A significant difference was observed in the clearance of SWCNT from the lungs in wild-type compared with MPO-knockout mice. The degradation of SWCNT (assessed by Raman spectroscopy) was significantly greater in wild-type mice and the volume of SWCNT aggregates per total lung volume (quantified in lung tissues by light microscopic imaging analysis) was significantly greater in MPO-knockout mice than in wild-type mice 28 days after exposure. [The Working Group noted that, consistent with the higher dose

of SWCNT retained, the MPO-deficient mice showed a greater degree of fibrosis, as measured by higher collagen content, and a greater average thickness of the alveolar connective tissue in the lungs than wild-type mice; however, wild-type mice also showed significant fibrosis.]

(g) Biokinetics of bioengineered CNT administered by intravenous administration

Much of the literature on the biokinetics of CNT in the body involves studies on their potential use in biomedical applications. The route of exposure has been shown to influence the biodistribution of CNT in the body (Ali-Boucetta & Kostarelos, 2013), with the highest initial dose observed at the site of administration. In medical imaging or therapeutical applications, the route of exposure is typically the intravenous injection.

CNT injected intravenously accumulate in the liver and spleen, while CNT administered orally are found primarily in the stomach and intestines (Ali-Boucetta & Kostarelos, 2013).

Well dispersed short MWCNT (length < 500 nm) injected intravenously into mice were excreted rapidly through the kidneys (no nephrotoxicity observed), while longer MWCNT were retained in the spleen, lungs, and liver (resulting in hepatotoxicity) (Jain et al., 2011).

Surface modification was considered to be the most important factor influencing the biodistribution of CNT (Ali-Boucetta & Kostarelos, 2013). The two main types of functionalization are the coating (i.e. non-covalent surface modification) of SWCNT and the covalent functionalization of SWCNT or MWCNT.

The coatings that have been studied include surfactant Pluronic F108, Tween 80, and PEG phospholipid. The blood clearance of Pluronic F108-coated CNT injected intravenously into rabbits was rapid (half-life $t_{1/2}$ < 1 h), which was attributed to the formation of SWCNT–protein complexes or SWCNT aggregates that accumulated primarily in the liver (Cherukuri et al., 2006). Tween 80-coated SWCNT were retained (for up to 28 days) in the liver, lungs, and spleen in injected mice (the CNT had a ^{13}C-enriched backbone) (Yang et al., 2007). The circulation of PEGylated CNT in the blood was longer (half-life $t_{1/2}$, 5 h) and was further extended (half-life $t_{1/2}$, 12–22 hours) by increasing the branching of the PEG and liver uptake was reduced in injected mice (Liu et al., 2008a, 2011a; Prencipe et al., 2009). PEGylated CNT were eliminated through biliary excretion (over 2 months). Pristine, non-covalently functionalized SWNCT mostly accumulated in the liver.

The covalent functional groups that have been studied include hydroxyl, ammonium, glucosamine, and taurine (Ali-Boucetta & Kostarelos, 2013). Many of these studies used radiolabelled CNT. Higher degrees of functionalization facilitated the dispersion of individual CNT that led to predominantly urinary excretion (Singh et al., 2006; Lacerda et al., 2008a, b, c). However, MWCNT–taurine accumulated in the liver, heart, and lung (Deng et al., 2007).

Many of these studies reported qualitative estimates of the amount of CNT in various organs (e.g. by whole-body imaging). The techniques used showed the relative amount of CNT, although small amounts may have been missed due to limits of sensitivity. The most typically reported quantitative measure was the half-life $t_{1/2}$ in blood circulation. While these studies provide valuable insights into the factors that influence the biodistribution of CNT, they focused on medical applications of CNT and thus have limited direct relevance to occupational or environmental exposures.

4.2 Physico-chemical properties associated with toxicity

The physico-chemical properties of CNT may be modulated by varying the method of synthesis, by applying modification processes

after synthesis, and/or by the covalent functionalization of their external surface. A large variety of CNT forms may thus be produced that exhibit different features that influence their pathogenicity. CNT cannot be considered as a single well defined substance but as families of different materials, the number of which is growing dramatically.

Evidence has been found that the responses of cells to CNT are modulated by their physico-chemical properties. The variability of the CNT employed in different studies gives rise to the discrepancies observed in biological outcomes (Muller et al., 2005; Kagan et al., 2006; Elgrabli et al., 2008; Poland et al., 2008; Takagi et al., 2008; Ma-Hock et al., 2009; Sakamoto et al., 2009; Fubini et al., 2010, 2011).

Major studies on the effects of relevant physico-chemical characteristics on the adverse responses to CNT in various experimental models are summarized in Table 4.2.

4.2.1 Crystal structure and defects

Purification and functionalization can induce defects in CNT and may modify or increase their toxicity. Nitric acid, which is involved in purification and functionalization, destroys SWCNT, resulting in the production of amorphous carbon and a reduction in the amount of the transition metal catalyst used in their production (Hu et al., 2003).

Perfectly crystalline CNT are formed only by hexagonal rings of sp^2 hybridized carbons. However, the graphene layers contain a variable number and degree of defects that may arise directly from the process of synthesis or may be introduced or eliminated during treatments after synthesis (Galano et al., 2010). The CNT that are currently produced are far from perfect and may include various numbers and types of defect, such as non-hexagonal rings, atom vacancies (topological defects), carbon with sp^3 hybridization, incomplete bonding, and oxygenated

groups (Ebbesen & Takada, 1995; Charlier, 2002; Galano, 2010). After systematic variation of the physical and chemical features of a given MWCNT specimen with or without defects, genotoxicity in vitro and inflammogenicity and fibrogenicity in vivo (Muller et al., 2008a), but not carcinogenicity (Muller et al., 2009; see Section 3), were correlated with the presence of defects. [The Working Group noted that only a single type of defect (i.e. broken C–C bonding generated by grinding) was evaluated in these studies.]

Defects impart the potential to quench free radicals to both MWCNT and SWCNT (Galano, 2010). CNT retard the oxidation of polystyrene, polyethylene, polypropylene, and poly(vinylidene) fluoride due to their strong ability to accept radicals, which may interrupt chain propagation, leading to antioxidant effects in polymeric material (Watts et al., 2003). Pristine SWCNT were demonstrated to be powerful antioxidants (Lucente-Schultz et al., 2009) and a variety of modified CNT exhibited different defective sites.

4.2.2 Form and size

A fibre shape associated with high durability has been proposed as a critical factor in CNT-induced pleural toxicity and carcinogenicity (Donaldson et al., 2011 and references therein). Poland et al. (2008) reported an "asbestos-like" pathogenicity of long, rigid CNT in the induction of inflammation while tangled CNT were less potent. Similarly to short amphibole asbestos fibres, shorter CNT induced less inflammation. In addition to dimensions and shape, other physico-chemical features are involved in fibre toxicity, suggesting that the fibre paradigm is not the only mechanism (Jaurand et al., 2009; Sanchez et al., 2009; Fubini et al., 2011). The physico-chemical properties of asbestos fibres and CNT differ substantially, correlating with the marked differences in their chemical

Table 4.2 Physico-chemical properties of carbon nanotubes that are relevant to toxicity: summary of the most pertinent studies

Property	Type of CNT	End-points/models	Effects	References	Characteristics
Diameter	MWCNT	Cellular viability, phagocytosis, apoptosis/guinea-pig alveolar macrophages	Greater toxicity of thick CNT	Wang et al. (2009)	Length, 1–5 μm; diameter: 10–20 nm, 40–60 nm, and 60–100 nm; purity: different nickel content
	MWCNT	Cytotoxicity, uptake/human mesothelial cells; inflammation, cellular viability, carcinogenicity/rats	Greater toxicity of 50-nm CNT compared with thicker and thin/tangled	Nagai et al. (2011)	Length, ~5 μm; diameter: 15 nm (tangled), 50 nm, and 100–250 nm; purity: iron and copper (amounts not reported)
	MWCNT	Cytotoxicity, uptake, oxidative stress induction/murine alveolar macrophages; lung inflammation/rats	Greater toxicity of thin CNT	Fenoglio et al. (2012)	Length, < 5 μm; diameter, 9.4 and 70 nm; purity: metal contaminants < 0.08%
	MWCNT/SWCNT	Cytotoxicity/human EAhy926, human A549, human HepG2, mouse DMBM-2, hamster V79, and human TK-6 cells	Thin CNT more cytotoxic than thick CNT	Fröhlich et al. (2013)	Length, 0.5–2 μm; diameter of SWCNT, 1–2 μm; diameter of MWCNT, < 8, 20–30, and > 50 nm; purity: SWCNT > 90% and MWCNT > 95%
Length	MWCNT	Lung inflammation, granuloma formation/mice	Long CNT induced inflammatory and granulomatous response	Poland et al. (2008)	Length, 1–5 and 5–20 μm (tangled), 13 μm, and 56 μm; diameter: 15 nm, 10 nm, 85 nm, and 165 nm; purity: iron, copper, vanadium, nickel, zinc, and cobalt content
	MWCNT	Cytotoxicity, DNA damage/A459 cells; lung inflammation/mice	Long and thick CNT, but not short and thin CNT, caused DNA damage/inflammation	Yamashita et al. (2010)	Length, 5–15 μm and 1–2 μm; diameter: 20–100 nm and < 10 nm
	SWCNT	Lung inflammation, granuloma formation/mice	CNT > 10 μm induced granuloma formation; CNT < 300 nm excreted from the body	Kolosnjaj-Tabi et al. (2010)	Length, > 1–2 μm and 20–80 nm; diameter, ~1 nm; purity: different iron content (1.5–25%)
	MWCNT	Pleural inflammation, cellular viability in the mesothelium/mice	Greater toxicity of longer CNT	Murphy et al. (2011)	Length: 0.5–2 μm (short), 5–20, and 1–5 μm (tangled), 13 and ≤ 56 μm (long); diameter: 20–30 nm, 15 and 15 nm, 40–50, and 20–100 nm
Defects	MWCNT	Genotoxicity/rat lung epithelial cells; lung inflammation, fibrosis/rats	Defects increased the inflammatory and genotoxic potential	Fenoglio et al. (2008), Muller et al. (2008a)	Length, 0.7 μm; diameter, 11 nm; purity: aluminium, cobalt, and iron < 0.08%
	MWCNT	Carcinogenicity/rats	Carcinogenicity not affected by defects	Muller et al. (2009)	Length, 0.7 μm; diameter, 11 nm; purity: aluminium, cobalt, and iron < 0.08%

Table 4.2 (continued)

Property	Type of CNT	End-points/models	Effects	References	Characteristics
Surface functionalities: oxidation/	MWCNT	Cytotoxicity/human T-cells	Surface functionalities (oxidized) increased the toxicity	Bottini et al. (2006)	Length, 1–5 μm; diameter, 20–40 nm; purity: > 95%
functionalization/ carboxylation	MWCNT	Cytotoxicity, oxidative stress/ human neuroblastoma cells	Surface functionalities (oxidized) and impurities increased the toxicity	Vittorio et al. (2009)	Length, 0.5–2 μm; diameter, > 35–40 nm and 20–40 nm; purity: 97–99%
	SWCNT	Embryotoxicity/mice, mouse embryonic stem cells, NIH3T3 cells	Surface functionalities (oxidized) increased the embryotoxicity	Pietroiusti et al. (2011)	Length, 0.37–0.85 μm; diameter, ~2 nm; purity: calcium, chromium, iron, and cobalt < 4% (higher in pristine)
	MWCNT	Profibrogenic markers/BEAS-2B cells, human monomyelocytic leukaemia THP-1 cells; fibrosis/ mice	Carboxylation of MWCNT decreased the fibrogenicity	Wang et al. (2011d)	Length, 10–30 μm; diameter, 20–30 nm; purity: ≈99%; nickel and iron not detected
	SWCNT/ MWCNT	Cytotoxicity/mammalian CHO cells, human HeLa cells	No cytotoxicity with F-SWCNT:DNA complexes	Pantarotto et al. (2004)	No characterization
	SWCNT/ MWCNT	Cytotoxicity/human EAhy926, human A549, human HepG2, mouse DMBM-2, hamster V79, and human TK-6 cells	Carboxylated CNT more cytotoxic than pristine CNT	Fröhlich et al. (2013)	Length, 0.5–2 μm; diameter of SWCNT, 1–2 μm; diameter of MWCNT, < 8, 20–30, and > 50 nm; purity: SWCNT > 90% and MWCNT > 95%
	SWCNT	Osteoblast proliferation/ osteosarcoma rat ROS 17/2.8 cells	Cells growth depended on the type of functionalization	Zanello et al. (2006)	Length, from nm to μm; diameter, 1.5 nm
	MWCNT, raw and metal-purified	Cell viability, inflammasome activation/freshly isolated alveolar macrophages from C57Bl/6 mice	Carboxylation after surface oxidation reduced cytotoxicity and inflammasome activation	Hamilton et al. (2013b)	Dimensions not reported
	MWCNT	Inflammation, fibrosis in vivo, inflammasome activation/ C57BL/6 mice	Carboxylation after surface oxidation decreased inflammation, fibrosis, and inflammasome activation	Sager et al. (2014)	Dimensions not reported
Metals from residual catalyst	SWCNT	Oxidative stress/mouse RAW 264.7 macrophages	Iron increased oxidative stress	Kagan et al. (2006)	Diameter: 1–4 nm; purity: iron, 0.23–26%
	SWCNT/ MWCNT	Cytotoxicity, release of inflammatory mediators, oxidative stress/rat NR8383 cells, human A549 lung cells	Metals increased oxidative stress	Pulskamp et al. (2007)	Diameter: 1–2 nm, 10–20 nm, and 30–50 nm; purity: different content of cobalt, iron, nickel, copper, and molybdenum

Table 4.2 Physico-chemical properties of carbon nanotubes that are relevant to toxicity: summary of the most pertinent studies (continued)

Property	Type of CNT	End-points/models	Effects	References	Characteristics
	MWCNT	Genotoxicity/rat lung epithelial cells; lung inflammation, fibrosis/rats	Metals residues contributed to an increase in toxicity	Muller et al. (2008a)	Length, 0.7 μm; diameter, 11 nm; purity: cobalt (~0.50%), and iron (0.48%)
	SWCNT	Oxidative stress, inflammation/EpiDerm FT engineered human skin; collagen accumulation/mice	Metals residues contributed to an increase in toxicity	Murray et al. (2009)	Iron, 30% and 0.23%
	MWCNT	Cell viability, inflammasome activation/freshly isolated alveolar macrophages from C57Bl/6 mice	Slight reduction in cytotoxicity and inflammasome activation after purification	Hamilton et al. (2013b)	Dimensions not reported
Residual catalyst support/amorphous carbon	MWCNT	Cell viability, inflammasome activation/freshly isolated alveolar macrophages from C57Bl/6 mice	Slight reduction in cytotoxicity and inflammasome activation after removal of amorphous carbon	Hamilton et al. (2013b)	Dimensions not reported
Chirality		No studies			

CNT, carbon nanotubes; F-SWCNT, functionalized SWCNT; MWCNT, multiwalled carbon nanotubes; SWCNT, single-walled carbon nanotubes
Adapted with permission from Ghiazza et al. (2014). Copyright (2014), with permission from Elsevier

composition and structure ([Fubini et al., 2010](#), [2011](#)) which are illustrated in [Table 4.3](#) ([Fubini et al., 2011](#)).

(a) Length

[Schinwald et al. (2012)](#) reported that CNT over 4 µm in length are pathogenic to the pleura in mice and proposed a threshold length value (4–5 µm) for the induction of an acute inflammatory response in a mouse model. Pleural inflammation and fibrosis are induced only by long (> 10 µm) CNT after intraperitoneal ([Kolosnjaj-Tabi et al., 2010](#)) or intrapleural ([Murphy et al., 2011](#)) injection. The adverse effects of long (> 10 µm), rigid CNT were related to their physical interaction with cells resulting in incomplete internalization and "frustrated phagocytosis", which activate an inflammatory response. Stomata (diameter, 3–10 µm) in the parietal pleura act as a "sieve" in drainage from the pleural space and fail to clear the long CNT ([Murphy et al., 2011](#)).

[Manshian et al. (2013)](#) investigated the role of the length of SWCNT in the induction of genotoxicity in human bronchial epithelial BEAS-2B and lymphoblastoid MCL-5 cells. SWCNT induced significant levels of chromosomal damage at subcytotoxic concentrations, the potency of which, according to the length of the SWCNT, was 400–800 nm > 5–30 µm > 1–3 µm. The authors hypothesized that surface area is an important determinant in cellular response, as well as the secondary structure of CNT under experimental conditions. In contrast, only SWCNT 1–3 µm in length were found to be mutagenic in mammalian cells (see Section 4.3).

(b) Thickness

A study of two MWCNT of similar length (< 5 µm) and surface reactivity but different diameter (9.4 and 70 nm) showed that thinner MWCNT appeared to be significantly more toxic than their thicker counterparts in vivo (rat lung)

and in vitro (murine alveolar macrophages) ([Fenoglio et al., 2012](#)). [Nagai et al. (2011)](#) also reported an effect of the diameter of CNT on mesothelial toxicity and carcinogenicity in rats (see also Section 3). Short CNT with different diameters that had or had not been subjected to carboxyl surface functionalization were assessed for cytotoxicity in phagocytic and non-phagocytic cells. The role of oxidative stress was evaluated by assessing the intracellular glutathione (GSH) levels and protection by N-acetyl cysteine (NAC). CNT < 8 nm in diameter were more cytotoxic than CNT ≥ 20 nm in diameter and carboxylated CNT were more toxic than as-produced CNT. Protection by NAC was maximal for larger-diameter as-produced CNT and minimal for small-diameter carboxylated CNT. Thinner (diameter < 8 nm) CNT acted mainly through the disruption of membrane integrity, and CNT with a larger diameter mainly induced apoptotic changes ([Fröhlich et al., 2013](#)).

4.2.3 Surface reactivity

The variability in the toxicity elicited by CNT can mostly be ascribed to both differences in shape and modifications to the chemical composition/structure of the CNT employed in the different studies ([Fubini et al., 2011](#) and references therein). Differences in surface state between asbestos and CNT (in contrast to asbestos, CNT quench radicals, are hydrophobic, and may be fully freed from metal impurities) suggest that these two fibrous materials might induce toxicity by different mechanisms ([Fubini et al., 2011](#))

Physical and chemical properties are generally accepted to modulate the cell responses to CNT. The introduction of surface oxygenated functionalities increased the toxicity of CNT in some models ([Bottini et al., 2006](#); [Vittorio et al., 2009](#); [Pietroiusti et al., 2011](#)). In contrast, [Cheng et al. (2008)](#) reported that purified PEGylated SWCNT, although reversibly internalized and translocated into the nucleus, were

Table 4.3 Comparison of the major physico-chemical features of carbon nanotubes and asbestos

Feature	Carbon nanotubes	Asbestos	
		Amphibole asbestos	Chrysotile serpentine
Origin	Manufactured	Natural	Natural
Chemical composition	Carbon	Silicate framework including Mg^{2+}, $Fe^{2+/3+}$, Na^+, and Ca^{2+} as structural or substitution unit	Silicate framework including Mg^{2+}, $Fe^{2+/3+}$, Na^+, and Ca^{2+} as structural or substitution unit
Structure	Single or multiple rolled graphene sheets	Octahedrally coordinated cation layers sandwiched between tetrahedral silicate layers	Multilayered brucite intercalated with rolled silicate sheets
Nature of the chemical bond	Fully covalent	Mixed, covalent-polar and ionic	Mixed, covalent-polar and ionic
Structural defects	Ring shapes other than hexagon, sp^3 hybridized carbon, dangling bonds at lattice defects, and end caps	Framework defects, absence or substitution of metal ions	Framework defects, absence or substitution of metal ions
Agglomeration	High	Naturally in bundles	Naturally in bundles
Durability in water	High	High in all media	High in neutral media, lower in acidic media
Hydrophilicity/ hydrophobicity	Highly hydrophobic if not functionalized	Highly hydrophilic	Highly hydrophilic
Bio-available metals	Highly variable (cobalt, nickel, iron – metallic or ionic)	Stoichiometric Fe^{2+} and Fe^{3+} ions in crystal structure	Substitutional Fe^{2+} ions
Surface charge (physiological pH)	Very low, negative if not functionalized	High, negative	High, positive
Free radicals	Scavenging of free radicals and reactive oxygen species	Generation of free radicals and reactive oxygen species	Generation of free radicals and reactive oxygen species
Dissolution/ degradation	Enzymatic degradation in neutrophils (SWCNT) and degradation in phagolysosomal fluid (carboxylated SWCNT)	Selective leaching of iron ions only in the presence of strong chelators	Selective leaching of iron ions only in the presence of strong chelators

Ca, calcium; Fe, iron; Mg, magnesium; Na, sodium; SWCNT, single-walled carbon nanotubes
Created by the Working Group with data from Fubini et al. (2011)

non-genotoxic in mammalian cells in terms of cell-cycle distribution and mitosis after 5 days of continuous exposure, suggesting that intensive purification and functionalization improves the biocompatibility of CNT.

Li et al. (2013) reported the role of surface charge in determining the pulmonary fibrogenic effects of MWCNT. Anionic functionalization with carboxylate and PEG decreased pulmonary fibrogenic potential compared with as-prepared MWCNT; strong cationic functionalization with polyetherimide induced a greater degree of pulmonary fibrosis. Neutral and weakly cationic (sidewall amine) functionalized CNT had similar fibrogenic potential to as-produced CNT. The mechanism of these effects involves differences in the cellular uptake of MWCNT, lysosomal damage, and cathepsin B release in macrophages, associated with the activation of NOD-like receptor family, pyrin domain containing 3 (NLRP3) inflammasome (Li et al., 2013).

Hamilton et al. (2013b) examined the consequences of surface carboxylation of MWCNT on bioactivity. Hydrochloric acid refluxing was used to purify raw "as-received" MWCNT by removing the amorphous carbon layer on their surface and reducing the metal impurities (e.g. nickel). The sidewall of raw and hydrochloric acid-purified MWCNT was further functionalized with the carboxyl moiety using nitric acid oxidation, a common approach that imparts the carboxyl functional group to the MWCNT. No structural damage was observed. Four distinct MWCNT were compared for their bioactivity: raw "as-received", purified, carboxyl-terminated raw MWCNT, and carboxyl-terminated purified MWCNT. Raw and hydrochloric acid-purified MWCNT are poorly soluble in water. In contrast, after nitric acid oxidation, both carboxylated forms of MWCNT showed very good water solubility. Freshly isolated alveolar macrophages from C57Bl/6 mice were exposed to these nanomaterials to determine the effects

of these modifications on cell viability and inflammasome activation, which was confirmed using inhibitors of cathepsin B and caspase-1. Purification slightly reduced cell toxicity and inflammasome activation compared with raw MWCNT. In contrast, functionalization of MWCNT with carboxyl groups dramatically reduced cytotoxicity and inflammasome activation. Similar results were seen in human monocytic THP-1 cells. All nanomaterials, regardless of modification, were taken up by alveolar macrophages. However, the manner in which the nanomaterials were processed within the cells differed. Purified MWCNT were taken up in large vacuoles or phagolysosomes and did not appear to be free in the cytoplasm. In contrast, the two functionalized MWCNT did not appear to be incorporated in large vacuoles, but were more evenly distributed in smaller phagolysosomal structures or free in the cytoplasm. The results confirmed that MWCNT activate NLRP3 inflammasome through a process that involves phagolysosomal permeabilization, the release of cathepsin B, and the activation of caspase-1 (Hamilton et al., 2013b).

Sager et al. (2014) investigated whether MWCNT (same nanomaterial as that used in Hamilton et al., 2013b) with different surface functionalities would exhibit different bioactivity profiles in vivo. Unmodified (bare) MWCNT and MWCNT that were surface functionalized with the carboxyl group (F-MWCNT) were instilled intratracheally into C57BL/6 mice. Mice were then examined for biomarkers of inflammation and injury, as well as histologically for the development of pulmonary disease as a function of dose and time. Biomarkers for pulmonary inflammation included cytokines (interleukin [IL]-1β, IL-18, and IL-33), profibrotic mediators, the presence of inflammatory cells (neutrophils), lysosomal release of cathepsin B, and markers of injury (albumin and lactate dehydrogenase [LDH]). The results showed that surface modification of the MWCNT by the addition of the

carboxyl group significantly reduced bioactivity and pathogenicity. Bare MWCNT were more bioactive, causing more inflammation, lung pathology, and fibrosis than the F-MWCNT. This difference in bioactivity correlated with the activation of NLRP3 inflammasome (Sager et al., 2014).

(a)   Generation of free radicals

Unlike other toxic particulates (e.g. asbestos), CNT modified by grinding to introduce structural defects have been reported not to generate but to quench free radicals in cell-free systems. This scavenging activity was eliminated in CNT that were fully divested of their defects (i.e. by heating at 2400 °C) (Fenoglio et al., 2008). CNT in composites (CNT-polymer) have been employed to preserve the polymeric matrix from oxidative degradation by their radical scavenging ability (Watts et al., 2003). The susceptibility of CNT to attack by radicals has been exploited to introduce functionalities at their surface (Ghiazza et al., 2014 and references therein). However, SWCNT with different iron contents displayed different redox activity in a cell-free model system, as revealed by the formation of ascorbate radicals resulting from ascorbate oxidation detected by electron paramagnetic resonance (Kagan et al., 2006). In the presence of zymosan-stimulated RAW 264.7 macrophages, non-purified iron-rich SWCNT were more effective in generating hydroxyl radicals (documented by electron paramagnetic resonance spin-trapping with 5,5-dimethyl-1-pyrroline-N-oxide) than purified SWCNT (Kagan et al., 2006). Exposure of immortalized human epidermal HaCaT keratinocytes to SWCNT induced oxidative stress, which was confirmed by the formation of free radical species, the accumulation of peroxidation products and thiobarbituric acid-reactive substances, the reduction of low-molecular-weight thiols and protein sulfhydryls, and a decrease in vitamin E and total antioxidant reserves in the cells. As-produced unrefined SWCNT contain up to 30% iron, and the authors hypothesized a Fenton-like reaction resulting in HO• generation, which increased in the presence of hydrogen peroxide and decreased in the presence of catalase (a hydrogen peroxide scavenger) or desferoxamine (a strong iron chelator) (Shvedova et al., 2003).

Whether CNT in cell-free media do not generate hydroxyl radicals and/or other reactive oxygen species (ROS) per se or whether what is hypothetically generated would immediately be quenched by defects is not clear (Fenoglio et al., 2006, 2008). Purified MWCNT scavenge hydroxyl radicals generated by different sources (Fenoglio et al., 2006). A local decrease in ROS was observed in vivo after intratracheal instillation of DWCNT in mice (Crouzier et al., 2010). However, CNT and other graphene materials have been reported to deplete the cellular antioxidant defences of cells by oxidizing GSH through a reaction with oxygen at the surface (Liu et al., 2011b). Therefore, CNT interact with the cellular antioxidant defence system in several ways. [The overall effect of CNT on the homeostasis of ROS in cells still needs to be clarified.]

(b)   Bioavailability and biodeposition of metals

After synthesis, CNT generally contain amorphous carbon and metals – iron and other different redox active metals (e.g. cobalt, nickel, and molybdenum) – as a residue of the catalyst employed in their synthesis. The amounts are highly variable and may reach 20% in unpurified, as-produced CNT (see also Section 1). Metals may be present in different oxidation states as ions, clusters, or even organized in metal nanoparticles. The iron in CNT has been reported to be a mixture of α-Fe^0, γ-Fe^0, and carbide phases; much of the metal appears by TEM to be at least superficially encapsulated by carbon (Guo et al., 2007). Most of the iron is located within the tube, and is thus not readily accessible to target cells. The metal residues may be extracted from the CNT, e.g. by acid treatment, but often a fraction remains inside. Toxicologically significant

amounts of iron can be mobilized from a diverse set of commercial nanotube samples in the presence of ascorbate and the chelating agent, ferrozine. This mobilized iron is redox active and induces single-strand breaks in plasmid DNA in the presence of ascorbate. Iron bioavailability is not fully suppressed by vendor "purification" and is sensitive to partial oxidation, mechanical stress, sample ageing, and intentional chelation (Guo et al., 2007). Because iron sealed within the graphene layers cannot be released in physiological media, the amount of bioavailable iron in CNT varies greatly from sample to sample and cannot be predicted from the total iron content (Guo et al., 2007, Fubini et al., 2011 and references therein).

Redox active metals associated with CNT (e.g. iron) have been reported to induce oxidative stress and toxicity (Kagan et al., 2006; Pulskamp et al., 2007). Clear evidence on the role of iron in the toxicity of CNT was obtained by showing that simple removal of most of the iron residues caused a remarkable decrease in the toxicity of SWCNT (Kagan et al., 2006) and MWCNT (Aldieri et al., 2013). Iron-rich SWCNT caused a significant loss of intracellular low-molecular-mass thiols (predominantly GSH) and accumulation of lipid hydroperoxides in both zymosan- and phorbol myristate acetate-stimulated RAW 264.7 macrophages (Kagan et al., 2006). Two MWCNT differing only in the presence or absence of iron were compared at dose ranges of 25–100 $\mu g/cm^2$. While iron-rich MWCNT (50 $\mu g/cm^2$) were significantly cytotoxic and genotoxic and induced a potent cellular oxidative stress response, iron-free MWCNT (50 $\mu g/cm^2$) did not exert any of these adverse effects (Aldieri et al., 2013).

Complete elimination of any metal trace can be achieved only by heating CNT to a very high temperature (2400 °C) at which metal vapourizes. Lung toxicity in vivo but not genotoxicity in vitro induced by MWCNT was decreased, but not completely eliminated, by heating at 600 °C, when metals are fully vapourized but

defects remain (Fenoglio et al., 2008; Muller et al., 2008a).

4.2.4 Fibre durability (leaching, dissolution, and breakage)

CNT are highly insoluble due to their graphitic structure (Lam et al., 2004) and they have been suggested to be as biopersistent as amphiboles (Sanchez et al., 2009). However, several studies reported that the carbon structure may be attacked and degraded, mainly by endogenous oxidants in biological simulation fluids or in vivo (Kagan et al., 2010; Shvedova et al., 2012a, b).

(a)   In vivo

Using MPO-deficient mice, Shvedova et al. (2012a) showed that MPO contributes to the pulmonary oxidative biodegradation of SWCNT in vivo (see also Section 4.1.2 (f)).

(b)   In vitro

Two different routes of attack and degradation of CNT by endogenous oxidants were reported in studies in vitro (see Section 4.1.2 (f)). One enzymatic route is through degradation by several peroxidases, such as MPO (Kagan et al., 2010), lactoperoxidase, and EPO (Shvedova et al., 2012b), while the second route follows non-enzymatic degradation when CNT are in contact with simulated phagolysosomal fluid (Liu et al., 2010). Degradation of SWCNT after incubation with human EPO and hydrogen peroxide has been reported; the biodegradation was greater in the presence of sodium bromide. However, neither EPO nor hydrogen peroxide alone caused SWCNT degradation (Andón et al., 2013).

Surface functionalization affects the biodegradability of CNT (Liu et al., 2010; Bianco et al., 2011). The rate of degradation is associated with both the degree of surface functional groups and the type of CNT; MWCNT are more resistant

than SWCNT and thus require a longer time for degradation (Bianco et al., 2011).

4.2.5 Physico-chemical determinants of defined biological end-points

Because of the extreme variability of the features of CNT, the method to be adopted to associate a physico-chemical feature to a given effect in vivo is to modify one single property at a time of a well defined specimen of CNT and test all modified specimens using exactly the same procedure. Two typical examples of this type of procedure taken from Table 4.2 are highlighted below.

This approach showed clearly that a slight modification in cytotoxicity and inflammogenicity occurred after purification, while acute inflammogenicity (demonstrated by inflammasome activation in MWCNT in vitro and in vivo) was dramatically reduced, with a consequent reduction in pathogenicity after functionalization of the surface with carboxyl (Hamilton et al., 2013b; Sager et al., 2014).

Modification of MWCNT by progressive heating during which metals and defects are gradually eliminated (see Table 4.4) enabled an association of genotoxicity in vitro with defects and respiratory toxicity in vivo with both metals and defects (Fenoglio et al., 2008; Muller et al., 2008a).

4.3 Genetic and related effects

4.3.1 Humans

(a) Exposed humans

No data were available to the Working Group.

(b) Human cells in vitro

See Section 4.3.2 (b)

4.3.2 Experimental systems

(a) In vivo

(i) DNA damage

Investigations on the direct genotoxicity of CNT have focused on end-points measured by the comet assay and oxidatively generated DNA lesions. Table 4.5 lists the in-vivo studies that have assessed levels of DNA damage in rodent tissues after exposure to CNT.

Intratracheal instillation of SWCNT into mice (54 µg/animal) increased the levels of DNA strand breaks in BALF cells 3 hours after exposure (Jacobsen et al., 2009). Another study showed that a single intratracheal instillation of MWCNT (50 or 200 µg/mouse) was associated with increased levels of DNA strand breaks in lung tissues of mice 3 hours after exposure, and also documented increased levels of 8-oxodeoxyguanosine (8-oxodG) and lipid peroxidation-derived DNA lesions in lung tissues of mice 3–168 hours after exposure. However, the baseline level of 8-oxodG was 4.8 lesions/10^6 nucleotides (corresponding to 22 lesions/10^6 deoxyguanosine [dG]), indicating spurious oxidation of DNA during the processing or analysis of samples (Kato et al., 2013). Another study showed that pulmonary exposure to MWCNT once every 2 weeks for 24 weeks was associated with an increased level of 8-oxodG in lung tissues of rats [the detection method was not described and the basal level of 8-oxodG was very high (1.3 ng/µg DNA, corresponding to 7600 lesions/10^6 dG)] (Xu et al., 2014).

Nose-only inhalation of 0.17–0.96 mg/m³ of MWCNT for 6 hours per day on 5 days per week for 28 days was associated with increased levels of DNA strand breaks in the lung tissues of rats (Kim et al., 2014). A similar study by the same authors in which rats were exposed by whole-body inhalation of 0.16–0.94 mg/m³ of MWCNT for 6 hours per day for 5 days also showed increased levels of DNA strand breaks in lung tissues (Kim et al., 2012a). Weekly intratracheal

Table 4.4 Example of an experimental mechanistic approach to evaluate specific physico-chemical determinants of biological activity for ground multiwalled carbon nanotubes

Multiwalled carbon nanotubes	Defects	Metals	Quenching activity	In-vivo respiratory toxicity		In-vitro genotoxicity
				Lung response	Cytokines	
Ground	Yes	Yes (in oxidized form)	Positive	Positive	Positive	Positive
600 °C vacuum	Yes (less)	Yes (in reduced form)	Positive	Reduced	Negative	Positive
Heated 2400 °C air	No	No	Negative	Negative	Negative	Negative
Heated 2400 °C ground	Yes	No	Positive	Positive	Negative	Positive
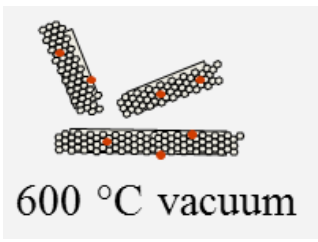
Created by the Working Group with data from Fenoglio et al. (2008) and Muller et al. (2008a)

Table 4.5 Studies of DNA damage and mutation in tissues of experimental animals exposed to carbon nanotubes in vivo

Material tested[a]	Species, strain	End-point, test system	Exposure	Result[b]	Reference
SWCNT (diameter, 0.9–1.7 nm; length, < 1 μm; SSA, 731 m²/g)	Mouse, C57BL/6 ApoE−/− knockout	DNA strand breaks in BALF, comet assay	54 μg/mouse, intratracheal instillation	+	Jacobsen et al. (2009)
SWCNT (diameter, 0.9–1.7 nm; length, < 1 μm; SSA, 731 m²/g; iron, 2%)	Mouse, C57BL/6 ApoE−/− knockout	DNA strand breaks and FPG-sensitive sites in lung, comet assay	0.5 mg/kg bw twice (24 h interval) (total dose, 1 mg/kg), intratracheal instillation	− DSB − FPG	Vesterdal et al. (2014a)
SWCNT (diameter, 1.8 nm; length, 4.4 μm; SSA, 878 m²/g; iron, 4.4%)	Rat, Crl: CD (SD)	DNA strand breaks in lung, comet assay	0.2 or 1 mg/kg bw (single dose), or 0.04 or 0.2 mg/kg bw once/wk, 5 wk, intratracheal instillation	−	Naya et al. (2012)
MWCNT (diameter, 90 nm; length, 2 μm)	Mouse, ICR	DNA strand breaks in lung, comet assay	50 or 200 μg/mouse, intratracheal instillation	+	Kato et al. (2013)
MWCNT (NM400: diameter, 5–35 nm; length, 0.7–3.0 μm; SSA, 298 m²/g; NM402: diameter, 6–20 nm; length, 0.7–4.0 μm; SSA, 225 m²/g)	Mouse, C57BL/6 ApoE−/− knockout	DNA strand breaks and FPG-sensitive sites in lung, comet assay	25.6 μg/mouse once/wk, 5 wk, intratracheal instillation	+ DSB − FPG	Cao et al. (2014)
MWCNT (diameter, 12 nm; length, up to 12 μm; SSA, 41–42 m²/g), non-functionalized or functionalized (acid-treated)	Mouse, Swiss-Webster	DNA strand breaks in peripheral blood leukocytes, comet assay	0.25–0.75 mg/kg bw once/day, 5 days, intraperitoneal injection	+	Patlolla et al. (2010)
MWCNT (diameter, 7–15 nm; length, 0.5–200 μm)	Mouse, Swiss albino	DNA strand breaks in bone marrow cells, comet assay	2, 5, or 10 mg/kg bw, intraperitoneal injection	+	Ghosh et al. (2011)
MWCNT (diameter, 44 nm; length, 2.7 μm; SAA, 69 m²/g; iron, 5.3%)	Rat, Crl/CD (SD)	DNA strand breaks in lung, comet assay	0.2 or 1 mg/kg bw (single dose), or 0.04 or 0.2 mg/kg bw once/wk, 5 wk, intratracheal instillation	−	Ema et al. (2013a)
MWCNT (diameter, 10–15 nm; length, 20 μm; SSA, 225 m²/g; iron, 2%)	Rat, Sprague-Dawley	DNA strand breaks in lung immediately and 1 mo after the last exposure, comet assay	0.16, 0.34, or 0.94 mg/m³, 6 h/day, 5 days, whole-body inhalation	+	Kim et al. (2012a)
MWCNT (diameter, 10–15 nm; length, 330 nm; SSA, 225 m²/g; iron, 2%)	Rat, F344	DNA strand breaks in lung immediately and 90 days after the last exposure, comet assay	0.17, 0.49, or 0.96 mg/m³, 6 h/day, 5 days/wk, 6 wk, nose-only inhalation	+	Kim et al. (2014)
MWCNT (diameter, 90 nm; length, 2 μm)	Mouse, ICR	DNA adduct HεdC in lung, LC-MS/MS	200 μg/mouse, intratracheal instillation	+	Kato et al. (2013)
SWCNT (diameter, 0.8–1.2 nm; length, 0.1–1 μm; iron < 23%; diameter, 1.2–2 nm; length, 1–15 μm; iron, 0.05%)	Mouse, ICR [with allergic pulmonary inflammation (ovalbumin-sensitized) or normal counterparts]	DNA adduct 8-oxodG in lung, immunohistochemistry	50 μg/mouse, once/wk, 6 wk, intratracheal instillation	+	Inoue et al. (2010)

Table 4.5 (continued)

Material tested[a]	Species, strain	End-point, test system	Exposure	Result[b]	Reference
SWCNT (diameter, 0.9–1.7 nm; length, < 1 μm; SSA, 731 m²/g; iron, 2%)	Rat, F344	DNA adduct 8-oxodG in lung, liver, and colon mucosa, HPLC-ECD	0.064 or 0.64 mg/kg bw, gavage	+ lung and liver – colon mucosa	Folkmann et al. (2009)
MWCNT (diameter, 90 nm; length, 2 μm)	Mouse, ICR	DNA adduct 8-oxodG in lung, LC-MS/MS	200 μg/mouse, intratracheal instillation	+[c]	Kato et al. (2013)
MWCNT described as "short" (diameter, 15 nm; length, 3 μm) or "long" (diameter, 150 nm; length, 8 μm)	Rat, F344	DNA adduct 8-oxodG in lung	0.125 mg/rat once every other wk, 24 wk (total dose, 1.6 mg/kg), trans-tracheal intrapulmonary spraying	(+)[d]	Xu et al. (2014)
SWCNT (diameter, 0.8–1.2 nm; length, 0.1–1 μm; iron, 17.7%)	Mouse, C57BL/6	K-*ras* gene mutation in lung, PCR	5 mg/m³, 5 h/day, 4 days, inhalation	+	Shvedova et al. (2008)
SWCNT (diameter, 0.8–1.2 nm; length, 0.1–1 μm; iron, 17.7%)	Mouse, C57BL/6	K-*ras* gene mutation in lung, PCR	5–20 μg/mouse, pharyngeal aspiration	–	Shvedova et al. (2008)
MWCNT (diameter, 90 nm; length, 2 μm)	Mouse, *Gpt* delta transgenic	*Gpt* gene mutant frequency in lung	0.2 mg/mouse once/wk, 4 wk, intratracheal instillation	+	Kato et al. (2013)

[a] Nanomaterial characteristics include diameter, length, specific surface area (SSA), and content of transition metals

[b] +, positive; –, negative; (+), weakly positive

[c] The baseline levels of DNA lesions were rather high (approximately 4.8 lesions/10⁶ nucleotides, corresponding to 22 lesions/10⁶ dG)

[d] The detection method was not described and the basal levels of 8-oxodG (1.3 ng/mg DNA) corresponded to 7600 lesions/10⁶ dG, assuming that the molecular weight of 8-oxodG is 283 g/mol and 1 fmol/μg DNA is equal to 1.64 lesions/10⁶ dG)

BALF, bronchoalveolar lavage fluid; bw, body weight; CNT, carbon nanotubes; dG, deoxyguanosine; DSB, DNA strand breaks; FPG, formamidopyrimidine glycosylase; *Gpt*, guanine phosphoribosyltransferase; HedC, heptanone etheno-deoxyribocytosine (DNA adduct, lipid peroxidation product-derived); HPLC-ECD, high-performance liquid chromatography-electrochemical detection; LC-MS/MS, liquid chromatography-tandem mass spectrometry; MWCNT, multiwalled carbon nanotubes; 8-oxodG, 8-oxodeoxyguanosine; PCR, polymerase chain reaction; SWCNT, single-walled carbon nanotubes; wk, week

instillations of 25.6 μg of MWCNT for 5 weeks were associated with elevated levels of DNA strand breaks in the lung tissues of mice, whereas unaltered levels of formamidopyrimidine glycosylase (FPG)-sensitive sites were found in the same tissues (Cao et al., 2014). Two intratracheal instillations of 0.5 mg/kg bw of SWCNT at an interval of 24 hours did not increase the level of DNA strand breaks or FPG-sensitive sites in mice 2 hours after the last injection (Vesterdal et al., 2014a). No difference in the levels of DNA strand breaks was observed in the lung tissues of rats after intratracheal instillation of a single dose of 0.2 or 1 mg/kg bw or of 0.04 or 0.2 mg/kg bw once per week for 5 weeks of MWCNT (Ema et al., 2013a) or SWCNT (Naya et al., 2012). Increased immunostaining of 8-oxodG was seen in the lung tissues of mice exposed to SWCNT by intratracheal instillation of 50 μg/mouse per week for 6 weeks (Inoue et al., 2010).

Intraperitoneal injection of 0.25–0.75 mg/kg bw of MWCNT once per day for 5 days resulted in increased levels of DNA strand breaks in the peripheral blood leukocytes of mice 24 hours after the last exposure (Patlolla et al., 2010). A single intraperitoneal injection of 2–10 mg/kg bw of MWCNT was also associated with an increased level of DNA strand breaks in the bone marrow cells of mice 3 hours after exposure (Ghosh et al., 2011).

Gastrointestinal exposure by gavage to 0.064 or 0.64 mg/kg bw of SWCNT in either saline suspension or corn oil was associated with increased levels of 8-oxodG in the liver and lung tissues of rats, whereas the same doses did not affect the level of 8-oxodG in colon mucosa cells (Folkmann et al., 2009).

(ii) Gene mutation

See Table 4.5

Inhalation exposure to 5 mg/m³ of SWCNT for 5 hours per day for 4 days enhanced mutation of the proto-oncogene K-*ras* in the lung of C57BL/6 mice. Mutations were found 1 day after the end of inhalation and progressed at 28 days (compared with sham-exposed controls, $P = 0.045$), but mutations were not increased after a single pharyngeal aspiration of 5–20 μg/mouse (Shvedova et al., 2008). One year after exposure, karyotypic changes were shown by micronuclei and multinucleated cells in type II pneumocytes (Shvedova et al., 2014). A study of the intratracheal instillation of 0.2 mg/mouse of MWCNT once per week for 4 weeks showed enhanced guanine phosphoribosyltransferase *Gpt* gene mutation frequencies in the lungs (Kato et al., 2013).

(iii) Chromosomal alterations

Table 4.6 lists the studies that have assessed chromosomal alterations (micronucleus formation and chromosomal aberration) in rodents after exposure to CNT.

Only one investigation examined CNT-induced chromosomal aberrations in rodents. In this study, Swiss-Webster mice (age, 6 weeks) received intraperitoneal injections of 0.25–0.75 mg/kg bw of native and acid-washed MWCNT (diameter, 12 nm; length, < 12 μm) once per day for 5 days. The bone marrow cells were prepared for cytogenetic analysis 24 hours after the exposure, which was associated with a dose-dependent increase in the levels of chromosome gaps, chromatid and isochromatid breaks, fragments, and structural rearrangements, including centromeric fusions and dicentric chromosomes (Patlolla et al., 2010).

Studies on the formation of micronuclei in experimental animals have mainly explored effects after non-pulmonary exposures, although one study in Wistar rats showed an increased frequency of micronuclei in type II pneumocytes isolated 3 days after intratracheal instillation of 0.5–2 mg/rat of MWCNT (Muller et al., 2008b). Oral exposure to 60–200 or 5–20 mg/kg bw of SWCNT once per day for 2 days did not affect the frequency of micronucleated polychromatic

Table 4.6 Studies of micronucleus frequency and chromosomal aberrations in cells of experimental animals exposed to carbon nanotubes in vivo

Material[a]	Species, strain	End-point, test system	Exposure	Results[b]	Reference
SWCNT (diameter, 1.8 nm; SSA, 878 m²/g; iron, 4.4%)	Mouse, ICR	Micronucleus formation in immature erythrocytes in bone marrow cells	5–20 mg/kg bw once/day, 2 days, oral gavage	–	Ema et al. (2013b)
SWCNT (diameter, 3 nm; length, 1.2 µm; SSA, 1064 m²/g)	Mouse, CD-1	Micronucleus formation in polychromatic erythrocytes in bone marrow cells	60 or 200 mg/kg bw once/day, 2 days, oral gavage	–	Naya et al. (2011)
MWCNT (diameter, 11 nm; length, 0.7 µm; 2% impurities)	Rat, Wistar	Micronucleus formation in type II pneumocytes	0.5 and 2 mg/rat, intratracheal instillation	+[c]	Muller et al. (2008b)
MWCNT (diameter, 12 nm; length, up to 12 µm; SSA, 41–42 m²/g), non-functionalized or functionalized (acid-treated)	Mouse, Swiss-Webster	Micronucleus formation in femoral bone marrow cells	0.25–0.75 mg/kg bw once/day, 5 days, intraperitoneal injection	+[d]	Patlolla et al. (2010)
MWCNT (diameter, 7–15 nm; length, 0.5–200 µm)	Mouse, Swiss albino	Micronucleus formation in polychromatic erythrocytes in bone marrow cells	2, 5, or 10 mg/kg bw, intraperitoneal injection	+	Ghosh et al. 2011
MWCNT (diameter, 10–15 nm; length, 0.15 or 10 µm; SSA, 178 or 195 m²/g; iron, 1% or 5%)	Mouse, ICR	Micronucleus formation in polychromatic erythrocytes in femoral bone marrow cells	50 mg/kg bw, intraperitoneal injection	–	Kim et al. (2011)
MWCNT (diameter, 12 nm; length, up to 12 µm; SSA, 41–42 m²/g), non-functionalized or functionalized (acid-treated)	Mouse, Swiss-Webster	Chromosomal aberrations in femoral bone marrow cells	0.25–0.75 mg/kg bw once/day, 5 days, intraperitoneal injection	+[e]	Patlolla et al. (2010)

[a] Nanomaterial characteristics include diameter, length, specific surface area (SSA), and content of transition metals
[b] +, positive; –, negative
[c] Occurring concurrently with pulmonary inflammation (assessed as increased number of macrophages and neutrophils in bronchoalveolar lavage fluid)
[d] Dose-dependent increase in micronucleus frequency
[e] Dose-dependent increase in structural chromosomal aberrations
bw, body weight; CNT, carbon nanotubes; MWCNT, multiwalled carbon nanotubes; SWCNT, single-walled carbon nanotubes

or immature erythrocytes in the bone marrow cells of ICR or CD-1 mice (Naya et al., 2011; Ema et al., 2013b). Intraperitoneal injection of 0.25–0.75 mg/kg bw of MWCNT once per day for 5 days was associated with an increased frequency of micronuclei in bone marrow cells in one study in Swiss-Webster mice (Patlolla et al., 2010). Intraperitoneal injection of 2–10 mg/kg bw of MWCNT in Swiss albino mice increased the frequency of micronuclei in bone marrow cells, whereas the percentage of polychromatic erythrocytes was unaltered (Ghosh et al., 2011). Another study showed no increase in the frequency of micronuclei and no alteration in the frequency of polychromatic erythrocytes in the bone marrow cells of ICR mice after a single intraperitoneal injection of 12.5–50 mg/kg bw of MWCNT (Kim et al., 2011).

(b)   In vitro

(i)   DNA damage

Studies that have assessed the levels of DNA damage in cell cultures after exposure to CNT are presented in Table 4.7. The neutral version of the comet assay showed unaltered levels of double-strand breaks in human alveolar basal epithelial adenocarcinoma A549 cells after exposure to MWCNT (Ju et al., 2014).

Several studies have documented that exposure to SWCNT or MWCNT increased the levels of DNA strand breaks in human colon carcinoma tissue HT29 cells (Pelka et al., 2013), bronchial epithelial BEAS-2B cells (Lindberg et al., 2009, 2013), lung adenocarcinoma A549 cells (Karlsson et al., 2008; Cavallo et al., 2012), mesothelial cells (Pacurari et al., 2008b; Lindberg et al., 2013), human gingival fibroblasts (Cicchetti et al., 2011), Chinese hamster V79 fibroblasts and primary mouse embryo fibroblasts (Kisin et al., 2007, 2011; Yang et al., 2009), human lymphocytes (Ghosh et al., 2011), phytohaemagglutinin-stimulated human lymphocytes (Kim & Yu, 2014), murine macrophages (Migliore et al.,

2010; Di Giorgio et al., 2011; Aldieri et al., 2013), human and rat kidney epithelial cells (Barillet et al., 2010; Kermanizadeh et al., 2013), and human hepatocytes (Kermanizadeh et al., 2012; Alarifi et al., 2014; Vesterdal et al., 2014b). Increased levels of DNA strand breaks were also observed in rat aortic endothelial and human lung adenocarcinoma A549 cells after exposure to CNT, but the statistical analysis appeared to have been based on the total number of comets from a single experiment rather than the mean values from independent experiments (Yamashita et al., 2010; Cheng et al., 2012). However, another study used all comets in the statistical analysis and showed no alteration in DNA strand breaks in human peripheral lymphocytes exposed to SWCNT (Zeni et al., 2008). [The Working Group noted the uncertainty that replicates were independent experiments.] Other studies have shown no alterations in the levels of DNA strand breaks in human lung adenocarcinoma A549 cells and human HaCaT keratinocytes after exposure to MWCNT (Thurnherr et al., 2011; McShan & Yu, 2014) or in FE1 MML mouse lung epithelial cells exposed to SWCNT (Jacobsen et al., 2008).

The protocol of the alkaline comet assay that measures DNA strand breaks can be extended using an additional DNA digestion step with DNA repair enzymes from bacterial or human cells. The bacterial enzymes include FPG and endonuclease III (ENDOIII). The FPG enzyme also cleaves DNA at ring-opened formamidopyrimidine lesions, including 2,6-diamino-4-hydroxy-5-formamidopyrimidine and 4,6-diamino-5-formamidopyrimidine. ENDOIII lesions comprise oxidized pyrimidines, such as uracil glycol, thymine glycol, 5-hydroxycytosine, and 5-hydroxyuracil. Results from these enzyme-modified comet assay measurements have been reported either as total sites (DNA strand breaks plus extra breaks generated by the enzyme) or enzyme-sensitive sites (breaks generated by the enzyme minus the basal level of DNA strand breaks).

Table 4.7 Studies of DNA damage and mutation in experimental systems after exposure to carbon nanotubes in vitro

Material[a]	Cells	End-point, test system	Concentration (LEC or HIC)[b]	Results[c]	Comments	Reference
MWCNT (diameter, 10–20 nm; length, 0.3–0.7 μm; iron, 0.06%)	Human lung adenocarcinoma A549 cells	DNA strand breaks, neutral comet assay	30 μg/mL	–		Ju et al. (2014)
SWCNT (diameter, 1.8 nm; length, 0.5 μm)	Human colon carcinoma HT29 cells	DNA strand breaks and FPG-sensitive sites, comet assay	0.00001 μg/mL	+ DSB – FPG	Incubation with FPG did not increase the level of FPG-sensitive sites above that of DNA strand breaks over the whole range (0.00001–0.2 μg/mL)	Pelka et al. (2013)
Mixed CNT (more than 50% SWCNT; diameter, 1.1 nm; length, 0.5–100 μm)	Human bronchial epithelial BEAS-2B cells	DNA strand breaks, comet assay	1 μg/cm²	+	Dose-dependent increase in DNA strand breaks over the whole range (1–100 μg/cm²)	Lindberg et al. (2009)
SWCNT (diameter < 2 nm; length, 1–5 μm)	Human bronchial epithelial BEAS-2B or mesothelial MeT-5A cells	DNA strand breaks, comet assay	5–200 μg/cm²	+		Lindberg et al. (2013)
MWCNT (diameter, 10–30 nm; length, 1–2 μm)	Human bronchial epithelial BEAS-2B or mesothelial MeT-5A cells	DNA strand breaks, comet assay	5–200 μg/cm²	– BEAS-2B + MeT-5A		Lindberg et al. (2013)
MWCNT (diameter, 20–40 nm; length, 0.5–200 μm; iron, 0.55%)	Human lung adenocarcinoma A549 cells	DNA strand breaks and FPG-sensitive sites, comet assay	5–100 μg/mL	+ DSB – FPG	No change in FPG-sensitive sites; uncertainty about the result because of lack of positive control	Cavallo et al. (2012)
MWCNT (diameter, 100–200 nm; length, few μm)	Human lung adenocarcinoma A549 cells	DNA strand breaks and FPG-sensitive sites, comet assay	1–40 μg/cm²	+ DSB – FPG	Dose–response trend for DNA strand breaks; no change in FPG-sensitive sites	Karlsson et al. (2008)
SWCNT (diameter, 1.4 nm; length, 2–5 μm; SSA, 293 m²/g; iron, 0.07%)	Human mesothelial cells	DNA strand breaks, comet assay	25–50 mg/cm²	+		Pacurari et al. (2008a)
SWCNT (diameter, 1.6 nm; length, 0.8 μm; SSA, 407 m²/g; purity > 90%)	Human gingival fibroblasts	DNA strand breaks, comet assay	50–150 μg/mL	+		Cicchetti et al. (2011)

Table 4.7 Studies of DNA damage and mutation in experimental systems after exposure to carbon nanotubes in vitro (continued)

Material[a]	Cells	End-point, test system	Concentration (LEC or HIC)[b]	Results[c]	Comments	Reference
MWCNT (diameter, 20–40 nm; length, 1–5 μm; 1% impurities), and pristine or amide-functionalized SWCNT (30% impurities)	Human fibroblasts	DNA strand breaks, γH2AX foci	25–150 μg/mL	+	Increased DNA double-strand breaks determined by γH2AX foci	Cveticanin et al. (2010)
MWCNT (diameter, 7–15 nm; length, 0.5–200 μm)	Human lymphocytes	DNA strand breaks, comet assay	2 μg/mL	+	Increased levels at 2 μg/mL, but not at 1, 5, or 10 μg/mL	Ghosh et al. (2011)
SWCNT (diameter, 1–1.2 nm; length, 20 μm)	Human lymphocytes	DNA strand breaks, comet assay	25–100 μg/mL	+		Kim & Yu (2014)
MWCNT (NM400: diameter, 5–35 nm; length, 0.7–3.0 μm; SSA, 298 m²/g; NM402: diameter, 6–20 nm; length, 0.7–4.0 μm; SSA, 225 m²/g)	Human renal proximal tubule epithelial HK-2 cells	DNA strand breaks and FPG-sensitive sites, comet assay	1.25–5 μg/cm²	+ DSB − FPG	Increased levels of DNA lesions; subtraction of DNA strand break levels from the total sites after treatment with FPG indicated negative values of FPG-sensitive sites	Kermanizadeh et al. (2013)
SWCNT (diameter, 1.2–1.7 nm; length, 0.1–4 μm)	Human hepatocyte HepG2 cells	DNA strand breaks, comet assay	5–20 μg/mL	+		Alarifi et al. (2014)
MWCNT (NM400: diameter, 5–35 nm; length, 0.7–3.0 μm; SSA, 298 m²/g; NM402: diameter, 6–20 nm; length, 0.7–4.0 μm; SSA, 225 m²/g)	Human hepatoblastoma C3A cells	DNA strand breaks and FPG-sensitive sites, comet assay	5–20 μg/cm²	+ DSB + FPG with NM402 − FPG with NM400	Levels of FPG-sensitive sites increased with NM402; subtraction of DNA strand break levels from the total sites after treatment with FPG indicated negative values for FPG-sensitive sites with NM400	Kermanizadeh et al. (2012)
SWCNT (diameter, 0.9–1.7 nm; length < 1 μm; SSA, 731 m²/g; iron, 2%)	Human hepatocyte HepG2 cells	DNA strand breaks and FPG-sensitive sites, comet assay	25 μg/mL	+ DSB + FPG	Increased levels of both DNA strand breaks and FGP-sensitive sites	Vesterdal et al. (2014b)
MWCNT (M1: diameter, 20–60 nm; length, 5–15 μm; M2: diameter, 60–100 nm; length, 1–2 μm; M3: diameter < 10 nm; length, 1–2 μm)	Human lung adenocarcinoma A549 cells	DNA strand breaks, comet assay	50 μg/mL	+ with M1 + with M2 − with M3	Uncertainty about replicates being independent experiments	Yamashita et al. (2010)
SWCNT (diameter < 2 nm; length, 5–15 μm)	Human lung adenocarcinoma A549 cells	DNA strand breaks, comet assay	50 μg/mL	−	Uncertainty about replicates being independent experiments	Yamashita et al. (2010)

Table 4.7 (continued)

Material[a]	Cells	End-point, test system	Concentration (LEC or HIC)[b]	Results[c]	Comments	Reference
MWCNT (diameter, 6–24 nm; length, 2–5 μm; < 0.4% impurities)	Human lung adenocarcinoma A549 cells	DNA strand breaks, comet assay	7.5–30 μg/mL	–		Thurnherr et al. (2011)
SWCNT (diameter < 2 nm; length, 5–15 μm) and MWCNT (diameter, 10–30 nm; length, 5–15 μm)	Human pleural mesothelial Met-5A cells	DNA strand breaks, comet assay	20 μg/mL	+	Statistical analysis based on the total number of comets	Ogasawara et al. (2012)
SWCNT (diameter, 1.1 nm; length, 50 μm; 3.7% impurities)	Human peripheral lymphocytes	DNA strand breaks, comet assay	1–10 μg/mL	–	Statistical analysis based on the total number of comets	Zeni et al. (2008)
MWCNT (characteristics not reported, used as pristine, purified and carboxyl-functionalized samples)	Human HaCaT keratinocytes	DNA strand breaks and FPG-sensitive sites, comet assay	20 μg/mL	– DSB + FPG	Unaltered level of DNA strand breaks; increased levels of FPG-sensitive sites with all MWCNT tested	McShan & Yu (2014)
SWCNT (diameter < 2 nm; length, 5–15 μm) and MWCNT (diameter, 10–30 nm; length, 5–15 μm)	Human pleural mesothelial Met-5A cells	DNA adduct 8-oxodG, HPLC-ECD	20 μg/mL	–	Uncertainty about replicates being independent experiments; high baseline level of 8-oxodG	Ogasawara et al. (2012)
SWCNT (diameter < 2 nm; length, 1–5 μm)	Human bronchial epithelial BEAS-2B or mesothelial MeT-5A cells	DNA adduct M1dG, immune-slot blot	1–160 μg/cm²	+	Increase in adducts in both cell lines after 48-h treatment; decrease in adducts in MeT-5A cells after 72-h treatment	Lindberg et al. (2013)
MWCNT (diameter, 10–30 nm; length: 1–2 μm)	Human bronchial epithelial BEAS-2B or mesothelial MeT-5A cells	DNA adducts M1dG, immune-slot blot	1–160 μg/cm²	–	Decrease in adducts in both cell lines after 72-h treatment	Lindberg et al. (2013)
SWCNT (diameter, 1–2 nm; length, 0.4–0.8 μm or 5–30 μm)	Human lymphoblastoid MCL-5 cells	*HGPRT* locus gene mutation frequency (forward mutation)	25–100 μg/mL	+ with short CNT – with long CNT		Manshian et al. (2013)
SWCNT (diameter, 12 nm; length < 5 μm; < 1% impurities)	Primary mouse embryo fibroblasts	DNA strand breaks, comet assay	5 μg/mL	+		Yang et al. (2009)
MWCNT (diameter, 67–70 nm; length, 1.1–1.2 μm; SSA, 52–60 m²/g) either pristine (iron, 0.5%) or purified (iron, 0.002%)	Mouse alveolar macrophage MH-S cells	DNA strand breaks, comet assay	50 μg/cm²	+ with pristine – with purified		Aldieri et al. (2013)

Table 4.7 Studies of DNA damage and mutation in experimental systems after exposure to carbon nanotubes in vitro (continued)

Material[a]	Cells	End-point, test system	Concentration (LEC or HIC)[b]	Results[c]	Comments	Reference
SWCNT (diameter, 0.9–1.7 nm; length < 1 µm; SSA, 731 m²/g; iron, 2%)	Mouse lung epithelial FE1-MML cells	DNA strand breaks and FPG-sensitive sites, comet assay	100 µg/mL	– DSB + FPG	Unaltered level of DNA strand breaks; increased levels of FPG-sensitive sites	Jacobsen et al. (2008)
SWCNT (diameter, 1.2–1.5 nm; length, 2–5 µm; nickel, 1.5%)	Mouse macrophage RAW 264.7 cells	DNA strand breaks, comet assay	3–50 µg/mL	+	Bell-shaped concentration–response relationship	Di Giorgio et al. (2011)
MWCNT (diameter, 10–25 nm; length, 0.5–50 µm; SSA, 400 m²/g; nickel, 1.5%)	Mouse macrophage RAW 264.7 cells	DNA strand breaks, comet assay	3–50 µg/mL	+	Bell-shaped concentration–response relationship	Di Giorgio et al. (2011)
SWCNT (diameter, 0.7–1.2 nm; length, 0.5–100 µm; SSA, 400 m²/g) and MWCNT (diameter, 110–170 nm; length, 5–9 µm; SSA, 22 m²/g; iron < 0.1%)	Mouse macrophage RAW 264.7 cells	DNA strand breaks, ENDOIII- and FPG-sensitive sites, comet assay	1–100 µg/mL	+ DSB + FPG + ENDOIII	Increased levels of DNA strand breaks and ENDOIII- and FPG-sensitive sites (increase in oxidized purines and pyrimidines) with both CNT	Migliore et al. (2010)
MWCNT defined as "short" (diameter, 7–180 nm; length, 0.1–5 µm) and "long" (diameter, 8–177 nm; length, 0.1–20 µm)	Rat kidney epithelial NRK-52E cells	DNA strand breaks, comet assay	20–200 µg/mL	+ with long CNT – with short CNT	Levels of DNA strand breaks in unexposed cells not reported	Barillet et al. (2010)
SWCNT (diameter, 0.8–12 nm; length, several µm; iron, 0.62%)	Rat aortic endothelial cells	DNA strand breaks, comet assay	50–200 µg/mL	+	Dose–response increase; uncertainty about replicates being independent experiments	Cheng et al. (2012)
SWCNT (diameter, 0.4–1.2 nm; length, 1–3 µm; SSA, 1040 m²/g; iron, 0.23%)	Chinese hamster lung V79 fibroblasts	DNA strand breaks, comet assay	24–96 µg/cm²	+		Kisin et al. (2007; 2011)
MWCNT (length, 7.4 µm)	Chicken DT40 lymphoid cells	DNA adduct 8-oxodG, immunostaining	5 µg/mL	+		Mohiuddin et al. (2014)
MWCNT (characteristics not given)	Mouse embryonic stem cells	Aprt locus, gene mutation frequency	5 µg/mL	+		Zhu et al. (2007)
SWCNT (diameter, 0.9–1.7 nm; length < 1 µm;	FE1-Muta™ mouse lung epithelial cells	cII locus, gene mutation frequency	100 µg/mL	–		Jacobsen et al. (2008)

Table 4.7 (continued)

Material[a]	Cells	End-point, test system	Concentration (LEC or HIC)[b]	Results[c]	Comments	Reference
MWCNT (diameter, 88 nm; length, 5 μm)	Chinese hamster lung CHL/IU cells	*Hgprt* locus, gene mutation frequency	3.3–100 μg/mL	–		Asakura et al. (2010)

[a] Nanomaterial characteristics include diameter, length, specific surface area (SSA), and content of transition metals

[b] LEC, lowest effective concentration; HIC, highest ineffective concentration

[c] +, positive; –, negative

Aprt, adenine phosphoribosyltransferase; CNT, carbon nanotubes; DSB, DNA strand breaks; ENDO-III, endonuclease-III; FPG, formamidopyrimidine glycosylase; *Hgprt*, hypoxanthine–guanine phosphoribosyltransferase; HPLC-ECD, high-performance liquid chromatography-electrochemical detection; M1dG, *N*1-*N*2malondialdehyde-2′-deoxyguanosine; MWCNT, multiwalled carbon nanotubes; 8-oxodG, 8-oxodeoxyguanosine; SWCNT, single-walled carbon nanotubes

Exposure to SWCNT increased the level of FPG-sensitive sites in FE1-MML mouse lung epithelial and human hepatoblastoma HepG2 cells (Jacobsen et al., 2008; Vesterdal et al., 2014b). Both SWCNT and MWCNT increased the level of ENDOIII- and FPG-sensitive sites in rat RAW 264.7 macrophages (Migliore et al., 2010), but the levels of FPG-sensitive sites in human lung adenocarcinoma A549 cells were unaltered after exposure to MWCNT, although the validity of this observation is questionable due to the lack of a positive control (Cavallo et al., 2012). Another study also found unaltered levels of FPG-sensitive sites in A549 cells after exposure to MWCNT (Karlsson et al., 2008). [The Working Group noted that the increased levels of FPG-sensitive sites were observed in cells after exposure to zinc oxide and copper oxide nanoparticles, indicating a reliable methodology for measuring oxidative damage to DNA.]

Exposure of human colon carcinoma cells to SWCNT did not increase the level of extra FPG sites (Pelka et al., 2013). Exposure to two different types of MWCNT increased the levels of total sites in human hepatoblastoma cells after treatment with FPG, whereas the FPG-modified assay generated fewer lesions compared with DNA strand breaks with one type of MWCNT (NM 402) but not with the other (NM 400) (Kermanizadeh et al., 2012). The same authors also showed increased levels of total sites in renal cells exposed to the same types of MWCNT, but the net level of FPG-sensitive sites did not appear to differ between exposed and unexposed cells (Kermanizadeh et al., 2013), indicating that the exposure to MWCNT was not associated with specific oxidative damage to DNA nucleobases but did seem to generate DNA strand breaks. Exposure of human HaCaT keratinocytes to MWCNT was associated with increased levels of total FPG sites (McShan & Yu, 2014).

Increased levels of lipid peroxidation product-derived 3-(2′-deoxy-β-D-erythropentofuranosyl)-pyrimido[1,2-α]-purin-10(3H)-one] adducts [M1dG or $N1N^2$malondialdehyde-2′-deoxyguanosine] were detected by immunoblot in human bronchial epithelial BEAS-2B and human pleural mesothelial Met-5A cells, after 48 hours of exposure to SWCNT but decreased levels 72 hours after exposure (Lindberg et al., 2013). No increase in the levels of 8-oxodG, measured by high-performance liquid chromatography with electrochemical detection, were observed in human pleural mesothelial Met-5A cells after exposure to SWCNT or MWCNT (Ogasawara et al., 2012). [The Working Group noted the uncertainty that replicates were independent experiments.] However, the baseline level of 8-oxodG (8 lesions/10^6 dG) was high, indicating spurious oxidation of DNA during the processing or analysis of samples (Ogasawara et al., 2012). [In keeping with the recommendations of the European Committee on Oxidative DNA Damage, reports with baseline levels of 8-oxodG higher than 5 lesions/10^6 dG in unexposed cells or animals should be interpreted with caution because of the risk of flawed methodology (ESCODD, 2003).] One study investigated oxidative damage to DNA in cells using antibody-based techniques, and showed increased levels of 8-oxodG by immunostaining in chicken lymphoid cells after exposure to MWCNT (Mohiuddin et al., 2014).

(ii)   Gene mutations

Exposure of mouse embryonic stem cells to MWCNT increased the mutation frequency in the adenine phosphoribosyltransferase (*Aprt*) gene (Zhu et al. 2007). However, mutation frequency in the hypoxanthine-guanine phosphoribosyltransferase (*Hgprt*) gene was unaltered after Chinese hamster lung cells were exposed to MWCNT (Asakura et al., 2010). Increased levels of mutations in the *Hgprt* gene were observed in human lymphoblastic MCL-5 cells after exposure to SWCNT with a length of 1–3 μm, whereas shorter (0.4–0.8 μm) and longer (5–30 μm) nanotubes were not associated with mutagenicity (Manshian et al., 2013). Long-term

exposure (24 days) of FE1-Muta™Mouse lung epithelial cells to SWCNT (length < 1 μm) did not increase the frequency of mutation in the *cII* gene (Jacobsen et al., 2008).

(iii) Micronucleus formation

The results on the induction of micronuclei in cultured cells after exposure to CNT have been conflicting. No difference between the distribution of studies showing an increased formation of micronuclei or a null effect was apparent, with regard to the use of the cytokinesis-block micronucleus protocol or other protocols to score micronuclei. Specific assay protocols have therefore not been highlighted in the descriptions of the findings in cell cultures. Table 4.8 lists the studies that have assessed chromosomal alterations in cell cultures after exposure to CNT.

The assessment of micronucleus frequency in human lymphocytes after exposure to six different types of MWCNT did not show a monotonic concentration–response relationship, although one sample with a short fibre length (0.4 μm) gave statistically significant results at all concentrations tested and one other sample yielded increased micronucleus frequencies at a low concentration of 2.5 μg/mL. The diameter and length of the tubes could not explain the observed results and other structural differences, including surface area and transition metal content, might be implicated (Tavares et al., 2014). Observations from cultured lymphocytes indicated no effect on micronucleus formation after exposure to MWCNT (Szendi & Varga, 2008), whereas both MWCNT and SWCNT increased the frequency of micronuclei in another study in lymphocytes (Cveticanin et al., 2010). Exposure to SWCNT was also associated with an increased frequency of micronuclei in phytohaemagglutinin-stimulated human lymphocytes (Kim & Yu, 2014). Increased frequencies of micronuclei (Kato et al., 2013) or no increase in micronuclei (Thurnherr et al., 2011) were observed in human lung adenocarcinoma A549 cells after exposure

to MWCNT. Exposure of human immortalized bronchial epithelial BEAS-2B cells to SWCNT yielded either a null effect (Lindberg et al., 2009, 2013) or an increased frequency of micronuclei (Manshian et al., 2013). Similarly, hamster lung V79 fibroblasts responded with unaltered micronucleus frequency (Kisin et al., 2007; Pelka et al., 2013) or increased micronucleus frequency (Asakura et al., 2010; Cicchetti et al., 2011; Kisin et al., 2011) after exposure to either SWCNT or MWCNT. Increased micronucleus frequencies were also observed in human breast epithelial MCF-7 and lung adenocarcinoma A549 cells, rat lung epithelial cells, mouse RAW 264.7 macrophages, and human B-lymphoblastoid MCL-5 cells after exposure to either MWCNT or SWCNT (Muller et al., 2008b; Di Giorgio et al., 2011; Kato et al., 2013; Manshian et al., 2013). A sample of MWCNT with a relatively short fibre length (0.7 μm) and low transition metal content (iron, 0.48%; cobalt, 0.49%) was used to study the impact of structural defects and metals content on the formation of micronuclei in rat lung epithelial cells. Ground MWCNT (producing structural defects) increased the micronucleus frequency, whereas heated (2400 °C) ground MWCNT (which ablates the structural defects and eliminates metals) did not (Muller et al., 2008a).

[Collectively, cell culture studies document the ability of MWCNT and SWCNT to increase the frequency of micronuclei in proliferating cells, although substantial differences in effects were seen between studies, possibly originating from differences in cell types, characteristics of the CNT, dispersion protocols, and assay conditions.]

(iv) Chromosomal aberrations

Table 4.8 lists in-vitro investigations in which established cell lines were exposed to SWCNT and MWCNT.

Increased chromosome breakage and aneuploid cells were demonstrated in mouse

Table 4.8 Studies of micronucleus frequency, chromosomal aberrations, and sister-chromatid exchange in experimental systems after exposure to carbon nanotubes in vitro

Material[a]	Cells	End-point, test system	Concentration (LEC or HIC)[b]	Result[c]	Comments	Reference
MWCNT (six different samples): NM400 (diameter, 11 nm; length, 0.7 µm; SSA, 280 m²/g), NM401 (diameter, 63 nm; length, 3.4 µm; SSA, 300 m²/g), NM402 (diameter, 11 nm; length, 1.1 µm; SSA, 250 m²/g), NM403 (diameter, 11 nm; length, 0.4 µm), NRCWE (diameter, 69 nm; length, 44 µm; SSA, 24–28 m²/g), and NRCWE-007 (diameter, 15 nm; length, 0.4 µm; SSA, 233 m²/g)	Human lymphocytes	Micronucleus, CBMN assay	2.5–250 µg/mL	+ with NM403 + with NRCWE (+) with NM402 – with NM400, NM401, and NRCWE-007	Increased frequency of micronuclei at all concentrations of NM403; NRCWE associated with increased micronucleus frequency at two low concentrations (2.5 and 15 µg/mL); micronucleus frequency increased at one concentration of NM402 (15 µg/mL), but regarded as an equivocal result	Tavares et al. (2014)
MWCNT (diameter, 10–30 nm; length, 1–2 µm)	Human lymphocytes	Micronucleus formation, CBMN assay	1000 µg/mL	–	No changes in micronucleus frequency (CBMN on samples from three different donors)	Szendi & Varga (2008)
MWCNT (diameter, 20–40 nm; length, 1–5 µm; 1% impurities), and pristine or amide-functionalized SWCNT (30% impurities)	Human lymphocytes	Micronucleus formation, CBMN assay	25–150 µg/mL	+	Increased micronucleus frequency by MWCNT and SWCNT (both pristine and functionalized form); decreased CBPI at high concentrations	Cveticanin et al. (2010)
SWCNT (diameter, 1–1.2 nm; length, 20 µm)	Human lymphocytes	Micronucleus formation	25–100 µg/mL	+		Kim & Yu (2014)
MWCNT (diameter, 6–24 nm; length, 2–5 µm; < 0.4% impurities)	Human lung adenocarcinoma A549 cells	Micronucleus formation	2.8–11.3 µg/mL	–		Thurnherr et al. (2011)
MWCNT (diameter, 90 nm; length, 2 µm)	Human lung adenocarcinoma A549 cells	Micronucleus formation	20–200 µg/mL	+		Kato et al. (2013)
Mixed CNT (more than 50% SWCNT; diameter, 1.1 nm; length, 0.5–100 µm)	Human bronchial epithelial BEAS-2B cells	Micronucleus formation	1–100 µg/cm²	–	Decreased CBPI at high concentrations	Lindberg et al. (2009)

Table 4.8 (continued)

Material[a]	Cells	End-point, test system	Concentration (LEC or HIC)[b]	Result[c]	Comments	Reference
SWCNT (diameter < 2 nm; length, 1–5 μm) and MWCNT (diameter, 10–30 nm; length, 1–2 μm)	Human bronchial epithelial BEAS-2B cells	Micronucleus formation	5–200 μg/cm^2	–	Decreased CBPI at high concentrations with MWCNT	Lindberg et al. (2013)
SWCNT: short (diameter, 1–2 nm; length, 0.4–0.8 μm; SSA, 585 m^2/g), medium (diameter, 1–2 nm; length, 1–3 μm; SSA, 337 m^2/g), or long (diameter, 1–2 nm; length, 5–30 μm; SSA, 310 m^2/g); with few impurities	Human bronchial epithelial BEAS-2B or lymphoblastoid MCL-5 cells	Micronucleus formation	1–100 μg/mL	+	Increased micronucleus frequency in both BEAS-2B and MCL-5; unaltered CBPI	Manshian et al. (2013)
MWCNT (diameter, 11 nm; length, 0.7 μm; 2% impurities)	Human breast epithelial MCF-7 cells	Micronucleus formation, CBMN and FISH using a pancentrometric probe	10–50 μg/mL	+	Dose-dependent increase in micronucleus frequency, induction of both centromere-positive and -negative micronuclei; no clear dose-dependent effect on CBPI	Muller et al. (2008b)
MWCNT (diameter, 1.6 nm; length, 0.8 μm; SSA, 407 m^2/g; 10% impurities)	Human gingival fibroblasts	Micronucleus formation, CBMN assay	50–150 μg/mL	+	Bell-shaped dose–response curve (maximal micronucleus frequency at 100 μg/mL); decreased CBPI at high concentrations	Cicchetti et al. (2011)
SWCNT (diameter, 1–4 nm; length, 0.5–1.0 μm; SSA, 1040 m^2/g; iron, 0.23%)	Primary human respiratory epithelial SAEC or human bronchial epithelial BEAS-2B cells	Chromosomal aberrations, aneuploidy (FISH), and multipolar mitotic spindles (dual-label immunofluorescence)	24–96 μg/cm^2	+	Significant dose-response relationship for aneuploidy and multipolar mitotic spindles	Sargent et al. (2009)
SWCNT (diameter, 1.0 nm; length, 0.5–1.0 μm; SSA, 1040 m^2/g; iron, 0.23%)	Primary human respiratory epithelial SAEC or human bronchial epithelial BEAS-2B cells	Chromosomal aberrations, aneuploidy (FISH), and multipolar mitotic spindles (dual-label immunofluorescence)	0.024–24 μg/cm^2	+	Significant dose-response relationship for aneuploidy including an equal number of chromosome losses and gains; a dose–response relationship for multipolar mitotic spindles	Sargent et al. (2012a)

Table 4.8 Studies of micronucleus frequency, chromosomal aberrations, and sister-chromatid exchange in experimental systems after exposure to carbon nanotubes in vitro (continued)

Material[a]	Cells	End-point, test system	Concentration (LEC or HIC)[b]	Result[c]	Comments	Reference
MWCNT (diameter, 10–20 nm; length, 1 μm; iron, 0.03%; no cobalt or nickel content)	Human bronchial epithelial BEAS-2B cells	Chromosomal aberrations, disrupted mitotic spindle	0.024–24 μg/mL	+	Dose–response relationship for aneuploidy and polyploidy; errors in chromosome number included more chromosome gains than losses; dose–response relationship for disrupted mitotic spindle predominantly with a single pole	Sargent et al. (2012b), Siegrist et al. (2014)
SWCNT (diameter < 2 nm; length, 1.5 μm; SSA, 436 m²/g) and MWCNT (diameter, 10–30 nm; length, 1–2 μm; SSA, 60 m²/g)	Human lymphocytes	Chromosomal aberrations	6.25–300 μg/mL	+	Increased chromatid and chromosome-type breakage with both CNT	Catalán et al. 2012
MWCNT (diameter, 10–30 nm; length, 1–2 μm)	Human lymphocytes	Sister-chromatid exchange, 5-BrdU incorporation	1000 μg/mL	–		Szendi & Varga (2008)
MWCNT (diameter, 10–25 nm; length, 0.5–50 μm; SSA, 400 m²/g; nickel, 1.5%) and SWCNT (diameter, 1.2–1.5 nm; length, 2–5 μm; nickel, 1.5%)	Mouse macrophage RAW 264.7 cells	Micronucleus formation	1–10 μg/mL	+	Dose-dependent increase; same effect with both CNT	Di Giorgio et al. (2011)
MWCNT (diameter, 11 nm; length, 0.7 μm; 2% impurities)	Rat lung epithelial cells	Micronucleus formation, CBMN assay	10–50 μg/mL	+	Dose-dependent increase	Muller et al. (2008b)
MWCNT (diameter, 20–50 nm; length, 0.7 μm; iron, 0.48%; cobalt, 0.49%) ground to produce structural defects and/or heated (2400 °C) to eliminate metals and defects	Rat lung epithelial cells	Micronucleus formation, CBMN assay	25 μg/mL	+ with CNTg – with CNTg before heating + with heating before CNTg	Ground CNT (CNTg) increased micronucleus frequency, whereas ground and subsequently heated (2400 °C) sample did not; MWCNT that were heated (2400 °C) and subsequently ground increased the micronucleus frequency	Muller et al. (2008a)

Table 4.8 (continued)

Material[a]	Cells	End-point, test system	Concentration (LEC or HIC)[b]	Result[c]	Comments	Reference
SWCNT (diameter, 0.4–1.2 nm; length, 1–3 μm; SSA, 1040 m²/g; iron, 0.23%)	Hamster lung V79 fibroblasts	Micronucleus formation	12–96 μg/cm²	–	No increase in micronucleus formation (cytotoxicity up to ~70%)	Kisin et al. (2007)
SWCNT (diameter, 0.4–1.2 nm; length, 1–3 μm; SSA, 1040 m²/g; iron, 0.23%)	Hamster lung V79 fibroblasts	Micronucleus formation	12–48 μg/cm²	+		Kisin et al. (2011)
SWCNT (diameter, 1.8 nm; length, 0.5 μm)	Hamster lung V79 fibroblasts	Micronucleus formation	10 pg/mL– 0.2 μg/mL	–	Unaltered micronucleus frequency, assessed by similar number of kinetochore-negative cells in SWCNT-treated and control groups	Pelka et al. (2013)
MWCNT (diameter, 88 nm; length, 5 μm)	Chinese hamster lung CHL/IU cells	Micronucleus formation	0.02–5 μg/mL	+	Significant dose-dependent increase in the number of micronuclei, especially related to bi- and multinucleated cells	Asakura et al. (2010)
MWCNT (diameter, 10–25 nm; length, 0.5–50 μm; SSA, 400 m²/g; nickel, 1.5%) and SWCNT (diameter, 1.2–1.5 nm; length, 2–5 μm; nickel, 1.5%)	Mouse macrophage RAW 264.7 cells	Chromosomal aberrations	1–10 μg/mL	+	Increased percentage of cells with chromosomal aberrations: acentric fragments, centrometric fusion, breaks, chromatid separation, and polyploidy with both CNT	Di Giorgio et al. (2011)
MWCNT (diameter, 88 nm; length, 5 μm)	Chinese hamster lung CHL/IU cells	Chromosomal aberrations	0.8–5 μg/mL	+	Dose-dependent increase in polyploidy (numerical chromosomal aberrations); no structural chromosomal changes	Asakura et al. (2010)
SWCNT (diameter, 1.8 nm; SSA, 878 m²/g; iron, 4.4%)	Chinese hamster lung fibroblast CHL/IU cells	Chromosomal aberrations with and without S9	6.25–100 μg/mL	–	No increase in the number of structural or numerical chromosomal aberrations (polyploidy) with or without S9	Ema et al. (2013b)

Table 4.8 Studies of micronucleus frequency, chromosomal aberrations, and sister-chromatid exchange in experimental systems after exposure to carbon nanotubes in vitro (continued)

Material[a]	Cells	End-point, test system	Concentration (LEC or HIC)[b]	Result[c]	Comments	Reference
MWCNT (high- or low-aspect-ratio: diameter, 10–15 or ~10 nm; length, 0.15 or 10 μm; SSA, 178 or 195 m²/g; iron, 1% or 5%; respectively)	Chinese hamster ovary CHO-k1 cells	Chromosomal aberrations with and without S9	1.6–12.5 μg/mL	–	No increase in chromatid-type breakage or exchange with or without S9	Kim et al. (2011)
SWCNT (diameter, 3 nm; length, 1.2 μm; SSA, 1064 m²/g)	Chinese hamster lung fibroblast CHL/IU cells	Chromosomal aberrations with and without S9	300–1000 μg/mL	–	No increase in chromosomal gaps or polyploidy with or without S9	Naya et al. (2011)
MWCNT (diameter, 90 nm; length, 2 μm)	Chinese hamster ovary CHO AA8 cells	Sister-chromatid exchange	0.1–2 μg/mL	+		Kato et al. (2013)

[a] Nanomaterial characteristics include diameter, length, specific surface area (SSA), and content of transition metals
[b] LEC, lowest effective concentration; HIC, highest ineffective concentration
[c] +, positive; –, negative; (+), weakly positive
5-BrdU, 5-bromo-2′-deoxyuridine; CBMN; cytokinesis-block micronucleus assay; CBPI, cytokinesis-block proliferation index; CNT, carbon nanotubes; FISH, fluorescence in situ hybridization; MWCNT, multiwalled carbon nanotubes; S9, metabolic activation system; SWCNT, single-walled carbon nanotubes

macrophage RAW 264.7 cell lines, Chinese hamster lung (CHL/IU) cell lines, primary human respiratory epithelial SAEC cell lines, and human bronchial epithelial BEAS-2B cells (Sargent et al., 2009, 2012a; Asakura et al., 2010; Di Giorgio et al., 2011; Siegrist et al., 2014). Other investigations in immortalized Chinese hamster lung fibroblasts and Chinese hamster ovary cells did not show increased aneuploidy or chromosomal aberrations after exposure to SWCNT (Naya et al., 2011; Ema et al., 2013b) or MWCNT (Kim et al., 2011). Both SWCNT and MWCNT increased chromosome and chromatid breakage in phytohaemagglutinin-stimulated human lymphocytes (Catalán et al., 2012).

Chromosome breakage and translocations between chromosomes were observed in an immortalized mouse macrophage RAW 264.7 cell line after exposure to 10 µg/mL of SWCNT or MWCNT. The modal number of the macrophage cell line karyotype was 40 chromosomes; however, the mean number of chromosomes per cell after exposure to either SWCNT or MWCNT was 20–60 with no distinct modal number, indicating a high degree of aneuploidy in the original cell line (Di Giorgio et al., 2011). Asakura et al. (2010) demonstrated an 8–34-fold increase in polyploidy in Chinese hamster lung cells treated with MWCNT (diameter, 88 nm; length, 5 µm). The authors of both studies attributed the increase in polyploid cells to a failure of cytokinesis (Asakura et al., 2010; Di Giorgio et al., 2011).

Chromosome breakage and errors in chromosome number were observed in cultured primary human respiratory epithelial cells after exposure to either SWCNT or MWCNT determined by analysis of chromosomes spreads or fluorescence in situ hybridization. The analysis of cultured primary human respiratory cells exposed to SWCNT demonstrated significantly increased aneuploidy, which was due to an equal number of gains and losses of chromosomes, while MWCNT-exposed cells had a significantly greater number of chromosomal gains than

losses, indicating polyploidy (Sargent et al., 2009, 2012a, b; Siegrist et al., 2014).

[Collectively, in-vitro investigations in immortalized and primary cells documented the ability of CNT to increase the frequency of chromosomal damage and aneuploidy in proliferating cells. Similar to the results from studies of micronucleus frequency after exposure to CNT, substantial effect differences between studies were found, possibly originating from differences in cell types, characteristics of CNT, dispersion protocols, and assay conditions.]

(v) Alterations in the mitotic spindle, cell cycle, and sister-chromatid exchange

The data that demonstrated chromosomal damage and errors in chromosomes after in-vitro exposure to either SWCNT or MWCNT (see Table 4.8) suggested an alteration in the integrity of the mitotic spindle, which was investigated by exposure to SWCNT (diameter, 1.0 nm) or MWCNT (diameter, 10–20 nm). The exposure to 1-nm SWCNT resulted in mitotic spindles with multiple poles (Sargent et al., 2009, 2012a), while cells treated with 10–20-nm MWCNT had mitotic spindles with one pole (Sargent et al., 2012b; Siegrist et al., 2014). Three-dimensional reconstructions of 0.1-µm optical sections showed CNT integrated with microtubules, DNA and within the centrosome structure. Further analysis by confocal microscopy and TEM demonstrated fragmented centrosomes after exposure to either SWCNT or MWCNT (Sargent et al., 2009, 2012a, b; Siegrist et al., 2014). The mitotic disruption associated with SWCNT treatment resulted in a G2/M block in the cell cycle while MWCNT treatment was associated with a block in G1/S (Sargent et al., 2009, 2012b; Siegrist et al., 2014). [When mammalian cells are exposed to agents that cause a block in the S-phase, the DNA is repaired by homologous recombination. The increased recombination between sister chromatids can be observed by the incorporation of 5-bromodeoxyuridine. The

increase in sister chromatid exchange suggests genotoxicity (Pfuhler et al., 2013).] The observation of increased sister-chromatid exchange in Chinese hamster ovary AA8 cells after exposure to MWCNT 90 nm in diameter further suggests a block in the S-phase (Kato et al., 2013).

[To date, four studies have shown CNT-induced mitotic spindle and cell-cycle disruption and three investigations demonstrated CNT-mediated centrosome disruption. These investigations documented the ability of CNT to disrupt the mitotic spindle, fragment the centrosome, and cause a block in the cell cycle in cultured cells.]

(vi) Mutation in bacteria

See Table 4.9

The mutagenic effect of MWCNT was evaluated in the bacterial reverse mutation assay (Ames test) in *Salmonella typhimurium* TA98 and TA100 and in *Escherichia coli* WP2uvrA in the presence and in absence of a metabolic activation system. MWCNT did not produce mutagenic effects at any concentration tested. In *S. typhimurium* TA98 in absence of metabolic activation, a reduction in the number of spontaneous revertant colonies was observed at concentrations ranging from 0.13 to 9.0 µg/plate, which was not concentration-dependent. In this bacterial strain, spontaneous mutational DNA damage is reverted to wild-type by specific mechanisms of frameshift (Di Sotto et al., 2009).

Kim et al. (2011) studied high-aspect-ratio (diameter, 10–15 nm; length, ≈10 nm) and low-aspect-ratio (diameter, 10–15 nm; length, ≈150 nm) MWCNT. Neither the high- nor the low-aspect-ratio MWCNT induced genotoxicity in the bacterial reverse mutation test in *Salmonella typhimurium* TA98, TA100, TA1535 and TA1537, and in *Escherichia coli* WP2uvrA in the presence and in absence of a metabolic activation system.

4.4 Other mechanisms of carcinogenesis

No published studies concerning the health effects of CNT in exposed humans were available to the Working Group. The body of relevant literature primarily comprises in-vivo studies in experimental animals, in-vitro studies using human cell lines, and a limited number of studies of occupational exposure (see Section 1, Table 1.5).

There were no studies in humans exposed to CNT only. However, four studies have been published in which several biological end-points of an occupational cohort (in Taiwan, China) exposed to engineered nanomaterials (*n* = 241) were compared with those of an unexposed control group (*n* = 196). Among the population exposed to engineered nanomaterials, a subgroup of workers (*n* = 57) was exposed to CNT originating from three facilities that used CNT and one facility that used and produced CNT. [The Working Group noted that the number of subjects in each individual study varied, probably due to missing data on specific end-points or follow-up. With the exception of the study describing the results on fractional exhaled nitric oxide, the studies did not report results separately for the CNT-exposed population.] Wu et al. (2014) described an increase in fractional exhaled nitric oxide in workers exposed to nanomaterials, that was limited to the population exposed to titanium dioxide (β = 0.351, SE = 0.166; *P* = 0.035). Results among CNT-exposed workers (*n* = 57) were null (β = 0.045, SE = 0.124; *P* = 0.715). Liou et al. (2012) studied approximately the same population and measured antioxidant enzyme activities, markers of inflammation and oxidative damage, cardiovascular biomarkers, genotoxicity, lung function, and neurobehavioural functions. In a cross-sectional evaluation, associations were found with significantly lower antioxidant enzyme activity (i.e. superoxide dismutase [SOD]), elevated markers of

Table 4.9 Studies of mutation in bacteria exposed to carbon nanotubes

Material[a]	Cells	End-point	Concentration (LEC or HIC)[b]	Results[c] Without metabolic activation system	With metabolic activation system	Reference
MWCNT (diameter, 110–170 nm; length, 5–9 µm)	*Salmonella typhimurium* TA98 and TA100 and *Escherichia coli* WP2 uvrA	Reverse mutation	9.0 µg/plate	–	–	Di Sotto et al. (2009)
MWCNT (high-aspect-ratio: diameter, 10–15 nm; length, ≈10 µm; low-aspect-ratio: diameter, 10–15 nm; length, ≈150 nm)	*Salmonella typhimurium* TA98, TA100, TA1535, and TA1537	Reverse mutation	1000 µg/plate	–	–	Kim et al. (2011)
MWCNT (diameter, 110–170 nm; length, 5–9 µm)	*Escherichia coli* WP2 uvrA	Reverse mutation	9.0 µg/plate	–	–	Di Sotto et al. (2009)
MWCNT (high-aspect-ratio: diameter, 10–15 nm; length, ≈10 µm; low-aspect-ratio: diameter, 10–15 nm; length, ≈150 nm)	*Escherichia coli* WP2 uvrA	Reverse mutation	1000 µg/plate	–	–	Kim et al. (2011)

[a] Nanomaterial characteristics include diameter and length
[b] LEC, lowest effective concentration; HIC, highest ineffective concentration
[c] +, positive; –, negative
MWCNT, multiwalled carbon nanotubes

cardiovascular disease (i.e. fibrinogen and intercellular adhesion molecule-1), and reduced neurobehavioural function. No specific analyses for the CNT-exposed population (n = 52) were presented. In a longitudinal analysis of a subpopulation of the same population with a follow-up of 6 months, Liao et al. (2014a) reported a significant association between exposure to engineered nanomaterials and an increase in antioxidant enzymes (SOD and GSH peroxidase [GPx]) and cardiovascular markers (vascular cell adhesion molecule and paraoxonase) among exposed workers compared with control workers over the follow-up period. The results were not presented by subtype of engineered nanomaterials. Liao et al. (2014b) studied the same exposed population for work-related symptoms and diseases and reported a significant worsening of allergic dermatitis among workers exposed to engineered

nanomaterial. No specific results for workers exposed to CNT were presented.

[The Working Group noted that the exposure assessments of Liao et al. (2014a, b), Liou et al. (2012), and Wu et al. (2014) were based on the control-banding approach of Paik et al. (2008). The exposure scores were based on both an estimate of nano-toxicity and the expected probability of exposure. The selection of controls for the above studies was not clearly described, although confounding factors did not seem to differ between the exposed and unexposed workers except for sex and level of education.]

4.4.1 Inflammasome activation

(a) Human cells in vitro

An interlaboratory validation study confirmed the extracellular release of IL-1β from the human THP-1 macrophage cell line exposed to as-produced MWCNT (Cheap Tubes Inc., Brattleboro, VT, USA) at non-cytotoxic doses (Xia et al., 2013). A comprehensive analysis of surface functionalization of the as-produced MWCNT (Li et al., 2013), and the dispersion of MWCNT in bovine serum albumin or by the triblock copolymer Pluronic F108 (Wang et al., 2012a) showed that surface charge, chemical functionalization, and dispersal state were important determinants of inflammasome activation and release of IL-1β from THP-1 macrophages. Anionic functionalization (carboxylate or PEG) decreased, cationic functionalization (polyetherimide) increased (Li et al., 2013), and dispersion (using Pluronic F108) prevented (Wang et al., 2012a) the release of IL-1β from THP-1 macrophages .

Platelet-derived growth factor (PDGF), in combination with transforming growth factor (TGF)-β, activates the "epithelial-mesenchymal trophic unit" in the lungs resulting in collagen deposition and fibrosis (reviewed in Bonner et al., 2013). These reciprocal interactions of cytokines and growth factors, initiated by inflammasome activation and the release of IL-1β from macrophages, were repeated in transwell co-cultures of human THP-1 macrophages and immortalized human BEAS-2B lung epithelial cells exposed to as-produced or cationic functionalized MWCNT (Wang et al., 2012a; Li et al., 2013).

Hamilton et al. (2013b) used the same as-produced MWCNT with variable diameters and lengths to assess the role of dimensions in the release of IL-1β from human THP-1 macrophages or murine primary alveolar macrophages. MWCNT with a greater diameter (30–50 nm) or length (10–30 μm) were more potent in inducing the release of IL-1β than shorter (length < 2 μm) or thinner (diameter, 10–20 nm) MWCNT. These investigators also studied a panel of nine MWCNT (including the as-produced sample from Cheap Tubes) and compared their potency for inflammasome activation and IL-1β and IL-18 release in primary murine alveolar macrophages co-stimulated with 20 ng/mL of lipopolysaccharide (LPS). Linear regression analysis demonstrated a significant correlation between the nickel content of the MWCNT samples and the release of IL-1β (Hamilton et al., 2012). Removal of nickel contaminants from the as-produced MWCNT sample slightly decreased the release of IL-1β in this in-vitro assay (Hamilton et al., 2013a). Haniu et al. (2011) confirmed that another commercial MWCNT sample (VGCF; Showa Denko, Tokyo, Japan) also induced IL-1β as well as the release of tumour necrosis factor (TNF)-α from human THP-1 macrophages. Inflammasome activation and IL-1β and IL-18 release was also induced by CNT (80% DWCNT; DWCNT, 0.1–100 μm in length) synthesized by CVD in human peripheral blood monocytes primed with LPS (Meunier et al., 2012).

(b) Experimental systems in vivo

See Table 4.10

(i) Inhalation

Three 13-week studies of two MWCNT and one CNF in Wistar rats showed that exposure to MWCNT induced persistent inflammation. In the studies of Ma-Hock et al. (2009) and Pauluhn (2010b), these inflammatory responses to MWCNT were observed in the lungs of males and females. The response to CNF was observed at high concentration (Delorme et al., 2012). The minimum concentrations that induced persistent or moderate inflammation were 2.5 mg/m^3 and 1.5 mg/m^3 of MWCNT and 25 mg/m^3 of CNF (Ma-Hock et al., 2009; Pauluhn, 2010b). Histopathological analysis of the 13-week inhalation study of MWCNT of Ma-Hock et al.

Table 4.10 Studies of persistent inflammation, granulomatosis, and fibrosis in experimental animals after exposure to carbon nanotubes

Route of administration	Species, strain (sex)	Type of CNT	Exposure concentration or dose, duration	Recovery	Characterization of CNT	Inflammation	Fibrosis or granulomatosis	Reference
Inhalation								
Head/nose-only	Rat, Wistar (M, F)	MWCNT	0.1, 0.5, or 2.5 mg/m³, 6 h/day, 5 days/wk, 13 wk	None	Metal oxide, 10%; diameter, 5–15 nm; length, 0.1–10 μm; BET, 250–300 m²/g; MMAD, 0.5–1.3 μm	0.1 mg/m³ (minimal), 0.5 mg/m³ (slight), 2.5 mg/m³ (moderate)	Granulomatous inflammation: 0.1 mg/m³ (minimal), 0.5 mg/m³ (slight), 2.5 mg/m³ (moderate)	Ma-Hock et al. (2009)
Nose-only	Rat, Wistar (M, F)	MWCNT	0.1, 0.4, 1.5, or 6 mg/m³, 6 h/day, 5 days/wk, 13 wk	6 mo	Cobalt, 0.46–0.53%; BET, 253 m²/g; length, 200–300 nm	0.1 mg/m³ (none), 0.4 mg/m³ (transient), 1.5 mg/m³ (persistent), 6 mg/m³ (persistent)	0.1 mg/m³ (none), 0.4 mg/m³ (persistent), 1.5 mg/m³ (persistent), 6 mg/m³ (persistent)	Pauluhn (2010b)
Nose-only	Rat, Sprague-Dawley (M, F)	VGCF-H CNF	0.54 mg/m³ (4.9 f/mL), 2.5 mg/m³ (56 f/mL), or 25 mg/m³ (252 f/mL), 6 h/day, 5 days/wk, 13 wk	90 days	Carbon > 99.5%; diameter, 158 nm; length, 5.8 μm; BET, 13.8 m²/g	25 mg/m³ (persistent)		Delorme et al. (2012)
Whole-body	Rat, Wistar (M)	SWCNT	0.03 mg/m³(5 × 10⁴ particles/cm³) or 0.13 mg/m³(6.6 × 10⁴ particles/cm³), 6 h/day, 5 days/wk, 4 wk	3 mo	Diameter, 3 nm; BET, 1064 m²/g; 0.03% impurities	No persistent inflammation	No fibrosis	Morimoto et al. (2012a)
Whole-body	Rat, Wistar (M)	MWCNT	0.37 mg/m³ (> 70% individual fibres), 6 h/day, 5 days/wk, 4 wk	1 or 3 mo	Diameter, 44 nm; length, 1.1 μm; BET, 69 m²/g; iron, 0.0005%	No persistent inflammation	No fibrosis	Morimoto et al. (2012b)
Nose-only	Rat, Sprague-Dawley (M, F)	MWCNT	0.17, 0.49, or 0.96 mg/m³, 6 h/day, 5 days/wk, 4 wk	28 or 90 days	Cobalt < wt 2%; diameter, 10–15 nm; length, 330.18 μm; BET, 224.9 m²/g	No change in the inflammatory cytokines levels in BALF	CNT were located in the lung and pleura after 28-day exposure and up to 90 days after exposure	Kim et al. (2014)

Table 4.10 Studies of persistent inflammation, granulomatosis, and fibrosis in experimental animals after exposure to carbon nanotubes (continued)

Route of administration	Species, strain (sex)	Type of CNT	Exposure concentration or dose, duration	Recovery	Characterization of CNT	Inflammation	Fibrosis or granulomatosis	Reference
Nose-only	Rat, Wistar (M)	MWCNT	11 or 241 mg/m³, 6 h	90 days	Cobalt, 0.53%; BET, 253 m²/g; length, 200–300 nm	241 mg/m³ (persistent)	241 mg/m³ (persistent or slight)	Ellinger-Ziegelbauer & Pauluhn (2009)
Whole-body	Rat, F344 (M, F)	MWCNT	0.2, 1, or 5 mg/m³, 6 h/day, 5 days/wk, 13 wk	None	Fibre-like BET, 24–28 m²/g; length, 5.7 µm	From 0.2 mg/m³	Granulomatous changes: M, from 0.2 mg/m³; F, from 1 mg/m³	Kasai et al. (2015)
Nose-only	Mouse, C57BL/6 (M)	MWCNT	1 or 30 mg/m³, 6 h	1 day, 2, 6, or 14 wk	Diameter, 10–30 nm; length, 0.5–40 µm; BET, 40–300 m²/g		Subpleural fibrosis	Ryman-Rasmussen et al. (2009a)
Intratracheal administration								
Instillation	Rat, F344 (M)	MWCNT	40 or 160 µg	Up to 91 days	Diameter, 88 nm; length, 5 µm; iron, 0.44%	Persistent	Persistent	Aiso et al. (2010)
Instillation	Rat, Sprague-Dawley (M)	MWCNT	0.04, 0.2, or 1 mg/kg bw	Up to 6 mo	BET, 23.0 m²/g; length < 20 µm	Transient	Minimal (1 mg/kg)	Kobayashi et al. (2010)
Instillation	Rat, Wistar (M)	SWCNT	0.04, 0.2, 1, or 2 mg/kg bw	6 mo (3 mo for 2 mg/kg)	BET, 1064 m²/g; 0.03% impurities	0.04 mg/kg (transient), 1 mg/kg (persistent), 2 mg/kg (persistent)	Minimal (1 mg/kg)	Kobayashi et al. (2011)
Instillation	Rat, Wistar (M)	MWCNT	0.66 or 3.3 mg/kg bw	Up to 6 mo	Diameter, 44 nm; length, 1.1 µm; BET, 69 m²/g; iron, 0.0005%	0.66 mg/kg (transient), 3.3 mg/kg (persistent)	Transient	Morimoto et al. (2012b)
Instillation	Rat, Wistar (M)	SWCNT	0.66 or 1.32 mg/kg bw	Up to 6 mo	Diameter, 1.8 nm; BET, 878 m²/g	Persistent	Minimal	Morimoto et al. (2012c)
Instillation	Rat, CD (M)	SWCNT	1 or 5 mg/kg bw	Up to 3 mo	Nominal diameter, 1.4 nm; length, > 1 µm; agglomerated ropes, ~30 nm	Transient	Multifocal granulomas	Warheit et al. (2004)

Table 4.10 (continued)

Route of administration	Species, strain (sex)	Type of CNT	Exposure concentration or dose, duration	Recovery	Characterization of CNT	Inflammation	Fibrosis or granulomatosis	Reference
Instillation	Rat, Wistar (M)	SWCNT	0.2 or 0.4 mg	Up to 754 days	BET, 877.7 m^2/g; diameter, 44 nm; length, 0.69 μm		Granuloma (disappeared at 365 days post-instillation)	Fujita et al. (2015)
Instillation	Rat, Sprague-Dawley (M)	MWCNT	4 mg/kg bw	21 days	BET, 109 m^2/g; length, 0.3–50 μm; diameter, 10–30 nm		Slight fibrosis	Cesta et al. (2010)
Instillation	Rat, Sprague-Dawley (F)	MWCNT	0.5, 2, or 5 mg	60 days	Length, 5.9 μm; ground: length, 0.7 μm	Inflammation (until 15 days)	Granuloma, fibrosis	Muller et al. (2005)
Pharyngeal aspiration								
	Mouse, C57Bl (F)	MWCNT	20 or 40 μg	7 days	Diameter, 31 nm; length, 20 μm; BET, 50 m^2/g; 3.5 wt% impurities	Transient		Han et al. (2010)
	Mouse, C57BL/6 J (M)	MWCNT	10, 20, 40, or 80 μg	Up to 56 days	GMI, 3.86 μm; CMD, 49 nm; 0.78% impurities	Persistent	80 μg (progressive)	Porter et al. (2010), Mercer et al. (2011)
	Mouse, C57BL/6 (M)	DWCNT	1, 10, or 40 μg	Up to 56 days	Diameter, 1–2 nm; length < 5 μm	10 and 40 μg (persistent alveolitis)	10 and 40 μg (interstitial fibrosis)	Sager et al. (2013)
	Mouse, C57BL/6 (F)	SWCNT	10, 20, or 40 μg	Up to 60 days	Diameter, 1–4 nm; BET, 1024 m^2/g; EC, 99.7%; iron, 0.23%	Persistent	Fibrosis	Shvedova et al. (2005)

Table 4.10 Studies of persistent inflammation, granulomatosis, and fibrosis in experimental animals after exposure to carbon nanotubes (continued)

Route of administration	Species, strain (sex)	Type of CNT	Exposure concentration or dose, duration	Recovery	Characterization of CNT	Inflammation	Fibrosis or granulomatosis	Reference
	Mouse, C57BL/6 (F)	SWCNT	40 μg	Up to 28 days	Diameter, 1–4 nm; length, 1–3 μm; BET, 1040 m²/g; iron, 0.23%	Persistent inflammation	Granuloma	Murray et al. (2012)
	Mouse, C57BL/6 J (M)	MWCNT	10, 20, 40, or 80 μg	Up to 56 days	GML, 3.86 μm; CMD, 49 nm; BET, 26 m²/g	Transient	Progressive fibrosis (granuloma)	Mercer et al. (2011)
Intraperitoneal administration								
	Rat, Wistar (M)	MWCNT	2 or 20 mg	24 mo	With and without defects; diameter, 11.3 nm; length, ~0.7 μm	Transient		Muller et al. (2009)
	Mouse, C57BL/6 (F)	Long MWCNT	50 μg	7 days	Mean length, 13 μm; maximal length, 56 μm		Granulomatous inflammation	Poland et al. (2008)
	Mouse, C57BL/6 (F)	Tangled MWCNT	50 μg	7 days	Length, 1–5 μm; length, 5–20 μm		Minimum	Poland et al. (2008)

BALF, bronchoalveolar lavage fluid; BET, Brunauer-Emmett-Teller surface area analysis; bw, body weight; CMD, count mean diameter; CNT, carbon nanotubes; DWCNT, double-walled carbon nanotubes; EC, elemental carbon; F, female; f/mL, fibres per millilitre; GML, geometric median length; M, male; MMAD, mass median aerodynamic diameter; mo, month; MWCNT, multiwalled carbon nanotubes; SWCNT, single-walled carbon nanotubes; VGCF-H CNF, vapour grown carbon nanofibres; wk, week

(2009) demonstrated focal granuloma formation and the accumulation of subpleural cells in a dose-dependent manner. Masson's stain established the presence of collagen within the sites of granuloma formation, while a reticulin fibre index further confirmed a dose-dependent increase in collagen within the alveolar walls (Treumann et al., 2013).

Two 4-week studies of SWCNT and MWCNT in Wistar rats showed evidence of transient (not persistent) inflammation. The maximum concentration that did not induce significant inflammation was 0.13 mg/m^3 of SWCNT and 0.37 mg/m^3 of MWCNT (Morimoto et al., 2012a, b).

A 4-week study of MWCNT (length, 330.18 nm; diameter, 10–15 nm) in Sprague-Dawley rats with a 90-day recovery period showed no statistically significant difference in the levels of inflammatory cytokines, bronchoalveolar cell distribution, or markers in the BALF or in histopathology (Kim et al., 2014).

Exposure to MWCNT for 6 hours provided evidence of persistent inflammation at high concentrations in male rats (Ellinger-Ziegelbauer & Pauluhn, 2009).

Kasai et al. (2015) reported a dose-independent increase in inflammatory parameters after exposure of male rats to a lower dose of MWCNT (0.2 mg/m^3). In male mice, subpleural fibrosis increased 2 and 6 weeks after inhalation of MWCNT (Ryman-Rasmussen et al., 2009a).

(ii) Intratracheal instillation

Fifteen studies of intratracheal instillation in rats and pharyngeal aspiration in mice have been reported (Lam et al., 2004; Warheit et al., 2004; Muller et al., 2005, 2008b; Shvedova et al., 2005; Aiso et al., 2010; Cesta et al., 2010; Han et al., 2010; Kobayashi et al., 2010, 2011; Mercer et al., 2011; Porter et al., 2010; Morimoto et al., 2012b, c; Murray et al., 2012; Sager et al., 2013; Fujita et al., 2015), most of which revealed that exposure to SWCNT and MWCNT led to persistent inflammation in the lung. In contrast, several studies in rats and mice revealed that exposure to SWCNT and MWCNT led to transient responses in the lung. [From the above studies, the Working Group considered that the pulmonary responses of rats and mice to SWCNT and MWCNT did not differ significantly.]

(c) Experimental systems in vitro

CNT, as well as asbestos fibres and poorly soluble crystalline particles (IARC, 2012), have been shown to induce inflammation, as assessed by the release of pro-inflammatory mediators (reviewed in Boyles et al., 2014). Two hypotheses have been proposed for the pro-inflammatory effects of high-aspect-ratio nanoparticles, including CNT and asbestos fibres: (1) frustrated phagocytosis; and (2) inflammasome activation (see Fig. 4.1). Frustrated phagocytosis is elicited in response to high-aspect-ratio, fibrous nanoparticles longer than ~15 µm that cannot be completely phagocytized by macrophages, resulting in their impaired clearance from the lungs and pleural linings and persistent inflammation accompanied by the prolonged release of ROS, pro-inflammatory mediators, and proteases (Johnston et al., 2010). Inflammasome activation triggered by lysosomal damage after the phagocytosis of crystalline minerals (e.g. silica, asbestos fibres) or CNT is the second mechanism that leads to the secretion of the pro-inflammatory mediators, IL-1β and IL-18 (Biswas et al., 2011; Palomäki et al., 2011). These two mechanisms are not exclusive and Hamilton et al. (2009) proposed that all high-aspect-ratio nanomaterials can induce frustrated phagocytosis and inflammasome activation similarly to asbestos fibres. The experimental evidence for inflammasome activation and the release of pro-inflammatory mediators based on in-vivo and in-vitro studies is summarized below.

Functionalized SWCNT produced by the HiPCO procedure (Unidym Inc., Sunnyvale, CA, USA) were evaluated for inflammasome activation and the release of IL-1β in LPS-primed,

Fig. 4.1 Inflammasome activation and inflammation induced by nanoparticles, including carbon nanotubes
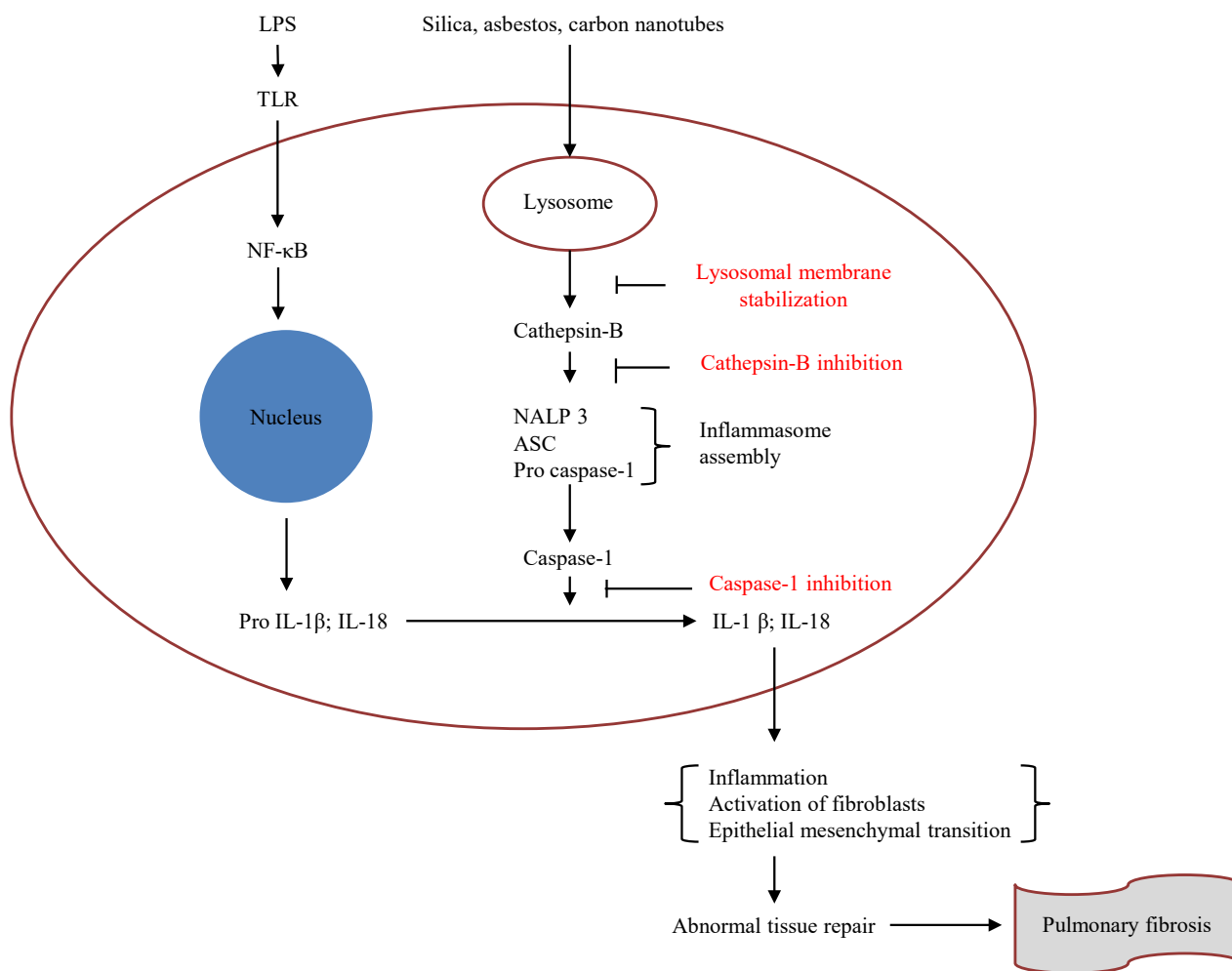
Adapted from Biswas et al. (2011). Copyright © 2011
ASC, apoptosis-associated specific-like protein containing a caspase recruitment domain (CARD); IL, interleukin; LPS, lipopolysaccharide; NALP3, a member of the NOD-like receptor family; NF-κB, nuclear factor-kappa B; TLR, toll-like receptor

immortalized, bone marrow-derived murine macrophages (Yang et al., 2013). Oxidized SWCNT increased the release of IL-1β while benzoic acid functionalization decreased the release of pro-inflammatory cytokines.

See also Hamilton et al. (2013a); discussed in Section 4.4.1 (b).

4.4.2 Release of cytokines, chemokines, and growth factors

(a) Exposed humans

Markers of inflammation and oxidative stress were monitored among workers handling engineered nanomaterials (Liao et al., 2014a, b). No effects were reported for IL-6 and IL-6 receptors, but depression of antioxidant enzymes was found among these workers (Liou et al., 2012).

(b)   Human cells in vitro

A panel of well-characterized MWCNT was investigated for their ability to stimulate cytokine release from human THP-1 macrophages and the immortalized human mesothelial Met-5A cell line. Only long CNT samples (mean length, 13–36 μm) at a sublethal dose of 5 μg/mL induced the release of TNF-α, IL-1β, and IL-6 from macrophages but not from mesothelial cells after 24 hours (Murphy et al., 2012). Immortalized human lung epithelial BEAS-2B cells were exposed to 30 μg/mL of highly purified (10 minutes at 37 °C) MWCNT (HTT2800 (see Haniu et al., 2010); diameter, 100–150 nm; length, 10–20 μm) and assessed for the release of TNF-α, IL-1β, IL-6, IL-8, IL-10, and IL-12 after 24 hours; only the release of IL-6 and IL-8 was detected (Tsukahara & Haniu, 2011). A dynamic cell growth model designed to mimic expansion and contraction during normal breathing was established using human lung adenocarcinoma A549 cells. Two samples of SWCNT (Cheap Tubes) were tested for the release of the cytokine, IL-8: a short CNT (diameter, 1–2 nm; length, 0.5–2 μm) and a long CNT (diameter, 1–2 nm; length, 5–30 μm). Only the long CNT induced the release of IL-8 after 24–72 hours and the levels were significantly higher in the dynamic cell growth model compared with static growth conditions (Patel & Kwon, 2013). A triple co-culture model of human lung epithelial 16HBE14o cells, primary human blood-derived dendritic cells, and primary human blood-derived macrophages in transwell cultures was used to evaluate the release of TNF-α and IL-8 after exposure to MWCNT (3 or 30 μg/mL) for 24 hours. As-produced and carboxylated MWCNT synthesized by CVD (Chengdu Carbon Nanomaterials R&D Center, Sichuan, China) were pre-coated with Curosurf 120 (porcine lung surfactant). Pre-coated, as-produced, and carboxylated MWCNT elicited the release of both TNF-α and IL-8 in this model system (Gasser et al., 2012). Transwell co-cultures of human THP-1 macrophages and immortalized human lung epithelial BEAS-2B cells exposed to MWCNT released the profibrotic mediators, TGF-β1 and PDGF (Wang et al., 2012a; Li et al., 2013).

[The use of in-vitro human or animal cell systems does not represent physiological routes of exposure for humans. The doses used in the in-vitro studies should be relevant to those to which humans are exposed, and the doses used in in-vitro studies may lead to mechanisms that differ from those that arise from the actual exposure concentrations of humans. Thus, interpretation of the data, including those on cytotoxicity and mechanisms, obtained from in-vitro studies should be evaluated cautiously.]

(c)   Experimental systems in vivo

Several studies have investigated the pulmonary effects of CNT after inhalation, intratracheal or intranasal instillation, and pharyngeal aspiration. The results of these studies are summarized and the characteristics of the CNT investigated are described in Table 4.11.

Inflammatory responses were assessed after the inhalation of MWCNT (Ma-Hock et al., 2009; Kim et al., 2014; Kasai et al., 2015). Ma-Hock et al. (2009) performed a 5-day range-finding inhalation study to select test concentrations for a 90-day inhalation toxicity study with MWCNT (Nanocyl NC 7000). Groups of male Wistar rats were exposed by head/nose-only inhalation to an aerosol of MWCNT dust for 6 hours per day on 5 consecutive days at target concentrations of 0, 2, 8, and 32 mg/m³. Treatment-related increases in BALF total cell counts (due to a significant increase in polymorphonuclear neutrophils), total protein content, and enzyme activities were observed in all treated groups 3 days after the last exposure. At the end of the 24-day recovery period, the same pattern of BALF findings was found. In the animals exposed to 2 mg/m³ (the lowest concentration), slight recovery was observed; protein

Table 4.11 Studies of pulmonary effects in experimental animals exposed to carbon nanotubes in vivo

Route of administration	Species, strain (sex)	Type of CNT	Exposure concentration or dose, duration	Recovery	Characterization of CNT	Effects	Reference
Inhalation							
Head/nose-only	Rat, Wistar (M)	MWCNT	0, 2, 8, or 32 mg/m³, 6 h/day, 5 days/wk	3 and 24 days	Diameter, 5–15 nm; length, 0.1–10 μm; metal oxide, 10%; BET, 250–300 m²/g; MMAD, 0.5–1.3 μm	Increases in BALF total cell counts, total protein content, and enzyme activities in all treated groups	Ma-Hock et al. (2009)
Whole-body	Rat, F344 (M, F)	MWCNT, fibre-like	0, 0.2, 1, or 5 mg/m³, 6 h/day, 5 days/wk, 13 wk	None	Diameter, 94.1–98 nm; length, 5.53–6.19 μm; purity > 99.6–99.8%; BET, 24–28 m²/g; MMAD, 1.4–1.6 μm	Increases in lung weights and inflammatory parameters in BALF, granulomatous changes, focal fibrosis of the alveolar wall, inflammatory infiltration in the visceral pleural and subpleural areas observed	Kasai et al. (2015)
Nose-only	Rat, Sprague-Dawley (M, F)	MWCNT, short	0, 0.17, 0.49, or 0.96 mg/m³, 6 h/day, 5 days/wk, 4 wk	28 and 90 days	Length, 330.18 m; diameter, 10–15 nm; BET, 224.9 m²/g	No increase in inflammatory cytokines levels, inflammatory cells, or inflammatory proteins	Kim et al. (2014)
Whole-body	Mouse, C57BL/6 (M)	MWCNT (mixture of MWCNT and graphitic nanofibres)	0.3, 1, or 5.3 mg/m³, 6 h/day, 7 or 14 days	None	Diameter, 10–20 nm; length, 5–15 μm; nickel and iron, 0.5%; BET, 100 m²/g; MMAD, 700–1000 nm/1800 nm	No local pulmonary effects but non-monotonic systemic immune suppression	Mitchell et al. (2007)
Whole-body	Mouse, C57BL/6 (M)	MWCNT	0.3 or 1 mg/m³, 6 h/day, 14 days	None	Mean diameter (based on particle mass), 146.3 nm²/cm³	Systemic immune suppression, not due to systemic uptake of MWCNT but to release of immune suppressing signals from the lung	Mitchell et al. (2009)
Intratracheal instillation							
	Rat, Sprague-Dawley (M)	MWCNT	0.04, 0.2, or 1 mg/kg bw	3, 7, 28, or 91 days	Diameter, 60 nm; length, 1.5 μm; 99.79% impurities; carbon, 7–8% (carbon soot); BET, 23.0 m²/g	Increase in BALF neutrophils and eosinophils, increased LDH and total protein levels; no change in levels of BALF cytokines	Kobayashi et al. (2010)
	Rat, Sprague-Dawley (M)	SWCNT	0.04, 0.2, 1, or 2 mg/kg bw	1, 3, 7, 28, 91, or 182 days	Diameter, 12 nm; length, 0.32 μm; total metal, 0.05%; BET, 1064 m²/g	Increases in BALF neutrophils, macrophages, lymphocytes, eosinophils, LDH, protein, IL-1β, and IL-6	Kobayashi et al. (2011)

Table 4.11 (continued)

Route of administration	Species, strain (sex)	Type of CNT	Exposure concentration or dose, duration	Recovery	Characterization of CNT	Effects	Reference
	Rat, Sprague-Dawley (M)	MWCNT	1, 10, or 100 µg	1, 7, 30, 90, or 180 days	Diameter, 20–50 nm; length, 0.5–2 µm; purity > 95%; BET, 280 m²/g	No inflammation; apoptosis of macrophages having phagocytosed MWCNT (elimination)	Elgrabli et al. (2008)
	Mouse, ICR (M)	SWCNT	0.5 mg/kg bw	3 or 14 days	Diameter, 1–2 nm; length, several µm (NR)	Release of cytokines (NF-κB)	Chou et al. (2008)
	Mouse, ICR (M)	MWCNT	5, 20, or 50 mg/kg bw	1, 3, 7, or 14 days	Diameter, 11–170 nm; length, 5–9 µm; carbon content > 90%; BET, 12.83 m²/g	Increase in immune cells and pro-inflammatory cytokines (IL-1, TNF-α, IL-6, IL-4, IL-5, IL-10, IL-12, and IFN-γ) and IgE; distribution of B-cells in the spleen	Park et al. (2009)
Intranasal instillation							
	Mouse, Swiss (M)	Purified DWCNT (80% DWCNT, 20% SWCNT)	1.5 mg/kg bw	6, 24, or 48 h	Diameter, 1.2–3.2 nm; length, 1–10 µm (bundles up to 100 µm)	Local and systemic inflammation; no increase in TNF-α; decrease in local oxidative stress	Crouzier et al. (2010)
Pharyngeal aspiration							
	Mouse, C57BL/6J (M)	MWCNT	10, 20, 40, or 80 µg	1, 7, 28, or 56 days	Diameter, 49 nm; length, 3.86 µm; total metals, 0.78%	Increase in PMN, LDH, and albumin in BALF	Porter et al. (2010)
	Mouse, C57BL/6 (F)	Purified SWCNT	10, 20, or 40 µg (0.5, 1, or 2 mg/kg bw)	1, 3, 7, 28, or 60 days	Diameter, 1–4 nm; iron, 0.23%; BET, 1040 m²/g	Inflammation (TNF-α and IL-1β increased)	Shvedova et al. (2005)
	Mouse, C57BL/6 (F)	Purified SWCNT	40 µg (1.9 mg/kg bw)	1, 7, or 28 days	Diameter, 1–4 nm; EC, 99.7%; iron, 0.23%; BET, 1040 m²/g	Robust, acute inflammation (PMN, TNF-α, IL-6, and LDH increased)	Shvedova et al. (2007)
	Mouse, C57BL/6 (F)	SWCNT	5, 10, or 20 µg (0.25, 0.5, or 1 mg/kg bw)	1, 7, or 28 days	Diameter, 0.8–1.2 nm; length, 100–1000 nm; EC, 82% wt; iron, 17.7%; BET, 508 m²/g	Inflammation (TNF-α, IL-6, and TGF-β increased), GSH depletion, lipid peroxidation, and oxidized proteins	Shvedova et al. (2008)

BALF, bronchoalveolar lavage fluid; BET, Brunauer-Emmett-Teller surface area analysis; bw, body weight; CNT, carbon nanotubes; DWCNT, double-walled carbon nanotubes; EC, elemental carbon; F, female; GSH, glutathione; IgE, immunoglobulin E; IL, interleukin; IFN, interferon; LDH, lactate dehydrogenase; M, male; MMAD, mass median aerodynamic diameter; MWCNT, multiwalled carbon nanotubes; NF-κB, nuclear factor kappa B; NR, not reported; PMN, polymorphonuclear leukocytes; SWCNT, single-walled carbon nanotubes; TGF-β, transforming growth factor β; TNF-α, tumour necrosis factor α; wk, week

content and *N*-acetyl glucosaminidase activity returned to control levels, but the other parameters were still significantly increased. Kasai et al. (2015) conducted a 13-week study in male and female Fischer 344 rats exposed by whole-body inhalation to MWCNT (Hodogaya Chemical Co., Ltd, Tokyo, Japan) at concentrations of 0, 0.2, 1, and 5 mg/m^3 using a generation and exposure system based on the cyclone sieve method. In the BALF analyses, inflammatory parameters were increased in a concentration-dependent manner in both sexes from the lowest dose upwards (Kasai et al., 2015). A 4-week inhalation study of MWCNT (length, 330.18 nm; diameter, 10–15 nm) in Sprague-Dawley rats with a recovery period of up to 90 days showed that the levels of inflammatory cytokines (TNF-α, TGF-β, IL-1, IL-2, IL-4, IL-5, IL-10, IL-12, and interferon (IFN)-γ) and inflammatory proteins (albumin, total protein, and LDH) in the BALF did not differ significantly (Kim et al., 2014). No local pulmonary effects were observed in C57BL/6 mice exposed to a mixture of MWCNT and graphitic nanofibres (Mitchell et al., 2007).

Intratracheal or intranasal instillation and pharyngeal aspiration are not physiological routes of exposure for humans but have been used in mice and rats to investigate the potential pulmonary and systemic toxicity of high concentrations of CNT.

Biological responses to MWCNT (Mitsui & Co. Ltd) were assessed in male rats after a single intratracheal instillation (0.04–1 mg/kg bw) (Kobayashi et al., 2010). Transient pulmonary inflammatory responses were observed in the lungs of the rats exposed to 1 mg/kg bw of MWCNT. However, the levels of cytokines in BALF did not change significantly at any timepoint (3, 7, 28, or 91 days after exposure).

Pulmonary and systemic responses were assessed in male rats after the intratracheal instillation of highly pure, well dispersed, and well-characterized SWCNT. The numbers of BALF inflammatory cells (neutrophils, macrophages, lymphocytes, and eosinophils) were increased in a dose-dependent manner. LDH values and the protein contents in BALF were significantly greater in the groups exposed to doses of SWCNT of 0.2 mg/kg bw and higher compared with those in the control group up to 3 months after instillation. Only small differences were observed between the SWCNT-exposed groups and the control group for the cytokines IL-1α, IL-2, IL-4, IL-10, granulocyte macrophage colony-stimulating factor, IFN-γ, and TNF-α at any of the time-points, but significant increases were observed for IL-1β and IL-6 at several time-points (Kobayashi et al., 2011).

Intratracheal instillation of 0.5 mg of SWCNT into male ICR mice induced alveolar macrophage activation, various chronic inflammatory responses, and severe pulmonary granuloma formation. Affymetrix microarrays were used to investigate the molecular effects on the macrophages exposed to SWCNT. A biological pathway analysis, a literature survey, and experimental validation suggested that the uptake of SWCNT into the macrophages can activate various transcription factors, such as nuclear factor kappa B (NF-κB) and activator protein 1 (AP-1), and that this leads to oxidative stress, the release of pro-inflammatory cytokines, the recruitment of leukocytes, the induction of protective and anti-apoptotic gene expression, and the activation of T-cells. [The resulting innate and adaptive immune responses may explain the chronic pulmonary inflammation and granuloma formation in vivo caused by SWCNT (Chou et al., 2008).]

Pulmonary and systemic immune responses induced by intratracheal instillation of 5, 20, and 50 mg/kg bw of MWCNT (Sigma-Aldrich, St. Louis, MO, USA (Cat. No. 659258)) into male mice were investigated (Park et al., 2009). Total numbers of immune cells in BALF were significantly increased in the treated groups and the distribution of neutrophils was elevated on day 1 after instillation. Pro-inflammatory cytokines

(IL-1, TNF-α, IL-6, IL-4, IL-5, IL-10, IL-12, and IFN-γ) were also increased in a dose-dependent manner in both BALF and blood. The highest levels of the cytokines were seen on day 1 after instillation and then decreased. The levels of T-helper (Th) 2-type cytokines (IL-4, IL-5, and IL-10) in the treated group were higher than those of the Th1-type cytokines (IL-12 and IFN-γ).

Male Swiss mice were intranasally instilled with 1.5 mg/kg bw of CNT (DWCNT, 80%; SWCNT, 20%). Local oxidative perturbations were investigated using electronic spin resonance (ESR) spin trapping experiments, and systemic inflammation was assessed by measuring the plasma concentrations of TNF-α, IL-1α, IL-1β, IL-6, insulin-like growth factor 1, leptin, granulocyte-colony stimulating factor, and vascular endothelial growth factor (Crouzier et al., 2010). Examination of the lungs and the elevation of pro-inflammatory cytokines in the plasma (leptin and IL-6 at 6 h) confirmed the induction of an inflammatory response, which was accompanied by a decrease in the local oxidative stress.

A dose–response and time-course study of MWCNT (Mitsui & Co. Ltd) was conducted in male mice exposed by pharyngeal aspiration. Examination of the BALF demonstrated that pulmonary inflammation and damage were dose-dependent and peaked at 7 days after exposure. By 56 days after exposure, markers of pulmonary inflammation and damage began returning to control levels, except in mice exposed to the 40-µg MWCNT dose which still had significantly higher levels than vehicle controls (Porter et al., 2010).

Pharyngeal aspiration of SWCNT (CNI, Inc.) by female C57BL/6 mice elicited unusual pulmonary effects that combined robust but acute inflammation with early-onset, progressive fibrosis and granulomas. A dose-dependent increase in LDH and γ-glutamyl transferase activities was found in the BALF, together with an accumulation of 4-hydroxynonenal [an oxidative biomarker] and the depletion of GSH in the lungs. An early accumulation of neutrophils, followed by lymphocyte and macrophage influx, was accompanied by an early elevation of pro-inflammatory cytokines (TNF-α and IL-1β) followed by fibrogenic TGF-β1 (Shvedova et al., 2005).

Female C57BL/6 mice were maintained on vitamin E-sufficient or vitamin E-deficient diets and were exposed by aspiration to SWCNT (CNI, Inc.) to explore and compare their pulmonary inflammatory reactions. The vitamin E-deficient diet caused a 90-fold depletion of α-tocopherol in the lung tissue and resulted in a significant decline of other antioxidants (reduced GSH and ascorbate) as well as an accumulation of lipid peroxidation products. A greater decrease in pulmonary antioxidants was detected in SWCNT-treated vitamin E-deficient mice compared with controls. The lower levels of antioxidants in vitamin E-deficient mice were associated with a higher sensitivity to SWCNT-induced acute inflammation (increases in the total number of inflammatory cells, the number of polymorphonuclear leukocytes, the release of LDH, total protein content, and the levels of pro-inflammatory cytokines, TNF-α and IL-6) and enhanced profibrotic responses (elevation of TGF-β and collagen deposition). Exposure to SWCNT also markedly shifted the ratio of cleaved to full-length extracellular SOD (Shvedova et al., 2007).

In female C57BL/6 mice, the inhalation of stable and uniform dispersions of 5 mg/m³ of unpurified SWCNT (CNI, Inc.; iron, 17.7% wt) for 5 hours per day for 4 days was compared with the pharyngeal aspiration of varying doses (5–20 g/mouse) of the same SWCNT. Overall, the outcomes of inhalation exposure to respirable SWCNT were very similar to those of pharyngeal exposure, both of which led to pulmonary toxicity. However, inhalation of SWCNT was more effective than aspiration in causing inflammatory response, oxidative stress, collagen

deposition, and fibrosis, as well as mutations at the *K-ras* gene locus in the lung (Shvedova et al., 2008).

(d) Experimental systems in vitro

No data were available to the Working Group

4.4.3 Immune effects

(a) Exposed humans

No data were available to the Working Group.

(b) Human cells in vitro

In in-vitro test systems, macrophages and other relevant mammalian cells are frequently used as test cells for nanomaterials because they are primarily responsible for surveillance in the body. However, they are highly reactive with endotoxins and the distinction between the response to endotoxins and that to nanomaterials is difficult to make. Consequently, contamination with endotoxins confounds the result of tests in vitro. A preliminary examination for endotoxins is therefore required to minimize contamination or confirm an insignificant level in the test sample. Their quantification is also important for an adequate interpretation of data obtained in in-vitro biological test systems (ISO, 2010e).

Exposure to CNT may alter innate immune responses by triggering the complement system, the clearance of apoptotic cells by macrophages, and the induction of adaptive immune responses (reviewed by Andersen et al., 2012). Different responses have been reported for as-produced versus functionalized or coated CNT, and deliberate surface modifications have been attempted to enhance biocompatibility for drug delivery applications (Hamad et al., 2010; Moghimi et al., 2010). The complement system is present in the lining fluid of the lung, and inhaled particles and fibres have been shown to induce complement-generating chemotactic activity that correlates with macrophage accumulation in vivo

(Warheit et al., 1985, 1988). Direct binding of as-produced CNT to Clq protein, which leads to the classical pathway of complement activation, has been described in some studies while other investigators reported that complement proteins were bound to CNT but were not activated (Ling et al., 2011). The macrophage-mediated clearance of apoptotic cells is important for the regulation of immune responses and the suppression of macrophage function, and may lead to impaired clearance of particle-laden neutrophils from the lungs (Wiethoff et al., 2003) and chronic inflammation (Witasp et al., 2008). Human peripheral blood monocyte-derived macrophages exposed to purified SWCNT (CNI, Inc.) at non-toxic doses impaired the chemotaxis and phagocytosis of apoptotic target cells – human Jurkat T lymphoblastic leukaemia cells (Witasp et al., 2009). In an in-vitro three-dimensional model of granuloma formation, three commercial samples of MWCNT (MWCNT-7, Mitsui & Co. Ltd; other MWCNT, MER Corp., AZ, USA) or crocidolite asbestos fibres (UICC) altered the phenotype with the co-expression of pro-inflammatory (M1) and profibrotic (M2) markers of murine bone marrow-derived macrophages after 7–14 days (Sanchez et al., 2011).

Exposure of innate immune cells or lymphocytes to CNT in vitro may also impair the presentation of antigens and the activation of lymphocytes with variable results depending on the physical properties and surface functionalization of the CNT tested (Andersen et al., 2012). For example, carboxylated MWCNT have been reported to enhance cytokine secretion by purified human peripheral blood lymphocytes and stimulate lymphocyte-mediated tumour cell cytotoxicity (Sun et al., 2011), while amino-functionalized or oxidized MWCNT activated human monocytes and natural killer cells (Delogu et al., 2012). Purified samples (SES Research) of short SWCNT (length, 1–5 μm) and short MWCNT (length, 1–2 μm) caused minimal activation of antigen-presenting cells in vitro in contrast to

titanium dioxide (rutile) or zinc nanoparticles ([Palomäki et al., 2010](#)).

(c)   Experimental systems in vivo

See [Table 4.11](#)

[The Working Group noted that, as in the case of in-vitro experiments on immune effects, the number of published in-vivo studies on CNT is too limited to draw any general conclusions, and the wide variation in the CNT used impedes any comparison of the reports from different studies.]

The pulmonary and systemic immune responses of male C57BL/6 mice to the inhalation of MWCNT were assessed ([Mitchell et al., 2007](#)). Analysis by TEM revealed that the material used was a mixture of MWCNT and graphitic nanofibres ([Lison & Muller, 2008](#); [McDonald & Mitchell, 2008](#)). After whole-body inhalation for 14 days, MWCNT were engulfed by alveolar macrophages and were distributed throughout the lung. However, no increases in inflammatory cell infiltration were found and no inflammation, granuloma formation, fibrosis, or tissue injury occurred up to the highest dose (5.3 mg/m^3) tested. Despite the lack of local pulmonary effects, systemic immunity was affected at all concentrations tested. The measurement of immune function in spleen-derived cells showed a suppressed T-cell-dependent antibody response, a decreased proliferation of T-cells after mitogen stimulation, and altered natural killer cell killing. These results were accompanied by increased gene expression of indicators of oxidative stress and altered immune function [nicotinamide adenine dinucleotide phosphate (NADPH) dehydrogenase quinone 1 and IL-10] in the spleen, but not in the lung. Immune suppression persisted for up to 30 days after exposure ([Mitchell et al., 2007](#)). A follow-up study investigated the mechanism of the suppressed systemic immune function. Mice exposed to a dose of 1 mg/m^3 of MWCNT by whole-body inhalation presented suppressed immune function, which involved

the activation of cyclooxygenase enzymes in the spleen in response to a signal from the lung. Inhaled MWCNT were shown to activate the release of TGF-β in the lung, which was postulated to have a direct effect on prostaglandin production in spleen cells, leading to immune suppression. However, to induce this altered systemic immunity, an additional [yet unknown] signalling mechanism from the lung would be necessary because not all observed systemic effects could be explained by this pathway ([Mitchell et al., 2009](#)).

Based on the results from these two studies ([Mitchell et al., 2007](#), [2009](#)), [Aschberger et al. (2010)](#) concluded that systemic immune effects are related to relatively short-term exposures to MWCNT. [The Working Group noted that the translocation of CNT from the lung does not appear to be necessary for such effects, although further investigation is required to confirm this hypothesis.]

In the study conducted by [Park et al. (2009)](#), distributions of B-cells in the spleen and blood were significantly increased on day 1 after intratracheal instillation of MWCNT into ICR mice, indicating that Th2-type cytokines had activated B-cells and caused them to proliferate. Together with the increased number of B-cells, granuloma formation in the lung tissue and the production of immunoglobulin (Ig) E were also observed with an intensity that was dependent on the dose of MWCNT instilled. [The Working Group noted that this study suggested that MWCNT may induce allergic responses in mice through B-cell activation and the production of IgE.]

(d)   Experimental systems in vitro

Murine bone marrow-derived dendritic cells exposed to purified SWCNT (CNI, Inc.) in vitro and co-cultured with splenic T lymphocytes suppressed T-cell proliferation ([Tkach et al., 2011](#)). SWCNT (Chengdu Organic Chemicals Co., Ltd) also suppressed lymphocyte proliferation

in co-cultures of primary murine peritoneal macrophages and T lymphocytes activated by concanavalin A (Dong et al., 2012).

4.4.4 Apoptosis

(a) Exposed humans

No data were available to the Working Group.

(b) Human cells in vitro

Several mechanisms have been shown to cause cell death in target cells exposed to engineered nanoparticles in vitro, including apoptosis, necrosis, and autophagic cell death (reviewed in Andón & Fadeel, 2013). In general, acute exposure to high concentrations (~30–400 µg/mL) of engineered nanoparticles can cause mitochondrial injury, increased intracellular generation of ROS, impaired adenosine triphosphate synthesis, and lysosomal damage leading to cell death. Therefore, the selection of doses of CNT for short-term in-vitro toxicity testing is problematic. Ideally, the doses should reflect the mass dose retained in workers exposed to CNT expressed as dose per alveolar epithelial cell surface area (Gangwal et al., 2011).

For a lifetime exposure to an airborne concentration of 1 mg/m^3 over 45 years, the relevant in-vitro dose would be ~50–70 µg/mL. However, short-term in-vitro toxicity testing is usually conducted after 24 hours of exposure and the equivalent dose for a 24-hour exposure of workers to an airborne concentration of 1 mg/m^3 would be ~0.2–0.6 µg/mL, which is two orders of magnitude lower, and doses > 50 µg/mL have been considered to be an "extraordinary high concentration" for use as a bolus dose in short-term in-vitro toxicity assays (Oberdörster, 2012).

The mechanistic pathways leading to cell death vary depending on the dose as well as the physical and chemical characteristics of the nanoparticles and the target cell type (see Section 4.2). Additional caveats in short-term in-vitro toxicity studies include other variables in experimental design (Table 4.12) and the variability and purity of the sample (Table 4.13).

Various mechanisms have been proposed for the induction of cell death by CNT, including direct membrane damage, intracellular generation of ROS, and destabilization of lysosomal membranes. Thin, rigid MWCNT (Mitsui & Co., Ltd) directly penetrated human mesothelial cells and induced the depletion of adenosine triphosphate and cell death at a dose of 5 µg/cm^2 after 4 days (Nagai et al., 2011). In normal and malignant human mesothelial cell lines, exposure to MWCNT prepared by the CVD process (Mitsui & Co., Ltd) induced low levels of intracellular ROS and induced apoptosis at doses ≥ 50 µg/cm^2 after 24 hours (Pacurari et al., 2008a, b). A commercial sample of carboxylated SWCNT (Sigma-Aldrich) induced autophagic cell death in the human lung adenocarcinoma A549 cell line at a dose of 1 mg/mL after 24 hours (Liu et al., 2011).

(c) Experimental systems in vivo

After the intratracheal instillation of 0, 1, 10, or 100 µg of MWCNT (dispersed with albumin) into rats, inflammation, apoptosis, fibrosis, respiratory function, and granuloma formation were assessed after 1, 7, 30, 90, and 180 days. The results were obtained by plethysmography, soluble collagen quantification, quantitative real-time polymerase chain reaction (qRT–PCR), luminex measurement of cytokine expression, and histopathological examination. Only evidence of apoptosis of the alveolar macrophages was shown (Elgrabli et al., 2008).

(d) Experimental systems in vitro

High-aspect-ratio fibrous nanomaterials, including MWCNT, have been shown to cause direct plasma membrane penetration and increased permeability in the murine J774.1 (Hirano et al., 2008) and RAW 264 (Shimizu et al., 2013) macrophage cell lines after exposure to ~100 µg/mL. Acid-functionalized SWCNT synthesized by the CVD process (Chengdu Organic

Table 4.12 Limitations of in-vitro assays for nanoparticle-induced toxicity

Experimental design		Examples and selected references
Target cells:	primary, immortalized or malignant cell lines	Stress induced by isolation of primary cells (Stone et al., 2009)
Culture format:	monolayer, suspension, transwell, or three-dimensional (3-D) culture	Transwell models (Snyder-Talkington et al., 2012) 3-D models (Movia et al., 2011; Sanchez et al., 2011)
	single-cell, multicellular	Co-cultures more predictive for in-vivo end-points (Müller et al., 2010; Clift et al., 2014)
Use of dispersants to prevent agglomeration in cell culture medium: influence on cell uptake		Inhibition of cell uptake after dispersal with pluronic F127 (Ali-Boucetta et al., 2011) or pluronic F108 (Wang et al., 2012a)
Secondary modification of nanoparticles during dispersion		Sonication-induced damage (Bussy et al., 2012)
Failure to confirm toxicity through morphology or different assays		Monteiro-Riviere et al. (2009)

Physical or chemical interference	Examples and selected references
Physical adsorption to probes or reaction products	Neutral red assay (Davoren et al., 2007)
	Formazan product of the MTT assay (Wörle-Knirsch et al., 2006)
Blocking or quenching of transmitted or emitted light	Thiobarbituric acid assay (Fenoglio et al., 2006; Creighton et al., 2013)
Direct oxidation of probed or substrates by nanoparticles	Surface generation of radicals (Fenoglio et al., 2008; Tournebize et al., 2013)
Adsorption or inactivation of cellular enzymes	Inactivation of lactate dehydrogenase (Karajanagi et al., 2004; Zhang et al., 2011)
Adsorption of secreted cytokines	Val et al. (2009), Horie et al. (2013)
Contamination with endotoxin	Adsorption to carbon surfaces (Delogu et al., 2010)
Adsorption of micronutrients from cell culture media	Medium depletion (Casey et al., 2008) Micronutrient depletion (Guo et al., 2012)

Compiled by the Working Group with data from Stone et al. (2009) and Tournebize et al. (2013)

Chemicals Co.) induced autophagy and cell death in primary murine peritoneal macrophages at doses of 10–50 μg/mL after 24 hours (Wan et al., 2013).

4.4.5 Activation of intracellular signalling pathways

(a) Exposed humans

No data were available to the Working Group.

(b) Human cells in vitro

In addition to inflammasome activation, other intracellular signalling pathways have been shown to be activated by the exposure of macrophages in vitro to CNT.

In human THP-1 macrophages, MWCNT (XNRI, Bussan Nanotech Research, Ibaraki, Japan) at a dose of 10 μg/mL for 24 hours induced the release of IL-1β via the activation of the Rho-kinase pathway (Kanno et al., 2014). In human lung fibroblast (IMR-90 or CRL-1490) cell lines, exposure to MWCNT prepared by the CVD method or SWCNT (CNI, Inc.) prepared by the HiPCO method activated the mitogen-activated protein kinase (MAPK)/p38 pathway at low doses ≤ 5 μg/mL, leading to the upregulation of pro-inflammatory gene expression and collagen deposition (Ding et al., 2005; Azad et al., 2013). In normal and malignant human mesothelial cell lines, MWCNT (Mitsui & Co., Ltd) induced the activation of the MAPK/p38 pathway at a dose of 25 μg/cm^2 after 30–120 minutes (Pacurari et al., 2008a). Exposure of normal and malignant human mesothelial cell lines to unpurified SWCNT (National Institute

Table 4.13 Minimal criteria required for the interpretation of in-vitro nanotoxicology assays

Criteria	Selected references
Complete physico-chemical characterization of nanoparticles	Warheit (2008)
Sample variability depending on batch, synthesis technique, and later processing	Fubini et al. (2011)
Consideration of contaminants (e.g. amorphous carbon)	Wang et al. (2011c)
Bioavailability of metal catalyst residues	Kagan et al. (2006), Pulskamp et al. (2007), Liu et al. (2008b), Aldieri et al. (2013)
Agglomeration state	Wick et al. (2007), Murray et al. (2012)
Comparison with positive and negative reference particles	Stone et al. (2009)
Positive controls for toxicity assays	Stone et al. (2009)
Use of doses that reflect potential human inhalation exposures	Oberdörster et al. (2013)
Consideration of dose-dependent mechanisms of adaptation and toxicity	Slikker et al. (2004), Bhattacharya et al. (2011)

Compiled by the Working Group with data from Warheit (2008) and Stone et al. (2009)

of Standards and Technology, Gaithersburg, MD, USA) induced the intracellular generation of ROS and activation of the AP-1 and NF-κB pathways at a dose of 25 µg/cm² after 1–4 hours (Pacurari et al., 2008b).

(c) Experimental systems in vivo

Some studies revealed that a Th2-associated response to CNT is activated through both adaptive and innate immune responses. In studies of MWCNT (NanoTechLabs, Inc., Yadkinville, USA)-exposed mice, the expression of IL-33 was accompanied by lung dysfunction and the upregulation of Th2-associated cytokines, such as IL-5 and eotaxin (Katwa et al., 2012; Beamer et al., 2013). The exposure of mice to SWCNT or MWCNT produced a dose-dependent increase in ovalbumin (OVA)-specific IgE and IgG1 in the serum (Nygaard et al., 2009).

With regard to signal transduction, the expression of four genes (coiled-coil domain containing-99, muscle segment homeobox gene-2, nitric oxide synthase-2, and wingless-type inhibitory factor-1) among 63 genes in the lung of mice exposed to MWCNT (Mitsui & Co. Ltd) was altered at two time-points, as determined by a quantitative PCR assay (Pacurari et al., 2011). In a study in mice, exposure to semi-SWCNT [semi-conductive components of SWCNT] (metal content approximately 10% wt, selectively separated from a mixture of metallic and semi-metallic SWCNT) induced phosphorylation of the signal transducer and activator of transcription-3, which forms part of the Janus kinase/signal transducers and activators of transcription signalling cascade, at two time-points (Park et al., 2011a). With regard to transcription factors, cFos mRNA levels in whole blood were increased in SWCNT-exposed mice (Erdely et al., 2009). In another study in mice, although the dose used for intratracheal instillation was excessive (1 mg/mouse, 10 mg/kg bw), NF-κB and AP-1 transcription factors were activated in the lung after exposure to SWCNT (Chou et al., 2008; Zhang et al., 2013).

(d) Experimental systems in vitro

The MAPK/extracellular signal-regulated kinase 1,2 pathway was upregulated in the murine macrophage RAW 264.7 cell line exposed to MWCNT (Helix Material Solutions, Inc., Richardson, TX, USA) at doses ≥ 50 µg/mL for 24 hours, resulting in an increased expression of cyclooxygenase-2 and inducible nitric oxide synthase (Lee et al., 2012). The exposure of murine epidermal JB6P+ cells to partially purified SWCNT produced by the HiPCO process (CNI, Inc.) at doses > 60 µg/mL for 24 hours, activated the NF-κB pathway dose-dependently (Murray et al., 2009).

Exposure of Chinese hamster ovary K1 cells (transfected with an NF-κB reporter gene construct) to MWCNT (XNRI, Bussan Nanotech Research) prepared by the CVD process at doses between 1 and 10 μg/mL for 20 hours upregulated the NF-κB pathway (Hirano et al., 2010).

4.4.6 Resistance to apoptosis

(a)   Exposed humans

No data were available to the Working Group.

(b)   Human cells in vitro

No data were available to the Working Group.

(c)   Experimental systems in vivo

The formation of large tumours from injected SWCNT-transformed cells (which were also reported to be resistant to apoptosis due to a low level of p53 phosphorylation in an in-vitro study) was observed in immunodeficient mice (Wang et al., 2011a). The expression of LC3B and the autophagy-related proteins p62 and Beclin-1 was upregulated and the expression of proliferating cell nuclear antigen was also elevated in mice exposed intratracheally to 100 μg of MWCNT (Yu et al., 2013). In another study, the expression of anti-apoptotic genes, such as cIAP2, SOD2, and A20, was induced in mouse lung by an [excessive] dose of SWCNT (1 mg/mouse) (Chou et al., 2008).

(d)   Experimental systems in vitro

No data were available to the Working Group.

4.4.7 Cell proliferation

(a)   Exposed humans

No data were available to the Working Group.

(b)   Human cells in vitro

Human cell lines were exposed to titanium dioxide nanobelts or purified MWCNT (Cheap Tubes, Inc.) at doses of 10 or 100 μg/mL for 1 and 24 hours. The target cell lines included human THP-1-derived macrophages and primary cultures of small airway epithelial cells. Total RNA was isolated and used for microarray analysis using Human Genome U133A 2.0 GeneChips (Affymetrix, Sana Clara, CA, USA). An analysis of the Global proteomics was conducted using liquid chromatography tandem mass spectrometry on tryptic digested cell lysates. The short exposure elicited similar proteomic responses to titanium dioxide nanobelts and MWCNT with different patterns of expression in various cell types. THP-1 macrophages showed the most significant transcriptional responses in 272 genes after 24 hours of exposure to MWCNT with unique patterns of gene expression in pathways related to cell-cycle regulation and cell proliferation (MYC and CDK1), as well as anti-apoptosis (survivin). Genes involved in the Sp1/AhR-dependent stress response were downregulated by exposure to MWCNT (Tilton et al., 2014).

In a study in human lung small airway epithelial cells exposed to SWCNT or MWCNT, occupationally relevant concentrations of CNT produced a neoplastic-like transformation phenotype depicted by increased cell proliferation, anchorage-independent growth, invasion, and angiogenesis (Wang et al., 2014).

(c)   Experimental systems in vivo

(i)   Bronchiolar and alveolar epithelial cells

Some, but not all, studies provided evidence of the proliferation of bronchiolar and alveolar epithelial cells.

In a 13-week inhalation study, exposure to CNF (VGCF-H) induced cell proliferation in the terminal bronchioles, alveolar ducts, and subpleural region of the respiratory tract in the lungs of male and female rats; however, this proliferation was not persistent and was absent in the subpleural region in females 3 months after exposure (Delorme et al., 2012).

Two studies of exposure by intratracheal instillation of rats to MWCNT (Roda et al., 2011) and mice to SWCNT (Murray et al., 2012) were performed. Exposure to as-produced or functionalized MWCNT induced proliferation of the alveolar and bronchiolar epithelial cells and alveolar macrophages in rats (Roda et al., 2011). Exposure to SWCNT decreased the proliferation of splenic T cells in mice (Murray et al., 2012). In another study in rats (Warheit et al., 2004), intratracheal instillation of SWCNT did not induce the proliferation of lung parenchymal cells assessed by 5-bromo-2-deoxyuridine.

(ii)   Other cells

The proliferation of T-cells was induced in mice exposed to MWCNT in one study (Grecco et al., 2011) but was decreased in another study (Murray et al., 2012).

Exposure of mice to SWCNT increased the occurrence of epithelial-derived fibroblasts. The aberrant activation of TGF-β/p-Smad2 or β-catenin was postulated to induce epithelial–mesenchymal transition during SWCNT-induced fibrosis (Chang et al., 2012). In rats, MWCNT induced visceral mesothelial cell proliferation, (assessed by proliferating cell nuclear antigen immunostaining), accompanied by increases in the number of macrophages and of the concentration of protein in the pleural lavage (Xu et al., 2012).

(d)   Experimental systems in vitro

Murine lung epithelial FE1 cells are a spontaneously immortalized cell line isolated from a Muta™ Mouse (Søs Poulsen et al., 2013). These cells were exposed to 12.5, 25, or 100 µg/mL of MWCNT (Mitsui-7; MWCNT-XNRI-7, lot 05072001K28, Hadoga Chemical Industry, Japan) suspended by sonication in cell culture medium. After 24 hours, the cells were harvested and total RNA was extracted for microarray analysis (Agilent 8 × 66K oligonucleotide microarrays); selected genes were verified using qRT–PCR. A total of 565 genes were differentially expressed at all concentrations. Classification of gene ontology revealed that most of the differentially expressed genes were involved in cell proliferation. At the highest exposure concentration, differentially expressed genes were related to cell death, cell-cycle arrest, oxidation reduction, and other metabolic pathways. Genes involved in fibrosis, cholesterol biosynthesis, GSH-mediated detoxification, and aryl hydrocarbon receptor signalling molecular canonical pathways were downregulated.

4.4.8 Granuloma formation and fibrosis

(a)   Exposed humans

No data were available to the Working Group.

(b)   Human cells in vitro

No data were available to the Working Group.

(c)   Experimental systems in vivo

See Table 4.10

(i)   Inhalation

Two 13-week studies of MWCNT in Wistar rats provided evidence of granulomatous inflammation and fibrosis in the lungs of male and female rats. The minimum concentrations of MWCNT that induced the persistent or slight fibrotic responses were 0.5 mg/m³ (Pauluhn, 2010b) and 0.4 mg/m³ (Treumann et al., 2013), respectively.

Two 4-week studies of MWCNT and SWCNT in Wistar rats showed no evidence of fibrosis in the lung at maximal concentrations of 0.37 mg/m³ of MWCNT and 0.13 mg/m³ of SWCNT (Morimoto et al., 2012a, b).

Two 6-hour exposure studies to MWCNT provided evidence of persistent fibrosis at high concentrations (241 and 30 mg/m³) in male rats (Ellinger-Ziegelbauer & Pauluhn, 2009) and mice (Ryman-Rasmussen et al., 2009a).

(ii) Intratracheal instillation

Fifteen studies of intratracheal instillation in rats and pharyngeal aspiration in mice have been reported (Lam et al., 2004; Muller et al., 2005; Warheit et al., 2004; Shvedova et al., 2005; Aiso et al., 2010; Cesta et al., 2010; Han et al., 2010; Kobayashi et al., 2010, 2011; Porter et al., 2010; Mercer et al., 2011; Morimoto et al., 2012b, c; Murray et al., 2012; Sager et al., 2013; Fujita et al., 2015). Most of the studies revealed that exposure to SWCNT and MWCNT resulted in persistent or progressive fibrosis in the lung (Muller et al., 2005; Shvedova et al., 2005; Aiso et al., 2010; Cesta et al., 2010; Porter et al., 2010; Mercer et al., 2011; Murray et al., 2012; Sager et al., 2013), whereas some studies in rats and one study in mice demonstrated transient or minimal fibrosis in the lung (Kobayashi et al., 2010, 2011; Morimoto et al., 2012b, c). In a long-term study, the formation of granuloma in the lungs disappeared over time (Fujita et al., 2015). [No significant differences in pulmonary responses were observed between rats and mice.]

(iii) Intraperitoneal injection

Exposure to long MWCNT led to granulomatous inflammation in the peritoneal cavity but exposure to tangled MWCNT induced weak or slight responses (Poland et al., 2008). In another study, MWCNT did not induce sustained inflammatory responses (Muller et al., 2009).

(d) Experimental systems in vitro

No data were available to the Working Group.

4.4.9 Alterations in DNA damage-induced response pathways

(a) Exposed humans

No data were available to the Working Group.

(b) Human cells in vitro

See Table 4.14

Human cells were used to study the effect of SWCNT on the expression of stress-response genes. The target cells included primary normal human bronchial epithelial cells, diseased human bronchial epithelial cells from asthma patients or from patients with chronic obstructive pulmonary disease, lung adenocarcinoma A549 cells and pharyngeal carcinoma FaDu cells. Cells were exposed to 0.1 or 1.0 mg/mL of SWCNT (Meijo Nano Carbon Co., Ltd, Nagoya, Japan) for 6 hours. A PCR array was conducted to examine 84 stress-response genes. Expression levels of 11 stress-response genes, including ERCC1 encoding a DNA repair enzyme, were downregulated more than twofold after exposure to SWCNT. Other genes belonging to the inflammatory responses, IL-6 and TNF-α, were significantly downregulated in normal human bronchial epithelial cells indicating that inflammatory cytokines were not activated under these conditions (Hitoshi et al., 2012).

Protein expression was investigated in human monoblastic leukaemia U937 cells exposed to MWCNT (100 μg/mL) that had been thermally treated at 1800 °C or 2800 °C. An analysis of proteomics was performed after two-dimensional electrophoresis and protein identification by matrix-assisted laser desorption/ionization-time of flight mass spectrometry. The expression of proteins involved in stress responses and DNA repair (such as DNA mismatch repair protein Msh2 and DNA damage-binding protein 1) was enhanced, suggesting the induction of DNA repair; however, the efficiency of repair was not evaluated (Haniu et al., 2010).

Gene and protein expression was studied in three human cell lines exposed to two types of high-aspect-ratio nanoparticles: MWCNT and titanium dioxide nanobelts that are known to exert low and high toxicity, respectively, in other cell systems. The sizes of the MWCNT and titanium dioxide nanobelts were 375 ± 23 nm and 1590 ± 126 nm in RPMI medium and 458 ± 16 nm and 634 ± 86 nm in DMEM medium,

Table 4.14 Studies of impaired DNA repair in human cells exposed to carbon nanotubes in vitro

Cell types	Type of carbon nanotube, treatment, duration	Assay/result	Reference
NHBE cells, and DHBE cells from asthma and COPD lung adenocarcinoma A549 and pharynx carcinoma FaDu cell lines	SWCNT, 0.1 or 1.0 mg/mL for 6 h	Measurement of gene expression using PCR array evaluating 84 stress-response genes Downregulation of 11 genes, including ERCC1 encoding a DNA repair enzyme	Hitoshi et al. (2012)
Human monoblastic leukaemia U937 cells	MWCNT, 50 μL (10 mg/mL) added to 5 mL of culture medium that contained 2.5×10^5 cells	Analysis of proteomics performed by two-dimensional electrophoresis and protein identification by MALDI-TOF MS Enhancement of the expression of proteins in response to stress and DNA repair (such as DNA mismatch repair protein Msh2 and DNA damage-binding protein 1)	Haniu et al. (2010)
Macrophage-like THP-1 cells, primary small airway epithelial cells, and Caco-2/HT29-MTX co-cultures	Cells exposed to 10 or 100 μg/mL MWCNT or titanium oxide nanobelts (TiO_2-NB) for 1 h and 24 h or 3 h and 24 h MWCNT and TiO_2-NB sizes: 375 ± 23 nm and 1590 ± 126 nm, respectively, in RPMI medium and 458 ± 16 nm and 634 ± 86 nm, respectively, in DMEM medium	Transcriptomic and proteomic analyses: comparison of elicited signatures induced by TiO_2-NB and MWCNT THP-1 cells were the most responsive cells. Three pathways were upregulated specifically by MWCNT, but not by TiO_2-NB: DNA damage checkpoint, DNA damage (double-strand breakage) repair and cytoskeleton spindle microtubules, consistent with DNA damage and mitotic perturbations induced by MWCNT	Tilton et al. (2014)

COPD, chronic obstructive pulmonary disease; DHBE, diseased human bronchial epithelial; ERCC1, excision repair cross-complementary rodent repair deficiency complementation group 1; MALDI-TOF MS, matrix-assisted laser desorption/ionization time-of-flight mass spectrometry; MWCNT, multiwalled carbon nanotubes; NHBE, primary normal human bronchial epithelial; PCR, polymerase chain reaction; SWCNT, single-walled carbon nanotubes

respectively. The cell lines were human THP-1 cells, primary small airway epithelial cells, and Caco-2/HT29-MTX co-cultures. The Caco-2 is a malignant human intestinal epithelial cell line and HT29-MTX is a goblet cell line. This co-culture mimics the intestinal epithelium. The cells were exposed to 10 or 100 µg/mL for 1 and 24 hours and 3 and 24 hours for transcriptomic and proteomic analyses, respectively. Titanium dioxide nanobelts were more cytotoxic than MWCNT, but the toxicity was low at early time-points. THP-1 cells were the most responsive and showed time-, concentration-, and particle type-dependent responses; the highest responses occurred at 100 µg/mL. Fewer genes were differentially expressed between untreated and treated cells in the other cell types. Cells responded to these nanoparticles by differentially regulating both common and unique sets of biological processes. In this study, the results were analysed by a comparison of the changes in regulatory pathways. When comparing signatures induced by titanium dioxide nanobelts and MWCNT in THP-1 cells, three pathways were upregulated specifically by MWCNT and not by titanium dioxide nanobelts: DNA damage checkpoint, DNA strand break repair, and cytoskeleton spindle microtubules. These results were consistent with others that demonstrated DNA damage and mitotic perturbations caused by MWCNT (Tilton et al., 2014). [Globally, these data showed common differential expression across the cell types and common pathways in response to exposure to titanium dioxide nanobelts or MWCNT, possibly linked to a common mechanism. However, they also showed cell-specific responses and particle-specific effects, thus addressing the question of target cell specificity.]

(c)   Experimental systems in vivo and in vitro

See Table 4.15

Female Fischer 344 rats received a single intragastric dose of SWCNT (Thomas Swan and Co. Ltd, Consett, United Kingdom) or C_{60}

fullerenes by gavage (0.064 or 0.64 mg/kg bw). Both C_{60} fullerenes (highest dose only) and SWCNT significantly enhanced the 8-oxodG level in the liver and lung tissues of rats in comparison with controls. SWCNT did not produce a significant increase in the gene expression of the DNA repair enzyme 8-oxoguanine DNA glycosylase in the liver. DNA repair activity was assessed in the liver using substrate nuclei containing 8-oxodG, and the level of 8-oxoguanine DNA glycosylase was not significantly altered (Folkmann et al., 2009).

In RAW 264.7 macrophages, SWCNT (Chengdu Organic Chemicals Co., Ltd) downregulated several genes involved in the DNA repair process (Dong et al., 2012).

The assessment of MWCNT genotoxicity in rats (Kim et al., 2012a, 2014) and mice (Ghosh et al., 2011) showed a persistence of DNA damage up to 90 days after exposure. [The findings may suggest a low or lack of DNA repair.]

Pregnant heterozygous p53 mice ($p53^{+/-}$) received an intravenous injection of MWCNT (200 µL, 2 mg/kg bw). DNA integrity was assessed using a long PCR assay. In general, DNA damage was found in the fetuses and in placental cells, with an enhancement of the mRNA expression of bax and p21. Nonetheless, DNA damage was higher in $p53^{-/-}$ and $p53^{+/-}$ fetuses than in $p53^{+/+}$ fetuses and neither *Bax* nor *p21* expression levels were modified in $p53^{-/-}$ fetuses, in agreement with a defective DNA repair system in these mice cells due to the absence of p53 (Huang et al., 2014). [These results were consistent with the induction of p53-dependent apoptosis in this test system, and showed that the repair of DNA damage and apoptosis are dependent on the p53 status resulting from the intravenous injection of MWCNT into mice. They did not directly demonstrate that DNA repair was impaired by MWCNT, but showed an impaired response in p53-deficient mice.]

Table 4.15 Studies of impaired DNA repair in tissues of experimental animals exposed to carbon nanotubes in vivo or in vitro

Species, strain (sex), or cell types (in vitro)	Route of administration (in vivo)/exposure concentration or dose, duration	Recovery	Result	Reference
Rat, F344 (F)	Intragastric (gavage) SWCNT or C_{60} fullerenes at 0.064 or 0.64 mg/kg bw Diameter, 0.9–1.7 nm; length < 1 μm (SWCNT); diameter, 0.7 nm (fullerenes)	24 h	Enhancement of 8-oxodG levels in the liver and lung tissues Increased gene expression of *OGG1* in the liver by C_{60} fullerenes (not significant with SWCNT) DNA repair activity assessed in the liver, using substrate nuclei containing 8-oxodG: no altered level of *OGG1* repair activity	Folkmann et al. (2009)
Rat, Sprague-Dawley (M)	Inhalation (in inhalation chambers) MWCNT: 0.16, 0.34, and 0.94 mg/m³, 6 h/day, 5 days/wk, 5 days	1 mo or none	Comet assay in lung cells Significant DNA damage at 0.94 mg/m³ Similar patterns of DNA damage at both time-points after exposure The persistence of DNA damage at 1 mo may suggest a lack of DNA repair.	Kim et al. (2012a)
Rat, Sprague-Dawley (M, F)	Nose-only inhalation MWCNT: 0.17, 0.49, and 0.96 mg/m³, 6 h/day, 5 days/wk, 28 days Diameter, 10–15 nm	28 or 90 days	Comet assay in lung cells Significant DNA damage at 0.94 mg/m³ Similar patterns of DNA damage at 28 and 90 days after exposure may suggest a lack of DNA repair	Kim et al. (2014)
Mouse, Swiss albino (M)	Intraperitoneal injection MWCNT: 2, 5, and 10 mg/kg bw at 0 and 24 h	3 h (comet assay) or 24 h (micronucleus)	Micronucleus and comet assay in bone marrow cells Results suggested low or lack of DNA repair during the recovery period	Ghosh et al. (2011)
Mouse, pregnant heterozygous *p53* (*p53+/−*)	Intravenous injection MWCNT: 2 mg/kg bw (single injection)		Studies of fetuses and placenta cells; measurement of DNA integrity using the L-PCR assay and mRNA expression of *Bax* and *p21* DNA damage greater in *p53−/−* and *p53+/−* fetuses than in *p53+/+* fetuses Neither *Bax* nor *p21* expression levels were modified in *p53−/−* fetuses, in agreement with an absence of DNA repair in the cells of these mice	Huang et al. (2014)

Table 4.15 (continued)

Species, strain (sex), or cell types (in vitro)	Route of administration (in vivo)/exposure concentration or dose, duration	Recovery	Result	Reference
Murine RAW 264.7 macrophages	Acid-functionalized SWCNT: 1, 10, and 50 µg/mL for 24 h	None	Gene expression profiles analysed by cDNA microarray Several genes from the DNA repair processes were downregulated (e.g. *XPA, XRCC1,* and *XRCC4*) Results suggest that acid-functionalized SWCNT may induce resistance to apoptosis and DNA damage repair deficiencies in these cells	Dong et al. (2012)

bw, body weight; F, female; L-PCR, long polymerase chain reaction; M, male; mo, month; MWCNT, multiwalled carbon nanotubes; *OGG1*, 8-oxoguanine glycosylase; 8-oxo-dG, 8-oxo-2′-deoxyguanosine; SWCNT, single-walled carbon nanotubes; wk, week

4.4.10 Depletion of antioxidants

As described previously, CNT have been shown to generate (or catalyse the formation of) ROS directly; however, this does not exclude a secondary generation of ROS by target cells in vitro or in vivo after exposure to CNT (Stone et al., 2009; Fubini et al., 2010, 2011).

(a) Exposed humans

No data were available to the Working Group.

(b) Human cells in vitro

See Table 4.16

(i) SWCNT

The effects of SWCNT (NASA-JSC, TX, USA) were determined in cell cultures of immortalized human epidermal HaCaT keratinocytes. The generation of HO• was observed in HaCaT keratinocytes exposed to SWCNT at 0.24 mg/mL, using the ESR spin trapping technique. Both GSH and the antioxidant levels of the HaCaT keratinocytes were decreased at doses of 0.06, 0.12, and 0.24 mg/mL. In parallel, a significant increase in the accumulation of lipid peroxidation products (thiobarbituric acid-reactive substances) was seen in cells exposed to SWCNT (Shvedova et al., 2003).

Human BJ foreskin cells were exposed to SWCNT (Sigma) dispersed in dimethyl formamide. ROS production was determined using the 2,7-dichlorofluorescein diacetate assay, and was induced by exposure to SWCNT at doses of 6, 8, and 10 µg/mL after 3 hours of incubation. Antioxidant defences were assessed in BJ cells co-incubated with exogenous antioxidants, NAC and GSH, in the presence or absence of SWCNT (6 µg/mL). Exogenous NAC and GSH decreased the induction of ROS by SWCNT approximately two- and 2.5-fold, respectively (Sarkar et al., 2007). [These results suggested that compromised cellular antioxidant defences may be responsible for the generation of excess ROS in response to SWCNT in BJ foreskin cells.]

The effects of SWCNT were investigated in human macrophage-like cells differentiated from a human monocytic leukaemia THP-1 cell line. Affymetrix microarrays were performed to investigate the changes in gene expression after exposure to SWCNT. Cells were exposed to 0.05 µg/mL of SWCNT for 24 hours, which resulted in an increased expression of SOD2; the levels of catalase, GPx1, GSH reductase, GSH synthetase, and NADPH-dependent oxidase were not altered (Chou et al., 2008).

Human hepatoma HepG2 cells were exposed to purified HiPCO SWCNT (Unidym) produced by the CVD process or to graphene. Proteins were extracted and their profile analysed using the iTRAQ-coupled two-dimensional liquid chromatography tandem mass spectrometry approach. Peptides and proteins were identified automatically using the Spectrum Proteomics Workbench software. Protein ratios were determined in treated and untreated control HepG2 cells. Only quantification data on proteins with relative changes in expression of > 1.25 or < 0.8 were considered. After exposure to 1 µg/mL for 48 hours, 37 differentially expressed proteins were found in cells exposed to SWCNT or to graphene. Differentially expressed proteins involved in metabolic pathways, redox regulation, and cytoskeletal dynamics were identified. The antioxidant protein SOD2 was downregulated (Yuan et al., 2011).

Human colon adenocarcinoma Caco-2 cells were exposed to 0, 5, 10, 50, 100, 500, and 1000 µg/mL of F-SWCNT (Sigma-Aldrich, Madrid, Spain). The production of ROS and biomarkers of oxidation were quantified, including lipid peroxidation, generation of ROS, GSH levels, and SOD, GPx, GSH reductase, and catalase activities. ROS generation was increased at a dose of 100 µg/mL and lipid peroxidation at a dose of 50 µg/mL. Catalase activity increased at doses up to 500 µg/mL, then significantly

Table 4.16 Depletion of antioxidants in cultured cells exposed to carbon nanotubes

Cell type	Type of carbon nanotube; treatment; duration	Assay/result	Reference
Human HaCaT keratinocytes	SWCNT; 0.24 mg/mL (ESR assay), and 0.06, 0.12, and 0.24 µg/mL (oxidation assay); 2, 4, 6, 8, and 18 h	Generation of HO• using ESR spin trapping technique; measurement of GSH, antioxidant levels and LPO products (TBARS) GSH and antioxidant levels decreased versus control cells, and the accumulation of LPO products significantly increased	Shvedova et al. (2003)
Human BJ foreskin cells	SWCNT; 6, 8, and 10 µg/mL; 3 h	Induction of ROS by SWCNT compared with control cells (dispersion medium) using DCF Antioxidants (NAC and GSH) reduced ROS production by SWCNT (6 µg/mL)	Sarkar et al. (2007)
Human macrophage-like cells differentiated from a human monocytic leukaemia THP-1 cell line	SWCNT; 0.05 µg/mL; 24 h	Molecular effects investigated using Affymetrix microarrays Expression of SOD2 increased, but levels of catalase, GPx1, GR, GS, and NOX not modified	Chou et al. (2008)
Human hepatoma HepG2 cells	SWCNT; 1 µg/mL; 48 h	Protein expression profile using the iTRAQ-coupled 2D LC-MS/MS approach; protein ratios determined for treated and untreated control HepG2 cells Differential expression of 37 proteins observed in treated cells, among which SOD2 was downregulated	Yuan et al. (2011)
Human colon adenocarcinoma Caco-2 cells	Carboxylic acid-functionalized SWCNT (F-SWCNT); 0, 5, 10, 50, 100, 500, and 1000 µg/mL; 48 h	Determination of ROS, LPO, and GSH levels, and SOD, GPx, GR, and catalase activities Generation of ROS increased from 100 µg/mL and that of LPO from 50 µg/mL; catalase activity increased up to 500 µg/mL, but significantly decreased at 1000 µg/m; SOD also enhanced (maximum up to 100 µg/mL); GPx activity enhanced at the highest concentrations and GR at 1000 µg/mL; level of GSH depleted (significant at 1000 µg/mL)	Pichardo et al. (2012)
Human bronchial epithelial BEAS-2B cells	Three samples of SWCNT (diameter, 1–2 nm; lengths, 400–800 nm, 1–3 µm, or 5–30 µm); 1 and 100 µg/mL; 24 or 48 h	Investigation of intracellular production of ROS and gene expression profiling using a pathway-specific RT-PCR array of 84 oxidative stress and antioxidant defence pathway genes ROS detected in cells treated with the two shortest SWCNT samples; with the 1–3-µm sample, several genes strongly upregulated, including EPHX2; expression level of few genes modified by the other SWCNT samples, but 400–800-nm SWCNT produced a low level of upregulation of CCS, MT3, and NOS2 All samples induced downregulation of GPx4, GPx7, and the peroxidase cytoglobin, and upregulation of NCF1	Manshian et al. (2013)

147

Table 4.16 Depletion of antioxidants in cultured cells exposed to carbon nanotubes (continued)

Cell type	Type of carbon nanotube; treatment; duration	Assay/result	Reference
Human colon carcinoma HT29 cell line	SWCNT; nine concentrations from 0.01 ng to 0.2 µg/mL; 3 or 24h	Determination of total GSH levels The range of 0.0001–0.01 µg/mL increased intracellular total GSH levels in comparison with control cells (significant at 0.001 and 0.01 µg/mL) at 24 h	Pelka et al. (2013)
Rat lung epithelial cells	SWCNT; 2.5, 5, and 10 µg/mL; up to 72 h	Determination of ROS (using the DCF assay), GSH, SOD-1, and SOD-2 levels ROS production was enhanced in a dose-dependent manner; GSH levels decreased in cells treated with 10 µg/mL for 6 h; SOD-1 and SOD-2 protein expression decreased after treatment for 24 h in comparison with control cells	Sharma et al. (2007)
Rat PC12 cells (adrenal gland pheochromocytoma)	SWCNT; 5–600 µg/mL; 24 and 48 h	Induction of mitochondrial membrane damage and the formation of increased levels of ROS and MDA Decreased levels of GSH and decreased activities of SOD, GPx, and catalase were observed at cytotoxic concentrations in a concentration-dependent manner	Wang et al. (2011b)
Rat PC12 cells (adrenal gland pheochromocytoma)	SWCNT; 50 µg/mL; 24 and 48 h	Determination of SOD, catalase, and GPx activities and of GSH content ROS generation enhanced in comparison with control cells, but MDA levels not modified; activities of SOD, catalase, and GPx were decreased	Wang et al. (2012b)
RAW 264.7 macrophages	Unpurified (iron, 26.0 wt %) or purified (iron, 0.23 wt %) SWCNT; 0.12–0.5 mg/mL without or with zymosan (0.25 µg/mL); 1–2 h	Determination of specific free radical intermediates by EPR spectroscopy Neither purified nor unpurified SWCNT generated intracellular ROS In the presence of zymosan, production of HO• more effective with unpurified than with purified SWCNT; LPO enhanced and GSH content decreased; both levels decreased by the addition of SWCNT in comparison with macrophages stimulated with zymosan only	Kagan et al. (2006)
Murine epidermal JB6 P+ cells	SWCNT; 0.06, 0.12, and 0.24 mg/mL; 24 h	A significant dose-dependent decrease in GSH observed after incubation of cells with partially purified SWCNT for 24 h; exposure to unpurified (iron, 30 wt%) SWCNT induced a greater reduction in GSH than exposure to partially purified (iron, 0.23 wt%) SWCNT	Murray et al. (2009)

Table 4.16 (continued)

Cell type	Type of carbon nanotube; treatment; duration	Assay/result	Reference
Primary mouse embryo fibroblasts	SWCNT (or carbon black, silicon dioxide, and zinc oxide); 5, 10, 20, 50, and 100 µg/mL; 24 h	Measurement of intracellular ROS, GSH and MDA levels, and SOD activity ROS production enhanced with all particles, in a dose-dependent manner up to 50 µg/mL; dose-dependent decrease in intracellular GSH level and SOD activity observed in comparison with control cells; with SWCNT, LPO was significantly enhanced only at 100 µg/mL	Yang et al. (2009)
Human epidermal keratinocytes	MWCNT; 0.4 mg/mL; 24 and 48h	Protein expression analysed by two-dimensional gel electrophoresis and mass spectrometry Significant differential expression of 152 proteins, among which the expression of SOD2 was decreased by 1.4- and 1.9-fold at 24 and 48 h, respectively, in comparison with untreated cells	Witzmann & Monteiro-Riviere (2006)
Human embryonic kidney HEK 293 cell line	MWCNT produced by electric arc process using graphite as a source (MWCNT1) and chemical vapour deposition using methane as hydrocarbon (MWCNT2); 10–100 µg/mL; for 48 h	Measurement of cellular levels of reduced GSH and MDA content The level of MDA increased and that of intracellular GSH decreased	Reddy et al. (2010b)
Human monocytic THP-1 cells differentiated into macrophages with phorbol myristate acetate	Three types of MWCNT: long (approximately 50 µm) straight MWCNT (diameter, 20–100 nm; NT1), micron-sized aggregated relatively straight MWCNT (diameter, approximately 150 nm; NT2), and MWCNT with an aggregated entangled structure (individual diameter, approximately 20 nm; NT3); 62.5 µg/mL; 4 h Control particles of carbon black (diameter, 260 nm or 14 nm) and LFA (length, > 5 mm; diameter, < 200 nm); 62.5 µg/mL; 4 h	Determination of *GSTpi* and *HO-1* expression (RT-PCR), HO-1 protein expression (ELISA), and GST activity *GSTpi* expression not modified after any treatment; *HO-1* expression enhanced by NT1 (significant) and NT2 (not significant), and reduced by NT3, 260-nm carbon black and LFA; HO-1 protein and GST activity (no significant difference)	Brown et al. (2010)
Human umbilical vein endothelial cells	MWCNT: 0, 5, and 20 µg/mL; 2 h	Measurement of LPO and antioxidant levels: MDA, SOD and GPx; the antioxidant NAC was used to explore the involvement of ROS in cell injury ROS levels significantly increased by 20 µg/mL MWCNT; SOD and GPx activities enhanced at the lowest doses, but reduced at 20 µg/mL; pretreatment with NAC reduced ROS in comparison with exposure to MWCNT only	Guo et al. (2011)

Table 4.16 Depletion of antioxidants in cultured cells exposed to carbon nanotubes (continued)

Cell type	Type of carbon nanotube; treatment; duration	Assay/result	Reference
Human embryonic kidney HEK 293 cell line	Four different MWCNT (CNM1, CNM2, CNM4, and CNM3; size: 100–800, 200–500, 150–750, and 230–1700 nm, respectively); 3, 10, 30, 100, and 300 µg/mL; 48 h	Measurement of cellular levels of GSH (colorimetric assay) and LPO (MDA content) Cytotoxicity and oxidative stress induced in a concentration-dependent manner; increased MDA content and decreased intracellular GSH levels observed with 30 and 100 µg/mL	Rama Narsimha Reddy et al. (2011)
Human lung adenocarcinoma epithelial A549 cells	MWCNT; 0.5, 1, 5, 10, 50, and 100 µg/mL; 6–72 h	Measurement of cellular levels of GSH (colorimetric assay), LPO (Lipid Peroxidation Assay Kit), and catalase activity (commercial kit) Significant ROS production at 10 and 50 µg/mL; enhancement of LPO significant at all MWCNT concentrations (for 24 h); significant decreases in intracellular GSH level and catalase activity at 50 µg/mL	Srivastava et al. (2011)
Human hepatoblastoma C3A cell line	Two types of MWCNT (NM 400, Nanocyl; diameter, 30 nm; length, 5 µm; and NM 402, Arkema Graphistrength C100; diameter, 30 nm; length, 20 µm); 0.5–256 µg/mL; 2–24 h	Determination of intracellular ROS level (using the DCF assay) and GSH (using OPT) Generation of ROS with both MWCNT and a decrease in total GSH and GSH cell content at 24 h; pretreatment with an antioxidant (Trolox) prevented MWCNT-induced ROS production	Kermanizadeh et al. (2012)
Telomerase-immortalized human keratinocytes (N-hTERT)	MWCNT; 100 µg/mL; 30 min–24 h	Determination of intracellular ROS level and oxidative stress (using DCF oxidation), and reduced GSH (commercial kit) Increased DCF oxidation induced by MWCNT stirred or sonicated in water; in contrast, no effects seen with MWCNT sonicated in dispersive agents (HPC, Fagron or Pluronic F108); addition of the antioxidant Trolox prevented DCF oxidation; significant reduction in GSH level compared with controls	Vankoningsloo et al. (2012)
Rat glioma C6 cell line	MWCNT1 (diameter, 10–20 nm; average length, 2 µm) and MWCNT2 (diameter, 40–100 nm; average length, 10 µm); 25–400 µg/mL; 24 h	Determination of cytotoxicity, MDA levels and SOD activity MWCNT1 more cytotoxic than MWCNT2; increased levels of oxidative stress observed; both CNT induced a significant increase in MDA level (at 100 µg/mL) compared with that in controls and lowered the activity of SOD	Han et al. (2012)

CCS, copper chaperone for superoxide dismutase; DCF, 2,7-dichlorofluorescein; ELISA, enzyme-linked immunosorbent assay; EPHX2, epoxide hydrolase 2; ESR, electronic spin resonance; GPx, glutathione peroxidase; GR, glutathione reductase; GS, glutathione synthetase; GSH, reduced glutathione; GST, glutathione S-transferase; HO-1, haeme-oxygenase-1; HPC, hydroxypropylcellulose; iTRAQ-coupled 2D LC-MS/MS, iTRAQ-coupled two-dimensional liquid chromatography tandem mass spectrometry; LFA, long fibre amosite asbestos; LPO, lipid peroxidation; MDA, malondialdehyde; MT3, metallothionein 3; MWCNT, multiwalled carbon nanotubes; NAC, N-acetylcysteine; NOS2, nitric oxide synthase 2; NOX, NADPH-dependent oxidase; OPT, fluorescent substrate o-phthalaldehyde; ROS, reactive oxygen species; RT-PCR, real-time polymerase chain reaction; SOD, superoxide dismutase; SWCNT, single-walled carbon nanotubes; TBARS, thiobarbituric acid-reactive substance

decreased at 1000 µg/mL. SOD activity was also increased at doses up to 100 µg/mL. GPx activity was enhanced at the highest doses and GSH reductase at a dose of 1000 µg/mL. GSH level was depleted at all doses tested (significant at 1000 µg/mL) (Pichardo et al., 2012). [These results showed the induction of antioxidant defences in response to exposure to F-SWCNT and an increase in lipid peroxidation products, possibly causing toxic effects.]

Intracellular generation of ROS and expression profiles of oxidative stress response genes were assessed in human bronchial epithelial BEAS-2B cells exposed to SWCNT. Three SWCNT samples were tested (diameter, 1–2 nm ; length, 400–800 nm, 1–3 µm or 5–30 µm). Crocidolite asbestos fibres were used as positive control. Gene expression profiles were studied using a pathway-specific RT-PCR array (SuperArray) comprising primers for 84 oxidative stress and antioxidant defence pathway genes. All SWCNT samples and crocidolite asbestos fibres induced the formation of micronuclei; the generation of ROS was detected in cells exposed to the two shortest SWCNT samples and crocidolite asbestos fibres. The 1–3-µm SWCNT sample upregulated the expression of several genes: epoxide hydrolase 2, surfactant protein D, and neutrophil cytosolic factor 1. Few genes showed differential expression with the other SWCNT samples; however, 400–800-nm SWCNT induced the upregulation of three proteins: copper chaperone for SOD, metallothionein 3, and nitric oxide synthase 2. Differentially expressed genes common to all SWCNT included the upregulation of titin and copper chaperone for SOD and downregulation of the GPxs, *GPX4* and *GPX7*, and the peroxidase cytoglobin that may be involved in protection against oxidative stress; neutrophil cytosolic factor 1 (required for the activation of latent NADPH oxidase, which is necessary for superoxide anion production) was also upregulated by all samples (Manshian et al., 2013).

The effects of SWCNT dispersed in sodium cholate on total GSH levels was evaluated in the human colon carcinoma HT29 cell line. Nine doses of SWCNT were tested (from 0.01 ng/mL to 0.2 µg/mL). Exposure to SWCNT in a dose range of 0.0001 µg/mL to 0.01 µg/mL increased the intracellular level of total GSH (significant at 0.001 and 0.01 µg/mL) (Pelka et al., 2013).

(ii)   MWCNT

Human epidermal keratinocytes were exposed to MWCNT manufactured using a microwave plasma-enhanced CVD system. After exposure to 0.4 mg/mL for 24 and 48 hours, proteins were extracted and analysed by two-dimensional gel electrophoresis and mass spectrometry. Of these, 152 were observed to be differentially expressed and to be associated with several pathways: metabolism, cell signalling, stress, the expression of cytoskeletal components, and vesicular trafficking. Among them, SOD2 protein was decreased by 1.4- and 1.9-fold at 24 and 48 hours, respectively, in comparison with untreated cells (Witzmann & Monteiro-Riviere, 2006).

MWCNT produced by an electric arc process using graphite as a source (MWCNT1) and by CVD using methane as the hydrocarbon (MWCNT2) were obtained from the Centre for Environment, Institute of Science and Technology, JNTU, Hyderabad, India. Cytotoxicity and oxidative stress were studied in the human embryonic kidney HEK 293 cell line. Cellular levels of reduced GSH and MDA content were measured to assess lipid peroxidation. Exposure of HEK 293 cells to MWCNT (10–100 µg/mL) for 48 hours resulted in concentration-dependent cytotoxicity, increased levels of MDA, and decreased intracellular levels of GSH (Reddy et al., 2010b). [These findings suggested that MWCNT induced oxidative stress and cytotoxicity in these target cells.]

Oxidative stress was studied after exposure to MWCNT of the human monocytic

THP-1 cell line differentiated into macrophages using phorbol myristate acetate. Three types of MWCNT were used: long straight MWCNT (length, approximately 50 μm; diameter, 20–100 nm; NT1); micron-sized aggregated MWCNT (relatively straight MWCNT; diameter, approximately 150 nm; NT2); and MWCNT with an aggregated entangled structure (individual diameter, approximately 20 nm; NT3). Control particles were carbon black 260 nm in diameter, carbon black 14 nm in diameter and long fibre amosite asbestos (length > 5 μm; diameter < 200 nm). Investigations included the assessment of gene expression using RT-PCR (GSH S-transferase [GST]pi and haeme oxidase 1[HO-1]), expression of HO-1 protein (enzyme-linked immunosorbent assay) and GST activity. After exposure of THP-1 cells to 62.5 μg/mL of particles for 4 hours, GSTpi expression was not modified after any treatment; HO-1 expression was enhanced in cells exposed to NT1 (statistically significant) and NT2 (not statistically significant), and reduced in cells exposed to NT3, 260-nm carbon black and long fibre amosite asbestos. No significant difference from the control was observed with any of the treatments for either GST activity or HO-1 protein expression. However, an enhancement of the Nrf2 protein expression was found in the nucleus of cells treated with NT1, which was eradicated by the addition of antioxidants (Brown et al., 2010). [This study suggested that the activation of the antioxidant response pathway is mediated by the antioxidant response element and Nrf2.]

Human umbilical vein endothelial cells were exposed for 2 hours to 0, 5, and 20 μg/mL of MWCNT (from Dr F. Chen, Lawrence Berkeley National Laboratory, Berkeley, CA) synthesized using a CVD method. Lipid peroxidation and antioxidant defences were determined by the quantification of MDA, and the activity of SOD and GPx. These cells were also incubated with the antioxidant NAC to explore the role of ROS in the induction of cell injury. Cellular ROS levels were significantly increased by exposure to 20 μg/mL of MWCNT. The activities of SOD and GPx were enhanced at the lowest concentrations but reduced at 20 μg/mL. When human umbilical vein endothelial cells were pretreated with NAC before exposure to MWCNT, ROS production was reduced compared with the groups exposed to MWCNT only, and cytotoxicity and DNA damage (DNA breakage by quantification of γH2AX foci) were also reduced (Guo et al., 2011). [These results showed that depletion of antioxidants was associated, at least partially, with cytotoxicity and DNA damage.]

Cellular levels of GSH were determined in the human embryonic kidney HEK 293 cell line exposed to four MWCNT with different dimensions (CNM1, CNM2, CNM4, and CNM3; size: 100–800, 200–500, 150–750, and 230–1700 nm, respectively) from the Centre for Environment (Institute of Science and Technology, JNTU, Hyderabad). In-vitro exposure of HEK 293 cells to 3–300 μg/mL of these MWCNT for 48 hours produced cytotoxicity and oxidative stress in a concentration-dependent manner. Increased lipid peroxidation (measured by MDA content) and decreased intracellular GSH levels were observed at concentrations of 30 and 100 μg/mL (Rama Narsimha Reddy et al., 2011).

Human lung adenocarcinoma epithelial A549 cells were exposed to MWCNT (provided by Professor D.G. Weiss, Department of Biological Sciences, Institute of Cell Biology and Biosystems Technology, Rostock University, Germany) at 0.5–100 μg/mL for 6–72 hours. Apoptotic cells were detected after exposure to 50 μg/mL for 72 hours. Significant ROS production was found at doses of 10 and 50 μg/mL, which was not due to mitochondrial activity. Lipid peroxidation was determined using a Lipid Peroxidation Assay Kit, and GSH levels determined using a colorimetric assay. Increased lipid peroxidation was significant at all concentrations of MWCNT after 24 hours of treatment, and both intracellular GSH levels

and catalase activity were significantly reduced at a dose of 50 µg/mL (Srivastava et al., 2011).

The effects of two types of MWCNT – NM 400 (Nanocyl; diameter, 30 nm; length, 5 µm) and NM 402 (Arkema Graphistrength C100 ; diameter, 30 nm; length, 20 µm) – were assessed in the human hepatoblastoma C3A cell line. Intracellular ROS generation was measured using the 2,7-dichlorofluorescein diacetate assay, and GSH was quantified by the reaction of sulfhydryl groups with the fluorescent substrate ortho-phthalaldehyde. Both samples of MWCNT induced the generation of ROS and decreased total GSH and cellular GSH content after 24 hours. Pretreatment with the antioxidant, Trolox, prevented MWCNT-induced production of ROS. Cytotoxicity was also reduced in C3A cells pretreated with Trolox before exposure to MWCNT (Kermanizadeh et al., 2012).

The intracellular level of GSH was quantified in telomerase-immortalized human keratinocytes (N-hTERT) exposed to 100 µg/mL of MWCNT (NanocylTM NC7000 MWCNT from Nanocyl, produced by catalytic CVD) for 30 minutes or 24 hours. Oxidative stress was assessed using 2,7-dichlorofluorescein oxidation. MWCNT stirred or sonicated in water were marked by increased dichlorofluorescein fluorescence, suggesting an increased intracellular generation of ROS. In contrast, MWCNT sonicated in dispersants (HPC, Fagron, or Pluronic F108) showed no significant effects. The addition of the antioxidant, Trolox, a hydrophilic analogue of the lipophilic antioxidant vitamin E, prevented 2,7-dichlorofluorescein oxidation. Moreover, GSH was significantly decreased compared with untreated controls (Vankoningsloo et al., 2012).

(c)   Experimental systems in vivo

See Table 4.17

(i)   SWCNT

C57BL/6 mice were maintained on vitamin E-sufficient or vitamin E-deficient diets and were exposed to SWCNT (CNI, Inc.) by pharyngeal aspiration. Antioxidant levels were determined in lung homogenates 28 days after exposure to 40 µg/mouse of SWCNT. Treatment with SWCNT induced greater increase in lipid peroxidation products and greater decrease in GSH levels in mice fed a vitamin E-deficient diet than in those fed basal diet, showing that SWCNT produced antioxidant depletion which was associated with a higher sensitivity to SWCNT-induced acute inflammation (Shvedova et al., 2007).

C57BL/6 mice were exposed to 5 mg/m³ of SWCNT in inhalation chambers for 5 hours per day for 4 days. The level of oxidative damage produced was measured in the lung homogenates. GSH levels were significantly depleted, and the level of lipid peroxidation products – measured as malondialdehyde (MDA) – showed a significant accumulation compared with controls 7 and 28 days after exposure. Total antioxidant capacity was reduced 1 and 7 days after treatment, but returned to the control level by 28 days after exposure (Shvedova et al., 2008).

SKH-1 immune competent hairless mice were exposed to SWCNT (CNI, Inc.) by daily skin application at doses of 40, 80, or 160 µg/mouse for 5 days. A reduction in GSH levels was found in skin homogenates of mice treated with the highest dose, but no change was found with the other doses (Murray et al., 2009).

Male BALB/c mice were exposed to 5 µg/g bw of aerosolized SWCNT (diameter, 1–2 nm; length, 0.5–2.0 µm; from Aldrich) in PBS or to PBS only, for 20 minutes per day on 7 consecutive days in a nose-only exposure system. The animals were killed at the end of the exposure period and lung tissues were collected. The intracellular levels of MDA and ROS, and the activities of SOD, catalase, and GPx were measured. Apoptosis was assessed by the measurement of

Table 4.17 Depletion of antioxidants in experimental animals exposed to carbon nanotubes

Species, strain (sex)	Route of administration exposure concentration or dose, duration	Recovery	Assay/result	Reference
Mouse, C57BL/6 fed vitamin E-sufficient or vitamin E-deficient diets (F)	Pharyngeal aspiration SWCNT: single dose of 40 μg/mouse	28 days	Measurement of lipid peroxidation products and GSH levels in lung homogenates SWCNT produced antioxidant depletion; higher increase in lipid peroxidation products and greater decrease in GSH levels found in mice fed vitamin E-deficient diets	Shvedova et al. (2007)
Mouse, C57BL/6 (F)	Inhalation (in inhalation chambers) SWCNT: 5 mg/m³, 5 h/day, 4 days	1, 7 or 28 days	Level of oxidative damage (lipid peroxidation measured as MDA and GSH levels) measured in lung homogenates Significant accumulation of lipid peroxidation products compared with controls 7 and 28 days after exposure; GSH levels significantly depleted; total antioxidant capacity reduced 1 and 7 days after treatment, but returned to the control level by 28 days after exposure	Shvedova et al. (2008)
Mouse, SKH-1 immune competent hairless (NR)	Skin application SWCNT: 40, 80, or 160 μg/mouse, once/day, 5 days	24 h	Measurement of GSH levels in skin homogenates Reduction of GSH levels in mice treated with the highest dose; no change with the other doses	Murray et al. (2009)
Mouse, BALB/c (M)	Inhalation (nose-only exposure) SWCNT: 5 μg/g bw, 20 min/day, 7 days	None	Measurement of intracellular levels of MDA and ROS, and activities of SOD, catalase, and GPx in the lung; caspase-3 and -8 activities for apoptosis in lung homogenates; and MPO activity in BALF ROS and MDA levels significantly higher in the lungs of SWCNT-exposed mice versus controls; reduced activities of SOD, catalase, and GPx; apoptosis induction; MPO activity higher in the BALF from SWCNT-exposed than control animals	Ravichandran et al. (2011)
Rat, Wistar albino (M)	Intratracheal instillation Two MWCNT samples: single dose of 0.2, 1, or 5 mg/kg bw or quartz-crystalline silica particles (positive control)	1, 7, 30, and 90 days	Antioxidant capacity determined in blood samples: measurement of GSH, lipid peroxidation product (MDA), and SOD and catalase activities Total antioxidant capacity assessed by the ability to scavenge the free radical, α,α-diphenyl-β-picryl hydrazyl With both MWCNT and quartz: significant dose-dependent depletion of GSH levels and decrease in SOD activity; transient dose-dependent decrease in catalase activity; dose-dependent increase in amount of MDA 1 day after instillation, that decreased later; decreased total antioxidant capacity	Reddy et al. (2011)
Rat, Wistar (M)	Intraperitoneal injection MWCNT functionalized with single-strand DNA: single dose of 270 mg/L		Levels of GSH measured in the plasma and liver after 1, 3, 6, 24, 48, or 144 h Significant decrease in the levels of GSH in plasma at all time points after exposure, and in the liver after 3 and 24 h, but not at 48 or 144 h; GSH level returned to normal within 6 days; decreased activity of MnSOD (SOD2) in the liver at 1, 24, and 48 h, but not at 144 h	Clichici et al. (2012)

Table 4.17 (continued)

Species, strain (sex)	Route of administration exposure concentration or dose, duration	Recovery	Assay/result	Reference
Mouse, BALB/c (M)	Inhalation (nose-only exposure) MWCNT: 5 µg/g bw, 20 min/day, 7 days	None	Measurement of intracellular levels of MDA and ROS, and activities of SOD, catalase and GPx in the lung; caspase-3 and -8 activities for apoptosis in lung homogenates; and MPO activity in BALF ROS and MDA levels significantly higher in lungs of MWCNT-exposed mice; reduced activities of SOD, catalase, and GPx; apoptosis induction; MPO activity higher in the BALF from MWCNT-exposed mice	Ravichandran et al. (2011)
Mouse, pregnant heterozygous *p53* (*p53*+/−)	Intravenous injection MWCNT: 2 mg/kg bw on gestational days 10.5, 12.5, and 15.5		Investigation of MEF Treatment of dams with MWCNT and an antioxidant, *N*-acetylcysteine, abolished MWCNT-only induced DNA breakage observed in MEF	Huang et al. (2014)

BALF, bronchoalveolar lavage fluid; bw, body weight; GPx, glutathione peroxidase; GSH, glutathione; MDA, malondialdehyde; MEF, mouse embryo fibroblasts; MnSOD, manganese superoxide dismutase; MPO, myeloperoxidase; MWCNT, multiwalled carbon nanotubes; NR, not reported; ROS, reactive oxygen species; SOD, superoxide dismutase; SWCNT, single-walled carbon nanotubes

caspase-3 and -8 activities in lung homogenates. MPO activity was measured in the BALF. MPO activity was higher in the BALF from SWCNT-exposed mice compared with controls. ROS and MDA levels were significantly higher in the lungs of SWCNT-exposed mice compared with controls, and SOD, catalase, and GPx were reduced. In parallel, apoptosis was demonstrated by the enhancement of caspase-3 and -8 activities (Ravichandran et al., 2011).

(ii) MWCNT

The antioxidant status of rat serum was evaluated after intratracheal instillation of MWCNT into male Wistar albino rats. Two MWCNT samples were used (from the Centre for Environment, Institute of Science and Technology, JNTU, Hyderabad), produced either by the electric arc process using graphite as a source or CVD using methane as the hydrocarbon. The rats received a single dose of 0.2, 1, or 5 mg/kg bw of MWCNT or quartz-crystalline silica particles (positive control). Blood samples were collected at 1, 7, 30, and 90 days after the instillation. Antioxidant capacity was determined by the measurement of GSH, a lipid peroxidation product (MDA), and SOD and catalase activities. Both MWCNT induced a significant dose-dependent depletion of GSH levels, decrease in SOD activity, and a transient dose-dependent decrease in catalase activity. Similarly, the amount of MDA was increased by both MWCNT in a dose-dependent manner 1 day after instillation and later decreased. Total antioxidant capacity, assessed by the ability to scavenge the free radical α,α-diphenyl-β-picryl hydrazyl, was decreased after exposure to MWCNT (Reddy et al., 2011). [These results indicated a reduction in antioxidant defence mechanisms after an instillation of MWCNT.]

Wistar rats received a single intraperitoneal injection of 270 mg/L of MWCNT (exterior diameter, 15–25 nm; interior diameter, 10–15 nm; surface, 88 m^2/g) synthesized by the CVD technique and functionalized with single-strand DNA. The level of GSH was measured in the plasma and liver 1, 3, 6, 24, 48, and 144 hours later. A significant decrease in the level of GSH was observed in the plasma at all timepoints after exposure, and after 3 and 24 hours (but not after 48 or 144 hours) in the liver. This result was consistent with a depletion of antioxidants by this single-strand DNA–MWCNT sample. The GSH level returned to normal within 6 days. The activity of manganese SOD (SOD2) in the liver was decreased after 1, 24, and 48 hours, but not after 144 hours (Clichici et al., 2012). [These results could be consistent with a decrease in antioxidant defence after exposure to this single strand DNA–MWCNT sample.]

In a transplacental study carried out on mouse embryo fibroblasts from fetuses of p53$^{+/-}$ heterozygous mice, the treatment of dams with MWCNT and an antioxidant, NAC, abolished the MWCNT-only induced DNA breakage observed in these cells (Huang et al., 2014). [This result was consistent with the generation of ROS in cells exposed to MWCNT.]

Male BALB/c mice were exposed daily to 5 µg/g bw of aerosolized MWCNT (diameter, 20–50 nm; length, 6–13 nm; from Sigma) in PBS or to PBS only for 20 minutes on 7 consecutive days, in a nose-only exposure system. Animals were killed at the end of the exposure period and lung tissues were collected. The intracellular levels of MDA and ROS, and the activities of SOD, catalase, and GPx were measured. Apoptosis was assessed by the measurement of caspase-3 and -8 activities in lung homogenates. MPO activity was measured in the BALF. MPO activity was higher in the BALF from MWCNT-exposed mice compared with controls. ROS and MDA levels were significantly higher in the lungs of MWCNT-exposed mice compared with controls, and SOD, catalase, and GPx were reduced. In parallel, apoptosis was demonstrated by the enhancement of caspase-3 and -8 activities (Ravichandran et al., 2011).

(c)   Experimental systems in vitro

See Table 4.16

(i)   SWCNT

Rat lung epithelial cell cultures were exposed to SWCNT (Sigma Chemical Co.). The levels of ROS (2,7-dichlorofluoroscein diacetate assay), GSH content, and the levels of SOD1 and SOD2 antioxidant enzymes were quantified. The results showed the production of ROS in a concentration-dependent manner. GSH levels were decreased in cells treated with 10 µg/mL for 6 hours. Expression of SOD1 and SOD2 proteins was decreased after 24 hours in comparison with control cells (Sharma et al., 2007). [Globally, exposure to SWCNT induced oxidative stress and depletion of antioxidants.]

Rat adrenal gland pheochromocytoma PC12 cells were exposed to SWCNT (diameter, 1–2 nm; length, ~20 µm) (Beijing Nachen Technology & Development Co. Ltd, Beijing, China) at concentrations of 5–600 µg/mL for 24 and 48 hours. Exposure to SWCNT induced mitochondrial membrane damage, the formation of ROS, and increased levels of the lipid peroxidation product MDA. GSH levels, and activities of SOD, GPx, and catalase were decreased at cytotoxic concentrations in a concentration-dependent manner (Wang et al., 2011b). [These findings revealed that SWCNT induced oxidative stress in these target cells.]

The effects of SWCNT (diameter, 1–2 nm; length, ~20 µm; Beijing Nachen Technology & Development Co. Ltd) were studied in rat adrenal gland pheochromocytoma PC12 cells. The activities of catalase, SOD, and GPx and the GSH content were determined 24 and 48 hours after exposure to 50 µg/mL. The generation of ROS was enhanced in SWCNT-treated PC12 cells, but the level of the lipid peroxidation product, MDA, did not appear to be elevated. The activities of SOD, catalase, and GPx were all decreased (Wang et al., 2012b).

Oxidative stress was assessed in RAW 264.7 macrophages exposed to SWCNT produced by the HiPCO disproportionation technique, with iron carbonyl as the iron-containing catalyst precursor (CNI, Inc.). The SWCNT used were unpurified (iron, 26.0 wt%) or purified (iron, 0.23 wt%) to determine the effects of iron. Specific free radical intermediates produced by RAW 264.7 cells exposed to 0.12–0.5 mg/mL for 1–2 hours were determined using electron paramagnetic resonance spectroscopy. Neither purified nor unpurified SWCNT induced the intracellular production of superoxide radicals or nitric oxide in RAW 264.7 macrophages. The production of radicals was observed when RAW 264.7 cells were stimulated with zymosan (0.25 mg/mL), an agent known to activate the generation of ROS in macrophages. Under these conditions, HO• production was enhanced in zymosan-treated cells, and unpurified iron-rich SWCNT were more potent than purified SWCNT. Lipid peroxidation assessed by MDA levels was enhanced and GSH content was decreased in zymosan-stimulated RAW 264.7 macrophages. The addition of SWCNT lowered both lipid peroxidation and GSH content in comparison with zymosan-stimulated macrophages (Kagan et al., 2006).

Murine epidermal JB6 P+ cells were exposed to SWCNT (CNI, Inc.) produced by the HiPCO disproportionation process. A significant concentration-dependent decrease in GSH content was observed after a 24-hour incubation of JB6 P+ cells with 0.06 mg/mL, 0.12 mg/mL, and 0.24 mg/mL of partially purified SWCNT. Exposure to unpurified (iron, 30 wt%) SWCNT induced a greater reduction in GSH than exposure to partially purified (iron, 0.23 wt%) SWCNT (Murray et al., 2009).

Primary mouse embryo fibroblasts were exposed to various manufactured nanoparticles: SWCNT (diameter, 8 nm; length < 5 µm), carbon black, silicon dioxide, and zinc oxide. Intracellular generation of ROS, GSH and MDA levels, and SOD activity were determined after exposure to

particle suspensions at doses of 5, 10, 20, 50, and 100 µg/mL for 24 hours. ROS production was enhanced by all particles in a concentration-dependent manner up to 50 µg/mL. Intracellular GSH levels decreased dose-dependently and the activity of SOD was decreased in treated fibroblasts in comparison with untreated control cells. Lipid peroxidation was significantly enhanced in cells exposed to SWCNT at a dose of 100 µg/mL only. In this study, SWCNT exhibited greater genotoxicity than zinc oxide nanoparticles, although zinc oxide induced more oxidative stress (Yang et al., 2009).

(ii) MWCNT

Two types of MWCNT – MWCNT1 (diameter, 10–20 nm; average length, 2 µm) and MWCNT2 (diameter, 40–100 nm; average length, 10 µm) – were studied in the C6 rat glioma cell line with regard to effects on MDA levels and SOD activity. Exposure of C6 rat glioma cells to MWCNT (25–400 µg/mL) for 24 hours resulted in an increased level of oxidative stress, and MWCNT1 was more cytotoxic than MWCNT2. MDA levels increased significantly after treatment with 100 µg/mL of both MWCNT1 and MWCNT2 compared with those in untreated controls. SOD activity was decreased by both MWCNTs (Han et al., 2012).

4.4.11 Activation of oncogenes and inactivation of tumour-suppressor genes

The expression of an important number of oncogenes and tumour-suppressor genes has been analysed in CNT-exposed experimental animals. Overall, most of these genes had different expression levels compared with unexposed control animals.

Lists of oncogenes, tumour-suppressor genes and cancer genes are available in the supplementary tables in Vogelstein et al. (2013).

(a) Exposed humans

No data were available to the Working Group.

(b) Human cells in vitro

See Table 4.18

(i) SWCNT

Cell-cycle regulation was investigated using microarray analysis in human embryo kidney HEK 293 cells exposed to 25 µg/mL of SWCNT (Carbon Nanotechnologies, Inc.) for 48 hours. Under these experimental conditions, cell viability was approximately 84%. Exposure to SWCNT was associated with the induction of apoptosis and cell-cycle control genes, and several oncogenes or tumour-suppressor genes were either downregulated (e.g. *CDK2*, *CDK4*, *CDK6*), or upregulated (e.g. *CDKN2A*, *TP53*), consistent with the activation of an apoptotic response and cell-cycle arrest (Cui et al., 2005). [A discrepancy was noted by the Working Group between the text and Table 2 in Cui et al. (2005) regarding the up- or downregulation of *TP53*.]

Human BJ foreskin CRL-2522 cells were exposed to 0 (control) or 6 µg/mL of SWCNT (Sigma) in dimethylformamide vehicle for 24 hours. Gene expression was assessed using a Stress and Toxicity Array (Super Array, Frederick, MD, USA) and was altered in 96 genes in SWCNT-treated cells compared with controls; 28 of these genes showed significant upregulation, with a ratio ranging from 1.5 to 3. The altered genes were involved in several pathways – apoptosis, xenobiotic metabolism, DNA repair, and oxidative stress – and may represent potential oncogenes or tumour-suppressor genes (i.e. *DNAJB4*, *ATM*, *CCNC*) (Sarkar et al., 2007). [These genes play a role in the response to stress, DNA repair and apoptosis, and cell-cycle progression. Their activation in SWCNT-exposed cells was not indicative of damage to these cells but signified the activation of defence mechanisms by BJ cells.]

Table 4.18 Expression of genes and proteins in human cells and experimental systems exposed to carbon nanotubes in vitro

Cell types	Type of carbon nanotube: treatment	Assay/result	Reference
Human embryo kidney HEK 293 cells	Unpurified SWCNT: 25 μg/mL, 48 h	Cell cycle regulation investigated by microarray analysis Several oncogenes or tumour-suppressor genes such as *CDK2, CDK4,* and *CDK6,* downregulated; *CDKN2A* and *TP53,* upregulated [discrepancy between the text and Table 2 in Cui et al. (2005) in which *TP53* was downregulated]	Cui et al. (2005)
Human BJ foreskin CRL-2522 cells	Unpurified SWCNT: 6 μg/mL, 24 h	Gene expression studied using Stress and Toxicity Array Modification of the expression of 96 genes in SWCNT-treated cells compared with controls, of which 28 showed significant upregulation; some genes may play a role as potential oncogenes or tumour-suppressor genes: *DNAJB4* (DnaJ (Hsp40) homologue), *ATM* (ataxia telangiectasia mutated), and *CCNC* (cyclin C)	Sarkar et al. (2007)
Human bronchial epithelial BEAS-2B cells	Purified SWCNT: 0.02 μg/cm² continuously, passaged weekly, 24 wk	Determination of p53 status by immunoblotting, using human apoptosis array After 24 wk of exposure, SWCNT-treated cells showed morphological features of malignant transformation Different expression profiles of apoptosis proteins in transformed SWCNT-treated cells compared with controls: differential expression of the phosphorylated forms of p53, which was lower in transformed SWCNT-treated BEAS-2B cells than in controls	Wang et al. (2011a)
Human colon carcinoma HT29 cell line	Purified SWCNT: eight concentrations from 0.05 ng/mL to 0.2 μg/mL, 3 or 24 h	Investigation of p53 phosphorylation by Western blot Induction of phospho-p53 observed at concentrations ≥ 5 ng/mL but declined at higher concentrations (0.1 and 0.2 μg/mL)	Pelka et al. (2013)
Human pleural mesothelial MeT-5A and peritoneal mesothelial LP-9 cells	Unpurified SWCNT: 0.02, 0.06, and 0.2 μg/cm² continuously, 2 mo	Protein expression of HRAS by Western blot, and activation of downstream signalling of the *HRAS* pathway Phenotypical changes characteristic of neoplastic transformation (cell growth in soft agar and invasion capability) Enhancement of HRAS protein expression and activation of the ERK1/2 pathway associated with more neoplastic phenotypes Exposure to SWCNT enhanced the expression of AKT (potential oncogenic protein) and lowered the expression level of genes involved in the epithelial–mesenchymal transition process (*TWIST* and *SNAI1,* [discrepancy between the text and Figure 5])	Lohcharoenkal et al. (2014)
Murine monocytic RAW 264.7 macrophages	AF-SWCNT: 0, 1, 10, and 50 μg/mL, 24 h	Determination of gene expression profiles by cDNA microarray A total of 130 genes differentially expressed; 126 were underexpressed and 4 were overexpressed, and *CHEK1* (potential tumour-suppressor gene) was downregulated	Dong et al. (2012)
Human skin HSF42 and human embryonic lung IMR-90 fibroblasts	MWCNO and unpurified MWCNT: 0.6 and 6 μg/mL, and 0.06 and 0.6 μg/mL, respectively, 48 h	Whole genome expression array Modification of the expression of numerous genes with both particles; no evidence of oncogene activation or tumour-suppressor gene inactivation seen with MWCNT	Ding et al. (2005)

Table 4.18 Expression of genes and proteins in human cells and experimental systems exposed to carbon nanotubes in vitro (continued)

Cell types	Type of carbon nanotube: treatment	Assay/result	Reference
Human lung adenocarcinoma A549 cells	Unpurified MWCNT: 1–50 μg/mL, 3, 6, 12, 24, and 48 h	Transcriptional gene expression determined by semiquantitative PCR analysis; protein expression by Western blot Increase in mRNA expression of *TP53*, *CDKN1A*, and *BAX*, in comparison with untreated cells at 10 and 50 μg/mL and decreased levels of *BCL2*; protein levels were similarly modified	Srivastava et al. (2011)
Normal human bronchial epithelial cell line	Unpurified MWCNT or crocidolite: 0.01–0.1%, 24 or 48 h	Gene expression analysis with whole human genome microarray (44 K) Upregulation of 1201 and 1252 genes by both asbestos and MWCNT observed after 6 and 24 h of exposure, respectively, and downregulation of 1977 and 1542 genes, respectively When compared with a list of genes known to be deregulated in human malignant mesothelioma or lung cancer, 12 and 22 genes were modulated by exposure to both MWCNT and crocidolite in malignant mesothelioma and lung cancers, respectively. Genes included oncogenes, tumour-suppressor genes or potential tumour-suppressor genes; *CDKN2A*, was downregulated, *CTGF* was upregulated, and *BCL2* oncogene expression was enhanced, similarly to both malignant mesothelioma and lung cancer	Kim et al. (2012b)
Human embryonic kidney epithelial HEK 293 cells, mouse mesenchymal C2C12 stem cells, and human neuroblastoma NB1691 cells	Purified carboxylated MWCNT: 100 μg/mL, 24 h	Expression of proteins by Western blot and mRNA expression by RT-PCR Expression of p21 protein enhanced in MWCNT-treated proliferating C2C12, HEK 293, and NB1691 cells; no change in p53 protein expression observed; enhancement of the unphosphorylated form of pRb and of *CDKN1A* gene expression found	Zhang & Yan (2012)
Telomerase-immortalized human keratinocytes (N-hTERT)	Unpurified MWCNT: 100 μg/mL, 24 h	Small-scale transcriptomic TLDA profiling Different expression levels of 46 mRNAs observed in treated cells compared with untreated cells; enhancement of *BCL2* expression	Vankoningsloo et al. (2012)
Rat PC12 cells (adrenal gland pheochromocytoma)	Unpurified SWCNT: 50 μg/mL, 24 or 48 h	Determination of the expression of proteins involved in apoptosis by flow cytometry, and of caspase activation Decreased expression of Bcl-2 observed in comparison with control cells	Wang et al. (2012b)
Rat lung epithelial RL 65 cells	Unpurified MWCNT: 5 μg/mL, 12 h	Analysis of protein expression levels by Western blot Increased levels of p53, p21$^{Cip1/Waf1}$, and bax proteins found in MWCNT-treated cells	Ravichandran et al. (2010)
Mouse embryonic J11 stem cells	Purified MWCNT: 5 and 100 μg/mL, 2, 4, and 24 h	Analysis of p53 protein expression levels by Western blot Expression of p53 protein observed within 2 h of exposure; p53 expression levels increased proportionally with the amount of MWCNT	Zhu et al. (2007)

Table 4.18 (continued)

Cell types	Type of carbon nanotube: treatment	Assay/result	Reference
Co-culture of mouse leukaemic monocyte macrophage RAW 264.7 and mouse embryonic fibroblast NIH 3T3 cell lines	Short or long unpurified MWCNT: 15 µg/mL, 24 h; RAW 264.7 cells seeded in the well below were treated first for 24 h and then co-cultured with NIH 3T3 cells attached on the top of the insert for another 24 h	Expression of *TGFβ1* measured by RT-PCR analysis Upregulation of mRNA levels of *TGFβ1* greater with long MWCNT than with short MWCNT; in parallel, long MWCNT induced more TGF-β1 protein than short MWCNT	Wang et al. (2013)
Lung epithelial FE1 cells	Unpurified MWCNT (Mitsui 7): 12.5, 25, or 100 µg/mL, 24 h	Microarray and pathway analyses Among the upregulated genes, several were known or potential oncogenes, or genes involved in cancer, such as *Jun*, *Ddit3*, and *Hmga2*, or *Ctgf*, *Runx1*, and *Fosl1*, some of which may also have suppressor functions in specific systems Among the downregulated genes, several were known or potential tumour-suppressor genes, or genes involved in cancer (*Pdgfrl*, *Id4*, *Cdkn2c*, *Cdkn2d*, or *Tgfβ2*, *Gstm2*, and *Gstt1*), some of which may also have oncogenic functions in specific systems	Søs Poulsen et al. (2013)

AF-SWCNT, acid-functionalized, further purified SWCNT; mo, month; MWCNO, multiwalled carbon nano-onions; MWCNT, multiwalled carbon nanotubes; RT-PCR, real-time polymerase chain reaction; SWCNT, single-walled carbon nanotubes; TGF, tumour growth factor; TLDA, Taghmon low density array; wk, week

The effects of SWCNT (CNI, Inc.) produced by the HiPCO technique were evaluated in human bronchial BEAS-2B cells using the Human Apoptosis Array (R&D Biosystems) which detects the 35 most common apoptosis-regulatory proteins by immunoblotting. The cells were continuously exposed to a subcytotoxic concentration (0.02 µg/cm²) of SWCNT in culture and were passaged weekly. After 24 weeks of exposure, SWCNT-treated cells showed the morphological features of malignant transformation. Transformed SWCNT-exposed cells exhibited differential expression of apoptosis-related proteins compared with controls. A differential expression of the phosphorylated forms of p53 was observed which was lower in SWCNT-treated cells than in untreated cells. [Because the phosphorylation of p53 is an indicator of the activation of the p53 tumour suppressor, these results suggested a loss of p53 activity.] (Wang et al., 2011a). [This SWCNT sample can be assumed to have impaired the apoptotic potential of p53. However, these results should be interpreted with caution because BEAS-2B cells are immortalized with SV40 viral oncoproteins and express large SV40 T-antigen, a protein that binds to and inactivates p53 protein.]

Toxicity (cell growth, ROS production, DNA damage assessed by the comet and micronucleus assays, and p53 induction) of SWCNT dispersed in sodium cholate was studied in the human colon carcinoma HT29 cell line. Eight doses from 0.05 ng/mL to 0.2 µg/mL were tested. Phosphorylation of the tumour-suppressor protein p53 was investigated in exposed and untreated control cells using Western blot analysis. After 3 and 24 hours of exposure, the phospho-p53 protein was induced at concentrations ≥ 5 ng/mL. A decline was observed at higher concentrations (0.1 and 0.2 µg/mL) (Pelka et al., 2013). [These results are consistent with the activation of DNA repair at subcytotoxic doses.]

Human mesothelial cells were continuously exposed to SWCNT synthesized by HiPCO (CNI, Inc.) at concentrations of 0.02, 0.06, or 0.2 µg/cm² for 2 months. Expression of the *HRAS* oncogene was assessed using HRAS protein analysis by Western blot and the activation of downstream signalling of the *HRAS* pathway. In parallel, phenotypical changes characteristic of neoplastic transformation were studied (cell growth in soft agar and invasion capability). Increased HRAS protein expression and activation of the ERK1/2 pathway were found to be associated with more neoplastic phenotypes. SWCNT enhanced the expression of a potential oncogenic protein (AKT) and downregulated expression of genes (*TWIST* and *SNAI1*) known to be involved in the epithelial–mesenchymal transition process (Lohcharoenkal et al., 2014).

(ii) MWCNT

A whole genome expression array (GeneChip® assay) was performed using human skin HSF42 fibroblasts and human embryonic lung IMR-90 fibroblasts exposed for 48 hours to 0.6 and 6 µg/mL of multiwalled carbon nano-onions and 0.06 and 0.6 µg/mL of MWCNT synthesized by the CVD method. Numerous genes showed changes in expression after treatment with the different particles. Similar to multiwalled carbon nano-onions, exposure to MWCNT upregulated the expression of genes involved in pathways related to cellular transport, metabolism, cell-cycle regulation, and stress response, but no evidence of oncogene activation or tumour-suppressor gene inactivation was found (Ding et al., 2005).

Human lung adenocarcinoma A549 cells were exposed to 1–50 µg/mL of MWCNT (provided by Professor D.G. Weiss, Department of Biological Sciences, Institute of Cell Biology and Biosystems Technology, Rostock University, Germany) for 3, 6, 12, 24, and 48 hours. Gene expression was analysed using semiquantitative PCR (RT-PCR). mRNA expression of *TP53* and *CDKN1A* (that encode p53 and p21[Cip1/Waf1], respectively) and the apoptotic gene *BAX*, was

increased in comparison with untreated cells at doses of 10 and 50 μg/mL, and the expression of the anti-apoptotic and potential oncogene *BCL2* was decreased. Protein levels were determined using Western blot analysis and confirmed differential mRNA expression. Apoptotic cells were detected after exposure to a dose of 50 μg/mL of MWCNT for 72 hours (Srivastava et al., 2011). [These results were consistent with a change in the expression of tumour-suppressor genes/oncogenes related to the induction of apoptosis.]

Normal human bronchial epithelial cells were exposed to MWCNT or crocidolite asbestos fibres at doses of 0.01–0.1% for 24 or 48 hours. Gene expression was investigated using the Whole Human Genome Microarray (44 K) (Agilent Technology). A total of 1201 and 1252 genes were upregulated and 1977 and 1542 genes were downregulated by both asbestos and MWCNT after 6 and 24 hours of exposure, respectively. These lists were compared with a list of genes known to be deregulated in human malignant mesothelioma or human lung cancers, using a data mining database (GeneCards). The authors found 12 and 22 genes modulated by exposure to both MWCNT and crocidolite in malignant mesothelioma and lung cancers, respectively, some of which were oncogenes and known or potential tumour-suppressor genes. One tumour-suppressor gene – *CDKN2A* – was downregulated 24 hours after exposure to each of the particles; and *CTGF* was upregulated similarly to human lung cancers. In addition, the expression of the *BCL2* oncogene was enhanced in comparison with control cells, similarly to both malignant mesothelioma and lung cancers (Kim et al., 2012b). [These results demonstrated that exposure to MWCNT in vitro (i) downregulated or upregulated some tumour-suppressor genes and oncogenes, respectively, and (ii) modified the expression of cancer genes also found to be deregulated in human lung cancers and malignant mesotheliomas with similar effects produced by exposure to crocidolite asbestos.]

A transcriptomic analysis was performed in telomerase-immortalized human keratinocytes (N-hTERT) exposed to MWCNT (NanocylTM NC7000 MWCNT; from Nanocyl) produced by catalytic CVD. Cells were exposed to a dose of 100 μg/mL for 24 hours and mRNA expression was investigated using small-scale transcriptomic TaqMan low density array profiling (TLDA, Applied Biosystems). The relative expression levels of 46 mRNAs in treated cells compared with untreated cells were reported. Expression of the *BCL2* oncogene was increased after exposure to water-sonicated MWCNT (Vankoningsloo et al., 2012). [The authors did not discuss the statistical analysis of these results.]

Carboxylated MWCNT were studied in human embryonic kidney epithelial HEK 293 cells, mouse mesenchymal stem C2C12 cells, and human neuroblastoma NB1691 cells. The expression of cell-cycle regulatory proteins was analysed using Western blot and mRNA expression was assessed using RT-PCR after exposure to 100 μg/mL of MWCNT for 24 hours. Expression of the protein p21, encoded by *CDKN1A* (a potential tumour-suppressor gene), was enhanced in MWCNT-exposed proliferating C2C12, HEK 293, and NB1691 cells. This was associated with an increased expression of the unphosphorylated form of pRb, concordant with cell-cycle downregulation. The expression of *CDKN1A* (an inhibitor of cell-cycle progression) was also enhanced at the transcriptional level as assessed using RT-PCR. Interestingly, expression of the p53 protein was not found to be enhanced, consistent with the absence of apoptosis (Zhang & Yan, 2012). [These results suggested the p53-independent induction of p21 in this experimental model.]

(c)   *Experimental systems in vivo*

See Table 4.19

Table 4.19 Activation of oncogenes and inactivation of tumour-suppressor genes in experimental animals exposed to carbon nanotubes

Species, strain (sex)	Route of administration/dose, duration	Recovery	Assay/result	Reference
Mouse, C57BL/6 (F)	Inhalation, in inhalation chambers, or pharyngeal aspiration Unpurified (iron, 17.7%) SWCNT: 5 mg/m³, 5 h/day, 4 days (inhalation) or 10 µg (pharyngeal aspiration)	1, 7, and 27 days	Investigation of K-ras mutations in DNA from lung sections Three different types of mutation detected in K-ras after inhalation: two at codon 12 and one double mutation at codons 12 and 8; pharyngeal aspiration did not significantly enhance the mutation rate in K-ras	Shvedova et al. (2008)
Mouse, ICR (NR)	Intratracheal instillation Purified SWCNT: 100 µg/kg bw	1, 7, 14, and 28 days	Proteins extracted from lung tissue; protein analyses performed by Western blot Expression of p53 was enhanced as early as 1 day after exposure	Park et al. (2011a)
Mouse, ICR (M)	Intratracheal instillation Unpurified SWCNT: 100 µg/kg bw	1, 7, and 14 days	Determination of the expression of several proteins by Western blot in lung tissue Expression of p53, Cox-2 and caspase-3 enhanced in the lungs of exposed mice in comparison with controls, then decreased at 28 days, consistent with an increase in p53 tumour-suppressor gene expression related to apoptosis	Park et al. (2011b)
Mouse, CCR5⁺/⁺ (wild-type) and CCR5⁻/⁻ (knockout)	Intratracheal instillation Unpurified SWCNT: 100 µg/kg	7 days	Expression of apoptosis-related proteins, caspase-9, caspase-3, and cleaved PARP, and p21$^{Cip1/Waf1}$, cyclin D1, and TGF-β by cell-cycle analysis in the lungs Expression of caspase-9, caspase-3, and cleaved PARP increased in the lung tissue of knockout mice relative to wild-type mice; phospho-p53, p21$^{Cip1/Waf1}$, and cyclinD1 expression was also increased in knockout mice	Park et al. (2013)
Mouse, C57BL/6J (M)	Pharyngeal aspiration Unpurified MWCNT: 0, 10, 20, 40, or 80 µg	7 and 56 days	Extraction of total RNA from frozen lung; quantification of 63 genes by qRT-PCR, including 47 signature genes of human non-small cell lung cancer and 16 hallmarks genes of cancer signalling pathways Differential expression of seven genes (by day 7) and 11 genes (by day 56) was observed in the exposed and control groups, including the downregulation of both Wif1 and Bcl2; among these, four were differentially expressed at both time-points: Ccdc99, Msx2, and Nos2 (upregulated), and Wif (downregulated)	Pacurari et al. (2011)
Mouse, C57BL/6J (M)	Pharyngeal aspiration Unpurified MWCNT: 0, 10, 20, 40, or 80 µg	1, 7, 28, and 56 days	Genome-wide mRNA expression profiles in lungs analysed through Ingenuity Pathway Twenty-four genes consistently differentially expressed; after 56 days, 38 genes were associated with cancer; when matched in human genomes, 16 genes (all time-points) and 35 genes (56 days) were predictive of human lung cancer risk and prognosis. The MWCNT signature was represented by 35 genes; two were potential oncogenes (BCL3 and EGFR) involved in lung cancer development, but were downregulated	Guo et al. (2012)

Table 4.19 (continued)

Species, strain (sex)	Route of administration/ dose, duration	Recovery	Assay/result	Reference
Mouse, C57BL/6J (M)	Pharyngeal aspiration Unpurified MWCNT: 0, 10, 20, 40, or 80 µg	1, 7, 28, and 56 days	Genome-wide mRNA expression profiles and pathological analysis of lungs, referring to inflammatory and fibrotic pathways analysed through Ingenuity Pathway Differential expression of 67 genes involved in the inflammatory process and 69 involved in fibrosis was observed; 23 genes were involved in both processes; two genes were potential oncogenes: *egfr* (downregulated) and *junb* (overexpressed at all time-points at most doses)	Snyder-Talkington et al. (2013a)
Rat, spontaneously hypertensive [derived from WKY rat] (M)	Intratracheal instillation Short (0.5–2 µm) and long (20–50 µm) unpurified MWCNT particles: 0.6 mg/rat, once/day, 2 days	1, 7, and 30 days	Investigation of TGF-β1 protein expression (immunohistochemistry in the lungs) and by qRT-PCR analysis; mRNA expression of genes involved in the TGF-β/ Smad signalling pathway In MWCNT-exposed rats, TGF-β1 protein expressed in macrophages and near the bronchiolar epithelium; gene expression of *Tgfβ1* and *Tgfbr2* enhanced at day 7; stimulation of the TFG-β/Smad signalling pathway only observed in rats treated with long MWCNT	Wang et al. (2013)
Mouse, pregnant heterozygous *p53* (*p53+/−*)	Intravenous injection Unpurified MWCNT: 2 mg/kg bw (single injection)	24 h	RNA isolated from mouse fetal liver and mouse embryo fibroblasts with different *p53*-status; *Cdkn1a* (encoding p21^Cip1) and *Bax* gene expression quantified by RT-PCR; protein expression determined in mouse embryo fibroblasts with the different types of *p53*-status MWCNT induced the mRNA transcription of two tumour-suppressor genes (*Cdkn1a* and *Bax*) in *p53+/+* fetuses but to a lesser extent in *p53+/−* and *p53−/−* mice; expression of *p21* and *Bax* triggered in a p53 status-dependent manner	Huang et al. (2014)
Mouse, C57BL/6 (F)	Intratracheal instillation Unpurified MWCNT (Mitsui 7): 18, 54, or 162 µg/mouse	24 h	Microarray analyses of gene expression in the lungs Referring to human orthologous genes, some oncogenes were upregulated (*Aurka* and *Bcl3*); downregulated genes also included known or potential oncogenes (*Wnt1*, *Myb*, and *Dnaja4*)	Sos Poulsen et al. (2013)

bw, body weight; Cox-2, cyclooxygenase 2; F, female; M, male; MWCNT, multiwalled carbon nanotubes; NR, not reported; PARP, poly(ADP-ribose) polymerase; qRT-PCR, quantitative real time-polymerase chain reaction; SWCNT, single-walled carbon nanotubes; TGF, tumour growth factor

(i) SWCNT

C57BL/6 mice were exposed to 5 mg/m^3 of SWCNT by inhalation for 5 hours per day for 4 days, or to 10 µg of SWCNT delivered by pharyngeal aspiration, after which DNA was isolated from lung sections. Three different types of mutation were detected in the K-*ras* gene after inhalation; two at codon 12, one of the most common mutation sites in human lung cancer, and one double mutation at codons 12 and 8. Pharyngeal aspiration did not significantly enhance K-*ras* gene mutations (Shvedova et al., 2008).

ICR mice were exposed to 100 µg/kg bw of SWCNT (ASP-100F from Hanhwa Nanotech, Republic of Korea) delivered by intratracheal instillation. The lungs were harvested 1, 7, 14, and 28 days after injection, and proteins were extracted from the lung tissue and analysed using Western blots. The expression of p53 protein was enhanced as early as 1 day after exposure (Park et al., 2011a). [The authors did not discuss the origin of the cell or the mechanism responsible for increased p53 protein expression.]

Exposure of male ICR mice to 100 µg/kg bw of SWCNT (metal content, approximately 10% wt; diameter, 1.2 nm; length, 2–10 µm; ASP-100F, Hanhwa Nanotech) by intratracheal instillation resulted in the modification of the expression of several proteins assessed by Western blot. One, 7, and 14 days after exposure, the expression of p53, cyclooxygenase 2, and caspase-3 proteins was increased in the lungs of exposed mice in comparison with controls, then decreased after 28 days (Park et al., 2011b). [These findings were consistent with an increase in the expression of the p53 tumour-suppressor gene that is related to the induction of apoptosis.]

The effects of SWCNT (diameter, 1.2 nm; length, 2–10 µm; ASP-100 F, Hanhwa Nanotech) were studied in CCR5$^{+/+}$ (wild-type) and CCR5$^{-/-}$ (knockout) mice exposed to a dose of 100 µg/kg bw delivered by intratracheal instillation. CCR5 is a chemokine receptor that plays a role in inflammatory responses. The cell cycle was analysed to determine the expression of apoptosis-related proteins, and p21$^{Cip1/Waf1}$, cyclin D1 (ccd1), and TGF-β in the lungs 7 days after instillation. The expression of apoptosis-related proteins – caspase-9, caspase-3, and cleaved poly(ADP-ribose) polymerase – and phospho-p53 protein was more markedly increased in the lung tissue of knockout mice than in that of wild-type mice. The expression of other proteins – p21$^{Cip1/Waf1}$ and ccd1 (both potential oncogenes) – was also increased in knockout mice (Park et al., 2013). [These results were consistent with SWCNT-induced apoptosis, but also showed that the expression of some known or potential oncogenes (*Cdkn1a* and *Ccnd1* encoding p21$^{Cip1/Waf1}$ and ccd1, respectively) can be altered in the lungs of mice exposed to SWCNT.]

(ii) MWCNT

Male C57BL/6J mice were exposed to 10, 20, 40, or 80 µg of MWCNT (MWCNT-7, lot # 05072001K28, from Mitsui & Co.) or vehicle by pharyngeal aspiration for 7 or 56 days. Total RNA was extracted from frozen lung and quantified using qRT-PCR. A total of 63 genes were investigated, 47 of which were selected from previous studies that had identified gene expression signatures of human non-small cell lung cancers, determined using genome-wide DNA microarray analyses as being potentially associated with lung cancer risk, and 16 of which were hallmarks of cancer signalling pathways. At 7 and 56 days after exposure, a set of seven and 11 genes, respectively, showed differential expression in the lungs of mice exposed to MWCNT compared with the vehicle-treated control group. Among these, *Wif1* (a gene functioning as a tumour-suppression gene that has been found to be epigenetically silenced in various cancers) was downregulated and an oncogene, *Bcl-2*, was also downregulated. Four genes from these two subsets of genes showing significant differential

mRNA expression at both time-points were either upregulated (*Ccdc99*, *Ms×2*, and *Nos2*) or downregulated (*Wif1*) ([Pacurari et al., 2011](#)). [These results demonstrated that exposure to this sample of MWCNT could modify the expression of genes that have been shown to be prognostic biomarkers in human lung cancers, including persistent downregulation of a putative tumour-suppressor gene.]

C57BL/6J mice were exposed to 0 (vehicle control), 10, 20, 40, or 80 μg of MWCNT (MWCNT-7, lot # 05072001K28; from Mitsui & Co.) by pharyngeal aspiration. RNA extracted 1, 7, 28, and 56 days after exposure was analysed for gene expression profiling using Agilent Mouse Whole Genome Arrays (Agilent, Santa Clara, CA). Selected genes showed significant changes at a minimum of two time-points and with a more than 1.5-fold change at all doses, and were significant in the linear model for dose or interaction of time and dose. The authors compared the list of differentially expressed genes from the microarray gene expression data with two published studies on microarray profiles in human lung carcinomas. In treated mice, 24 genes were consistently differentially expressed. From data at 56 days after exposure, 38 genes were selected as being associated with cancer. When matched in human genomes using gene symbols, 16 and 35 genes were found to predict the risk and prognosis of human lung cancer from data obtained at all time-points and at 56 days, respectively. Among the proteins encoded by the list of 35 genes with differential expression induced by exposure to MWCNT, several were implicated in lung cancer development, including two potential oncogenes – *BCL3* and *EGFR*. However, both genes were downregulated after exposure to MWCNT ([Guo et al., 2012](#)).

Microarray gene expression profiling was investigated using RNA isolated from the lungs of male C57BL/6J mice exposed to 0 (vehicle control), 10, 20, 40, or 80 μg of MWCNT (MWCNT-7, lot #05072001K28; from Mitsui &

Co.) delivered by pharyngeal aspiration for 1, 7, 28, or 56 days. The authors applied a novel computational model to generate genome-wide mRNA expression profiles that correlated with histopathological analysis of mouse lungs, focusing on inflammatory and fibrosis pathways identified using Ingenuity Pathway identification. Twenty-three genes were found to be involved in both MWCNT-induced inflammation and fibrosis – 67 in inflammation and 69 in fibrosis. Two of these genes are potential oncogenes; *egfr* was downregulated and *junb* was overexpressed across all days at most doses, possibly in relation to persistent inflammation ([Snyder-Talkington et al., 2013a](#)).

The expression of *Tgfβ1* was measured in spontaneously hypertensive male rats exposed to PBS (control) or 0.6 mg/rat of short (0.5–2 μm) or long (20–50 μm) unpurified MWCNT (Nanotech Port, Chengdu, China) suspended in PBS by non-surgical intratracheal instillation once per day for two consecutive days. *Tgfβ1* expression was evaluated by immunohistochemistry on the lung tissue sections and by qRT-PCR analysis. mRNA expression of other genes involved in the TGF-β Smad signalling pathway was also measured. [Several genes – *Tgfbr2*, *Smad2*, and *Smad3* – are potential tumour-suppressor genes.] TGF-β1 protein expression was detected in lung macrophages and near the bronchiolar epithelium in response to MWCNT; the expression of both *Tgfβ1* and *Tgfbr2* genes was increased after 7 days of exposure (other times tested: 1 and 30 days). Additional results suggested that the TGF-β/Smad signalling pathway was upregulated only in rats exposed to long MWCNT ([Wang et al., 2013](#)).

Pregnant heterozygous *p53*^{+/−} mice received an intravenous injection of 2 mg/kg bw of MWCNT. Exposure to MWCNT induced mRNA expression of two tumour-suppressor genes – *Cdkn1a* (encoding p21[Cip1]) and *Bax* – in *p53*^{+/+} fetuses, but to a lesser extent in *p53*^{+/−} and *p53*^{−/−} mice ([Huang et al., 2014](#)). [These results

suggested that exposure to MWCNT triggers apoptosis in mice, a process decreased or inactivated in p53-deficient mice, depending on their p53 status.]

Pulmonary responses of C57BL/6 mice after exposure to MWCNT (Mitsui 7) were compared with in-vitro studies using cultured lung epithelial FE1 cells at the global transcriptomic level. Mice were exposed by intratracheal instillation to doses of 18, 54, and 162 μg/mouse of MWCNT, and lung samples were collected 24 hours after exposure. Microarray analyses were performed using Agilent 8 × 66K oligonucleotide microarrays, and gene expression was analysed using the gene ontology classifications of all of the differentially expressed genes. After in-vivo exposure, several pathways were commonly (more than one dose) or uniquely (one dose) affected. Referring to human orthologous genes, expression of some oncogenes was upregulated (*Aurka* and *Bcl3*). Downregulated genes also included known or potential oncogenes (*Wnt1*, *Myb*, and *Dnaja4*) (Søs Poulsen et al., 2013). [When comparing in-vivo and in-vitro models, most of the genes associated with exposure to MWCNT involved the same pathways, but the number of differentially expressed genes, in comparison with untreated mice, was higher in vivo than in vitro, which was at least partly linked to the multicellular versus unicellular nature of these model systems.]

(d) Experimental systems in vitro

See Table 4.18

(i) SWCNT

Murine monocytic RAW 264.7 cells were exposed to 0, 1, 10 or 50 μg/mL of acid-functionalized SWCNT (AF-SWCNT) for 24 hours. Gene expression profiles were analysed using cDNA microarrays. Based on the criteria of significance ($P < 0.001$ and fold change > 2), differentially expressed genes were identified at a dose of 10 μg/mL. A total of 130 genes were differentially expressed: 126 were underexpressed and four were overexpressed. Among these genes, *MYC* (oncogene) mRNA expression was upregulated in AF-SWCNT-treated RAW 264.7 cells in comparison with controls, confirmed using RT-PCR analyses. Several genes involved in DNA repair were downregulated, including *XPA*, *XRCC1*, *XRCC4*, and *CHEK1* (potential tumour-suppressor genes). Globally, AF-SWCNT altered the expression of genes related to ribosome function, mitochondrial function, inflammatory response, cell cycle/apoptosis, and the proteasome pathway (Dong et al., 2012). [These results showed that AF-SWCNT may downregulate tumour-suppressor genes involved in the repair of DNA damage and stimulate the expression of oncogenes in RAW 264.7 cells.]

(ii) MWCNT

Rat lung epithelial RL 65 cells exposed to MWCNT (diameter, 6–13 nm; length, 2.5–20 μm; Sigma-Aldrich) showed increased levels of p53, p21$^{Cip1/Waf1}$, and bax protein expression after 12 hours of exposure to 5 μg/mL, probably related to the induction of apoptosis (Ravichandran et al., 2010).

SWCNT (outside diameter, 1–2 nm; length, ~20 μm; Beijing Nachen Technology & Development Co. Ltd) were studied in rat adrenal gland pheochromocytoma PC12 cells. After 24 and 48 hours of exposure to 50 μg/mL of SWCNT, the expression of proteins involved in apoptosis – Bcl-2, an oncogenic protein, and bax – was determined using flow cytometry. Bcl-2 expression was decreased and bax protein and caspase-3 activity were increased in comparison with control cells, consistent with the induction of apoptosis in SWCNT-treated PC12 cells (Wang et al., 2012b).

Mouse embryonic J11 stem cells were exposed to MWCNT (Tsinghua and Nanfeng Chemical Group Cooperation, China) and the DNA damage response induced was analysed by measuring p53 protein expression levels. The expression

of p53 protein was observed within 2 hours of exposure, and increased proportionally with the dose (5 and 100 µg/mL). Phosphorylation of p53 protein was assessed using the phospho-specific antibody to p53-Ser-23 and confirmed the activation of the p53 DNA damage-induced response pathway (Zhu et al., 2007). [Increased p53 protein expression suggests that MWCNT could cause DNA damage.]

The expression of *TGFβ1*, a tumour-suppressor gene that might also be an oncogene, was assessed in a co-culture of the mouse leukaemic monocyte macrophage RAW 264.7 cell line and the mouse embryonic fibroblast NIH 3T3 cell line, using RT-PCR analysis. RAW 264.7 cells seeded in the bottom well were first exposed to short (length, 0.5–2 µm) or long (20–50 µm) MWCNT (15 µg/mL) for 24 hours, and then NIH 3T3 cells that had attached on the top of the insert for 24 hours were co-cultured with RAW 264.7 for another 24 hours. mRNA expression of *TGF-β1* was more upregulated by exposure to long MWCNT in comparison with short MWCNT. In parallel, more TGF-β1 protein was expressed in co-cultures exposed to long MWCNT than those exposed to short MWCNT (Wang et al., 2013).

A comparison of the in-vivo pulmonary responses of C57BL/6 mice to MWCNT (Mitsui 7) with the in-vitro response of lung epithelial FE1 cells (a spontaneously immortalized lung epithelial cell line derived from a normal healthy MutaTM Mouse) was made at the global transcriptomic level (Søs Poulsen et al., 2013). This cell line retains key endogenous metabolic capacity and intact p53 signalling pathways, and expresses both type I and type II alveolar phenotypes (Berndt-Weis et al., 2009). FE1 cells were exposed to 12.5, 25, or 100 µg/mL of MWCNT for 24 hours. Microarray analyses were performed using Agilent 8 × 66K oligonucleotide microarrays and gene expression was analysed using the gene ontology classification of differentially expressed genes. After in-vivo exposure, several pathways were commonly (several doses) or uniquely (one dose) affected. In FE1 cells in vitro, genes commonly affected included pathways involving aryl hydrocarbon receptor signalling, GSH-mediated detoxification, acute phase response signalling, and the nuclear factor (erythroid-derived 2)-like 2-mediated oxidative stress response. Among the upregulated genes, several were known or potential oncogenes or genes involved in cancer, including *Jun*, *Ddit3*, *Hmga2*, *Ctgf*, *Runx1*, and *Fosl1*, some of which may also have tumour-suppressor functions in specific models. Among the downregulated genes, several were also known or potential tumour-suppressor genes or genes involved in cancer, such as *Pdgfrl*, *Id4*, *Cdkn2c*, *Cdkn2d* (p19), *Tgfβ2*, *Gstm2*, and *Gstt1*, some of which may also have oncogenic functions in specific systems (Pdgfra and Cdkn2d). In-vitro data showed a high degree of overlap across the exposure groups, with some exceptions at the highest concentration (Søs Poulsen et al., 2013). [When comparing the two in-vitro and in-vivo models after exposure to MWCNT, most of the genes were associated with the same pathways, but the number of differentially expressed genes was lower in vitro and in vivo in comparison with untreated mice, which was at least partly linked to the multicellular versus unicellular nature of the systems.]

(e) Acellular systems in vitro

The generation of radicals by MWCNT was studied in an acellular system. MWCNT were synthesized by the decomposition of ethylene on an alumina support doped with a cobalt–iron catalyst mixture and purified by subsequent treatment with sodium hydroxide. The potential of MWCNT to release free radicals in aqueous suspensions was thus monitored by ESR spectroscopy, using 5,5-dimethyl-1-pyrroline-*N*-oxide as a trapping agent. A suspension of 5 mg of MWCNT did not generate oxygen or carbon-centred free radicals in the presence of hydrogen peroxide or formate, respectively. In

contrast, MWCNT were able to scavenge radicals in the presence of an external source of hydoxyl radicals, •OH, or superoxide radicals, O2·⁻ (Fenoglio et al., 2006). [Although not formally demonstrated, it is possible that MWCNT might protect against antioxidant depletion.]

The ability of various types of MWCNT to generate/scavenge radical formation was studied in both cell-free systems and human bronchial BEAS-2B cells. Printex 90 carbon black, crocidolite asbestos, and glass wool were also used. Hydrogen peroxide-induced free radical formation was determined by ESR. All CNM were found to scavenge the induction of •OH, but the presence of bovine serum albumin abolished •OH production in some samples. In addition to a scavenging effect, two types of long, needle-like MWCNT (average diameter, > 74 and 64.2 nm; average length, 5.7 and 4.0 µm, respectively) induced the dose-dependent formation of a unique, as yet unidentified radical in both the absence and presence of cells, which also coincided with cytotoxicity. The ability of MWCNT to protect against oxidant formation also depended on the composition of the medium (Nymark et al., 2014).

4.5 Susceptible populations

See Table 4.20

No data on human populations were available to the Working Group. One study was carried out in transgenic animals with increased susceptibility to carcinogenic substances (Takanashi et al., 2012). Several experimental studies focused on the possible aggravation of airway disease and the effects of CNT on pulmonary vessels using models of asthma in mice.

Studies of genes related to inflammation in genetically deficient mice are also reported below. Although not related to cancer, these studies are summarized in relation to their pertinence to inflammatory processes.

4.5.1 Modification of risks for cancer of the lung

(a) MWCNT

The effects of MWCNT on allergic airway inflammation were studied in four groups of ICR mice that received intratracheal injections of vehicle, MWCNT (50 µg/animal; one of two types: Bussan Nanotech Research and SES Research), OVA, and OVA+MWCNT. Biological parameters were measured in the BALF (cellularity), lungs (histology, protein levels of cytokines related to allergic inflammation in lung homogenates and BALF), and serum (Ig levels). MWCNT exacerbated murine allergic airway inflammation, as demonstrated by an aggravation of allergen-induced airway inflammation and an increased number of goblet cells in the bronchial epithelium, and exhibited adjuvant activity for allergen-specific IgG1 and IgE. OVA+MWCNT amplified the lung levels of Th2 cytokines (e.g. IL-4, IL-5, and IL-13) and chemokines (e.g. thymus- and activation-regulated chemokine and macrophage-derived chemokine) compared with OVA (Inoue et al., 2009).

The effects of the inhalation of MWCNT on airway fibrosis were investigated in normal and OVA-sensitized mice with allergic asthma. Quantitative morphometry showed significant airway fibrosis in OVA-sensitized mice 14 days after exposure to MWCNT but not in mice treated with OVA or MWCNT alone. The levels of inflammatory factors in the BALF differed according to the exposure: IL-13 and TGF-β1 were elevated in OVA-sensitized mice while PDGF-AA was elevated in MWCNT-treated mice, suggesting that the airway fibrosis resulting from the combined effect of OVA and MWCNT required PDGF (a fibroblast mitogen) and TGF-β1 that stimulates collagen production (Ryman-Rasmussen et al., 2009b). [These findings indicated that individuals with pre-existing

Table 4.20 Susceptibility to cancer in experimental animals exposed to carbon nanotubes

Species, strain (sex)	Route of administration/treatment	Observation time	Result	Reference
Mouse, ICR (M)	Pharyngeal aspiration Vehicle control (PBS), once/wk, 6 wk MWCNT-treated group, 50 µg once/wk, 6 wk OVA-treated group, 1 µg every 2 wk then PBS every 2 wk, 6 wk OVA+MWCNT-treated group: same protocol as OVA- and MWCNT-treated groups	24 h	BALF: number of total cells significantly greater in MWCNT-, OVA-, and OVA+MWCNT-treated groups than in the vehicle controls Lung homogenates: moderate infiltration of neutrophils seen in the MWCNT- and OVA-treated groups, more marked in the OVA+MWCNT-treated group; significant induction of goblet cell hyperplasia in the airways of OVA- and MWCNT-treated groups compared with vehicle controls, with a marked progression in the OVA+MWCNT-treated group; a significant increase in the number of eosinophils, lymphocytes, and neutrophils in the MWCNT-, OVA-, and OVA+MWCNT-treated groups compared with vehicle controls; protein levels of cytokines and chemokines related to allergic inflammation greater in the OVA+MWCNT-treated group compared with the MWCNT- or OVA-treated groups Serum: allergen-specific IgG1 and IgE levels significantly greater in the OVA-treated or OVA+MWCNT-treated groups compared with controls, and higher in the OVA+MWCNT-treated group than in the OVA- or MWCNT-treated groups	Inoue et al. (2009)
Mouse, C57BL/6 (M)	Inhalation MWCNT: ~100 mg/m³, 6 h (10 mg/kg bw range) Prior sensitization to OVA: intraperitoneal injection of 10 µg, once/wk, 2 wk, then intranasal challenge with 100 µL of 1% OVA 1 day before exposure to MWCNT Intraperitoneal injection of 50 mg/kg bw 5'-bromodeoxyuridine 1 hour before euthanasia	1 or 14 days after exposure	OV+MWCNT: trend of increased neutrophils in BALF compared with a group treated with MWCNT alone; airway fibrosis noted at 14 days, but not in mice that received OVA or MWCNT alone OVA+MWCNT: increased IL-13 protein levels in BALF and of mRNA in lung tissue, compared with unsensitized or MWCNT-treated animals but not with animals treated with OVA alone OVA+MWCNT: both PDGF-AA and TGF-β1 increased (MWCNT alone: PDGF-AA increased) No focal areas of 5'-bromodeoxyuridine staining observed in the lung tissue of controls or MWCNT-treated animals	Ryman-Rasmussen et al. (2009a)
Mouse, BALB/c (M)	Intranasal instillation Sensitization with 30 µL of 0.01, 0.1, or 1 mg/mL MWCNT with or without 2.5 mg/mL OVA at 0, 1, 2, 14, 15, and 16 days Challenges by intratracheal administration of 20 µL of 1% OVA at 28, 29, 30, and 35 days		Enhancement of the degree of airway resistance in MWCNT+OVA-treated group compared with vehicle-, MWCNT-, and OVA-treated groups OVA+MWCNT (1 mg/mL): significant enhancement of IL-4, IL-5, IL-13, and IL-17 in the lung tissue, and of C3a in the BALF in comparison with control, MWCNT-treated, and OVA-treated groups; goblet cell hyperplasia observed OVA + MWCNT: increased levels of OVA-specific IgE, IgG1, and IgG2a in serum	Mizutani et al. (2012)

Table 4.20 Susceptibility to cancer in experimental animals exposed to carbon nanotubes (continued)

Species, strain (sex)	Route of administration/treatment	Observation time	Result	Reference
Mouse, BALB/cByJ (M)	Intranasal instillation Vehicle control group HDM (a *Dermatophagoides pteronyssinus* extract): 2 µg Der p1 on days 0, 7, 14, and 21 MWCNT (75 µg) or MWCNT (75 µg) + HDM on days 0, 7, and 14 MWCNT (225 µg) or MWCNT (225 µg) + HDM on days 0, 2, 4, 6, 8, 10, 12, 14, 16, and 18 Analyses of serum, BALF, and lung	day 23	Effects of MWCNT + HDM compared with HDM alone or control: Serum: increased level of specific and total IgG1 BALF: enhancement of allergen-induced airway inflammation Lungs: allergic and epithelium-derived cytokines significantly increased (TSLP, IL-33, and IL-25); tissue remodelling	Ronzani et al. (2014)
Mouse, C57BL/6J wild-type and macrophage-specific PPARγ knockout (NR)	Subcutaneous implantation MWCNT: 100 µg Analyses in BALF (cell counts; transcripts for IFN-γ, osteopontin, and CCL2; IFN-γ and CCL2 proteins) and lung histology: granulomas	60 days	Decreased PPARγ expression and activity in alveolar macrophages from MWCNT-instilled wild-type C57BL/6 mice bearing granulomas Granuloma formation in macrophage-specific PPARγ knockout mice exceeded that in wild-type animals Pro-inflammatory cytokines elevated in lung, granulomas and BALF from MWCNT-instilled macrophage-specific PPARγ knockout mice Minimal staining of CD3+ (T-cells), monocytes and macrophages in tissue sections from sham-treated C57/BL6 or PPARγ knockout control mice, but major staining in MWCNT-instilled mice	Huizar et al. (2013)
Mouse, C57BL/6J × 129/Ola wild-type or homozygous knockout (*Cox-2⁻/⁻*) (M + F)	Oropharyngeal aspiration Intranasal challenge with 20 mg OVA in saline on days 26, 28, and 32 MWCNT: 4 mg/kg bw on day 34	1 or 14 days after exposure	Exacerbation of OVA-induced airway inflammation Enhancement of OVA-induced mucus-cell metaplasia in *Cox-2* knockout mice Amplification of OVA-induced Th2, Th1, and Th17 mediators in *Cox-2* knockout mice	Sayers et al. (2013)
Mouse, transgenic rasH2 which express the *c-Ha-ras* proto-oncogene derived from humans (M)	Subcutaneous implantation MWCNT (VGCF-S; Showa Denko, Japan) produced by CVD (mean diameter, 100 nm; mean length, 10 µm; 99.9% carbon content), sterilized by autoclaving at 121 °C for 15 min, and dispersed in Tween 80 Black tattoo ink (diameter, 30–50 nm; carbon, 99.57 wt%; sodium, 0.43 wt%) Particles: 75 mg/kg bw injected into the tissue of the back of each mouse	26 wk	No tumour developed in animals treated with MWCNT Some neoplasms in carbon black-treated mice Tumours in all positive control mice treated with *N*-methyl-*N*-nitrosourea	Takanashi et al. (2012)

Table 4.20 (continued)

Species, strain (sex)	Route of administration/treatment	Observation time	Result	Reference
Rat, Wistar (M)	Intratracheal instillation SWCNT: 0.02, 0.2, or 2.0 mg/kg bw every 3 days (total 13 instillations) Vitamin E: 100 mg/kg bw 3 h after 0.2 or 2.0 mg/kg bw SWCNT Sensitization by subcutaneous injection of 200 mg OVA on days 6, 20, and 27; challenge with 1% OVA on days 33–39	24 h after final challenge	Exacerbation of OVA-induced allergic asthma by SWCNT Exacerbation was counteracted by concurrent administration vitamin E	Li et al. (2014)
Mouse, ICR (M)	Intratracheal instillation Vehicle control SWCNT: 50 μg/mice once/wk, 6 wk OVA: 1 μg/mice every 2 wk, 6 wk OVA+SWCNT: same protocol as that for OVA and SWCNT alone	24 h after the final administration	BALF cellularity and infiltration of inflammatory leukocytes in the lung significantly greater in OVA+SWCNT-treated group compared with SWCNT- or OVA-treated groups; SWCNT potentiated mucus hyperplasia Measurement of protein levels of allergic response-related cytokines and chemokines in lung tissue homogenates, and inflammatory cytokines in BALF: higher levels of almost all of the cytokines tested in the OVA+SWCNT-treated group relative to the other three groups Serum: significantly higher levels of allergen-specific IgG1, IgG2a, and IgE in OVA- and OVA+SWCNT-treated groups compared with vehicle controls; both IgG1 and IgE higher in OVA+SWCNT-treated compared with OVA- or SWCNT-treated mice SWCNT potentialized allergen-induced oxidative stress in the lung as measured by MPO, NO, and lipid hydroperoxide levels in the BALF/lung homogenates, HO-1 transcript level, and 8-hydroxy-dG staining, compared with SWCNT or OVA alone	Inoue et al. (2010)
Mouse, Ccr5+/+ (wild-type) and Ccr5−/− (knockout) (NR)	Intratracheal instillation SWCNT: 100 μg/kg bw Analyses in BALF (cell count, cell-cycle analysis, and cell distribution), lung histology, and expression of apoptotic and pro-inflammatory response-related proteins	7 days	Factors modified in BALF of Ccr5 knockout mice relative to wild-type mice: % of macrophages (% of neutrophils lower) % of cells in G0/G1 (higher; cell cycle arrest) Enhanced expression of apoptosis- and inflammatory response-related proteins CCR4 expression more markedly increased in lung tissue Factors enhanced in lungs of Ccr5 knockout mice relative to wild-type mice: Expression of the G1 arrest-related proteins, Cdk2, Ccnd1, and p21 Expression of TGF-β and mesothelin	Park et al. (2013)

Table 4.20 Susceptibility to cancer in experimental animals exposed to carbon nanotubes (continued)

Species, strain (sex)	Route of administration/treatment	Observation time	Result	Reference
Mouse, B6.129P2-Apoe^{tm1Unc} (*ApoE^{–/–}*) (M)	Intrapharyngeal instillation SWCNT: 20 µg/mouse once/2 wk, 8 wk Regular chow diet (regimen 1) or a high fat chow diet (regimen 2), 4 wk, followed by regular chow, 4 wk Controls exposed to vehicle Measurement of plasma levels of cholesterol, triglycerides, glucose, LDH, and inflammatory cytokines Quantification of plaque formation in brachiocephalic arteries Evaluation of mitochondrial DNA damage (quantitative polymerase chain reaction)		Plasma levels of cholesterol, glucose, and LDH comparable in SWCNT-treated and vehicle control mice regardless of diet regimens Plasma levels of inflammatory cytokines: no significant difference in *ApoE^{–/–}* mice treated with vehicle or SWCNT Exposure to SWCNT associated with considerably larger areas of atherosclerotic lesions; significant enhancement in *ApoE^{–/–}* mice fed regimen 2 compared with those fed regimen 1 SWCNT-exposed *ApoE^{–/–}* mice demonstrated significantly increased mitochondrial DNA damage	Li et al. (2007b)

ApoE, apolipoproteinase 2; BALF, bronchoalveolar lavage fluid; bw, body weight; CCL2, C–C motif chemokine ligand 2; Ccr5, chemokine (C–C motif) receptor 5; Cdk2, cyclin dependent-kinase 2; Ccnd1, cyclin D1; CVD, chemical vapour deposition; dG, deoxyguanosine; F, female; HMD, house dust mites; HO-1, haeme oxygenase 1; IFN, interferon; Ig, immunoglobulin; IL, interleukin; LDH, lactate dehydrogenase; M, male; min, minute; MPO, myeloperoxidase; MWCNT, multiwalled carbon nanotubes; NO, nitric oxide; NR, not reported; OVA, ovalbumin; p21, p21^{Waf1/Cip1} protein; PBS, phosphate-buffered saline; PDGF, platelet-derived growth factor; PPARγ, peroxisome proliferator-activated receptor gamma; SWCNT, single-walled carbon nanotubes; TGF-β, transforming growth factor β; Th, T helper; TSLP, thymic stromal lymphopoietin; wk, week

allergic inflammation may be susceptible to airway fibrosis from inhaled MWCNT.]

Whether sensitization by MWCNT (30 µL of 0.01, 0.1, or 1 mg/mL) and OVA (30 µL of 2.5 mg/mL) (combined) promotes an allergic asthmatic response was examined in mice. An increase in airway resistance was observed in the groups treated with OVA + 0.1 or 1 mg/mL of MWCNT compared with controls and those treated with OVA or MWCNT alone. In OVA + 1-mg/mL MWCNT-treated mice, the concentration of pro-inflammatory cytokines (IL-4, IL-5, IL-13, and IL-17) was increased in lung tissues and that of the anaphylatoxin C3a in the BALF. OVA-specific IgE, IgG1, and IgG2a were increased in the serum of mice sensitized with OVA and MWCNT (Mizutani et al., 2012).

The effects of MWCNT on the systemic immune response, airway inflammation, and remodelling induced by house dust mites (HDM) was investigated in BALB/cByJ mice. MWCNT increased the systemic immune response (significantly enhanced levels of specific and total IgG1 in the serum of HDM+MWCNT-treated mice compared with control mice and mice treated with the highest dose of HDM), airway inflammation (significantly enhanced number of eosinophils, neutrophils, and lymphocytes in the BALF of HDM+MWCNT-treated mice compared with control mice and mice treated with the highest dose of HDM), mucus production, and fibrotic response in a dose-dependent manner, as demonstrated by histological analyses of the lungs (Ronzani et al., 2014). [HDM are the most frequent allergens associated with asthma to date; using this model of asthma in mice, exposure to MWCNT was found to aggravate allergen-induced systemic immune responses, as well as airway inflammation and remodelling.]

The instillation of CNT has been shown to induce granulomatous changes and a study was performed to determine whether peroxisome proliferator-activated receptor gamma (PPARγ) deficiency would enhance granuloma formation after exposure to MWCNT (Huizar et al., 2013). PPARγ is a transcription factor that acts as a negative regulator of genes linked to inflammatory events. The alveolar macrophages of healthy individuals constitutively express PPARγ but PPARγ is deficient in the alveolar macrophages of patients with severe sarcoidosis, a granulomatous disease. PPARγ was therefore hypothesized to play a role in the formation of MWCNT-induced granulomas. Wild-type and macrophage-specific PPARγ knockout C57BL/6 mice received oropharyngeal instillations of 100 µg of MWCNT. The expression and activity of PPARγ by alveolar macrophages were significantly reduced in MWCNT-treated wild-type mice bearing granulomas. Granuloma formation was more extensive in MWCNT-treated macrophage-specific PPARγ knockout mice than in wild-type mice. PPARγ knockout mice exposed to MWCNT also demonstrated an elevated expression of pro-inflammatory cytokines in the lung tissues, laser-microdissected lung granulomas, and BALF cells. [These data suggested that PPARγ deficiency may promote inflammation and granuloma formation.]

Wild-type or cyclooxygenase 2 knockout mice were sensitized to OVA to induce allergic airway inflammation before exposure to 4 mg/kg bw of MWCNT by oropharyngeal aspiration. Exposure to MWCNT significantly increased OVA-induced lung inflammation and mucus-cell metaplasia in knockout mice compared with wild-type mice. Allergen-induced cytokines involved in Th2, Th1, and Th17 inflammatory responses were significantly enhanced in MWCNT-treated knockout but not in wild-type mice (Sayers et al., 2013).

MWCNT were implanted subcutaneously into transgenic rasH2 mice that overexpress the *c-Ha-ras* oncogene and are highly sensitive to carcinogens. Carbon black and *N*-methyl-*N*-nitrosourea were used as controls. No tumour developed in MWCNT-treated mice. In the carbon black-treated group, one mouse had a

haemangioma in the spleen and another had an adenoma in the lung. Neoplasms developed in all mice in the *N*-methyl-*N*-nitrosourea-treated group but in none of the solvent-treated group (Takanashi et al., 2012). [These results showed that carcinogen-sensitive rasH2 mice did not develop neoplasms after subcutaneous implantation of MWCNT under these experimental conditions.]

(b) SWCNT

OVA-sensitized rats were exposed to SWCNT by intratracheal instillation. SWCNT exacerbated OVA-induced allergic asthma and this exacerbation was counteracted by the concurrent administration of vitamin E (Li et al., 2014).

The effects of SWCNT on allergic airway inflammation was studied in four groups of ICR mice that received intratracheal instillations of vehicle, SWCNT (50 μg/animal), OVA, and OVA+SWCNT. Two types of SWCNT were administered: one type ranged from 0.8 to 1.2 nm in diameter and 100 to 1000 nm in length and contained < 35% (by weight) iron; the other type (SES Research) was formed in the arc process and ranged from 1.2 to 2 nm in diameter and 1 to 15 μm in length. Both types of SWCNT contained up to 75% nanotubes (the remaining material consisted of amorphous carbon and other carbon nanoparticles) and were autoclaved at 250 °C for 2 hours before use. SWCNT aggravated allergen-induced pulmonary inflammation with mucus hyperplasia. OVA+SWCNT enhanced the protein levels of Th cytokines and chemokines related to allergy in the lung and exhibited adjuvant activity for allergen-specific IgG1 and IgE compared with OVA alone. OVA+SWCNT-treated mice also had enhanced oxidative stress-related biomarkers in the airways (Inoue et al., 2010). [These results were consistent with an exacerbation of allergic airway inflammation in mice via the enhanced activation of Th immunity and increased oxidative stress.]

The effects of SWCNT were investigated in wild-type and *Ccr5* (a C-C chemokine receptor predominantly expressed on T-cells, macrophages, dendritic cells, and microglia, which plays an important role in inflammatory responses to infections) knockout mice. A comparison of wild-type and knockout mice exposed to SWCNT showed a significant decrease in the levels of neutrophils and an increase in the expression of apoptosis-related proteins, TGF-βl, and mesothelin in knockout mice. Histopathological lesions were also observed more frequently in knockout mice. The concentrations of the pro-inflammatory cytokines IL-6, IL-13, and IL-17 in BALF were significantly higher in knockout than in wild-type mice, but the levels of IL-1β, IL-10, and IFN-γ were similar in both models. Ccr5 deficiency may delay the resolution of inflammatory responses triggered by SWCNT and shifts the inflammatory response for SWCNT clearance from a Th1-type to a Th2-type (Park et al., 2013).

Nanoparticles have been reported to produce respiratory damage associated with adverse cardiovascular effects. To evaluate the effects of SWCNT on the progression of atherosclerosis, apolipoprotein E knockout (*ApoE*$^{-/-}$) C57BL/6 mice were fed normal or atherogenic diets and were exposed by intrapharyngeal instillation to SWCNT. *ApoE*$^{-/-}$ mice lack ApoE, a high-affinity ligand for lipoprotein receptors, and consequently have elevated plasma levels of cholesterol and triglycerides and develop atherosclerotic plaques. Exposure to SWCNT did not modify the lipid profiles of *ApoE*$^{-/-}$ mice but induced accelerated plaque formation in mice fed an atherogenic diet. This response was accompanied by increased mitochondrial DNA damage but not inflammation (Li et al., 2007b). [These findings suggested that ApoE deficiency may enhance sensitivity to SWCNT.]

4.6 Mechanistic considerations

4.6.1 Physical and chemical properties associated with biological activity

See Fig. 4.2

The physico-chemical properties of CNT may be modulated by their production method, by applying post-synthesis modification (purification), and/or by covalent functionalization of their external surface. The resulting large variety of CNT, their different features and their impact on biological activity and pathogenicity are reviewed in Section 4.2 and summarized in Table 4.2 and Fig. 4.2.

4.6.2 Deposition, biopersistence, translocation, and associated end-points

See Table 4.21

The lung interstitium and pleura were the target tissues for the carcinogenic (see Section 3), inflammogenic, and fibrotic effects that have been reported to be associated with exposure to MWCNT in rats and mice.

The biokinetic factors that relate to the mechanisms of carcinogenicity are those that influence the dose to the target tissue. These factors include the particle characteristics that determine the efficiency of their deposition in the respiratory tract, their clearance or retention, and their potential for translocation to distal sites. Airborne CNT include inhalable (capable of depositing in any region of the respiratory tract; 50% cut size, 10 μm) or respirable size particles (capable of depositing in the pulmonary or alveolar region of the lungs where gas exchange occurs; 3 and 5 μm for adults and children, respectively) (Brown et al., 2013). Particles that are deposited in the pulmonary region can be cleared from the lungs by alveolar macrophages, and those that are not cleared have the potential to translocate beyond the lungs.

CNT of respirable size have been shown to be deposited in the lungs of rats and mice exposed by inhalation, with estimated pulmonary deposition fractions of approximately 1–4% for SWCNT or MWCNT in mice (Shvedova et al., 2008; Mercer et al., 2013a) and approximately 5–20% for MWCNT in rats (Pauluhn, 2010b; Oyabu et al., 2011). Estimated human pulmonary deposition fractions for MWCNT or SWCNT studied in rodents were approximately 8 to 10% (NIOSH, 2013).

CNT can enter cells by passive internalization (diffusion or penetration of the cell membrane) or active internalization (phagocytosis or other types of endocytosis) (Kunzmann et al., 2011; Ye et al., 2013). The mechanisms of cell uptake depend on the surface properties of the CNT, the cell type encountered and its activation state. SWCNT uptake into alveolar macrophages was low (10% of alveolar burden in mice) (Shvedova et al., 2005) and 90% of dispersed SWCNT structures were observed in the lung interstitium (Mercer et al., 2008). More effective uptake of MWCNT has been observed (Mercer et al., 2010, 2011; Treumann et al., 2013). F-MWCNT significantly increased the alveolar macrophage uptake in comparison with O- or P-MWCNT (Silva et al., 2014).

CNT translocated from the lungs of mice and were observed in blood samples (Ingle et al., 2013). Two sizes of MWCNT (diameter, 60–80 nm or 90–150 nm) were observed as black pigments in liver tissue 1 day after intratracheal administration; dose-dependent toxicity and necrosis were observed in the liver and kidney (Reddy et al., 2010a). MWCNT seen by TEM were located in alveolar macrophages in the subpleural region, where focal subpleural fibrosis was also observed 2 weeks after inhalation exposure of 30 mg/m^3 in mice (Ryman-Rasmussen et al., 2009a). MWCNT administered to rats by intrapulmonary spraying were observed to penetrate directly from the lungs to the pleural cavity through the visceral pleura, where visceral

Fig. 4.2 Physical and chemical properties of carbon nanotubes associated with biological activity

---
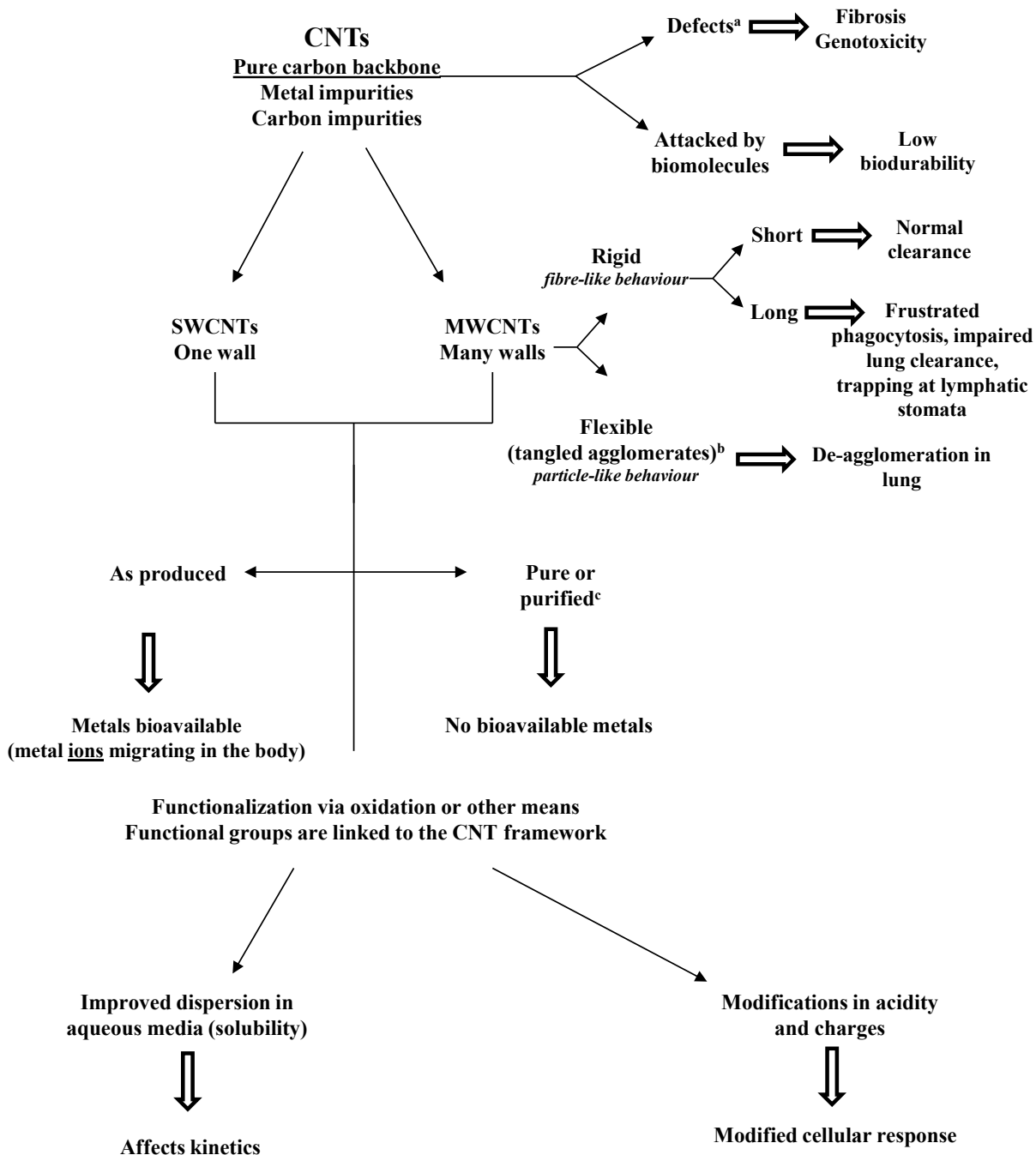
[a] CNTs do not generate radicals/reactive oxygen species (ROS) per se, but act as quenchers of radicals/ROS. When in contact with cells, an oxidative stress response may take place, but the radicals/ROS generated by cells may be totally or partially quenched by CNT. A balance between radicals/ROS generated or quenched depends on cell activity and the quenching potential of CNT, and is strictly related to defects
[b] Tangled or less dense material may lead to volumetric overload mechanism. Reagglomeration may occur dur to hydrophobic interaction
[c] Nitric acid purification may also lead to defects
CNT, carbon nanotube; MWCNT, multiwalled carbon nanotube; SWCNT, single-walled carbon nanotube
Prepared by the Working Group

Table 4.21 Studies of the kinetics of MWCNT or SWCNT[a] in vivo: deposition, biopersistence, translocation, and associated end-points

Target tissue	MWCNT[b]	SWCNT
Penetration of the lung interstitium	(+) MWCNT (Mitsui-7) penetrated the alveolar epithelium and visceral pleura at a high frequency: > 20 million alveolar epithelial cell penetrations throughout the lungs at doses ≥ 40 µg in mice (Mercer et al., 2010)	(+) Rapid translocation (1 day after PA) of dispersed SWCNT (HiPCO) (10 µg) and increased collagen in mice (Mercer et al., 2008) (±) Of the poorly dispersed SWCNT (HiPCO), 80% remained in airspaces/granulomas; 20% of the SWCNT material was sufficiently small to enter the alveolar wall and stimulate collagen production in mice (Mercer et al., 2008)
Translocation to the pleura	(+) MWCNT (Mitsui-7): 0.6% in subpleura on day 1 after PA in mice; MWCNT-loaded alveolar macrophages seen in the intralobular septa; MWCNT penetrated the visceral pleura (Mercer et al., 2010) (+) MWCNT (Helix Material Solutions) was seen in the subpleural lung tissue 1 day after inhalation in mice (30 mg/m³); focal pleural inflammation and fibrosis were seen 2 and 6 wk after exposure (Ryman-Rasmussen et al., 2009a) (+) MWCNT (Mitsui-7) penetrated the visceral pleura in the intrapleural space after PA (10 µg) in mice (Porter et al., 2010) (+) MWCNT (Mitsui-7): 1.6% of dose was observed in the subpleura 56 days after exposure (PA) (10–80 µg) in mice (Mercer et al., 2011) (+) MWCNT (diameter, 10–15 nm; length, 20 µm) caused persistent DNA damage in the rat lung 90 days after inhalation (Kim et al., 2014) [note: short length (330 ± 1.72 nm) administered]	(±) Dispersed SWCNT (HiPCO) observed "in the vicinity of the pleura" in mice (Mercer et al., 2008)
Translocation to the pleura and other organs	(+) MWCNT (Mitsui-7): inhaled particles (5 mg/m³, 12 days) penetrated the visceral pleura and were found in the pleural lavage as singlets with an average length of 6.9 µm, in close contact with or penetrating into the cytoplasm and/or nucleus of monocytes in mice; translocation to other organs was also observed: 15 371 and 109 885 fibres/g in the liver, kidney, heart, or brain 1 and 336 days after exposure, respectively; the number of singlet MWCNT in the lymph nodes, diaphragm, chest wall, and extrapulmonary organs was significantly higher 336 days after exposure compared with 1 day after exposure (Mercer et al., 2013a, b) (+) Translocation of MWCNT-N (Nikkiso Co.), MWCNT-M (Mitsui-7), or crocidolite asbestos was observed in rats after intrapulmonary spraying (5 times over 9 days; total dose, 1.25 mg/rat); MWCNT or crocidolite fibres were found in the mediastinal lymph nodes, liver sinusoid cells, blood vessel wall cells in the brain, renal tubular cells, spleen sinus, and macrophages; a few fibres penetrated directly from the lungs into the pleural cavity through the visceral pleura; no fibres were seen in the parietal pleura; visceral pleural cell proliferation was observed at the end of exposure on day 9 (Xu et al., 2012)	

Table 4.21 (continued)

Target tissue	MWCNT[b]	SWCNT
Bioersistence/ increased retention half-time	(+) MWCNT (Baytubes) had significantly increased retention half-times (at ≥ 0.4 mg/m³) in rats (Pauluhn, 2010a) (+) MWCNT (Mitsui-7): 65% of the dose remained in the lungs 336 days after inhalation (5 mg/m³), and the dispersion of multiple structures to single fibres over time was seen in mice (Mercer et al., 2013b) (+) MWCNT (Mitsui-7): 8% of a PA-administered dose (10–80 µg) was seen in the alveolar septa (Mercer et al., 2011)	

[a] The metal catalyst content in all CNT materials in these studies was reported to be < 2% (as-produced). No studies of the disposition of purified CNT in the lungs were found; no studies of CNT other than SWNT and MWCNT were found

[b] Studies of intrapleural and intraperitoneal injection in mice showed that short (~5 µm) or tangled MWCNT were effectively cleared through the lymphatic stomata, while long, rigid MWCNT were trapped in the stomata and induced inflammation and granuloma formation (Poland et al., 2008; Murphy et al., 2011).

(+) positive finding; (±) equivocal finding; CNT, carbon nanotubes; HiPCO, high-pressure carbon monoxide process; MWCNT, multiwalled carbon nanotubes; PA, pharyngeal aspiration; SWCNT, single-walled carbon nanotubes

pleural cell proliferation was apparent at the end of the 9-day exposure (Xu et al., 2012). MWCNT (as-produced, CM-100; diameter, ~10–15 nm; length, ~20 μm) were observed in the pleura 28 days after a 90-day exposure by inhalation in rats, and DNA damage was observed (by the comet assay) up to 90 days after exposure (Kim et al., 2014). [The Working Group noted the short length of the aerosol generated.]

The numbers of MWCNT in the lungs and other organs were quantified after a 12-day exposure of mice to 5 mg/m³ for 5 hours per day; most of the MWCNT in the lungs were agglomerated, but only singlet MWCNT structures (average length, 6.9 μm) were observed in the liver, kidney, heart, brain, chest wall, and diaphragm (Mercer et al., 2013a, b). Rapid translocation of MWCNT occurred and 0.6% of the dose administered by pharyngeal aspiration was seen in the subpleura of mice 1 day after exposure (Mercer et al., 2010). ¹⁴C-Radiolabelled MWCNT administered to mice by pharyngeal aspiration was detected in the spleen and liver 1 day after exposure, increasing to 0.1–1% of the administered dose by 6–12 months after exposure, while the lung dose decreased to 10–20% of the administered dose over that time (Czarny et al., 2014).

The length and rigidity of the MWCNT influenced their clearance from the pleura after intrapleural injection; mice given the longer structures (mean length, 13 μm) developed significant inflammation and fibrosis of the parietal pleura compared with those given the shorter MWCNT (length, 0.5–5 μm) (Murphy et al., 2011).

The rat lung retention rate of short MWCNT (geometric mean length, 1.1 μm; GSD, 2.7) was similar to that for respirable poorly soluble spherical particles, with a retention half-time of approximately 50 days after inhalation exposure to 0.37 mg/m³ of MWCNT (Oyabu et al., 2011). The rat lung retention half-times were greater for another MWCNT (Baytubes; MMAD, ~3 μm; GSD, ~2), ranging from 151 to 375 days in rats

exposed to inhalation concentrations ranging from 0.1 to 6 mg/ mg/m³ (Pauluhn, 2010a).

4.6.3 Persistent inflammation, granuloma formation, fibrosis, and pleural end-points

The studies on the toxicity of CNT in vivo are summarized in Table 4.22, in which the types of CNT and biological end-points are identified. Acute or persistent pulmonary inflammation (Fig. 4.3), pulmonary granuloma, fibrosis, and pleural end-points with well-defined effects were observed in the studies of MWCNT, SWCNT, and other CNT. Regardless of the number of walls or extent of purification, significant dose–response relationships were observed for these pulmonary end-points.

Occupational exposures to CNT may be to various types and forms of CNT that vary with respect to purity, especially in the content and bioavailability of metal catalyst residues. In general, MWCNT and SWCNT used in their "as-produced" or pure or purified forms produce a marked acute inflammatory response in the lungs after inhalation/aspiration. There is some evidence that "fully purified" MWCNT showed less severe responses than "as-produced" or partially purified MWCNT. Repeated exposure to CNT by inhalation/aspiration induces a persistent inflammatory response with concomitant focal granuloma formation and co-localization of fibrosis in a dose-dependent fashion. Even acute exposure to MWCNT can lead to their translocation to the pleura with subpleural cellular infiltration, collagen deposition, and pleural (mesothelial) cell hyperplasia.

4.6.4 Genotoxicity

See Table 4.23, Table 4.24, and Table 4.25 [The Working Group recognized the difficulties in evaluating the results of studies of genotoxicity due to the lack of standardized methods

Table 4.22 Summary of results for end-points related to persistent inflammation, granuloma formation, fibrosis, and pleural end-points after exposure to carbon nanotubes in vivo

End-point	MWCNT		SWCNT			Other CNT
	As-produced	Pure or purified	Fully purified[a]	As-produced	Pure or purified	
Acute pulmonary inflammation	(+) Muller et al. (2008a); (+D) Ma-Hock et al. (2009); (+D) Park et al. (2009); (–) Mitchell et al. (2007); (–) Elgrabli et al. (2008); (–) Mitchell et al. (2009)	(+D) Muller et al. (2005); (+) Han et al. (2010); (+D) Kasai et al. (2015); (+) Muller et al. (2008a); (–) Morimoto et al. (2012b) (inhalation exposure)	(–) Muller et al. (2008a)	(+) Warheit et al. (2004)	(–) Morimoto et al. (2012a)	(+D) Crouzier et al. (2010) (80% DWCNT/20% SWCNT)
Persistent pulmonary inflammation	(+D) Ma-Hock et al. (2009); (+D) Ellinger-Ziegelbauer & Pauluhn (2009); (+D) Aiso et al. (2010); (+D) Treumann et al. (2013); (+) Mercer et al. (2013a); (–) Elgrabli et al. (2008)	(+D) Ellinger-Ziegelbauer & Pauluhn (2009); (+D) Kobayashi et al. (2010); (+D) Porter et al. (2010); (+D) Mercer et al. (2011); (+D) Morimoto et al. (2012b) (intratracheal instillation); (+D) Kasai et al. (2015); (–) Morimoto et al. (2012b) (inhalation exposure)		(+D) Shvedova et al. (2008)	(+D) Shvedova et al. (2005); (+D) Shvedova et al. (2007); (+D) Kobayashi et al. (2011); (+D) Morimoto et al. (2012c); (+) Murray et al. (2012); (–) Morimoto et al. (2012a)	(+D) Delorme et al. (2012) (CNF); (+) Murray et al. (2012) (CNF); (+D) Sager et al. (2013) (DWCNT)
Pulmonary granuloma or fibrosis	(+) Muller et al. (2008a); (+D) Ma-Hock et al. (2009); (+D) Ryman-Rasmussen et al. (2009a); (+D) Aiso et al. (2010); (+) Cesta et al. (2010); (+D) Pauluhn (2010b); (+D) Treumann et al. (2013); (+) Mercer et al. (2013a)	(+D) Muller et al. (2005); (+D) Ellinger-Ziegelbauer & Pauluhn (2009); (+D) Porter et al. (2010); (+D) Mercer et al. (2011); (+D) Morimoto et al. (2012b) (intratracheal instillation; bolus); (+D) Kasai et al. (2015); (+) Muller et al. (2008a); (–) Morimoto et al. (2012b) (inhalation exposure)	(±) Muller et al. (2008a)		(+D) Shvedova et al. (2005); (+D) Kobayashi et al. (2011); (+D) Morimoto et al. (2012c); (+) Murray et al. (2012); (–) Morimoto et al. (2012a); (–) Fujita et al. (2015)	(+D) Delorme et al. (2012) (CNF); (+D) Sager et al. (2013) (DWCNT)
Other biological effects	(+) Poland et al. (2008) (peritoneal granuloma); (+) Murphy et al. (2011) (pleural inflammation); (+) Schinwald et al. (2012) (pleural inflammation)	(–) Muller et al. (2009)	(–) Muller et al. (2009)			

[a] Metal impurities and defects were eliminated by heating at high temperatures (2400 °C)

(+) positive findings were observed at the highest dose; (–) no positive findings were observed at the highest dose; (+D), positive dose–response relationship was observed; (±) equivocal findings were observed; CNF, carbon nanofibres; CNT, carbon nanotubes; DWCNT, double-walled carbon nanotubes; MWCNT, multiwalled carbon nanotubes; SWCNT, single-walled carbon nanotubes

Fig. 4.3 Persistent inflammation and exposure to carbon nanotubes
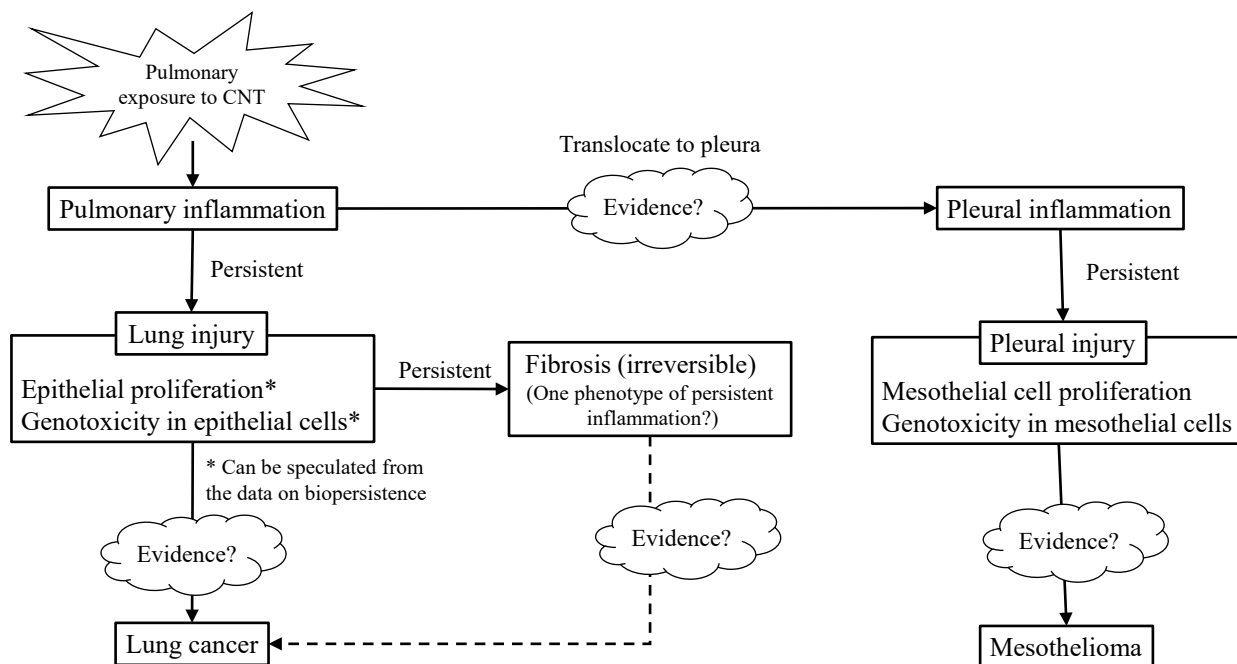
CNT, carbon nanotubes
Compiled by the Working Group with data from Morimoto et al. (2014)

for genotoxicity testing, and variations in sample preparations and characterization of CNT.]

The Working Group did not identify any studies on genotoxicity end-points in presumed target tissues, surrogate cells (peripheral blood leukocytes), or matrices (e.g. urine) in humans with well-defined exposure to CNT and therefore regarded the observations in cultured human cells as being the most relevant with regard to supporting mechanistic evidence for carcinogenicity. In particular, both MWCNT and SWCNT induced aneuploidy in primary or immortalized human airway epithelial cells (Sargent et al., 2009, 2012a). This mechanism, which is described as a physical interference between CNT and the mitotic apparatus or fragmentation of the centrosome, is considered to be relevant for (airway) exposure of humans in vivo. These observations of chromosomal damage are supported by positive findings for SWCNT in cultured primary human lymphocytes (Catalán et al., 2012) and for MWCNT in the bronchial

epithelial BEAS-2B cell line (Siegrist et al., 2014). Further supporting evidence in six out of eight studies showed an increased frequency of micronuclei in human cell lines after exposure to either SWCNT or MWCNT (Muller et al., 2008b; Cveticanin et al., 2010; Cicchetti et al., 2011; Thurnherr et al., 2011; Lindberg et al., 2013; Manshian et al., 2013; Kim & Yu, 2014; Tavares et al., 2014). Studies that gave negative results investigated the effects of pure MWCNT (length, 2–5 μm; diameter, 6–26 nm; 0.4% iron) (Thurnherr et al., 2011) and SWCNT (length, 1–5 μm; diameter, < 2 nm; impurities not reported) (Lindberg et al., 2013) that did not appear to differ from samples that caused the formation of micronuclei. In addition, one study showed that only two out of six MWCNT samples generated micronuclei, although they did not have overtly different physico-chemical characteristics compared with non-genotoxic samples (Tavares et al., 2014).

The strongest evidence of mutagenesis derives from animal studies that showed increased

Table 4.23 Summary of results for end-points related to genotoxicity, gene expression, and cellular transformation after exposure to carbon nanotubes in vitro

End-point	MWCNT	SWCNT
DNA oxidation products	± (FPG) Kermanizadeh et al. (2012, 2013)[a] + (FPG) McShan & Yu (2014)[a] + (FPG, ENDOIII) (iron, 0.1%) Migliore et al. (2010) − (FPG) Cavallo et al. (2012)[a] − (FPG) Karlsson et al. (2008)	+ (FPG) Vesterdal et al. (2014b)[a] + (FPG) (iron, 2%) Jacobsen et al. (2008) + (FPG, ENDOIII) Migliore et al. (2010) − (FPG) Pelka et al. (2013)[a]
DNA strand breaks	+ Lindberg et al. (2013)[b] + (iron, 0.55%) Cavallo et al. (2012)[a] + Karlsson et al. (2008)[a] + Cicchetti et al. (2011)[a] + Kermanizadeh et al. (2012, 2013)[a] + Alarifi et al. (2014)[a] + (iron, 0.420%) Aldieri et al. (2013) + (nickel, 1.5%) Di Giorgio et al. (2011) + (iron, 0.1%) Migliore et al. (2010) + (1% impurities) Cveticanin et al. (2010)[a] + Barillet et al. (2010)[c] − Ju et al. (2014) (neutral comet assay)[a] − Thurnherr et al. (2011) − McShan & Yu (2014) − Barillet et al. (2010)[d] − Lindberg et al. (2013)[a,e] − (iron, 0.002%) Aldieri et al. (2013)	+ Pelka et al. (2013)[a] + Lindberg et al. (2013)[a,b] + Kim & Yu (2014)[a] + Vesterdal et al. (2014b)[a] + (iron, 0.07%) Pacurari et al. (2008a)[a,b] + (> 50% SWCNT) Lindberg et al. (2009)[a] + (iron, 0.23%) Kisin et al. (2007) + (iron, 0.23%) Kisin et al. (2011) + (1% impurities) Yang et al. (2009) + (30% impurities, amide functionalized) Cveticanin et al. (2010)[a] + (nickel, 1.5%) Di Giorgio et al. (2011) + Migliore et al. (2010) − (iron, 2%) Jacobsen et al. (2008)
Chromosomal aberrations	+ Siegrist et al. (2014)[a] + Asakura et al. (2010) − (iron, 1 or 5%) Kim et al. (2011)	+ (iron, 0.23%) Sargent et al. (2009)[a] + (iron, 0.23%) Sargent et al. (2012a)[a] + Catalán et al. (2012)[a] − (iron, 4.4%) Ema et al. (2013b) − Naya et al. (2011)
Micronucleus formation	+ (1% impurities) Cveticanin et al. (2010)[a] + (1% impurities, amide functionalized) Cveticanin et al. (2010)[a] + (10% impurities) Cicchetti et al. (2011)[a] + Tavares et al. (2014)[a] + Asakura et al. (2010) + (nickel, 1.5%) Di Giorgio et al. (2011) + (2% impurities, ground sample) Muller et al. (2008b) + (iron, 0.48%; cobalt, 0.49%) Muller et al. (2008a)[f] + Kato et al. (2013)[a] − Szendi & Varga (2008)[a] − (0.4% impurities) Thurnherr et al. (2011)[a]	+ (30% impurities) Cveticanin et al. (2010)[a] + (30% impurities, amide-functionalized) Cveticanin et al. (2010)[a] + Kim & Yu (2014)[a] + Manshian et al. (2013)[a] + Kato et al. (2013) + (iron, 0.23%) Kisin et al. (2011) + (nickel, 1.5%) Di Giorgio et al. (2011) − (> 50% SWCNT) Lindberg et al. (2009)[a] − Lindberg et al. (2013)[a] − (iron, 0.23%) Kisin et al. (2007) − Pelka et al. (2013)

Table 4.23 (continued)

End-point	MWCNT	SWCNT
Sister-chromatid exchange	+ Kato et al. (2013)	
Mutations	+ Zhu et al. (2007) *Aprt* – Asakura et al. (2010) *Hgprt* – Di Sotto et al. (2009) *Escherichia coli* – Kim et al. (2011) *Salmonella* and *Escherichia coli*	– Manshian et al. (2013) *HGPRT* [a] – Jacobsen et al. (2008) *cII*
Gene expression[g]	+ Ravichandran et al. (2010) p53, p21 (up)[a] + Srivastava et al. (2011) *P53, CDKN1A* (up); *BCL2* (down)[a] + Kim et al. (2012b) *CDKN2A* (down), *BCL2* (up)[a] + Vankoningsloo et al. (2012) *Bcl2* (up) + Søs Poulsen et al. (2013) *Jun* (up), *Cdkn2c* (down) + Zhu et al. (2007) p53 (up) + Zhang & Yan (2012) *Cdkn1a* (up), *pRb* unphosphorylated (up) – Zhang & Yan (2012) *P53*[a]	+ Sarkar et al. (2007) *ATM* (up)[a] + Wang et al. (2011a) P53 phosphorylated (down)[a] + Pelka et al. (2013) P53 phosphorylated (up)[a] + Wang et al. (2012b) Bcl2 (down) + Lohcharoenkal et al. (2014) *H-RAS* (up)[a,b] + Wang et al. (2014) *MYC* (up), P53 (down)[a]
In-vitro cellular transformation	+ Wang et al. (2014)[a]	+ Wang et al. (2011a)[a] + Lohcharoenkal et al. (2014)[a] + Wang et al. (2014)[a]

[a] Measurements in human cells [the Working Group noted that the studies reported by Sargent et al. (2009, 2012a) were carried out on primary or immortalized human airway epithelial cells; the proposed mechanisms were supported by observations under acellular conditions (Li et al. 2006; Dinu et al. 2009), leading to physical interference with the mitotic apparatus or fragmentation of the centrosome in response to both SWCNT and MWCNT (approximately 1 μm); these interactions led to aneuploidy in the daughter cells.]

[b] Studied in mesothelial cells

[c] Defined as "long" MWCNT (0.1–20 μm)

[d] Defined as "short" MWCNT (0.1–5 μm)

[e] Studied in bronchial epithelial BEAS-2B cells

[f] Heating (2400 °C) of the ground sample abolished genotoxicity; samples that were heated and subsequently ground increased the formation of micronuclei

[g] Gene expression included oncogenes, tumour-suppressor genes, and genes involved in DNA repair and cell-cycle regulation; +, differential expression between control (untreated) and treated cells; –, unaltered

CNT, carbon nanotubes; ENDOIII, endonuclease III; FPG, formamidopyrimidine glycosylase; MWCNT, multiwalled carbon nanotubes; SWCNT, single-walled carbon nanotubes Levels of DNA damage, mutations, chromosome damage and cellular transformation were increased (+) or unaltered (–) in exposed cells compared with unexposed controls; (±), equivocal result

Table 4.24 Summary of results for end-points related to genotoxicity and gene expression after exposure to carbon nanotubes in vivo

End-point	MWCNT	SWCNT
DNA oxidation products (lung)	– (FPG) Cao et al. (2014)	– (FPG) (iron, 2%) Vesterdal et al. (2014a)
DNA breaks (lung)	+ Kato et al. (2013); + Cao et al. (2014); + (iron, 2%) Kim et al. (2012a); + (iron, 2%) Kim et al. (2014); – Ema et al. (2013a)	– (iron, 2%) Vesterdal et al. (2014a); – (iron, 4.4%) Naya et al. (2012)
Mutations (lung)	+ Kato et al. (2013) Gpt	+ (iron, 17.7%) Shvedova et al. (2008) K-Ras (inhalation exposure); – (iron, 17.7%) Shvedova et al. (2008) K-Ras (pharyngeal aspiration)
Micronuclei (lung)	+ (2% impurities) Muller et al. (2008b)	
Gene expression[a]	+ Snyder-Talkington et al. (2013b) Vegfa (down), Junb (up); + Guo et al. (2012) Bcl3 (down), EgFr (down); + Huang et al. (2014) Cdkn1, Bax (up); + Søs Poulsen et al. (2013) Bcl3, Aurka (up); Myb (down)	+ (Unpurified sample) Park et al. (2011a) p53 (up); + (Purified sample) Park et al. (2011b) p53 (up); + Park et al. (2013) p53 phosphorylated (up)
DNA oxidation products (gavage study)		+ (8-oxodG) (iron, 2%) Folkmann et al. (2009) liver, lung; – (8-oxodG) (iron, 2%) Folkmann et al. (2009) colon mucosa
Micronucleus formation (gavage study)		– (iron, 4.4%) Ema et al. (2013b) immature bone marrow erythrocytes; – Naya et al. (2011) polychromatic bone marrow erythrocytes
DNA breaks (intraperitoneal injection)	+ (Both pristine and acid-functionalized samples) Patlolla et al. (2010) leukocytes; + Ghosh et al. (2011) bone marrow cells	
Micronucleus formation (intraperitoneal injection)	+ (Both pristine and acid-functionalized samples) Patlolla et al. (2010) femoral bone marrow cells; + Ghosh et al. (2011) polychromatic erythrocytes, femoral bone marrow cells; – Kim et al. (2011) polychromatic erythrocytes	
Chromosomal aberrations (intraperitoneal injection)	+ (Both pristine and acid-functionalized samples) Patlolla et al. (2010) femoral bone marrow cells	

a Gene expression included oncogenes, tumour-suppressor genes, and genes involved in DNA repair and cell-cycle regulation; +, differential expression between control (untreated) and treated cells.

Levels of DNA damage, mutations, chromosome damage and cellular transformation were increased (+) or unaltered (–) in exposed cells compared with unexposed controls.

CNT, carbon nanotubes; FPG, formamidopyrimidine glycosylase; MWCNT, multiwalled carbon nanotubes; SWCNT, single-walled carbon nanotubes; 8-oxodG, 8-oxodeoxyguanosine; SWCNT, single-walled carbon nanotubes

Table 4.25 Overall summary of results for genetic and related end-points in studies of exposure to carbon nanotubes in vivo and in vitro

End-point	In vivo (studies in experimental animals only)		In vitro (studies in cells of humans and experimental animals only)	
	MWCNT	SWCNT	MWCNT	SWCNT
DNA oxidation products	1 negative (FPG, lung) at low-dose	1 negative (FPG, lung) at low doses 1 positive (8-oxodG) (gavage exposure)	2/5 positive (FPG)	3/4 positive (FPG)
DNA strand breaks	4/5 positive (lung), 2 positive (intraperitoneal injection)	2/2 negative (FPG, lung)	11/15 positive	11/13 positive
Mutations	1 positive (lung)	1 positive (lung)	2/2 negative	2/2 negative
Chromosomal aberrations	1 positive (intraperitoneal injection)	No information	2/3 positive	3/5 positive
Micronucleus formation	1 positive (lung), 2/3 positive (intraperitoneal injection)	2/2 negative	9/11 positive	7/9 positive
Sister-chromatid exchange	1 positive	No information	No information	No information
Gene expression	Modulation of genes involved in DNA repair, apoptosis, and cell-cycle control	Modulation of p53 expression (up)	Modulation of genes involved in DNA repair, apoptosis, and cell-cycle control	Modulation of p53 expression (up) and genes involved in DNA repair
Transformation	No information	No information	1 positive	3/3 positive

FPG, formamidopyrimidine glycosylase; MWCNT, multiwalled carbon nanotubes; 8-oxodG, 8-oxodeoxyguanosine; SWCNT, single-walled carbon nanotubes

Fig. 4.4 Mechanisms of genomic instability generated by carbon nanotubes
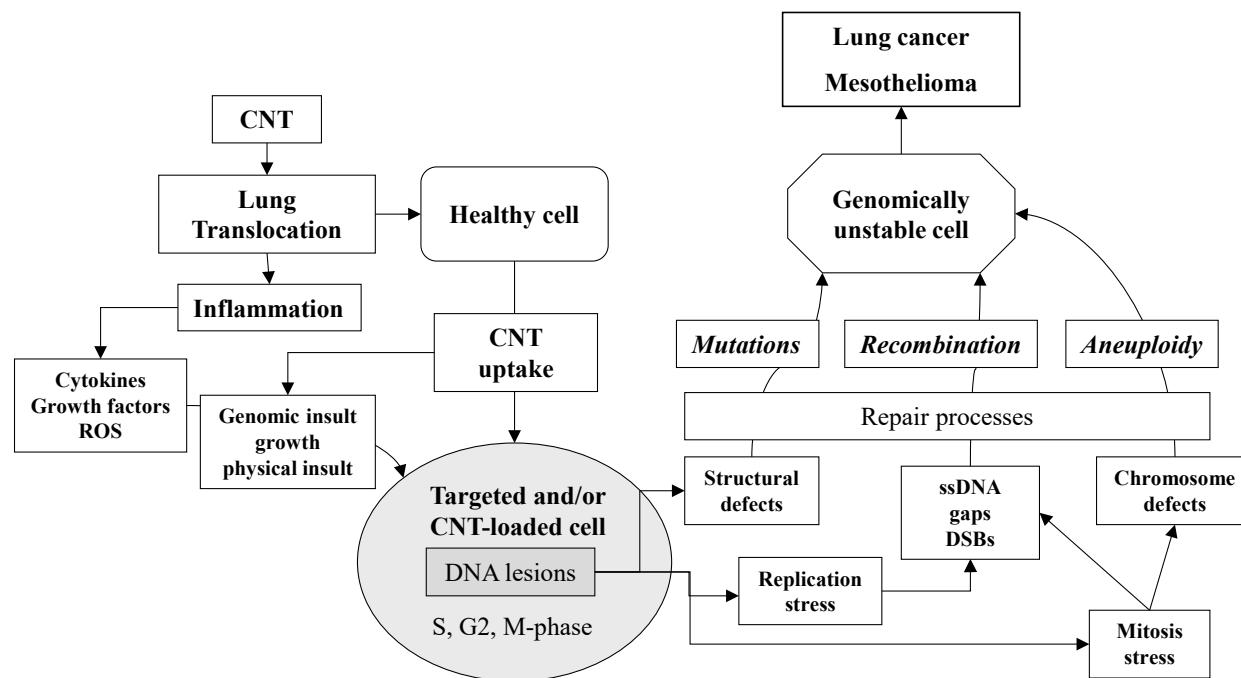
CNT, carbon nanotubes; ssDNA, single-strand DNA; DSB, double-strand break; ROS, reactive oxygen species
Cancer arises from genomic instability (GIN), and the genotoxic effects of carbon nanotubes (CNT) are consistent with an ability to generate GIN. Inhaled CNT may induce local inflammation associated with the production of cytokines, growth factors, and reactive oxygen species, which can induce genomic insult and stimulate cell growth. Alternatively, fibres can be internalized by many cell types, resulting in a physical insult due to fibre load. In these "targeted and/or fibre-loaded" cells, DNA lesions produce defects in DNA structure. DNA breakage is generated by replication stress, and mitosis stress generates both DNA breaks and chromosome defects. Various repair mechanisms and cell-cycle checkpoints are then activated to control genome integrity. Unrepaired or error-prone repair processes can entail mutations, chromosomal rearrangements and variations in chromosome number or morphology, which are the causes of GIN. Selection and amplification of genomically unstable cells can progress to lung cancer and mesothelioma.
Compiled by the Working Group

levels of guanine phosphoribosyltransferase (*Gpt*) mutations in the lung tissues of mice after intratracheal exposure to MWCNT (Kato et al., 2013) and of K-*Ras* mutations after inhalation exposure to SWCNT (Shvedova et al., 2008, 2014). The results for mutagenesis in cultured cells have been negative, including one study in human lymphoblastoid MCL-5 cells (Manshian et al., 2013). Genotoxicity studies have provided information on the mechanisms of genomic instability generated by CNT (Fig. 4.4). Studies of DNA damage – essentially DNA strand breaks and oxidatively damaged DNA measured by the comet assay – in cultured human cells have shown genotoxicity after exposure to either MWCNT or SWCNT. Increased levels of DNA strand breaks

in the lungs of rodents after pulmonary exposure to either MWCNT or SWCNT were found in four studies (Kim et al., 2012a; Kato et al., 2013; Cao et al., 2014; Kim et al., 2014) while no increase was found in three studies (Naya et al., 2012; Ema et al., 2013a; Vesterdal et al., 2014a); intraperitoneal injection of MWCNT yielded positive results in two studies (Patlolla et al., 2010; Ghosh et al., 2011). No data were available regarding the relationship between the characteristics of CNT and their ability to generate DNA damage in human cultured cells and organs of exposed animals. [These observations indicate that the mechanisms of genotoxicity involve chromosomal aberrations and oxidative stress, although a formal assessment of the inhibition of DNA damage

through supplementation with antioxidants in CNT-exposed cells has not been pursued.] This mechanism of DNA damage is known to occur in human cells after exposure to particulate matter. Two human mesothelial (pleural Met-5A and peritoneal LP-9) cell lines showed features of morphological transformation and *H-RAS* expression after continuous exposure to SWCNT (Lohcharoenkal et al., 2014).

Pulmonary exposure to MWCNT and SWCNT had no effect on oxidative DNA damage (i.e. FPG-sensitive sites) in studies that mainly focused on cardiovascular effects in atherosclerosis-prone (*ApoE*$^{-/-}$ knockout) mice, but the administered doses were low (maximal dose of 1 mg/kg bw as two intratracheal instillations (Vesterdal et al., 2014a) and 25.6 µg/mouse per week (Cao et al., 2014)). [Therefore, these studies cannot rule out the possibility that DNA damage is generated by oxidative stress in pulmonary tissues after airway exposure to MWCNT and SWCNT.] One study showed increased levels of pro-mutagenic 8-oxodG lesions in both lung and liver tissues after gastrointestinal administration of low doses (0.064 and 0.64 mg/kg bw) of SWCNT (Folkmann et al., 2009). [This study suggests the involvement of a genotoxic mechanism arising as a consequence of oxidative stress, although it is impossible to distinguish between direct and indirect genotoxic mechanisms.]

The MWCNT and SWCNT investigated originated from different manufacturing processes, leading to substantial differences in dimensions and residual transition metal content. The available literature supports the conclusion that exposure to a range of different MWCNT (including Mitsui-7) and SWCNT can generate DNA strand breaks, oxidized DNA nucleobases, micronuclei, and chromosomal aberrations in animal and human cells through various mechanisms according to the type of CNT material. Overall, there is strong evidence that a genotoxic mechanism in human cells leads to carcinogenesis after exposure to both MWCNT and SWCNT.

5. Summary of Data Reported

5.1 Exposure data

Carbon nanotubes (CNT) are comprised of graphene sheets rolled into cylinders, some of which may be hundreds of micrometres in length and be composed of either a single graphene cylinder (single-walled carbon nanotube; SWCNT) or many graphene cylinders inside one another in concentric layers (multiwalled carbon nanotubes; MWCNT). The outer diameter of SWCNT is generally 1–3 nm and that of MWCNT is 10–200 nm. The thickness of CNT mainly depends on the number of graphene layers contained therein and on the chirality of the tubes. The length of a typical CNT is a few micrometres, but their length can vary from only a few hundreds of nanometres to several tens of micrometres.

The production of CNT involves the use of a carbon source at a high temperature and/or pressure in the presence of transition metals. Both SWCNT and MWCNT are normally produced by one of three principal techniques: chemical vapour deposition, arc discharge, or laser ablation. Chemical vapour deposition is the most common production method. Depending on the production technique, the physical and chemical characteristics (e.g. diameter, length, atomic structure, surface chemistry, and defects) and the levels of impurities (such as metal catalysts, amorphous carbon, carbon black, fibres, soot, graphite, and non-tubular fullerenes) present in the final preparation may vary greatly.

Industrial-scale commercial production of CNT began in the twenty-first century. In 2006, global production of MWCNT and SWCNT was estimated at 300 and 7 tonnes, respectively. Because the industrial production and use of CNT material are relatively recent and the size of the workforce in CNT is still small, currently available data on occupational exposure are

limited. The main route of exposure in occupational settings is anticipated to be inhalation.

Due to the limitations of exposure assessment methods and the lack of a consensus on the most relevant exposure metrics, the available data do not allow complete characterization of occupational exposure to SWCNT and MWCNT and only permit a limited description of some occupational exposure situations. The operations that yield the highest release of CNT material include production, blending, transferral, sieving, pouring, weighing, and cleaning. CNT were more frequently found in the form of large entangled agglomerates; individual CNT were rarely observed and may be dependent on the work process or task.

CNT have a wide variety of applications, including incorporation into fabrics, plastics, rubbers, electronics, reinforced structures, composite materials, and other household products to improve their strength and water- and wear-resistance and reduce their weight. No quantitative data on consumer exposure to CNT have been identified, but exposure can occur in principle at all phases of the life-cycle of CNT, ranging from production to waste treatment. Several studies describing the release of CNT from consumer products have been conducted to estimate exposures from abrasion and weathering, but quantitative values of CNT or CNT composites released from the products have not been specified.

5.2 Human carcinogenicity data

No relevant data were available to the Working Group.

5.3 Animal carcinogenicity data

MWCNT-7 significantly increased the incidence of peritoneal mesothelioma in one study by intrascrotal injection in male rats, of mesothelioma in one study by intraperitoneal injection in male and female rats (combined), and of peritoneal mesothelioma in two studies by intraperitoneal administration in male p53$^{+/-}$ mice. In one inhalation study in male mice, MWCNT-7 was a promoter of 3-methylcholanthrene-initiated bronchiolo-alveolar adenoma and carcinoma.

In one study, intraperitoneal administration of two types of MWCNT with physical dimensions similar to those of MWCNT-7 (length, 1–19 μm; diameter, 40–170 nm) significantly increased the incidence of mesothelioma in male and female rats (combined).

One study of intraperitoneal administration of MWCNT in male rats and one study of subcutaneous administration of MWCNT in male mice gave negative results. One study of intratracheal instillation of MWCNT in male mice and one study of intraperitoneal implantation of MWCNT in rats were inadequate for an evaluation.

One study of intratracheal instillation and one study of intraperitoneal implantation of SWCNT in rats were inadequate for an evaluation.

5.4 Mechanistic and other relevant data

5.4.1 Biopersistence, pleural translocation, and injury

MWCNT have been associated with increased retention half-times in rat lungs at lower mass doses than those observed for other poorly soluble, respirable particles. MWCNT and SWCNT enter the lung interstitium in rodents exposed by inhalation.

In rodents, three types of long, rigid MWCNT (MWCNT-7, MWCNT-N, and Helix) reached the subpleural tissues after inhalation, and one of these (Helix) induced subpleural fibrosis in mice. The three types of MWCNT also translocated to lung-associated lymph nodes and distal

organs at increasing concentrations after inhalation or intrapulmonary spraying into the lungs. MWCNT-7 rapidly translocated to the pleura and intrapleural space in mice (small percentage of the dose within 1 day of administration).

No studies evaluated the pleural penetration, translocation, or injury of other types of CNT administered by lung instillation or inhalation.

5.4.2 Lung inflammation and fibrosis

Acute exposure to CNT was associated with transient inflammation that resolved over time, although CNT were able to persist in the tissues. Long-term exposure to CNT induced a sustained inflammatory response associated with granuloma formation, fibrosis, and subpleural thickening. Acute or persistent pulmonary inflammation, pulmonary granuloma or fibrosis, and bronchiolar or bronchoalveolar hyperplasia were observed in most of the studies with MWCNT, SWCNT, and other CNT. Regardless of the number of walls or extent of purification, statistically significant dose–response relationships were observed for these pulmonary end-points.

Lung epithelial cell proliferation was observed in one study in rats exposed to as-produced or functionalized MWCNT by pharyngeal aspiration.

5.4.3 Genotoxicity in vivo and in vitro

SWCNT and MWCNT induced genetic lesions in experimental animals and similar genetic injuries (end-points) in cultured human and animal cells. Positive and negative results were observed in human primary and immortalized lung and mesothelial cells in short-term assays in vitro. DNA strand breaks, oxidized DNA bases, mutations, micronucleus formation, and numerical and structural chromosomal abnormalities have been reported. SWCNT and MWCNT interacted with and perturbed the cellular mitotic apparatus, including microtubules and centrosomes, in human lung epithelial cells. K-*Ras* point mutations were observed in the lung tissues of mice 1 and 28 days and 1 year after a 4-day inhalation exposure to one type of SWCNT; 1 year after exposure, karyotypic changes were shown by micronuclei and multinucleated cells in type II pneumocytes. In two studies, MWCNT was genotoxic (by the comet assay) in rats after inhalation exposure. Overall, experimental studies are too limited to link the specific physical and chemical properties of SWCNT or MWCNT with genotoxicity. Consistent evidence indicated that SWCNT and MWCNT are genotoxic in vitro to relevant human target cells in the lungs and pleura.

5.4.4 Conclusion

The results of studies of genotoxicity in vivo and in vitro were positive for SWCNT and MWCNT. Lung inflammation, granuloma formation, and fibrosis were observed in rats and mice exposed by inhalation, intratracheal instillation, or pharyngeal aspiration to SWCNT, double-walled CNT, or MWCNT. Pleural inflammation or proliferation was observed in mice or rats exposed by inhalation or intrapulmonary spraying to three types of MWCNT (MWCNT-7, MWCNT-N, and Helix).

For end-points related to mesothelioma, the mechanistic evidence is *moderate* for MWCNT and is *weak* for SWCNT due to the lack of data.

For end-points related to cancer of the lung, the mechanistic evidence is *moderate* for MWCNT and *equivocal* for SWCNT.

The mechanistic evidence for other CNT is *weak* due to limited data.

The mechanistic events relevant to genotoxicity, lung inflammation, and fibrosis as well as translocation to the pleura, are liable to occur in humans exposed to CNT by inhalation.

Due to the heterogeneity of CNT and the limited long-term studies, significant data

gaps remain with regard to understanding the mechanisms of carcinogenicity.

6. Evaluation

6.1 Cancer in humans

There is *inadequate evidence* in humans for the carcinogenicity of carbon nanotubes.

6.2 Cancer in experimental animals

There is *sufficient evidence* in experimental animals for the carcinogenicity of MWCNT-7 multiwalled carbon nanotubes.

There is *limited evidence* in experimental animals for the carcinogenicity of two types of multiwalled carbon nanotube with dimensions similar to MWCNT-7.

There is *inadequate evidence* in experimental animals for the carcinogenicity of multiwalled carbon nanotubes other than MWCNT-7.

There is *inadequate evidence* in experimental animals for the carcinogenicity of single-walled carbon nanotubes.

6.3 Overall evaluation

MWCNT-7 multiwalled carbon nanotubes are *possibly carcinogenic to humans* (Group 2B).

Multiwalled carbon nanotubes other than MWCNT-7 are *not classifiable* as to their carcinogenicity to humans (Group 3).

Single-walled carbon nanotubes are *not classifiable* as to their carcinogenicity to humans (Group 3).

References

Abe S, Itoh S, Hayashi D, Kobayashi T, Kiba T, Akasaka T, et al. (2012). Biodistribution of aqueous suspensions of carbon nanotubes in mice and their biocompatibility. *J Nanosci Nanotechnol*, 12(1):700–6. doi:10.1166/jnn.2012.5391 PMID:22524043

Aiso S, Kubota H, Umeda Y, Kasai T, Takaya M, Yamazaki K, et al. (2011). Translocation of intratracheally instilled multiwall carbon nanotubes to lung-associated lymph nodes in rats. *Ind Health*, 49(2):215–20. doi:10.2486/indhealth.MS1213 PMID:21173528

Aiso S, Yamazaki K, Umeda Y, Asakura M, Kasai T, Takaya M, et al. (2010). Pulmonary toxicity of intratracheally instilled multiwall carbon nanotubes in male Fischer 344 rats. *Ind Health*, 48(6):783–95. doi:10.2486/indhealth.MS1129 PMID:20616469

Aitken RJ, Chaudhry MQ, Boxall AB, Hull M (2006). Manufacture and use of nanomaterials: current status in the UK and global trends. *Occup Med (Lond)*, 56(5):300–6. doi:10.1093/occmed/kql051 PMID:16868127

Al Faraj A, Bessaad A, Cieslar K, Lacroix G, Canet-Soulas E, Crémillieux Y (2010). Long-term follow-up of lung biodistribution and effect of instilled SWCNTs using multiscale imaging techniques. *Nanotechnology*, 21(17):175103. doi:10.1088/0957-4484/21/17/175103 PMID:20368681

Al Faraj A, Cieslar K, Lacroix G, Gaillard S, Canet-Soulas E, Crémillieux Y (2009). In vivo imaging of carbon nanotube biodistribution using magnetic resonance imaging. *Nano Lett*, 9(3):1023–7. doi:10.1021/nl8032608 PMID:19199447

Al Faraj A, Fauvelle F, Luciani N, Lacroix G, Levy M, Crémillieux Y, et al. (2011). In vivo biodistribution and biological impact of injected carbon nanotubes using magnetic resonance techniques. *Int J Nanomedicine*, 6:351–61. doi:10.2147/IJN.S16653 PMID:21499425

Alarifi S, Ali D, Verma A, Almajhdi FN, Al-Qahtani AA (2014). Single-walled carbon nanotubes induce cytotoxicity and DNA damage via reactive oxygen species in human hepatocarcinoma cells. *In Vitro Cell Dev Biol Anim*, 50(8):714–22. doi:10.1007/s11626-014-9760-3 PMID:24789727

Aldieri E, Fenoglio I, Cesano F, Gazzano E, Gulino G, Scarano D, et al. (2013). The role of iron impurities in the toxic effects exerted by short multiwalled carbon nanotubes (MWCNT) in murine alveolar macrophages. *J Toxicol Environ Health A*, 76(18):1056–71. doi:10.1080/15287394.2013.834855 PMID:24188191

Alexander AJ (2007). Carbon Nanotube Structures and Composition: Implications for Toxicological Studies. In: Monteiro-Riviere NA, Tran CL, editors. Nanotoxicology: Characterization, Dosing and Health Effects. New York (NY), USA: Informa Healthcare USA; pp. 7–18.

Ali-Boucetta H, Al-Jamal KT, Müller KH, Li S, Porter AE, Eddaoudi A, et al. (2011). Cellular uptake and cytotoxic impact of chemically functionalized and polymer-coated carbon nanotubes. *Small*, 7(22):3230–8. doi:10.1002/smll.201101004 PMID:21919194

Ali-Boucetta H, Kostarelos K (2013). Pharmacology of carbon nanotubes: toxicokinetics, excretion and tissue accumulation. *Adv Drug Deliv Rev*, 65(15):2111–9. doi:10.1016/j.addr.2013.10.004 PMID:24184372

Andersen AJ, Wibroe PP, Moghimi SM (2012). Perspectives on carbon nanotube-mediated adverse immune effects. *Adv Drug Deliv Rev*, 64(15):1700–5. doi:10.1016/j.addr.2012.05.005 PMID:22634159

Andón FT, Fadeel B (2013). Programmed cell death: molecular mechanisms and implications for safety assessment of nanomaterials. *Acc Chem Res*, 46(3):733–42. doi:10.1021/ar300020b PMID:22720979

Andón FT, Kapralov AA, Yanamala N, Feng W, Baygan A, Chambers BJ, et al. (2013). Biodegradation of single-walled carbon nanotubes by eosinophil peroxidase. *Small*, 9(16):2721–9, 2720. doi:10.1002/smll.201202508 PMID:23447468

Anjilvel S, Asgharian B (1995). A multiple-path model of particle deposition in the rat lung. *Fundam Appl Toxicol*, 28(1):41–50. doi:10.1006/faat.1995.1144 PMID:8566482

Antonelli A, Serafini S, Menotta M, Sfara C, Pierigé F, Giorgi L, et al. (2010). Improved cellular uptake of functionalized single-walled carbon nanotubes. *Nanotechnology*, 21(42):425101 doi:10.1088/0957-4484/21/42/425101 PMID:20858931

ARA (2011). Multiple-path particle deposition (MPPD 2.1): a model for human and rat airway particle dosimetry. Raleigh (NC), USA: Applied Research Associates, Inc.

Arrêté Royal (2014). [Arrêté royal relatif à la mise sur le marché des substances manufacturées à l'état nanoparticulaire.] C-2014/24329, 27 May 2014. Bruxelles, Belgium: Service Public Fédéral Santé Publique, Sécurité de la Chaîne Alimentaire et Environnement. Available from: http://www.nanotechia.org/sites/default/files/files/20140924_belgian_register_fr_nl.pdf.

Asakura M, Sasaki T, Sugiyama T, Takaya M, Koda S, Nagano K, et al. (2010). Genotoxicity and cytotoxicity of multi-wall carbon nanotubes in cultured Chinese hamster lung cells in comparison with chrysotile A fibers. *J Occup Health*, 52(3):155–66. doi:10.1539/joh.L9150 PMID:20379079

Aschberger K, Johnston HJ, Stone V, Aitken RJ, Hankin SM, Peters SA, et al. (2010). Review of carbon nanotubes toxicity and exposure–appraisal of human health risk assessment based on open literature. *Crit Rev Toxicol*, 40(9):759–90. doi:10.3109/10408444.2010.506638 PMID:20860524

Australian National Industrial Chemical Notification and Assessment Scheme (NICNAS) (2010). NICNAS working definition for 'industrial nanomaterial'. Available from: http://www.nicnas.gov.au/communications/issues/nanomaterials-nanotechnology/nicnas-working-definition-for-industrial-nanomaterial, accessed 1 October 2014.

Azad N, Iyer AKV, Wang L, Liu Y, Lu Y, Rojanasakul Y (2013). Reactive oxygen species-mediated p38 MAPK regulates carbon nanotube-induced fibrogenic and angiogenic responses. *Nanotoxicology*, 7(2):157–68. doi:10.3109/17435390.2011.647929 PMID:22263913

Barillet S, Simon-Deckers A, Herlin-Boime N, Mayne-L'Hermite M, Reynaud C, Cassio D, et al. (2010). Toxicological consequences of TiO2, SiC nanoparticles and multi-walled carbon nanotubes exposure in several mammalian cell types: an in vitro study. *J Nanopart Res*, 12(1):61–73. doi:10.1007/s11051-009-9694-y

Beamer CA, Girtsman TA, Seaver BP, Finsaas KJ, Migliaccio CT, Perry VK, et al. (2013). IL-33 mediates multi-walled carbon nanotube (MWCNT)-induced airway hyper-reactivity via the mobilization of innate helper cells in the lung. *Nanotoxicology*, 7(6):1070–81. doi:10.3109/17435390.2012.702230 PMID:22686327

Becker ML, Fagan JA, Gallant ND, Bauer BJ, Bajpai V, Hobbie EK, et al. (2007). Length-dependent uptake of DNA-wrapped single-walled carbon nanotubes. *Adv Mater*, 19(7):939–45. doi:10.1002/adma.200602667

Bello D, Hart AJ, Ahn K, Hallock M, Yamamoto N, Garcia EJ, et al. (2008). Particle exposure levels during CVD growth and subsequent handling of vertically-aligned carbon nanotube films. *Carbon*, 46(6):974–7. doi:10.1016/j.carbon.2008.03.003

Bello D, Hsieh SF, Schmidt DF, Rogers EJ (2009a). Nanomaterials properties vs. biological oxidative damage: Implications for toxicity screening and exposure assessment. *Nanotoxicology*, 3(3):249–61. doi:10.1080/17435390902989270

Bello D, Wardle BL, Yamamoto N, Guzman deVilloria R, Garcia EJ, Hart AJ, et al. (2009b). Exposure to nanoscale particles and fibers during machining of hybrid advanced composites containing carbon nanotubes. *J Nanopart Res*, 11(1):231–49. doi:10.1007/s11051-008-9499-4

Bello D, Wardle BL, Zhang J, Yamamoto N, Santeufemio C, Hallock M, et al. (2010). Characterization of exposures to nanoscale particles and fibers during solid core drilling of hybrid carbon nanotube advanced composites. *Int J Occup Environ Health*, 16(4):434–50. doi:10.1179/oeh.2010.16.4.434 PMID:21222387

Berndt-Weis ML, Kauri LM, Williams A, White P, Douglas G, Yauk C (2009). Global transcriptional characterization of a mouse pulmonary epithelial cell line for use in genetic toxicology. *Toxicol In Vitro*, 23(5):816–33. doi:10.1016/j.tiv.2009.04.008 PMID:19406224

Bernholc J, Roland C, Yakobson BI (1997). Nanotubes. *Curr Opin Solid State Mater Sci*, 2(6):706–15. doi:10.1016/S1359-0286(97)80014-9

Beyer G (2002). Short communication: carbon nanotubes and flame retardants for polymers. *Fire Mater*, 26(6):291–3. doi:10.1002/fam.805

Bhattacharya S, Zhang Q, Carmichael PL, Boekelheide K, Andersen ME (2011). Toxicity testing in the 21 century: defining new risk assessment approaches based on perturbation of intracellular toxicity pathways. *PLoS*

One, 6(6):e20887 doi:10.1371/journal.pone.0020887 PMID:21701582

Bhirde AA, Patel S, Sousa AA, Patel V, Molinolo AA, Ji Y, et al. (2010). Distribution and clearance of PEG-single-walled carbon nanotube cancer drug delivery vehicles in mice. *Nanomedicine (Lond)*, 5(10):1535–46. doi:10.2217/nnm.10.90 PMID:21143032

Bhushan B (2004). Springer handbook of nanotechnology. Berlin, Germany: Springer.

Bianco A, Kostarelos K, Prato M (2011). Making carbon nanotubes biocompatible and biodegradable. *Chem Commun (Camb)*, 47(37):10182–8. doi:10.1039/c1cc13011k PMID:21776531

Birch ME, Ku BK, Evans DE, Ruda-Eberenz TA (2011). Exposure and emissions monitoring during carbon nanofiber production–Part I: elemental carbon and iron-soot aerosols. *Ann Occup Hyg*, 55(9):1016–36. doi:10.1093/annhyg/mer073 PMID:21965464

Biswas R, Bunderson-Schelvan M, Holian A (2011). Potential role of the inflammasome-derived inflammatory cytokines in pulmonary fibrosis. *Pulm Med*, 2011:105707. doi:10.1155/2011/105707 PMID:21660282

Bonner JC, Silva RM, Taylor AJ, Brown JM, Hilderbrand SC, Castranova V, et al. (2013). Interlaboratory evaluation of rodent pulmonary responses to engineered nanomaterials: the NIEHS Nano GO Consortium. *Environ Health Perspect*, 121(6):676–82. doi:10.1289/ehp.1205693 PMID:23649427

Bottini M, Bruckner S, Nika K, Bottini N, Bellucci S, Magrini A, et al. (2006). Multi-walled carbon nanotubes induce T lymphocyte apoptosis. *Toxicol Lett*, 160(2):121–6. doi:10.1016/j.toxlet.2005.06.020 PMID:16125885

Boyles MSP, Stoehr LC, Schlinkert P, Himly M, Duschl A (2014). The significance and insignificance of carbon nanotube-induced inflammation. *Fibers.*, 2(1):45–74. doi:10.3390/fib2010045

Brody AR, Roe MW (1983). Deposition pattern of inorganic particles at the alveolar level in the lungs of rats and mice. *Am Rev Respir Dis*, 128(4):724–9. PMID:6625350

Brouwer D, Berges M, Virji MA, Fransman W, Bello D, Hodson L, et al. (2012). Harmonization of measurement strategies for exposure to manufactured nano-objects; report of a workshop. *Ann Occup Hyg*, 56(1):1–9. doi:10.1093/annhyg/mer099 PMID:22156566

Brouwer DH, Links IH, De Vreede SA, Christopher Y (2006). Size selective dustiness and exposure; simulated workplace comparisons. *Ann Occup Hyg*, 50(5):445–52. doi:10.1093/annhyg/mel015 PMID:16524926

Brown DM, Donaldson K, Stone V (2010). Nuclear translocation of Nrf2 and expression of antioxidant defence genes in THP-1 cells exposed to carbon nanotubes. *J Biomed Nanotechnol*, 6(3):224–33. doi:10.1166/jbn.2010.1117 PMID:21179939

Brown JS, Gordon T, Price O, Asgharian B (2013). Thoracic and respirable particle definitions for human health risk assessment. *Part Fibre Toxicol*, 10(1):12. doi:10.1186/1743-8977-10-12 PMID:23575443

Brown JS, Wilson WE, Grant LD (2005). Dosimetric comparisons of particle deposition and retention in rats and humans. *Inhal Toxicol*, 17(7–8):355–85. doi:10.1080/08958370590929475 PMID:16020034

BSI (2007). Nanotechnologies – Part 2: Guide to safe handling and disposal of manufactured nanomaterials. PD 6699–2:2008. London, United Kingdom: British Standardization Institution.

BSI (2010). Nanotechnologies – Part 3: Guide to assessing airborne exposure in occupational settings relevant to nanomaterials. London, United Kingdom: British Standardization Institution.

Bussy C, Pinault M, Cambedouzou J, Landry MJ, Jegou P, Mayne-L'hermite M, et al. (2012). Critical role of surface chemical modifications induced by length shortening on multi-walled carbon nanotubes-induced toxicity. *Part Fibre Toxicol*, 9(46):46 doi:10.1186/1743-8977-9-46 PMID:23181604

Canadian Environment Protection Act (2014). Proposed Regulatory Framework for nanomaterials under the Canadian Environmental Protection Act, 1999. Available from: http://www.ec.gc.ca/subsnouvelles-newsubs/default.asp?lang=En&n=FD117B60-1, accessed 9 April 2014.

Cao Y, Jacobsen NR, Danielsen PH, Lenz AG, Stoeger T, Loft S, et al. (2014). Vascular effects of multiwalled carbon nanotubes in dyslipidemic ApoE−/− mice and cultured endothelial cells. *Toxicol Sci*, 138(1):104–16. doi:10.1093/toxsci/kft328 PMID:24431218

Casey A, Herzog E, Lyng FM, Byrne HJ, Chambers G, Davoren M (2008). Single walled carbon nanotubes induce indirect cytotoxicity by medium depletion in A549 lung cells. *Toxicol Lett*, 179(2):78–84. doi:10.1016/j.toxlet.2008.04.006 PMID:18502058

Catalán J, Järventaus H, Vippola M, Savolainen K, Norppa H (2012). Induction of chromosomal aberrations by carbon nanotubes and titanium dioxide nanoparticles in human lymphocytes in vitro. *Nanotoxicology*, 6(8):825–36. doi:10.3109/17435390.2011.625130 PMID:21995283

Cavallo D, Fanizza C, Ursini CL, Casciardi S, Paba E, Ciervo A, et al. (2012). Multi-walled carbon nanotubes induce cytotoxicity and genotoxicity in human lung epithelial cells. *J Appl Toxicol*, 32(6):454–64. doi:10.1002/jat.2711 PMID:22271384

Cena LG, Peters TM (2011). Characterization and control of airborne particles emitted during production of epoxy/carbon nanotube nanocomposites. *J Occup Environ Hyg*, 8(2):86–92. doi:10.1080/15459624.2011.545943 PMID:21253981

Cesta MF, Ryman-Rasmussen JP, Wallace DG, Masinde T, Hurlburt G, Taylor AJ, et al. (2010). Bacterial lipopolysaccharide enhances PDGF signalling and pulmonary fibrosis in rats exposed to carbon nanotubes. *Am*

J Respir Cell Mol Biol, 43(2):142–51. doi:10.1165/rcmb.2009-0113OC PMID:19738159

Chakravarty P, Marches R, Zimmerman NS, Swafford AD, Bajaj P, Musselman IH, et al. (2008). Thermal ablation of tumor cells with antibody-functionalized single-walled carbon nanotubes. *Proc Natl Acad Sci USA*, 105(25):8697–702. doi:10.1073/pnas.0803557105 PMID:18559847

Chang CC, Tsai ML, Huang HC, Chen CY, Dai SX (2012). Epithelial-mesenchymal transition contributes to SWCNT-induced pulmonary fibrosis. *Nanotoxicology*, 6(6):600–10. doi:10.3109/17435390.2011.594913 PMID:21711127

Chang LY, Overby LH, Brody AR, Crapo JD (1988). Progressive lung cell reactions and extracellular matrix production after a brief exposure to asbestos. *Am J Pathol*, 131(1):156–70. PMID:2833103

Charlier JC (2002). Defects in carbon nanotubes. *Acc Chem Res*, 35(12):1063–9. doi:10.1021/ar010166k PMID:12484794

Chen BT, Schwegler-Berry D, McKinney W, Stone S, Cumpston JL, Friend S, et al. (2012). Multi-walled carbon nanotubes: sampling criteria and aerosol characterization. *Inhal Toxicol*, 24(12):798–820. doi:10.3109/08958378.2012.720741 PMID:23033994

Cheng J, Fernando KA, Veca LM, Sun YP, Lamond AI, Lam YW, et al. (2008). Reversible accumulation of PEGylated single-walled carbon nanotubes in the mammalian nucleus. *ACS Nano*, 2(10):2085–94. doi:10.1021/nn800461u PMID:19206455

Cheng WW, Lin ZQ, Ceng Q, Wei BF, Fan XJ, Zhang HS, et al. (2012). Single-wall carbon nanotubes induce oxidative stress in rat aortic endothelial cells. *Toxicol Mech Methods*, 22(4):268–76. doi:10.3109/15376516.2011.647112 PMID:22500782

Cherukuri P, Gannon CJ, Leeuw TK, Schmidt HK, Smalley RE, Curley SA, et al. (2006). Mammalian pharmacokinetics of carbon nanotubes using intrinsic near-infrared fluorescence. *Proc Natl Acad Sci USA*, 103(50):18882–6. doi:10.1073/pnas.0609265103 PMID:17135351

Cheung W, Pontoriero F, Taratula O, Chen AM, He H (2010). DNA and carbon nanotubes as medicine. *Adv Drug Deliv Rev*, 62(6):633–49. doi:10.1016/j.addr.2010.03.007 PMID:20338203

Chico L, Crespi VH, Benedict LX, Louie SG, Cohen ML (1996). Pure carbon nanoscale devices: Nanotube heterojunctions. *Phys Rev Lett*, 76(6):971–4. doi:10.1103/PhysRevLett.76.971 PMID:10061598

Chou CC, Hsiao HY, Hong QS, Chen CH, Peng YW, Chen HW, et al. (2008). Single-walled carbon nanotubes can induce pulmonary injury in mouse model. *Nano Lett*, 8(2):437–45. doi:10.1021/nl0723634 PMID:18225938

Chow JC, Watson JG, Pritchett LC, Pierson WR, Frazier CA, Purcell RG (1993). The DRI thermal/optical reflectance carbon analysis system: description, evaluation and applicaiton in US Ari quality studies. *Atmos Environ*, 27A(8):1185–201. doi:10.1016/0960-1686(93)90245-T

Chung KT, Sabo A, Pica AP (1982). Electrical permittivity and conductivity of carbon black-polyvinyl chloride composites. *J Appl Phys*, 53(10):6867–79. doi:10.1063/1.330027

Cicchetti R, Divizia M, Valentini F, Argentin G (2011). Effects of single-wall carbon nanotubes in human cells of the oral cavity: geno-cytotoxic risk. *Toxicol In Vitro*, 25(8):1811–9. doi:10.1016/j.tiv.2011.09.017 PMID:21968257

CIIT and RIVM (2006). Multiple-path particle dosimetry (MPPD, version 2.0): a model for human and rat airway particle dosimetry. Research Triangle Park (NC), USA: Centers for Health Research (CIIT) and the Netherlands: National Institute for Public Health and the Environment (RIVM).

Clichici S, Biris AR, Tabaran F, Filip A (2012). Transient oxidative stress and inflammation after intraperitoneal administration of multiwalled carbon nanotubes functionalized with single strand DNA in rats. *Toxicol Appl Pharmacol*, 259(3):281–92. doi:10.1016/j.taap.2012.01.004 PMID:22280989

Clift MJ, Endes C, Vanhecke D, Wick P, Gehr P, Schins RP, et al. (2014). A comparative study of different in vitro lung cell culture systems to assess the most beneficial tool for screening the potential adverse effects of carbon nanotubes. *Toxicol Sci*, 137(1):55–64. doi:10.1093/toxsci/kft216 PMID:24284789

Creighton MA, Rangel-Mendez JR, Huang J, Kane AB, Hurt RH (2013). Graphene-induced adsorptive and optical artifacts during in vitro toxicology assays. *Small*, 9(11):1921–7. doi:10.1002/smll.201202625 PMID:25018686

Crouzier D, Follot S, Gentilhomme E, Flahaut E, Arnaud R, Dabouis V, et al. (2010). Carbon nanotubes induce inflammation but decrease the production of reactive oxygen species in lung. *Toxicology*, 272(1–3):39–45. doi:10.1016/j.tox.2010.04.001 PMID:20381574

Cui D, Tian F, Ozkan CS, Wang M, Gao H (2005). Effect of single wall carbon nanotubes on human HEK293 cells. *Toxicol Lett*, 155(1):73–85. doi:10.1016/j.toxlet.2004.08.015 PMID:15585362

Cveticanin J, Joksic G, Leskovac A, Petrovic S, Sobot AV, Neskovic O (2010). Using carbon nanotubes to induce micronuclei and double strand breaks of the DNA in human cells. *Nanotechnology*, 21(1):015102. doi:10.1088/0957-4484/21/1/015102 PMID:19946169

Czarny B, Georgin D, Berthon F, Plastow G, Pinault M, Patriarche G, et al. (2014). Carbon nanotube translocation to distant organs after pulmonary exposure: insights from in situ (14)C-radiolabeling and tissue radioimaging. *ACS Nano*, 8(6):5715–24. doi:10.1021/nn500475u PMID:24853551

Dahl AR, Schlesinger RB, Heck HD, Medinsky MA, Lucier GW (1991). Comparative dosimetry of inhaled

materials: differences among animal species and extrapolation to man. *Fundam Appl Toxicol*, 16(1):1–13. doi:10.1016/0272-0590(91)90125-N PMID:2019334

Dahm MM, Evans DE, Schubauer-Berigan MK, Birch ME, Deddens JA (2013). Occupational exposure assessment in carbon nanotube and nanofiber primary and secondary manufacturers: mobile direct-reading sampling. *Ann Occup Hyg*, 57(3):328–44. doi:10.1093/annhyg/mes079 PMID:23100605

Dahm MM, Evans DE, Schubauer-Berigan MK, Birch ME, Fernback JE (2012). Occupational exposure assessment in carbon nanotube and nanofiber primary and secondary manufacturers. *Ann Occup Hyg*, 56(5):542–56. PMID:22156567

Dahm MM, Yencken MS, Schubauer-Berigan MK (2011). Exposure control strategies in the carbonaceous nanomaterial industry. *J Occup Environ Med*, 53(6):Suppl: S68–73. doi:10.1097/JOM.0b013e31821b1d3b PMID:21654421

Danish Environment Protection (2014). Danish Mandatory Nano-Register. Available from: https://www.retsinformation.dk/Forms/R0710.aspx?id=163367, accessed 10 January 2014.

Davoren M, Herzog E, Casey A, Cottineau B, Chambers G, Byrne HJ, et al. (2007). In vitro toxicity evaluation of single walled carbon nanotubes on human A549 lung cells. *Toxicol In Vitro*, 21(3):438–48. doi:10.1016/j.tiv.2006.10.007 PMID:17125965

Delogu LG, Stanford SM, Santelli E, Magrini A, Bergamaschi A, Motamedchaboki K, et al. (2010). Carbon nanotube-based nanocarriers: the importance of keeping it clean. *J Nanosci Nanotechnol*, 10(8):5293–301. doi:10.1166/jnn.2010.3083 PMID:21125885

Delogu LG, Venturelli E, Manetti R, Pinna GA, Carru C, Madeddu R, et al. (2012). Ex vivo impact of functionalized carbon nanotubes on human immune cells. *Nanomedicine (Lond)*, 7(2):231–43. doi:10.2217/nnm.11.101 PMID:22106855

Delorme MP, Muro Y, Arai T, Banas DA, Frame SR, Reed KL, et al. (2012). Ninety-day inhalation toxicity study with a vapor grown carbon nanofiber in rats. *Toxicol Sci*, 128(2):449–60. doi:10.1093/toxsci/kfs172 PMID:22581831

Deng X, Jia G, Wang H, Sun H, Wang X, Yang S, et al. (2007). Translocation and fate of multi-walled carbon nanotubes in vivo. *Carbon*, 45(7):1419–24. doi:10.1016/j.carbon.2007.03.035

DGCIS (2012). [Les réalités industrielles dans le domaine des nanomatériaux en France – Analyse de la réalité du poids des nanomatériaux dans la filière industrielle concernée.] Paris, France: Direction générale de la compétitivité, de l'industrie et des services. Available from: http://www.entreprises.gouv.fr/files/files/guides/realites-industrielles-nanomateriaux-france.pdf. [French]

Di Giorgio ML, Di Bucchianico S, Ragnelli AM, Aimola P, Santucci S, Poma A (2011). Effects of single and multi walled carbon nanotubes on macrophages: cyto and genotoxicity and electron microscopy. *Mutat Res*, 722(1):20–31. doi:10.1016/j.mrgentox.2011.02.008 PMID:21382506

Di Sotto A, Chiaretti M, Carru GA, Bellucci S, Mazzanti G (2009). Multi-walled carbon nanotubes: Lack of mutagenic activity in the bacterial reverse mutation assay. *Toxicol Lett*, 184(3):192–7. doi:10.1016/j.toxlet.2008.11.007 PMID:19063954

Ding L, Stilwell J, Zhang T, Elboudwarej O, Jiang H, Selegue JP, et al. (2005). Molecular characterization of the cytotoxic mechanism of multiwall carbon nanotubes and nano-onions on human skin fibroblast. *Nano Lett*, 5(12):2448–64. doi:10.1021/nl051748o PMID:16351195

Dinu CZ, Bale SS, Zhu G, Dordick JS (2009). Tubulin encapsulation of carbon nanotubes into functional hybrid assemblies. *Small*, 5(3):310–5. doi:10.1002/smll.200801434 PMID:19148890

Donaldson K, Aitken R, Tran L, Stone V, Duffin R, Forrest G, et al. (2006). Carbon nanotubes: a review of their properties in relation to pulmonary toxicology and workplace safety. *Toxicol Sci*, 92(1):5–22. doi:10.1093/toxsci/kfj130 PMID:16484287

Donaldson K, Murphy F, Schinwald A, Duffin R, Poland CA (2011). Identifying the pulmonary hazard of high aspect ratio nanoparticles to enable their safety-by-design. *Nanomedicine (Lond)*, 6(1):143–56. doi:10.2217/nnm.10.139 PMID:21182425

Donaldson K, Murphy FA, Duffin R, Poland CA (2010). Asbestos, carbon nanotubes and the pleural mesothelium: a review of the hypothesis regarding the role of long fibre retention in the parietal pleura, inflammation and mesothelioma. *Part Fibre Toxicol*, 7(1):5. doi:10.1186/1743-8977-7-5 PMID:20307263

Dong PX, Wan B, Guo LH (2012). In vitro toxicity of acid-functionalized single-walled carbon nanotubes: effects on murine macrophages and gene expression profiling. *Nanotoxicology*, 6(3):288–303. doi:10.3109/17435390.2011.573101 PMID:21486190

Dutch Social and Economic Council (2012). Provisional nano reference values for engineered nanomaterials. The Hague, the Netherlands: Social Economic Council.

Ebbesen TW, Takada T (1995). Topological and sp³ defect structures in nanotubes. *Carbon*, 33(7):973–8. doi:10.1016/0008-6223(95)00025-9

Elder A, Gelein R, Finkelstein JN, Driscoll KE, Harkema J, Oberdörster G (2005). Effects of subchronically inhaled carbon black in three species. I. Retention kinetics, lung inflammation, and histopathology. *Toxicol Sci*, 88(2):614–29. doi:10.1093/toxsci/kfi327 PMID:16177241

Elgrabli D, Abella-Gallart S, Robidel F, Rogerieux F, Boczkowski J, Lacroix G (2008). Induction of apoptosis and absence of inflammation in rat lung after

intratracheal instillation of multiwalled carbon nanotubes. *Toxicology*, 253(1–3):131–6. doi:10.1016/j.tox.2008.09.004 PMID:18834917

Ellinger-Ziegelbauer H, Pauluhn J (2009). Pulmonary toxicity of multi-walled carbon nanotubes (Baytubes) relative to alpha-quartz following a single 6h inhalation exposure of rats and a 3 months post-exposure period. *Toxicology*, 266(1–3):16–29. doi:10.1016/j.tox.2009.10.007 PMID:19836432

Ema M, Imamura T, Suzuki H, Kobayashi N, Naya M, Nakanishi J (2013b). Genotoxicity evaluation for single-walled carbon nanotubes in a battery of in vitro and in vivo assays. *J Appl Toxicol*, 33(9):933–9. doi:10.1002/jat.2772 PMID:22763644

Ema M, Masumori S, Kobayashi N, Naya M, Endoh S, Maru J, et al. (2013a). In vivo comet assay of multi-walled carbon nanotubes using lung cells of rats intratracheally instilled. *J Appl Toxicol*, 33(10):1053–60. doi:10.1002/jat.2810 PMID:22936419

ENRHES (2009). Engineered nanoparticles – Review of health and environmental safety (ENRHES). ENRHES project. ENRHES. Available from: http://ihcp.jrc.ec.europa.eu/whats-new/enhres-final-report, accessed 30 May 2013.

EPA (1988). Reference physiological parameters in pharmacokinetic modeling. Washington (DC), USA: Office of Health and Environment Assessment, Exposure Assessment Group, United States Environmental Protection Agency. EPA report no. EPA/600/6–88/004.

EPA (2006). Approaches for the application of physiologically based pharmacokinetic (PBPK) models and supporting data in risk assessment. Washington (DC), USA: National Center for Environmental Assessment, Office of Research and Development, United States Environmental Protection Agency. EPA/600/R.05/043F.

EPA (2011). Multi-walled carbon nanotubes: significant new use rule, 40 CFR Parts 9 and 721 [EPA–HQ–OPPT–2009–0686; FRL–8865–4] RIN 2070–AB27. *Fed Regist*, 76(88). Washington (DC), USA: United States Environmental Protection Agency.

EPA (2014). Control of nanoscale materials under the Toxic Substance Control Act. Washington (DC), USA: United States Environmental Protection Agency. Available from: http://www.epa.gov/opptintr/nano/, accessed 9 April 2014.

Erdely A, Dahm M, Chen BT, Zeidler-Erdely PC, Fernback JE, Birch ME, et al. (2013). Carbon nanotube dosimetry: from workplace exposure assessment to inhalation toxicology. *Part Fibre Toxicol*, 10(1):53. doi:10.1186/1743-8977-10-53 PMID:24144386

Erdely A, Hulderman T, Salmen R, Liston A, Zeidler-Erdely PC, Schwegler-Berry D, et al. (2009). Cross-talk between lung and systemic circulation during carbon nanotube respiratory exposure. Potential biomarkers.

Nano Lett, 9(1):36–43. doi:10.1021/nl801828z PMID:19049393

EU Commission (2011). EU Commission recommendation on the definition of nanomaterial (2011/696/EU). Official Journal of the European Union. 20.10.2011: L 275/38–40. Available from: http://eur-lex.europa.eu/legal-content/EN/TXT/PDF/?uri=CELEX:32011H0696&from=EN, accessed 1 October 2014.

European Standards Committee on Oxidative DNA Damage (ESCODD) (2003). Measurement of DNA oxidation in human cells by chromatographic and enzymic methods. *Free Radic Biol Med*, 34(8):1089–99. doi:10.1016/S0891-5849(03)00041-8 PMID:12684094

Evans DE, Turkevich LA, Roettgers CT, Deye GJ, Baron PA (2013). Dustiness of fine and nanoscale powders. *Ann Occup Hyg*, 57(2):261–77. doi:10.1093/annhyg/mes060 PMID:23065675

Fenoglio I, Aldieri E, Gazzano E, Cesano F, Colonna M, Scarano D, et al. (2012). Thickness of multiwalled carbon nanotubes affects their lung toxicity. *Chem Res Toxicol*, 25(1):74–82. doi:10.1021/tx200255h PMID:22128750

Fenoglio I, Greco G, Tomatis M, Muller J, Raymundo-Piñero E, Béguin F, et al. (2008). Structural defects play a major role in the acute lung toxicity of multi-wall carbon nanotubes: physicochemical aspects. *Chem Res Toxicol*, 21(9):1690–7. doi:10.1021/tx800100s PMID:18636755

Fenoglio I, Tomatis M, Lison D, Muller J, Fonseca A, Nagy JB, et al. (2006). Reactivity of carbon nanotubes: free radical generation or scavenging activity? *Free Radic Biol Med*, 40(7):1227–33. doi:10.1016/j.freeradbiomed.2005.11.010 PMID:16545691

Folkmann JK, Risom L, Jacobsen NR, Wallin H, Loft S, Møller P (2009). Oxidatively damaged DNA in rats exposed by oral gavage to C60 fullerenes and single-walled carbon nanotubes. *Environ Health Perspect*, 117(5):703–8. doi:10.1289/ehp.11922 PMID:19479010

Fröhlich E, Meindl C, Höfler A, Leitinger G, Roblegg E (2013). Combination of small size and carboxyl functionalisation causes cytotoxicity of short carbon nanotubes. *Nanotoxicology*, 7(7):1211–24. doi:10.3109/17435390.2012.729274 PMID:22963691

Fubini B, Fenoglio I, Tomatis M, Turci F (2011). Effect of chemical composition and state of the surface on the toxic response to high aspect ratio nanomaterials. *Nanomedicine (Lond)*, 6(5):899–920. doi:10.2217/nnm.11.80 PMID:21793679

Fubini B, Ghiazza M, Fenoglio I (2010). Physico-chemical features of engineered nanoparticles relevant to their toxicity. *Nanotoxicology*, 4(4):347–63. doi:10.3109/17435390.2010.509519 PMID:20858045

Fujita K, Fukuda M, Fukui H, Horie M, Endoh S, Uchida K, et al. (2015). Intratracheal instillation of single-wall carbon nanotubes in the rat lung induces time-dependent changes in gene expression. *Nanotoxicology*,

9(3):290–301. doi:10.3109/17435390.2014.921737 PMID:24911292

Galano A (2010). Carbon nanotubes: promising agents against free radicals. *Nanoscale*, 2(3):373–80. doi:10.1039/b9nr00364a PMID:20644818

Galano A, Francisco-Marquez M, Martinez A (2010). Influence of point defects on the free-radical scavenging capability of single-walled carbon nanotubes. *J Phys Chem C*, 114(18):8302–8. doi:10.1021/jp101544u

Gangwal S, Brown JS, Wang A, Houck KA, Dix DJ, Kavlock RJ, et al. (2011). Informing selection of nanomaterial concentrations for ToxCast in vitro testing based on occupational exposure potential. *Environ Health Perspect*, 119(11):1539–46. doi:10.1289/ehp.1103750 PMID:21788197

Gasser M, Wick P, Clift MJD, Blank F, Diener L, Yan B, et al. (2012). Pulmonary surfactant coating of multi-walled carbon nanotubes (MWCNTs) influences their oxidative and pro-inflammatory potential in vitro. *Part Fibre Toxicol*, 9(1):17. doi:10.1186/1743-8977-9-17 PMID:22624622

Ghiazza M, Vietti G, Fenoglio I (2014). Carbon nanotubes: properties, applications and toxicity. In: Pielichowski K, Zhu H, editors. Health and environmental risks of nanomaterials: Polymer nancomposites and other materials containing nanoparticles Woodhead Publishing Series in Composites Science and Engineering No. 49 Njuguna J. Woodhead Publishing U.K.; Chapter 8, pp. 147–74. doi:10.1533/9780857096678.3.147

Ghosh M, Chakraborty A, Bandyopadhyay M, Mukherjee A (2011). Multi-walled carbon nanotubes (MWCNT): induction of DNA damage in plant and mammalian cells. *J Hazard Mater*, 197:327–36. doi:10.1016/j.jhazmat.2011.09.090 PMID:21999988

Gottschalk F, Kost E, Nowack B (2013). Engineered nanomaterials in water and soils: a risk quantification based on probabilistic exposure and effect modeling. *Environ Toxicol Chem*, 32(6):1278–87. doi:10.1002/etc.2177 PMID:23418073

Gottschalk F, Sonderer T, Scholz RW, Nowack B (2009). Modeled environmental concentrations of engineered nanomaterials (TiO(2), ZnO, Ag, CNT, Fullerenes) for different regions. *Environ Sci Technol*, 43(24):9216–22. doi:10.1021/es9015553 PMID:20000512

Gottschalk F, Sonderer T, Scholz RW, Nowack B (2010). Possibilities and limitations of modeling environmental exposure to engineered nanomaterials by probabilistic material flow analysis. *Environ Toxicol Chem*, 29(5):1036–48. PMID:20821538

Grecco ACP, Paula RFO, Mizutani E, Sartorelli JC, Milani AM, Longhini AL, et al. (2011). Up-regulation of T lymphocyte and antibody production by inflammatory cytokines released by macrophage exposure to multi-walled carbon nanotubes. *Nanotechnology*, 22(26):265103. doi:10.1088/0957-4484/22/26/265103 PMID:21576788

Guo L, Morris DG, Liu X, Vaslet C, Hurt RH, Kane AB (2007). Iron bioavailability and redox activity in diverse carbon nanotube samples. *Chem Mater*, 19(14):3472–8. doi:10.1021/cm062691p

Guo NL, Wan YW, Denvir J, Porter DW, Pacurari M, Wolfarth MG, et al. (2012). Multiwalled carbon nanotube-induced gene signatures in the mouse lung: potential predictive value for human lung cancer risk and prognosis. *J Toxicol Environ Health A*, 75(18):1129–53. doi:10.1080/15287394.2012.699852 PMID:22891886

Guo T, Nikolaev P, Rinzler AG, Tomanek D, Colbert DT, Smalley RE (1995a). Self-assembly of tubular fullerenes. *J Phys Chem B*, 99(27):10694–7. doi:10.1021/j100027a002

Guo T, Nikolaev P, Thess A, Colbert DT, Smalley RE (1995b). Catalytic growth of single-walled carbon nanotubes by laser vaporization. *Chem Phys Lett*, 243(1–2):49–54. doi:10.1016/0009-2614(95)00825-O

Guo YY, Zhang J, Zheng YF, Yang J, Zhu XQ (2011). Cytotoxic and genotoxic effects of multi-wall carbon nanotubes on human umbilical vein endothelial cells in vitro. *Mutat Res*, 721(2):184–91. doi:10.1016/j.mrgentox.2011.01.014 PMID:21296185

Guseva Canu I, Bateson TF, Bouvard V, Debia M, Dion C, Savolainen K, et al. (2016). Human exposure to carbon-based fibrous nanomaterials: A review. *Int J Hyg Environ Health*, 219(2):166–75. doi:10.1016/j.ijheh.2015.12.005 PMID:26752069

Hamad I, Al-Hanbali O, Hunter AC, Rutt KJ, Andresen TL, Moghimi SM (2010). Distinct polymer architecture mediates switching of complement activation pathways at the nanosphere-serum interface: implications for stealth nanoparticle engineering. *ACS Nano*, 4(11):6629–38. doi:10.1021/nn101990a PMID:21028845

Hamilton RF Jr, Buford M, Xiang C, Wu N, Holian A (2012). NLRP3 inflammasome activation in murine alveolar macrophages and related lung pathology is associated with MWCNT nickel contamination. *Inhal Toxicol*, 24(14):995–1008. doi:10.3109/08958378.2012.745633 PMID:23216160

Hamilton RF Jr, Buford MC, Wood MB, Arnone B, Morandi M, Holian A (2007). Engineered carbon nanoparticles alter macrophage immune function and initiate airway hyper-responsiveness in the BALB/c mouse model. *Nanotoxicology*, 1(2):104–17. doi:10.1080/17435390600926939

Hamilton RF Jr, Wu N, Porter D, Buford M, Wolfarth M, Holian A (2009). Particle length-dependent titanium dioxide nanomaterials toxicity and bioactivity. *Part Fibre Toxicol*, 6(1):35. doi:10.1186/1743-8977-6-35 PMID:20043844

Hamilton RF Jr, Wu Z, Mitra S, Shaw PK, Holian A (2013b). Effect of MWCNT size, carboxylation, and purification on in vitro and in vivo toxicity, inflammation and lung pathology. *Part Fibre Toxicol*, 10(1):57. doi:10.1186/1743-8977-10-57 PMID:24225053

Hamilton RF Jr, Xiang C, Li M, Ka I, Yang F, Ma D, et al. (2013a). Purification and sidewall functionalization of multiwalled carbon nanotubes and resulting bioactivity in two macrophage models. *Inhal Toxicol*, 25(4):199–210. doi:10.3109/08958378.2013.775197 PMID:23480196

Han JH, Lee EJ, Lee JH, So KP, Lee YH, Bae GN, et al. (2008). Monitoring multiwalled carbon nanotube exposure in carbon nanotube research facility. *Inhal Toxicol*, 20(8):741–9. doi:10.1080/08958370801942238 PMID:18569096

Han SG, Andrews R, Gairola CG (2010). Acute pulmonary response of mice to multi-wall carbon nanotubes. *Inhal Toxicol*, 22(4):340–7. doi:10.3109/08958370903359984 PMID:20064106

Han YG, Xu J, Li ZG, Ren GG, Yang Z (2012). In vitro toxicity of multi-walled carbon nanotubes in C6 rat glioma cells. *Neurotoxicology*, 33(5):1128–34. doi:10.1016/j.neuro.2012.06.004 PMID:22728153

Haniu H, Matsuda Y, Takeuchi K, Kim YA, Hayashi T, Endo M (2010). Proteomics-based safety evaluation of multi-walled carbon nanotubes. *Toxicol Appl Pharmacol*, 242(3):256–62. doi:10.1016/j.taap.2009.10.015 PMID:19874835

Haniu H, Saito N, Matsuda Y, Kim YA, Park KC, Tsukahara T, et al. (2011). Elucidation mechanism of different biological responses to multi-walled carbon nanotubes using four cell lines. *Int J Nanomedicine*, 6:3487–97. doi:10.2147/IJN.S26689 PMID:22267932

Hedmer M, Isaxon C, Nilsson PT, Ludvigsson L, Messing ME, Genberg J, et al. (2014). Exposure and emission measurements during production, purification, and functionalization of arc-discharge-produced multi-walled carbon nanotubes. *Ann Occup Hyg*, 58(3):355–79. doi:10.1093/annhyg/met072 PMID:24389082

Hedmer M, Kåredal M, Gustavsson P, Rissler J (2013). 148 Carbon nanotubes. Report - The Nordic Expert Group for Criteria Documentation of Health Risks of Chemicals. Arbete och hälsa. 47(5):1-252. Available from: https://gupea.ub.gu.se/bitstream/2077/34499/1/gupea_2077_34499_1.pdf.

Hirano S, Fujitani Y, Furuyama A, Kanno S (2010). Uptake and cytotoxic effects of multi-walled carbon nanotubes in human bronchial epithelial cells. *Toxicol Appl Pharmacol*, 249(1):8–15. doi:10.1016/j.taap.2010.08.019 PMID:20800606

Hirano S, Kanno S, Furuyama A (2008). Multi-walled carbon nanotubes injure the plasma membrane of macrophages. *Toxicol Appl Pharmacol*, 232(2):244–51. doi:10.1016/j.taap.2008.06.016 PMID:18655803

Hirsch A, Vostronowsky O (2005). Functionalization of carbon nanotubes. In: Schluter AD, editor. Functional molecular nanostructures. Topics in current chemistry. Volume 245. Berlin, Heidelberg: Springer-Verlag; pp. 193–237.

Hitoshi K, Katoh M, Suzuki T, Ando Y, Nadai M (2012). Single-walled carbon nanotubes downregulate stress-responsive genes in human respiratory tract cells. *Biol Pharm Bull*, 35(4):455–63. doi:10.1248/bpb.35.455 PMID:22466547

Honnert B, Grzebyk M (2014). Manufactured nano-objects: an occupational survey in five industries in France. *Ann Occup Hyg*, 58(1):121–35. doi:10.1093/annhyg/met058 PMID:24142930

Horie M, Kato H, Iwahashi H (2013). Cellular effects of manufactured nanoparticles: effect of adsorption ability of nanoparticles. *Arch Toxicol*, 87(5):771–81. doi:10.1007/s00204-013-1033-5 PMID:23503611

Hou P-X, Xu S-T, Ying Z, Yang Q-H, Liu C, Cheng H-M (2003). Hydrogen adsorption/desorption behavior of multi-walled carbon nanotubes with different diameters. *Carbon*, 41(13):2471–6. doi:10.1016/S0008-6223(03)00271-9

Hu H, Zhao B, Itkis ME, Haddon RC (2003). Nitric acid purification of single-walled carbon nanotubes *J Phys Chem B*, 107(50):13838–42. doi:10.1021/jp035719i

Huang X, Zhang F, Sun X, Choi KY, Niu G, Zhang G, et al. (2014). The genotype-dependent influence of functionalized multiwalled carbon nanotubes on fetal development. *Biomaterials*, 35(2):856–65. doi:10.1016/j.biomaterials.2013.10.027 PMID:24344357

Huizar I, Malur A, Patel J, McPeek M, Dobbs L, Wingard C, et al. (2013). The role of PPARγ in carbon nanotube-elicited granulomatous lung inflammation. *Respir Res*, 14(1):7. doi:10.1186/1465-9921-14-7 PMID:23343389

Hussain F, Hojjati M, Okomoto M, Gorga RE (2006). Review article: Polymer-matrix nanocomposites, processing, manufacturing, and applications: An overview. *J Compos Mater*, 40(17):1511–75. doi:10.1177/0021998306067321

IARC (2012). Arsenic, metals, fibres, and dusts. *IARC Monogr Eval Carcinog Risks Hum*, 100C:1–499. Available from: http://monographs.iarc.fr/ENG/Monographs/vol100C/index.php. PMID:23189751

ICRP (International Commission on Radiological Protection) (1994). Human respiratory tract model for radiological protection. *Annals of the ICRP, Publication 66*. Tarrytown (NY), USA: Elsevier Science Ltd.

Iijima S (1991). Helical microtubules of graphite carbon. *Nature*, 354(6348):56–8. doi:10.1038/354056a0

Iijima S, Brabec C, Maiti A, Bernholc C (1996). Structural flexibility of carbon nanotubes. *J Chem Phys*, 104(5):2089–92. doi:10.1063/1.470966

Ingle T, Dervishi E, Biris AR, Mustafa T, Buchanan RA, Biris AS (2013). Raman spectroscopy analysis and mapping the biodistribution of inhaled carbon nanotubes in the lungs and blood of mice. *J Appl Toxicol*, 33(10):1044–52. doi:10.1002/jat.2796 PMID:23047664

Inoue K, Koike E, Yanagisawa R, Hirano S, Nishikawa M, Takano H (2009). Effects of multi-walled carbon nanotubes on a murine allergic airway inflammation model.

Toxicol Appl Pharmacol, 237(3):306–16. doi:10.1016/j. taap.2009.04.003 PMID:19371758

Inoue K, Yanagisawa R, Koike E, Nishikawa M, Takano H (2010). Repeated pulmonary exposure to single-walled carbon nanotubes exacerbates allergic inflammation of the airway: Possible role of oxidative stress. *Free Radic Biol Med*, 48(7):924–34. doi:10.1016/j. freeradbiomed.2010.01.013 PMID:20093178

Ishigami M, Choi HJ, Aloni S, Louie SG, Cohen ML, Zettl A (2004). Identifying defects in nanoscale materials. *Phys Rev Lett*, 93(19):196803. doi:10.1103/ PhysRevLett.93.196803 PMID:15600863

ISO (2008). ISO/TS 27687. Nanotechnologies – Terminology and definitions for nano-objects — Nanoparticle, nano-fibre and nanoplate. Geneva, Switzerland: International Organization for Standardization.

ISO (2010a). ISO/TS 80004–1. Nanotechnologies – Vocabulary Part 1: Core terms. Geneva, Switzerland: International Organization for Standardization.

ISO (2010b). ISO/TS 80004–3. Nanotechnologies – Vocabulary Part 3: Carbon nano-objects. Geneva, Switzerland: International Organization for Standardization.

ISO (2010c). ISO/TS 10867. Nanotechnologies – Characterization of single-wall carbon nanotubes using near infrared photoluminescence spectroscopy. Geneva, Switzerland: International Organization for Standardization.

ISO (2010d). ISO/TS 11251. Nanotechnologies – Characterization of volatile components in single-wall carbon nanotube samples using evolved gas analysis/gas chromatograph-mass spectrometry. Geneva, Switzerland: International Organization for Standardization.

ISO (2010e). ISO 29701. Nanotechnologies – Endotoxin test on nanomaterial samples in vitro systems-Liumulus amebocyte lysis (LAL) test. Geneva, Switzerland: International Organization for Standardization.

ISO (2011a). ISO/TS 10798. Nanotechnologies – Characterization of single-wall carbon nanotubes using scanning electron microscopy and energy dispersive X-ray spectrometry analysis. Geneva, Switzerland: International Organization for Standardization.

ISO (2011b). ISO/TS 11308. Nanotechnologies – Characterization of single-wall carbon nanotubes using thermogravimetric analysis. Geneva, Switzerland: International Organization for Standardization.

ISO (2012a). ISO/TR 13014. Nanotechnologies – Guidance on physico-chemical characterization of engineered nanoscale materials for toxicologic assessment. Geneva, Switzerland: International Organization for Standardization.

ISO (2012b). ISO/TS 10797. Nanotechnologies – Characterization of single-wall carbon nanotubes using transmission electron microscopy. Geneva,

Switzerland: International Organization for Standardization.

IUPAC (2014). Compendium of Chemical Terminology – Gold book. 1622 pp. Research Triangle Park (NC), USA: International Union of Pure and Applied Chemistry. Available from: http://goldbook.iupac.org/ PDF/goldbook.pdf.

Jacobsen NR, Møller P, Jensen KA, Vogel U, Ladefoged O, Loft S, et al. (2009). Lung inflammation and genotoxicity following pulmonary exposure to nanoparticles in ApoE−/− mice. *Part Fibre Toxicol*, 6(1):2. doi:10.1186/1743-8977-6-2 PMID:19138394

Jacobsen NR, Pojana G, White P, Møller P, Cohn CA, Korsholm KS, et al. (2008). Genotoxicity, cytotoxicity, and reactive oxygen species induced by single-walled carbon nanotubes and C(60) fullerenes in the FE1-Mutatrade markMouse lung epithelial cells. *Environ Mol Mutagen*, 49(6):476–87. doi:10.1002/ em.20406 PMID:18618583

Jain S, Thakare VS, Das M, Godugu C, Jain AK, Mathur R, et al. (2011). Toxicity of multiwalled carbon nanotubes with end defects critically depends on their functionalization density. *Chem Res Toxicol*, 24(11):2028–39. doi:10.1021/tx2003728 PMID:21978239

Jaurand MCF, Renier A, Daubriac J (2009). Mesothelioma: Do asbestos and carbon nanotubes pose the same health risk? *Part Fibre Toxicol*, 6(1):16. doi:10.1186/1743-8977-6-16 PMID:19523217

Ji JH, Woo D, Lee SB, Kim T, Kim D, Kim JH, et al. (2013). Detection and characterization of nanomaterials released in low concentrations during multi-walled carbon nanotube spraying process in a cleanroom. *Inhal Toxicol*, 25(14):759–65. doi:10.3109/08958378.20 13.846951 PMID:24304302

Jin H, Heller DA, Sharma R, Strano MS (2009). Size-dependent cellular uptake and expulsion of single-walled carbon nanotubes: single particle tracking and a generic uptake model for nanoparticles. *ACS Nano*, 3(1):149–58. doi:10.1021/nn800532m PMID:19206261

Johnson DR, Methner MM, Kennedy AJ, Steevens JA (2010). Potential for occupational exposure to engineered carbon-based nanomaterials in environmental laboratory studies. *Environ Health Perspect*, 118(1):49–54. PMID:20056572

Johnston HJ, Hutchison GR, Christensen FM, Peters S, Hankin S, Aschberger K, et al. (2010). A critical review of the biological mechanisms underlying the in vivo and in vitro toxicity of carbon nanotubes: The contribution of physico-chemical characteristics. *Nanotoxicology*, 4(2):207–46. doi:10.3109/17435390903569639 PMID:20795897

Jorio A, Saito R, Hafner JH, Lieber CM, Hunter M, McClure T, et al. (2001). Structural (n, m) determination of isolated single-wall carbon nanotubes by resonant Raman scattering. *Phys Rev Lett*, 86(6):1118–21. doi:10.1103/PhysRevLett.86.1118 PMID:11178024

Journal Officiel (2012). [Décret No 2012_232 du 17 février 2012 relatif à la déclaration annuelle des substances à l'état nanoparticulaire pris en application de l'article L. 523–4 du code de l'environnement.] Paris, France: Journal officiel de la République Française. [French]

Ju L, Zhang G, Zhang X, Jia Z, Gao X, Jiang Y, et al. (2014). Proteomic analysis of cellular response induced by multi-walled carbon nanotubes exposure in A549 cells. *PLoS One*, 9(1):e84974. doi:10.1371/journal.pone.0084974 PMID:24454774

Kagan VE, Konduru NV, Feng W, Allen BL, Conroy J, Volkov Y, et al. (2010). Carbon nanotubes degraded by neutrophil myeloperoxidase induce less pulmonary inflammation. *Nat Nanotechnol*, 5(5):354–9. doi:10.1038/nnano.2010.44 PMID:20364135

Kagan VE, Tyurina YY, Tyurin VA, Konduru NV, Potapovich AI, Osipov AN, et al. (2006). Direct and indirect effects of single walled carbon nanotubes on RAW 264.7 macrophages: role of iron. *Toxicol Lett*, 165(1):88–100. doi:10.1016/j.toxlet.2006.02.001 PMID:16527436

Kam NW, O'Connell M, Wisdom JA, Dai H (2005). Carbon nanotubes as multifunctional biological transporters and near-infrared agents for selective cancer cell destruction. *Proc Natl Acad Sci USA*, 102(33):11600–5. doi:10.1073/pnas.0502680102 PMID:16087878

Kanno S, Hirano S, Chiba S, Takeshita H, Nagai T, Takada M, et al. (2014). The role of Rho-kinases in IL-1β release through phagocytosis of fibrous particles in human monocytes *Arch Toxicol.* PMID:24760326

Karajanagi SS, Vertegel AA, Kane RS, Dordick JS (2004). Structure and function of enzymes adsorbed onto single-walled carbon nanotubes. *Langmuir*, 20(26):11594–9. doi:10.1021/la047994h PMID:15595788

Karlsson HL, Cronholm P, Gustafsson J, Möller L (2008). Copper oxide nanoparticles are highly toxic: a comparison between metal oxide nanoparticles and carbon nanotubes. *Chem Res Toxicol*, 21(9):1726–32. doi:10.1021/tx800064j PMID:18710264

Karthikeyan S, Mahalingam P, Karthik M (2009). Large scale synthesis of carbon nanotubes. *E-J Chem*, 6(1):1–12. doi:10.1155/2009/756410

Kasai T, Umeda Y, Ohnishi M, Kondo H, Takeuchi T, Aiso S, et al. (2015). Thirteen-week study of toxicity of fiber-like multi-walled carbon nanotubes with whole-body inhalation exposure in rats. *Nanotoxicology*, 9(4):413–22. doi:10.3109/17435390.2014.933903 PMID:25030099

Kato T, Totsuka Y, Ishino K, Matsumoto Y, Tada Y, Nakae D, et al. (2013). Genotoxicity of multi-walled carbon nanotubes in both in vitro and in vivo assay systems. *Nanotoxicology*, 7(4):452–61. doi:10.3109/17435390.2012.674571 PMID:22397533

Katwa P, Wang X, Urankar RN, Podila R, Hilderbrand SC, Fick RB, et al. (2012). A carbon nanotube toxicity paradigm driven by mast cells and the IL-$_{33}$/ST$_2$ axis.

Small, 8(18):2904–12. doi:10.1002/smll.201200873 PMID:22777948

Kermanizadeh A, Gaiser BK, Hutchison GR, Stone V (2012). An in vitro liver model–assessing oxidative stress and genotoxicity following exposure of hepatocytes to a panel of engineered nanomaterials. *Part Fibre Toxicol*, 9(1):28. doi:10.1186/1743-8977-9-28 PMID:22812506

Kermanizadeh A, Vranic S, Boland S, Moreau K, Baeza-Squiban A, Gaiser BK, et al. (2013). An in vitro assessment of panel of engineered nanomaterials using a human renal cell line: cytotoxicity, pro-inflammatory response, oxidative stress and genotoxicity. *BMC Nephrol*, 14(1):96. doi:10.1186/1471-2369-14-96 PMID:23617532

Kim JE, Lim HT, Minai-Tehrani A, Kwon JT, Shin JY, Woo CG, et al. (2010). Toxicity and clearance of intratracheally administered multiwalled carbon nanotubes from murine lung. *J Toxicol Environ Health A*, 73(21–22):1530–43. doi:10.1080/15287394.2010.511578 PMID:20954079

Kim JS, Lee K, Lee YH, Cho HS, Kim KH, Choi KH, et al. (2011). Aspect ratio has no effect on genotoxicity of multi-wall carbon nanotubes. *Arch Toxicol*, 85(7):775–86. doi:10.1007/s00204-010-0574-0 PMID:20617304

Kim JS, Song KS, Lee JK, Choi YC, Bang IS, Kang CS, et al. (2012b). Toxicogenomic comparison of multi-wall carbon nanotubes (MWCNTs) and asbestos. *Arch Toxicol*, 86(4):553–62. doi:10.1007/s00204-011-0770-6 PMID:22076105

Kim JS, Sung JH, Choi BG, Ryu HY, Song KS, Shin JH, et al. (2014). In vivo genotoxicity evaluation of lung cells from Fischer 344 rats following 28 days of inhalation exposure to MWCNTs, plus 28 days and 90 days post-exposure. *Inhal Toxicol*, 26(4):222–34. doi:10.3109/08958378.2013.878006 PMID:24568578

Kim JS, Sung JH, Song KS, Lee JH, Kim SM, Lee GH, et al. (2012a). Persistent DNA damage measured by comet assay of Sprague Dawley rat lung cells after five days of inhalation exposure and 1 month post-exposure to dispersed multi-wall carbon nanotubes (MWCNTs) generated by new MWCNT aerosol generation system. *Toxicol Sci*, 128(2):439–48. doi:10.1093/toxsci/kfs161 PMID:22543278

Kim JS, Yu IJ (2014). Single-wall carbon nanotubes (SWCNT) induce cytotoxicity and genotoxicity produced by reactive oxygen species (ROS) generation in phytohemagglutinin (PHA)-stimulated male human peripheral blood lymphocytes. *J Toxicol Environ Health A*, 77(19):1141–53. doi:10.1080/15287394.2014.917062 PMID:25119736

Kim YA, Hayashi T, Endo M, Dresselhaus MS (2013). 7. Carbon Nanofibers. In: Vajtai R editor. *Springer handbook of nanomaterials.* doi:10.1007/978-3-642-20595-8_7

Kisin ER, Murray AR, Keane MJ, Shi XC, Schwegler-Berry D, Gorelik O, et al. (2007). Single-walled carbon nanotubes: geno- and cytotoxic effects in lung fibroblast V79 cells. *J Toxicol Environ Health A*, 70(24):2071–9. doi:10.1080/15287390701601251 PMID:18049996

Kisin ER, Murray AR, Sargent L, Lowry D, Chirila M, Siegrist KJ, et al. (2011). Genotoxicity of carbon nanofibers: are they potentially more or less dangerous than carbon nanotubes or asbestos? *Toxicol Appl Pharmacol*, 252(1):1–10. doi:10.1016/j.taap.2011.02.001 PMID:21310169

Kitiyanan B, Alvarez WE, Harwell JH, Resasco DE (2000). Controlled production of single-wall carbon nanotubes by catalytic decomposition of CO on bimetallic Co-Mo catalysts. *Chem Phys Lett*, 317(3–5):497–503. doi:10.1016/S0009-2614(99)01379-2

Kobayashi N, Naya M, Ema M, Endoh S, Maru J, Mizuno K, et al. (2010). Biological response and morphological assessment of individually dispersed multi-wall carbon nanotubes in the lung after intratracheal instillation in rats. *Toxicology*, 276(3):143–53. doi:10.1016/j.tox.2010.07.021 PMID:20696199

Kobayashi N, Naya M, Mizuno K, Yamamoto K, Ema M, Nakanishi J (2011). Pulmonary and systemic responses of highly pure and well-dispersed single-wall carbon nanotubes after intratracheal instillation in rats. *Inhal Toxicol*, 23(13):814–28. doi:10.3109/08958378.2011.614968 PMID:22004357

Köhler AR, Som C, Helland A, Gottschalk F (2008). Studying the potential release of carbon nanotubes throughout the application life cycle. *J Clean Prod*, 16(8–9):927–37. doi:10.1016/j.jclepro.2007.04.007

Kolosnjaj-Tabi J, Hartman KB, Boudjemaa S, Ananta JS, Morgant G, Szwarc H, et al. (2010). In vivo behavior of large doses of ultrashort and full-length single-walled carbon nanotubes after oral and intraperitoneal administration to Swiss mice. *ACS Nano*, 4(3):1481–92. doi:10.1021/nn901573w PMID:20175510

Kostarelos K, Bianco A, Prato M (2009). Promises, facts and challenges for carbon nanotubes in imaging and therapeutics. *Nat Nanotechnol*, 4(10):627–33. doi:10.1038/nnano.2009.241 PMID:19809452

Ku BK, Maynard AD, Baron OA, Deye GJ (2007). Observation and measurement of anomalous responses in a differential mobility analyser caused by ultrafine fibrous carbon aerosols. *J Electrost*, 65(8):542–8. doi:10.1016/j.elstat.2006.10.012

Kumar M, Ando Y (2010). Chemical vapor deposition of carbon nanotubes: a review on growth mechanism and mass production. *J Nanosci Nanotechnol*, 10(6):3739–58. doi:10.1166/jnn.2010.2939 PMID:20355365

Kunzmann A, Andersson B, Thurnherr T, Krug H, Scheynius A, Fadeel B (2011). Toxicology of engineered nanomaterials: focus on biocompatibility, biodistribution and biodegradation. *Biochim Biophys Acta*, 1810(3):361–73. doi:10.1016/j.bbagen.2010.04.007 PMID:20435096

Lacerda L, Ali-Boucetta H, Herrero MA, Pastorin G, Bianco A, Prato M, et al. (2008b). Tissue histology and physiology following intravenous administration of different types of functionalized multiwalled carbon nanotubes. *Nanomedicine (Lond)*, 3(2):149–61. doi:10.2217/17435889.3.2.149 PMID:18373422

Lacerda L, Herrero MA, Venner K, Bianco A, Prato M, Kostarelos K (2008c). Carbon-nanotube shape and individualization critical for renal excretion. *Small*, 4(8):1130–2. doi:10.1002/smll.200800323 PMID:18666166

Lacerda L, Soundararajan A, Singh R, Pastorin G, Al-Jamal KT, Turton J, et al. (2008a). Dynamic imaging of functionalized multi-walled carbon nanotube systemic circulation and urinary excretion. *Adv Mater*, 20(2):225–30. doi:10.1002/adma.200702334

Lam CW, James JT, McCluskey R, Arepalli S, Hunter RL (2006). A review of carbon nanotube toxicity and assessment of potential occupational and environmental health risks. *Crit Rev Toxicol*, 36(3):189–217. doi:10.1080/10408440600570233 PMID:16686422

Lam CW, James JT, McCluskey R, Hunter RL (2004). Pulmonary toxicity of single-wall carbon nanotubes in mice 7 and 90 days after intratracheal instillation. *Toxicol Sci*, 77(1):126–34. doi:10.1093/toxsci/kfg243 PMID:14514958

Lee JH, Lee SB, Bae GN, Jeon KS, Yoon JU, Ji JH, et al. (2010). Exposure assessment of carbon nanotube manufacturing workplaces. *Inhal Toxicol*, 22(5):369–81. doi:10.3109/08958370903367359 PMID:20121582

Lee JH, Sohn EK, Ahn JS, Ahn K, Kim KS, Lee JH, et al. (2013). Exposure assessment of workers in printed electronics workplace. *Inhal Toxicol*, 25(8):426–34. doi:10.3109/08958378.2013.800617 PMID:23808635

Lee JK, Sayers BC, Chun KS, Lao HC, Shipley-Phillips JK, Bonner JC, et al. (2012). Multi-walled carbon nanotubes induce COX-2 and iNOS expression via MAP kinase-dependent and -independent mechanisms in mouse RAW264.7 macrophages. *Part Fibre Toxicol*, 9(1):14. doi:10.1186/1743-8977-9-14 PMID:22571318

Li J, Li L, Chen H, Chang Q, Liu X, Wu Y, et al. (2014). Application of vitamin E to antagonize SWCNTs-induced exacerbation of allergic asthma. *Sci Rep*, 4:4275. PMID:24589727

Li JG, Li WX, Xu JY, Cai XQ, Liu RL, Li YJ, et al. (2007a). Comparative study of pathological lesions induced by multiwalled carbon nanotubes in lungs of mice by intratracheal instillation and inhalation. *Environ Toxicol*, 22(4):415–21. doi:10.1002/tox.20270 PMID:17607736

Li R, Wang X, Ji Z, Sun B, Zhang H, Chang CH, et al. (2013). Surface charge and cellular processing of covalently functionalized multiwall carbon nanotubes

determine pulmonary toxicity. *ACS Nano*, 7(3):2352–68. doi:10.1021/nn305567s PMID:23414138

Li X, Peng Y, Qu X (2006). Carbon nanotubes selective destabilization of duplex and triplex DNA and inducing B-A transition in solution. *Nucleic Acids Res*, 34(13):3670–6. doi:10.1093/nar/gkl513 PMID:16885240

Li Z, Hulderman T, Salmen R, Chapman R, Leonard SS, Young SH, et al. (2007b). Cardiovascular effects of pulmonary exposure to single-wall carbon nanotubes. *Environ Health Perspect*, 115(3):377–82. doi:10.1289/ehp.9688 PMID:17431486

Liao HY, Chung YT, Lai CH, Lin MH, Liou SH (2014b). Sneezing and allergic dermatitis were increased in engineered nanomaterial handling workers. *Ind Health*, 52(3):199–215. doi:10.2486/indhealth.2013-0100 PMID:24492762

Liao HY, Chung YT, Lai CH, Wang SL, Chiang HC, Li LA, et al. (2014a). Six-month follow-up study of health markers of nanomaterials among workers handling engineered nanomaterials. *Nanotoxicology*, 8(S1):Suppl 1: 100–10. doi:10.3109/17435390.2013.858793 PMID:24295335

Lindberg HK, Falck GC, Singh R, Suhonen S, Järventaus H, Vanhala E, et al. (2013). Genotoxicity of short single-wall and multi-wall carbon nanotubes in human bronchial epithelial and mesothelial cells in vitro. *Toxicology*, 313(1):24–37. doi:10.1016/j.tox.2012.12.008 PMID:23266321

Lindberg HK, Falck GC, Suhonen S, Vippola M, Vanhala E, Catalán J, et al. (2009). Genotoxicity of nanomaterials: DNA damage and micronuclei induced by carbon nanotubes and graphite nanofibres in human bronchial epithelial cells in vitro. *Toxicol Lett*, 186(3):166–73. doi:10.1016/j.toxlet.2008.11.019 PMID:19114091

Ling WL, Biro A, Bally I, Tacnet P, Deniaud A, Doris E, et al. (2011). Proteins of the innate immune system crystallize on carbon nanotubes but are not activated. *ACS Nano*, 5(2):730–7. doi:10.1021/nn102400w PMID:21214219

Liou SH, Tsou TC, Wang SL, Li LA, Chiang HC, Li WF, et al. (2012). Epidemiological study of health hazards among workers handling engineered nanomaterials. *J Nanopart Res*, 14(8):878. doi:10.1007/s11051-012-0878-5

Lioy PJ, Lippmann M, Phalen RF (1984). Rationale for particle size-selective air sampling. In Particle size-selective sampling in the workplace: report of the ACGIH Technical Committee on Air Sampling Procedures *Ann Am Conf Ind Hyg*, 11:27–34.

Lison D, Muller J (2008). Lung and systemic responses to carbon nanotubes (CNT) in mice. *Toxicol Sci*, 101(1):179–80, author reply 181–2. doi:10.1093/toxsci/kfm249 PMID:17897971

Liu HL, Zhang YL, Yang N, Zhang YX, Liu XQ, Li CG, et al. (2011). A functionalized single-walled carbon nanotube-induced autophagic cell death in human lung cells

through Akt-TSC2-mTOR signalling. *Cell Death Dis*, 2(5):e159. doi:10.1038/cddis.2011.27 PMID:21593791

Liu X, Guo L, Morris D, Kane AB, Hurt RH (2008b). Targeted removal of bioavailable metal as a detoxification strategy for carbon nanotubes. *Carbon N Y*, 46(3):489–500. doi:10.1016/j.carbon.2007.12.018 PMID:19255622

Liu X, Hurt RH, Kane AB (2010). Biodurability of single-walled carbon nanotubes depends on surface functionalization. *Carbon N Y*, 48(7):1961–9. doi:10.1016/j.carbon.2010.02.002 PMID:20352066

Liu X, Sen S, Liu J, Kulaots I, Geohegan D, Kane A, et al. (2011b). Antioxidant deactivation on graphenic nanocarbon surfaces. *Small*, 7(19):2775–85. doi:10.1002/smll.201100651 PMID:21818846

Liu X, Tao H, Yang K, Zhang S, Lee S-T, Liu Z (2011a). Optimization of surface chemistry on single-walled carbon nanotubes for in vivo photothermal ablation of tumors. *Biomaterials*, 32(1):144–51. doi:10.1016/j.biomaterials.2010.08.096 PMID:20888630

Liu Z, Davis C, Cai W, He L, Chen X, Dai H (2008a). Circulation and long-term fate of functionalized, biocompatible single-walled carbon nanotubes in mice probed by Raman spectroscopy. *Proc Natl Acad Sci USA*, 105(5):1410–5. doi:10.1073/pnas.0707654105 PMID:18230737

Lohcharoenkal W, Wang L, Stueckle TA, Park J, Tse W, Dinu CZ, et al. (2014). Role of H-Ras/ERK signalling in carbon nanotube-induced neoplastic-like transformation of human mesothelial cells. *Front Physiol*, 5:222. doi:10.3389/fphys.2014.00222 PMID:24971065

Lu X, Chen Z (2005). Curved pi-conjugation, aromaticity, and the related chemistry of small fullerenes (< C60) and single-walled carbon nanotubes. *Chem Rev*, 105(10):3643–96. doi:10.1021/cr030093d PMID:16218563

Lucente-Schultz RM, Moore VC, Leonard AD, Price BK, Kosynkin DV, Lu M, et al. (2009). Antioxidant single-walled carbon nanotubes. *J Am Chem Soc*, 131(11):3934–41. doi:10.1021/ja805721p PMID:19243186

Ma-Hock L, Treumann S, Strauss V, Brill S, Luizi F, Mertler M, et al. (2009). Inhalation toxicity of multi-wall carbon nanotubes in rats exposed for 3 months. *Toxicol Sci*, 112(2):468–81. doi:10.1093/toxsci/kfp146 PMID:19584127

Mahar B, Laslau C, Yip R, Sun Y (2007). Development of carbon nanotube-based sensors – A rview. *IEEE Sens J*, 7(2):266–84. doi:10.1109/JSEN.2006.886863

Manshian BB, Jenkins GJS, Williams PM, Wright C, Barron AR, Brown AP, et al. (2013). Single-walled carbon nanotubes: differential genotoxic potential associated with physico-chemical properties. *Nanotoxicology*, 7(2):144–56. doi:10.3109/17435390.2011.647928 PMID:22263934

Matthews IP, Gregory CJ, Aljayyoussi G, Morris CJ, McDonald I, Hoogendoorn B, et al. (2013). Maximal

extent of translocation of single-walled carbon nanotubes from lung airways of the rat. *Environ Toxicol Pharmacol*, 35(3):461–4. doi:10.1016/j.etap.2013.02.002 PMID:23501606

Maynard AD, Baron PA, Foley M, Shvedova AA, Kisin ER, Castranova V (2004). Exposure to carbon nanotube material: aerosol release during the handling of unrefined single-walled carbon nanotube material. *J Toxicol Environ Health A*, 67(1):87–107. doi:10.1080/15287390490253688 PMID:14668113

Maynard AD, Ku BK, Emery M, Stolzenburg M, McMurry PH (2007). Measuring particle size-dependent physicochemical structure in airborne single walled carbon nanotube agglomerates. *J Nanopart Res*, 9(1):85–92. doi:10.1007/s11051-006-9178-2

McDonald J, Mitchell L (2008). Lung and systemic responses to carbon nanotubes (CNT) in mice. *Toxicol Sci*, 101(1):181–2. doi:10.1093/toxsci/kfm250 PMID:18281258

McShan D, Yu H (2014). DNA damage in human skin keratinocytes caused by multiwalled carbon nanotubes with carboxylate functionalization. *Toxicol Ind Health*, 30(6):489–98. doi:10.1177/0748233712459914 PMID:23012341

Mercer RR, Hubbs AF, Scabilloni JF, Wang L, Battelli LA, Friend S, et al. (2011). Pulmonary fibrotic response to aspiration of multi-walled carbon nanotubes. *Part Fibre Toxicol*, 8(1):21. doi:10.1186/1743-8977-8-21 PMID:21781304

Mercer RR, Hubbs AF, Scabilloni JF, Wang L, Battelli LA, Schwegler-Berry D, et al. (2010). Distribution and persistence of pleural penetrations by multi-walled carbon nanotubes. *Part Fibre Toxicol*, 7(1):28. doi:10.1186/1743-8977-7-28 PMID:20920331

Mercer RR, Scabilloni J, Wang L, Kisin E, Murray AR, Schwegler-Berry D, et al. (2008). Alteration of deposition pattern and pulmonary response as a result of improved dispersion of aspirated single-walled carbon nanotubes in a mouse model. *Am J Physiol Lung Cell Mol Physiol*, 294(1):L87–97. doi:10.1152/ajplung.00186.2007 PMID:18024722

Mercer RR, Scabilloni JF, Hubbs AF, Battelli LA, McKinney W, Friend S, et al. (2013b). Distribution and fibrotic response following inhalation exposure to multi-walled carbon nanotubes. *Part Fibre Toxicol*, 10(1):33. doi:10.1186/1743-8977-10-33 PMID:23895460

Mercer RR, Scabilloni JF, Hubbs AF, Wang L, Battelli LA, McKinney W, et al. (2013a). Extrapulmonary transport of MWCNT following inhalation exposure. *Part Fibre Toxicol*, 10(1):38. doi:10.1186/1743-8977-10-38 PMID:23927530

Methner M, Beaucham C, Crawford C, Hodson L, Geraci C (2012). Field application of the Nanoparticle Emission Assessment Technique (NEAT): task-based air monitoring during the processing of engineered nanomaterials (ENM) at four facilities. *J Occup Environ Hyg*, 9(9):543–55. doi:10.1080/15459624.2012.699388 PMID:22816668

Methner M, Hodson L, Dames A, Geraci C (2010). Nanoparticle Emission Assessment Technique (NEAT) for the identification and measurement of potential inhalation exposure to engineered nanomaterials–Part B: Results from 12 field studies. *J Occup Environ Hyg*, 7(3):163–76. doi:10.1080/15459620903508066 PMID:20063229

Meunier E, Coste A, Olagnier D, Authier H, Lefèvre L, Dardenne C, et al. (2012). Double-walled carbon nanotubes trigger IL-1β release in human monocytes through Nlrp3 inflammasome activation. *Nanomedicine*, 8(6):987–95. doi:10.1016/j.nano.2011.11.004 PMID:22100755

Migliore L, Saracino D, Bonelli A, Colognato R, D'Errico MR, Magrini A, et al. (2010). Carbon nanotubes induce oxidative DNA damage in RAW 264.7 cells. *Environ Mol Mutagen*, 51(4):294–303. PMID:20091701

Mitchell LA, Gao J, Wal RV, Gigliotti A, Burchiel SW, McDonald JD (2007). Pulmonary and systemic immune response to inhaled multiwalled carbon nanotubes. *Toxicol Sci*, 100(1):203–14. doi:10.1093/toxsci/kfm196 PMID:17660506

Mitchell LA, Lauer FT, Burchiel SW, McDonald JD (2009). Mechanisms for how inhaled multiwalled carbon nanotubes suppress systemic immune function in mice. *Nat Nanotechnol*, 4(7):451–6. doi:10.1038/nnano.2009.151 PMID:19581899

Mizutani N, Nabe T, Yoshino S (2012). Exposure to multi-walled carbon nanotubes and allergen promotes early- and late-phase increases in airway resistance in mice. *Biol Pharm Bull*, 35(12):2133–40. doi:10.1248/bpb.b12-00357 PMID:23207765

Moghimi SM, Andersen AJ, Hashemi SH, Lettiero B, Ahmadvand D, Hunter AC, et al. (2010). Complement activation cascade triggered by PEG-PL engineered nanomedicines and carbon nanotubes: the challenges ahead. *J Control Release*, 146(2):175–81. doi:10.1016/j.jconrel.2010.04.003 PMID:20388529

Mohiuddin , Keka IS, Evans TJ, Hirota K, Shimizu H, Kono K, et al. (2014). A novel genotoxicity assay of carbon nanotubes using functional macrophage receptor with collagenous structure (MARCO)-expressing chicken B lymphocytes. *Arch Toxicol*, 88(1):145–60. doi:10.1007/s00204-013-1084-7 PMID:23963510

Monteiro-Riviere NA, Inman AO, Zhang LW (2009). Limitations and relative utility of screening assays to assess engineered nanoparticle toxicity in a human cell line. *Toxicol Appl Pharmacol*, 234(2):222–35. doi:10.1016/j.taap.2008.09.030 PMID:18983864

Morimoto Y, Hirohashi M, Horie M, Ogami A, Oyabu T, Myojo T, et al. (2012c). Pulmonary toxicity of well-dispersed single-wall carbon nanotubes following intratracheal instillation. *J Nano Res*, 18–19:9–25. doi:10.4028/www.scientific.net/JNanoR.18-19.9

Morimoto Y, Hirohashi M, Kobayashi N, Ogami A, Horie M, Oyabu T, et al. (2012a). Pulmonary toxicity of well-dispersed single-wall carbon nanotubes after inhalation. *Nanotoxicology*, 6(7):766–75. doi:10.3109/17435390.2011.620719 PMID:21942532

Morimoto Y, Hirohashi M, Ogami A, Oyabu T, Myojo T, Todoroki M, et al. (2012b). Pulmonary toxicity of well-dispersed multi-wall carbon nanotubes following inhalation and intratracheal instillation. *Nanotoxicology*, 6(6):587–99. doi:10.3109/17435390.2011.594912 PMID:21714591

Morimoto Y, Izumi H, Kuroda E (2014). Significance of persistent inflammation in respiratory disorders induced by nanoparticles. *J Immunol Res*, 2014(962871):962871. PMID:25097864

Morrow PE (1988). Possible mechanisms to explain dust overloading of the lungs. *Fundam Appl Toxicol*, 10(3):369–84. doi:10.1016/0272-0590(88)90284-9 PMID:3286345

Morrow PE (1994). Mechanisms and significance of "particle overload". In: Toxic and Carcinogenic Effects of Solid Particles in the Respiratory Tract. Proceedings of the 4th International Inhalation Symposium, March 1993, Hanover, Germany, pp. 17–25. Washington (DC), USA: International Life Sciences Institute Press.

Movia D, Prina-Mello A, Bazou D, Volkov Y, Giordani S (2011). Screening the cytotoxicity of single-walled carbon nanotubes using novel 3D tissue-mimetic models. *ACS Nano*, 5(11):9278–90. doi:10.1021/nn203659m PMID:22017733

Muller J, Decordier I, Hoet PH, Lombaert N, Thomassen L, Huaux F, et al. (2008b). Clastogenic and aneugenic effects of multi-wall carbon nanotubes in epithelial cells. *Carcinogenesis*, 29(2):427–33. doi:10.1093/carcin/bgm243 PMID:18174261

Muller J, Delos M, Panin N, Rabolli V, Huaux F, Lison D (2009). Absence of carcinogenic response to multiwall carbon nanotubes in a 2-year bioassay in the peritoneal cavity of the rat. *Toxicol Sci*, 110(2):442–8. doi:10.1093/toxsci/kfp100 PMID:19429663

Muller J, Huaux F, Fonseca A, Nagy JB, Moreau N, Delos M, et al. (2008a). Structural defects play a major role in the acute lung toxicity of multiwall carbon nanotubes: toxicological aspects. *Chem Res Toxicol*, 21(9):1698–705. doi:10.1021/tx800101p PMID:18636756

Muller J, Huaux F, Moreau N, Misson P, Heilier JF, Delos M, et al. (2005). Respiratory toxicity of multi-wall carbon nanotubes. *Toxicol Appl Pharmacol*, 207(3):221–31. doi:10.1016/j.taap.2005.01.008 PMID:16129115

Müller L, Riediker M, Wick P, Mohr M, Gehr P, Rothen-Rutishauser B (2010). Oxidative stress and inflammation response after nanoparticle exposure: differences between human lung cell monocultures and an advanced three-dimensional model of the human epithelial airways. *J R Soc Interface*, 7:Suppl 1: S27–40. doi:10.1098/rsif.2009.0161.focus PMID:19586954

Murphy FA, Poland CA, Duffin R, Al-Jamal KT, Ali-Boucetta H, Nunes A, et al. (2011). Length-dependent retention of carbon nanotubes in the pleural space of mice initiates sustained inflammation and progressive fibrosis on the parietal pleura. *Am J Pathol*, 178(6):2587–600. doi:10.1016/j.ajpath.2011.02.040 PMID:21641383

Murphy FA, Schinwald A, Poland CA, Donaldson K (2012). The mechanism of pleural inflammation by long carbon nanotubes: interaction of long fibres with macrophages stimulates them to amplify pro-inflammatory responses in mesothelial cells. *Part Fibre Toxicol*, 9(1):8. doi:10.1186/1743-8977-9-8 PMID:22472194

Murr LE, Bang JJ, Esquivel EV, Guerrero PA, Lopez A (2004b). Carbon nanotubes, nano-crystal forms, and complex nanoparticle aggregates in common fuel-gas combustion sources and the ambient air. *J Nanopart Res*, 6(2/3):241–51. doi:10.1023/B:NANO.0000034651.91325.40

Murr LE, Esquivel EV, Bang JJ, de la Rosa G, Gardea-Torresdey JL (2004a). Chemistry and nanoparticulate compositions of a 10,000 year-old ice core melt water. *Water Res*, 38(19):4282–96. doi:10.1016/j.watres.2004.08.010 PMID:15491674

Murr LE, Guerrero PA (2006). Carbon nanotubes in wood soot *Atmosph Sci Lett*, 793–95.

Murr LE, Soto KF (2005). A TEM study of soot, carbon nanotubes, and related fullerene nanopolyhedra in common fuel-gas combustion sources. *Mater Charact*, 55(1):50–65. doi:10.1016/j.matchar.2005.02.008

Murr LE, Soto KF, Garza KM, Guerrero PA, Martinez F, Esquivel EV, et al. (2006). Combustion-generated nanoparticulates in the El Paso, TX, USA / Juarez, Mexico Metroplex: their comparative characterization and potential for adverse health effects. *Int J Environ Res Public Health*, 3(1):48–66. doi:10.3390/ijerph2006030007 PMID:16823077

Murray AR, Kisin E, Leonard SS, Young SH, Kommineni C, Kagan VE, et al. (2009). Oxidative stress and inflammatory response in dermal toxicity of single-walled carbon nanotubes. *Toxicology*, 257(3):161–71. doi:10.1016/j.tox.2008.12.023 PMID:19150385

Murray AR, Kisin ER, Tkach AV, Yanamala N, Mercer R, Young SH, et al. (2012). Factoring-in agglomeration of carbon nanotubes and nanofibers for better prediction of their toxicity versus asbestos. *Part Fibre Toxicol*, 9(1):10. doi:10.1186/1743-8977-9-10 PMID:22490147

Nagai H, Okazaki Y, Chew SH, Misawa N, Miyata Y, Shinohara H, et al. (2013). Intraperitoneal administration of tangled multiwalled carbon nanotubes of 15 nm in diameter does not induce mesothelial carcinogenesis in rats. *Pathol Int*, 63(9):457–62. doi:10.1111/pin.12093 PMID:24200157

Nagai H, Okazaki Y, Chew SH, Misawa N, Yamashita Y, Akatsuka S, et al. (2011). Diameter and rigidity of multiwalled carbon nanotubes are critical factors in

mesothelial injury and carcinogenesis. *Proc Natl Acad Sci USA*, 108(49):E1330–8. doi:10.1073/pnas.1110013108 PMID:22084097

Nanocyl (2009). Responsible care and nanomaterials case study Nanocyl. Presentation at European Responsible Care Conference, 21–23 October 2009, Prague, Czech Republic. Brussels, Belgium: The European Chemical Industry Council (CEFIC). Available from: http://www.cefic.org/Documents/ResponsibleCare/04_Nanocyl.pdf.

Naya M, Kobayashi N, Endoh S, Maru J, Honda K, Ema M, et al. (2012). In vivo genotoxicity study of single-wall carbon nanotubes using comet assay following intratracheal instillation in rats. *Regul Toxicol Pharmacol*, 64(1):124–9. doi:10.1016/j.yrtph.2012.05.020 PMID:22735368

Naya M, Kobayashi N, Mizuno K, Matsumoto K, Ema M, Nakanishi J (2011). Evaluation of the genotoxic potential of single-wall carbon nanotubes by using a battery of in vitro and in vivo genotoxicity assays. *Regul Toxicol Pharmacol*, 61(2):192–8. doi:10.1016/j.yrtph.2011.07.008 PMID:21821090

NIOSH (1994a). NIOSH Manual of Analytical Methods. 4th Edition, Method No. 7402. Cincinnati (OH), USA: United States Department of Health and Human Services, Public Health Service, Centers for Disease Control and Prevention, National Institute for Occupational Safety and Health.

NIOSH (1994b). NIOSH Manual of Analytical Methods. 4th Edition, Method No. 0500. Cincinnati (OH), USA: United States Department of Health and Human Services, Public Health Service, Centers for Disease Control and Prevention, National Institute for Occupational Safety and Health.

NIOSH (1999). NIOSH Manual of Analytical Methods. 4th Edition, Method No. 5040. Cincinnati (OH), USA: United States Department of Health and Human Services, Public Health Service, Centers for Disease Control and Prevention, National Institute for Occupational Safety and Health.

NIOSH (2003a). NIOSH Manual of Analytical Methods. 4th Edition, Method No. 7300. Cincinnati (OH), USA: United States Department of Health and Human Services, Public Health Service, Centers for Disease Control and Prevention, National Institute for Occupational Safety and Health.

NIOSH (2003b). NIOSH Manual of Analytical Methods. 4th Edition, Method No. 7303. Cincinnati (OH), USA: United States Department of Health and Human Services, Public Health Service, Centers for Disease Control and Prevention, National Institute for Occupational Safety and Health.

NIOSH (2003c). NIOSH Manual of Analytical Methods. 4th Edition, Method No. 7404. Cincinnati (OH), USA: United States Department of Health and Human Services, Public Health Service, Centers for Disease Control and Prevention, National Institute for Occupational Safety and Health.

NIOSH (2013). Current Intelligence Bulletin 65: Occupational Exposure to Carbon Nanotubes and Nanofibers. Publication No. 2013–145. Cincinnati (OH), USA: United States Department of Health and Human Services, Public Health Service, Centers for Disease Control and Prevention, National Institute for Occupational Safety and Health. Available from: http://www.cdc.gov/niosh/review/peer/HISA/nano-pr.html.

Nowack B, David RM, Fissan H, Morris H, Shatkin JA, Stintz M, et al. (2013). Potential release scenarios for carbon nanotubes used in composites. *Environ Int*, 59:1–11. doi:10.1016/j.envint.2013.04.003 PMID:23708563

NSTC (2011). The First Nanosafety Management Master Plan (2012–2016), National Science and Technology Commission. [in Korean]. Seoul, Republic of Korea: National Science and Technology Commission. Available from: http://www.nnpc.re.kr/knowledge/nano_policy/19/view?p_page=1&p_pagesize=10&o_field=&o_direction=&s_t_type=&s_keyword=&s_category, accessed 23 January 2016.

Nygaard UC, Hansen JS, Samuelsen M, Alberg T, Marioara CD, Løvik M (2009). Single-walled and multi-walled carbon nanotubes promote allergic immune responses in mice. *Toxicol Sci*, 109(1):113–23. doi:10.1093/toxsci/kfp057 PMID:19293371

Nymark P, Jensen KA, Suhonen S, Kembouche Y, Vippola M, Kleinjans J, et al. (2014). Free radical scavenging and formation by multi-walled carbon nanotubes in cell free conditions and in human bronchial epithelial cells. *Part Fibre Toxicol*, 11(1):4. doi:10.1186/1743-8977-11-4 PMID:24438343

Oberdörster G (1995). Lung particle overload: implications for occupational exposures to particles. *Regul Toxicol Pharmacol*, 21(1):123–35. doi:10.1006/rtph.1995.1017 PMID:7784625

Oberdörster G (2012). Nanotoxicology: in vitro-in vivo dosimetry. *Environ Health Perspect*, 120(1):A13–, author reply A13. doi:10.1289/ehp.1104320 PMID:22214547

Oberdörster G, Kane AB, Klaper RD, Hurt RH (2013). Nanotoxicology. In: Casarett and Doull's toxicology. Columbus (OH), USA: McGraw-Hill Companies, Inc.

Observatory Nano (2011). Briefing No. 23: Transport — Nanotechnology in automotive tyres. European Commission. Available from: http://nanopinion.eu/sites/default/files/briefing_no.23_nanotechnology_in_automotive_tyres.pdf.

OECD (2009a). Series on the safety of manufactured nanomaterials, preliminary analysis of exposure measurement and exposure mitigation in occupational settings: manufactured nanomaterials. Paris, France: Organisation for Economic Co-operation and Development (OECD).

OECD (2009b). Emission assessment for identification of sources and release of airborne manufactured

nanomaterials in the workplace: compilation of existing guidance. Paris, France: Organisation for Economic Co-operation and Development.

OECD (2009c). Identification, compilation and analysis of guidance information for exposure measurement and exposure mitigation: manufactured nanomaterials. Paris, France: Organisation for Economic Co-operation and Development.

OECD (2009d). Report of an OECD Workshop on Exposure Assessment and Exposure Mitigation: Manufactured Nanomaterials. Paris, France: Organisation for Economic Co-operation and Development.

OECD (2010). Compilation and Comparison of Guidelines Related to Exposure to Nanomaterials in Laboratories. Paris, France: Organisation for Economic Co-operation and Development.

Ogasawara Y, Umezu N, Ishii K (2012). [DNA damage in human pleural mesothelial cells induced by exposure to carbon nanotubes] *Nippon Eiseigaku Zasshi*, 67(1):76–83. doi:10.1265/jjh.67.76 PMID:22449827

Ogura I, Kotake M, Hashimoto N, Gotoh K, Kishimoto A (2013b). Release characteristics of single-wall carbon nanotubes during manufacturing and handling. *J Phys Conf Ser*, 429:012057. doi:10.1088/1742-6596/429/1/012057

Ogura I, Kotake M, Shigeta M, Uejima M, Saito K, Hashimoto N, et al. (2013a). Potential release of carbon nanotubes from their composites during grinding. *J Phys Conf Ser*, 429:012049. doi:10.1088/1742-6596/429/1/012049

Ono-Ogasawara M, Myojo T (2013). Characteristics of multi-walled carbon nanotubes and background aerosols by carbon analysis; particle size and oxidation temperature. *Adv Powder Technol*, 24(1):263–9. doi:10.1016/j.apt.2012.06.013

OSHA (2013). Fact Sheet: Working Safely with Nanomaterials. Washington (DC), USA: Occupational Safety and Health Administration, United States Department of Labor. Available from: https://www.osha.gov/Publications/OSHA_FS-3634.pdf, accessed 9 September 2014.

Oyabu T, Myojo T, Morimoto Y, Ogami A, Hirohashi M, Yamamoto M, et al. (2011). Biopersistence of inhaled MWCNT in rat lungs in a 4-week well-characterized exposure. *Inhal Toxicol*, 23(13):784–91. doi:10.3109/08958378.2011.608096 PMID:22035120

Pacurari M, Qian Y, Porter DW, Wolfarth M, Wan Y, Luo D, et al. (2011). Multi-walled carbon nanotube-induced gene expression in the mouse lung: association with lung pathology. *Toxicol Appl Pharmacol*, 255(1):18–31. doi:10.1016/j.taap.2011.05.012 PMID:21624382

Pacurari M, Yin XJ, Ding M, Leonard SS, Schwegler-berry D, Ducatman BS, et al. (2008a). Oxidative and molecular interactions of multi-wall carbon nanotubes (MWCNT) in normal and malignant human mesothelial cells. *Nanotoxicology*, 2(3):155–70. doi:10.1080/17435390802318356

Pacurari M, Yin XJ, Zhao J, Ding M, Leonard SS, Schwegler-Berry D, et al. (2008b). Raw single-wall carbon nanotubes induce oxidative stress and activate MAPKs, AP-1, NF-kappaB, and Akt in normal and malignant human mesothelial cells. *Environ Health Perspect*, 116(9):1211–7. doi:10.1289/ehp.10924 PMID:18795165

Paik SY, Zalk DM, Swuste P (2008). Application of a pilot control banding tool for risk level assessment and control of nanoparticle exposures. *Ann Occup Hyg*, 52(6):419–28. doi:10.1093/annhyg/men041 PMID:18632731

Palomäki J, Karisola P, Pylkkänen L, Savolainen K, Alenius H (2010). Engineered nanomaterials cause cytotoxicity and activation on mouse antigen presenting cells. *Toxicology*, 267(1–3):125–31. doi:10.1016/j.tox.2009.10.034 PMID:19897006

Palomäki J, Välimäki E, Sund J, Vippola M, Clausen PA, Jensen KA, et al. (2011). Long, needle-like carbon nanotubes and asbestos activate the NLRP3 inflammasome through a similar mechanism. *ACS Nano*, 5(9):6861–70. doi:10.1021/nn200595c PMID:21800904

Pantarotto D, Singh R, McCarthy D, Erhardt M, Briand JP, Prato M, et al. (2004). Functionalized carbon nanotubes for plasmid DNA gene delivery. *Angew Chem Int Ed Engl*, 43(39):5242–6. doi:10.1002/anie.200460437 PMID:15455428

Park EJ, Cho WS, Jeong J, Yi J, Choi K, Park K (2009). Pro-inflammatory and potential allergic responses resulting from B cell activation in mice treated with multi-walled carbon nanotubes by intratracheal instillation. *Toxicology*, 259(3):113–21. doi:10.1016/j.tox.2009.02.009 PMID:19428951

Park EJ, Roh J, Kim SN, Kang MS, Han YA, Kim Y, et al. (2011b). A single intratracheal instillation of single-walled carbon nanotubes induced early lung fibrosis and subchronic tissue damage in mice. *Arch Toxicol*, 85(9):1121–31. doi:10.1007/s00204-011-0655-8 PMID:21472445

Park EJ, Roh J, Kim SN, Kang MS, Lee BS, Kim Y, et al. (2011a). Biological toxicity and inflammatory response of semi-single-walled carbon nanotubes. *PLoS One*, 6(10):e25892. doi:10.1371/journal.pone.0025892 PMID:22016783

Park EJ, Roh J, Kim SN, Kim Y, Han SB, Hong JT (2013). CCR5 plays an important role in resolving an inflammatory response to single-walled carbon nanotubes. *J Appl Toxicol*, 33(8):845–53. doi:10.1002/jat.2744 PMID:22438032

Patel HJ, Kwon S (2013). Length-dependent effect of single-walled carbon nanotube exposure in a dynamic cell growth environment of human alveolar epithelial cells. *J Expo Sci Environ Epidemiol*, 23(1):101–8. doi:10.1038/jes.2012.75 PMID:22854519

Patlolla AK, Hussain SM, Schlager JJ, Patlolla S, Tchounwou PB (2010). Comparative study of the clastogenicity of functionalized and nonfunctionalized

multiwalled carbon nanotubes in bone marrow cells of Swiss-Webster mice. *Environ Toxicol*, 25(6):608–21. doi:10.1002/tox.20621 PMID:20549644

Pauluhn J (2010a). Multi-walled carbon nanotubes (Baytubes): approach for derivation of occupational exposure limit. *Regul Toxicol Pharmacol*, 57(1):78–89. doi:10.1016/j.yrtph.2009.12.012 PMID:20074606

Pauluhn J (2010b). Subchronic 13-week inhalation exposure of rats to multiwalled carbon nanotubes: toxic effects are determined by density of agglomerate structures, not fibrillar structures. *Toxicol Sci*, 113(1):226–42. doi:10.1093/toxsci/kfp247 PMID:19822600

Pelka J, Gehrke H, Rechel A, Kappes M, Hennrich F, Hartinger CG, et al. (2013). DNA damaging properties of single walled carbon nanotubes in human colon carcinoma cells. *Nanotoxicology*, 7(1):2–20. doi:10.3109/17435390.2011.626536 PMID:22007624

Petersen EJ, Zhang L, Mattison NT, O'Carroll DM, Whelton AJ, Uddin N, et al. (2011). Potential release pathways, environmental fate, and ecological risks of carbon nanotubes. *Environ Sci Technol*, 45(23):9837–56. doi:10.1021/es201579y PMID:21988187

Pfuhler S, Elespuru R, Aardema MJ, Doak SH, Maria Donner E, Honma M, et al. (2013). Genotoxicity of nanomaterials: refining strategies and tests for hazard identification. *Environ Mol Mutagen*, 54(4):229–39. doi:10.1002/em.21770 PMID:23519787

Piccinno F, Gottschalk F, Seeger S, Nowack B (2012). Industrial production quantities and uses of ten engineered nanomaterials in Europe and in the world. *J Nanopart Res*, 14(9):1109. doi:10.1007/s11051-012-1109-9

Pichardo S, Gutiérrez-Praena D, Puerto M, Sánchez E, Grilo A, Cameán AM, et al. (2012). Oxidative stress responses to carboxylic acid functionalized single wall carbon nanotubes on the human intestinal cell line Caco-2. *Toxicol In Vitro*, 26(5):672–7. doi:10.1016/j.tiv.2012.03.007 PMID:22449549

Pietroiusti A, Massimiani M, Fenoglio I, Colonna M, Valentini F, Palleschi G, et al. (2011). Low doses of pristine and oxidized single-wall carbon nanotubes affect mammalian embryonic development. *ACS Nano*, 5(6):4624–33. doi:10.1021/nn200372g PMID:21615177

Poland CA, Duffin R, Kinloch I, Maynard A, Wallace WAH, Seaton A, et al. (2008). Carbon nanotubes introduced into the abdominal cavity of mice show asbestos-like pathogenicity in a pilot study. *Nat Nanotechnol*, 3(7):423–8. doi:10.1038/nnano.2008.111 PMID:18654567

Pop E, Mann D, Wang Q, Goodson K, Dai H (2006). Thermal conductance of an individual single-wall carbon nanotube above room temperature. *Nano Lett*, 6(1):96–100. doi:10.1021/nl052145f PMID:16402794

Popov VN (2004). Carbon nanotubes: properties and applications. *Mater Sci Eng Rep*, 43(3):61–102. doi:10.1016/j.mser.2003.10.001

Porter DW, Hubbs AF, Chen BT, McKinney W, Mercer RR, Wolfarth MG, et al. (2013). Acute pulmonary dose-responses to inhaled multi-walled carbon nanotubes. *Nanotoxicology*, 7(7):1179–94. doi:10.3109/17435390.2012.719649 PMID:22881873

Porter DW, Hubbs AF, Mercer RR, Wu N, Wolfarth MG, Sriram K, et al. (2010). Mouse pulmonary dose- and time course-responses induced by exposure to multi-walled carbon nanotubes. *Toxicology*, 269(2–3):136–47. doi:10.1016/j.tox.2009.10.017 PMID:19857541

Prencipe G, Tabakman SM, Welsher K, Liu Z, Goodwin AP, Zhang L, et al. (2009). PEG branched polymer for functionalization of nanomaterials with ultralong blood circulation. *J Am Chem Soc*, 131(13):4783–7. doi:10.1021/ja809086q PMID:19173646

Pulskamp K, Diabaté S, Krug HF (2007). Carbon nanotubes show no sign of acute toxicity but induce intracellular reactive oxygen species in dependence on contaminants. *Toxicol Lett*, 168(1):58–74. doi:10.1016/j.toxlet.2006.11.001 PMID:17141434

Raabe OG, Al-Bayati MA, Teague SV, Rasolt A (1988). Regional deposition of inhaled monodisperse coarse and fine aerosol particles in small laboratory animals. *Ann Occup Hyg*, 32: inhaled particles VI: 53–63. doi:10.1093/annhyg/32.inhaled_particles_VI.53

Rama Narsimha Reddy A, Narsimha Reddy Y, Himabindu V, Rama Krishna D (2011). Induction of oxidative stress and cytotoxicity by carbon nanomaterials is dependent on physical properties. *Toxicol Ind Health*, 27(1):3–10. doi:10.1177/0748233710377780 PMID:20639279

Ravichandran P, Baluchamy S, Gopikrishnan R, Biradar S, Ramesh V, Goornavar V, et al. (2011). Pulmonary biocompatibility assessment of inhaled single-wall and multiwall carbon nanotubes in BALB/c mice. *J Biol Chem*, 286(34):29725–33. doi:10.1074/jbc.M111.251884 PMID:21705330

Ravichandran P, Baluchamy S, Sadanandan B, Gopikrishnan R, Biradar S, Ramesh V, et al. (2010). Multiwalled carbon nanotubes activate NF-κB and AP-1 signalling pathways to induce apoptosis in rat lung epithelial cells. *Apoptosis*, 15(12):1507–16. doi:10.1007/s10495-010-0532-6 PMID:20694747

Reddy AR, Rao MV, Krishna DR, Himabindu V, Reddy YN (2011). Evaluation of oxidative stress and anti-oxidant status in rat serum following exposure of carbon nanotubes. *Regul Toxicol Pharmacol*, 59(2):251–7. doi:10.1016/j.yrtph.2010.10.007 PMID:20955749

Reddy AR, Reddy YN, Krishna DR, Himabindu V (2010b). Multi wall carbon nanotubes induce oxidative stress and cytotoxicity in human embryonic kidney (HEK293) cells. *Toxicology*, 272(1-3):11–6. doi:10.1016/j.tox.2010.03.017 PMID:20371264

Reddy ARN, Krishna DR, Reddy YN, Himabindu V (2010a). Translocation and extra pulmonary toxicities of multi wall carbon nanotubes in rats. *Toxicol Mech*

Methods, 20(5):267–72. doi:10.3109/15376516.2010.484 077 PMID:20482408

Rinzler AG, Liu J, Dai H, Nikolaev P, Huffman CB, Rodriguez-Macias FJ, et al. (1998). Large-scale purification of single-wall carbon nanotubes: process, product, and characterization. *Appl Phys, A Mater Sci Process*, 67(1):29–37. doi:10.1007/s003390050734

Roda E, Coccini T, Acerbi D, Barni S, Vaccarone R, Manzo L (2011). Comparative pulmonary toxicity assessment of pristine and functionalized multi-walled carbon nanotubes intratracheally instilled in rats: morphohistochemical evaluations. *Histol Histopathol*, 26(3):357–67. PMID:21210349

Romero G, Rojas E, Estrela-Lopis I, Donath E, Moya SE (2011). Spontaneous confocal Raman microscopy–a tool to study the uptake of nanoparticles and carbon nanotubes into cells. *Nanoscale Res Lett*, 6(1):429. doi:10.1186/1556-276X-6-429 PMID:21711493

Ronzani C, Casset A, Pons F (2014). Exposure to multi-walled carbon nanotubes results in aggravation of airway inflammation and remodeling and in increased production of epithelium-derived innate cytokines in a mouse model of asthma. *Arch Toxicol*, 88(2):489–99. doi:10.1007/s00204-013-1116-3 PMID:23948970

Ruoff RS, Thersoff J, Lorents DC, Subramoney S, Chan B (1993). Radial deformation of carbon nanotubes by van-der-Waals forces. *Nature*, 364(6437):514–6. doi:10.1038/364514a0

Ryman-Rasmussen JP, Cesta MF, Brody AR, Shipley-Phillips JK, Everitt JI, Tewksbury EW, et al. (2009a). Inhaled carbon nanotubes reach the subpleural tissue in mice. *Nat Nanotechnol*, 4(11):747–51. doi:10.1038/nnano.2009.305 PMID:19893520

Ryman-Rasmussen JP, Tewksbury EW, Moss OR, Cesta MF, Wong BA, Bonner JC (2009b). Inhaled multiwalled carbon nanotubes potentiate airway fibrosis in murine allergic asthma. *Am J Respir Cell Mol Biol*, 40(3):349–58. doi:10.1165/rcmb.2008-0276OC PMID:18787175

Safe Work Australia (2010). Human health hazard assessment and classification of carbon nanotubes. Canberra, Australia: Safe Work Australia.

Sager TM, Wolfarth MW, Andrew M, Hubbs A, Friend S, Chen TH, et al. (2014). Effect of multi-walled carbon nanotube surface modification on bioactivity in the C57BL/6 mouse model. *Nanotoxicology*, 8(3):317–27. doi:10.3109/17435390.2013.779757 PMID:23432020

Sager TM, Wolfarth MW, Battelli LA, Leonard SS, Andrew M, Steinbach T, et al. (2013). Investigation of the pulmonary bioactivity of double-walled carbon nanotubes. *J Toxicol Environ Health A*, 76(15):922–36. doi:10.1080/15287394.2013.825571 PMID:24156695

Saito S, Zettl A (2008). Carbon nanotubes: Quantum cylinders and graphene. In: Burstein E, Cohen ML, Mills DL, Stiles PJ editors. Series: Contemporary concepts of condensed matter science. Volume 3: Oxford, United Kingdom: Elsevier; pp. 1–215.

Sakamoto Y, Nakae D, Fukumori N, Tayama K, Maekawa A, Imai K, et al. (2009). Induction of mesothelioma by a single intrascrotal administration of multi-wall carbon nanotube in intact male Fischer 344 rats. *J Toxicol Sci*, 34(1):65–76. doi:10.2131/jts.34.65 PMID:19182436

Sanchez VC, Pietruska JR, Miselis NR, Hurt RH, Kane AB (2009). Biopersistence and potential adverse health impacts of fibrous nanomaterials: what have we learned from asbestos? *Wiley Interdiscip Rev Nanomed Nanobiotechnol*, 1(5):511–29. doi:10.1002/wnan.41 PMID:20049814

Sanchez VC, Weston P, Yan A, Hurt RH, Kane AB (2011). A 3-dimensional in vitro model of epithelioid granulomas induced by high aspect ratio nanomaterials. *Part Fibre Toxicol*, 8(1):17. doi:10.1186/1743-8977-8-17 PMID:21592387

Sargent LM, Hubbs AF, Young SH, Kashon ML, Dinu CZ, Salisbury JL, et al. (2012a). Single-walled carbon nanotube-induced mitotic disruption. *Mutat Res*, 745(1–2):28–37. doi:10.1016/j.mrgentox.2011.11.017 PMID:22178868

Sargent LM, Porter DW, Staska LM, Hubbs AF, Lowry DT, Battelli L, et al. (2014). Promotion of lung adenocarcinoma following inhalation exposure to multi-walled carbon nanotubes. *Part Fibre Toxicol*, 11(1):3 doi:10.1186/1743-8977-11-3 PMID:24405760

Sargent LM, Reynolds SH, Lowry D, Kashon ML, Benkovic SA, Salisbury JL, et al. (2012b). Abstract 5464. Genotoxicity of multi-walled carbon nanotubes at occupationally relevant doses *Cancer Res*, 72(8):Suppl 1. doi:10.1158/1538-7445.AM2012-5464

Sargent LM, Shvedova AA, Hubbs AF, Salisbury JL, Benkovic SA, Kashon ML, et al. (2009). Induction of aneuploidy by single-walled carbon nanotubes. *Environ Mol Mutagen*, 50(8):708–17. doi:10.1002/em.20529 PMID:19774611

Sarkar S, Sharma C, Yog R, Periakaruppan A, Jejelowo O, Thomas R, et al. (2007). Analysis of stress responsive genes induced by single-walled carbon nanotubes in BJ Foreskin cells. *J Nanosci Nanotechnol*, 7(2):584–92. PMID:17450800

Sato Y, Yokoyama A, Shibata K, Akimoto Y, Ogino S, Nodasaka Y, et al. (2005). Influence of length on cytotoxicity of multi-walled carbon nanotubes against human acute monocytic leukemia cell line THP-1 in vitro and subcutaneous tissue of rats in vivo. *Mol Biosyst*, 1(2):176–82. doi:10.1039/b502429c PMID:16880981

Sayers BC, Taylor AJ, Glista-Baker EE, Shipley-Phillips JK, Dackor RT, Edin ML, et al. (2013). Role of cyclooxygenase-2 in exacerbation of allergen-induced airway remodeling by multiwalled carbon nanotubes. *Am J Respir Cell Mol Biol*, 49(4):525–35. doi:10.1165/rcmb.2013-0019OC PMID:23642096

Schinwald A, Murphy FA, Prina-Mello A, Poland CA, Byrne F, Movia D, et al. (2012). The threshold length for fiber-induced acute pleural inflammation: shedding

light on the early events in asbestos-induced mesothelioma. *Toxicol Sci*, 128(2):461–70. doi:10.1093/toxsci/kfs171 PMID:22584686

Schlesinger RB (1995). Interaction of gaseous and particulate pollutants in the respiratory tract: mechanisms and modulators. *Toxicology*, 105(2–3):315–25. doi:10.1016/0300-483X(95)03228-8 PMID:8571368

Schneider T, Jansson A, Alstrup JK, Kristjanson V, Luotamo M, Nygren O, et al. (2007). Evaluation and control of occupational health risks from nanoparticles. TemaNord: 581. Copenhagen, Denmark: Nordic Council of Ministers. 10.6027/tn2007-581 doi:10.6027/tn2007-581

Sharma CS, Sarkar S, Periyakaruppan A, Barr J, Wise K, Thomas R, et al. (2007). Single-walled carbon nanotubes induces oxidative stress in rat lung epithelial cells. *J Nanosci Nanotechnol*, 7(7):2466–72. doi:10.1166/jnn.2007.431 PMID:17663266

Shimizu K, Uchiyama A, Yamashita M, Hirose A, Nishimura T, Oku N (2013). Biomembrane damage caused by exposure to multi-walled carbon nanotubes. *J Toxicol Sci*, 38(1):7–12. doi:10.2131/jts.38.7 PMID:23358135

Shvedova AA, Castranova V, Kisin ER, Schwegler-Berry D, Murray AR, Gandelsman VZ, et al. (2003). Exposure to carbon nanotube material: assessment of nanotube cytotoxicity using human keratinocyte cells. *J Toxicol Environ Health A*, 66(20):1909–26. doi:10.1080/713853956 PMID:14514433

Shvedova AA, Kapralov AA, Feng WH, Kisin ER, Murray AR, Mercer RR, et al. (2012a). Impaired clearance and enhanced pulmonary inflammatory/fibrotic response to carbon nanotubes in myeloperoxidase-deficient mice. *PLoS One*, 7(3):e30923. doi:10.1371/journal.pone.0030923 PMID:22479306

Shvedova AA, Kisin E, Murray AR, Johnson VJ, Gorelik O, Arepalli S, et al. (2008). Inhalation vs. aspiration of single-walled carbon nanotubes in C57BL/6 mice: inflammation, fibrosis, oxidative stress, and mutagenesis. *Am J Physiol Lung Cell Mol Physiol*, 295(4):L552–65. doi:10.1152/ajplung.90287.2008 PMID:18658273

Shvedova AA, Kisin ER, Mercer R, Murray AR, Johnson VJ, Potapovich AI, et al. (2005). Unusual inflammatory and fibrogenic pulmonary responses to single-walled carbon nanotubes in mice. *Am J Physiol Lung Cell Mol Physiol*, 289(5):L698–708. doi:10.1152/ajplung.00084.2005 PMID:15951334

Shvedova AA, Kisin ER, Murray AR, Gorelik O, Arepalli S, Castranova V, et al. (2007). Vitamin E deficiency enhances pulmonary inflammatory response and oxidative stress induced by single-walled carbon nanotubes in C57BL/6 mice. *Toxicol Appl Pharmacol*, 221(3):339–48. doi:10.1016/j.taap.2007.03.018 PMID:17482224

Shvedova AA, Pietroiusti A, Fadeel B, Kagan VE (2012b). Mechanisms of carbon nanotube-induced toxicity: focus on oxidative stress. *Toxicol Appl Pharmacol*, 261(2):121–33. doi:10.1016/j.taap.2012.03.023 PMID:22513272

Shvedova AA, Yanamala N, Kisin ER, Tkach AV, Murray AR, Hubbs A, et al. (2014). Long-term effects of carbon containing engineered nanomaterials and asbestos in the lung: one year postexposure comparisons. *Am J Physiol Lung Cell Mol Physiol*, 306(2):L170–82. doi:10.1152/ajplung.00167.2013 PMID:24213921

Siegrist KJ, Reynolds SH, Kashon ML, Lowry DT, Dong C, Hubbs AF, et al. (2014). Genotoxicity of multi-walled carbon nanotubes at occupationally relevant doses. *Part Fibre Toxicol*, 11(6):6. doi:10.1186/1743-8977-11-6 PMID:24479647

Silva RM, Doudrick K, Franzi LM, TeeSy C, Anderson DS, Wu Z, et al. (2014). Instillation versus inhalation of multiwalled carbon nanotubes: exposure-related health effects, clearance, and the role of particle characteristics. *ACS Nano*, 8(9):8911–31. doi:10.1021/nn503887r PMID:25144856

Singh N, Manshian B, Jenkins GJ, Griffiths SM, Williams PM, Maffeis TG, et al. (2009). NanoGenotoxicology: the DNA damaging potential of engineered nanomaterials. *Biomaterials*, 30(23–24):3891–914. doi:10.1016/j.biomaterials.2009.04.009 PMID:19427031

Singh R, Pantarotto D, Lacerda L, Pastorin G, Klumpp C, Prato M, et al. (2006). Tissue biodistribution and blood clearance rates of intravenously administered carbon nanotube radiotracers. *Proc Natl Acad Sci USA*, 103(9):3357–62. doi:10.1073/pnas.0509009103 PMID:16492781

Sinha S, Barjami S, Iannacchione G, Schwab A, Muench G (2005). Off-axis thermal properties of carbon nanotube films. *J Nanopart Res*, 7(6):651–7. doi:10.1007/s11051-005-8382-9

Sinnott SB (2002). Chemical functionalization of carbon nanotubes. *J Nanosci Nanotechnol*, 2(2):113–23. doi:10.1166/jnn.2002.107 PMID:12908295

Slikker W Jr, Andersen ME, Bogdanffy MS, Bus JS, Cohen SD, Conolly RB, et al. (2004). Dose-dependent transitions in mechanisms of toxicity: case studies. *Toxicol Appl Pharmacol*, 201(3):226–94. doi:10.1016/j.taap.2004.06.027 PMID:15582646

Snipes MB (1989). Long-term retention and clearance of particles inhaled by mammalian species. *Crit Rev Toxicol*, 20(3):175–211. doi:10.3109/10408448909017909 PMID:2692607

Snyder-Talkington BN, Dymacek J, Porter DW, Wolfarth MG, Mercer RR, Pacurari M, et al. (2013a). System-based identification of toxicity pathways associated with multi-walled carbon nanotube-induced pathological responses. *Toxicol Appl Pharmacol*, 272(2):476–89. doi:10.1016/j.taap.2013.06.026 PMID:23845593

Snyder-Talkington BN, Pacurari M, Dong C, Leonard SS, Schwegler-Berry D, Castranova V, et al. (2013b). Systematic analysis of multiwalled carbon nanotube-induced cellular signalling and gene expression in human

small airway epithelial cells. *Toxicol Sci*, 133(1):79–89. doi:10.1093/toxsci/kft019 PMID:23377615

Snyder-Talkington BN, Qian Y, Castranova V, Guo NL (2012). New perspectives for in vitro risk assessment of multiwalled carbon nanotubes: application of coculture and bioinformatics. *J Toxicol Environ Health B Crit Rev*, 15(7):468–92. doi:10.1080/10937404.2012.736856 PMID:23190270

Søs Poulsen S, Jacobsen NR, Labib S, Wu D, Husain M, Williams A, et al. (2013). Transcriptomic analysis reveals novel mechanistic insight into murine biological responses to multi-walled carbon nanotubes in lungs and cultured lung epithelial cells. *PLoS One*, 8(11):e80452. doi:10.1371/journal.pone.0080452 PMID:24260392

Srivastava RK, Pant AB, Kashyap MP, Kumar V, Lohani M, Jonas L, et al. (2011). Multi-walled carbon nanotubes induce oxidative stress and apoptosis in human lung cancer cell line-A549. *Nanotoxicology*, 5(2):195–207. doi:10.3109/17435390.2010.503944 PMID:20804439

Stankovich S, Dikin DA, Piner RD, Kohlhaas KA, Kleinhammes A, Jia Y, et al. (2007). Wu y, Nguyen ST, Ruoff RS. Synthesis of graphene-based nanosheets via chemical reduction of exfoliated graphite oxide. *Carbon*, 45(7):1558–65. doi:10.1016/j.carbon.2007.02.034

Stone V, Johnston H, Schins RPF (2009). Development of in vitro systems for nanotoxicology: methodological considerations. *Crit Rev Toxicol*, 39(7):613–26. doi:10.1080/10408440903120975 PMID:19650720

Sun YP, Fu K, Lin Y, Huang W (2002). Functionalized carbon nanotubes: properties and applications. *Acc Chem Res*, 35(12):1096–104. doi:10.1021/ar010160v PMID:12484798

Sun Z, Liu Z, Meng J, Meng J, Duan J, Xie S, et al. (2011). Carbon nanotubes enhance cytotoxicity mediated by human lymphocytes in vitro. *PLoS One*, 6(6):e21073. doi:10.1371/journal.pone.0021073 PMID:21731651

Szendi K, Varga C (2008). Lack of genotoxicity of carbon nanotubes in a pilot study. *Anticancer Res*, 28:1A: 349–52. PMID:18383868

Takagi A, Hirose A, Futakuchi M, Tsuda H, Kanno J (2012). Dose-dependent mesothelioma induction by intraperitoneal administration of multi-wall carbon nanotubes in p53 heterozygous mice. *Cancer Sci*, 103(8):1440–4. doi:10.1111/j.1349-7006.2012.02318.x PMID:22537085

Takagi A, Hirose A, Nishimura T, Fukumori N, Ogata A, Ohashi N, et al. (2008). Induction of mesothelioma in p53+/− mouse by intraperitoneal application of multi-wall carbon nanotube. *J Toxicol Sci*, 33(1):105–16. doi:10.2131/jts.33.105 PMID:18303189

Takanashi S, Hara K, Aoki K, Usui Y, Shimizu M, Haniu H, et al. (2012). Carcinogenicity evaluation for the application of carbon nanotubes as biomaterials in rasH2 mice. *Sci Rep*, 2:498. doi:10.1038/srep00498 PMID:22787556

Takaya M, Ono-Ogasawara M, Shinohara Y, Kubota H, Tsuruoka S, Koda S (2012). Evaluation of exposure risk in the weaving process of MWCNT-coated yarn with real-time particle concentration measurements and characterization of dust particles. *Ind Health*, 50(2):147–55. doi:10.2486/indhealth.MS1312 PMID:22293727

Tavares AM, Louro H, Antunes S, Quarré S, Simar S, De Temmerman PJ, et al. (2014). Genotoxicity evaluation of nanosized titanium dioxide, synthetic amorphous silica and multi-walled carbon nanotubes in human lymphocytes. *Toxicol In Vitro*, 28(1):60–9. doi:10.1016/j.tiv.2013.06.009 PMID:23811260

Thomas T, Bahadori T, Savage N, Thomas K (2009). Moving toward exposure and risk evaluation of nanomaterials: challenges and future directions. *Wiley Interdiscip Rev Nanomed Nanobiotechnol*, 1(4):426–33. doi:10.1002/wnan.34 PMID:20049808

Thostenson ET, Li CY, Chou TW (2005). Nanocomposites in context. *Compos Sci Technol*, 65(3–4):491–516. doi:10.1016/j.compscitech.2004.11.003

Thostenson ET, Ren ZF, Chou TW (2001). Advances if the science and technology of carbon nanotubes and human fibroblasts and their composites: a review. *Compos Sci Technol*, 61:1899–912. doi:10.1016/S0266-3538(01)00094-X

Thurnherr T, Brandenberger C, Fischer K, Diener L, Manser P, Maeder-Althaus X, et al. (2011). A comparison of acute and long-term effects of industrial multi-walled carbon nanotubes on human lung and immune cells in vitro. *Toxicol Lett*, 200(3):176–86. doi:10.1016/j.toxlet.2010.11.012 PMID:21112381

Tilton SC, Karin NJ, Tolic A, Xie Y, Lai X, Hamilton RF Jr, et al. (2014). Three human cell types respond to multi-walled carbon nanotubes and titanium dioxide nanobelts with cell-specific transcriptomic and proteomic expression patterns. *Nanotoxicology*, 8(5):533–48. doi:10.3109/17435390.2013.803624 PMID:23659652

Tkach AV, Shurin GV, Shurin MR, Kisin ER, Murray AR, Young SH, et al. (2011). Direct effects of carbon nanotubes on dendritic cells induce immune suppression upon pulmonary exposure. *ACS Nano*, 5(7):5755–62. doi:10.1021/nn2014479 PMID:21657201

Tournebize J, Sapin-Minet A, Bartosz G, Leroy P, Boudier A (2013). Pitfalls of assays devoted to evaluation of oxidative stress induced by inorganic nanoparticles. *Talanta*, 116:753–63. doi:10.1016/j.talanta.2013.07.077 PMID:24148470

Treumann S, Ma-Hock L, Gröters S, Landsiedel R, van Ravenzwaay B (2013). Additional histopathologic examination of the lungs from a 3-month inhalation toxicity study with multiwall carbon nanotubes in rats. *Toxicol Sci*, 134(1):103–10. doi:10.1093/toxsci/kft089 PMID:23570993

Tsai SJ, Hofmann M, Hallock M, Ada E, Kong J, Ellenbecker M (2009). Characterization and evaluation of nanoparticle release during the synthesis of single-walled

and multiwalled carbon nanotubes by chemical vapor deposition. *Environ Sci Technol*, 43(15):6017–23. doi:10.1021/es900486y PMID:19731712

Tsukahara T, Haniu H (2011). Cellular cytotoxic response induced by highly purified multi-wall carbon nanotube in human lung cells. *Mol Cell Biochem*, 352(1–2):57–63. doi:10.1007/s11010-011-0739-z PMID:21298324

Val S, Hussain S, Boland S, Hamel R, Baeza-Squiban A, Marano F (2009). Carbon black and titanium dioxide nanoparticles induce pro-inflammatory responses in bronchial epithelial cells: need for multiparametric evaluation due to adsorption artifacts. *Inhal Toxicol*, 21(s1):Suppl 1: 115–22. doi:10.1080/08958370902942533 PMID:19558243

van Broekhuizen P, van Veelen W, Streekstra WH, Schulte P, Reijnders L (2012). Exposure limits for nanoparticles: report of an international workshop on nano reference values. *Ann Occup Hyg*, 56(5):515–24. PMID:22752096

Vankoningsloo S, Piret JP, Saout C, Noel F, Mejia J, Coquette A, et al. (2012). Pro-inflammatory effects of different MWCNTs dispersions in p16(INK4A)-deficient telomerase-expressing human keratinocytes but not in human SV-40 immortalized sebocytes. *Nanotoxicology*, 6(1):77–93. doi:10.3109/17435390.2011.558642 PMID:21352087

Varga C, Szendi K (2010). Carbon nanotubes induce granulomas but not mesotheliomas. *In Vivo*, 24(2):153–6. PMID:20363987

Velasco-Santos C, Martinez-Hernandez AL, Consultchi A, Rodriguez R, Castano VM (2003). Naturally produced carbon nanotubes. *Chem Phys Lett*, 373(3–4):272–6. doi:10.1016/S0009-2614(03)00615-8

Vesterdal LK, Danielsen PH, Folkmann JK, Jespersen LF, Aguilar-Pelaez K, Roursgaard M, et al. (2014b). Accumulation of lipids and oxidatively damaged DNA in hepatocytes exposed to particles. *Toxicol Appl Pharmacol*, 274(2):350–60. doi:10.1016/j.taap.2013.10.001 PMID:24121055

Vesterdal LK, Jantzen K, Sheykhzade M, Roursgaard M, Folkmann JK, Loft S, et al. (2014a). Pulmonary exposure to particles from diesel exhaust, urban dust or single-walled carbon nanotubes and oxidatively damaged DNA and vascular function in apoE(–/–) mice. *Nanotoxicology*, 8(1):61–71. doi:10.3109/17435390.2012.750385 PMID:23148895

Vittorio O, Raffa V, Cuschieri A (2009). Influence of purity and surface oxidation on cytotoxicity of multi-walled carbon nanotubes with human neuroblastoma cells. *Nanomedicine*, 5(4):424–31. doi:10.1016/j.nano.2009.02.006 PMID:19341817

Vogelstein B, Papadopoulos N, Velculescu VE, Zhou S, Diaz LA Jr, Kinzler KW (2013). Cancer genome landscapes. *Science*, 339(6127):1546–58. doi:10.1126/science.1235122 PMID:23539594

Walters DA, Ericson LM, Casavant MJ, Liu J, Colbert DT, Smith KA, et al. (1999). m Smalley RE. Elastic strain

of freely suspended single-wall carbon nanotube ropes. *Appl Phys Lett*, 74(25):3803–5. doi:10.1063/1.124185

Wan B, Wang ZX, Lv QY, Dong PX, Zhao LX, Yang Y, et al. (2013). Single-walled carbon nanotubes and graphene oxides induce autophagosome accumulation and lysosome impairment in primarily cultured murine peritoneal macrophages. *Toxicol Lett*, 221(2):118–27. doi:10.1016/j.toxlet.2013.06.208 PMID:23769962

Wang J, Sun P, Bao Y, Dou B, Song D, Li Y (2012b). Vitamin E renders protection to PC12 cells against oxidative damage and apoptosis induced by single-walled carbon nanotubes. *Toxicol In Vitro*, 26(1):32–41. doi:10.1016/j.tiv.2011.10.004 PMID:22020378

Wang J, Sun P, Bao Y, Liu J, An L (2011b). Cytotoxicity of single-walled carbon nanotubes on PC12 cells. *Toxicol In Vitro*, 25(1):242–50. doi:10.1016/j.tiv.2010.11.010 PMID:21094249

Wang L, Luanpitpong S, Castranova V, Tse W, Lu Y, Pongrakhananon V, et al. (2011a). Carbon nanotubes induce malignant transformation and tumorigenesis of human lung epithelial cells. *Nano Lett*, 11(7):2796–803. doi:10.1021/nl2011214 PMID:21657258

Wang L, Stueckle TA, Mishra A, Derk R, Meighan T, Castranova V, et al. (2014). Neoplastic-like transformation effect of single-walled and multi-walled carbon nanotubes compared to asbestos on human lung small airway epithelial cells. *Nanotoxicology*, 8(5):485–507. doi:10.3109/17435390.2013.801089 PMID:23634900

Wang P, Nie X, Wang Y, Li Y, Ge C, Zhang L, et al. (2013). Multiwall carbon nanotubes mediate macrophage activation and promote pulmonary fibrosis through TGF-β/Smad signalling pathway. *Small*, 9(22):3799–811. doi:10.1002/smll.201300607 PMID:23650105

Wang R, Mikoryak C, Li S, Bushdiecker D 2nd, Musselman IH, Pantano P, et al. (2011c). Cytotoxicity screening of single-walled carbon nanotubes: detection and removal of cytotoxic contaminants from carboxylated carbon nanotubes. *Mol Pharm*, 8(4):1351–61. doi:10.1021/mp2001439 PMID:21688794

Wang X, Jia G, Wang H, Nie H, Yan L, Deng XY, et al. (2009). Diameter effects on cytotoxicity of multi-walled carbon nanotubes. *J Nanosci Nanotechnol*, 9(5):3025–33. doi:10.1166/jnn.2009.025 PMID:19452965

Wang X, Xia T, Duch MC, Ji Z, Zhang H, Li R, et al. (2012a). Pluronic F108 coating decreases the lung fibrosis potential of multiwall carbon nanotubes by reducing lysosomal injury. *Nano Lett*, 12(6):3050–61. doi:10.1021/nl300895y PMID:22546002

Wang X, Xia T, Ntim SA, Ji Z, Lin S, Meng H, et al. (2011d). Dispersal state of multiwalled carbon nanotubes elicits profibrogenic cellular responses that correlate with fibrogenesis biomarkers and fibrosis in the murine lung. *ACS Nano*, 5(12):9772–87. doi:10.1021/nn2033055 PMID:22047207

Warheit DB (2008). How meaningful are the results of nanotoxicity studies in the absence of adequate material

characterization? *Toxicol Sci*, 101(2):183–5. doi:10.1093/toxsci/kfm279 PMID:18300382

Warheit DB, George G, Hill LH, Snyderman R, Brody AR (1985). Inhaled asbestos activates a complement-dependent chemoattractant for macrophages. *Lab Invest*, 52(5):505–14. PMID:3990243

Warheit DB, Laurence BR, Reed KL, Roach DH, Reynolds GAM, Webb TR (2004). Comparative pulmonary toxicity assessment of single-wall carbon nanotubes in rats. *Toxicol Sci*, 77(1):117–25. doi:10.1093/toxsci/kfg228 PMID:14514968

Warheit DB, Overby LH, George G, Brody AR (1988). Pulmonary macrophages are attracted to inhaled particles through complement activation. *Exp Lung Res*, 14(1):51–66. doi:10.3109/01902148809062850 PMID:2830106

Watts PCP, Fearon PK, Hsu WK, Billingham NC, Kroto HW, Walton DRM (2003). Carbon nanotubes as polymer antioxidants. *J Mater Chem*, 13(3):491–5. doi:10.1039/b211328g

Wick P, Manser P, Limbach LK, Dettlaff-Weglikowska U, Krumeich F, Roth S, et al. (2007). The degree and kind of agglomeration affect carbon nanotube cytotoxicity. *Toxicol Lett*, 168(2):121–31. doi:10.1016/j.toxlet.2006.08.019 PMID:17169512

Wiethoff AJ, Reed KL, Webb TR, Warheit DB (2003). Assessing the role of neutrophil apoptosis in the resolution of particle-induced pulmonary inflammation. *Inhal Toxicol*, 15(12):1231–46. doi:10.1080/08958370390229898 PMID:14515224

Wildoer JWG, Venema LC, Rinzler AG, Smalley RE, Decker C (1998). Electronic structure of atomically resolved carbon nanotubes. *Nature*, 391(6662):59–62. doi:10.1038/34139

Witasp E, Kagan V, Fadeel B (2008). Programmed cell clearance: molecular mechanisms and role in autoimmune disease, chronic inflammation, and anti-cancer immune responses. *Curr Immunol Rev*, 4(2):53–69. doi:10.2174/157339508784325064

Witasp E, Shvedova AA, Kagan VE, Fadeel B (2009). Single-walled carbon nanotubes impair human macrophage engulfment of apoptotic cell corpses. *Inhal Toxicol*, 21(s1):Suppl 1: 131–6. doi:10.1080/08958370902942574 PMID:19558245

Witzmann FA, Monteiro-Riviere NA (2006). Multi-walled carbon nanotube exposure alters protein expression in human keratinocytes. *Nanomedicine*, 2(3):158–68. [Lond Print] doi:10.1016/j.nano.2006.07.005 PMID:17292138

Wohlleben W, Brill S, Meier MW, Mertler M, Cox G, Hirth S, et al. (2011). On the lifecycle of nanocomposites: comparing released fragments and their in-vivo hazards from three release mechanisms and four nanocomposites. *Small*, 7(16):2384–95. doi:10.1002/smll.201002054 PMID:21671434

Wörle-Knirsch JM, Pulskamp K, Krug HF (2006). Oops they did it again! Carbon nanotubes hoax scientists in viability assays. *Nano Lett*, 6(6):1261–8. doi:10.1021/nl060177c PMID:16771591

WTEC (2007). Panel report on international assessment of carbon nanotube manufacturing and applications. Baltimore (MD), USA: World Technology Evaluation Center, Inc.

Wu M, Gordon RE, Herbert R, Padilla M, Moline J, Mendelson D, et al. (2010). Case report: Lung disease in World Trade Center responders exposed to dust and smoke: carbon nanotubes found in the lungs of World Trade Center patients and dust samples. *Environ Health Perspect*, 118(4):499–504. doi:10.1289/ehp.0901159 PMID:20368128

Wu WT, Liao HY, Chung YT, Li WF, Tsou TC, Li LA, et al. (2014). Effect of nanoparticles exposure on fractional exhaled nitric oxide (FENO) in workers exposed to nanomaterials. *Int J Mol Sci*, 15(1):878–94. doi:10.3390/ijms15010878 PMID:24413755

Xia T, Hamilton RF Jr, Bonner JC, Crandall ED, Elder A, Fazlollahi F, et al. (2013). Interlaboratory evaluation of in vitro cytotoxicity and inflammatory responses to engineered nanomaterials: the NIEHS Nano GO Consortium. *Environ Health Perspect*, 121(6):683–90. doi:10.1289/ehp.1306561 PMID:23649538

Xiao Y, Gao X, Taratula O, Treado S, Urbas A, Holbrook RD, et al. (2009). Anti-HER2 IgY antibody-functionalized single-walled carbon nanotubes for detection of brest cancer cells. *BMC Cancer*, 9:351. doi:10.1186/1471-2407-9-351 PMID:19799784

Xu J, Alexander DB, Futakuchi M, Numano T, Fukamachi K, Suzui M, et al. (2014). Size- and shape-dependent pleural translocation, deposition, fibrogenesis, and mesothelial proliferation by multiwalled carbon nanotubes. *Cancer Sci*, 105(7):763–9. doi:10.1111/cas.12437 PMID:24815191

Xu J, Futakuchi M, Shimizu H, Alexander DB, Yanagihara K, Fukamachi K, et al. (2012). Multi-walled carbon nanotubes translocate into the pleural cavity and induce visceral mesothelial proliferation in rats. *Cancer Sci*, 103(12):2045–50. doi:10.1111/cas.12005 PMID:22938569

Yamashita K, Yoshioka Y, Higashisaka K, Morishita Y, Yoshida T, Fujimura M, et al. (2010). Carbon nanotubes elicit DNA damage and inflammatory response relative to their size and shape. *Inflammation*, 33(4):276–80. doi:10.1007/s10753-010-9182-7 PMID:20174859

Yang H, Liu C, Yang D, Zhang H, Xi Z (2009). Comparative study of cytotoxicity, oxidative stress and genotoxicity induced by four typical nanomaterials: the role of particle size, shape and composition. *J Appl Toxicol*, 29(1):69–78. doi:10.1002/jat.1385 PMID:18756589

Yang M, Flavin K, Kopf I, Radics G, Hearnden CH, McManus GJ, et al. (2013). Functionalization of carbon nanoparticles modulates inflammatory cell

recruitment and NLRP3 inflammasome activation. *Small*, 9(24):4194–206. doi:10.1002/smll.201300481 PMID:23839951

Yang ST, Guo W, Lin Y, Deng XY, Wang HF, Sun HF, et al. (2007). Biodistribution of pristine single-walled carbon nanotubes in vivo. *J Phys Chem C*, 111(48):17761–4. doi:10.1021/jp070712c

Ye R, Wang S, Wang J, Luo Z, Peng Q, Cai X, et al. (2013). Pharmacokinetics of CNT-based drug delivery systems. *Curr Drug Metab*, 14(8):910–20. doi:10.2174/138920021131400113 PMID:24016105

Ye SF, Wu YH, Hou ZQ, Zhang QQ (2009). ROS and NF-kappaB are involved in upregulation of IL-8 in A549 cells exposed to multi-walled carbon nanotubes. *Biochem Biophys Res Commun*, 379(2):643–8. doi:10.1016/j.bbrc.2008.12.137 PMID:19121628

Ye Y, Ahn CC, Witham C, Fultz B, Liu J, Rintzer AG, et al. (1999). Hydrogen absorption and cohesive energy of single-walled carbon nanotubes. *Appl Phys Lett*, 74(16):2307–9. doi:10.1063/1.123833

Yeganeh B, Kull CM, Hull MS, Marr LC (2008). Characterization of airborne particles during production of carbonaceous nanomaterials. *Environ Sci Technol*, 42(12):4600–6. doi:10.1021/es703043c PMID:18605593

Yu IJ, Ichihara G, Ahn K (2014). In: Njuguna J, Pielichowski K, Zhu H, editors. Health and Environmental Safety of Nanomaterials: Nanoparticle exposure assessment: methods, sampling techniques, and data analysis. Salt Lake City (UT), USA: Woodland Publishing; pp. 47–62. doi:10.1533/9780857096678.2.47

Yu KN, Kim JE, Seo HW, Chae C, Cho MH (2013). Differential toxic responses between pristine and functionalized multiwall nanotubes involve induction of autophagy accumulation in murine lung. *J Toxicol Environ Health A*, 76(23):1282–92. doi:10.1080/15287394.2013.850137 PMID:24283420

Yu MF, Files BS, Arepalli S, Ruoff RS (2000). Tensile loading of ropes of single wall carbon nanotubes and their mechanical properties. *Phys Rev Lett*, 84(24):5552–5. doi:10.1103/PhysRevLett.84.5552 PMID:10990992

Yuan J, Gao H, Ching CB (2011). Comparative protein profile of human hepatoma HepG2 cells treated with graphene and single-walled carbon nanotubes: an iTRAQ-coupled 2D LC-MS/MS proteome analysis. *Toxicol Lett*, 207(3):213–21. doi:10.1016/j.toxlet.2011.09.014 PMID:21963432

Zanello LP, Zhao B, Hu H, Haddon RC (2006). Bone cell proliferation on carbon nanotubes. *Nano Lett*, 6(3):562–7. doi:10.1021/nl051861e PMID:16522063

Zeni O, Palumbo R, Bernini R, Zeni L, Sarti M, Scarfi MR (2008). Cytotoxicity investigation on cultured human blood cells treated with single-wall carbon nanotubes. *Sensors (Basel Switzerland)*, 8(1):488–99. doi:10.3390/s8010488

Zhang F, Wang N, Kong J, Dai J, Chang F, Feng G, et al. (2011). Multi-walled carbon nanotubes decrease lactate dehydrogenase activity in enzymatic reaction. *Bioelectrochemistry*, 82(1):74–8. doi:10.1016/j.bioelechem.2011.04.007 PMID:21612987

Zhang H, Cao CP, Wang ZY, Yang YS, Shi ZJ, Gu ZA (2010). Carbon nanotube array anodes for high-rate Li-ion batteries. *Electrochim Acta*, 55(8):2873–7. doi:10.1016/j.electacta.2010.01.028

Zhang MF, Yudasaka M, Koshio A, Iijima S (2002). Thermogravimetric analysis of single-wall carbon nanotubes ultrasonicated in monochlorobenzene. *Chem Phys Lett*, 364(3–4):420–6. doi:10.1016/S0009-2614(02)01347-7

Zhang Y, Deng J, Zhang Y, Guo F, Li C, Zou Z, et al. (2013). Functionalized single-walled carbon nanotubes cause reversible acute lung injury and induce fibrosis in mice. *J Mol Med (Berl)*, 91(1):117–28. doi:10.1007/s00109-012-0940-x PMID:22878607

Zhang Y, Yan B (2012). Cell cycle regulation by carboxylated multiwalled carbon nanotubes through p53-independent induction of p21 under the control of the BMP signalling pathway. *Chem Res Toxicol*, 25(6):1212–21. doi:10.1021/tx300059m PMID:22428663

Zhao Y, Wei J, Vajtai R, Ajayan PM, Barrera EV (2011). Iodine doped carbon nanotube cables exceeding specific electrical conductivity of metals. *Sci Rep*, 1:83. doi:10.1038/srep00083 PMID:22355602

Zhu L, Chang DW, Dai L, Hong Y (2007). DNA damage induced by multiwalled carbon nanotubes in mouse embryonic stem cells. *Nano Lett*, 7(12):3592–7. doi:10.1021/nl071303v PMID:18044946

FLUORO-EDENITE

1. Exposure Data

1.1 Chemical and physical properties

1.1.1 Nomenclature

Mineral name: Fluoro-edenite [in allusion to its composition with dominant fluorine and its relationship with edenite] ([Mindat, 2014](#))

Agreed name: Fluoro-edenite fibrous amphibole, with compositional variability appearing to be similar to that of calcic amphiboles such as tremolite, winchite, and richterite

Synonyms: Fluor edenite; fluoredenite; IMA1994-059; IMA2000-049 ([Jambor et al., 1999](#); [Mindat, 2014](#))

Chemical formula: $NaCa_2Mg_5Si_7AlO_{22}(F,OH)_2$ ([INS-Europa, 2014](#))

Empirical formula:
$Na_{0.9}K_{0.2}Ca_{1.6}Mg_{4.7}Fe^{2+}_{0.2}Fe^{3+}_{0.1}Si_{7.4}Al_{0.6}O_{22}F_2$ ([INS-Europa, 2014](#))

Relative molecular mass: 837.63 ([INS-Europa, 2014](#))

1.1.2 General description

Fluoro-edenite occurs in the volcanic products of the Monte Calvario locality of Biancavilla on the flanks of Mount Etna, Sicily, Italy, and is found in the cavities of benmoreitic lava metasomatized by hot fluids rich in fluorine. The "Monte Calvario" quarry has been mined extensively for a sandy volcanic material that is used in the local building industry. This geological area is made up of domes and dikes associated with "autoclastic breccia," a fine-grained material in which fluoro-edenite has been found that was initially classified as intermediate phases between tremolite and actinolite ([Comba et al., 2003](#); [Mazziotti-Tagliani et al., 2009](#)). Fluoro-edenite is found as both prismatic and acicular millimetre-scale crystals and asbestiform (fibrous) fibres that are present as loose materials in rock cavities. The National Institute for Occupational Safety and Health (NIOSH) of the USA provided definitions for the morphology of elongated mineral particles: acicular – a mineral comprised of fine needle-like crystals; prismatic – a crystal with one dimension markedly longer than the other two; asbestiform – a mineral that is fibrous and composed of separable fibres ([NIOSH, 2011](#)).

Fluoro-edenite is generally associated with potassium feldspars and plagioclase, quartz, clino- and orthopyroxenes, fluoro-apatite, ilmenite, and abundant haematite ([Gianfagna & Oberti, 2001](#)). Due to its high content of fluorine and sodium, in comparison with that of tremolite and actinolite fibres, a new end-member of the amphibole calcic group of the edenite → fluoro-edenite series has been approved by the Commission on New Minerals and Mineral Names of the International Mineralogical Association (IMA, code 2000-049) ([Gianfagna & Oberti, 2001](#); [Comba et al., 2003](#)). The

mineralization process of fluoro-edenite has been suggested to have occurred elsewhere in other volcanic areas (Comba et al., 2003).

Fluoro-edenite is found in materials extracted from the Il Calvario quarry that are used in the local building industry (walls, plaster, mortar, and concrete) and in soil used to pave roads, plazas, and other areas (Paoletti et al., 2000; Burragato et al., 2005). The quarry has been mined since at least the 1950s, with a peak in production around the 1960s and 1970s (Gianfagna et al., 2003; Bruno et al., 2006), and fibrous amphiboles have also been found outside the quarry around Biancavilla (Bruni et al., 2014).

Biancavilla is the first area in which the occurrence of amphiboles fibres in a volcanic environment was reported (Burragato et al., 2005). However, a "fluor-edenite" compound was also found in the cavities of the Ishigamiyama lava dome of the Kimpo volcano, Kumamoto, southwestern Japan, as acicular crystals several millimetres in length and associated with tridymite and magnetite (Tomita et al., 1994; Makino et al., 1996; Jambor et al., 1999).

1.1.3 Chemical and physical properties

Density (specific gravity): D_{cal} = 3.09 g/cm³

Hardness (Mohs' scale): 5–6 (between apatite and orthoclase)

Cleavage: perfect on {110}

Fracture: conchoidal

Lustre: vitreous to resinous

Diaphaneity (transparency): transparent

Colour: yellow to intense yellow (prismatic); yellowish and grey-whitish (fibrous)

Streak: grey-white, yellowish white, parallel to the *c*-axis

Tenacity: brittle

Refractive index: 1.60–1.63

From Mindat (2014)

(a) Chemical properties

(i) Chemical composition

The chemical composition of fluoro-edenite crystals from Biancavilla is variable, as shown by scanning electron microscopy (SEM)-X-ray microanalysis in several different studies (see Table 1.1). The chemical composition of "fluor-edenite" acicular crystals from Kumamoto which differs to a certain extent from that of Biancavilla is (wt%): SiO_2, 48.92; TiO_2, 1.32; Al_2O_3, 5.43; FeO, 7.17; MnO, 0.18; MgO, 19.14; CaO, 11.01; Na_2O, 2.77; K_2O, 1.03; F, 3.19; and Cl, 0.12 (Makino et al., 1996; Jambor et al., 1999). The chemical formula of the Kumamoto fluor-edenite is $K_{0.190}$ $Na_{0.776}$ $Ca_{1.704}$ $Mg_{4.121}$ $Fe^{2+}_{0.866}$ $Ti_{0.143}$ $Mn_{0.022}$ $Al_{0.924}$ $Si_{7.066}$ O_{22} $F_{1.455}$ $OH_{0.545}$ (Tomita et al., 1994) and the crystal-chemical formula of the fluoro-edenite from Biancavilla is $^A(Na_{0.56}$ $K_{0.15})$ $^B(Na_{0.30}$ $Ca_{1.62}$ $Mg_{0.03}$ $Mn_{0.05})$ $^C(Mg_{4.68}$ $Fe^{2+}_{0.19}$ $Fe^{3+}_{0.10}$ $Ti^{4+}_{0.03})$ $^T(Si_{7.42}$ $Al_{0.58})$ O_{22} $^{O3}(F_{1.98}$ $Cl_{0.02})_2$ (Gianfagna & Oberti, 2001). Although fibrous and prismatic fluoro-edenite have similar chemical compositions, some compositional differences exist between prismatic fluoro-edenite and fibres with regard to their contents of magnesium and calcium (higher in the prismatic variety) and silica and iron (higher in fibres), and the variability in composition is greater in fibrous species (Gianfagna et al., 2007). Despite these differences, optical, chemical, and X-ray analyses of the fibres confirm their similarity to the yellow prismatic fluoro-edenite. According to the Leake amphibole classification (Leake et al., 1997), the composition of the fibres ranged from fluoro-edenite (60%) to a lower proportion of winchite (24%), tremolite (12%), and richterite (4%) (Fig. 1.1). The variable chemical composition of fluoro-edenite and the presence of different components complicate the classification of the fibres and the definition of their mineral species (Andreozzi et al., 2009), similarly to the amphiboles observed in Montana (USA) and Libby amphiboles (winchite, ~84%;

Table 1.1 Chemical composition of samples of fluoro-edenite from Biancavilla, Sicily, Italy (wt%)

Component	Sample 1	Sample 2	Sample 3 F[a]	Sample 3 P[b]	Sample 4[c]	Sample 5 F[a,d]	Sample 5 P[b,e]
SiO_2	52.92	53.08	54–56	52.31	52.66–54.12	53.85	52.83
TiO_2	0.29	NR	ND	0.28	ND–0.06, 0.02–0.03	0.59	0.55
Al_2O_3	3.53	3.65	3.8–4.2	3.87	1.95–2.91	3.55	3.81
FeO_t	2.60	2.67[f]	2.6–3.2	2.65	3.59–5.98[g]	4.25[h]	2.25[i]
MnO	0.46	NR	ND	0.40	0.44–0.56	0.53	0.46
MgO	22.65	22.62	19–23	22.78	20.50–22.63	20.44	23.60
CaO	10.83	10.71	7–8	10.86	8.48–10.20	10.06	10.73
Na_2O	3.20	3.33	4.2–5	3.10	2.29–3.10	2.96	3.04
K_2O	0.84	1.12	1.2–1.4	0.89	0.52–0.54	0.88	0.82
F	4.35	4.54	4.2–4.7	4.47	4.40	4.46	4.11
Cl	0.07	NR	ND	0.08	0.06	0.08	0.05

[a] F, amphibole fibres

[b] P, prismatic fluoro-edenite

[c] Range of average chemical composition of four samples of fibrous amphiboles corresponding to 52 (1st sample), 40 (2nd sample), 42 (3rd sample), and 58 (4th sample) analyses

[d] Average chemical composition derived from 25 analyses of the fibrous amphibole

[e] Average chemical composition from three analyses of the prismatic fluoro-edenite crystal

[f] FeO, 1.71%; Fe_2O_3, 0.95%

[g] FeO, 0.29–2.50%; Fe_2O_3, 3.26–5.25

[h] FeO, 1.39%; Fe_2O_3, 3.17%

[i] FeO, 0.19%; Fe_2O_3, 2.29%

Al_2O_3, aluminium oxide; CaO, calcium oxide; Cl, chlorine; F, fluorine; FeO, ferrous oxide; FeO_t, iron oxides; Fe_2O_3, ferric oxide; K_2O, potassium oxide; MgO, magnesium oxide; MnO, manganese oxide; Na_2O, sodium oxide; ND, not detected; NR, not reported; SiO_2, silicon dioxide; TiO_2, titanium dioxide; wt, weight

Sample 1, From Gianfagna & Oberti (2001); Sample 2, From INS-Europa (2014); Sample 3, From Gianfagna et al. (2003); Sample 4, From Pacella (2009), Mazziotti-Tagliani et al. (2009); Sample 5, From Gianfagna et al. (2007)

Compiled by the Working Group

richterite, ~11%; and tremolite, ~6%) (Meeker et al., 2003).

The Fe^{3+}/Fe_{total} ratios evaluated by Mössbauer spectroscopy reflect the different iron oxidation states, with a greater prevalence of Fe^{3+} than Fe^{2+} (Mazziotti-Tagliani et al., 2009). The reactivity of the fibrous samples, measured by the production of the [DMPO, HO]· radical adduct in electron paramagnetic resonance spectroscopy, was lower than that of UICC crocidolite (highly reactive) but comparable with that of fibrous tremolite (Fantauzzi et al., 2012).

(ii) Crystal structure

Relevant mineralogical data (unit-cell parameters) for prismatic and fibrous fluoro-edenite described in various studies are presented in Table 1.2. Fluoro-edenite is monoclinic, with space group C2/m and a space group number of 12. In plane-polarized light, fluoro-edenite is birefringent (first order), biaxial negative, α = 1.6058(5), β = 1.6170(5), γ = 1.6245(5), $2V_{calc}$ = 78.09°, with no visible pleochroism (Gianfagna & Oberti, 2001), and refractive indices vary from 1.60 to 1.63. Fibrous and prismatic fluoro-edenite are quite similar according to optical, chemical, and Rietveld analyses (Burragato et al., 2005).

(b) Physical properties

Different morphologies that have been found for fluoro-edenite are shown in Fig. 1.2. Biancavilla fluoro-edenite is transparent, deep yellow with prismatic to acicular properties. Fibrous and asbestiform fluoro-edenite amphibole fibres are also found in abundance as loose

Fig. 1.1 Composition of four samples of fluoro-edenite fibrous amphibole from Biancavilla, plotted against A(Na+K)/BNa, according to the classification of Leake et al. (1997)
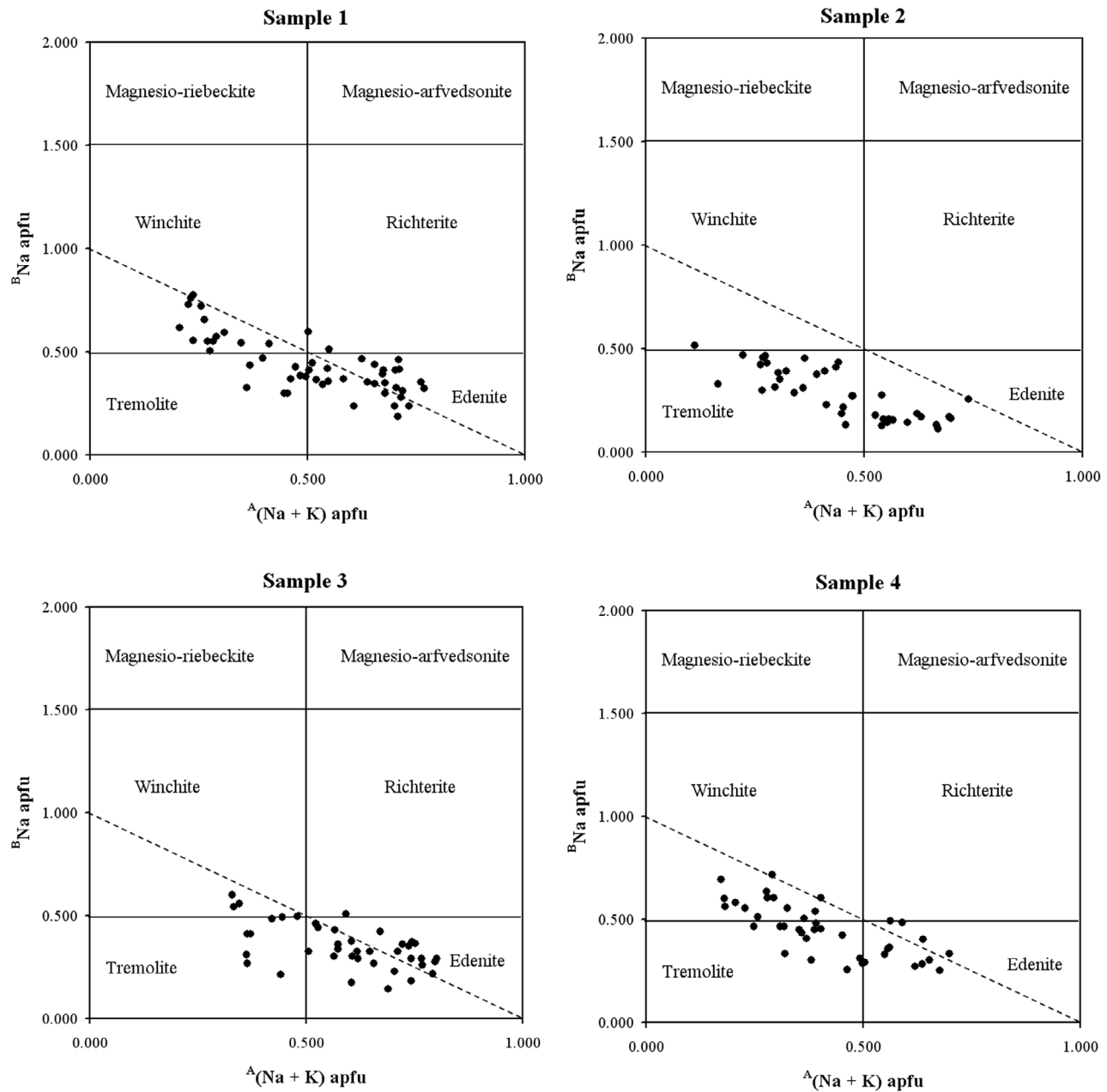
From Mazziotti-Tagliani et al. (2009) © Mazziotti-Tagliani et al. 2009. License: CC BY 4.0

Table 1.2 Unit-cell parameters for fluoro-edenite

Lattice parameters (Å)			Crystallographic axe β	Volume (Å³)	Morphology	References
a	**b**	**c**				
9.847(2)	18.017(3)	5.268(2)	104.84(2)°	903.45	Prismatic	Gianfagna & Oberti (2001)
9.8445(3)	18.0091(6)	5.2772(2)	104.813(2)°	904.5(6)	Prismatic	Gianfagna et al. (2003)
9.815(1)	17.992(3)	5.2733(6)	104.547(9)°	901.4(3)	Fibrous	Gianfagna et al. (2003)
9.8125(3)	18.0188(6)	5.2781(2)	104.620(2)°	903.00(5)	Fibrous	Gianfagna et al. (2007)
9.8056(4)	18.0105(7)	5.2725(2)	104.406(3)°	901.86(6)	Fibrous	Andreozzi et al. (2009)
9.8112(3)	18.0162(6)	5.2774(2)	104.624(2)°	902.61(5)	Fibrous	Andreozzi et al. (2009)
9.8272(1)	17.9899(2)	5.2756(1)	104.596(1)°	902.57(2)	Fibrous	Andreozzi et al. (2009)
9.7935(3)	17.9728(5)	5.2746(1)	104.403(2)°	899.23(5)	Fibrous	Andreozzi et al. (2009)
9.861(4)	18.05(1)	5.282(1)	104.841(1)°	908.9(6)	Acicular	Tomita et al. (1994), Jambor et al. (1999)

Å, 0.1 mm
Compiled by the Working Group

fibres with variable lengths of up to 100–150 μm and a thickness or width < 1 μm (200–600 nm) in the pores of grey-red altered benmoreitic lavas (Gianfagna et al., 2003; Mazziotti-Tagliani et al., 2009).

Fluoro-edenite fibres are highly asymmetrical (thickness, < 1 μm; length, > 10 μm); the shorter fibres are rigid and hard, whereas longer fibres are tensile, elastic, and flexible. The dimensions of the fibres are micrometric to submicrometric and correspond to respirable fibres (Mazziotti-Tagliani et al., 2009).

1.2 Sampling and analytical methods

See Table 1.3

The sampling and analytical methods for fluoro-edenite are identical to those for conventional asbestos. Bulk samples are prepared by removing the debris and grinding the remainder in an agate mortar to produce fine particles, followed by further processing with a mesh or gravimetric sedimentation in water. The resulting suspension is filtered and then mounted for observation using an appropriate analytical device. Air samples are obtained using a vacuum pump equipped with a membrane filter to obtain a representative air volume, and the filter is then processed according to the analytical method. Biological specimens, such as lung tissues, lymph nodes, and sputum, are digested with sodium hypochlorite or hydrogen peroxide or a combination thereof, and the mineral components are recovered on a filter for analysis. The tissue samples are ashed using a low-temperature plasma and then filtered before analysis.

All processed samples on filters can be analysed using a phase-contrast microscope to count the fibres, according to WHO (1997) or NIOSH method 7402 (NIOSH, 1994a).

The sample-loaded filters can also be mounted on a stub and analysed using SEM-energy dispersive X-ray analyser (EDX) (Bruni et al., 2006; Putzu et al., 2006) or mounted on a transmission electron microscopy (TEM) grid and analysed using TEM-EDX according to NIOSH method 7402 (NIOSH, 1994a). TEM allows the analysis of crystal structure and the identification of mineral fibres using electron diffraction and a comparison with reference minerals.

Powdered bulk samples can be analysed using X-ray diffraction based on NIOSH method 9000 (NIOSH, 1994b). To obtain the weight percentage

Fig. 1.2 Morphology of fluoro-edenite crystals: (a) prismatic; (b) acicular; (c) fibrous
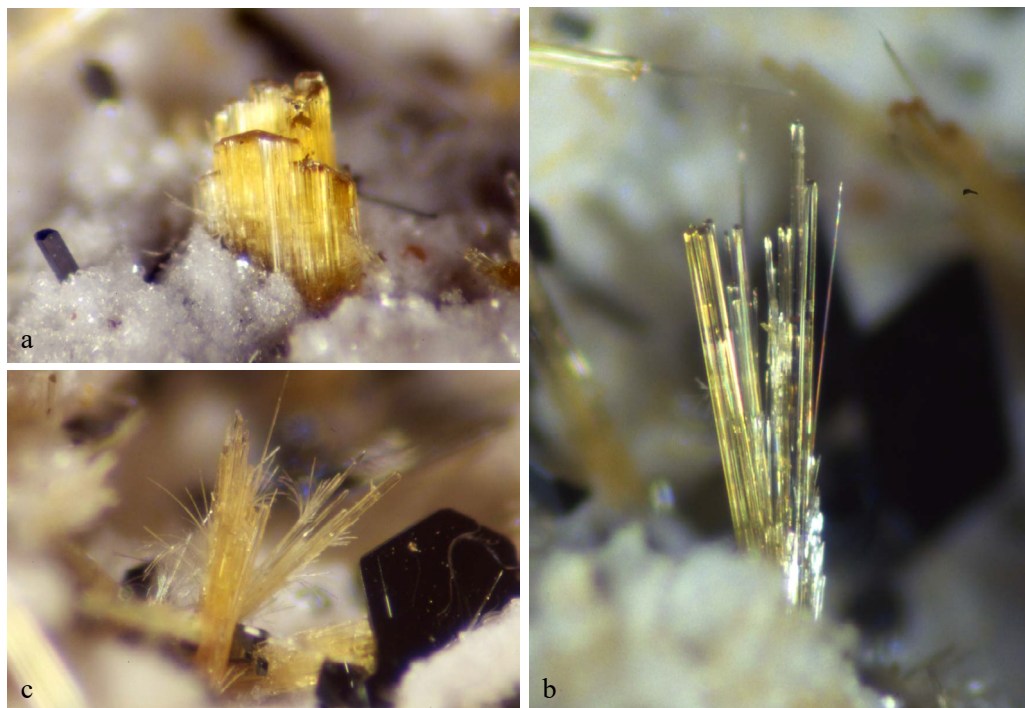
From Gianfagna et al. (2003)

of fluoro-edenite or other amphiboles, standard fluoro-edenite or amphiboles should be prepared.

1.3   Production and use

Fluoro-edenite only occurs naturally. It is a contaminant of an ore that is extensively used in the building industry in Sicily, Italy (see Section 1.1.2).

1.4   Environmental occurrence

1.4.1   Natural occurrence

Fluoro-edenite is a newly defined mineral species (Gianfagna & Oberti, 2001; Comba et al., 2003; Gianfagna et al., 2003) that is found near Biancavilla in eastern Sicily, Italy, located in a volcanic area near Mount Etna. Early environmental investigations of the area in and around

Biancavilla identified local quarries in a nearby area called Monte Calvario as the primary source of fluoro-edenite in the locality (Paoletti et al., 2000). Fluoro-edenite fibres have also been identified occurring naturally in and around the larger Biancavilla area (Bruni et al., 2006). According to Comba et al. (2003), the complex volcanic processes that produced the fluoro-edenite near Biancavilla may not be unique and may have occurred elsewhere.

1.4.2 Air

Fluoro-edenite fibres have been found in air samples in Biancavilla (Famoso et al., 2012; Bruni et al., 2014) and are considered to originate from the local quarry products (Manna & Comba, 2001) that have been used in building materials for local structures since at least the 1950s (Bruni et al., 2006). Unpaved roads made

Table 1.3 Selected methods of analysis of fluoro-edenite in various matrices

Sample matrix	Sample preparation	Assay method	Reference
Bulk sample			
Volcanic materials	Suspension filtered on polycarbonate filter 25 mm (0.4 μm pore), mounted on SEM-stub	SEM-EDX	Bruni et al. (2006)
Plasters and mortar	Suspension filtered on polycarbonate filter 25 mm (0.4 μm pore), mounted on SEM-stub	SEM-EDX	Bruni et al. (2006)
Air sample			
	Polycarbonate filter 25 mm (0.8 μm pore), mounted on SEM-stub	SEM-EDX	Bruni et al. (2006), Famoso et al. (2012)
	Acetone–triacetin-treated filter	PCOM	Famoso et al. (2012)
Biological sample			
Human lung	Digestion of lung tissue; filtration on polycarbonate filter 25 mm (0.45 μm pore), mounted on SEM-stub	SEM-EDX	Bruni et al. (2006)
Sputum	Digestion of sputum; filtration through mixed cellulose ester filter (25 mm, 0.45 μm pore), mounted on SEM-stub or slide	PCOM SEM-EDX	Putzu et al. (2006) Putzu et al. (2006)
Sheep lung sample	Chopped with scissors and lancet; lipid dissolution by acetone; filtration through polycarbonate filter 25 mm (0.8 μm pore), washed in pure water	SEM-EDX	DeNardo et al. (2004)
Sheep lung lymph nodes	SEM-stub	SEM-EDX	Rapisarda et al. (2005)

EDX, energy dispersive X-ray analyser; PCOM, phase contrast optical microscopy; SEM, scanning electron microscopy
Compiled by the Working Group

from local quarry products have also been a primary source of airborne fluoro-edenite fibres (Manna & Comba, 2001). Bruni et al. (2014) described three environmental sampling surveys that were conducted in Biancavilla, in 2000, 2004–05, and 2009–13 and limited the analyses to those with data obtained by SEM. Outdoor samples taken in 2000 (before mitigation efforts) showed amphibole concentrations (of unknown average age) ranging from 0.4 to 8.2 fibres/L, with a mean of 1.76 fibres/L. Peak concentrations were associated with the use of unpaved roads by heavy traffic with concentrations as high as 93–183 fibres/L. Indoor sampling during the same period identified concentrations ranging from < 0.4 fibres/L to 4.8 fibres/L, with a mean of 1.18 fibres/L. The outdoor sampling conducted in 2004–05 demonstrated amphibole concentrations ranging from 0.01 fibres/L to 4.19 fibres/L, with a mean of 0.35 fibres/L, and more recent

samplings yielded mean concentrations of 0.46 fibres/L in 2009 and 0.1 fibres/L in 2013.

Although the sampling period was not noted, and therefore these sample may not be independent of those mentioned by Bruni et al. (2014), Famoso et al. (2012) reported the results obtained from 860 air samples collected in a 3.3-km² area of Biancavilla and analysed by phase-contrast optical microscopy and SEM-EDX; in 21% of samples, concentrations greater than 0.4 fibres/L were detected while 6% of samples contained concentrations greater than 0.8 fibres/L.

1.4.3 Water

Water flow is undoubtedly important to the fate and transport of fibres from the quarries near the Monte Calvario locality of Biancavilla, and from the anthropogenic use and dispersion of these materials over decades of construction activities and road building. However, few data

are available that describe the detection of fluoro-edenite fibres in and around Biancavilla. In one report, all of 10 samples from five water sources in Biancavilla, including two springs and three wells, contained fluoro-edenite fibres (Famoso et al., 2012).

1.4.4 Soil

As mentioned above, environmental investigations have identified the quarries near Monte Calvario as a primary source of fluoro-edenite fibres (Paoletti et al., 2000; Bruni et al., 2006). Analysis of 840 samples of top soil and 90 samples of roadside dust in Biancavilla showed that approximately 90% contained fluoro-edenite (Famoso et al., 2012).

1.5 Exposure of the general population

Exposure to fluoro-edenite mainly occurs via inhalation and ingestion. Inhalation is the primary route of exposure for the general population in Biancavilla, where outdoor air is contaminated with fluoro-edenite fibres (Famoso et al., 2012). Indoor air may also be contaminated from the use of contaminated local quarry products in plaster and mortar. Bruni et al. (2006) took friable plaster samples from 38 local buildings known to have been constructed using materials from the Monte Calvario quarries and found that 71% of these buildings were contaminated. Although the local quarries that are thought to be the primary source of fluoro-edenite were closed in 2001, historical exposures could also include those of family members of quarry and construction workers exposed to dust from working clothes.

Of 12 long-term residents of Biancavilla who were at least 45 years of age and had been hospitalized for exacerbation of their symptoms of chronic obstructive pulmonary disease, six had detectable fluoro-edenite fibres in their sputum

samples (Putzu et al., 2006). Of these, four were women who were all housewives, one was a man who was a farmer and the other was a man who was a mason. The fibre concentrations found in the sputum ranged from 0.04 to 10 fibres/g, with a length of 20–40 μm and a diameter of < 0.5 μm (Putzu et al., 2006).

Several mineral fibres identified as the tremolite/actinolite amphibole fibres found in the quarries and building materials in Biancavilla were also detected in the lung tissue of a woman aged 86 years who died from mesothelioma and was a housewife who had always lived in Biancavilla (Paoletti et al., 2000).

2. Cancer in Humans

2.1 Introduction

The available epidemiological evidence on the risk of cancer in humans associated with exposure to fibres composed of fluoro-edenite resulted from a sequence of community studies of the mortality from and incidence of pleural mesothelioma, and from two case series of individual patients with mesothelioma, all of which were conducted and reported in the same location – Biancavilla, a municipality of about 20 000 inhabitants situated in a rural setting on the slopes of the Mount Etna volcano in Sicily, Italy.

After the publication of several reports on pleural mesothelioma in Biancavilla, a few studies also investigated the occurrence of other asbestos-related diseases, namely lung cancer, in the same community, but no case–control or cohort studies have been conducted to date.

2.2 Mesothelioma

The first indication of an excess of mesothelioma in Biancavilla was given in a 1996 report of the national programme of epidemiological

surveillance of mesothelioma mortality in Italy for the period 1988–92 (Di Paola et al., 1996); the programme examined mortality from malignant pleural neoplasms in all 8000 Italian municipalities to detect cases with ascertained or suspected exposure to asbestos. The excess of mesothelioma in Biancavilla was based on four observed deaths versus 0.96 expected [standardized mortality ratio (SMR), 4.17; 95% confidence interval (CI), 1.13–10.67] using the Sicilian region as a reference population. Subsequent reports of this programme confirmed the original findings. Mastrantonio et al. (2002) reported an SMR of 5.80 (95% CI, 2.99–10.13) based on 12 observed deaths for the period 1988–97, and Fazzo et al. (2012) reported SMRs of 4.39 (90% CI, 1.91–8.67 [95% CI, 1.61–9.55]) based on six observed deaths in men and 6.12 (90% CI, 2.09–14.01 [95% CI, 1.67–15.66]) based on four observed cases in women, for the period 1995–2002. All of these studies used the Ninth Revision of the International Classification of Diseases that has a category of "malignant pleural neoplasms" (code 163). Subsequently, Italy began to use the 10th Revision, which includes a more specific code for pleural mesothelioma (code 45.1). Thus, for the time window of 2003–09, Fazzo et al. (2012) reported the mortality from pleural mesothelioma and found SMRs of 6.54 (90% CI, 2.58–13.75 [95% CI, 1.61–9.55]) in men and 22.93 (90% CI, 9.04–48.22 [95% CI, 2.72–15.70]) in women based on five cases in each sex.

As a consequence of the first report on mortality from pleural mesothelioma (Di Paola et al., 1996), Biancavilla was included in the list of Italian municipalities at risk for mesothelioma, for which an assessment of exposure to asbestos was recommended. Pending this assessment, the occurrence of additional cases that died in 1993–97 was examined and their pathological diagnoses were reviewed.

In a report of a case series of mesothelioma, Paoletti et al. (2000) emphasized that the process of case ascertainment might not have been exhaustive due to the absence (before 1998) of a validated system of mesothelioma surveillance in Sicily. The source of the cases included the mortality records of the municipality of Biancavilla, family doctors, and hospital records; histological specimens, where available, were reviewed by an expert pathologist; and information on the occupation and residence of the cases was collected by physicians in the local health unit through interviews with the cases (when alive) or, more frequently, with closest relatives. The case series included 10 men and seven women; histology slides were available for nine of the 17 cases, and all diagnoses were confirmed by the pathologist. One case was diagnosed at the age of 29 years, four cases were aged between 40 and 50 years, and the remaining 12 cases were aged over 50 years. All cases except one were long-term residents in Biancavilla. Information on occupation was available for all cases; none had confirmed occupational exposure to asbestos, but two had been employed in industries where exposure was considered to be probable. Asbestiform fibres were detected at a large stone quarry located close to the urbanized area of Biancavilla, from which materials used in the local building industry and road paving were extracted. Several mineral fibres were detected in the lung autopsy samples from a woman aged 86 years who died from pleural mesothelioma and was a resident in Biancavilla, and were identified as the fibrous amphiboles found in the quarries and building materials used in Biancavilla. The patient was a housewife who had been married to a farmer. No chrysotile, crocidolite, or amosite fibres were found in her lung tissue. The fibres were regarded as mineralogical phase intermediates between sodium- and fluorine-rich tremolites and actinolites (Paoletti et al., 2000). This material was subsequently identified as a new mineral species that was called fluoro-edenite (Gianfagna & Oberti, 2001). Further analyses of the mineral material demonstrated that amphibole fibres from Biancavilla had a dominant fluoro-edenite

component with significant tremolite and minor winchite components (Bruni et al., 2014).

Since 1998, the surveillance of mesothelioma in Sicily has been conducted by the Sicilian Operative Regional Centre of the Italian National Mesothelioma Registry; the procedures used by the centre for case ascertainment have been discussed extensively elsewhere (INAIL, 2010). A total of 28 cases were detected during the period 1998–2011 (Bruno et al., 2014). Two of these were not resident in Biancavilla at the time of diagnosis, and thus did not meet the criterion to be included in the case series of Biancavilla residents reported by the centre or in the subsequent computation of incidence rates; one had lived in Biancavilla from birth until the age of 53 years and the other from birth until the age of 28 years. Of the remaining 26 cases, two were peritoneal (one man and one woman) and 24 were pleural (12 men and 12 women). One case was diagnosed at the age of 27 years, one at the age of 33 years, one at the age of 39 years, two cases between the ages of 40 and 50 years, and the remaining cases after 50 years of age. Only environmental exposure to Biancavilla fibres was established for eight subjects. None of the cases had definite occupational exposure to asbestos, but one had worked in an industrial sector where asbestos had been used and three had been employed in industries where exposure could occur. Occupational information was insufficient for two cases, although there was an indication that one had worked temporarily in the Biancavilla quarry. No information about past exposures could be obtained for the remaining 12 cases. [Although observations in case series generally provide weak evidence of causality, the young ages of the cases, the equal numbers of men and women, and the lack of documented history of exposure to asbestos for most cases are consistent with an environmental cause.]

The incidence of mesothelioma in Biancavilla was computed and compared with that of the Sicilian region by estimating standardized incidence ratios (SIRs) with their 95% CIs. Table 2.1 shows a large excess of both pleural (SIR, 5.65; 95% CI, 3.62–8.41) and peritoneal (SIR, 7.92; 95% CI, 0.96–20.0) mesothelioma, although the latter was based on only two cases and had a wide confidence interval (Bruno et al., 2014). SIRs for pleural mesothelioma were particularly elevated in women and were highest in the younger age groups: 21.34 (95% CI, 6.93–50.00; 5 cases) and 62.88 (95% CI, 13.00–180.00; 3 cases) for women under the ages of 50 years and 40 years, respectively.

[No data on individual exposures were available for the population of Biancavilla. However, the high incidence of mesothelioma in younger age groups and women is suggestive of environmental exposure. The consistently larger rate ratios for mesothelioma in women than those in men could most probably be explained by the much higher background rate of mesothelioma in men than in women; thus relative rates would be higher in women than in men even if the absolute excess rates were the same. This explanation is strongly supported by the observation of the same number of cases of mesothelioma in men and women in the reports of the Epidemiological Study of Residents in National Priority Contaminated Sites (SENTIERI). These findings are also unlikely to be explained by a greater susceptibility of women than that of men to the effects of exposure, which has not been observed in studies of populations exposed to asbestos.]

2.3 Cancer of the lung

The occurrence of cancer of the lung in the municipality of Biancavilla, where exposure to fibres composed of fluoro-edenite can occur, has been the object of geographical studies of mortality, cancer incidence, and hospitalization (Table 2.1).

Mortality from lung cancer in Biancavilla during the periods 1995–2002 and 2003–10 was

Table 2.1 Occurrence of mesothelioma, and cancers of the lung, larynx, and ovary among Biancavilla (Italy) residents

Reference, follow-up period	Total No. of subjects	Exposure assessment	Organ site	Exposure categories	No. of exposed cases	Relative risk	Covariates	Comments
Bruno et al. (2014) 1998–2011		Residence in Biancavilla at time of death/diagnosis	Pleural mesothelioma	Men and women	24	5.65 (95% CI, 3.62–8.41)	Age, socioeconomic deprivation index	
				Men	12	3.63 (95% CI, 1.87–6.34)		
				Women	12	12.75 (95% CI, 6.59–22.00)		
				Age < 40 yr	3	62.88 (95% CI, 13.00–180.00)		
				Age < 50 yr	5	21.34 (95% CI, 6.93–50.00)		
				Age > 50 yr	19	4.74 (95% CI, 2.85–7.39)		
				Men, age > 50 yr	8	2.55 (95% CI, 1.10–5.02)		
				Women, age > 50 yr	11	12.56 (95% CI, 6.27–22.00)		
			Peritoneal mesothelioma		2	7.92 (95% CI, 0.96–20.00)		
Conti et al. (2014) 2003–2010	23 703 (2011 national census)		Pleural mesothelioma	*Mortality:* Men	5	3.79 (90% CI, 1.49–7.97)		
				Women	6	11.28 (90% CI, 4.91–22.26)		
				Hospitalization (2005–10): Men	7	2.61 (90% CI, 1.22–4.89)		
				Women	7	7.80 (90% CI, 3.66–14.64)		
			Lung	*Mortality:* Men	35	0.86 (90% CI, 0.63–1.14) [95% CI, 0.62–1.20]		
				Women	11	1.28 (90% CI, 0.72–2.12) [95% CI, 0.70–2.31]		
				Hospitalization (2005–10): Men	53	1.10 (90% CI, 0.87–1.39) [95% CI, 0.84–1.44]		
				Women	13	1.16 (90% CI, 0.68–1.84) [95% CI, 0.67–2.00]		
			Larynx	*Hospitalization (2003–10):* Men	7	0.86 (90% CI, 0.40–1.62)		
			Ovary	Mortality	4	0.77 (90% CI, 0.26–1.77)		
				Hospitalization	11	0.80 (90% CI, 0.45–1.32)		

Table 2.1 (continued)

Reference, follow-up period	Total No. of subjects	Exposure assessment	Organ site	Exposure categories	No. of exposed cases	Relative risk	Covariates	Comments
Pirastu et al. (2014) 2003–2005	23 703 (2011 national census)	Residence in Biancavilla at time of diagnosis	Lung	Men	21	0.72 (90% CI, 0.48–1.03) [95% CI, 0.47–1.10]	Age and socioeconomic status	Incidence
				Women	10	1.67 (90% CI, 0.91–2.84) [95% CI, 0.90–3.10]		
			Mesothelioma	Women	4	14.41 (90% CI, 4.90–32.94)		Mesothelioma incidence not reported for men
			Ovary	Women	3	0.65 (90% CI, 0.18–1.67)		

CI, confidence interval; yr, year
Compiled by the Working Group

investigated as a part of the SENTIERI project (Pirastu et al., 2011, 2014). Sicilian regional mortality rates were used as the reference population and SMRs were adjusted for socioeconomic status. In 1995–2002, a deficit in mortality from lung cancer in men (SMR, 0.80; 90% CI, 0.60–1.04 [95% CI, 0.59–1.09]; 40 cases) and an excess in women (SMR, 1.33; 90% CI, 0.72–2.26 [95% CI, 0.72–2.47]; 10 cases) were observed. A more detailed report based on data from the 2003–10 SENTIERI project (Conti et al., 2014) showed moderate but imprecise increases in mortality from lung cancer (SMR, 1.28; 90% CI, 0.72–2.12 [95% CI, 0.70–2.31]) and hospitalization (standardized hospitalization ratio, 1.16; 90% CI, 0.68–1.84 [95% CI, 0.67–2.00]) in women and a deficit in mortality (SMR, 0.86; 90% CI, 0.63–1.14 [95% CI, 0.62–1.20]) and a small excess of hospitalization (standardized hospitalization ratio, 1.10; 90% CI, 0.87–1.39 [95% CI, 0.84–1.44]) in men. [The Working Group calculated that the pooled SMRs for lung cancer for the entire 1995–2010 period were 0.83 (95% CI, 0.66–1.03) in men and 1.30 (95% CI, 0.85–1.60) in women.]

A recent report by the Sicilian Region Department of Health (Cernigliaro et al., 2013) showed that mortality from lung cancer (2004–11) in Biancavilla was lower than that expected from local reference populations in men (SMR, 0.91; 95% CI, 0.69–1.18) but was higher than that expected compared with a local reference population in women (SMR, 1.77; 95% CI, 1.10–2.71).

The incidence of lung cancer (2003–05) was also examined in the SENTIERI project and showed a moderate excess in women (SIR, 1.67; 90% CI, 0.91–2.84 [95% CI, 0.90–3.10]) and a deficit in men (SIR, 0.72; 90% CI, 0.48–1.03 [95% CI, 0.47–1.10]) (Pirastu et al., 2014). [The only statistically significant finding for lung cancer was in women when local reference rates were used. An apparent deficit in lung cancer was observed among men when regional reference rates were used, but this was largely removed when local reference rates were used.

Significantly, an excess of lung cancer has not been consistently observed in other community studies of exposure to asbestos. The possible role of smoking as a confounder or effect modifier in these studies cannot be assessed directly because no data were available on smoking habits in Biancavilla. However, available reports have indicated that the proportion of current smokers in Catania Province, which includes Biancavilla, corresponded with the regional average in Sicily (Regione Sicilia, 2014).]

2.4 Other neoplasms

A non-significant deficit in hospitalization for laryngeal cancer based on seven observed cases in men was reported by Conti et al. (2014) (Table 2.1). Data on hospitalizations for women and mortality data for both sexes were not available because the observations were based on fewer than three cases and thus could not be published due to privacy regulations. No figures on mortality from laryngeal cancer were available in the previous edition of the SENTIERI project report for 1995–2002 (Pirastu et al., 2011). The incidence of laryngeal cancer was investigated in the most recent SENTIERI report for 2003–05 (Pirastu et al., 2014), but fewer than three cases per sex were observed, thus precluding publication of the data on this cancer.

A deficit in ovarian cancer based on four observed deaths (SMR, 0.77; 90% CI, 0.26–1.77) and 11 observed cases of hospitalization (standardized hospitalization ratio, 0.80; 90% CI, 0.45–1.32) was reported by Conti et al. (2014) for the period 2005–10 (Table 2.1). In the previous SENTIERI project report relative to 1995–2002, a deficit in mortality from ovarian cancer based on five cases was reported (Pirastu et al., 2011); a deficit in the incidence of ovarian cancer based on three observed cases (SIR, 0.65; 90% CI, 0.18–1.67) was reported in the last edition of the SENTIERI project that included data for the years 2003–05 (Pirastu et al., 2014; Table 2.1).

[Potential confounding by tobacco smoking and alcohol consumption is a concern for laryngeal cancer, but data on these risk factors were not available for the study population. Although based on small numbers and statistically non-significant, the deficit in ovarian cancer appeared to be consistent.]

[The Working Group noted that 90% CIs rather than the more commonly adopted 95% CIs were used in the Biancavilla epidemiological studies that were included in the SENTIERI project. This choice was motivated by the focus on sites where specific, exposure-related conditions were expected to be in excess; the rationale was further elaborated by Pirastu et al. (2014). The Working Group computed 95% CIs for the associations that were reported to be statistically significant on the basis of 90% CIs, and all of them excluded unity.]

3. Cancer in Experimental Animals

See Table 3.1 and Table 3.2

Rat

Only one study, described in two reports, was conducted to examine the potential carcinogenicity of fluoro-edenite in rats (Soffritti et al., 2004; Belpoggi et al., 2011).

One group of 40 male and 40 female Sprague-Dawley rats (age, 8 weeks) received a single intraperitoneal injection of 25 mg of fibrous fluoro-edenite (the fibrous sample contained 25–30% of fluoro-edenite fibres [diameter, 0.5–1 μm; length > 10 μm] in addition to feldspars, haematite, and pyroxenes; in 1 mL of water) sampled from a quarry in Biancavilla, Sicily, Italy; a second group of 40 males and 40 females received a single intrapleural injection of 25 mg of fibrous fluoro-edenite (in 1 mL of water) through the chest wall into the pleural cavity; a third group of 15 male and 15 female rats received a single intraperitoneal injection of 25 mg of powdered prismatic fluoro-edenite; and a fourth group of 40 males and 40 females received a single intraperitoneal injection of 1 mL of water only and served as vehicle controls. [No vehicle control group for intrapleural injection was provided.] The animals were observed until all those in group 1 that were treated with fibrous fluoro-edenite by intraperitoneal injection had died (109 weeks). At 109 weeks, 70 of the 80 rats treated by intrapleural injection (group 2) had died. The average time to the appearance of tumours in group 1 was 61.6 weeks for males and 66.4 weeks for females (see Table 3.1); a total of 37 out of 40 (92.5%) [$P < 0.0001$, Fisher exact test] males and 29 out of 40 (72.5%) [$P < 0.0001$, Fisher exact test] females developed mesothelioma. The average latency for the group that received an intrapleural injection of fibrous fluoro-edenite was 71.0 weeks in males and 72.8 weeks in females; 4 out of 37 (10.8%) males and 6 out of 33 (18.2%) females developed mesothelioma. None of the rats given water or powdered prismatic fluoro-edenite intraperitoneally had developed mesothelioma at 109 weeks (Soffritti et al., 2004).

The rats in group 2 (intrapleural injection of fluoro-edenite), group 3 (intraperitoneal injection of powdered prismatic fluoro-edenite), and group 4 (intraperitoneal injection of water) were further followed for a total of 122 weeks, at which time all of the rats had died or were killed (see Table 3.2). At 122 weeks, only 1 (female) out of 80 rats that received a single intraperitoneal injection of water alone had developed mesothelioma. None of the males or females exposed to powdered prismatic fluoro-edenite developed mesothelioma, but 6 out of 40 (15%) males and 7 out of 40 (17.5%) females in group 3 (intrapleural injection of fibrous fluoro-edenite) were found to have mesothelioma (Belpoggi et al., 2011). As reported in Soffritti et al. (2004), the incidence of mesothelioma was increased in males (37 out of 40) and females (29 out of 40) that

Table 3.1 Induction of mesotheliomas by fluoro-edenite in Sprague-Dawley rats followed for up to 109 weeks

Material	Route of administration (dose)	No. of rats (sex)	No. of deceased rats at 109 wk	Incidence of mesotheliomas (%)	Significance[a]	Mean latency (wk)
Fibrous fluoro-edenite	Intraperitoneal injection (25 mg/rat)	40 (M)	40	92.5 (37/40)	[P < 0.0001]	61.6
Fibrous fluoro-edenite	Intraperitoneal injection (25 mg/rat)	40 (F)	40	72.5 (29/40)	[P < 0.0001]	66.4
Fibrous fluoro-edenite	Intrapleural injection (25 mg/rat)	40 (M)	37	10.8 (4/37)	NA	71.0
Fibrous fluoro-edenite	Intrapleural injection (25 mg/rat)	40 (F)	33	18.2 (6/33)	NA	72.8
Powdered prismatic fluoro-edenite	Intraperitoneal injection (25 mg/rat)	15 (M)	13	0 (0/13)	[NS]	NA
Powdered prismatic fluoro-edenite	Intraperitoneal injection (25 mg/rat)	15 (F)	13	0 (0/13)	[NS]	NA
Water (control)	Intraperitoneal injection (1 mL)	40 (M)	33	0 (0/33)	–	NA
Water (control)	Intraperitoneal injection (1 mL)	40 (F)	32	0 (0/32)	–	NA

[a] Calculated by the Working Group, Fisher exact test
F, female; M, male; NA, not applicable; NS, not significant; wk, week
From Soffritti et al. (2004)

Table 3.2 Induction of mesotheliomas by fluoro-edenite in Sprague-Dawley rats followed for up to 122 weeks

Material	Route of administration (dose)	Total No. of rats (sex)	No. of rats deceased or killed at 122 weeks	Incidence of mesotheliomas (%)	Significance[a]	Mean latency (wk)
Fibrous fluoro-edenite	Intrapleural injection (25 mg/rat)	40 (M)	40	15 (6/40)	NA[b]	82.3
Fibrous fluoro-edenite	Intrapleural injection (25 mg/rat)	40 (F)	40	17.5 (7/40)	NA[c]	77.4
Powdered prismatic fluoro-edenite	Intraperitoneal injection (25 mg/rat)	15 (M)	15	0 (0/15)	[NS]	NA
Powdered prismatic fluoro-edenite	Intraperitoneal injection (25 mg/rat)	15 (F)	15	0 (0/15)	[NS]	NA
Water (control)	Intraperitoneal injection (1 mL)	40 (M)	40	0 (0/40)	–	NA
Water (control)	Intraperitoneal injection (1 mL)	40 (F)	40	2.5 (1/40)	–	122

[a] Calculated by the Working Group, Fisher exact test
[b] Historical incidence in vehicle controls: 0/20 male Sprague-Dawley rats (Maltoni & Minardi, 1989)
[c] Historical incidence in vehicle controls: 0/20 female Sprague-Dawley rats (Maltoni & Minardi, 1989)
F, female; M, male; NA, not applicable; NS, not significant; wk, week
From Belpoggi et al. (2011)

received an intraperitoneal injection of fibrous fluoro-edenite. The authors characterized the fluoro-edenite-induced mesotheliomas as epithelial, mixed, or sarcomatous. Rats given fibrous fluoro-edenite by intraperitoneal injection developed mesotheliomas of predominantly sarcomatous or mixed histology. In contrast, half of the mesotheliomas that resulted from pleural administration in males were morphologically epithelial. Many of the mesotheliomas had metastasized into the lung, lymph nodes, and throughout the abdomen. The incidence and latency were comparable with those of many types of fibre that have been demonstrated to cause mesothelioma (e.g. crocidolite and amosite) in Sprague-Dawley rats in that laboratory (Maltoni & Minardi, 1989). [The study described by Soffritti et al. (2004) and Belpoggi et al. (2011) was limited by the lack of statistical analysis and an appropriate control for the intrapleural injection experiment. However, the authors presented the mesothelioma response as a simple description to demonstrate the extent of an obvious effect. The Working Group also noted that 20 male and 20 female Sprague-Dawley rats that served as controls in a lifetime study conducted in the same laboratory (Maltoni & Minardi, 1989) did not develop mesotheliomas after a single intrapleural injection of water.]

4. Mechanistic and Other Relevant Data

4.1 Deposition, phagocytosis, retention, translocation, and clearance

4.1.1 Humans

Paoletti et al. (2000) reported fluoro-edenite fibrous amphiboles (i.e. intermediate phases between tremolite and actinolite) in 71–72% of the samples of sand and other building materials in Biancavilla, Sicily, Italy, that had the same type of amphibole phases observed in the local quarries. Similar fibrous amphiboles were also observed in the lung tissue from the autopsy of a woman aged 86 years who had been diagnosed with pleural mesothelioma, had lived in Biancavilla for her entire life, and did not have any reported occupational exposure to fibrous amphiboles. The fibre dimensions observed in the lung tissue were similar to those reported in sheep (Rapisarda et al., 2005), with diameters ranging from 0.4 μm to 1 μm and lengths ranging from 12 μm to 40 μm (Paoletti et al., 2000; Rapisarda et al., 2005).

4.1.2 Experimental animals

Limited data are available on the mechanisms related to the deposition or disposition of inhaled fluoro-edenite in experimental animals. DeNardo et al. (2004) and Rapisarda et al. (2005) measured the burden of fluoro-edenite fibres in the lungs of sheep (Table 4.1) because of their anatomical and physiological similarity to human lungs (Bégin et al., 1981), and because the animals had potentially been exposed environmentally to fluoro-edenite amphibole fibres from a stone quarry near the town of Biancavilla.

DeNardo et al. (2004) studied the lung burden of fibres in 27 sheep (age, 3 years or older) that lived and grazed near (1–3 km) the Monte Calvario stone quarries to the south east of Biancavilla. The sheep (all ewes) were selected on the basis of age and the longest air exposure in a flock of approximately 200 animals. Tissue samples from the lung tracheal lobes were analysed by SEM-EDX and the fibres were identified as fluoro-edenite by their chemical composition and the presence of fluorine, magnesium, and calcium. A positive identification of fluoro-edenite was based on an observed ratio of 2 ≤ magnesium/calcium ≤ 3, and a probable identification based on a ratio of

Table 4.1 Toxicokinetics of fluoro-edenite fibres in sheep

Particle dimensions and surface area	Species (age and sex), number of animals	Route of exposure and dose/exposure concentration	Duration of study	Findings	Comments	Reference
NR Fluoro-edenite: confirmed, identified if ratio of $2 \leq$ Mg/Ca ≤ 3; probable, identified if 1.5 $\leq$ Mg/Ca ≤ 2	Sheep (≥ 3 yr, F), 27 exposed	Inhalation (environmental)	Sheep had lived and grazed near (1–3 km) the Monte Calvario stone quarries to the South-eastern of Biancavilla	Fluoro-edenite content was identified as 7.5% of the mineral species (2.7% confirmed and 4.8% probable)	Mineral species in lung tracheal lobe tissue samples (approximately 50 g) from each of 27 animals obtained from slaughterhouse	DeNardo et al. (2004)
Fluoro-edenite: fibre length, 8–41 μm; fibre width: 0.4–1.39 μm	Sheep (NR), 60 exposed and 10 controls	Inhalation (environmental)	Exposed sheep randomly selected from six flocks that regularly grazed 3 km from the town of Biancavilla	Lymph nodes of all the exposed sheep contained fibres; no fibres found in lymph nodes of the controls Mean fibre number: $0.08 \pm 0.04 \times 10^6$ fibres/g of dry tissue		Rapisarda et al. (2005)

F, female; NR, not reported; yr, year
Compiled by the Working Group

1.5 ≤ magnesium/calcium ≤ 2. Tissue analyses revealed the presence of 14 mineral species in the recovered particulate matter, and most of the minerals isolated from the lungs corresponded to those occurring geologically in the area; 5% of the total mineral species identified from the sheep were from exogenous materials, including man-made mineral fibres, and fluoro-edenite content was identified as 7.5% (2.7% confirmed and 4.8% probable).

Rapisarda et al. (2005) measured the concentration of fluoro-edenite in the lymph nodes because they considered that this site provided a better indication of previous exposure to asbestos than lung parenchymal tissues (Dodson et al., 2000). [Inhaled fibres may be cleared from the lungs by various processes, whereas the fibres that enter the lymph system would be retained and persist in the lymph nodes.] The lymph nodes examined were from the tracheobronchial area and one from the middle mediastinum that drains the lung lobes. Sixty healthy sheep from six flocks that commonly grazed 3 km from the town of Biancavilla were randomly selected together with 10 unexposed (control) sheep. Using light microscopy, SEM, and EDX, the lymph nodes of all of the exposed sheep were found to contain fibres, while none were found in those of the control (unexposed) sheep. Some fibres were identified as fluoro-edenite by their crystallo-chemical characteristics, the dimensions of which were reported as 0.4–1.39 μm in width and 8–41 μm in length; the mean number of fibres was $0.08 \pm 0.04 \times 10^6$ fibres/g of dry tissue.

4.2 Physico-chemical properties associated with toxicity

Because of the similarity between asbestos, fluoro-edenite, and some asbestiform minerals, the physico-chemical properties of mineral fibres associated with toxicity are briefly summarized below, but were reported in detail for asbestos in Volume 100C of the *IARC Monographs* (IARC, 2012).

4.2.1 Crystal structure and chemical composition

Fluoro-edenite exhibits considerable compositional variability, ranging from edenite [$NaCa_2Mg_5Si_7AlO_{22}F_2$] to winchite [$NaCaMg_4(Al,Fe^{3+})Si_8O_{22}(OH)_2$], with a variable content of tremolite [$Ca_2(Mg,Fe^{2+})_5Si_8O_{22}(OH)_2$] (Andreozzi et al., 2009). The variability, which may influence pathogenic potency, has been ascribed to small differences in ambient conditions during the crystallization of the fluorine fibrous amphiboles (Mazziotti-Tagliani et al., 2009).

A set of three fibrous samples (Biancavilla) with variable compositions was tested to assess cytotoxicity using the MTT assay on human lung adenocarcinoma (A549) and human mesothelial (MeT-5A) cells (Pacella, 2009). Both cell lines were cultured in the presence of fibres (50 μg/mL) for 24 and 48 hours. On the basis of the average chemical formula, the three samples were identified as 25% tremolite and 30% winchite (a), 25% tremolite and 20% winchite (b), and 30% tremolite and 30% winchite (c). The iron content ranged from 3.6 to 6.0 wt% as ferrous oxide and the Fe^{3+}/Fe_{total} ratio was 92, 54, and 94% in the three samples, respectively. Despite the differences in composition, the three samples exhibited similar cytotoxic potency towards both cell lines.

Two specimens (length, 30 μm; average diameter, 5 μm) of fluoro-edenite fibres (Biancavilla) with a low (Fe^{3+}, 50%) and a high (Fe^{3+}, 70%)

total content of iron were tested using Met-5A and monocyte-macrophage J774 cells (Cardile et al., 2007). Reduction in cell viability (lactate dehydrogenase release and MTT assay) were investigated together with the induction of the heat shock protein 70, stimulation of reactive oxygen species (ROS) (dichloro-dihydro-fluorescein diacetate fluorescence assay) and nitrogen monoxide formation (analysis of nitrite release). Cells were exposed to 5, 50, or 100 μg of fibres/mL for 72 hours. An iron-free fibrous tremolite was used as a reference sample. High-iron fibres were more potent than low-iron fibres in stimulating ROS release; conversely, the low-iron sample had a remarkably stronger effect on nitrogen monoxide formation. Such differences were more pronounced in J774 macrophages than in Met-5A mesothelial cells. Low-iron fluoro-edenite was slightly more effective than high-iron fluoro-edenite in eliciting an increase in heat shock protein 70 expression in both cell lines and in reducing viability of Met-5A mesothelial cells. Both forms of fluoro-edenite were more potent than tremolite in eliciting all adverse cell responses. The authors inferred that the observed effects were mainly related to the differences in iron content.

Both low- and high-iron fluoro-edenite increased phospholipase C (PLC)β1 and PLCγ1 expression in A549 cells after exposure to 50 μg/mL for 48 hours; low-iron fluoro-edenite was more active than high-iron fluoro-edenite, crocidolite, and tremolite in the induction of PLCγ1 expression (Loreto et al., 2009). PLC expression did not depend on the total iron content of each fibre, but the increased level of PLCβ1 was associated with the highest content of ferrous ions. Both samples also induced the release of tumour necrosis factor (TNF)-α, interleukin (IL)-1β, and IL-6. The induction of cytokines was positively correlated with the total iron content of the fibres in the following order: crocidolite > high-iron fluoro-edenite > low-iron fluoro-edenite > tremolite.

Edenite and fluoro-edenite fibres induced functional modifications (cell motility and distribution of polymerized actin) and the synthesis of vascular endothelial growth factor (VEGF) and β-catenin in A549 and MeT-5A cells. The level of cyclooxygenase (COX-2) and prostaglandin (PGE2) was examined in J774 cells (Pugnaloni et al., 2007). The fibre width ranged from about 1 μm (mostly 0.5 μm) to 2–3 μm (edenite) up to several millimetres (fluoro-edenite), and the length ranged from about 6–80 μm (edenite) up to some hundred micrometres (fluoro-edenite). Differential alteration of cytoplasmic actin networks, cell motility, and the expression of VEGF and β-catenin was observed in treated A549 and MeT-5A cells, according to the different sensitivity of the two cell lines. Exposed J774 cells exhibited a significantly increased expression of COX-2 and PGE2 concentrations. [No information on the role of the two minerals (edenite/fluoro-edenite) was provided.]

4.2.2 Form and size

Fluoro-edenite may have prismatic, acicular, or fibrous properties.

A pilot study (Putzu et al., 2006) on spontaneous sputum as an indicator of exposure to fluoro-edenite fibres was carried out on 12 subjects (age, > 45 years) who had been resident in Biancavilla for at least 30 years. In six subjects, fluoro-edenite fibres ranging between 20 and 40 μm in length, and < 0.5 μm in diameter were observed. Fibres of similar length (8–41 μm) and width (0.4–1.4 μm) were detected in sheep lymph nodes (Rapisarda et al., 2005). Fibres > 5 μm in length were also detected in the lung and pleural tissues of residents of Biancavilla who died from pleural mesothelioma (Paoletti & Bruni, 2009); 95% and 98% of the fibres found in the lung and pleura were > 5 μm in length, respectively.

Travaglione et al. (2006) showed that fibrous fluoro-edenite (average length, 15.5 μm; average diameter, 0.45 μm) can induce multinucleation and spreading, which are common features related to cellular transformation, in A549 cells in contrast with prismatic (length, 20 μm; diameter, nearly 3 μm) fluoro-edenite (Travaglione et al., 2003).

Both prismatic fluoro-edenite and fibrous fluoro-edenite were cytotoxic. The cytotoxicity induced by prismatic fluoro-edenite was not accompanied by changes in morphology (Travaglione et al., 2003); in contrast, fibrous fluoro-edenite produced dramatic changes in cell morphology, similar to those caused by crocidolite (Travaglione et al., 2006).

Both prismatic and fibrous fluoro-edenite promoted the secretion of IL-6 [a multifunctional cytokine with immuno-regulatory and pro-inflammatory effects], within 48 hours of exposure; the fibrous form showed greater potency (Travaglione et al., 2003, 2006).

Fibrous, but not prismatic, fluoro-edenite induced mesotheliomas in Sprague-Dawley rats after intraperitoneal administration (Soffritti et al., 2004). The fibrous sample contained 25–30% of fluoro-edenite fibres [diameter, 0.5–1 μm; length > 10 μm] in addition to feldspars, haematite, and pyroxenes. [No information on the features of the prismatic sample was provided.]

The cytotoxicity of two samples of fluoro-edenite with a diameter of < 1 μm (200–600 nm) and acicular-fibrous morphology, with an average length of ~50 μm, or filamentous-asbestiform morphology, with a length of up to 150 μm, was compared in A549 and in MeT-5A cells. Both cell lines were cultured in presence of 50 μg/mL of fibres for 24 and 48 hours, and cell viability was evaluated using the MTT assay. All samples reduced the time-dependent loss of cell viability, but no significant differences in potency were noted (Pacella, 2009).

4.2.3 Surface reactivity

Fantauzzi et al. (2012) compared samples of fibres from Biancavilla and Libby, MT, USA. Comparison of the oxidation state (X-ray photo-electron spectroscopy) of surface iron with that of bulk iron revealed that the sample with the lowest bulk iron oxidation state was the most affected by surface oxidation. Biancavilla samples were highly heterogeneous (tremolite and winchite; see Section 4.2.1 samples (a) and (c); Pacella, 2009). Both samples had comparable iron content but with different oxidation states at the surface. Sample (a) had both ferrous and ferric ions ($Fe^{2+}/Fe_{total} = 0.13$) and sample (c) had only fully oxidized iron. On both surfaces, ferric ions were predominantly in the form of oxyhydroxide (Fe^{3+}_{hydr}), formed by weathering of the silicate surface: $Fe^{3+}_{ox}/Fe_{total} = 0.33$ and $Fe^{3+}_{hydr}/Fe_{total} = 0.54$ for sample (a), and $Fe^{3+}_{ox}/Fe_{total} = 0.13$ and $Fe^{3+}_{hydr}/Fe_{total} = 0.87$ for sample (c).

(a) Generation of free radicals

Surface reactivity was investigated by the production of hydroxyl (HO·) radicals released in the presence of hydrogen peroxide using the spin trapping technique (Fantauzzi et al., 2012). The two specimens from Biancavilla showed no significant difference in the production of HO· radicals, but produced less HO· than the Libby amphibole; crocidolite asbestos was used as a positive control. [The Working Group noted that HO· release was evaluated at equal mass, but no data on the surface area of fluoro-edenite were provided.]

A quarry rock dust (Brunauer–Emmett–Teller area = 0.5 m²/g) and a house plaster dust (Brunauer–Emmett–Teller area = 4.4 m²/g) from Biancavilla were tested for their ability to generate HO· radicals using the deoxyribose assay (Rapisarda et al., 2003). Both samples contained fluoro-edenite fibres and other minerals, including feldspar, quartz, haematite, ilmenite, and fluoro-apatite. The content of fluoro-edenite was not quantified but the authors noted that the quarry rock dust was richer in fluoro-edenite than the house plaster dust. The two samples, tested at an equal surface area (doses ranging from 2.5 cm²/mL to 60 cm²/mL), generated HO· and the quarry rock dust was more reactive than the house dust.

(b) Bioavailability and biodeposition of metals

No data were available to the Working Group.

4.2.4 Fibre durability

No data on fibre durability (leaching, phagocytosis, dissolution, or breakage) were available to the Working Group.

4.3 Genetic and related effects

DNA strand breaks (assessed using the alkaline comet assay) were elevated in primary human lung fibroblasts, immortalized human lung adenocarcinoma (A549) cells, and mouse monocyte-macrophage (J774) cells exposed to 5–100 µg/mL of fluoro-edenite (Biancavilla) for 72 hours (Cardile et al., 2004b).

4.4 Other mechanistic data relevant to carcinogenesis

4.4.1 Release of cytokines, chemokines, and growth factors

(a) Experimental animals

Apoptosis was investigated in the lungs of healthy sheep grazing near Biancavilla through the detection of TNF-related apoptosis-inducing ligand (TRAIL) and its death receptor, DR5, and through the expression and localization of collagenases-3 (matrix metalloproteinase, MMP-13) [MMP-13 is an extracellular matrix component that plays an important role in the remodelling of the lung in inflammatory diseases]. The results

showed that MMP-13 was overexpressed, mainly in fibroblasts and epithelial cells, while positivity for TRAIL and DR5 was detected on alveolar cell surfaces and in the vascular stroma. In the lungs of sheep exposed to fluoro-edenite, the expression of the TRAIL receptor was most pronounced in areas of inflammatory cell infiltration and active fibrosis, revealed by the expression of MMP-13. These changes may reflect the activation of apoptotic processes through exposure to fluoro-edenite (Martinez et al., 2006). [TRAIL selectively induces apoptosis in a variety of tumour and transformed cells, but not in most normal cells (Wang & El-Deiry, 2003).]

(b)   Experimental systems in vitro

Using the mouse monocyte-macrophage J774 cell line, Pugnaloni et al. (2007) found time-dependent increased expression of COX-2 and release of PGE2 after exposure to fluoro-edenite fibres (Monte Calvario) and edenite fibres with a wide range of diameters (from 0.5 µm to several micrometres) and lengths (6 µm to several hundred micrometres). Exposure to fluoro-edenite also increased the expression of VEGF in human lung adenocarcinoma A549 cells and in the immortalized human mesothelial Met-5A cell line, as assessed by immunocytochemistry (Pugnaloni et al., 2007). Exposure of J774 macrophages or Met-5A cells to two types of fluoro-edenite fibre from Biancavilla (sample 19, low-iron (50% Fe^{3+}) or sample 27, high-iron (about 70% Fe^{3+}); length, 30 µm; diameter, ~ 5 µm) also induced the generation of ROS as indicated by dichlorofluorescein fluorescence and extracellular release of nitrite (Cardile et al., 2007). In J774 macrophages, exposure to fluoro-edenite (Biancavilla) in combination with lipopolysaccharide significantly enhanced the release of nitrite and increased the expression of inducible nitric oxide synthase (Cardile et al., 2004a).

Travaglione et al. (2003, 2006) compared the response of the human lung adenocarcinoma (A549) cell line to prismatic or fibrous forms of fluoro-edenite (Monte Calvario) compared with crocidolite asbestos fluoro-edenite fibres. Prismatic fibres (length, 20 µm; diameter, ~3 µm) were taken up by the cells and induced the cellular release of the cytokine IL-6 after 24–72 hours [no reference particles were included in this study] (Travaglione et al., 2003). Fibrous fluoro-edenite (length, 15.5 µm; diameter, 0.45 µm), as well as standard crocidolite asbestos fibres (NIOSH, USA) as a positive reference, at equivalent toxic doses were taken up by the cells resulting in a time-dependent release of the cytokines IL-6 and IL-8 (Travaglione et al., 2006). Loreto et al. (2009) confirmed the release of cytokines (IL-1β, TNF-α, and IL-6) from A549 cells after exposure to two samples of fluoro-edenite (sample 19, low-iron, or sample 27, high-iron) from Biancavilla, tremolite, or crocidolite asbestos fibres (OSHA standard) at a dose of 50 µg/mL for 48 hours.

4.4.2 Apoptosis

(a)   Experimental animals

Programmed cell death in vivo was investigated by analysing the immuno-expression of bax protein and bcl-2 oncoprotein (which are involved in the early stages of apoptosis), caspase 3, poly (ADP-ribose) polymerase, and DNA fragmentation in lung tissues from sheep grazing near Biancavilla (Loreto et al., 2008). The results showed epithelial and interstitial overexpression of bax, especially in cells that were directly in contact with the fibres, and negative bcl-2 immuno-expression. Terminal deoxynucleotidyl transferase dUTP nick end labelling-positive cells characteristic of apoptosis were detected in the alveoli and in areas of fibrosis. [These data suggested an increase in the concentration of bax homodimers that enable apoptosis and were in agreement with the findings of Narasimhan et al. (1998), who documented nearly absent bcl-2 expression and uniform bax expression in malignant pleural mesothelioma cell lines. Plataki et al. (2005) found an increased expression

of pro-apoptotic and a reduced expression of anti-apoptotic molecules in epithelial cells from diseased lungs that may be responsible for inadequate and delayed re-epithelialization, which in turn contributes to fibroblast proliferation. Some evidence has also suggested that apoptosis is directly involved in the loss of alveolar epithelial cells (Yokohori et al., 2004). Recent studies indicated that epithelial apoptosis could be a key profibrotic event in lung fibrogenesis (Li et al., 2004), and that tumour growth is a result of cell resistance to apoptotic death (Niehans et al., 1997).]

[These results support the hypothesis that apoptosis is an important mechanism for removing cells with irreparable fluoro-edenite-induced genetic changes that may result in a predisposition to the development of neoplasia.]

(b)   Experimental systems in vitro

The exposure of several lung target cells (primary human fibroblasts, human lung adenocarcinoma A549 cells, murine monocyte-macrophage J774 cells, or Met-5A mesothelial cells) to fibrous fluoro-edenite from Monte Calvario (Travaglione et al., 2006), or Biancavilla (Cardile et al., 2004b), decreased cell viability, increased the intracellular generation of ROS, as indicated by dichlorofluorescein fluorescence, decreased mitochondrial activity, as indicated by the MTT assay, and induced plasma membrane damage, as indicated by the extracellular release of lactate dehydrogenase.

When compared on a mass basis, crocidolite asbestos fibres (OSHA standard) were more toxic at doses between 5 and 100 µg/mL after 24–72 hours (Cardile et al., 2007). Fluoro-edenite fibres (sample 19, low-iron, or sample 27, high-iron; Biancavilla) were more potent than fibrous tremolite (Val di Susa, Piemonte, Italy) in inducing the generation of ROS and mitochondrial and plasma membrane damage; fluoro-edenite sample 19 was more potent than fluoro-edenite sample 27 in inducing plasma membrane damage in mesothelial Met-5A cells. All of the fibrous minerals induced the expression of heat shock protein 70 as a marker of a generalized stress-response pathway (Cardile et al., 2007). Exposure of A549 cells to fibrous fluoro-edenite (Monte Calvario) or standard crocidolite asbestos fibres (NIOSH, USA) induced time-dependent decreases in viability assessed by trypan blue exclusion, but no induction of apoptosis or altered expression of the pro-apoptotic protein, Bax, or the anti-apoptotic proteins, Bcl-2 or Bcl-X$_L$, were detected (Travaglione et al., 2006).

4.4.3 Activation of intracellular signalling pathways

Human cells in vitro

Loreto et al. (2009) demonstrated that exposure to fluoro-edenite samples 19 and 27 (low- and high-iron, respectively) from Biancavilla, tremolite, or crocidolite asbestos fibres induced PLCγ1 and -β1 protein expression in lung adenocarcinoma A549 cells; [this enzyme activates the signalling pathway that leads to the mobilization of intracellular calcium and activation of protein kinase C].

4.4.4 Cell proliferation

Human cells in vitro

Exposure of human lung adenocarcinoma A549 cells to the prismatic (Travaglione et al., 2003) or fibrous (Travaglione et al., 2006) forms of fluoro-edenite (Monte Calvario) reduced cell proliferation for up to 72 hours with no disruption in cell-cycle progression, as assessed by flow cytometry. Neither fibrous fluoro-edenite nor standard crocidolite asbestos fibres (NIOSH, USA) altered the expression of p53, p21, or cyclin D1, as assessed by Western blot (Travaglione et al., 2006).

4.4.5 Formation of granulomas and fibrosis

Experimental animals

Histopathological examination of the lung tissues collected from healthy sheep grazing near a town in the eastern region of Sicily where environmental exposure to fluoro-edenite was reported to occur revealed fibrosis, including the loss of alveolar architecture with honeycombing that are characteristic of the final stage of fibrosis (Martinez et al., 2006).

4.4.6 Activation of oncogenes and inactivation of tumour-suppressor genes

(a)   Experimental animals

The lungs of 10 ewes grazing 3 km from Biancavilla and 10 ewes grazing approximately 30 km from the local stone quarry were examined for apoptotic cell death in situ and the expression of Bax. Microscopic analyses detected the presence of fluoro-edenite fibres in the lungs of the exposed sheep. Focal Bax overexpression was observed in the alveolar epithelium and interstitium, particularly in alveolar epithelial cells in close contact with the fibres, and in the mucosal epithelium lining the terminal bronchioles. Increased expression of tumour-suppressor genes and Bax are consistent with increased apoptosis, as confirmed by the increased expression of caspase 3 and poly (ADP-ribose) polymerase immunoreactivity (Loreto et al., 2008).

The lungs of 10 sheep grazing 3 km from Biancavilla and 10 ewes grazing approximately 30 km from the local stone quarry were examined immunohistochemically for the expression of unphosphorylated (Rb) and phosphorylated (pRb) proteins. Microscopic analyses detected the presence of fibres in the lungs of exposed animals and pRb was overexpressed in the lungs of exposed sheep, especially in the cytoplasm of fibroblasts and epithelial cells, in comparison with those of control animals. pRb overexpression was also detected in the alveolar epithelium and in the interstitium, especially in proximity to the fluoro-edenite fibres in the tissues, whereas Rb immunostaining was faint or absent (Musumeci et al., 2010). [These data suggested that the altered balance between pRb and Rb expression could favour the upregulation of the *RB* tumour-suppressor gene.]

(b)   Human cells in vitro

The expression of several oncogenes and tumour-suppressor genes (cyclin D1, p21$^{WAF1/CIP1}$, and p53) and pro- and anti-apoptotic genes was studied immunohistochemically in human lung carcinoma A549 cells exposed to fluoro-edenite or to NIOSH crocidolite fibres (Travaglione et al., 2006). No change in the levels of expression of p53, p21$^{WAF1/CIP1}$, or cyclin D1 was found. The number of viable epithelial cells was decreased, but the loss of cell viability was not associated with apoptosis, as demonstrated by flow cytometry and the absence of changes in the expression of Bax, Bcl-2, and Bcl-X$_L$. [These results demonstrated no alterations in the expression of oncogenes and tumour-suppressor genes under these experimental conditions.]

Human immortalized mesothelial MeT-5A and human lung adenocarcinoma A549 cells were incubated with fluoro-edenite at concentrations of 10, 50, and 100 µg/mL (2.12, 10.6, and 21.2 µg/cm^2) and the expression of several proteins involved in cell-cycle regulation (Rb [unphosphorylated Rb], pRb [phosphorylated Rb], p27, and cyclin D1) was studied by Western blot analysis. In A549 cells, the two higher concentrations induced greater pRb expression in comparison with control cultures. In Met-5A cells, increased pRb expression was induced at the highest concentration only. The expression of cyclin D1, the product of the oncogene *CCND1*, was significantly increased in both A549 and Met-5A cells exposed to 50 and 100 µg/mL. Fluoro-edenite reduced the expression of p27^{Kip1}, a negative regulator of cell-cycle progression

at G1 ([Musumeci et al., 2011](#)). [These results suggested that Rb phosphorylation could be upregulated to counteract the stimulation of cell-cycle progression.]

4.4.7 Other mechanisms lacking evidence

No data on inflammasome activation, persistent inflammation, resistance to apoptosis, or depletion of antioxidants were available to the Working Group.

4.5 Susceptible populations

No data were available to the Working Group.

4.6 Mechanistic considerations

The environmental exposure of sheep to fluoro-edenite leads to the deposition and retention of these fibres in the lungs. Fluoro-edenite samples from Biancavilla can generate hydroxyl radicals directly in acellular assays. In-vitro exposure to fluoro-edenite induces DNA breaks and is associated with cytokine release in human epithelial cells and fibroblasts, and murine monocyte-macrophages. Overall, there is a paucity of mechanistic data for the carcinogenicity of fluoro-edenite.

5. Summary of Data Reported

5.1 Exposure data

Fluoro-edenite fibrous amphiboles – a new end-member of the calcic amphibole group composed of most fluoro-edenite – have been identified in the volcanic products of Mount Etna near Biancavilla in Sicily, Italy, and represent the first occurrence of amphibole fibres in a volcanic environment; a "fluoro-edenite" compound was also found in the lava dome of the Kimpo volcano, Kumamoto, Japan. Fluoro-edenite is found as prismatic or acicular crystals or as asbestiform (fibrous) fibres.

The composition of samples of the amphibole fibres from Biancavilla included fluoro-edenite (60%), winchite (24%), tremolite (12%), and richterite (4%). The variable chemical composition of fluoro-edenite and the presence of different components complicate the classification of these fibres and the definition of their mineral species.

Fluoro-edenite and the associated fibrous amphiboles from Biancavilla occur naturally, and early environmental investigations identified the source as local quarry products that had been used in building materials for local structures since at least the 1950s. Unpaved roads made from the local quarry products have also been recognized as a primary source for airborne fluoro-edenite fibres.

Comparison of outdoor air samples taken before mitigation efforts were begun in 2000 with those taken in 2013 showed that mean amphibole concentrations have diminished from 1.76 fibres/L to 0.1 fibres/L. Indoor air may also be contaminated from the use of local quarry products in plaster and mortar. Few data are available to determine the occurrence of fluoro-edenite fibres in water supplies in and around Biancavilla other than one study, in which all 10 samples taken from several local wells and springs were reported to contain fluoro-edenite fibres. Analysis of samples of top soil and roadside dust in Biancavilla showed that approximately 90% of samples contained fluoro-edenite fibres.

5.2 Human carcinogenicity data

An excess of mortality from and incidence of mesothelioma has been documented in several surveillance studies in the Biancavilla municipality of Sicily, Italy, where exposure to fluoro-edenite from naturally occurring sources has been found. Although the exposure assessments were essentially ecological in nature, these studies provided strong evidence for a causal

association for several reasons. First, the magnitude of the rate ratios for mesothelioma was large and statistically stable, and thus chance is unlikely to explain these findings. Second, most of these cases did not have any history of occupational or environmental exposure to asbestos. Approximately 70–90% of cases of mesothelioma in the general population are believed to be attributable to exposure to asbestos; therefore, the fact that the majority of the cases in Biancavilla had no known exposure to asbestos strongly suggests another local exposure. The excess observed was similar in both sexes and was most prominent in young adults, which strongly indicates an environmental rather than an occupational cause. Finally, the cases were identified through a national surveillance programme using standardized procedures and their diagnoses were based on extensive pathological review; thus biases of ascertainment and diagnosis are unlikely to explain the findings.

The findings for cancer of the lung were much weaker than those for mesothelioma. A modest excess of mortality from cancer of the lung was observed in women and a modest deficit was observed in men, both with wide confidence intervals. The lack of any strong evidence of an effect on cancer of the lung may reflect that, in contrast to mesothelioma, the background rate of lung cancer is high and its causes are multiple. Furthermore, several studies of environmental exposure to asbestos in other countries have also failed to demonstrate an excess of lung cancer. The Working Group considered that the evidence for carcinogenicity in the lung was inadequate because of the small number of studies, the weak indication of an association, and the lack of controls for potential confounding.

5.3   Animal carcinogenicity data

The carcinogenicity of fluoro-edenite fibrous amphibole has been investigated in only one study in experimental animals. Intraperitoneal injection of fibrous fluoro-edenite caused a significant increase in the incidence of mesothelioma in male and female rats. In the same study, intrapleural injection of fluoro-edenite resulted in a high incidence of mesotheliomas in male and female rats relative to historical controls from that laboratory.

5.4   Mechanistic and other relevant data

Fluoro-edenite is biopersistent in the lungs of sheep and is detected in the sputum of exposed humans. In-vitro exposure to fluoro-edenite induces DNA breaks and is associated with the release of cytokines in human epithelial cells and fibroblasts, and murine monocyte-macrophages. The available studies are consistent with the mechanisms proposed for fibre carcinogenicity (see IARC, 2012). Overall, the mechanistic data for the carcinogenicity of fluoro-edenite are moderate.

6.   Evaluation

6.1   Cancer in humans

There is *sufficient evidence* in humans for the carcinogenicity of fluoro-edenite fibrous amphibole. Fluoro-edenite fibrous amphibole causes mesothelioma.

6.2   Cancer in experimental animals

There is *sufficient evidence* in experimental animals for the carcinogenicity of fluoro-edenite fibrous amphibole.

6.3   Overall evaluation

Fluoro-edenite fibrous amphibole is *carcinogenic to humans (Group 1).*

References

Andreozzi GB, Ballirano P, Gianfagna A, Mazziotti-Tagliani S, Pacella A (2009). Structural and spectroscopic characterization of a suite of fibrous amphiboles with high environmental and health relevance from Biancavilla (Sicily, Italy). *Am Mineral*, 94(10):1333–40. doi:10.2138/am.2009.3214

Bégin R, Rola-Pleszczynski M, Sirois P, Masse S, Nadeau D, Bureau MA (1981). Sequential analysis of the broncho-alveolar milieu in conscious sheep. *J Appl Physiol Respir Environ Exerc Physiol*, 50(3):665–71. PMID:7251456

Belpoggi F, Tibaldi E, Lauriola M, Bua L, Falcioni L, Chiozzotto D, et al. (2011). The efficacy of long-term bioassays in predicting human risks: mesotheliomas induced by fluoro-edenitic fibres present in lava stone from Etna volcano in Biancavilla Italy. *Eur J. Oncol*, 16:185–95.

Bruni BM, Pacella A, MazziottiTagliani S, Gianfagna A, Paoletti L (2006). Nature and extent of the exposure to fibrous amphiboles in Biancavilla. *Sci Total Environ*, 370(1):9–16. doi:10.1016/j.scitotenv.2006.05.013 PMID:16806404

Bruni BM, Soggiu ME, Marsili G, Brancato A, Inglessis M, Palumbo L, et al. (2014). Environmental concentrations of fibers with fluoro-edenitic composition and population exposure in Biancavilla (Sicily, Italy). *Ann Ist Super Sanita*, 50(2):119–26. PMID:24968909

Bruno C, Comba P, Zona A (2006). Adverse health effects of fluoro-edenitic fibers: epidemiological evidence and public health priorities. *Ann N Y Acad Sci*, 1076(1):778–83. doi:10.1196/annals.1371.020 PMID:17119254

Bruno C, Tumino R, Fazzo L, Cascone G, Cernigliaro A, De Santis M, et al. (2014). Incidence of pleural mesothelioma in a community exposed to fibres with fluoro-edenitic composition in Biancavilla (Sicily, Italy). *Ann Ist Super Sanita*, 50(2):111–8. PMID:24968908

Burragato F, Comba P, Baiocchi V, Palladino DM, Simei S, Gianfagna A, et al. (2005). Geo-volcanological, mineralogical and environmental aspects of quarry materials related to pleural neoplasm in the area of Biancavilla, Mount Etna (Eastern Silicy, Italy). *Environ Geol*, 47(6):855–68. doi:10.1007/s00254-004-1217-7

Cardile V, Lombardo L, Belluso E, Panico A, Renis M, Gianfagna A, et al. (2007). Fluoro-edenite fibers induce expression of Hsp70 and inflammatory response. *Int J Environ Res Public Health*, 4(3):195–202. doi:10.3390/ijerph2007030001 PMID:17911657

Cardile V, Proietti L, Panico A, Lombardo L (2004a). Nitric oxide production in fluoro-edenite treated mouse monocyte-macrophage cultures. *Oncol Rep*, 12(6):1209–15. PMID:15547739

Cardile V, Renis M, Scifo C, Lombardo L, Gulino R, Mancari B, et al. (2004b). Behaviour of the new asbestos amphibole fluor-edenite in different lung cell systems. *Int J Biochem Cell Biol*, 36(5):849–60. doi:10.1016/j.biocel.2003.09.007 PMID:15006637

Cernigliaro A, Marras A, Addario SP, Scondotto S (2013). [Stato di salute della popolazione residente nelle aree a rischio ambientale e nei siti di interesse nazionale per le bonifiche della Sicilia. Analisi dei dati ReNCaM (anni 2004-2011) e dei ricoveri ospedalieri (anni 2007–2011). Rapporto 2012. Supplemento numero monografico notiziario gennaio 2013; pp. 1–76.] Regione Siciliana, Sicily: OE Notiziario dell'Osservatorio Epidemiologico Regionale. Available from: http://nomuos.org/documents/stato_salute_popolazione_Gela-Niscemi-Butera_2012.pdf, accessed 2 October 2014. [Italian]

Comba P, Gianfagna A, Paoletti L (2003). Pleural mesothelioma cases in Biancavilla are related to a new fluoro-edenite fibrous amphibole. *Arch Environ Health*, 58(4):229–32. doi:10.3200/AEOH.58.4.229-232 PMID:14655903

Conti S, Minelli G, Manno V, Iavarone I, Comba P, Scondotto S, et al. (2014). Health impact of the exposure to fibres with fluoro-edenitic composition on the residents in Biancavilla (Sicily, Italy): mortality and hospitalization from current data. *Ann Ist Super Sanita*, 50(2):127–32. PMID:24968910

DeNardo P, Bruni B, Paoletti L, Pasetto R, Sirianni B (2004). Pulmonary fibre burden in sheep living in the Biancavilla area (Sicily): preliminary results. *Sci Total Environ*, 325(1-3):51–8. doi:10.1016/j.scitotenv.2003.11.018 PMID:15144777

Di Paola M, Mastrantonio M, Carboni M, et al. (1996). [Mortality from malignant pleural neoplasms in Italy in the years 1988–1992.] Rapporti ISTISAN 96/40. Rome, Italy: Istituto Superiore di Sanità. [Italian]

Dodson RF, Huang J, Bruce JR (2000). Asbestos content in the lymph nodes of nonoccupationally exposed individuals. *Am J Ind Med*, 37(2):169–74. doi:10.1002/(SICI)1097-0274(200002)37:2<169::AID-AJIM2>3.0.CO;2-V PMID:10615097

Famoso D, Mangiameli M, Roccaro P, Mussumeci G, Vagliasindi FGA (2012). Asbestiform fibers in the Biancavilla site of national interest (Sicily, Italy): review of environmental data via GIS platforms. *Rev Environ Sci Biotechnol*, 11(4):417–27. doi:10.1007/s11157-012-9284-9

Fantauzzi M, Pacella A, Fournier J, Gianfagna A, Andreozzi GB, Rossi A (2012). Surface chemistry and surface reactivity of fibrous amphiboles that are not regulated as asbestos. *Anal Bioanal Chem*, 404(3):821–33. doi:10.1007/s00216-012-6190-5 PMID:22763717

Fazzo L, De Santis M, Minelli G, Bruno C, Zona A, Marinaccio A, et al. (2012). Pleural mesothelioma mortality and asbestos exposure mapping in Italy. *Am J Ind Med*, 55(1):11–24. doi:10.1002/ajim.21015 PMID:22025020

Gianfagna A, Andreozzi GB, Ballirano P, Mazziotti-Tagliani S, Bruni BM (2007). Structural and chemical

Contrasts between prismatic and fibrous fluoro-edenite from Biancavilla, Sicily, Italy. *Can Mineral*, 45(2):249–62. doi:10.2113/gscanmin.45.2.249

Gianfagna A, Ballirano P, Bellatreccia F, Bruni B, Paoletti L, Oberti R (2003). Characterization of amphibole fibres linked to mesothelioma in the area of Biancavilla, eastern Sicily, Italy. *Min Mag (Lond)*, 67(6):1221–9. doi:10.1180/0026461036760160

Gianfagna A, Oberti R (2001). Fluoro-edenite from Biancavilla (Catania, Sicily, Italy): Crystal chemistry of a new amphibole end-member. *Am Mineral*, 86(11-12):1489–93. doi:10.2138/am-2001-11-1217

IARC (2012). Arsenic, metals, fibres, and dusts. *IARC Monogr Eval Carcinog Risks Hum*, 100C:1–499. Available from: http://monographs.iarc.fr/ENG/Monographs/vol100C/index.php PMID:23189751

INAIL (2010). Mesothelioma National Register (Article 36, D.Lgs.n°277/91–Dpcm 308/02). Guidelines for the identification and definition of malignant mesothelioma cases and the transmission to ISPESL by Regional Operating Centres. Rome, Italy: Istituto nazionale Assicurazione Infortuni sul Lavoro (INAIL). Available from: http://www.ispesl.it/dml/leo/download/RenamGuidelines. [Italian]

INS-Europa (2014). Fluoro-edenite mineral data. Barcelona, Spain: Institut Europa (INS-Europa). Available from: http://www.ins-europa.org/mineralia/php-scripts/Alphabetical/Fitxes/FitxaFrame.php?Id=3692&Mineral=Fluoro-edenite, accessed 18 July 2014.

Jambor JL, Kovalenker VA, Roberts A (1999). New Mineral Names. *Am Mineral*, 84:1685–8.

Leake BE, Woolley AR, Arps CES, Birch WD, Gilbert MC, Grice JD, et al. (1997). Nomenclature of amphiboles: report of the Subcommittee on Amphiboles of the International Mineralogical Association, Commission on New Minerals and Mineral names. *Can Mineral*, 35:219–46.

Li X, Shu R, Filippatos G, Uhal BD (2004). Apoptosis in lung injury and remodeling. *J Appl Physiol (1985)*, 97(4):1535–42. doi:10.1152/japplphysiol.00519.2004 PMID:15358756

Loreto C, Carnazza ML, Cardile V, Libra M, Lombardo L, Malaponte G, et al. (2009). Mineral fiber-mediated activation of phosphoinositide-specific phospholipase c in human bronchoalveolar carcinoma-derived alveolar epithelial A549 cells. *Int J Oncol*, 34(2):371–6. PMID:19148471

Loreto C, Rapisarda V, Carnazza ML, Musumeci G, Valentino M, Fenga C, et al. (2008). Fluoro-edenite fibres induce lung cell apoptosis: an in vivo study. *Histol Histopathol*, 23(3):319–26. PMID:18072089

Makino K, Yamaguchi Y, Tomita K (1996). Fluor edenite from the Ishigamiyama lava dome of the Kimpo volcano, Kumamoto, southwest Japan. *GANKO*, 91:419–23.

Maltoni C, Minardi F (1989). Recent results of carcinogenicity biassays of fibres and other particulate materials. In: Bignon J, Pato J, Saracci R editors. Non-occupational exposure to mineral fibres. Lyon. *IARC Scientific Publications*. Volume 90: pp. 46–53.

Manna P, Comba P (2001). [Asbestos risk: communicating with health authorities and the public : the case of Biancavilla (CT).] *Epidemiol Prev*, 25(1):28–30. [Italian] PMID:11296533

Martinez G, Loreto C, Rapisarda V, Masumeci G, Valentino M, Carnazza ML (2006). Effects of exposure to fluoro-edenite fibre pollution on the respiratory system: an in vivo model. *Histol Histopathol*, 21(6):595–601. PMID:16528669

Mastrantonio M, Belli S, Binazzi A, et al. (2002). La mortalità per tumore maligno della pleura nei comuni italiani (1988–1997). Rapporti Istisan 02/12. [Italian]

Mazziotti-Tagliani S, Andreozzi GB, Bruni BM, et al. (2009). Quantitative chemistry and compositional variability of fluorine fibrous amphiboles from Biancavilla (Sicily, Italy). *Period Mineral*, 78:65–74.

Meeker GP, Bern AM, Brownfield IK, Lowers HA, Sutley SJ, Hoefen TM, et al. (2003). the composition and morphology of amphiboles from the rainy creek complex, near Libby, Montana. *Am Mineral*, 88(11-12):1955–69. doi:10.2138/am-2003-11-1239

Mindat (2014). Fluoro-edenite. Hudson Institute of Mineralogy. Available from: http://www.mindat.org/min-6950.html, accessed 18 July 2014.

Musumeci G, Cardile V, Fenga C, Caggia S, Loreto C (2011). Mineral fibre toxicity: expression of retinoblastoma (Rb) and phospho-retinoblastoma (pRb) protein in alveolar epithelial and mesothelial cell lines exposed to fluoro-edenite fibres. *Cell Biol Toxicol*, 27(3):217–25. doi:10.1007/s10565-011-9183-9 PMID:21327865

Musumeci G, Loreto C, Cardile V, Carnazza ML, Martinez G (2010). Immunohistochemical expression of retinoblastoma and phospho-retinoblastoma protein in sheep lung exposed to fluoro-edenite fibers. *Anat Sci Int*, 85(2):74–8. doi:10.1007/s12565-009-0059-5 PMID:19680741

Narasimhan SR, Yang L, Gerwin BI, Broaddus VC (1998). Resistance of pleural mesothelioma cell lines to apoptosis: relation to expression of Bcl-2 and Bax. *Am J Physiol*, 275(1 Pt 1):L165–71. PMID:9688948

Niehans GA, Brunner T, Frizelle SP, Liston JC, Salerno CT, Knapp DJ, et al. (1997). Human lung carcinomas express Fas ligand. *Cancer Res*, 57(6):1007–12. PMID:9067260

NIOSH (1994a). NIOSH Manual of Analytical Methods. 4th Edition, Method No. 7402. Cincinnati (OH), USA: National Institute for Occupational Safety and Health.

NIOSH (1994b). NIOSH Manual of Analytical Methods. 4th Edition, Method No. 9000. Cincinnati (OH), USA: National Institute for Occupational Safety and Health.

NIOSH (2011). Current Intelligence Bulletin 62, Asbestos Fibers and Other Elongate Mineral Particles: State of the Science and Roadmap for Research. DHHS (NIOSH) Publication No. 2011–159. Cincinnati (OH), USA: National Institute for Occupational Safety and Health.

Pacella A (2009). Crystal chemistry and reactivity of fibrous amphiboles of environmental and health interest [PhD Thesis]. Rome, Italy: Sapienza University of Rome, Department of Earth Sciences; Paris, France: University Pierre et Marie Curie, Paris 6, Laboratory of Surface Reactivity.

Paoletti L, Batisti D, Bruno C, Di Paola M, Gianfagna A, Mastrantonio M, et al. (2000). Unusually high incidence of malignant pleural mesothelioma in a town of eastern Sicily: an epidemiological and environmental study. *Arch Environ Health*, 55(6):392–8. doi:10.1080/00039890009604036 PMID:11128876

Paoletti L, Bruni BM (2009). [Size distribution of amphibole fibres from lung and pleural tissues sampled from mesothelioma cases due to environmental exposure.] *Med Lav*, 100(1):11–20. PMID:19263868

Pirastu R, Ricci P, Comba P, Bianchi F, Biggeri A, Conti S, et al. (2014). SENTIERI - Epidemiological Study of Residents in National Priority Contaminated Sites: mortality, cancer incidence and hospital discharges. *Epidemiol Prev*, 38(2 Suppl 1):43–7. Available from: http://www.epiprev.it/materiali/2014/EP2/S1/EPv38i2S1_SENTIERIind.pdf PMID:24986501

Pirastu R, Zona A, Ancona C, Bruno C, Fano V, Fazzo L, et al. (2011). [Mortality results in SENTIERI Project.] *Epidemiol Prev*, 35(5-6 Suppl 4):29–152. [Italian] PMID:22166295

Plataki M, Koutsopoulos AV, Darivianaki K, Delides G, Siafakas NM, Bouros D (2005). Expression of apoptotic and antiapoptotic markers in epithelial cells in idiopathic pulmonary fibrosis. *Chest*, 127(1):266–74. doi:10.1378/chest.127.1.266 PMID:15653994

Pugnaloni A, Lucarini G, GiantomassI F, Lombardo L, Capella S, Belluso E, et al. (2007). In vitro study of biofunctional indicators after exposure to asbestos-like fluoro-edenite fibres. *Cell Mol Biol (Noisy-le-grand)*, 53(Suppl):OL965–80. PMID:17695086

Putzu MG, Bruno C, Zona A, Massiccio M, Pasetto R, Piolatto PG, et al. (2006). Fluoro-edenitic fibres in the sputum of subjects from Biancavilla (Sicily): a pilot study. *Environ Health*, 5(1):20. doi:10.1186/1476-069X-5-20 PMID:16780574

Rapisarda V, Amati M, Coloccini S, Bolognini L, Gobbi L, Duscio D (2003). [The in vitro release of hydroxyl radicals from dust containing fluoro-edenite fibers identified in the volcanic rocks of Biancavilla (eastern Sicily).] *Med Lav*, 94(2):200–6. PMID:12852202

Rapisarda V, Rapisarda G, Vico GD, Gobbi L, Loreto C, Valentino M (2005). Monitoring of fluoro-edenite fibre pollution through the study of sheep lymph nodes as a model of a biological indicator. *Occup Environ Med*, 62(9):656. doi:10.1136/oem.2005.020727 PMID:16109823

Regione Sicilia (2014). [Regione Sicilia Dipartimento Attività Sanitarie e Osservatorio Epidemiologico Sistema di Sorveglianza PASSI Rapporto Regionale 2009–2012; Notiziario OE Supplemento Monografico Luglio.] Available from: http://pti.regione.sicilia.it/portal/page/portal/PIR_PORTALE/PIR_LaStrutturaRegionale/PIR_AssessoratoSalute/PIR_AreeTematiche/PIR_Epidemiologia/PIR_PASSI2005. [Italian]

Soffritti M, Minardi F, Bua L, Degli Esposti D, Belpoggi F (2004). First experimental evidence of peritoneal and pleural mesotheliomas induced by fluoro-edenite fibres present in Etnean volcanic material from Biancavilla (Sicily, Italy). *European J Oncol*, 9:169–75.

Tomita K, Makino K, Yamaguchi Y (1994). Fluor-edenite: its occurrence and crystal chemistry. In: Physics and Chemistry of Minerals. International Mineralogical Association 16th General Meeting, 3–8 September 1994, Pisa, Italy. Berlin, Germany: Springer Berlin Heidelberg; p. 410.

Travaglione S, Bruni B, Falzano L, Paoletti L, Fiorentini C (2003). Effects of the new-identified amphibole fluoro-edenite in lung epithelial cells. *Toxicol In Vitro*, 17(5-6):547–52. doi:10.1016/S0887-2333(03)00118-8 PMID:14599443

Travaglione S, Bruni BM, Falzano L, Filippini P, Fabbri A, Paoletti L, et al. (2006). Multinucleation and pro-inflammatory cytokine release promoted by fibrous fluoro-edenite in lung epithelial A549 cells. *Toxicol In Vitro*, 20(6):841–50. doi:10.1016/j.tiv.2005.12.010 PMID:16480849

Wang S, El-Deiry WS (2003). TRAIL and apoptosis induction by TNF-family death receptors. *Oncogene*, 22(53):8628–33. doi:10.1038/sj.onc.1207232 PMID:14634624

WHO (1997) Determination of airborne fibre number concentrations. A recommended method, by phase-contrast optical microscopy (membrane filter method). Geneva, Switzerland: World Health Organization.

Yokohori N, Aoshiba K, Nagai A; Respiratory Failure Research Group in Japan (2004). Increased levels of cell death and proliferation in alveolar wall cells in patients with pulmonary emphysema. *Chest*, 125(2):626–32. doi:10.1378/chest.125.2.626 PMID:14769747

SILICON CARBIDE

1. Exposure Data

1.1 Chemical and physical properties

1.1.1 Nomenclature

(a) Silicon carbide fibres

Chem. Abst. Serv. Reg. No.: 308076-74-6

Chemical name: Synthetic fibres, silicon carbide

Synonyms: Ceramic fibres, silicon carbide; silicon carbide ceramic; silicon carbide ceramic synthetic fibres; silicon carbide fibres; silicon carbide synthetic fibres

Trade names: Dow X; Enhanced Nicalon; Hi-Nicalon; Nicalon NP 1616; SCS 6; SM; Sigma; Sylramic; Textron SCS 6; Tokamax; Tokawhisker S200; Tyranno ZX ([Chemical Book, 2014](#)).

(b) Non-fibrous silicon carbide

Chem. Abst. Serv. Reg. No.: 409-21-2
EINECS: 206-991-8
Chemical name: Silicon carbide
IUPAC systematic name: Silicon carbide
Chemical formula: SiC ([ACGIH, 2003](#))
Molecular formula:

$$Si^+ \equiv C^-$$
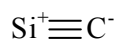
Relative molecular mass: 40.097

Synonyms: Carbon silicide; carborundum, a commercial name for silicon carbide abrasives, is sometimes used as a common name for silicon carbide dust; silicon monocarbide

Trade names: Annanox, Betarundum, Carbofrax, Carbogran, Carbolon, Crystar, Crystolon, Densic, DU-A, Ekasic, Green densic, Halsik, Hexoloy, Hitaceram, Ibiden, Lonza, Norton, Polisher, Shinano Rundum, Sika, Silundum, Sixcy, Supersic, Tokawhisker, Ultrafine (carbide) ([CAMEO Chemicals, 2014](#)) [this list is not intended to be exhaustive].

1.1.2 General description

Silicon carbide appears in two different crystalline forms: hexagonal α-silicon carbide is the main product, while cubic β-silicon carbide is formed at lower temperatures ([Føreland et al., 2008](#)). Silicon carbide occurs in several forms: as "non-fibrous," as "polycrystalline fibres," or as one of more than 150 different single-crystal modifications (or polytypes) of "whiskers" ([Health Council of the Netherlands, 2012](#)). A "whisker" is a type of single-crystal fibre, whereas a "fibre" may be single- or polycrystalline, or non-crystalline ([ASTM, 2011](#)).

Non-fibrous silicon carbide or the particulate material – also called silicon carbide dust, silicon carbide particles, or granular silicon carbide – has an average particle size of 1–20 μm. Exposure to silicon carbide dust can occur during the

manufacture or use of synthetic abrasive materials (Health Council of the Netherlands, 2012).

Silicon carbide fibres – also known as silicon carbide continuous fibres or silicon carbide ceramic fibres, which are mostly polycrystalline materials (ASTM, 2011) – are unwanted by-products of silicon carbide particle production and are considered to be pollutants (Bye et al., 1985; Dufresne et al., 1987a, b; Bégin et al., 1989; Scansetti et al., 1992; Dufresne et al., 1993, 1995; Dion et al., 2005; Gunnæs et al., 2005; Skogstad et al., 2006; Føreland et al., 2008; Bye et al., 2009; Føreland et al., 2013). The length and diameter of these fibres are variable, but fulfil the definition of WHO fibres (particles > 5 μm with a width of < 3 μm and an aspect ratio of > 3) (Rödelsperger & Brückel, 2006).

Fibrous silicon carbide may exist as whiskers or continuous fibres (Bye et al., 1985). Silicon carbide whiskers often have a diameter < 5 μm and a length > 20 μm and are thus respirable fibres similar to amphibole asbestos. Silicon carbide whiskers are single-crystal structures that are cylindrical in shape (ACGIH, 2003).

Silicon carbide fibres are unwanted by-products from the Acheson process and are morphologically heterogeneous, whereas silicon carbide whiskers are intentionally produced and have homogeneous morphology. Skogstad et al. (2006) reported the close resemblance of the morphology and size distribution of silicon carbide whiskers to those of the Norwegian airborne industrial by-product fibres used by Stanton & Layard (1978), Stanton et al. (1981) and Johnson et al. (1992) to carry out in-vivo and in-vitro tests.

1.1.3 Chemical and physical properties

From ASTM (1998), ACGIH (2003), Health Council of the Netherlands (2012), Chemical Book (2014)

Density (specific gravity): 3.22 g/mL at 25 °C

Crystalline form: Hexagonal or cubic

Refractive index: 2.650

Oxidation: Occurs above 700 °C

Sublimes and then decomposes: 2700 °C

Solubility: Insoluble in water, alcohol, and acid; soluble in molten alkalis (sodium hydroxide or potassium hydroxide) and molten iron

Reactivity: Chemical reactions do not take place at ordinary temperatures

Appearance: Variable, exceedingly hard, green to bluish-black, iridescent, sharp crystals

Odour: None

Conversion factor: 1 mg/m³ = 0.5990 ppm at 20 °C.

(a) Chemical properties

Silicon carbide is a crystalline material, the colour of which is determined by the level of impurities. Pure silicon carbide is colourless and transparent. The green to black colour of the industrial product results from impurities, mostly iron. The green specimen is a somewhat purer, slightly harder, but more friable form (Wright, 2006).

Although silicon carbide has a very simple chemical formula, it can exist as numerous different structures (polytypes) (Shaffer, 1969). These structures are composed of a single basic unit, a tetrahedral (SiC_4 or CSi_4) layer, with different stacking arrangements for silicon and carbon atoms (Kordina & Saddow, 2006; Oliveros et al., 2013). The distance between the carbon and silicon atom is 0.189 nm, and the distance between the carbon atoms is 0.308 nm (Fig. 1.1; Kordina & Saddow, 2006).

The polytypes are represented by a number showing how many tetrahedra are stacked along a specific direction in the unit cell and by a letter for the crystal symmetry: cubic (C) and hexagonal (H) (Fig. 1.2). The polytypes of silicon carbide are defined by the stacking order of the double layers of silicon and carbon atoms. The polytypes 3C-, 4H-, and 6H-silicon carbide are

Fig. 1.1 Silicon carbide tetrahedron formed by covalently bonded carbon and silicon
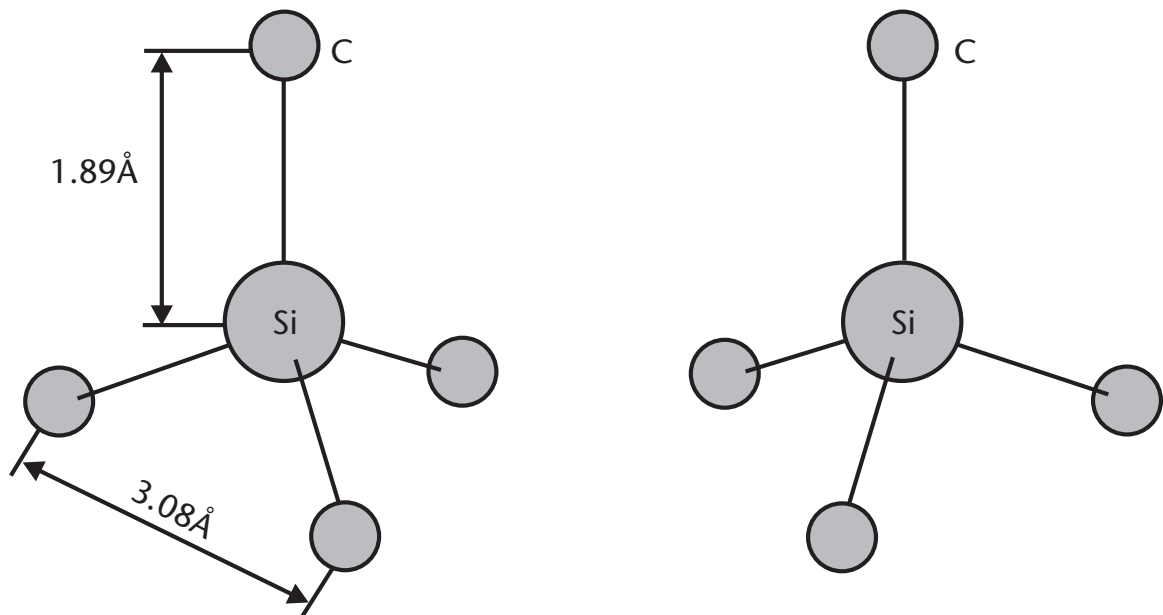
The characteristic tetrahedron building block of all silicon carbide crystals. Four carbon atoms are covalently bonded with a silicon atom in the centre. Two types exist. One is rotated 180 ° around the c-axis with respect to the other, as shown.
From Kordina & Saddow (2006). Reproduced with permission from Saddow SE and Agarwal A, Advances in Silicon Carbide Processing and Applications, Norwood, MA: Artech House, Inc., 2003. © 2003 by Artech House, Inc.

Fig. 1.2 Atomic stacking for silicon carbide polytypes
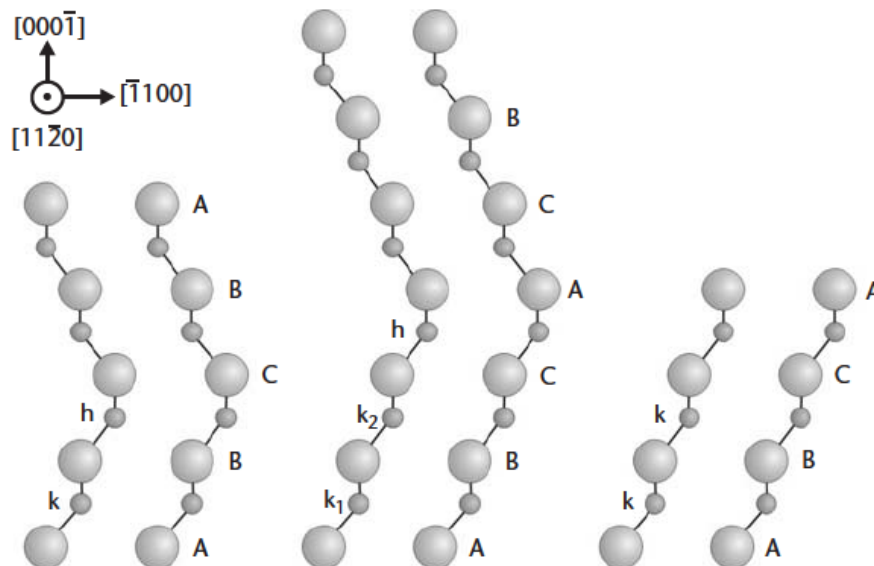
The three most common polytypes in silicon carbide viewed in the [1120] plane. From left to right: 4H-silicon carbide, 6H-silicon carbide, and 3C-silicon carbide; k and h denote crystal symmetry points that are cubic and hexagonal, respectively.
From Kordina & Saddow (2006). Reproduced with permission from Saddow, Stephen E, and Agarwal, Anant, Advances in Silicon Carbide Processing and Applications, Norwood, MA: Artech House, Inc., 2003. © 2003 by Artech House, Inc.

the most frequent. The simplest cubic structure is referred to as β-silicon carbide, whereas the hexagonal structure is referred to as α-silicon carbide (Gunnæs et al., 2005). All polytypes have equal proportions of silicon and carbon atoms but, because the stacking sequences between the planes differ, their electronic and optical properties differ (Kordina & Saddow, 2006; Wright, 2006).

Silicon carbide is very stable, but can nevertheless react violently when heated with a mixture of potassium dichromate and lead chromate. Chemical reactions between silicon carbide and oxygen as well as a variety of compounds (e.g. sodium silicate, calcium, and magnesium oxides) are possible at relatively high temperatures. Indeed, silicon carbide undergoes active or passive oxidation depending on the ambient oxygen potential. Passive oxidation occurs under conditions of high partial pressure of oxygen, producing a protective layer of silicon dioxide on the surface:

$$2SiC\ (s) + 3O_2\ (g) \rightarrow 2SiO_2\ (s) + 2CO\ (g)$$

[where s = solid and g = gaseous]
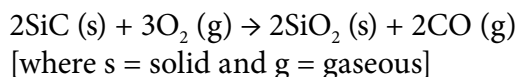
Accordingly, silicon carbide crystals take the form of a rainbow-like cluster caused by the layer of silicon dioxide produced by passive oxidation, which is determined primarily by the nature and concentration of impurities.

Active oxidation takes place under conditions of low partial pressure (30 Pa) of oxygen at 1400 °C and gaseous oxidation products are formed:

$$SiC\ (s) + O_2\ (g) \rightarrow SiO\ (g) + CO\ (g)$$
$$SiC\ (s) + 2SiO_2\ (s) \rightarrow 3SiO\ (g) + CO\ (g)$$

[where s = solid and g = gaseous]
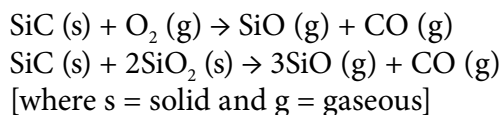
Fresh surfaces of silicon carbide are thus exposed to the oxidizing atmosphere (Wright, 2006), and can be covered largely by silicon dioxide film or islets, heterogeneously distributed at the surface (Dufresne et al., 1987b; Boudard et al., 2014).

(b) Physical properties

The physical parameters of fibres (density, length, and diameter) as well as their aerodynamic behaviour are important factors that affect their respirability, deposition, and clearance in the respiratory tract (Cheng et al., 1995).

(i) By-product fibres from the Acheson process and cleavage fragments

The generation of fibres as a by-product has been demonstrated during the industrial production of silicon carbide in a Norwegian plant (Bye et al., 1985). Characterization of the airborne fibres from the furnace department in the silicon carbide industry showed that more than 93% of fibres consisted of silicon carbide fibres which were divided into eight categories based on their morphology. In addition, less than 2% of the fibres constituted silicon carbide fragments probably resulting from the cleavage of non-fibrous silicon carbide crystals and corresponding to WHO fibres; these fragments were mostly found during sorting operations. In the processing department, 25% of fibres consisted of silicon carbide fibres and 57% of cleavage fragments. The geometric mean (GM) length of all fibres > 5 μm was 9.5 μm (range, 5–900 μm) and the GM diameter of all fibres was 0.39 μm (range, 0.07–2.90 μm); 33% of the fibres had a diameter between 0.07 and 0.25 μm, and 15% corresponded to Stanton fibres (length, 8 μm; diameter ≤ 0.25 μm) (Skogstad et al., 2006). The occurrence of silicon carbide fibres was also confirmed in a Canadian silicon-carbide production factory (Dufresne et al., 1987b; Dion et al., 2005).

Silicon carbide cleavage fragments are elongated particles produced by the splintering of larger crystals during the grinding and classifying of silicon carbide. They can be distinguished from fibrous particles, such as asbestos, glass fibres, and whiskers, by their irregular shape. Typically they fulfil the WHO criteria for respirable fibres. Even granular or powdered silicon carbide may

Table 1.1 Typical parameters of three characterized types of silicon carbide whisker

Type	Fibre (total/µg)	Percentage of fibres with length > 5 µm	Percentage of fibres with diameter < 0.3 µm and length > 8.0 µm
SiC-W 1	7.6×10^6	31.0	3.8
SiC-W 2	1.61×10^5	93.7	6.9
SiC-W 3	1.05×10^7	30.8	10.8

SiC-W, silicon carbide whisker

Adapted from Johnson et al. (1992), by permission of John Wiley & Sons

contain traces of cleavage fragments that fulfil the definition of WHO fibres (Rödelsperger & Brückel, 2006).

(ii) Synthetic silicon carbide whiskers

Exposure to silicon carbide whiskers may occur during the manufacture of the whiskers or during the production, machining, and finishing of composite materials (Beaumont, 1991).

Silicon carbide whiskers have diameters of a few micrometres (average, 0.5 µm) and lengths of up to 5 cm (average, 10 µm) and occur mostly as hair- or ribbon-like crystals (Wright, 2006). Because whiskers are single crystals, they fracture across and not along the long dimension. They meet the dimensional criteria for a fibre (length:diameter (aspect) ratio, > 3) (Beaumont, 1991) but can exceed an aspect ratio of 10:1 (Rödelsperger & Brückel, 2006). Several types of silicon carbide whisker exist, some of which have been well characterized, and their typical parameters are presented in Table 1.1.

During the manufacture of discontinuously reinforced composites, silicon carbide whiskers are combined with metal or ceramic powders and formed into the desired shape. The metal composites can be extruded, forged, rolled, bent, and machined in a fashion similar to the base alloy. The ceramic composites can be machined on lathes, drill presses, and milling machines and finished by abrasive grinding in a manner similar to that of common metals. Some whiskers

are released during the machining of ceramic and metal matrix composites (Beaumont, 1991).

(iii) Polycrystalline silicon carbide fibres

Polycrystalline silicon carbide fibres (diameter, generally < 2 µm; length, generally ≤ 30 µm) can also be manufactured for commercial purposes by various methods (i.e. polymer pyrolysis, chemical vapour deposition, or sintering) (Wright, 2006).

1.2 Sampling and analytical methods

The sampling and analytical methods for silicon carbide fibres are very similar to those for asbestos and man-made mineral fibres. Bulk samples are prepared and ground in an agate mortar to produce fine particles, and further processed using a mesh or gravimetric sedimentation in water. This suspension is then filtered and mounted for observation using appropriate analytical devices. Air samples are obtained using a vacuum pump equipped with a membrane filter to obtain a representative air volume, and the filters are then processed for the analytical methods. Biological specimens, such as lung tissues, lymph nodes, sputum, and bronchoalveolar lavage fluid (BALF), are digested using sodium hypochlorite or hydrogen peroxide or a combination thereof, and the mineral components are recovered on a filter for analysis. Tissue

samples can be ashed using a low-temperature plasma asher, and the ashed solutions are then filtered for further analysis.

All the processed samples on the filters can be analysed using a phase-contrast optical microscope (PCOM) to count the fibres according to WHO (1997) or National Institute for Occupational Safety and Health (NIOSH) method 7400 (NIOSH, 1994a). The sample-loaded filters can also be mounted on a stub and analysed using scanning electron microscopy with an energy dispersive X-ray analyser (SEM-EDX) (Funahashi et al., 1984; Bye et al., 1985) or mounted on a transmission electron micros-copy (TEM) grid and analysed using TEM-EDX according to NIOSH method 7402 (NIOSH, 1994b). TEM allows analysis of the crystal structures and identification of the mineral fibres using electron diffraction and comparing them with reference minerals (Bye et al., 1985). Powdered bulk samples can be analysed using X-ray diffraction to observe the different crystal-line compounds, based on NIOSH method 9000 (NIOSH, 1994c). To obtain the weight percentage of silicon carbide or other amphiboles, standards for silicon carbide should be prepared. Selected methods for the analysis of silicon carbide fibres in various matrices are presented in Table 1.2.

1.3 Production and use

1.3.1 History

Silicon carbide was first created syntheti-cally by Edward Acheson in 1891 by heating quartz sand and carbon in a large electric furnace. Acheson called the new compound "carborundum", which became a trademark for a silicon carbide abrasive (Encyclopaedia Britannica, 2014). Subsequently, in 1905, silicon carbide was observed in its natural form by the chemist Henri Moissan, in a meteor crater located in Canyon Diablo, Arizona, USA. Moissanite, named in honour of its discoverer,

is a transparent mineral that is as brilliant and almost as hard as diamond. Only synthetically produced silicon carbide is used for commercial applications because natural moissanite is very scarce (Wright, 2006).

The available information on history and production levels mostly concerns the Acheson production industry, involving mainly powdered and granular silicon carbide particulates. Thus data on the history and production levels of silicon carbide fibres and whiskers are limited.

1.3.2 Production levels

The world production capacity of silicon carbide was 1 010 000 tonnes in 2013. Of these, the Norwegian plants produced 8%, Japan produced 6%, Brazil produced approximately 4%, the USA and Canada produced 4%, and China was the world's leading producer of abrasive silicon carbide, accounting for 45% of the production capacity (Table 1.3).

Production and salient statistics for abra-sive silicon carbide in the USA and Canada for 2013 are shown in Table 1.4. Silicon carbide was produced by two companies at two plants in the USA, and bonded and coated abrasive prod-ucts accounted for most abrasive uses of silicon carbide (USGS, 2014). [These data were not avail-able for other countries.]

During 2009–12, the USA imported 72% of the silicon carbide demand mainly from China (58%), South Africa (17%), the Netherlands (7%), Romania (7%), and others (11%) for crude prod-ucts, and China (44%), Brazil (24%), the Russian Federation (8%), Norway (7%), and others (17%) for grains. About 5% of silicon carbide is recycled (USGS, 2014).

Table 1.2 Selected methods of analysis of silicon carbide fibres in various matrices

Sample matrix	Sample preparation	Assay method	Detection limit	Reference
Bulk samples				
	Direct transfer to SEM-stub	SEM-EDX	NR	Governa et al. (1997)
	Suspension filtration; mounting on SEM stub	SEM-EDX	NR	Johnson et al. (1992), Governa et al. (1997), Yamato et al. (1998)
	Suspension filtration; mounting on TEM grid	TEM-EDX	NR	Johnson et al. (1992)
	Deposition of fibrous dusts onto filter	PCOM	0.01 fibres/mL	HSE (1995, 1988), Miller et al. (1999)
	Deposition of fibrous dusts onto filter	SEM	NR	WHO (1985), Miller et al. (1999), Rödelsperger & Brückel (2006)
	Powder (for density)	Helium pycnometer	NR	Cheng et al. (1995)
	Powder (for surface area)	BET	NR	Governa et al. (1997)
Air samples				
	Direct reading instrument	Dust monitor	NR	Akiyama et al. (2003, 2007)
	Polycarbonate filter (25 mm, 0.4 µm pore)	SEM-EDX	NR	Bye et al. (1985), Skogstad et al. (2006)
	MCE filter (25 mm, 0.3 µm pore)	TEM-EDX-SAED	NR	Bye et al. (1985)
	MCE filter (25 mm, 0.8–1.2 µm pore)	PCOM	13 fibres/mm^2	Scansetti et al. (1992), WHO (1997); Dion et al. (2005), Føreland et al. (2013)
	Sampling with nylon cyclone (or HD cyclone, or aluminum cyclone); ashing with plasma asher; redeposition on silver membrane	XRD	0.005 mg per sample	Dufresne et al. (1987a), NIOSH (2003), Dion et al. (2005), Bye et al. (2009), Føreland et al. (2013)
		XRD	12 µg	Scansetti et al. (1992), NIOSH (1998)
	MCE filter (37 mm, 5 µm pore) with cyclone	Gravimetry	0.06 mg	Bye et al. (2009), Føreland et al. (2013)
	Aerosol generation by small scale particle disperser	Cascade impactor (MMAD)	NR	Cheng et al. (1995)
	Heubach, MRI dustiness tester	Cascade impactor (dustiness)	NR	Plinke et al. (1992)
Biological samples				
Human lung and bronchoalveolar lavage fluid	Digestion with sodium hypochlorite, hydrogen peroxide or low temperature ashing	TEM-EDX	NR	Hayashi & Kajita (1988), Dufresne et al. (1995)
		SEM-EDX	NR	Funahashi et al. (1984), De Vuyst et al. (1986)
Animal lung	Digestion and filtration	XRD	NR	Akiyama et al. (2003, 2007)
		SEM	NR	Davis et al. (1996)
		TEM-EDX	NR	Dufresne et al. (1992)

BET, Brunauer–Emmett–Teller; EDX, energy dispersive X-ray analyser; HD, Higgins–Dewell; MCE, mixed cellulose esters; MMAD, mass median aerodynamic diameter; MRI, Midwest Research Institute; NR, not reported; PCOM, phase-contrast optical microscopy; SAED, selected area electron diffraction; SEM, scanning electron microscopy; TEM, transmission electron microscopy; XRD, X-ray diffraction

Table 1.3 World production capacity for silicon carbide in 2013

Country	Production capacity (tonnes)
China	455 000
Norway	80 000
Japan	60 000
Mexico	45 000
Brazil	43 000
USA and Canada	42 600
Germany	36 000
Venezuela	30 000
France	16 000
Argentina	5 000
India	5 000
Other countries	190 000
World total (rounded)	1 010 000

Compiled by the Working Group with data from USGS (2014)

1.3.3 Production methods

Silicon carbide is intentionally manufactured by several processes depending on the levels of purity, crystal structure, particle size, and shape required.

(a) Acheson process

The Acheson process is most frequently used for the production of silicon carbide by the carbothermal reaction of a mixture of petroleum coke (carbon) and high purity crystalline silica (quartz) in an open electrical resistance furnace (Gunnæs et al., 2005). A silicon carbide plant can be divided into four different departments: material storage, preparation areas, the furnace department where the crude silicon carbide is produced, and the processing department where the silicon carbide grits are manufactured, as presented in Fig. 1.3 (Føreland et al., 2008).

Sawdust is occasionally added to the mixture to reduce its density, to facilitate the escape of evolved gaseous carbon monoxide, and to improve the porosity of the furnace mix (Smith et al., 1984; Føreland et al., 2008). Silica reacts with carbon to produce silicon carbide and

Table 1.4 Production volume and salient statistics for abrasive silicon carbide in the USA and Canada, 2013

Salient statistic	Amount (tonnes)
Production, USA and Canada (crude)	35 000
Imports for consumption (USA)	108 000
Exports (USA)	17 700
Consumption, apparent (USA)	125 000

Compiled by the Working Group with data from USGS (2014)

carbon monoxide according to the following overall reaction:

$SiO_2 + 3C \rightarrow SiC + 2CO$ (Føreland et al., 2008)

The Acheson furnace is heated by a direct current passing through powdered graphite within the charge mixture (Fig. 1.4). The furnace is fired for 40–48 hours, during which temperatures in the core vary from > 1700 to 2700 °C, and is < 140 °C at the outer edge. Silicon carbide develops as a cylindrical ingot around the core, with radial layers growing from graphite in the inside (which can be recycled to the next furnace) to hexagonal α-silicon carbide (the highest grade material with a coarse crystalline structure, 98% silicon carbide), cubic β-silicon carbide (metallurgical grade, 90% silicon carbide), firesand (80% silicon carbide, recycled to the next furnace), the crust (a condensation layer of silicon dioxide and other oxide impurities), and finally partly and unreacted material (sand and coke) on the outside (Saint-Gobain, 2014).

After the heating cycle, the furnace is disassembled and the side walls are removed to allow cooling (up to 2 weeks). A cross-sectional view of the resistor furnace after cooling is given in Fig. 1.5 (Indian Institute of Science, 2014).

The outer layer of non-reacted mixture is removed from the crude and returned to the mix area, exposing the core of green or black silicon carbide crystals. The crude silicon carbide is transported to the sorting area where β-silicon carbide is removed from α-silicon carbide. The final α-silicon carbide product is an aggregate of

Fig. 1.3 Flow diagram depicting production of silicon carbide by the Acheson process

SiC, silicon carbide

Fig. 1.4 The Acheson furnace and the crude silicon carbide product
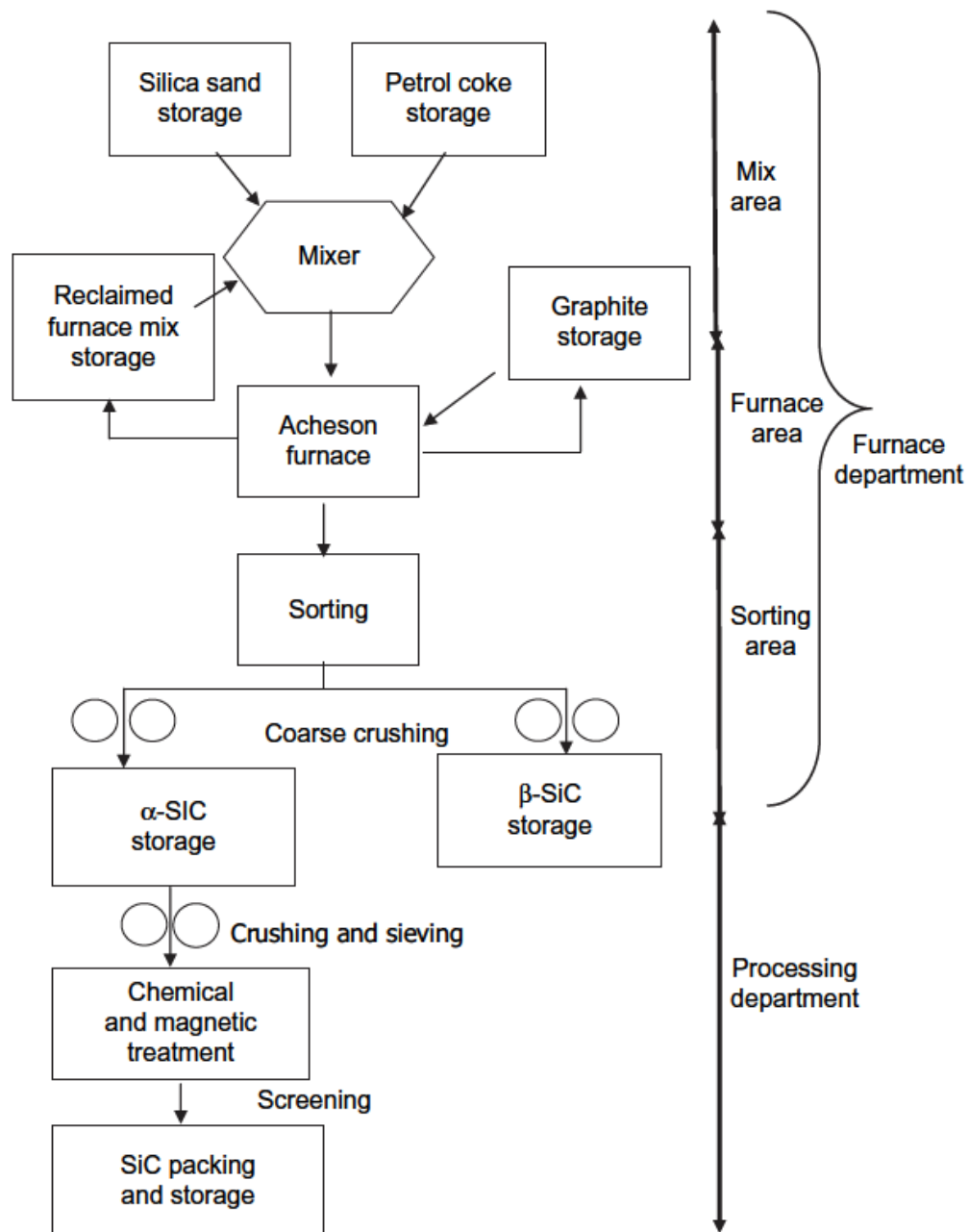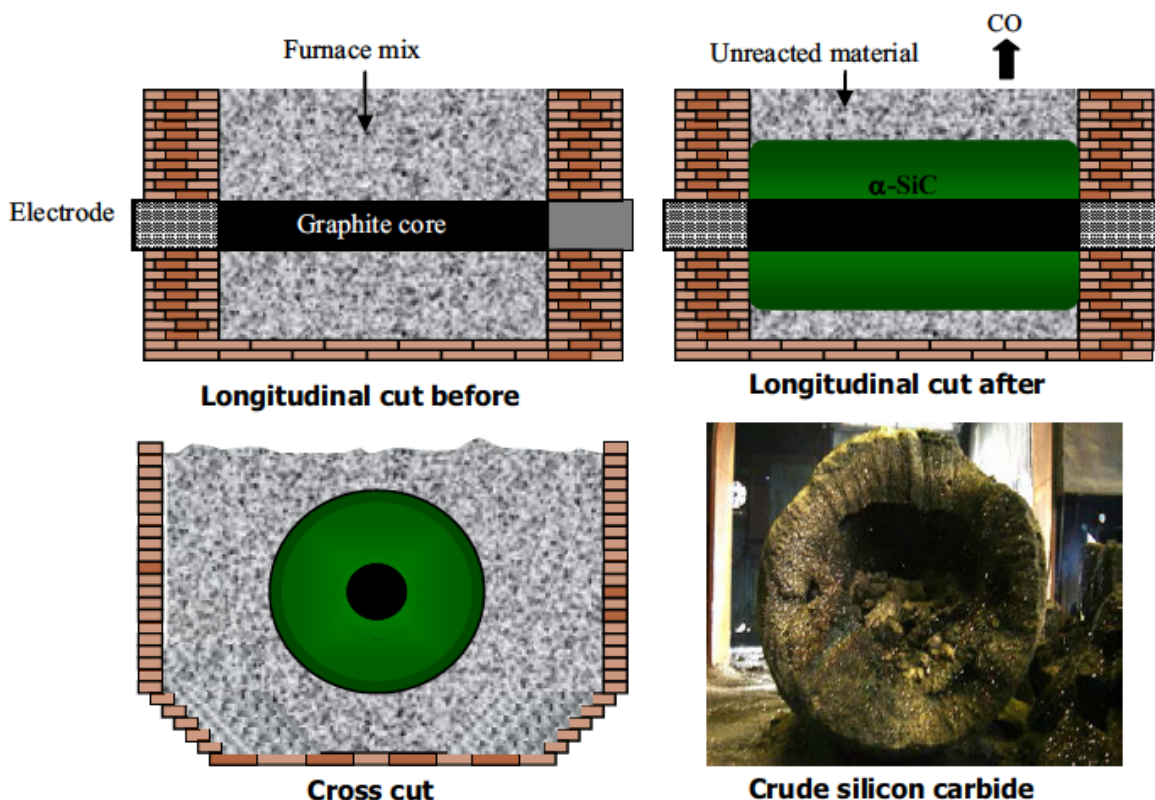
SiC, silicon carbide; CO, carbon monoxide
Reproduced from Føreland (2012), with permission of the author

iridescent crystals, due to a thin layer of silica from superficial oxidation of the carbide, which is transported to the processing department for crushing, grounding, magnetic and chemical treatments to remove impurities, and screening into the size required for the end-use (Wright, 2006; Føreland et al., 2008). Two different types of silicon carbide crystal may be obtained: green silicon carbide is the purest material with > 99% silicon carbide, while the black material contains ~98% silicon carbide (Bye et al., 2009).

Formation of silicon carbide fibres

Silicon carbide fibres are formed during the Acheson process in the intermediate region, where the partly reacted material is found (Bye et al., 1985). The fibres are believed to be formed

when a blow of gas escapes the baking lump of silicon dioxide–petroleum coke in the electric furnace (Bégin et al., 1989). Different morphologies of fibrous silicon carbide in this layer have been observed by SEM and TEM (Gunnæs et al., 2005; Skogstad et al., 2006). The high concentration of fibres during the handling of the raw material is consistent with the fibres encountered in recycled material. Silicon carbide fibres have not been observed in the final abrasive products, but have been observed in products for refractory and metallurgical purposes (firesand) (Føreland et al., 2008; Bye et al., 2009; Bruch et al., 2014).

In addition to silicon carbide fibres (including whiskers), the production of silicon carbide generates many airborne contaminants including

Fig. 1.5 Cross-sectional view of the Acheson furnace after cooling
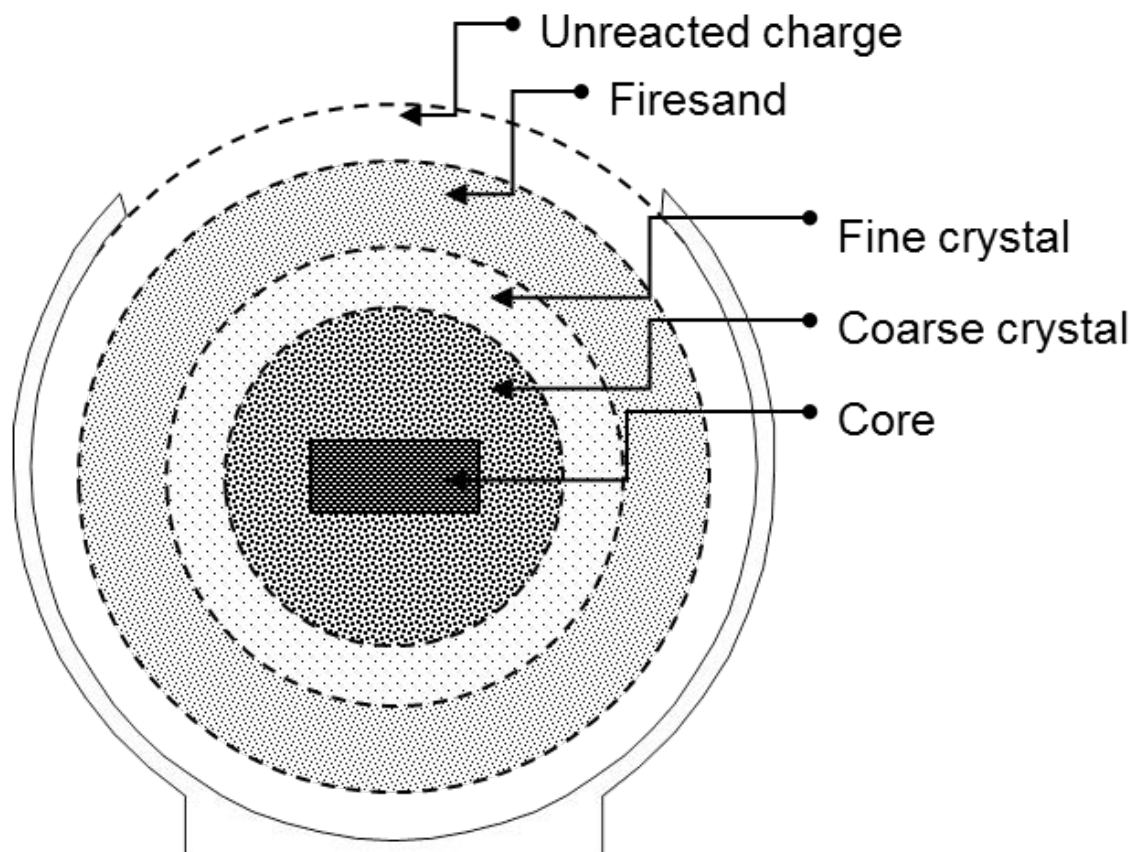
quartz, cristobalite, graphite, and non-fibrous silicon carbide dust (Bye et al., 2009). Sulfur dioxide (from the oxidation of sulfur contained in the petroleum coke) and polycyclic aromatic hydrocarbons are also found in the environment of the Acheson furnace (Bye et al., 1985; Dufresne et al., 1987a; Føreland et al., 2008).

(b)   Synthesis of silicon carbide powder and whiskers from rice hulls

The conversion of silicon dioxide particles in plant material (as rice hulls) to silicon carbide is carried out by heating in the excess carbon from the organic material. Rice hulls contain 16–26% by weight of silica. The silica is amorphous and is transformed into β-silicon carbide by pyrolysis. High quality silicon carbide powder and whiskers are produced from rice hulls without catalysts using an inexpensive method. The rice hulls are preheated at 750–850 °C in the absence of air for 3 hours. The temperature is gradually increased to 1300 and 1400 °C over 12 hours in an argon atmosphere. Different structures are found: needles with a diameter of 0.25 μm; fibres of about 0.16 μm in diameter; spherical particles of 1 μm in diameter; and structures with the original morphology. Excess carbon is eliminated by burning in an air atmosphere at 850 °C for 6 hours and residual silicon oxide is

removed by washing with a solution of fluoric acid (Rodriguez-Lugo et al., 2002).

(c) Synthesis of silicon carbide whiskers from waste serpentine

Serpentine rock can be used as a raw material for the production of a high-reactivity amorphous silica powder, which can then be used for the synthesis of silicon carbide. Amorphous silica is obtained by the extraction of waste serpentine at 80 °C in 5M sulfuric acid for 48 hours. The amorphous silica powder is then reacted with carbon black at 1550 °C for 5 hours to obtain β-silicon carbide whiskers for use as a raw material in industry (Cheng & Hsu, 2006).

(d) Other production methods

Silicon carbide is also produced, for special applications, by other advanced processes (Wright, 2006).

(i) Physical vapour transport (or modified Lely process)

Large single crystals of silicon carbide are produced from a form of physical vapour transport growth in which silicon and carbon are transported at high temperatures through a reactor to a growing seed crystal. The silicon carbide crystals can then be sliced into wafers up to 100 mm in diameter (Wright, 2006).

(ii) Chemical vapour deposition

Wear-resistant layers of silicon carbide as well as silicon carbide fibres or whiskers for reinforcing metals or other ceramics can be formed by chemical vapour deposition, a process in which volatile compounds containing carbon and silicon are reacted at high temperatures in the presence of hydrogen. The silicon carbide whiskers produced by chemical vapour deposition with silicon oxide and carbon monoxide as the primary reactants are similar to those produced by pyrolysis or the thermal decomposition of rice hulls (Sharma et al., 1984).

(iii) Vapour–liquid–solid process

Silicon carbide whiskers of high purity are produced by this process, in which the crystal growth occurs by precipitation from the supersaturated liquid at the solid–liquid surface. The vapour contains a carbon-bearing gas (methane) and silicon monoxide (Milewski et al., 1985).

1.3.4 Use

Silicon carbide has been produced on a large scale since 1893 for use as an abrasive. This was followed by electronic applications, in light-emitting diodes and detectors in early radios (Wright, 2006).

Most of the silicon carbide produced worldwide today is in the form of grains or powder for use as an abrasive. Additional silicon carbide applications are: refractories, electrical devices, electronics (semiconductor), diesel particles filters, ceramics, industrial furnaces, structural materials, and metallurgy (Wright, 2006). Silicon carbide is also used by the aerospace, automotive, and power generation industries as a reinforcing material in advanced ceramic composites (ACGIH, 2003; USGS, 2014). Although no application has been found for the unwanted fibres from the Acheson process, metallurgical grade silicon carbide that contains silicon carbide fibres may be sold to the industry.

Silicon carbide whiskers have a wide range of industrial uses related to its high tensile strength, weight advantage over metals, and stability at high temperatures. They are used for ceramic seals, sandblast nozzles, and structural materials for applications at high temperatures, as durable asbestos substitutes (Health Council of the Netherlands, 2012).

1.4 Natural occurrence

Only minute quantities of silicon carbide exist in nature.

1.5 Exposure

1.5.1 Exposure of the general population

No data have been reported on the levels of silicon carbide fibres in non-occupational environmental matrices such as air, water, and soil.

1.5.2 Occupational exposure

Silicon carbide in fibrous and non-fibrous forms has been detected in occupational environments. Various forms of silicon carbide can comply with the WHO definition of a fibre (i.e. a particle longer than 5 μm with a diameter of less than 3 μm and an aspect ratio of more than 3), including intentionally manufactured monocrystalline silicon carbide whiskers, intentionally manufactured polycrystalline silicon carbide fibres, unwanted silicon carbide fibres resulting as by-products of the manufacture of silicon carbide (partially reacted materials), and cleavage fragments of crude silicon carbide (Lockey, 1996; Rödelsperger & Brückel, 2006; Wright, 2006).

Inhalation is the primary route of exposure to fibrous silicon carbide in occupational settings, but data on the number of workers occupationally exposed to silicon carbide fibres are lacking. However, the United States National Occupational Exposure Survey (1981–83) estimated that about 250 900 workers were exposed to silicon carbide. The industries with the largest number of exposed workers included machinery (except for electrical), and electric and electronic equipment. The United States National Occupational Exposure Survey also estimated that about 17 500 and 8700 workers were exposed to silicon carbide powder and silicon carbide dust, respectively (NIOSH, 2014).

(a) Manufactured silicon carbide fibres

The term "silicon carbide whiskers" specifically refers to monocrystalline forms produced at high cost for targeted high technology use,

such as in the aerospace industry (Wright, 2006). To characterize silicon carbide whiskers, Cheng et al. (1995) aerosolized them and took samples from a filter. The count median length of the aerosol samples was 3.43 μm and the count median diameter was 0.198 μm. Thus, only a fraction of the aerosol could be defined as WHO fibres. According to the aerodynamic size, 65% (cascade impactor) to 76% (aerosol centrifuge) of the silicon carbide aerosol particles were respirable.

Exposures to both these respirable manufactured silicon carbide whiskers and silicon carbide fibres may occur during their production and the manufacturing/machining/finishing/use of composite materials (Johnson et al., 1992; Lockey, 1996; Cook, 2006; Wright, 2006; Malard & Binet, 2012). However, limited information on the quantification of such exposures has been reported in the literature.

Beaumont (1991) monitored total fibre occurrence during the machining of silicon carbide whisker-reinforced metals and ceramics. Calculated 8-hour time-weighted average (TWA) exposures ranged from 0.031 fibres/mL to 0.76 fibres/mL, depending on the processes used. Control improvements to optimize the local exhaust ventilation and/or cleaning coolant provided a substantial reduction in the exposure to fibres (see Table 1.5).

Possible airborne fibre release from silicon carbide cutting tips used on some machine tools was investigated by on-site monitoring and during simulated work activities in a laboratory (Revell & Bard, 2005). All airborne fibre concentrations for each sample were below the limit of quantification during on-site monitoring. SEM analysis of a fractured surface silicon carbide ceramic tip showed a large number of fibres, typically about 2 μm in length and 0.5 μm in diameter. Using fractured tips could lead to exposures to fibres because protruding fibres could feasibly be broken off easily. However, laboratory tests to simulate a cutting action using silicon carbide

Table 1.5 Calculated 8-hour time-weighted average exposures to fibres during machining of silicon carbide whisker-reinforced composite materials before and after control improvements

Description	Concentration (fibres/mL)	
	Before	**After**
Machining of metal matrix composites	0.031	NA[a]
Lathe machining of green ceramic composites	0.26	0.034
Lathe machining of pre-sintered ceramic composites	0.76	0.038
Cutting pre-sintered ceramic composites with tool post grinder	NC[b]	0.031
Surface grinding of fired ceramic	0.21	0.0062
Inside/outside grinding of fired ceramic	0.075	0.016

[a] NA, not applicable because no changes were made in the metal machining area

[b] NC, this value could not be calculated from the data collected

Adapted from: Reduction in airborne silicon carbide whiskers by process improvements, Beaumont (1991), *Journal of Occupational and Environmental Hygiene*, reprinted by permission of the publisher (Taylor & Francis Ltd, http://www.tandfonline.com)

whisker ceramic tips indicated that very few fibres were released; concentrations were below the limit of quantification of 0.04 fibres/mL.

Several other forms of silicon carbide are used in industries. Nixdorf (2008) indicated that new non-respirable silicon carbide (diameter, 5–10 μm) can be used as a substitute for other respirable silicon carbide particles. Malard & Binet (2012) reported the use of the silicon carbide Nicalon® (diameter, typically 14 μm) in reinforced composite materials. However, these silicon carbide forms do not comply with the WHO definition of a fibre. The possibility of releases of submicron airborne particles could be investigated during machining operations on these reinforced materials.

(b) By-products of silicon carbide production

(i) Studies of exposed workers

Silicon carbide fibres also appear and were mainly investigated as unwanted by-products generated during the production of silicon carbide crystals through the Acheson furnace process (Lockey, 1996). Results from field studies are summarized in Table 1.6.

Quantification of these undesired airborne silicon carbide fibres was first reported in three Norwegian silicon carbide production plants by Bye et al. (1985). Short-term (15–50 minutes) personal or stationary samples were collected at various workplaces and fibres were counted using PCOM. The concentrations of silicon carbide fibres reported in the three plants were 0.1–4.9 fibres/mL during the mixing of raw material, 0–3.6 fibres/mL during furnace operations, 0.2–2.7 fibres/mL during the separation of raw products, and 0–0.2 fibres/mL during the preparation of final products. The analysis of an airborne dust sample (100 fibres evaluated) by SEM showed fibres with diameters and lengths ranging from 0.5 μm to 2.5 μm and from 1 μm to 50 μm, respectively. The presence of long (length, up to 20 μm) and thin (diameter, 0.2–0.5 μm) airborne fibres in the silicon carbide industries was later confirmed (but not quantified) by Dufresne et al. (1987b) using SEM.

Scansetti et al. (1992) measured fibre concentrations by PCOM or SEM in samples obtained by static sampling in an Italian plant operating 24 Acheson furnaces. GMs of respirable fibre concentrations determined by PCOM for the different working operations are given in Table 1.6. GMs of respirable fibre concentrations were also determined by SEM and the ratios of SEM to PCOM ranged from 1.15 to 2.02 indicating the presence of thin fibres below the PCOM limit of detection. High variability in

Table 1.6 Reported personal and/or static measurements of fibres (fibres/mL) in silicon-carbide production plants

Reference	Country, year of study	Plant	Furnace department			Processing department	Maintenance department
			Mixing of raw material (No.)	Furnace operations (No.)	Separation of material /sorting (No.)	Preparation of final product/refinery (No.)	
Bye et al. (1985)	Norway, 1985	A	0.3 (1)	0–3.6 (16)	0.2–0.7 (6)	0–0.1 (2)	
		B	0.1–1.9 (7)	0.1–1.9 (4)	0.2–2.7 (6)	0.1–0.2 (3)	
		C	1.8–4.9 (4)	0.1–0.7 (7)	0.2 (3)	0–0.1 (3)	
Romundstad et al. (2001)[a]	Norway, 1982–88	A	0.9 (6)	0.3 (29)	0.8 (24)	0.04 (3)	
		B	1.1 (15)	0.5 (29)	1.1 (19)		
		C		0.4 (14) and 0.9 (12)	1.8 (13)		
Scansetti et al. (1992)[b]	Italy, 1990	–	0.07 (9)	0.11 (6) (loading) 0.14 (4) (heating) 0.63 (6) (side-opening) 0.14 (4) (cooling)	0.58 (6) (cylinder breaking) 2.40 (6) (unreacted material removing)	0.71 (11) (selection) 0.41 (12) (crushing)	
Dion et al. (2005)[c]	Canada, 2000	–	–	0.03–0.11 (3) (assistant operator) 0.16–0.39 (3) (furnace attendant) 0.23–0.67 (3) (subproduct attendant)	0.25–0.89 (12) (carboselector)	0.42–0.77 (3) (crusher) 0.06–0.15 (4) (millwright)	
Foreland et al. (2008)[b]	Norway, 2002–03	A	0.097 (14)	0.082–2.7 (54)	0.13 (19)	0.011–0.030 (94)	0.034–0.086 (69)
		B	–	0.025–0.062 (44)	0.19 (21)	0.007–0.037 (102)	0.017–0.041 (69)
		C	0.046 (10)	0.039–0.36 (72)	0.43 (21)	0.011–0.021 (100)	0.017–0.049 (37)

[a] Estimates based directly on measurements
[b] Geometric mean values
[c] Values are 8-hour time-weighted averages
Compiled by the Working Group

the workplace environment was reported in the majority of the working operations studied.

To study cancer incidence among 2620 men employed in all three Norwegian silicon carbide plants, Romundstad et al. (2001, 2002) estimated exposures to silicon carbide fibres for different occupations from 1912 to 1996 for plant A, from 1965 to 1996 for plant B, and from 1963 to 1996 for plant C. Estimated exposures, presented in Table 1.6, were based on industrial hygiene measurements carried out between 1982 and 1988 and on descriptions of changes in the process technology and work practices over time. Arithmetic means of silicon carbide fibre concentrations calculated by job over the whole sampling period are presented in Table 1.7. The highest levels were reached during mixing raw materials, oven work, and sorting. Estimated exposures indicated a continual decrease in workplace levels of silicon carbide fibres from the 1910s to the 1990s in plant A.

Gunnæs et al. (2005) investigated the chemical composition, structure, surface properties, and morphology of clustered silicon carbide fibres in one of the three industrial silicon carbide plants in Norway. Fibres were collected both by personal sampling in the furnace hall and by collecting material containing fibres from the zone between the silicon carbide crust and the outer firesand layer. A large variety of silicon carbide fibres was found both in the air samples and in the samples taken from the furnace. The authors described a complex morphology of needles with branches based on a face-centred cubic structure and covered by a thin amorphous layer of carbon.

Additional investigations in the three Norwegian plants by Skogstad et al. (2006) provided a detailed description of the morphological variation of the fibres by classifying their types by shape, chemical composition, and dimensions and exploring possible determinants of the occurrence of these various types. A total of 32 short-term (0.5–2 hours) personal samples were analysed by SEM The authors classified the silicon carbide fibres into categories (K1–K8 and CF) according to their morphologies, including a category for fibres that could not easily be assigned to one of the seven previous groups (K8) and one for those that satisfied the fibre counting criteria (CF). The category K4 comprises around 50% of all fibres identified. These thin fibres were "rectilinear but often tapered along the fibre axis." In addition, approximately 15% and 10% of the fibres counted were classified as K1 ("straight fibres [that] looked like a staple of discs perpendicular to the fibre axis") and K2 ("straight fibres with variable diameter along the fibre axis") categories, respectively. Fewer than 10% of the fibres counted were not silicon carbide fibres, but were carbon fibres, silicon oxide fibres, silicon fibres, vanadium-rich fibres, and man-made vitreous fibres. The proportions of the various silicon carbide categories were shown to differ between plants, jobs, and production parameters. For all categories, the arithmetic means of the diameter, length, and aspect ratio of counted fibres were 0.51 µm, 12 µm, and 36, respectively.

Dion et al. (2005) examined nearly 100 measurements of silicon carbide fibre concentrations in one Canadian factory producing silicon carbide abrasive material (grains or particles). Fibres were counted from personal samples following the WHO method (using PCOM) and the 8-hour TWA concentrations were calculated for six groups of workers: assistant operators of station 01, Acheson furnace attendants (loading mix into the furnace), subproduct attendants, crusher and backhoe operators, carboselectors, and millwrights. The 8-hour TWA concentrations ranged from 0.03 fibres/mL (for assistant operators at station 01) to 0.89 fibres/mL (for carboselectors breaking up and sorting silicon carbide lumps). Crushers, who also screen all grades of the silicon carbide produced into several sizes, had the second highest exposure (8-hour TWA of between 0.42 and 0.77 fibres/mL).

Table 1.7 Comparison of estimated retrospective exposure assessment to silicon carbide fibres for selected job groups and study periods from the studies of Romundstad et al. (2001) and Føreland et al. (2012)

Job group	Study period	Fibre concentrations (fibres/mL), arithmetic mean	
		Romundstad et al. (2001)	Føreland et al. (2012)
Plant A			
Mix	1912–36	4.4	0.37
	1936–52	2.2	0.29
	1953–79	1.6	0.23
	1980–96	0.9[a]	0.15
Charger	1915–38	3.3	0.89
	1939–52	2.8	0.67
	1953–59	2.1	0.55
	1960–79	1.2	0.49
	1980–96	0.3[a]	0.36
Crane	1938–52	2.8	0.33
	1953–58	1.3	0.22
	1959–96	0.3	0.15
Sorter	1913–33	3.2	1.0
	1934–52	2.4	0.76
	1953–96	0.8[a]	0.26
Refinery	1914–43	0.06	0.06
	1947–96	0.04[a]	0.05
Fines	1931–43	0	0.02
	1947–96	0	0.02
Packer	1914–43	0.06	0.25
	1947–96	0.04	0.20
Plant B			
Mix	1965–81	2.8	0.13
	1982–96	1.1[a]	0.1
Crane	1965–81	0.2	0.12
	1982–96	0.2	0.09
Sorter	1965–81	1.1	0.65
	1982–96	1.1[a]	0.46
Refinery	1965–96	0.06	0.05
Fines	1965–96	0	0.03
Plant C			
Mix	1963–96[b] or 1964–96[c]	0.6	0.07
Charger	1963–96[b] or 1964–96[c]	0.4[a]	0.47
Payloader	1963–96[b] or 1964–96[c]	0.9[a]	0.39
Crane	1963–79[b] or 1964–96[c]	0.4	0.10
Sorter	1963–96[b] or 1964–96[c]	1.8[a]	0.67
Refinery	1963–96	0.05	0.03
Fines	1963–96	0	0.02

[a]   Measured data
[b]   Romundstad et al. (2001)
[c]   Føreland et al. (2012)
Adapted from Føreland et al. (2012)

In the three Norwegian plants producing silicon carbide, Føreland et al. (2008) assessed personal exposure to silicon carbide fibres for 13 different job groups classified in three departments (furnace, processing, and maintenance). Approximately 720 new short-term (0.5–3.5 hours) personal measurements were taken during the period 2002–03 and counted according to the WHO counting criteria (WHO, 1997). GMs of fibre levels were in the range 0.007–2.7 fibres/mL for all jobs and plants. The highest exposures were monitored in the furnace department. The Norwegian exposure limit for fibres (0.1 fibres/mL) was exceeded by 53%, 17%, and 0.2% of the samples from the furnace, maintenance, and processing departments, respectively. The authors reported that 78% of the workers in the furnace department used respirators.

To construct a retrospective job–exposure matrix (JEM) for the Norwegian silicon carbide industry, Føreland et al. (2012) combined historical exposure data from company records, the Norwegian Labour Inspectorate records, and studies performed by the National Institute of Occupational Health (NIOH). Mixed-effect models were used to estimate the exposure to silicon carbide fibres for each plant which is expected to give more accurate assessments. Arithmetic means of exposures were estimated for several job groups depending on the plant: mix, charger, payloader, crane, sorter, refinery, fines, and packer (see Table 1.7). The new estimated exposure data were compared with the original JEM developed by Romundstad et al. (2001). The fibre exposure estimates using the novel method (Føreland et al., 2012) were 3.2 times lower on average than those in the previous JEM, and this method was used by Bugge et al. (2011, 2012) to update previous Norwegian epidemiological investigations.

To identify the determinants of exposure to dust and dust constituents in the Norwegian silicon carbide industry, Føreland et al. (2013) assessed exposures to silicon carbide fibres in the three Norwegian plants, and data formerly presented in Føreland et al. (2008) for each plant were grouped for the three plants. As previously reported, work in the furnace department was associated with the highest exposure and that in the processing department with the lowest exposure to fibres. Job group was an important predictor of exposure to silicon carbide fibres and accounted for up to 82% of the between-worker variance. For maintenance workers, increased exposure to fibres was also associated with work in the furnace department.

(ii) Studies with biological samples from exposed workers

Some case studies have evaluated biological samples from workers and the studies of Dufresne et al. (1993, 1995) are particularly relevant regarding exposures to silicon carbide fibres in the Canadian silicon carbide industry. Dufresne et al. (1993) reported a concentration of 39 300 fibres/mg of dry lung tissue for fibres longer than 5 μm (mean diameter, 0.49 μm; mean length, 11 μm) and a concentration of 105 243 fibres/mg of dry lung tissue for fibres shorter than 5 μm (mean diameter, 0.22 μm; mean length, 2.86 μm) in the lung parenchyma of a retired silicon-carbide plant worker (see Table 1.8). The worker was diagnosed with pneumoconiosis and lung cancer and had been exposed for 42 years near an Acheson furnace. The authors noted that the concentration of total pulmonary fibres in this study greatly exceeded (approximately by a factor of 10) the fibre concentrations reported in the lungs of subjects exposed to asbestos in mining activities (Case & Sebastien, 1987). In a subsequent study, Dufresne et al. (1995) examined post-mortem lung material from 15 deceased men who had worked for between 15 and 42 years in the silicon carbide industry. The GM concentrations of fibres shorter than 5 μm were 48 529 fibres/mg of dry lung tissue in workers without lung fibrosis and lung cancer, and up to 147 911 fibres/mg in workers with lung fibrosis but no lung cancer. GM concentrations of fibres longer than 5 μm

Table 1.8 Biological levels of fibres in the lung parenchyma of workers in the silicon carbide industry in Canada

Reference	Subjects	Geometric mean (± geometric standard deviation)		
		Silicon carbide fibres (length, < 5μm) per mg of dry lung	Silicon carbide fibres (length, ≥ 5μm) per mg of dry lung	Ferruginous bodies per g of dry lung
Dufresne et al. (1993)	1 male worker with silicon carbide pneumoconiosis and lung cancer, exposed for 42 yrs, retired for 2 yrs, and smoked 1.5 packs of cigarettes per day for > 40 yrs	105 243	39 300	800 000
Dufresne et al. (1995)	5 male workers with no lung fibrosis or lung cancer exposed for 23.4 ± 6.9 yrs, no longer exposed for the past 7.9 ± 7.1 yrs, and smoked 50.6 ± 30 cigarette pack–yrs	48 529 (± 3.5)	7 586 (± 3.9)	39 903 (± 4.0)
	6 male workers with lung fibrosis but no lung cancer, exposed for 28.8 ± 5.5 yrs, no longer exposed for the past 7.0 ± 1.6 yrs, and smoked 59.8 ± 32.2 cigarette pack–yrs	147 911 (± 2.5)	53 951 (± 3.5)	305 492 (± 3.8)
	4 male workers with lung fibrosis and lung cancer, exposed for 32.3 ± 9.0 yrs, no longer exposed for the past 5.0 ± 3.5 yrs, and smoked 39.2 ± 25.8 cigarette pack–yrs	100 925 (± 1.8)	27 353 (± 1.8)	583 445 (± 2.4)

yr, year
Compiled by the Working Group

were up to 53 951 fibres/mg of dry lung tissue in workers with lung fibrosis but no lung cancer (see Table 1.8). No statistical differences were observed in the dimensions of silicon carbide fibres between each group. Fibres < 5 μm long were approximately 2 μm in length and 0.2 μm in diameter with an aspect ratio of approximately 10. Fibres ≥ 5 μm long were approximately 8 μm in length and 0.3 μm in diameter with an aspect ratio of approximately 25. Ferruginous bodies were also counted in this study. Other types of particle and fibre were also reported, including mica, clays, amosite, and cleavage fragments of tremolite.

(iii)   Co-exposures

As shown in the Norwegian silicon carbide industry, workers are also co-exposed to total dust (GM range, < 0.29–21 μg/m³), respirable dust (GM range, < 0.12–1.3 μg/m³), respirable quartz (GM range, < 0.44–20 μg/m³), and respirable cristobalite (GM range, < 0.33– 35 μg/m³). Some other low-level contaminants, such as sulfur dioxide and polycyclic aromatic hydrocarbons, have also been reported (Føreland et al., 2008). The highest levels of fibres were reached for workers in the furnace department where high exposure to respirable dust also occurs (Føreland et al., 2012).

1.6   Regulations and guidelines

TWA values, short-term exposure limits, and other regulations or guidelines worldwide are summarized in Table 1.9.

Table 1.9 Regulations and guidelines for silicon carbide worldwide

Type of silicon carbide	Country or region	Concentration	Interpretation	Carcinogenicity
Non-fibrous silicon carbide		*(mg/m³)*		
	USA			
	OSHA (PEL)			
	Total dust	15	TWA	
	Respirable fraction	5	TWA	
	ACGIH (TLV)			
	Inhalable fraction[a]	10	TWA	
	Respirable fraction[a]	3	TWA	
	NIOSH (REL)			
	Total dust	10	10-h TWA	
	Respirable fraction	5	10-h TWA	
	United Kingdom			
	Total inhalable	10	TWA	
	Respirable fraction	4	TWA	
Fibrous silicon carbide		*(fibres/cm³)*		
	USA			
	ACGIH (TLV)[b]	0.1	TWA	A2
	Europe			
	SCOEL (OEL)[c]	1	TWA	
	Sweden			
	LLV	0.2		C

[a] Particulate matter containing no asbestos and < 1% crystalline silica

[b] Including whiskers: respirable fibres (length, > 5 μm; aspect ratio, ≥ 3:1) as determined by the membrane filter method at 400–450 × magnification (4 mm objective), using phase-contrast illumination

[c] Refractory ceramic fibres, including fibres of silicon carbide

A2, suspected human carcinogen; ACGIH, American Conference of Governmental Industrial Hygienists; C, carcinogenic; LLV, level limited value; NIOSH, National Institute for Occupational Safety and Health; OEL, occupational exposure limit; OSHA, Occupational Safety and Health Administration; PEL, permissible exposure limit; REL, recommended exposure limit; SCOEL, Scientific Committee on Occupational Exposure Limits; TLV, threshold limit value; TWA, 8-hour time-weighted average (unless otherwise specified)

From HSE (2011), NIOSH (2011), Swedish Work Environment Authority (2011), SCOEL (2012), OSHA (2015)

2. Cancer in Humans

2.1 Introduction

Only a few studies that refer directly to exposure to silicon carbide fibres have been published (see Table 2.1) and concerned workers were engaged in the production of silicon carbide, using the Acheson production process, where exposure to silicon carbide fibres was combined with exposure to a range of other dusts and gases, including non-fibrous silicon carbide. The Acheson process remains the dominant method of producing silicon carbide; the process

and related exposure conditions are described in Section 1. No studies were found of workers engaged in the production of silicon carbide whiskers. Other studies of workers exposed to silicon carbide include cohort studies of downstream users of the product, especially of workers in the abrasives industry. These studies were reviewed but were regarded as uninformative with respect to silicon carbide fibres because the Working Group had no evidence that workers producing or using abrasive materials were exposed to the fibres.

2.2 Silicon-carbide production industry

The first study to be published on a cohort from the silicon-carbide production industry was conducted in Canada by Infante-Rivard et al. (1994). A cohort of silicon-carbide production workers was subsequently studied in Norway by Romundstad et al. (2001) with updates and exposure–response analyses of lung cancer carried out by Bugge et al. (2010, 2012). Due to the similarities between silicon carbide fibres and asbestos, and also due to the observed induction of mesothelioma by silicon carbide whiskers in experimental animals, whether an increased incidence of mesothelioma was observed in the cohort studies was of special interest. Only the two Norwegian studies reported the incidence of pleural cancer or results for cancer sites other than lung and stomach.

In the Canadian study by Infante-Rivard et al. (1994), 585 silicon carbide industry workers employed for more than 2 years during 1950–80 were identified and their vital status, job history, and smoking histories were ascertained until 1989. A JEM on total dust was developed. No information on exposure to silicon carbide fibres specifically was available. Mortality from total and site-specific cancer was compared with that of the general population of the Province of Québec, and also related to cumulative exposure to total dust. The standardized mortality ratio (SMR) for lung cancer was 1.69 (95% confidence interval [CI], 1.09–2.52). Mortality from lung cancer showed a moderate increase with increasing cumulative exposure to total dust (see Table 2.1). Increased mortality from stomach cancer (SMR, 2.18; 95% CI, 0.88–4.51) was also observed. Data for other cancer sites were not presented. [One strength of this study was the collection of information concerning job history and smoking, either from the worker personally or from relatives. Weaknesses were mainly that the cohort was small and that only total dust

estimates were available. In addition, the method used to account for a minimum latency period (ignoring both years at risk and deaths during the first 15 years of employment) may have reduced the power of the study.]

A cohort of 2620 male workers employed for more than 6 months in 1913–96 in the Norwegian silicon carbide industry was established by Romundstad et al. (2001) and followed up from 1953 to 1996. Data on cancer incidence were obtained from the Norwegian Cancer Registry and comparisons were made with the general Norwegian population. A JEM on total dust, crystalline silica, silicon carbide fibres, and inorganic dust other than quartz and cristobalite, and potentially including silicon carbide particles and cleavage fragments, was constructed. Exposure assessments were mainly based on total dust measurements. An estimation of exposures other than those to total dust was based on a few measurements of these factors, and an estimation of the relative content of these factors in total dust was also made. [Uncertainties regarding exposure assessment due to the strong correlation between the different exposure factors and the small number of measurements precluded any firm conclusions based on the available data.]

Bugge et al. (2010) performed an update of the Norwegian cohort study (Romundstad et al., 2001), with the addition of employment information until 2003 and a further 9 years of cancer incidence follow-up (until 2005). A full report of cancer incidence in the silicon carbide industry was given in the study, but no exposure–effect analyses were performed. In a second study of the Norwegian cohort by Bugge et al. (2012), which included data on cancer incidence until 2008, a detailed JEM was constructed, based on new exposure measurements and mathematical modelling of historical exposure levels of total and respirable dust, non-fibrous and fibrous silicon carbide, quartz, and cristobalite (Føreland et al., 2012). In this last study (Bugge et al., 2012), the relative influence of different exposure factors

Table 2.1 Cohort studies of workers in the silicon-carbide production industry

Reference, location, follow-up period	Total No. of subjects	Exposure assessment	Organ site (ICD code)	Exposure categories	No. of exposed cases	Relative risk (95% CI)	Covariates; comments
Infante-Rivard et al. (1994), Québec (Province), Canada, 1950–89	585	Job-exposure matrix in 1984, total dust	Lung	Overall	24	SMR 1.69 (1.09–2.52)	Compared with age- and calendar-specific death rates among Québec (Province) men
				Total dust (mg-yr/m³)		IRR	
				< 105	5	1.00	SIRs from internal analysis; no latency
				105–275	9	1.48 (0.47–4.58)	
				> 275	10	1.67 (0.57–4.83)	
				< 105	5	1.00	SIRs from internal analysis; 15-yr latency
				105–275	9	1.25 (0.40–3.90)	
				> 275	10	1.36 (0.47–3.95)	
			Stomach	Overall	7	SMR 2.18 (0.88–4.51)	Compared with age- and calendar-specific death rates among Québec (Province) men
Bugge et al. (2010). Norway, 1953–2005	2612	Personnel records, duration of employment	Lung	Overall	103	2.0 (1.6–2.4)	Compared with age- and period-specific cancer incidence rates among Norwegian men
	1687		Lung	Overall	60	1.7 (1.3–2.2)	Long-term workers (≥ 3 yr of employment)
			Stomach	Overall	25	1.3 (0.9–1.9)	
			Lip	Overall	7	2.4 (1.2–5.1)	
			Oral cavity and pharynx (ICD-7: 141, 143–8)	Overall	10	2.1 (1.1–3.9)	
			Larynx	Overall	3	0.9 (0.3–2.8)	
			Pleura	Overall	1	0.8 (0.1–6.0)	
			Prostate	Overall	77	1.2 (1.0–1.5)	
			Leukaemia (ICD-7: 204)	Overall	6	2.8 (1.2–6.1)	

Table 2.1   (continued)

Reference, location, follow-up period	Total No. of subjects	Exposure assessment	Organ site (ICD code)	Exposure categories	No. of exposed cases	Relative risk (95% CI)	Covariates; comments
Bugge et al. (2012), Norway, 1953–2008	1687		Lung	Overall	62	1.6 (1.3–2.1)	Long-term workers (≥ 3 yr of employment)
		Department	Lung	Low exposure	3	1.0	Adjusted for age and smoking
				Furnace	20	3.8 (1.1–13)	
				Processing	9	1.6 (0.4–5.9)	
				Maintenance	9	1.5 (0.4–5.7)	
				Mixed	21	2.2 (0.7–7.5)	
	1166	Job-exposure matrix (Foreland et al., 2012)	Lung	Silicon carbide fibres (fibre–yrs/mL)		IRR	Ever-smoking, long-term workers; adjusted for age
				0–0.50	11	1.0	No lag
				0.50–2.0	14	1.0 (0.5–2.2)	
				2.0–93	33	1.7 (0.8–3.3)	
				0–0.50	21	1.0	20-yr exposure lag
				0.50–2.0	14	1.4 (0.7–2.9)	
				2.0–93	23	2.3 (1.2–4.4)	

CI, confidence interval; ICD, International Classification of Diseases; IRR, incidence rate ratio; SIR, standardized incidence ratio; SMR, standardized mortality ratio; yr, year

(including silicon carbide fibres) was estimated, but only for lung cancer incidence.

In Bugge et al. (2012), the standardized incidence ratio (SIR) for lung cancer in long-term workers (≥ 3 years of employment) was 1.6 (95% CI, 1.3–2.1). The results from the two earlier studies from this cohort showed similar SIRs of 1.9 (95% CI, 1.5–2.3; Romundstad et al., 2001) and 2.0 (95% CI, 1.6–2.4; Bugge et al., 2010) for lung cancer in the entire cohort. The highest incidence of lung cancer was observed among workers in the furnace department (SIR, 2.3; 95% CI, 1.5–3.5) and among workers with employment in more than one department (including furnace work) (SIR, 1.9; 95% CI, 1.3–2.9). Among workers in the processing and maintenance departments the SIR was 1.4 for both groups (95% CI, 0.7–2.7 and 0.7–2.6, respectively). Similar patterns of relative risks were observed in analyses using workers with low exposure as the referent group (Table 2.1). The SIR for lung cancer increased with increasing cumulative exposure to silicon carbide fibres, but also with indicators of other exposures, including cristobalite. Due to a high correlation between the different exposure factors, especially in the furnace halls, Poisson regression models were built to estimate the relative effect of the different exposure factors. The incidence of lung cancer was most strongly associated with exposure to cristobalite (incidence rate ratio, 1.9; 95% CI, 1.2–2.9 per log mg–years/m³ unadjusted; and 1.6; 95% CI, 0.8–3.3 per log mg–years/m³ adjusted for silicon carbide fibres and non-fibrous silicon carbide). The unadjusted incidence rate ratio with silicon carbide fibres was 1.9 (95% CI, 1.2–2.9 per log fibre–years/mL), but when adjusted for cristobalite and non-fibrous silicon carbide showed a weaker non-significant association (incidence rate ratio, 1.3; 95% CI, 0.7–2.6 per log fibre–years/mL).

Data for all other cancer sites were reported by Bugge et al. (2010). Only one case of cancer of the pleura (ICD-9 163) was reported among long-term workers, resulting in an SIR of 0.8 (95% CI, 0.1–6.0), but two cases were observed among the short-term workers (SIR, 3.7; 95% CI, 0.9–14.7). [The Working Group noted that the report did not provide information on the time elapsed between exposures in the silicon carbide industry and the diagnosis of mesothelioma.] The SIR for stomach cancer was 1.3 (95% CI, 0.9–1.9), while that for larynx cancer was 0.9 (95% CI, 0.3–2.8). An increased incidence of cancer of the oral cavity and pharynx (SIR, 2.1; 95% CI, 1.1–3.9; 10 cases), lip cancer (SIR, 2.4; 95% CI, 1.2–5.1; 7 cases), prostate cancer (SIR, 1.2; 95% CI, 1.0–1.5; 77 cases), and leukaemia (SIR, 2.8; 95% CI, 1.2–6.1; 6 cases) was also observed among the long-term workers. SIRs did not differ significantly from unity for other cancer sites in this group (Bugge et al., 2010). [Although elevated SIRs were observed for several cancers other than the lung, the confidence intervals were wide, the cancer sites are not known to be specific for exposure to fibres, and numerous comparisons were made. In light of these considerations, the Working Group concluded that a causal interpretation was not possible.]

[The strengths of this study were the access to a detailed JEM, based on a large number of new parallel measurements of total dust, respirable dust, respirable quartz, cristobalite, and non-fibrous silicon carbide, and fibrous silicon carbide. Mathematical modelling of historical exposure to several agents present in the industry allowed analyses of the exposures that were most strongly associated with cancer incidence. However, uncertainties still existed because historical total dust exposures before the late 1960s were estimated based only on knowledge about changes in the work organization and working hours. Correlations between estimated exposures to several agents, including silicon carbide particles and crystalline silica, challenged the interpretation of associations with silicon carbide fibres.]

2.3 Silicon-carbide user industry

Five studies on the incidence of or mortality from cancer with data from industries that use silicon carbide were found, two of which were carried out in the abrasives producing industries. Wegman & Eisen (1981) conducted a proportionate mortality study of abrasives manufacturers in Massachusetts, USA, and Edling et al. (1987) studied cancer incidence among Swedish workers manufacturing abrasives. The other three studies were performed in industries using abrasives for polishing. Sparks & Wegman (1980) studied proportionate mortality among jewellery polishers in Massachusetts, USA, Järvholm et al. (1982) studied cancer incidence among steel polishers in Sweden, and Jakobsson et al. (1997) studied cancer incidence among workers in a Swedish stainless steel factory.

[These studies contained very little information on levels of exposure to dust in general and no information on exposure to silicon carbide fibres specifically. Because the Working Group had no evidence that workers producing or using abrasive silicon carbide products have significant exposure to silicon carbide fibres, these studies were not considered to be relevant for the evaluation.]

3. Cancer in Experimental Animals

Studies of fibrous silicon carbide in experimental animals were available only for silicon carbide whiskers and only in rats.

3.1 Inhalation

See Table 3.1

Two groups of 40 AF/Han specific pathogen-free rats [sex and age unspecified] were exposed by inhalation for 7 hours per day on 5 days a week for approximately 12 months to silicon carbide whiskers (Advanced Composite Materials Corporation (ACMC), Greer, SC, USA; mean diameter, 0.45 µm; 984 whiskers/mL, > 5 µm in length in airborne dust clouds). After exposure, the rats were allowed to live their full life-span, although the study was terminated when the number of survivors in each group decreased to 6. Moribund animals and those surviving to the end of the study were killed and the lungs were examined microscopically for tumours. In the silicon carbide whisker-exposed rats, pulmonary carcinomas were present in 5 out of 42 (12%) [not significant] animals, pulmonary adenomas in 5 out of 42 (12%) [not significant] animals, and pleural mesotheliomas in 10 out of 42 (24%) [$P = 0.0003$] animals (Davis et al., 1996). A concurrent control group was not included in the study; however, the authors stated that in a group of control rats of the same strain and maintained in the same laboratory from a previous study with a similar study design, the incidence of pulmonary adenoma was 1 out of 47 (2%), that of pulmonary carcinoma was 1 out of 47 (2%), and that of mesothelioma was 0 out of 47 (Davis et al., 1991). [The Working Group noted the absence of a concurrent control group. Statistical analysis was not performed by the authors, but statistics were calculated by the Working Group based on the incidence of tumours reported for the control group of the previous study.]

Two groups of 42 male Wistar rats (age, 4 weeks) were exposed by inhalation for 6 hours per day on 5 days a week for 12 months to silicon carbide whiskers (GM length, 2.8 µm; GM diameter, 0.5 µm; mass median aerodynamic diameter [MMAD], 2.4 µm; daily average fibre count, 98 ± 19 whiskers/mL) or clean air (control) and were killed 6 days, or 3, 6, or 12 months after exposure. No lung tumours were reported. However, 12 months after exposure, fibrotic changes were present in the lungs and bronchiolo-alveolar hyperplasia was observed in two exposed animals (Akiyama et al., 2007). [The Working Group noted that this study was designed to evaluate the biopersistence of silicon

Table 3.1 Studies of carcinogenicity with silicon carbide whiskers in rats

Strain (sex) Duration Reference	Dosing regimen, Animals/group at start	For each target organ: incidence (%)	Significance	Comments
AF/Han (SPF) (NR) Lifetime Davis et al. (1996)	7 h/day, 5 days/wk, by inhalation, for about 12 mo, then held for life SiC-W (ACMC): mean diameter, 0.45 μm; length, > 5 μm; 984 whiskers/mL 2 × 40/group	Pulmonary carcinoma: control, 1/47 (2%); SiC-W, 5/42 (12%) Pulmonary adenoma: control, 1/47 (2%), SiC-W, 5/42 (12%) Pleural mesothelioma: control, 0/47; SiC-W, 10/42 (24%)	[NS] [NS] [P = 0.0003]	Statistics, Fisher exact test; age at start, NR; no concurrent control group; a group of control animals of the same strain and maintained in the same laboratory from a previous study with a similar design (Davis et al., 1991) was used by the Working Group for statistical analysis instead of a concurrent control group
Wistar (M) 24 mo Akiyama et al. (2007)	6 h/day, 5 days/wk, by inhalation, for 12 mo, then held for up to an additional 12 mo 0 (clean air, control) or 98 ± 19 whiskers/ mL (GM diameter, 0.5 μm; GM length, 2.8 μm; MMAD, 2.4 μm) 42/group	Lung tumours: 0/33, 0/31 Bronchiolo-alveolar hyperplasia at 24 mo: 0/13, 2/11	NS NS	Rats (exposed and control) killed at 6 days (n = 10 and 10), 3 mo (n = 5 and 5), 6 mo (n = 5 and 5) or 12 mo (n = 11 and 13) after the 12 mo exposure period; although the study was 2 yr in duration, the exposure duration may have been too short to evaluate carcinogenicity
F344/ NTacBR (F) 18 mo Vaughan et al. (1993)	Single administration, by intratracheal instillation, then held for 18 mo SiC-W-1 (GM diameter, 0.8 μm; GM length, 18.1 μm)/SiC-W-2 (GM diameter, 1.5 μm; GM length, 19.0 μm) suspended in PBS and instilled at doses of 1.0 or 5.0 mg/100 mL MRV; controls received PBS 25/dose per group	No treatment-related mesotheliomas or other malignant tumours reported	NS	The duration of the study was probably too short to evaluate carcinogenicity; the Working Group noted the limited reporting of the study and the low dose used
Osborne-Mendel (F) 2 yr Stanton et al. (1981)	Single dose of 40 mg SiC-W or one of 71 mineral fibres and particles dispersed in hardened gelatin and implanted onto the left pleural surface (intrapleural implantation) after thoracotomy, then held for 2 yr 30–50/group	Pleural sarcoma [sarcomatoid mesothelioma]: Untreated controls, 1/248 (0.4%); sham controls, 8/267 (3.0%); negative controls, 16/562 (2.8%); combined controls, 25/1077 (2.3%); SiC-W-treated, 17/26 (65%)	[P = 0.0001]	Statistics, Fisher exact test; fibre dimensions NR; statistics calculated by the Working Group, based on a combination of controls (untreated), sham controls (thoracotomy, no implant), and negative controls (thoracotomy with non-fibrous implant) that were controls (from numerous experiments) of the same species, sex, and age, from the same laboratory

Table 3.1 (continued)

Strain (sex) Duration Reference	Dosing regimen, Animals/group at start	For each target organ: incidence (%)	Significance	Comments
F344/N (F) Up to 28 mo Johnson & Hahn (1996)	Single dose by intrapleural injection (in 4 mL saline) of 0 (50 rats) or 20 mg of SiC-W-1 (length, 4.5 μm; diameter, 0.42 μm), SiC-W-2 (length, 20.1 μm; diameter, 0.75 μm), or SiC-W-3 (length, 6.6 μm; diameter, 0.32 μm) 30/group unless otherwise specified	Pleural mesothelioma: control, 0/50; SiC-W-1, 27/30; SiC-W-2, 26/30; SiC-W-3, 7/30	[P = 0.0001], [P = 0.0001], [P = 0.0006]	Statistics, Fisher exact test; survival of rats treated with SiC-W-1 or SiC-W-2 lower than that of controls
Wistar (F) At least up to 130 wk Pott et al. (1991)	Single dose 0 (72 rats), 0.05, 0.25, 1.25, 6.25, or 25 (48 rats) mg of SiC-W (diameter, 0.31 μm; length, 3.1 μm) by intraperitoneal injection in 2 mL of saline, then held at least up to 130 wk 36/group unless otherwise specified	Mesothelioma or sarcoma in the abdominal cavity: control: 2/50 (4%); 0.05 mg, 2/16 (12.5%); 0.25 mg, 5/23 (21.7%), 1.25 mg, 13/21 (61.9%); 6.25 mg, 23/30 (76.7%); 25 mg, 36/37 (97.3%)	[NS], [P = 0.0285], [P = 0.0001], [P = 0.0001], [P = 0.0001]	Statistics, Fisher exact test; age at start NR; weight, 160 g; statistical analyses not reported by the authors; the study was compromised by an infectious disease of the lung in experimental months 12 and 13 that significantly reduced the mean life span; the Working Group judged that this did not influence the induction of abdominal cavity tumours
F344/ NTacfBR (F) 18 mo Vaughan et al. (1993)	Single dose of 0 or 20 mg of SiC-W-2 (GM diameter, 1.5 μm; GM length, 19.0 μm) by intraperitoneal injection in 1 mL PBS, then held for 18 mo 20/group	No malignant mesothelioma in SiC-W-2-treated or control groups and no treatment-related tumours reported at other sites	NS	SiC-W-2 from American Matrix, Knoxville, KY, USA
AF/Han (NR) Lifetime Davis et al. (1996)	Single dose of 10⁹ fibres/2 mL of SiC-W (ACMC, mean diameter, 0.45 μm) or glass microfibres (C100/475; mean diameter, 0.32 μm) by intraperitoneal injection in PBS, then held for life Fibres all > 5 μm long 24/group	Mesothelioma: SiC-W, 22/24 (92%); glass microfibre, 8/24 (33%)	NA	Age at start NR; mesotheliomas appeared most rapidly in SiC-W-treated rats; time at which 50% survival was achieved, 257 days for SiC-W and 679 days for glass microfibres; no vehicle control group included in this study, so statistical analysis could not be performed; the Working Group noted the limited reporting of the study
F344/Nslc (F) Up to 2 yr Adachi et al. (2001)	Intraperitoneal injection 5 or 10 mg (mean ± SD: 414 × 10³ whiskers/μg; length, 6.40 ± 2.45 μm; diameter, 0.30 ± 1.58 μm) of SiC-W or 10 mg of UICC chrysotile B (positive control) fibres suspended in saline (1 mg/mL) by intraperitoneal injection; animals were held up to 2 yr 330 rats divided into 24 groups [estimate, 13–14/group]	Peritoneal mesothelioma (epithelial or sarcomatous): 10 mg SiC-W, 100% (within 1 yr); 5 mg SiC-W, 70% (within 1 yr); UICC chrysotile B, 85% (within 2 yr)	NA	Highest volume of an administration to rat in a week was 5 mL; no vehicle controls in the study, therefore statistical analyses could not be performed; the Working Group noted the limited reporting of the study; length and diameter reported by Kohyama et al. (1997)

ACMC, Advanced Composite Materials Corporation; d, day; F, female; GM, geometric mean; M, male; MMAD, mass median aerodynamic diameter; MRV, minute respiratory volume; mo, month; NA, not applicable; NR, not reported; NS, not significant; PBS, phosphate-buffered saline; SD, standard deviation; SiC-W, silicon carbide whisker; wk, week; yr, year

carbide whiskers and not as a carcinogenicity study.]

3.2 Intratracheal instillation

Groups of female Fischer 344/NTacfBR rats (age, 9 weeks) received a single intratracheal instillation of one of two samples of silicon carbide whiskers: SiC-W-1 (GM diameter, 0.8 μm; GM length, 18.1 μm; Tateho, Inc., Japan) and SiC-W-2 (GM diameter, 1.5 μm; GM length, 19.0 μm; American Matrix, Knoxville, KY, USA). The minute respiratory volume (MRV) was estimated for each animal, and the test materials were suspended in phosphate buffered saline (PBS) and diluted to 1.0 mg/100 mL MRV (low dose) and 5.0 mg/100 mL MRV (high dose). Each of the two samples was administered to a minimum of 50 rats, half of which received the low dose and half received the high dose. A group of control animals of similar size received the PBS vehicle. The animals were killed 18 months after treatment, and the lungs, liver, spleen, kidneys, heart, and incidental tumours were collected for histopathological evaluation. Exposure to SiC-W-1 and SiC-W-2 induced the development of pulmonary granulomas, and exposure to SiC-W-1 also produced bronchiolar mucosal hyperplasia. However, no mesotheliomas or other malignant tumours that could be attributed to treatment were observed (Vaughan et al., 1993). [The Working Group noted the limited reporting of the study, the low dose used, and the duration of the study that was probably too short for an evaluation of carcinogenicity.]

3.3 Intrapleural implantation

In a study to evaluate the relationship between fibre dimension and carcinogenicity, groups of 30–50 female Osborne-Mendel rats (age, 12–20 weeks) were implanted with a hardened gelatin pellet containing 40 mg of one of 72 uniformly distributed mineral fibres, including silicon carbide whiskers [fibre dimensions unspecified], into the left pleura after thoracotomy and were followed for 2 years, at which time the survivors were killed and necropsied. Three groups of controls from numerous experiments from the same laboratory were also available: untreated rats, sham controls that underwent thoracotomy but no fibre implant, and rats that received implants of non-fibrous materials. Fibrosarcomas of the left mammary gland and subcutaneous fibrosarcomas were considered to be spontaneous tumours or to be induced by the suture material. At 2 years, pleural sarcomas [sarcomatoid mesotheliomas] were present in 25 out of 1077 (2.3%) animals of the three control groups (combined). The incidence of pleural sarcomas in silicon carbide whisker-treated rats was 17 out of 26 (65%) [$P = 0.0001$] (Stanton et al., 1981). [Statistical analysis was not reported by the authors, but statistics were calculated by the Working Group, based on the combination of controls from numerous experiments from the same laboratory.]

Another study was conducted to determine the potential of three samples of silicon carbide whiskers to induce mesothelioma after intrapleural injection. Groups of female Fischer 344/N rats (age, 6–8 weeks) were given a single intrapleural injection of either 4 mL saline (vehicle controls; 50 rats), 20 mg of SiC-W-1 (length, 4.5 μm; diameter, 0.42 μm; 30 rats) in 4 mL saline, SiC-W-2 (length, 20.1 μm; diameter, 0.75 μm; 30 rats) in 4 mL saline, or SiC-W-3 (length, 6.6 μm; diameter, 0.32 μm; 30 rats) in 4 mL saline. The rats were killed when moribund or after 28 months. Animals were necropsied and the incidence of pleural mesotheliomas was determined after microscopical examination. The survival of rats treated with SiC-W-1 or SiC-W-2 was significantly shorter than that of saline controls ($P < 0.05$). The incidence of pleural mesothelioma in rats treated with SiC-W-1 or SiC-W-2 was 27 out of 30 [$P = 0.0001$] and 26

out of 30 [P = 0.0001], respectively. SiC-W-3 caused pleural mesotheliomas in 7 out of 30 rats [P = 0.0006]. No pleural mesotheliomas were identified in the 50 saline controls (Johnson & Hahn, 1996).

3.4 Intraperitoneal injection

Groups of female Wistar rats [age not reported] (weight, 160 g) were given a single intraperitoneal injection of 0.05 (36 rats), 0.25 (36 rats), 1.25 (36 rats), 6.25 (36 rats) or 25 (48 rats) mg of silicon carbide whiskers (length, 3.1 μm; diameter, 0.31 μm) in 2 mL saline. A control group of 72 rats received weekly intraperitoneal injections of 2 mL of saline for 5 weeks. Animals surviving until termination of the experiment were observed for up to 130 weeks. The number of rats with mesothelioma or sarcoma in the abdominal cavity relative to the number of rats examined that survived at least 56 weeks or died earlier with tumours was: control, 2 out of 50 (4%); 0.05 mg, 2 out of 16 (12.5%) [not significant]; 0.25 mg, 5 out of 23 (21.7%) [P = 0.0285]; 1.25 mg, 13 out of 21 (61.9%) [P = 0.0001]; 6.25 mg, 23 out of 30 (76.7%) [P = 0.0001]; and 25 mg, 36 out of 37 (97.3%) [P = 0.0001] (Pott et al., 1991). [The study was compromised by an infectious disease of the lung that occurred during experimental months 12 and 13 and significantly reduced the mean lifespan. The Working Group judged that this did not influence the induction of abdominal cavity tumours. Statistical analyses were not reported by the authors.]

Groups of 20 female Fischer F344/NTacfBR rats (age, 9 weeks) received a single intraperitoneal injection of 0 or 20 mg of silicon carbide whiskers (SiC-W-2; GM diameter, 1.5 μm; GM length, 19.0 μm; American Matrix) in 1 mL of PBS and were killed 18 months later, at which time the lungs, liver, spleen, kidneys, heart, and incidental tumours were collected for histopathological evaluation. Peritoneal fibrosis occurred in 90% of the silicon carbide whisker-treated animals; however, no malignant mesotheliomas were found. No treatment-related tumours were reported at other sites (Vaughan et al., 1993).

A study was conducted to assess the ability of SiC-W to produce mesotheliomas. Groups of 24 AF/Han rats [sex and age unspecified] received a single intraperitoneal injection of 10^9 fibres (length, > 5 μm) of silicon carbide whiskers (ACMC) or glass microfibres (C100/475) suspended in 2 mL PBS. The incidence of mesotheliomas was 22 out of 24 (92%) for silicon carbide whiskers and 8 out of 24 (33%) for glass microfibres. Mesotheliomas appeared more rapidly in silicon carbide whisker-treated rats. The time at which 50% survival was achieved was 257 days for silicon carbide whiskers and 679 days for glass microfibres (Davis et al., 1996). [A vehicle control group was not included in this study and statistical analysis was not performed. The Working Group also noted the limited reporting of the study.]

Groups of 13–14 female Fischer 344/Nslc rats (age, 5 weeks) received intraperitoneal injections of 5 or 10 mg of silicon carbide whiskers (length, (mean ± standard deviation [SD]), 6.40 ± 2.45 μm; diameter (mean ± SD), 0.30 ± 1.58 μm (reported by Kohyama et al., 1997); 414 × 10^3 whiskers/μg) suspended in saline (1 mg/mL). A third group of rats was injected with 10 mg of UICC chrysotile B as a positive control. The greatest volume administered to rats in a week was 5 mL. The animals were observed for up to 2 years. Dead and moribund animals were necropsied and fixed tissues were examined microscopically for peritoneal mesothelioma. All rats given 10 mg of silicon carbide whiskers and 70% of rats injected with 5 mg of silicon carbide whiskers developed peritoneal mesotheliomas within 1 year. Microscopically, the tumour cells exhibited a variety of characteristics including epithelial or sarcomatous structures. UICC chrysotile B produced peritoneal mesotheliomas in 85% of treated rats by the end of the study (2 years)

(Adachi et al., 2001). [The Working Group noted the limited reporting of the study. The authors stated that 330 rats were divided into 24 groups, but the exact number of rats per treatment group was not reported and was assumed to be 13–14 per group. No vehicle controls were available and statistical analyses could therefore not be performed.]

4. Mechanistic and Other Relevant Data

4.1 Deposition, phagocytosis, retention, translocation, and clearance

The characteristics of the silicon carbide forms employed in experimental studies are reported in Table 4.1.

4.1.1 Humans

Several studies have been published concerning the occupational exposure of humans to silicon carbide (see Table 4.2). In the human setting, very little is known regarding the specific deposition, phagocytosis, and translocation of silicon carbide fibres in the lungs, with the exception of studies of silicon carbide in human monocytes in vitro (Nordsletten et al., 1996). However, it is clear that silicon carbide fibres are highly respirable (Funahashi et al., 1984; Dufresne et al., 1993, 1995).

4.1.2 Experimental animals

See Table 4.3

(a) Deposition

The deposition fraction of silicon carbide whiskers (TWS-100; 98% silicon carbide; CAS No. 409-21-2) was estimated in the lungs of male Wistar rats exposed by whole-body inhalation for 6 hours per day on 5 days per week for 4 weeks to 10.4 (± 0.5) mg/m³ (214 ± 31 fibres/mL). The GM fibre length was 2.2 µm (GSD, 1.9), indicating that > 90% of fibres were less than 10 µm in length, the GM fibre diameter was 0.4 µm (GSD, 1.6), and the MMAD was 2.5 µm (GSD, 2.7). A total of 77 rats (42 exposed, 35 unexposed controls) were studied, and groups of 5 or 12 rats were killed 3 days, 2 weeks, and 1, 2, 3, 6, and 12 months after exposure. The average lung burdens of silicon carbide measured at each time-point after exposure were: 0.60, 0.52, 0.44, 0.36, 0.34, 0.19, and 0.07 mg, respectively. The deposition fraction of silicon carbide whiskers in the lungs was estimated by calculating the ratio of the measured mass of silicon carbide in the lungs divided by the mass of silicon carbide whiskers inhaled during the exposure. The mass of inhaled silicon carbide was calculated by multiplying the average exposure concentration by the total exposure time by the respiratory volume. The estimated average total mass inhaled was reported as 12.5 mg, and the apparent deposition fraction (as a percentage) was reported as 4.8%. [These reported values can be calculated as follows: total mass inhaled – 12.5 mg = 10.4 mg/m³ × (6 h/day × 5 days/week × 4 weeks × 60 min/h) × 0.167 L/min × (1 m³/1000 L); deposition fraction – 4.8% = (0.6 mg (silicon carbide lung burden on day 3 after exposure)/12.5 mg) × 100.] The minute ventilation of 0.167 L/min used in the calculations herein was estimated to obtain the reported total inhaled mass of silicon carbide (i.e. 12.5 mg) (Akiyama et al., 2003). This was lower by a factor of 4 than the value of 0.037 L/min for mice reported by the Environmental Protection Agency (EPA, 1988, 2006), but was very similar to the value of 0.165 L/min (165 cm³/min) for mice reported by Shvedova et al. (2008).

In a 1-year whole-body inhalation study (with exposure conditions similar to those in Akiyama et al. (2003)), the mass of silicon carbide whiskers deposited in each rat lung 6 days after exposure (measured by X-ray diffraction) was 5.3 ± 1.4 mg. The lung deposition fraction (as a percentage)

Table 4.1 Main characteristics of the forms of silicon carbide employed in experimental studies

Silicon carbide form	Particle/fibre type	Purity
Abrasive dust from the Acheson process[a]	Mixture of particles, fibres and fibre fragments	High level of impurities
Whiskers	Needle-like single crystals	Pure
Nanoparticles	Isometric nanoparticles	Pure

[a] In one study (Dufresne et al., 1992), the angular fragments and fibres isolated from the Acheson process were studied separately

was estimated to be 12.9% (calculated as in Akiyama et al. (2003)), which was higher than the estimated 4.8% deposition estimated after 4 weeks of inhalation exposure (Akiyama et al., 2007). [In the calculation of deposition fractions in Akiyama et al. (2003, 2007), the use of the measured lung dose at the end of the 4-week or 12-month exposure period would not have accounted for the portion of deposited silicon carbide whiskers that were cleared from the lungs during the exposure period. Thus, the deposition fraction would be underestimated by the amount that was cleared during the exposure period (and therefore not measured in the lungs at the end of the exposure).]

See Sections 4.1.2 (d) and 4.1.2 (e) for more information on the retention and clearance of silicon carbide in the 4-week and 1-year inhalation studies (Akiyama et al., 2003, 2007), each with follow-up examinations at up to 12 months after exposure.

(b)   Phagocytosis

Inhaled fibres can be deposited in the pulmonary (alveolar) region of the lungs, depending on their aerodynamic or diffusion diameter, their shape, and orientation in the air stream (Asgharian & Yu, 1989a, b). Alveolar macrophages can phagocytize shorter fibres (e.g. < 5 μm) and clear them from the lungs via the mucociliary escalator. However, fibres that are physically longer than macrophages cannot be fully engulfed or effectively cleared (Lippmann, 1993; Oberdörster, 1994). Rat macrophages are approximately 10–13 μm long (human alveolar macrophages are approximately 14–21 μm long) (Stone et al., 1992; Oberdörster, 2000). Fibres that are not cleared by macrophages could undergo dissolution and breakage over time (depending on their solubility in biological fluids) or enter the lymphatic system if shorter (e.g. < 5 μm in length) (Oberdörster et al., 1988; Murphy et al., 2011). Fibres may also be actively transported to the lymphatic system by alveolar macrophages, as was shown for particles in dogs, in which macrophages carried red fluorescent microspheres (diameter, 1.3 μm; 5×10^{10} particles instilled per lung) to the regional tracheobronchial lymph nodes (Harmsen et al., 1985).

Studies of silicon carbide have reported that most structures are < 10 μm in length and insoluble (Dufresne et al., 1992; Searl et al., 1999; Akiyama et al., 2003). Thus, macrophage-mediated clearance of these structures would be expected at lung doses that do not cause overloading (e.g. 0.6 mg in rats) (Akiyama et al., 2003). However, a proportion of silicon carbide fibres may be longer; Akiyama et al. (2003) reported that approximately 10% of silicon carbide whiskers were > 10 μm in length and Miller et al. (1999) estimated that approximately 30% of silicon carbide whiskers were > 10 μm in length. Longer insoluble fibres that are inhaled and deposited in the alveolar region would be unlikely to be cleared by macrophages or to dissolve, and would therefore have long retention half-times in the lungs.

A study in Syrian golden hamsters showed that silicon carbide whiskers were taken up by primary alveolar macrophages obtained from the BALF. SEM showed that some of the macrophages were penetrated by fibres that were longer than the cells. A dose-dependent effect of the silicon carbide whiskers on the cell

273

Table 4.2 Studies of occupational exposure to silicon carbide

Setting	Activity	Sampling event parameters	Concentration of silicon carbide	Reference
Two workers in a factory using silicon carbide	Manufacturing refractory bricks	Personal exposure over many years; bilateral reticulonodular densities on chest radiograms; biopsy from one patient revealed fibrosed alveolar septums; X-ray powder diffraction analysis of the lung tissue revealed at least 6 different types of silicon carbides, traces of tungsten carbide, and an insignificant amount of quartz	NR	Funahashi et al. (1984)
Silicon-carbide factory workers with low levels of exposure to sulfur dioxide	145 production workers with an average of 13.9 (range, 3–41) yr of employment in this industry	Respiratory symptoms (phlegm, wheeze, and mild exertional dyspnea) were more closely associated with exposure to sulfur dioxide than exposure to silicon carbide	Cumulative exposure to sulfur dioxide averaged 1.94 (range, 0.02–19.5) ppm–years; low-level exposures to respirable dust also occurred (0.63 ± 0.26 mg/m^3); cumulative exposure to dust was significantly associated with chronic wheeze in the 10–20 mg-yrs/m^3 exposure category (odds ratio, 3.45; $P < 0.05$, chi-squared statistics)	Osterman et al. (1989)
267 silicon carbide factory workers	Production of silicon carbide abrasive (carborundum)	Chest opacities (profusion q1/0 and q2/1) on X-ray film were correlated with cumulative exposure to dust; pulmonary function was affected by cumulative dust exposure, profusion of opacities, and smoking	No exposure concentrations exceeded the permissible limits during the study period. (0.30–1.0 mg/m^3)	Marcer et al. (1992)
Silicon carbide factory worker	Working near a Acheson furnace of a silicon carbide plant for 42 yr	At autopsy, the concentration of silicon carbide fibres longer than 5 μm was 39 300 fibres/mg dry lung; the fibres had a similar morphology to those observed in the working environment	NR	Dufresne et al. (1993)
Silicon carbide factory workers	15 Canadian men who worked in the primary silicon carbide industry	Five men had neither lung fibrosis nor lung cancer (NFNC), 6 had lung fibrosis (LF), and 4 had lung fibrosis and lung cancer (LFLC); the workers had 23–32 yr of exposure, with means of 23.4 (SD, 6.9) yr in the NFNC group, 28.8 (SD, 5.5) yr in the LF, and 32.3 (SD, 9.0) yr in the LFLC group	Excess pulmonary retention of silicon carbide fibres ≥ 5 μm in LF and LFLC cases	Dufresne et al. (1995)
Three Norwegian silicon carbide plants	Identification and quantification of airborne fibrous particles in the plants	Silicon carbide fibres generated during the industrial production of silicon carbide; most fibres found during the mixing of the raw material; 47 different dust samples examined; several α-silicon carbide polytypes were present along the axis in each single fibre particle; no fibrous particles were observed in the final abrasive products	Fibre concentration (10^6 fibres/m^3) during mixing of raw material (0.3 in plant A; 0.1–1.9 in plant B; 1.8–4.9 in plant C)[a]	Bye et al. (1985)

Table 4.2 (continued)

Setting	Activity	Sampling event parameters	Concentration of silicon carbide	Reference
Canadian silicon-carbide production plants	Report on the concentration of silicon carbide fibres, crystalline silica, and respirable dust in the plants	In the Canadian silicon-carbide production plants, two silica polymorphs, quartz, and cristobalite, were present as respirable particulates; respirable silicon carbide fibres were present in Norwegian and Italian occupational settings at a higher concentration than in the Canadian industries	Highest 8-h time-weighted average concentrations of fibres were found among crusher and backhoe attendants and carboselectors (arithmetic means of 0.63 fibres/mL and 0.51 fibres/mL, respectively)	Dion et al. (2005)
Norwegian silicon carbide industry	1687 long-term Norwegian silicon carbide workers employed from 1913 to 2003	Lifetime occupational exposure of workers based on total dust, silicon carbide, and crystalline silica concentrations found in the silicon carbide industry associated with increased mortality from non-malignant respiratory diseases (obstructive lung disease); exposure–response relationships were found for both silicon carbide and crystalline silica (twofold risk)	Total dust: low, 0–28.6 mg–yrs/m³; medium, 28.7–86.1 mg–yrs/m³; high, > 86.2 mg–yrs/m³; Silicon carbide dust: low, 0–0.7 mg–yrs/m³; medium, 0.8–2.6 mg–yrs/m³; high, > 2.7 mg–yrs/m³	Bugge et al. (2011)
Norwegian silicon carbide industry	Silicon carbide workers (see Bugge et al. 2011)	Cumulative exposure to total and respirable dust, respirable quartz, cristobalite, and silicon carbide particles and silicon carbide fibres was assessed	Exposure level and lung cancer risk most significant for total dust and cristobalite; a moderate association with silicon carbide	Bugge et al. (2012)
Employees in Norwegian silicon carbide plants	All employees, age 20–55 yr at inclusion ($n = 456$), were examined annually for up to 5 yr (1499 examinations)	The annual change in forced expiratory volume (FEV) in one second per squared height (FEV1/height²) per mg/m³ increase in dust exposure was −2.3 (95% confidence interval, −3.8 to −0.79) (mL/m²)/yr	Dust exposure, expressed by a quantitative job–exposure matrix, was found to be associated with an increased yearly decline in FEV1 in employees of Norwegian silicon carbide plants	Johnsen et al. (2013)

[a] Number of samples: plant A, 1; plant B, 7; plant C, 4

NR, not reported; yr, year

275

Table 4.3 Kinetics of silicon carbide in experimental animals

Type of silicon carbide	Dimensions and surface area	Species (age and sex)	Route of exposure and dose/exposure concentration	Duration of study	Findings	Comments	Reference
Silicon carbide whiskers (CAS No. 409-21-2), TWS-100 (Tokai Carbon Co.); 98% silicon carbide	GM length, 2.2 μm (GSD, 1.9); GM diameter, 0.4 μm (GSD, 1.6); MMAD, 2.5 μm (GSD, 2.7)	Wistar rat (male; age, 9 wk)	Whole-body inhalation; 10.4 (± 0.5) mg/m³ (214 ± 31 fibres/mL)	4-wk exposure (6 h/day, 5 days/wk); animals killed 3 days, 2 wk, 1, 2, 3, 6, or 12 mo after exposure	Average lung burdens of silicon carbide whiskers were 0.60, 0.52, 0.44, 0.36, 0.34, 0.19, and 0.07 mg, respectively, at the time-points after exposure; estimated total mass inhaled was 12.5 mg; lung deposition fraction estimated at 4.8%; estimated biological $t_{1/2}$ of 4 mo		Akiyama et al. (2003)
Silicon carbide whiskers, TWS-100 (Tokai Carbon Co.) [same as Akiyama et al. (2003)]	GM length, 2.4 μm (GSD, 2.3); GM diameter, 0.5 μm (GSD, 1.5); MMAD, 2.4 μm (GSD 2.4)	Wistar rat (male; age, 4 wk)	Whole-body inhalation; 2.6 (± 0.4) mg/m³ (98 ± 19 fibres/mL)	1-yr exposure (6 h/day, 5 days/wk); animals killed 6 days, 3, 6, or 12 mo after exposure	Lung burden of silicon carbide whiskers 6 days after exposure was 5.3 ± 1.4 mg; lung deposition fraction was estimated at 12.9%. At 6 days, 3, 6, and 12 mo after exposure, respectively: mean fibre diameter: 0.32, 0.29, 0.35, and 0.32 μm; mean fibre length: 1.55, 1.40, 1.90, and 2.62 μm; estimated biological $t_{1/2}$ of 16 mo		Akiyama et al. (2007)

Table 4.3 (continued)

Type of silicon carbide	Dimensions and surface area	Species (age and sex)	Route of exposure and dose/exposure concentration	Duration of study	Findings	Comments	Reference
Silicon carbide whiskers (ACMC)	Fibre distribution injected: 821, 577, 387, 307, 185, and 121 × 10⁶ for cumulative length categories of > 0.4, > 5, > 8, > 10, > 15, and > 20 μm, respectively (fibre diameter < 0.95 μm); 1–4 × 10⁶ fibres per cumulative length category (fibre diameter > 0.95 μm)	Wistar rat (male; age NR)	Intratracheal instillation (Searl et al., 1999); intraperitoneal injection (Miller et al., 1999) [intratracheal instillation also mentioned in Miller et al. (1999)]; 14.2 mg (821 × 10⁶ fibres > 0.4 μm long)	3 days, 1, 6, and 12 mo after exposure	Mean fibre number in the lungs was 80.9 × 10⁶ at 3 days and 29.3 × 10⁶ at 12 mo after exposure by intratracheal instillation; retention of fibres 1 yr after exposure was 36%; mean fibre diameter for all fibres > 0.4 μm long was 0.48 μm at 3 days and 0.50 μm at 12 mo after exposure; that for fibres > 20 μm long was 0.53 μm at 3 days and 0.55 μm at 12 mo; no significant change in the length of whiskers up to 12 mo after exposure; the ratio of complex whiskers (i.e. > 1 fibrous component) to single whiskers was unchanged over the 12 mo period; the estimated retention of fibres in the cumulative length categories (> 0.4, > 5, > 8, > 10, > 15, and > 20 μm) was 52.6, 53.7, 47.7, 49.2, 54.5, and 59.2%, respectively		Searl et al. (1999), Miller et al. (1999)

Table 4.3 (continued)

Type of silicon carbide	Dimensions and surface area	Species (age and sex)	Route of exposure and dose/exposure concentration	Duration of study	Findings	Comments	Reference
Silicon carbide (carborundum)	Non-fibrous (angular) or fibrous; largest fibres, ~30 μm in length and 0.5 μm in diameter; mean diameter of non-fibrous particles, 0.92 μm	Sheep [see Bégin et al. (1985, 1989) for more details]	Injection of 100 mg of either fibrous or non-fibrous silicon carbide (in 100 mL saline) into the tracheal lung lobe	BALF was obtained before and 2, 4, 6, and 8 mo after exposure	Mass concentration of carborundum in BALF at 2 mo was ~60 and 200 ng/mL for fibrous and non-fibrous silicon carbide, respectively; estimated clearance $t_{1/2}$ of 1.7 or 5.8 mo, respectively, for the sheep in the fibrous or non-fibrous groups; average retained lung dose in tracheal lobe 8 mo after exposure was 219 ng/mg dry lung in the non-fibrous group, and 4.6 and 58 ng/mg dry lung for fibrous and angular silicon carbide, respectively, in the fibrous group	Samples collected from a workplace furnace; fibrous sample contained several morphological types of fibre as well as angular particles (27% by wt) and graphite (5% by wt); non-fibrous sample was ~90% silicon carbide and 10% aluminium oxide	Dufresne et al. (1992)
Silicon carbide (carborundum)	Information on size NR [carborundum dust separated from powder, suggesting fine-sized (vs ultrafine-sized) fraction was used]	Mouse (strain, sex, and age NR)	Intraperitoneal injection; ~4 mg of carborundum silica (as silicon dioxide) in peanut oil	14 days after exposure	Elevated mass levels of silicon dioxide measured in liver, spleen, and abdominal lymph glands 14 days after injection; those in kidney were slightly elevated relative to those in controls; carborundum (expressed as silicon dioxide) not measurably excreted in urine during the 14 days after exposure		Holt (1950)

ACMC, Advanced Composite Materials Corporation; BALF, bronchoalveolar lavage fluid; MMAD, mass median aerodynamic diameter; mo, month; GM, geometric mean; GSD, geometric standard deviation; NR, not reported; $t_{1/2}$, retention half-life; wk, week; wt, weight; yr, year

cytoskeleton function was observed by magnetometry (a technique involving pretreatment of cells with magnetite). Impaired cytoskeleton function was observed at the lowest dose tested (20 μg/mL) ([Watanabe et al., 2000](#)). [Loss of function of the macrophage cytoskeleton (which includes microtubules, microfilaments, and intermediate filaments) could alter mobility of the cells as well as cell polarity, the integrity of the cytoplasm, and transport of organelles, resulting in a reduced ability of alveolar macrophages to phagocytize and clear silicon carbide (and other exogenous materials) from the lungs.]

(c) Translocation

The disposition of various silica compounds, including carborundum (silicon carbide), was evaluated in mice [strain and sex unspecified]; solubility in vivo was determined by measuring the amount excreted in the urine after intraperitoneal injection of the dust samples. [Information on particle size was not provided. The statement that the carborundum dust was separated from carborundum powder using a commercial type elutriator suggests that a fine-sized rather than an ultrafine-sized fraction was used.] Approximately 4 mg of carborundum silica (expressed as silica dioxide) in peanut oil was injected intraperitoneally. Elevated mass levels of silica dioxide were measured in the liver, spleen, and abdominal lymph glands (para-aortic, iliac, and mesenteric) 14 days after the injection of carborundum. The mass levels of silica dioxide in the kidney were also elevated relative to those in control (unexposed) mice, but to a much lesser degree compared with the elevated levels in the liver, spleen, and lymph nodes. Carborundum (as expressed by silica dioxide content) was not measurably soluble or excreted in urine during a 14-day period after exposure in mice ([Holt, 1950](#)). [The Working Group noted that the relationship between the administered dose of carborundum and the expression of the carborundum administered

or tissue dose as silica dioxide is unclear; in the publication, the footnote to Table 2 states that values are expressed as silica dioxide for easy comparison. The Working Group also noted that, in the publication, the rows within dust material in Tables 1, 2, and 3 are not labelled but might be assumed to be individual mouse data; the units of "Dust injected" in Table 2 are not specified, and what those values represent is therefore not clear.]

(d) Retention

(i) Rats

The biopersistence of silicon carbide whiskers was studied in male Wistar rats after a 1-year whole-body inhalation exposure for 6 hours per day on 5 days per week to an average daily exposure concentration of 2.6 (± 0.4) mg/m^3 (98 ± 19 fibres/mL) ([Akiyama et al., 2007](#)). The GM fibre length was 2.4 μm (GSD, 2.3), the GM fibre diameter was 0.5 μm (GSD, 1.5), and the MMAD was 2.4 μm (GSD, 2.4). Groups of rats were killed 6 days and 3, 6, or 12 months after the exposure, and the lungs were processed for measurement of the silicon carbide mass retained as well as the determination of fibre sizes. The average deposited mass of silicon carbide in rat lungs (6 days after exposure) was 5.3 ± 1.4 mg. The deposition fraction (as a percentage) was estimated to be 12.9% [calculated as in [Akiyama et al. (2003)](#)]. The mean fibre dimensions of silicon carbide measured in the lungs were: 0.32, 0.29, 0.35, or 0.32 μm in diameter and 1.55, 1.40, 1.90, and 2.62 μm in length, at 6 days, 3, 6, or 12 months, respectively. These results show that the mean diameter of fibres retained in the lungs did not change appreciably during the observation period after exposure. However, the mean length of the fibres retained appeared to increase at the 6- and 12-month time-points after exposure ([Akiyama et al., 2007](#)). These findings are consistent with those of other studies that showed reduced clearance and increased retention of the longer fibres

for some types of fibres (e.g. amosite) ([Searl et al., 1999](); [Yamato et al., 2003]()). However, [Searl et al. (1999)]() found no significant change in the length of silicon carbide whiskers in the lungs of rats 12 months after intratracheal instillation. [The estimated deposition fraction was calculated from the ratio of the measured silicon carbide lung burden at the end of the exposure to the estimated total inhaled mass of silicon carbide. As such, the amount of silicon carbide that was cleared from the lungs during the exposure period (e.g. by macrophage-mediated clearance) was not considered, which would result in an underestimation of the daily deposition fraction. The higher estimated deposition fraction after the 1-year exposure ([Akiyama et al., 2007]()) compared with that estimated after the 4-week exposure ([Akiyama et al., 2003]()) may in part be due to the higher total lung burden and reduced clearance rate of the rats in the 1-year exposure study.]

[Searl et al. (1999)]() measured the biopersistence of nine mineral fibre types, including silicon carbide whiskers, for up to 12 months after intratracheal injection in male specific pathogen-free Wistar rats [as reported in [Miller et al. (1999)]()]. The silicon carbide whiskers (Advanced Composite Materials Corporation (ACMC)) were described as semi-crystalline often with small hooks at one end and/or buds along their length. Approximately 40% of the fibres consisted of two or more "fully developed, bonded" whiskers. The silicon carbide was used in high-temperature composite materials and was supplied as a fine powder of whiskers, which was reportedly entirely within the respirable size range [the particle size distribution of the powder was not reported, but fibres in the rat lungs were reported to be up to 20 µm in length or greater]. After injection of 14.2 mg (821×10^6 fibres > 0.4 µm in length) [reported in [Miller et al. (1999)]()], the lung fibre burdens of silicon carbide (recovered by bleach digestion of lung tissue) were measured 3 days, and 1, 6, and 12 months after injection.

The fibres were counted and sized using SEM. The mean (standard error) number of silicon carbide fibres in the lungs was 80.9 (14) $\times 10^6$ at 3 days and 29.3 (6.6) $\times 10^6$ at 12 months after injection. Retention of 36% of silicon carbide fibres was measured in rat lungs 1 year after intratracheal exposure. The mean diameter of the silicon carbide fibres recovered was similar throughout the observation period. The mean diameter for all fibres > 0.4 µm in length was 0.48 µm at 3 days and 0.50 µm at 12 months after exposure, and that for fibres > 20 µm in length was 0.53 µm at 3 days and 0.55 µm at 12 months after exposure. The persistence rates of silicon carbide showed no length specificity.

The retention of length fibres in the lungs at 12 months after exposure by intratracheal instillation was reported as the percentage of fibres in the same cumulative length categories ([Miller et al., 1999]()). Four rats per group were killed 3 days after injection and at three additional time-points, and the retained fibre number in the lungs was determined using the same counting and sizing criteria as for the injected samples. The biopersistence was estimated by fitting an exponential decay model to the fibre count and data on time after exposure. These data were re-expressed as the expected percentage of fibres remaining in the lungs 12 months after exposure. The estimated percentages of retained silicon carbide whiskers in the cumulative length categories (i.e. > 0.4, > 5, > 8, > 10, > 15, and > 20 µm) were 52.6, 53.7, 47.7, 49.2, 54.5, and 59.2%, respectively. Among the nine fibre types examined, silicon carbide whiskers showed the greatest percentage of retained total fibres (53% weighted average) 12 months after exposure. [The Working Group noted the difference in the 36% versus 53% weighted average retention.] The ratio of complex silicon carbide whiskers (i.e. more than one fibrous component) to single silicon carbide whiskers reportedly remained unchanged over the 12 months experiments because their dissolution was expected to be "immeasurably small."

Miller et al. (1999) studied factors such as biopersistence and fibre dimensions as predictors of mesothelioma, which was measured as survival time in rats exposed by intraperitoneal injection to nine different fibre types, including silicon carbide whiskers [the experimental data were reported in Searl et al. (1999)]. The silicon carbide whiskers were prepared as a respirable size sample and counted and sized by optical and electron microscopy. Fibres were counted if their length:diameter aspect ratio was greater than 3:1 and the length was greater than 0.4 μm. The counted fibres were sized by diameter and length (in 0.1 μm increments). The silicon carbide whiskers included structures with complex shapes (e.g. multiple branches), which required a more detailed system of quantification that involved recording the dimensions of each branch (as if a separate fibre) as well as estimating these structures as rectangles (with length measured parallel to the longest branch and width at the thickest branch). Miller et al. (1999) used the estimated rectangular dimensions of silicon carbide in their analysis. The target fibre doses were 10^9 fibres ≥ 5 μm in length, which resulted in different mass doses across fibre types. The injected mass dose of length whiskers was 14.2 mg (suspended in sterile physiological saline). Most of the length fibres had diameters of less than approximately 1 μm. The length distribution of injected fibres was reported as: 821, 577, 387, 307, 185, or 121×10^6 fibres in cumulative length categories of > 0.4, > 5, > 8, > 10, > 15, and > 20 μm, respectively. Fibre numbers with diameters greater than approximately 1 μm were: 4, 3, 3, 3, 3, or 1×10^6 fibres, respectively, in the same length categories.

Combining the data from all nine fibre types examined in a regression analysis, Miller et al. (1999) estimated the most predictive factors of survival of rats for deaths from all causes or mesothelioma were the number of fibres > 20 μm in length injected and the biopersistence of fibres

> 5 μm in rat lungs. The lowest median survival of rats injected with the nine fibre types examined was found for silicon carbide whiskers in this study.

(ii)   Sheep

During the production of silicon carbide, also known commercially as carborundum, both fibrous and angular particles can be emitted. Samples of two types of silicon carbide were obtained from the Acheson furnaces of a silicon carbide plant (Dufresne et al., 1992). The silicon carbide was reportedly obtained from the field because no reference material was available. The non-fibrous (angular) silicon carbide sample was collected from the centre of the hot material at the end of the firing process, and the fibrous silicon carbide sample was collected from the outside of the cylindrical lump near the graphite core. The non-fibrous sample was ground, sieved, and micronized (10 μm), while the fibrous sample was disaggregated by grinding at cold temperature (near liquid nitrogen).

The prepared samples were analysed by SEM, TEM, and energy dispersive spectrometer of X-rays. At least five morphological types of particle were identified: isolated fibrils, aggregated fibrils, rectilinear fibres, corrugated fibres, and angular particles. All particles in the non-fibrous sample were reported to be angular in shape (Dufresne et al., 1992). The non-fibrous material consisted of a particular polymorph of carborundum as well as an aluminium oxide corundum (estimated at approximately 90 and 10%, respectively). In contrast, the fibrous sample contained several morphological types of fibre as well as angular particles (27% by weight) and graphite (5% by weight). The size distribution of the particles in the fibrous sample was not measured, although the largest fibres were reported to be approximately 30 μm in length and 0.5 μm in diameter. The size distribution of the non-fibrous particles was measured by a Coulter Counter; 95% of the particles were

less than 2 μm in "equivalent" diameter and the mean diameter was 0.92 μm.

Groups of eight sheep (weighing 25–45 kg) were studied for the pulmonary clearance of silicon carbide up to 8 months after injection of 100 mg of either fibrous or non-fibrous silicon carbide (in 100 mL of saline) into the tracheal lobe. The administered dose ("exposure") of non-fibrous (angular silicon carbide) was estimated to be 90 mg [i.e. by subtraction of the 10% aluminium oxide corundum], and the administered dose of fibrous silicon carbide was estimated to be 95 mg [i.e. by subtraction of the 5% carbon], which comprised 27 mg of angular and 68 mg of fibrous silicon carbide. BALF was obtained before and 2, 4, 6, and 8 months after exposure by slow infusion of four 50-mL aliquots of PBS through the bronchoscope and by gentle aspiration of the effluent. The fourth syringe of BALF was retained for particle analysis. [The rationale for not including the first three syringes of BALF is unclear because that approach would seem to reduce the yield of particles and cells from the BALF, resulting in lower estimates of the carborundum in the BALF.] Sheep were killed 8 months after exposure, the lungs were removed, and nine tissue samples were taken from the tracheal lobe for particle analysis (Dufresne et al., 1992).

The mass concentration of carborundum in the BALF at the first time-point after exposure (2 months) was approximately 60 and 200 ng/mL of fibrous and non-fibrous silicon carbide, respectively. [To what extent this difference was due to a faster clearance of the fibrous silicon carbide, greater deposition efficiency of the non-fibrous silicon carbide, or possibly differential recovery of the BALF cannot be determined from the available data. If BALF had been obtained earlier (e.g. 1–3 days) after the tracheal lobe injection, data could have been obtained on the initial deposition efficiency of each material as noted by the authors in the Discussion section of the article.] However, the data from 2–8 months after exposure show a faster rate of clearance in the fibrous group. From these data, the authors estimated the clearance half-time ($t_{1/2}$) [i.e. the time required to reduce the lung dose by half] to be 1.7 or 5.8 months, respectively, for the sheep in the fibrous or non-fibrous groups. Lower retention of fibrous versus angular silicon carbide was also reported in the lung parenchyma (tracheal lobe tissue), i.e. the retention of silicon carbide in the lung tissue in the fibrous group was approximately 30 times lower than that in the non-fibrous group. The "retention rate" of the angular fraction of the fibrous silicon carbide was nearly the same as that of the non-fibrous (angular) silicon carbide. The average retained lung tissue dose measured in the tracheal lobe at 8 months after exposure was 219 ng/mg of dry lung tissue in the non-fibrous (angular) silicon carbide group, and 4.6 and 58 ng/mg for fibrous and angular silicon carbide, respectively, in the fibrous group (Dufresne et al., 1992). The "retention rate" was calculated as the ratio of the "retention" (ng/mg)/"exposure" (mg) (i.e. the administered dose of silicon carbide).

[The Working Group noted that the "retention rate" column in Table 1 of Dufresne et al. (1992) is not clear. The reported values of 2.43 for angular (non-fibrous group) and 0.07 and 2.15 for angular and fibrous silicon carbide, respectively, in the fibrous group can be calculated directly from the "exposure" (mg of silicon carbide) and "lung retention" (ng of silicon carbide/mg of dry tracheal lobe tissue) columns, as follows: retention/exposure = "retention rate." However, the units were apparently not taken into account, i.e. the calculation should be: (ng/mg)/(mg × 106 ng/mg). Moreover, the total dry mass of the tracheal lobe into which the silicon carbide was injected did not seem to be taken into account, i.e. the correct calculation would be: lung retention (mass silicon carbide/mass tracheal lobe tissue)/exposure (mass silicon carbide/total mass of tracheal lobe). Also, as calculated, the "retention rate" is

a proportion (not a rate) because it is described as the retained mass at the 8-month time-point after exposure. Finally, values greater than 1 do not make sense for a proportion. Thus, the values in "retention rate" are apparently reported incorrectly. Nevertheless, the relative values reported (if they are correct) are approximately 30 times higher for the angular silicon carbide in either the fibrous or non-fibrous group compared with the fibrous silicon carbide value; another error is that, for angular silicon carbide, the exposure is listed as 100 versus 90 in the "retention rate" column, although the resulting value of 2.24 is arithmetically correct if 90 is substituted for 100; in addition, the issues on units and total tracheal lobe mass are still not resolved.]

[Despite the lack of clarity of the values reported for "retention rate" (see Table 1 of Dufresne et al. (1992)), the data on BALF are consistent in showing a faster rate of clearance from 2 to 8 months after exposure and a lower retained proportion of fibrous silicon carbide at 8 months compared with "particulate" (angular) silicon carbide (see Fig. 5 of Dufresne et al. (1992)). The lower estimated retention of fibrous silicon carbide (ng/mg lung tissue) might be explained by the fibrotic lung response – which occurred in sheep exposed to fibrous (with 27% angular) silicon carbide but not in sheep exposed to the non-fibrous (angular) silicon carbide – and the associated increased lung tissue weight, resulting in a low mass of silicon carbide per mass of lung tissue. However, the similar reported lung tissue retention for the angular silicon carbide fraction in either the non-fibrous or fibrous group were considered to provide evidence against a fibrotic lung response explaining the different retention rates (assuming the reported values are correct). The fate of the fibrous or non-fibrous silicon carbide after clearance from the lungs was not reported, due to the lack of data on doses of silicon carbide in other organ tissues (including lymph nodes) or in the urine/faeces.]

In summary, the Dufresne et al. (1992) study reported shorter retention half-times for fibrous silicon carbide in the lungs of sheep than for non-fibrous (angular) silicon carbide at approximately equal administered mass doses.

[The findings of Dufresne et al. (1992) would appear to contradict those from other studies that showed greater lung retention with increasing length of biopersistent amosite fibres (Searl et al., 1999), which would suggest greater retention of the fibrous versus angular silicon carbide. A higher dissolution rate of the fibrous silicon carbide might be a possible explanation, given the smaller diameter of the fibrous silicon carbide (0.5 μm maximum reported diameter) compared with that of angular silicon carbide (mean diameter, 0.92 μm) (Dufresne et al., 1992). However, the dissolution of silicon carbide was found to be very low in either cell-free assays (simulated physiological saline) (Searl et al., 1999) or in mice (Holt, 1950). Experimental data and modelling of other fibre types found that dissolution and breakage of non-biopersistent fibres results in a decrease in longer fibres and an increase in shorter fibres. Although shorter fibres can be cleared more effectively than longer fibres by alveolar macrophages, the fibre breakage resulted in a higher proportion of fibres in the shorter size categories 1 year after exposure (Searl et al., 1999; Tran et al., 2003). However, a breakage of the silicon carbide fibres would not explain the lower mass retention of fibrous silicon carbide because the angular silicon carbide would also be expected to be cleared effectively by alveolar macrophages. In addition, the fibrogenic response in sheep to fibrous silicon carbide is not consistent with its lower retained lung dose compared with angular silicon carbide, which did not cause fibrosis (Dufresne et al., 1992). A possible explanation for the findings in Dufresne et al. (1992) might be that the fibrous silicon carbide had more highly reactive surfaces (as well as a greater total surface area) than the angular silicon carbide, resulting in greater

reactivity with lung tissues, as well as to faster translocation from the lungs to the lymph nodes (where the silicon carbide would pass through the epithelial cells and could damage cells in the process). Some support for this explanation is the finding that toxic crystalline silica causes adverse lung effects at lower mass doses and is translocated to the lung-associated lymph nodes at a faster rate than less toxic particles (Tran et al., 2002). This possibility cannot be evaluated from the data available in Dufresne et al. (1992), however, because no measurements were reported of the surface reactivity of the fibrous versus angular silicon carbide particle surfaces, nor was the translocation of silicon carbide to the lymph nodes measured.]

(e)   Clearance

The clearance of silicon carbide whiskers was studied in rats after a 4-week whole-body inhalation exposure (Akiyama et al., 2003) [see experimental details in Section 4.1.2(a)]. The mass lung burden of silicon carbide 3 days, 2 weeks, and 1, 2, 3, 6, and 12 months after exposure was used to estimate the clearance of fibres. A one-compartment exponential decay model was shown to fit the retained lung burden and data on time after exposure adequately (R^2 = 0.90). A biological half-time ($t_{1/2}$) of 4 months was calculated from that model.

In a 1-year whole-body inhalation study of silicon carbide whiskers by the same group (Akiyama et al., 2007), the mass lung burden was measured 6 days, 3, 6, and 12 months after exposure [see Section 4.1.2(d) for the values measured]. A biological half-time ($t_{1/2}$) of 16 months was calculated from these data.

The authors argued that one of the reasons for the longer retention half-time may have been due to the lung dose of silicon carbide exceeding the alveolar macrophage-mediated clearance capacity (i.e. overloading; Morrow et al., 1991). From the measured lung dose of 5.4 mg of silicon carbide whiskers 6 days after the end of the

1-year exposure and a specific gravity of silicon carbide whiskers of 3.2 g/cm³, Akiyama et al. (2007) calculated that the retained volumetric dose of silicon carbide whiskers in the lungs was approximately 1600 nL, which exceeds the 1000-nL dose associated with overloading of lung clearance in rats reported by Morrow et al. (1991). In comparison, the mass retained lung dose of silicon carbide whiskers after a 4-week inhalation exposure (Akiyama et al., 2003) was approximately 190 nL [calculated from 0.6 mg/ (3.2 g/mL × 1000 mg/g × 1 mL/10⁶ nL)].

4.2 Physico-chemical properties associated with toxicity

4.2.1 Crystal structure

Silicon carbide may occur in several crystalline forms (polymorphs) after a different stacking of silicon and carbon atoms. In the non-fibrous form, silicon carbide particles may be amorphous. Traditional industrial production via the Acheson process yields polydispersed particulates with particles from several micron- to nano-size, often containing quartz, cristobalite, and carbon particles (Scansetti et al., 1992; Boumahdi, 2009).

The nature of the crystalline phases (α- versus β-silicon carbide) in nano-size (α-silicon carbide, 16 nm; β-silicon carbide, 4 nm; β-silicon carbide with α-silicon carbide < 10% and iron impurities ≈500 ppm, 14 or 26 nm) influenced tumour necrosis factor (TNF)-α production. α-Silicon carbide induced higher TNF-α production than β-silicon carbide. When the presence of α-silicon carbide was detected by X-ray diffraction analysis, a moderate or elevated level of TNF-α was found, while this pro-inflammatory cytokine was not elicited by exposure to pure β-silicon carbide (Pourchez et al., 2012).

Silicon carbide may be prepared in a non-stoichiometric form, i.e. with a variable silicon/carbon ratio, which influenced the in-vitro

cellular responses to micron- and nano-size particles (Boumahdi, 2009; Barillet et al., 2010a). A comparison of the cellular responses induced in human A549 lung adenocarcinoma cells by a panel of silicon carbide nanoparticles (for details, see Section 4.2.2) led to the conclusion that silicon carbide nanoparticles with a high silicon/carbon ratio induced the production of reactive oxygen species (ROS) and inhibited glutathione (GSH) reductase activity earlier than those with a low silicon/carbon ratio. They also induced more persistent genotoxicity. The authors considered that the presence of silicon dioxide residues on the surface of these nanoparticles renders them more toxic (Barillet et al., 2010a).

Conversely, three silicon carbide nanoparticles showing similar crystallite size (4 nm), Brunauer–Emmett–Teller (BET) size (14–15 nm), specific surface area (125–139 m²/g), and oxidation state of the surface (7–8% of O1s) but increasing carbon/silicon atomic ratios from 0.88 to 1.21 did not differ in their cytotoxicity or pro-inflammatory response (TNF-α values at the same level as the negative control), showing no influence of the carbon/silicon atomic ratio on the in-vitro cellular responses (Pourchez et al., 2012).

4.2.2 Form and size

Silicon carbide may assume a large variety of forms from isometric particles to fibres and whiskers. Most silicon carbide industrial dusts may contain some particles with a fibrous shape. The material is usually comprised of particles of different sizes, some of which may be of greater concern than others. The term whiskers is confined to monocrystals with a fine fibre morphology, resembling amphibole asbestos or erionite. Being single crystals, silicon carbide whiskers have sharp tips and high tensile strength (Svensson et al., 1997).

(a)   Silicon carbide particles (Acheson process)

Five silicon carbide industrial powders (silicon carbide C1, C2, F1, F2, and I) were collected after their production in the Acheson process in industrial plants (see Table 4.4 for the characteristics of the particles used in this study). Silicon carbide C1 and C2 are coarser than silicon carbide F1 and F2. They are mostly constituted by the α-silicon carbide phase. Silicon carbide I is a metallurgically impure dust representative of airborne dusts inhaled in the workplace environment. Free radical release but also iron content increased with particle size. Hydrogen peroxide production by RAW 264.7 macrophage cells was induced to a greater extent by exposure to fine silicon carbide F1 and F2 particles than that to coarse silicon carbide C1 or C2 or to silicon carbide I and was proportional to surface area (Boudard et al., 2014).

(b)   Silicon carbide whiskers

Five whiskers (four silicon carbide whiskers, SiCW-1, -2, -3, and -4, and one silicon nitride, SiNW) and two powders (one silicon carbide, SiCP, and one silicon nitride, SiNP) were studied (Svensson et al., 1997; see Table 4.5 for the characteristics of the particles/whiskers used in this study). One of the silicon carbide whiskers, SiCW-3, was also ball-milled in water for 3 hours (SiCW-3S, short-milled) and 58 hours (SiCW-3L, long-milled). The cloning efficiency of Chinese hamster V79 cells was inhibited in a concentration-dependent manner by all materials. At least five different concentrations (range, 0.25–80 μg/cm²) of each material were tested for 20 hours. The dose–response curves were linear and the concentration resulting in 50% survival (EC_{50}) was calculated. A clear difference in viability was observed after exposure to milled whiskers and powders. The EC_{50} for the whiskers ranged from 0.9 to 4.2 μg/cm², whereas that for crocidolite asbestos (positive control) was 1.4 μg/cm². The milled whiskers

Table 4.4 Physico-chemical characteristics of different microparticles comprised of silicon carbide from the study by Boudard et al. (2014)

Sample	Specific surface area (m²/g)	Median diameter D_{50} (μm)	Crystallite phases	O1s (% atomic)	Carbon/silicon (atomic ratio)	Iron (ppm)	Aluminium (ppm)
SiC C1	4.0	2.5	SiC-6H (91%), SiC-4H (7%), SiC-15R (< 1%)	17 (presence of a SiO_2 layer)	0.98	2 370	350
SiC F1	11.0	0.5	SiC-6H (91%), SiC-4H (7%), SiC-15R (2%)	22 (presence of a SiO_2 layer)	1	1 570	560
SiC I	3.0	6.0	SiC-6H (53%), SiC-4H (7%), SiC-15R (5%), SiO_2 quartz (9%), SiO_2 cristobalite (5%)	23 (presence of a SiO_2 layer)	1.66	20 000	1 300
SiC C2	3.5	2.5	SiC-6H (90%), SiC-4H (7%), SiC-15R (2%)	17 (presence of a SiO_2 layer)	0.99	2 230	730
SiC F2	8.5	0.8	SiC-6H (90%), SiC-4H (3%), SiC-15R (7%)	23 (presence of a SiO_2 layer)	0.98	1 370	0

SiC, silicon carbide; SiO_2, silicon dioxide

Adapted from *Toxicol In Vitro*, Volume 28, issue 5, Boudard et al. (2014) In vitro cellular responses to silicon carbide particles manufactured through the Acheson process: Impact of physico-chemical features on pro-inflammatory and pro-oxidative effects, Page Nos 856–865, Copyright (2014), with permission from Elsevier

and powders were less potent than the whiskers. Milling SiCW-3 for 3 and 58 hours decreased its toxicity (EC_{50}) from 4.2 μg/cm² to 6.9 μg/cm² and 10.7 μg/cm², respectively. The powders of both silicon nitride and silicon carbide were much less toxic in this test system, although the silicon nitride powder was more toxic than the silicon carbide powder, in line with the toxicity of the whiskers.

Three well-characterized whiskers of different sizes (SiCW 1, SiCW 2, and SiCW 3; characteristics reported in Table 4.6) were tested in vivo (Johnson & Hahn, 1996) and their effects were compared with those of continuous silicon carbide ceramic filaments. Crocidolite asbestos fibres were used as a positive control. A size analysis of the morphology of the three whiskers is illustrated in Table 1.1 (Health Council of the Netherlands, 2012). Silicon carbide whiskers, but not continuous silicon carbide ceramic filaments, induced mesotheliomas after intrapleural injection into rats (see also Section 3.3). A difference in the biological activity of the three samples of whiskers (SiCW 1, SiCW 2 >> SiCW 3) was observed, which could not be explained on the basis of their physical dimensions.

(c)   Silicon carbide nanoparticles

Five silicon carbide nanoparticles (characteristics reported in Table 4.7) with varying diameters and silicon/carbon ratios that were synthesized by laser pyrolysis of gaseous precursors were taken up by human A549 lung adenocarcinoma cells, in which their cytotoxicity was low (Barillet et al., 2010a). [The low cytotoxicity of silicon carbide nanoparticles has also been demonstrated in studies of silicon carbide nanocrystals (Fan et al., 2008) or microscaled silicon carbide particles (Bruch et al., 1993a, b), suggesting that the absence of cytotoxicity after contact with a silicon carbide surface is unrelated to particle size.] However, silicon carbide nanoparticles induced major redox alterations. Cell redox status was markedly affected: silicon carbide nanoparticles caused the production of ROS, the depletion of GSH and the inactivation of some antioxidant enzymes (GSH reductase and superoxide dismutase) (Barillet et al., 2010a).

Table 4.5 Characteristics[a] of silicon carbide and silicon nitride particles and whiskers from the study by Svensson et al. (1997)

Composition and sample No.[b]	Manufacturer/ type	Content of discriminated whiskers × 10^10/g	Content of long fibres (≥ 20 μm) × 10^10/g	Length (μm)	Diameter (μm)	Length/ diameter	Specific area (m²/g)
SiCW-1	Tokai 100	1.2	0.23	14 ± 10	0.8 ± 0.4	18 ± 11	3.0
SiCW-2	Tokai 400	0.9	0.20	14 ± 9	0.9 ± 0.4	17 ± 10	1.5
SiCW-3	Tateho SCW10	4.3	0.52	12 ± 10	0.7 ± 0.4	19 ± 13	4.2
SiCW-4	Tateho SCW1S	1.1	0.14	12 ± 9	0.7 ± 0.4	21 ± 12	4.9
SiCW-3L[c]	Tateho SCW10	3.9	0.12	9 ± 5	0.6 ± 0.3	16 ± 10	11.7
SiCW-3S[d]	Tateho SCW10	5.2	0.44	11 ± 7	0.7 ± 0.4	16 ± 9	5.2
SiNW	UBE	2.2	0.42	13 ± 8	0.9 ± 0.4	16 ± 8	2.2
SiNP	UBE E10				0.4 ± 0.4		10.9
SiCP	UF 15, Lonza				0.4 ± 0.3		14.9

[a] Further information on measurement and characterization in Nyberg et al. (1995); data comprise mean ± standardard deviation

[b] Length/diameter ≥ 5 μm, diameter ≤ 3 μm. Discrimination limit in image analysis

[c] L, long-milled (for 58 h)

[d] S, short-milled (for 3 h)

SiCW, silicon carbide whiskers; SiNW, silicon nitride whiskers; SiNP, silicon nitride powder; SiCP, silicon carbide powder

Reproduced from Svensson et al. (1997). Toxicity in vitro of some silicon carbides and silicon nitrides: whiskers and powders, *Am J Ind Med*, 1997, volume 31, issue 3, pages 335–343, by permission of John Wiley & Sons

Table 4.6 Characteristics of silicon carbide particles/whiskers and crocidolite from the study by Johnson & Hahn (1996)

Sample	Mean length (in μm) (standard error of the mean)	Mean diameter (in μm) (standard error of the mean)	Fibre (n/mg)	Specific surface area (m²/g)	Specific gravity
SiCW 1	4.5 (0.23)	0.42 (0.02)	7.6×10^6	3.0	3.4
SiCW 2	20.1 (1.01)	0.75 (0.02)	1.6×10^5	1.4	3.3
SiCW 3	6.6 (0.40)	0.32 (0.01)	1.1×10^7	3.6	3.2
Crocidolite	2.1 (0.31)	0.12 (0.01)	3.6×10^9	7.0	3.2
CCF (PRD-166)[a]	40–100	12	ND	1.5	4.3

[a] Values determined approximately by light microscopy

CCF, continuous silicon carbide ceramic filament; ND, not determined; SiCW, silicon carbide whiskers

Reproduced from *Occup Environ Med*, Johnson & Hahn (1996), volume 53, page 813–816, copyright (1996), with permission from BMJ Publishing Group Ltd

Six ultrafine silicon carbide nanoparticles were prepared using both sol-gel and a laser (the physical characteristics, including size, crystallinity, silicon/carbon ratio, and oxygen or iron contaminants, of which are reported in Table 4.8; Pourchez et al., 2012). None of the nanoparticles tested induced cytotoxicity in RAW 264.7 cells derived from murine peritoneal macrophages. Conversely, other adverse cellular responses elicited (see Section 4.4) were markedly dependent upon crystal phase, silicon/carbon ratio, and level of contaminants. The nature of the surface oxidation layer (silica versus silicon oxycarbide) did not modulate the pro-inflammatory response (TNF-α production) while a linear correlation was observed (R^2 = 0.97) between TNF-α production and the total surface area exposed to silicon carbide nanoparticles. Such

Table 4.7 Characteristics[a] of silicon carbide nanoparticles from the study by Barillet et al. (2010a)

Sample	SSA (m²/g)	BET size (nm)	TEM size (nm)	Silicon/carbon	ζ (mV)	Hydrodynamic diameter (nm)
SiC-A	125	15	17 ± 3	0.8	–24	168 (100%)
SiC-B	134	14	13 ± 3	1.0	–22	125 (100%)
SiC-C	140	13	12 ± 3	1.2	–31	97 (100%)
SiC-D	52	36	31 ± 8	1.1	–28	190 (100%)
SiC-E	33	58	45 ± 18	1.1	–28	280 (100%)

[a] SSA, specific surface area, measured according to Brunauer–Emmett–Teller (BET); BET size, diameters of silicon carbide nanoparticles calculated from SSA; TEM size, diameters of silicon carbide nanoparticles measured by transmission electron microscopy; ζ, zeta potential measured just before nanoparticle dilution into cell culture medium; hydrodynamic diameter measured by photon correlation spectroscopy after nanoparticle dilution into cell culture medium

Reprinted from *Toxicol Lett*, Volume 198, issue 3, Barillet et al. (2010a). In vitro evaluation of SiC nanoparticles impact on A549 pulmonary cells: Cyto-, genotoxicity and oxidative stress, Page Nos 324–330, Copyright (2010), with permission from Elsevier

a correlation was obtained for β-silicon carbide nanoparticles with the presence of α-silicon carbide, confirming the impact of both crystalline phase and the specific surface area.

4.2.3 Surface reactivity

Because the bonding energy between silicon and oxygen is higher than that between silicon and carbon, the silicon atoms exposed at the surface of silicon carbide are highly likely to react with oxygen, particularly if loosely bound to the underlying crystal structure. The particles obtained by using the Acheson process had the following surface species (as shown by X-ray photoelectron spectroscopy): silicon dioxide, silicon oxycarbure, carbon residues (C–C), silicon impurities (Si–Si) and oxidized carbon forms (C–O, C=O) (Boumahdi, 2009).

All forms of silicon carbide that are exposed to the atmosphere tend in the long-term to be covered by one or more layers of silica over time. However, this process may occur through different kinetics and is greatly accelerated by heating (Deal & Grove, 1965; Boch, 2001; Boumahdi, 2009). Consequently, heated silicon carbide particles may be covered with a thick external layer of silicon dioxide, while unheated particles may be only partially covered by a few silicon–oxygen patches, e.g. only on some crystal faces or at steps, kinks, and corners, thus exposing the silicon–carbon structure to fluids, cells, and tissues. This is fairly relevant to the fate of the particles in vivo as various studies have shown that cells react quite differently to a silicon–carbon surface than to a silica-like surface. While the silica-like surface always induces a substantial level of cytotoxicity, the silicon–carbon surface appears to be non-cytotoxic in the RAW 264.7 cell line derived from murine peritoneal macrophages (toxicity assessed as cell membrane damage (release of lactate dehydrogenase; Pourchez et al., 2012; Boudard et al., 2014)) or in the human A549 lung adenocarcinoma cells (toxicity assessed by impaired mitochondrial activity as detected using the 3-[4,5-dimethylthiazol-2-yl]-2,5-diphenyl tetrazolium bromide assay (Barillet et al., 2010a)). Boudard et al. (2014) compared several cellular responses to unheated and heated silicon carbide dust, taking into account that the oxidation of silicon to silica is favoured on heating and that heated particles were almost completely covered by a thick layer of silica. Although the starting material was non-toxic, heating increased cytotoxicity which was assessed by the release of lactate dehydrogenase.

Conversely, both oxidized silicon carbide C1 and F1 particles treated at 1400 °C induced lower

Table 4.8 Characteristics of silicon carbide nanoparticles from the study by Pourchez et al. (2012)

Sample	ρ (g/cm³)	SSA (m²/g)	BET size (nm)	Crystallite size	Crystalline phases	O1s (% atomic)	Iron (ppm)	Carbon/silicon (atomic ratio)
SG	3.2	125	15	14-nm monocrystalline nanograins	β-SiC (SiC-3C), α-SiC < 10% (SiC-6H)	8	0	0.88
LP1	3.2	139	14	4-nm polycrystalline nanograins	β-SiC (SiC-3C)	8	105	1.00
LP2	3.1	125	15	4-nm polycrystalline nanograins	β-SiC (SiC-3C)	7	200	1.21
LP3	3.0	140	14	4-nm polycrystalline nanograins	β-SiC (SiC-3C)	14 (presence of a SiO₂ layer)	605	0.81
LP4	3.1	52	37	16-nm nanograins with stacking faults	β-SiC (SiC-3C), α-SiC < 10% (SiC-6H)	8	592	0.88
LP5	3.1	33	59	26-nm nanograins with stacking faults	β-SiC (SiC-3C), α-SiC < 10% (SiC-6H), Si (< 2%)	22 (presence of a SiO₂ layer)	415	0.88
M	3.0	62	32	16-nm nanograins with stacking faults	α-SiC (SiC-6H)	25 (presence of a SiO₂ layer)	2830	0.70

BET, Brunauer–Emmett–Teller; LP1, typical nanoparticles of β-SiC synthesized by laser pyrolysis; LP2 and LP3, SiC nanoparticles enriched in carbon and silicon, respectively; LP4 and LP5, nanopowders with coarse grains of larger size; M, pure α-SiC nanoparticles; SG, nanopowder synthesized chemically; SiO₂, silicon dioxide; SSA, specific surface area
Adapted from *J Nanopart Res*, In vitro cellular responses to silicon carbide nanoparticles: impact of physico-chemical features on pro-inflammatory and pro-oxidative effects, volume 14, 2012, page 1143, Pourchez et al. (2012), with permission of Springer

levels of TNF-α than their unheated counterparts. Cellular production of hydrogen peroxide was unrelated to surface oxidation (Boudard et al., 2014).

(a) Generation of free radicals and depletion of antioxidants

Conflicting evidence has been shown for the direct generation of free radicals by silicon carbide particles. An earlier study reported that both the supercoiled plasmid assay for DNA scission and high-performance liquid chromatography using salicylate as an hydroxyl radical trap gave negative results with silicon carbide fibre (ACMC) but positive results with amosite asbestos (Brown et al., 1998).

(i) Silicon carbide particles (Acheson process)

The ability of silicon carbide particles to generate HO• and COO•- radicals was assessed under cell-free conditions using electron paramagnetic resonance spectroscopy (Boudard et al., 2014). All particles were able to generate free radicals and were more effective in generating COO•- than HO•. Free radical production increased with particle size and was 3–5-fold higher with coarse silicon carbide C1/C2 particles than with fine silicon carbide F1/F2 particles (maximal COO•- production with silicon carbide C2). The silicon carbide I powder was characterized by the generation of HO• radicals, with a 5-fold greater production compared with silicon carbide F1/F2. This behaviour may be related to the large amount of iron in the coarse particles compared with the fine particles, especially silicon carbide I, which also exhibited a partially crystallized surface layer of silica. The potential to release the particle-derived free radicals HO• and COO•- decreases with surface oxidation but, at very high temperatures (> 1400 °C), the specific surface area markedly decreases and the external silica layer that was originally amorphous crystallizes into cristobalite. The amount of free radical released per unit surface under these circumstances markedly increases in respect to the original material. The decrement in radical yield upon heating up to 850 °C is caused by both development of an amorphous surface layer and the conversion of Fe^{2+} into Fe^{3+} after oxidation [as reported for other toxic particulates (Tomatis et al., 2002)].

(ii) Silicon carbide whiskers

The generation of hydroxyl radicals by a panel of silicon carbide whiskers was investigated using three independent assays: deoxyguanosine hydroxylation, dimethyl sulfoxide as a scavenger, and deoxyribose assays. Table 4.9 summarizes the release of free radicals from silicon carbide whiskers and Table 4.5 shows the characteristics of the whiskers (Svensson et al., 1997). The HO• radical tests showed that only crocidolite (positive control) and silicon carbide whiskers-4 could potentiate the formation of hydroxyl radicals. The other materials tested did not differ from the control. [Analysis using the nick translation assay detected DNA strand breaks with all fibres except silicon carbide whiskers-2 and silicon nitride whiskers. Taking into account the concentration used, exposure to all of the silicon carbide whiskers induced DNA breaks (of the same magnitude as crocidolite) compared with a low rate for the other material. The highest activity was found for silicon carbide whiskers-3S.]

(iii) Silicon carbide nanoparticles

In the study by Pourchez et al. (2012) (see Table 4.8 for characteristics of the particles), in which free radicals were measured directly using electron paramagnetic resonance spectroscopy under cell-free conditions, no radical release was observed with LP1 and SG. LP2 and LP3 were able to generate COO•-, but not HO• radicals. Significant HO• radical release was observed with LP4 (21 nmol/m²) and more importantly with LP5. This sample exhibited the highest activity for COO•- (400 nmol/m²) and HO• generation

Table 4.9 Free radical release from silicon carbide and nitride whiskers/particles[a]

Sample	8-OHdG/10³dG	Deoxyribose (A_{532})	DMSO/MSA (A_{425})
Control	0.28 ± 0.1	0.05 ± 0.03	0.40 ± 0.17
SiCW-1	0.28 ± 0.09	0.09 ± 0.02	0.34 ± 0.09
SiCW-2	0.35 ± 0.10	0.09 ± 0.04	0.36 ± 0.11
SiCW-3	0.54 ± 0.16	0.15 ± 0.14	0.33 ± 0.14
SiCW-4	2.34 ± 1.80	0.64 ± 0.58	0.68 ± 0.11
SiCW-3L	0.46 ± 0.19	0.17 ± 0.06	0.61 ± 0.02
SiCW-3S	0.71 ± 0.21	0.15 ± 0.09	0.56 ± 0.02
SiNW	0.31 ± 0.17	0.13 ± 0.03	0.19 ± 0.06
SiNP	0.49 ± 0.24	0.05 ± 0.03	0.31 ± 0.09
SiCP	0.32 ± 0.16	0.07 ± 0.02	0.26 ± 0.06
Crocidolite	3.59 ± 1.20	1.73 ± 0.04	Not measured

[a] Data are given as mean of three experiments ± standard deviation. Values represent number of molecules of 8-hydroxydeoxyguanosine per 10^3 deoxyguanosine and absorbence at A_{532} and A_{425}, respectively

dG, deoxyguanosine; DMSO, dimethyl sulfoxide; 8-OHdG, 8-hydroxydeoxyguanosine; MSA, methanesulfonic acid; SiCP, silicon carbide particles; SiCW, silicon carbide whiskers; SiNP, silicon nitride particles; SiNW, silicon nitride whiskers

Reproduced from Svensson et al. (1997). Toxicity in vitro of some silicon carbides and silicon nitrides: whiskers and powders, *Am J Ind Med*, 1997, volume 31, issue 3, pages 335–343, by permission of John Wiley & Sons

per unit surface (47 nmol/m²). LP5 contained the highest amount of surface iron. The authors concluded that free radical production under acellular conditions is associated with the iron content at the nanoparticles surface; in contrast to other cases (e.g. silica and asbestos) in which even traces of iron ions are able to trigger the Fenton reaction (Fubini et al., 2001; Turci et al., 2011), a threshold effect of surface iron of around 11 μg/m² has been observed for silicon carbide nanoparticles.

(b)   Bioavailability and biodeposition of metals

Substantial amounts of iron or other metal impurities are present at the surface of particles produced by the Acheson process, which are probably bioavailable although bioavailability per se has not been measured. Metal ion bioavailability has not been reported for whiskers. Iron was present at the surface of the silicon carbide nanoparticles studied by Pourchez et al. (2012), while Barillet et al. (2010a) considered the particles they studied to be free from any metal-based impurities, thus ruling out any effect caused by Fenton-like and Haber-Weiss reactions.

(c)   Antioxidant depletion

The ability of several types of fibre, including silicon carbide, to deplete the antioxidants, ascorbic acid and GSH, was investigated in the lining fluid of rat lung epithelial cells. Silicon carbide whiskers (ACMC), as well as other fibres, were able to deplete GSH in lung lining fluid and depletion was dependent on the number of fibres (Brown et al., 2000).

Silicon carbide nanoparticles (Barillet et al., 2010a) caused the depletion of cellular GSH, the major antioxidant cellular defence mechanism. GSH may either be released from cells to the extracellular medium or oxidized intracellularly to oxidized GSH (GSSG) by GSH peroxidase, which is coupled to the reduction of hydrogen peroxide to water. Because high levels of ROS accumulate in cells exposed to silicon carbide nanoparticles, the oxidation of GSH to GSSG by GSH peroxidase was hypothesized. However, the total glutathione content (GSH + GSSG) decreased. Consequently, GSH may be oxidized to GSSG, but GSH and/or GSSG must also be released from cells to the extracellular medium. To support this hypothesis,

Brown et al. (2000) demonstrated that silicon carbide whiskers (ACMC) deplete GSH from lung lining fluid. Moreover, Zhang et al. (1999) suggested that GSH was released from alveolar macrophages exposed to silica as a consequence of GSH depletion in the extracellular fluid, and hypothesized that silicon carbide nanoparticles deplete GSH and/or GSSG from the extracellular fluid and that the cells then release these molecules to re-establish the GSH intra-/extracellular balance. GSH reductase, which is responsible for the reduction of GSSG to GSH, is inactivated (see also Barillet et al., 2010a). The GSH pool is thus not re-established, leading to the accumulation of hydrogen peroxide in the cells. Superoxide dismutase, which is responsible for $O_2^{\cdot-}$ dismutation to hydrogen peroxide, was also partially inactivated in cells exposed to silicon carbide nanoparticles, resulting in the intracellular accumulation of $O_2^{\cdot-}$.

4.2.4 Fibre durability (leaching, phagocytosis, dissolution, and breaking)

Silicon carbide is a very durable material that is poorly dissolved in aqueous media. Biopersistence is linked not only to durability in biological fluids, but also to the form of the material (see Table 4.1).

(a) In vivo

(i) Silicon carbide whiskers

Silicon carbide whiskers (mean diameter, 0.45 μm), as a very durable material, were compared with less durable glass microfibres (code 100/475), relatively soluble man-made vitreous fibres (Davis et al., 1996). Amosite asbestos was used as a positive control. After inhalation for 1 year, fewer very long glass microfibres (length, > 20 μm) remained in rats lungs at the end of the exposure compared with amosite or silicon carbide. After exposure, amosite and glass microfibres were removed from the lungs at rates similar to those of most fibre dimensions whereas

the clearance of silicon carbide was much slower. When dust was administered by intratracheal instillation, the differences in length with regard to fibre removal from the lung tissue were less marked.

Silicon carbide whiskers exhibit high biopersistence and are not modified in vivo. Over the long-term, longer whiskers are more biopersistent than shorter whiskers. Akiyama et al. (2003) reported an exponential clearance of deposited silicon carbide whiskers (MMAD, 2.5 μm; GM diameter, 0.4 μm; GM length, 2.2 μm) from rat lungs after 4 weeks of inhalation. The apparent deposition fraction was 4.8% ± 0.7%. During the clearance period, the amount of silicon carbide whiskers deposited in the rat lungs decreased exponentially with increasing duration of clearance. The biological half-time in the one-compartment model was determined to be 4.0 months, similar to that of other biopersistent inorganic fibres.

The biopersistence of deposited silicon carbide whiskers was measured after a longer inhalation exposure in rats (Akiyama et al., 2007). A group of 42 male Wistar rats was exposed by inhalation to daily average concentrations of 2.6 ± 0.4 mg/m³ (98 ± 19 fibres/mL) of silicon carbide whiskers (MMAD, 2.4 μm (GSD, 2.4); GM diameter, 0.5 μm (GSD, 1.5); GM length, 2.8 μm (GSD, 2.3)) for 6 hours per day on 5 days per week for 1 year; the rats were killed 6 days and 3, 6, and 12 months after the exposure. The amount of silicon carbide whiskers deposited in each rat lung 6 days after the exposure, determined by an X-ray diffraction method, was 5.3 ± 1.4 mg. The biological half-time was 16 months, calculated from the amount of deposited silicon carbide whiskers at 6 days and 3, 6, and 12 months, and was more prolonged than normal physiological clearance. The diameter of the silicon carbide whiskers in the lung at each time-point during the 12 months of clearance after inhalation did not change. However, longer silicon carbide whiskers tended to be retained in

the lung as the clearance time increased, especially after 6 months. Histopathological examination revealed bronchoalveolar hyperplasia in 2 rats 1 year after the exposure and severe fibrotic changes around aggregated silicon carbide whiskers.

(ii) Silicon carbide particles, fibres, and angular particles

Pioneer studies on the fate of siliceous dusts in the body compared the in-vivo solubility of cement, carborundum, quartz, and moulding sand by estimating urinary silica values after intraperitoneal injection of different dusts into mice. An increase in the excretion of silica was found only with exposure to cement (Holt, 1950).

The lung tissue of a worker exposed for 10 years in an abrasive manufacturing plant was analysed by bulk analysis and in situ analytical electron microanalysis. Total dust in the lung was 120 mg/g of the dried lung tissue, 43% of which was silicon carbide (Hayashi & Kajita, 1988).

Materials taken in the field (carborundum from Acheson furnaces at a silicon carbide plant) contained both angular and fibrous silicon carbide particulates emitted by the silicon-carbide production operations. The pulmonary retention of the two morphological types was studied in sheep. Animals were injected in the tracheal lobe with an equal mass (100 mg) of particulates prepared from silicon carbide materials collected in the workplace. Particles were measured by analytical TEM in samples of BALF obtained 2, 4, 6, and 8 months after the injection and also in samples of lung parenchyma obtained at 8 months. Measurements in BALF and lung samples both indicated a much lower retention of fibrous than of angular silicon carbide. The retention rate in lung parenchyma at 8 months was 30 times lower for fibrous silicon carbide. The half-life of the decrease in concentrations was 3.4 times shorter for fibrous silicon carbide (Dufresne et al., 1992).

A study on pulmonary dust retention in a worker who had a lung lobectomy for an epidermoid carcinoma and who had been employed for 42 years in the vicinity of an Acheson furnace in a silicon carbide plant reported silicon carbide fibres in the lung parenchyma. The concentration of silicon carbide fibres longer than 5 μm was 39 300 fibres/mg of dry lung (Dufresne et al., 1993).

Particle-induced X-ray emission is a technique used to measure X-rays induced by proton irradiation that requires minimal sample preparation, can yield a detection limit as low as a few parts per million, and is based on the excitation of the electronic levels of atoms by means of an ion beam, producing X-ray emissions. These X-rays are characteristic and proportional to every element. Doses of 0.5 and 5 mg of silicon carbide nanoparticles were instilled into female Wistar rat lungs and were investigated using this technique for 60 days. The biopersistence of silicon carbide at a dose of 5 mg showed the typical trend reported for larger amounts of nanoparticles during the first few days after exposure to high doses. For lower doses (0.5 mg), only 0.074 mg of silicon carbide remained in the lungs 1 hour after instillation, representing 14.8% of the original dose. After 60 days, the biopersistence of the lower dose (0.5 mg) was 2.84%. The higher dose (5 mg) resulted in the retention of 1.834 mg in the lungs, representing 36.68% of the administered dose, 1 hour after instillation. After 60 days, only 1.17% of the higher dose was retained in the lungs (Lozano et al., 2012).

(b) In vitro

An examination of the in-vitro solubility of silicon carbide whiskers and their chemical composition after extraction from lung tissues showed almost no change in chemical composition (Davis et al., 1996).

4.3 Genetic and related effects

See Table 4.10

4.3.1 Human cells in vitro

Silicon carbide whiskers were reported to increase the level of DNA strand breaks and DNA–DNA interstrand crosslinks in human A549 lung adenocarcinoma cells after exposure at 200 μg/mL for 1 hour (Wang et al., 1999). [The Working Group noted that the report lacked information on the number of independent replicates.]

DNA strand breaks were measured using the alkaline comet assay in human A549 lung adenocarcinoma cells after exposure to 50 μg/mL of five different silicon carbide nanomaterials for 4, 24, or 48 hours (Barillet et al., 2010a). The silicon carbide nanoparticles were synthesized by laser pyrolysis of gaseous silane and acetylene precursors to materials with different sizes and ratios between silicon and carbon. Measurements of size included the specific surface area (33–140 m²/g), BET size (13–58 nm), TEM size (12–45 nm), and hydrodynamic diameter (97–280 nm, measured by photon correlation spectrometry in cell culture medium). All of five silicon carbide materials were reported to increase the level of DNA strand breaks 4 hours after exposure, whereas genotoxicity was less evident after 24 and 48 hours. No difference in the generation of DNA strand breaks between the silicon carbide samples was observed after 4 hours of exposure, whereas one sample with a large specific surface area (125 m²/g), median hydrodynamic diameter (168 nm), and low silicon:carbon ratio (0.8) was not genotoxic at 24 or 48 hours. [The data appear to have been obtained from only a single experiment and the statistical analysis was based on 50 comets from this experiment.]

Silicon carbide whiskers were reported to increase the number of chromosomal aberrations (acentric fragments, chromosome breaks, chromosome fragments, chromatid breaks, chromatid exchanges, and structural chromosomal aberrations) in human embryo lung cells after exposure to 2.5 or 5 μg/mL for 24 hours (Wang et al., 1999).

4.3.2 Experimental systems in vitro

Svensson et al. (1997) measured DNA strand breaks using the nick translation assay in Chinese hamster lung fibroblast V79 cells treated with 0.3–15 μg/mL whiskers (four silicon carbides, SiCW-1, -2, -3, and -4, and one silicon nitride, SiNW) and powders (one silicon carbide, SiCP, and one silicon nitride, SiNP) for 20 hours. The length of the silicon carbide whiskers ranged between 12 ± 10 μm and 14 ± 10 μm and the diameters between 0.7 ± 0.4 and 0.9 ± 0.4 μm. Accordingly, their length:diameter ratios were similar. The SiCW-3 whiskers were also ball-milled in water for 3 hours (SiCW-3S, short-milled) or 58 hours (SiCW-3L, long-milled). The mean length of SiCW-3S and SiCW-3L was 11 ± 7 μm and 9 ± 5 μm, respectively. High rates of DNA strand breaks were observed for all of the silicon carbide whiskers (of the same magnitude as crocidolite). The highest effect was found for SiCW-3S and the lowest for SiCP.

The induction of DNA strand breaks was investigated by alkaline comet assay in rat kidney proximal tubule NRK-52E cells 24 hours after exposure to 2–200 μg/mL of a silicon carbide nanopowder. The silicon carbide nanoparticles, synthesized by pyrolysis, were described as having a spherical morphology with a specific surface area of 125 m²/g and a particle size of 15 nm (BET) or 17 nm (TEM). The results were not statistically significant. The authors also reported that the silicon carbide sample did not generate DNA double-strand breaks although the results were not shown (Barillet et al., 2010b).

Using the M3E3/C3 lung epithelial cell line from Syrian golden hamsters, exposure to silicon carbide fibres for 48–96 hours at doses between

Table 4.10 Studies of genotoxicity in human cells and in experimental systems in vitro after exposure to silicon carbide

Material[a]	Dose and cells	Effect	Comments	Reference
Human cells in vitro				
5 SiC-NP (SiC-A–E) with diameters of 13–68 nm and silicon/carbon ratio of 0.8–1.3	50 µg/mL for 4–48 h in human A549 lung adenocarcinoma cells	Increase in DNA strand breaks with all SiC-NP (assessed by the alkaline version of comet assay; genotoxicity appeared to be transient in cells exposed to SiC-A and SiC-B, and permanent in cells exposed to the other SiC-NP (higher silicon/carbon ratio)	Uncertainty about number of independent replicates and statistical analysis	Barillet et al. (2010a)
SiCW	200 µg/mL for 1 h in human A549 lung adenocarcinoma cells or 2.5 or 5 µg/ml for 24 h in human embryo lung cells	Increase in DNA strand breaks and DNA–DNA interstrand crosslinks in A549 cells; increased frequency of chromosomal aberration in human embryo lung cells	Lack of information on the number of independent replicates	Wang et al. (1999)
Other experimental systems				
SiC nanoparticles synthetized by pyrolysis, with spherical morphology, a specific surface area of 125 m²/g and particle size of 15 nm (BET) or 17 nm (TEM)	2–200 µg/mL for 24 h in rat kidney proximal tubule NRK-52E cells	No increase in DNA strand breaks (measured by alkaline comet assay)		Barillet et al. (2010b)
SiC fibres	0.1–2 µg /mL for 48–96 h in Syrian golden hamster M3E3/C3 lung epithelial cells	Increase in micronuclei frequency; both kinetophore-positive and -negative micronuclei were detected, evocative of chromosomal aberration and breakage and aneuploidy	Fibre characteristics NR	Peraud & Riebe-Imre (1994)
Five SiC (SiCW-1, -2, -3, and -4 and 1 SiCP); diameter, 0.4–0.8 µm	0.3–15 µg/mL for 20 h in Chinese hamster lung fibroblast V79 cells	Increase in DNA strand breaks (assessed by nick translation assay); high rate of breakage for all SiCW (of the same magnitude as crocidolite); highest effect found for SiCW-3S and the lowest for the SiCP		Svensson et al. (1997)

BET, Brunauer–Emmett–Teller; NR, not reported; SiCP, silicon carbide powder; SiC-NP, silicon carbide nanoparticles; SiCW, silicon carbide whiskers; TEM, transmission electron microscopy

0.1 and 2 µg/mL increased the frequency of micronuclei (Peraud & Riebe-Imre, 1994). [The Working Group noted that no information was available on fibre characteristics in this study.]

4.4 Other mechanisms of carcinogenesis

4.4.1 Humans

See also Section 4.1, Table 4.2

Several studies have been published concerning occupational exposure to silicon carbide in humans. In contrast, information in humans on cellular mechanisms such as apoptosis, with the exception of studies in human monocytes in vitro after exposure to silicon carbide (Nordsletten et al., 1996), is limited. A dose–response has been demonstrated for decreased lung function and increased incidence of obstructive lung disease with particle mass (Bugge et al., 2011, 2012; Johnsen et al., 2013). Table 4.2 provides a summary of studies conducted among workers within the silicon carbide industry and the adverse health outcomes observed, including decreased lung function and increased incidence of obstructive lung disease (Bugge et al., 2010, 2012).

Fibrosis

Two men exposed only to silicon carbide powder for many years in a factory manufacturing refractory bricks developed bilateral reticulonodular densities as detected by chest radiography. An open lung biopsy from one patient showed a large amount of black material in the fibrosed alveolar septa. X-Ray diffraction revealed silicon carbide powder to which they had been exposed, but not quartz; X-ray diffraction analysis of the lung tissue confirmed at least six different types of silicon carbide, traces of tungsten carbide, and an insignificant amount of quartz (Funahashi et al., 1984).

No data on persistent inflammation, activation of intracellular signalling pathways, resistance to apoptosis, or cell proliferation in humans were available to the Working Group.

4.4.2 Experimental animals

(a) Inflammasome activation

Persistent inflammation accompanied by epithelial cell injury and repair by cell proliferation are important in the development of diseases associated with the inhalation of fibres (Bissonnette & Rola-Pleszczynski, 1989; McGavran & Brody, 1989; Rom et al., 1991; Donaldson & Brown, 1993; Barrett, 1994; Davis et al., 1996).

In a short-term inhalation experiment silicon carbide whiskers caused the recruitment of inflammatory cells and increased protein levels in BALF similarly to code 100/475 glass fibres and amosite asbestos fibres. Rats were exposed by whole-body inhalation to the fibre types at a concentration of 1000 WHO fibres/mL for 7 hours per day. The granulocyte response, commonly used as a measure of inflammation, showed a different pattern of time dependence for each fibre type but no clear differences between fibre types was found for BALF protein levels (Cullen et al., 1997). The bronchiolar alveolar deposition of fibres results in increased proliferation in epithelial and interstitial cells in the lung (Chang et al., 1988; Brody & Overby, 1989; Warheit et al., 1992). In the study of Cullen et al. (1997), the proliferative response to code 100/475 glass fibres was no greater than that in unexposed control animals, whereas amosite and silicon carbide whiskers both produced significant increases in cell proliferation.

Nine groups of eight sheep were exposed to saline, latex, graphite, raw silicon carbide particles, ashed silicon carbide particles, quartz, crocidolite, raw silicon carbide fibres, and ashed silicon carbide fibres by instillation once into the tracheal lobe (Bégin et al., 1989). BALF was

obtained at 2-month intervals and animals were necropsied after 8 months. Analyses of cellularity and cytotoxicity in the BALF in association with histopathology to assess fibrosis demonstrated that all particles except for quartz were inert.

(b)   Biomarkers of lung injury

Studies on intratracheal instillation have shown that exposure to silicon carbide whiskers produces pulmonary fibrotic changes, suggesting that these whiskers might have fibrogenic potential (Morimoto et al., 2003a, b).

Male Wistar rats were given a single intratracheal instillation of 2 or 10 mg of silicon carbide whiskers suspended in saline and were killed after 3 days, 1 week, 1 month, 3 months, or 6 months of recovery time. Expression of Clara cell secretory protein (CCSP) was detected using reverse transcriptase-polymerase chain reaction (RT-PCR), Western blot, and immunostaining. Exposure to 10 mg of silicon carbide whiskers decreased CCSP mRNA expression at 3 days, 1 week, 1 month, and 6 months after intratracheal instillation. Protein levels of CCSP in rats were decreased at 1 day, 3 days, and 1 month after a single instillation of 2 or 10 mg of silicon carbide whiskers (Morimoto et al., 2003b). CCSP is one of the major secretory products specifically produced by Clara cells and is hypothesized to inhibit inflammation and fibrosis because it is homologous with lipocortin (Mantile et al., 1993). CCSP has also been hypothesized to play a role as a phospholipase A_2 inhibitor in suppressing inflammation and fibrosis (Mango et al., 1998). [The results obtained by Morimoto et al. (2003b) suggest that CCSP is involved not only in the acute phase but also in the chronic phase of the lung injury induced by silicon carbide whiskers.]

Surfactant protein (SP) is a biomarker of lung injury and pulmonary fibrotic activity. SP mainly produced by type II alveolar epithelial cells, acts as a control tower responsible for guiding the secretion and re-uptake of phospholipids, which decrease alveolar surface tension, and prevent alveolar collapse, which are thought to play contributory roles in limiting the progression of fibrosis (Hawgood & Clements, 1990; Batenburg, 1992; McCormack et al., 1995). The expression of SP-A, SP-C, and thyroid transcription factor-1 (TTF-1), a common transcription factor of SP-A and SP-C mRNA in lungs exposed to silicon carbide whiskers, was examined in male Wister rats given a single intratracheal instillation of 2 or 10 mg of silicon carbide whiskers suspended in saline and killed 3 days, 1 week, 1 month, 3 months, and 6 months after the exposure. RNA was subsequently extracted from the lungs and the expression of SP-A, SP-C, and TTF-1 mRNA from the lungs was quantified using RT–PCR. Exposure to 2 mg of silicon carbide whiskers decreased mRNA expression of SP-A and TTF-1 at 6 months, and exposure to 10 mg of silicon carbide whiskers decreased the levels of SP-A and TTF-1 mRNA after 3 days and 6 months. In contrast, no clear alteration in the expression of SP-C was observed (Morimoto et al., 2003a). [These data suggest that SP-A and TTF-1 are associated not only with the acute phase but also the chronic phase of lung injury induced by silicon carbide whiskers.]

The expression of calcitonin gene-related peptide (CGRP) was quantified using RT–PCR and the enzyme immunometric assay in the lungs of male Wistar rats given a single intratracheal instillation of 2 mg of crystalline silica, crocidolite, silicon carbide whiskers, or potassium octatitanate whiskers suspended in saline and killed after recovery periods of 3 days, 1 week, 1 month, 3 months, and 6 months. CGRP protein levels in the lungs of rats exposed to silicon carbide whiskers and potassium octatitanate whiskers were higher after 3 days of recovery than those in rats exposed to silica and crocidolite (Morimoto et al., 2007). CGRP, which is found in the central and peripheral nerves, pancreatic Langerhans cells, adrenal cortex, and hypophysis, is a 37-amino acid neuropeptide (Dakhama et al., 2004). In the lung, it is secreted

from the neuroendocrine cells and nerve endings (Russwurm et al., 2001). The reported functions of CGRP include strong vasodilation, inhibition of inflammatory mediator activity, modulation of macrophage function, and maintenance of airway responsiveness (Dakhama et al., 2002, 2004). CGRP has also been reported to stimulate the proliferation of epithelial and endothelial cells in various organs (White et al., 1993; Kawase et al., 1999). In the lung, CGRP facilitates the proliferation of alveolar and airway epithelial cells; the proliferation of alveolar epithelial cells stimulated by CGRP is mediated by the mitogen-activated protein kinase signalling pathway (Kawanami et al., 2009). In animal models of airway and alveolar epithelial injury, pulmonary neuroepithelial cells and neuroepithelial bodies producing CGRP have been reported to undergo hyperplasia these cells produce CGRP in a paracrine fashion and proliferate in this lung microenvironment (Elizegi et al., 2001).

(c) Persistent inflammation

See Table 4.11

Persistent inflammation in the lung has been reported in experimental animals exposed to asbestos or silica, and is an important mechanism that leads to the production of irreversible chronic lesions, including fibrosis and tumours.

(i) Inhalation

Inhalation exposure of female Wistar rats to silicon carbide powder (mean diameter, < 3 μm) for two periods of 5 days did not induce inflammation (Bruch et al., 1993a).

(ii) Intratracheal instillation

Two studies of silicon carbide administered by intratracheal instillation of fibres in sheep and of whiskers in rats showed fibrosing alveolitis in sheep lungs (Bégin et al., 1989), and transient alveolitis in rat lungs (Ogami et al., 2007).

(d) Cell proliferation

Bronchiolar and alveolar epithelial cells in vivo

Studies of acute and chronic inhalation of silicon carbide whiskers and intratracheal instillation of silicon carbide powder and whiskers all showed that the proliferation of bronchiolar and alveolar epithelial cells was induced by exposure to silicon carbide whiskers but not to silicon carbide powder. In the 1-year study of Akiyama et al. (2007), histopathological examination revealed hyperplasia of bronchoalveolar epithelial cells in 2 out of 11 Wistar rats exposed to silicon carbide whiskers. In a 13-week study (Lapin et al., 1991), adenomatous hyperplasia of the lung was observed in male and female Sprague-Dawley rats exposed to silicon carbide whiskers.

In two studies of acute exposure to silicon carbide whiskers (Davis et al., 1996; Cullen et al., 1997), analysis of the expression of 5-bromo-2-deoxyuridine revealed the induction of hyperplasia of the bronchiolar and alveolar epithelial cells in rat lungs after 1 and 7 days, respectively.

In sheep that were instilled intratracheally with non-fibrous silicon carbide and two types of silicon carbide fibres, a fibroblast proliferation assay using BALF recovered from the lungs revealed that both fibres, but not particles, induced the proliferation of sheep lung fibroblasts (Bégin et al., 1989).

(e) Granuloma formation and fibrosis

See Table 4.11

(i) Inhalation

Exposure of rats to silicon carbide whiskers for 1 year induced severe fibrotic changes in the lung in two studies (Davis et al., 1996; Akiyama et al., 2007).

Inhalation exposure of Sprague-Dawley rats to silicon carbide whiskers for 13 weeks induced minimal or slight pleural fibrosis (Lapin et al., 1991). [Although this study also

Table 4.11 Studies on persistent inflammation, granuloma formation, and fibrosis in experimental animals

Route of administration	Type of silicon carbide	Species, strain, (sex)	Dosing regimen	Duration of exposure/ recovery	Bulk sample	Inflammation	Fibrosis or granulomatosis	Reference
Inhalation	Whiskers	Rat, Wistar (M)	2.6 ± 0.6 mg/m³ (98 ± 19 fibres/mL)/day	Exposure, 1 yr; recovery, 1 yr	Tokai Carbon Co.; purity, 98%		Hyperplasia, severe fibrosis	Akiyama et al. (2007)
	Whiskers	Rat, Sprague-Dawley (M, F)	0.09, 3.93, 10.7, 60.5 mg/m³ (0, 630, 1746, 7276 fibres/mL)/day	Exposure, 13 wk; recovery, 26 wk	Whiskers, 80–90%; mean diameter, 0.555 ± 0.197 µm; mean length, 10 ± 11.2 µm	Adenomatous hyperplasia (minimum/slight)	Pleural fibrosis (minimum/ slight)	Lapin et al. (1991)
	Whiskers	Rat, AF/HAN (NR)	1000 fibres/mL, 7 h/day, 5 days/wk for 1 yr	Exposure, 1 yr; recovery, lifespan (1 yr)	Mean diameter, 0.45 µm including fibres > 20 µm		Fibrosis (Wagner scale 4)	Davis et al. (1996)
	Powder	Rat, Wistar (F)	20 mg/m³, 5 h/day, 5 days/wk followed by a rest period of 2 days and a re-exposure period of 5 days	Exposure, 2 × 5 days; recovery, 90 days	Mean diameter, < 3 µm	No inflammation		Bruch et al. (1993a)
Intratracheal instillation	Powder	Rat, Wistar (F)	50 mg	Single dose; recovery, 3 and 8 mo	Mean diameter, < 3 µm	No inflammation		Bruch et al. (1993b)
	Whiskers	Rat, F344 (F)	1 or 5 mg/rat	Recovery, 18 mo	Sample 1: GM diameter, 0.8 µm (SD, 0.3); GM length, 18.1 µm (SD, 14.3) Sample 2: GM diameter, 1.5 µm (SD, 0.6); GM length, 15.3 µm (SD, 11.2)		Multiple nodular granulomas	Vaughan et al. (1993)
	Whiskers	Rat, Wistar (M)	2 mg/rat	Recovery, 6 mo	GM diameter, 0.3 µm (SD, 1.5); GM length, 5.1 µm (SD, 2.3)	Inflammation (transient)		Ogami et al. (2007)
	Non-fibrous and fibres	Sheep (NR)	100 mg/sheep	Recovery, 8 mo	99.5% < 5 µm	Nodular fibrosing alveolitis: fibres only		Bégin et al. (1989)
	Silicon carbide	Rat, Wistar (M)	50 mg/rat	Recovery, 12 months	Average size < 3 µm		No fibrosis	Bruch et al. (1993b)

F, female; GM, geometric mean; M, male; mo, month; NR, not reported; SD, standard deviation; wk, week; yr, year

revealed persistent alveolar wall thickening, it is unclear whether this finding was associated with pulmonary fibrosis.]

(ii)   Intratracheal instillation

A single dose of 50 mg of silicon carbide powder did not induce fibrosis in the lung [even though the dose was excessive] (Bruch et al., 1993b).

Two studies of silicon carbide whiskers provided evidence of various degrees of granuloma formation or fibrosis (Vaughan et al., 1993; Morimoto et al., 2003a).

No data on immunosuppression, apoptosis, activation of intracellular signalling pathways, or resistance to apoptosis were available to the Working Group.

4.4.3 Experimental systems in vitro

(a)   Release of cytokines, chemokines, and growth factors

Macrophages exposed to toxic and carcinogenic dusts and fibres in vitro release pro-inflammatory mediators, and the release of TNF-α is commonly used as a biomarker for acute pro-inflammatory effects. Primary rat alveolar macrophages were exposed to two samples of silicon carbide whiskers (ACMC) in comparison with amosite or crocidolite asbestos fibres and a variety of man-made mineral fibres at equal fibre numbers (length, > 5 μm) for 24 hours. Both samples of silicon carbide whiskers were as potent as or more potent than asbestos fibres in eliciting TNF-α release (Cullen et al., 1997).

Nuclear translocation of the transcription factor nuclear factor (NF)-κB is associated with pro-inflammatory gene activation (Mossman et al., 1997). In the human A549 lung adeno-carcinoma cell line, exposure to silicon carbide whiskers (ACMC) for 8 hours induced the activation of NF-κB in 38% of cells compared with 55% of cells exposed to long-fibre amosite asbestos at equal fibre numbers (Brown et al.,

1999). Translocation of NF-κB was significantly decreased by antioxidants (curcumin, pyrrolidine dithiocarbamate, or nacystelin).

(b)   Apoptosis and necrosis

In explants of dog tracheal epithelium, a dose of 10 μg/cm^2 of one of three samples of silicon carbide whiskers (Tateho, Japan, or American Matrix, Inc., Tennessee, USA) induced necrosis of non-ciliated cells after 3 days (Vaughan et al., 1991b). At doses of between 5 and 20 μg/cm^2, two of these samples also induced acute toxicity in BALB/3T3 mouse embryonic cells, as assessed by trypan blue exclusion, ^{51}Cr release, and colony-forming efficiency, that was comparable with that of crocidolite asbestos fibres (Los Alamos National Laboratory, New Mexico, USA) (Vaughan et al., 1991a).

Three samples of silicon carbide whiskers (Alcan Aluminum Corp., Pennsylvania; ACMC; American Matrix Inc.) were compared with crocidolite asbestos fibres (UICC), erionite fibres (Rome, Oregon, USA), and JM Code 100 glass-fibres (Johns Manville Corp., Colorado, USA). At doses between 5 and 50 μg/mL, all fibrous samples induced toxicity in primary rat alveolar macrophages, as assessed by trypan blue exclusion, and decreased colony-forming efficiency in primary rat tracheal epithelial cells, lung epithelial cells, and the human lung adenocarcinoma A549 cell line (Johnson et al., 1992). The authors noted that these toxicity end-points based on mass doses may not correlate with toxicity ranked on the basis of equal fibre numbers.

Svensson et al. (1997) assessed the effects of silicon carbide whiskers (Tokai Carbon Co., Ltd, Japan; Tateho Chemical Co., Ltd), silicon carbide powder (UF15, Lonza) and crocidolite asbestos fibres (UICC) on colony-formation efficiency in the V79 Chinese hamster lung fibroblast cell line exposed to 0.25–80 μg/cm^2 for 20 hours. The silicon carbide whiskers and crocidolite asbestos fibres showed highest potency; milled silicon

carbide whiskers and silicon carbide powder were less potent.

In primary cultures of hamster alveolar macrophages, silicon carbide whiskers (Japan Fibrous Materials Research Association) induced apoptosis after exposure to 20–60 μg/mL for 18 hours assessed by the detection of a DNA ladder and nuclear morphology using TEM (Watanabe et al., 2000). Using the same sample of silicon carbide whiskers in comparison with chrysotile asbestos fibres (Japan Association for the Working Environment Measurement) at doses of 20–60 μg/mL, Shibata et al. (2007) detected plasma membrane injury assessed by lactate dehydrogenase release in primary cultures of rat alveolar macrophages and the murine peritoneal macrophage RAW 264.7 cell line.

(c) Impaired DNA repair

No data on impaired DNA repair were available to the Working Group.

DNA breakage was detected in M3E3/C3 lung epithelial cells exposed to silicon carbide, as measured by the detection of micronuclei (Peraud & Riebe-Imre, 1994). Both kinetochore positive and kinetochore negative micronuclei were detected as evidence for chromosome breakage and aneuploidy.

(d) Depletion of antioxidants

No direct data on the depletion of antioxidants in cells were available to the Working Group.

In an acellular test system, the effects of five whiskers (four silicon carbides, SiCW-1, -2,-3, and -4, and one silicon nitride, SiNW) and two powders (one silicon carbide, SiCP, and one silicon nitride, SiNP) were determined. SiCW-3 was also ball-milled in water for 3 hours (SiCW-3S, short-milled) or 58 hours (SiCW-3L, long-milled). The lengths of the silicon carbide whiskers ranged between 12 ± 10 and 14 ± 10 μm and the diameters between 0.7 ± 0.4 and 0.9 ± 0.4 μm and their length/diameter ratios were therefore similar.

The mean length of SiCW-3S and SiCW-3L was 11 ± 7 μm and 9 ± 5 μm, respectively. The assay detected the reaction product, 8-hydroxydeoxyguanosine, formed in the presence of hydrogen peroxide and deoxyguanosine. The 8-hydroxydeoxyguanosine/deoxyguanosine ratio was taken as an index of hydroxyl radical formation. Only SiCW-4 and crocidolite, used as positive control, could potentiate the formation of hydroxyl radicals. In the presence of the scavenger dimethyl sulfoxide, the hydroxyl radical production of these samples was lowered (Svensson et al., 1997). In an acellular system, silicon carbide whiskers (ACMC) had the ability to deplete both GSH and ascorbate from pure solutions of GSH or ascorbate, and GSH from Wistar rat lung lining fluid (Brown et al., 2000).

The formation of oxygen radicals by human neutrophils treated with samples of silicon carbide whiskers and silicon nitride whiskers was assessed by chemiluminescence and the formation of hydrogen peroxide was determined (Svensson et al., 1997). Several samples – SiCW-1, SiCW-3, SiCW-4, SiCW-3S, and SiCW-3L – induced chemiluminescence and a relatively good correlation was found between the magnitude of chemiluminescence and the neutrophil-mediated formation of hydrogen peroxide. [These results showed that some samples could trigger the intracellular production of ROS and suggest that silicon carbide whiskers may disturb the cellular oxidant/antioxidant balance.]

Another study demonstrated the production of ROS by silicon carbide-exposed cells. In addition, the authors suggested that the generation of ROS was dependent on NF-κB activation. In this study, human A549 lung adenocarcinoma cells were exposed to silicon carbide (60.86% > 10 μm in length; ACMC). The effects on hydrogen peroxide formation of silicon carbide, long amosite asbestos fibres, and refractory ceramic fibres were compared. All fibres produced positive nuclear staining of NF-κB in A549 cells, as well as generation of hydrogen peroxide. Several

Table 4.12 Summary of the results of mechanistic studies for the three categories of silicon carbide

Category of silicon carbide	End-point			Reference
	Biopersistence	Inflammation/ fibrosis in lung	Genotoxicity	
Abrasive dust from the Acheson process	Weak	Weak	No data	Dufresne et al. (1992)
Silicon carbide whiskers	Strong	Strong	Moderate[a]	Akiyama et al. (2003, 2007)
Silicon carbide nanoparticles	No data	No data	Inadequate data	Barillet et al. (2010a)

[a] Chromosomal aberrations in human cells

antioxidant inhibitors and a specific inhibitor of NF-κB activation inhibited the effect of the fibres (Brown et al., 1999). [These results showed the involvement of oxidants in silicon carbide-dependent activation of the transcription factor NF-κB and also suggest that silicon carbide fibres could perturb the cellular oxidant/antioxidant balance.]

No data on inflammasome activation, immunosuppression, alteration of DNA methylation, or the activation of oncogenes and tumour-suppressor genes in other experimental systems were available to the Working Group.

4.5 Susceptible populations

No data were available to the Working Group.

4.6 Mechanistic considerations

The summary of the relevant data available are reported separately in Table 4.12 for the three categories of silicon carbide and for the three most relevant end-points: biopersistence, inflammation and fibrosis, and genotoxicity.

5. Summary of Data Reported

5.1 Exposure data

Silicon carbide occurs in several forms: non-fibrous or granular particulate material (dust, crude, and grains), fibres, and whiskers. A fibre is typically polycrystalline, whereas the name whisker is applied only to monocrystalline (or single-crystal) fibres. Whiskers are intentionally produced and have a homogeneous morphology whereas silicon carbide fibres are morphologically heterogeneous. Silicon carbide whiskers are cylindrical in shape, similar in size to asbestos amphiboles, and may meet the definition of WHO fibres.

Silicon carbide is very stable, but chemical reactions between silicon carbide and oxygen occur at relatively high temperatures. Fresh surfaces of silicon carbide exposed to an oxidizing atmosphere could thus be covered by a film of silicon dioxide.

Silicon carbide can be manufactured by several processes, resulting in different levels of purity, crystal structure, particle size, and shape; the most frequently used method is the Acheson process for the production of silicon carbide particles, in which silicon carbide fibres are unwanted by-products. Different morphologies of silicon carbide fibres formed during the Acheson process have been observed by electron microscopy. Their length and diameter

are variable, but can fulfil the WHO definition of fibres, and may include fibres that are indistinguishable from whiskers. Silicon carbide fragments (probably derived from the cleavage of non-fibrous silicon carbide crystals), also corresponding to the WHO definition of fibres, were found in the processing department and in sorting operations.

Other methods for the production of silicon carbide particulates, fibres, or whiskers exist but have not been well documented with respect to the generation of fibrous silicon carbide in the air.

Silicon carbide production began in the early twentieth century mostly for use as abrasives. Carborundum is a commercial name for silicon carbide abrasives and is occasionally used as a common name for silicon carbide dust. In 2013, the global production capacity was estimated to more than 1 000 000 metric tonnes, of which China was the leading producer. The available information on production levels mostly concerns the Acheson process. Additional applications of silicon carbide include: refractories, electrical devices, electronics, diesel particle filters, ceramics, industrial furnaces, structural materials, metallurgy, and in the aerospace, automotive, and power generation industries as reinforcing materials in advanced ceramic composites. Unwanted fibres from the Acheson process are usually recycled in further reactions in the Acheson furnace; they may also occasionally be sold as part of metallurgical-grade silicon carbide. Silicon carbide whiskers are used as a durable industrial substitute for asbestos.

Insufficient data have been reported to reach a conclusion on the exposure of workers to whiskers and silicon carbide dust used as abrasive products. However, high levels of silicon carbide fibres have been measured in the Acheson process during the mixing of materials, furnace operations, and the separation of products with average concentrations of > 0.1 fibres/cm^3. The majority of the silicon carbide fibres were thin with an average diameter < 1 µm and an aspect ratio > 35. Lower levels of fibres have been measured in the processing department, but cleavage fragments were present at higher concentrations. Exposures to respirable silicon carbide fibres were confirmed by the analysis of human lung tissues. Most of the fibres in lung samples were < 5 µm in length. In silicon carbide industries, workers are also co-exposed to quartz and cristobalite.

5.2 Human carcinogenicity data

The carcinogenic risk associated with exposure to silicon carbide fibres has been investigated in two cohort studies of occupational exposure among workers using the Acheson process in silicon-carbide manufacturing plants. This process is characterized by multiple exposures, among them fibrous and non-fibrous silicon carbide, quartz, and cristobalite. The first cohort study included workers in the Canadian silicon-carbide manufacturing industry. An excess of mortality from lung cancer was observed in comparison with the general population. Mortality from mesothelioma was not reported for this cohort. In the second cohort, the incidence of lung cancer was investigated among workers in the Norwegian silicon-carbide manufacturing industry. In a series of studies, the most informative analysis was limited to long-term workers with at least 3 years of employment, and was based on a detailed job–exposure matrix taking into account total and respirable dust, non-fibrous and fibrous silicon carbide, quartz, and cristobalite. Overall, the incidence of lung cancer was increased, with the highest risk for workers in the furnace department who were believed to have the highest exposures to fibrous silicon carbide and crystalline silica dust. In multivariate modelling, an exposure–response effect was observed for silicon carbide fibres. The effect was weakened and no longer statistically significant after adjustment for concurrent exposure to cristobalite. The Working Group noted

that the strong correlation between exposures to silicon carbide fibres and cristobalite made the disentanglement of their respective effects difficult. Silicon carbide particles were not associated with cancer of the lung independently of silicon carbide fibres or cristobalite. No excess in the incidence of mesothelioma was observed in the Norwegian cohort. No data were available on cancer in populations exposed to manufactured silicon carbide whiskers.

5.3 Animal carcinogenicity data

Studies of fibrous silicon carbide in experimental animals were available only for silicon carbide whiskers.

Silicon carbide whiskers significantly increased the incidence of mesothelioma in three studies in female rats treated by intrapleural injection, intrapleural implantation, or intraperitoneal injection, and the increase was dose-related in rats treated by intraperitoneal injection. In a study in female rats treated by intratracheal instillation with two types of silicon carbide whiskers, judged by the Working Group to be limited because of its short duration, no treatment-related neoplasms were observed. One study of inhalation in male rats and one study of intraperitoneal injection in female rats gave negative results.

Mesotheliomas were reported in one study of intraperitoneal injection in female rats and in one study each of inhalation and intraperitoneal injection in rats (sex unspecified); however, these studies did not include concurrent controls. Because the background incidence of mesotheliomas is very low in rats, some consideration was given to these three studies that gave positive results, despite their lack of concurrent controls.

5.4 Mechanistic and other relevant data

5.4.1 Silicon carbide produced by the Acheson process

Airborne silicon carbide from the Acheson process, containing silicon carbide dust and fibres, can be deposited and retained in the human lung. After intratracheal instillation, silicon carbide dust and fibres were retained in the lungs of sheep. Mechanistic studies on silicon carbide materials in humans are lacking. The few available studies in experimental animals do not provide any insight into the mechanisms of carcinogenicity.

5.4.2 Silicon carbide whiskers

Studies on silicon carbide whiskers demonstrated biopersistence in the rat lung. The Working Group noted the lack of studies on the translocation of silicon carbide materials to the pleural cavity in experimental animals. Pulmonary exposure to silicon carbide whiskers in experimental animals has been associated with lung cell injury, inflammation, and fibrotic responses. Oxidative stress has been reported in studies in vitro. Genotoxicity measurements were limited to in-vitro studies. One study of genotoxicity demonstrated chromosomal aberrations in human embryonic lung cells exposed to silicon carbide whiskers. The few available studies reported data which are fully consistent with the mechanisms of carcinogenicity proposed for asbestos and erionite (see *IARC Monographs* Volume 100C).

5.4.3 Silicon carbide nanoparticles

Mechanistic studies of silicon carbide nanoparticles are sparse. The production of reactive oxygen species and the depletion of antioxidants have been reported in a few in-vitro studies, which have not been independently replicated

across different cell cultures or in in-vivo models and thus do not provide conclusive evidence that oxidative stress is a mechanism of the toxicity of silicon carbide nanoparticles. The results from experimental models do not provide adequate information to support a conclusion regarding the potential mechanisms of carcinogenicity of silicon carbide nanoparticles.

6. Evaluation

6.1 Cancer in humans

There is *sufficient evidence* in humans for the carcinogenicity of occupational exposures associated with the Acheson process. Occupational exposures associated with the Acheson process cause cancer of the lung.

There is *limited evidence* in humans for the carcinogenicity of fibrous silicon carbide. Positive associations have been observed between exposure to fibrous silicon carbide and cancer of the lung.

6.2 Cancer in experimental animals

There is *sufficient evidence* in experimental animals for the carcinogenicity of silicon carbide whiskers.

6.3 Overall evaluation

Occupational exposures associated with the Acheson process are *carcinogenic to humans (Group 1)*.

Fibrous silicon carbide is *possibly carcinogenic to humans (Group 2B)*.

Silicon carbide whiskers are *probably carcinogenic to humans (Group 2A)*.

6.4 Rationale

Rationale for a separate evaluation of whiskers and fibres – majority view

The rationale for a separate evaluation of whiskers and fibres is based on differences in the nature of the agents.

The cohort of workers at plants using the Acheson process was occupationally exposed to non-fibrous and fibrous silicon carbide, potentially including some fibres that could be defined as whiskers, whereas exposure in most of the studies in experimental animals and in experimental systems was to silicon carbide whiskers.

Silicon carbide whiskers are monocrystalline and homogeneous in form, while fibrous silicon carbide is mostly polycrystalline and heterogeneous in form. The physico-chemical characteristics of these fibres were considered to be distinct, and therefore the fibres and whiskers warrant separate evaluations.

Rationale for a combined overall evaluation of whiskers and fibres – minority view

The argument for a combined overall evaluation of silicon carbide whiskers and fibres was that a proportion of the fibres in the epidemiological study in Norway had dimensions that were consistent with silicon carbide whiskers, and were morphologically indistinguishable from silicon carbide whiskers under electron microscopy. Thus, the excess of cancer of the lung observed was relevant for evaluating the carcinogenicity of silicon whiskers as well as other fibrous silicon carbide. Had the minority view been adopted, it would have supported an overall evaluation of *probably carcinogenic to humans (Group 2A)*.

Rationale for classification in Group 2A – majority view

A narrow majority of the Working Group voted for the classification of silicon carbide whiskers as *probably carcinogenic to humans (Group 2A)* rather than as *possibly carcinogenic to humans (Group 2B)*.

The majority view was primarily based on their expert opinion that the major physical properties of silicon carbide whiskers resembled those of asbestos and erionite fibres, which are classified as *carcinogenic to humans (Group 1)*. This information was used to upgrade the overall evaluation of carcinogenicity to humans to Group 2A.

Rationale for classification in Group 2B – minority view

A minority of the Working Group voted for the classification of silicon carbide whiskers as *possibly carcinogenic to humans (Group 2B)* because:

- the evidence for the carcinogenicity of silicon carbide whiskers in experimental animals was based on direct bolus delivery into the pleura or peritoneum at high mass doses;

- only one study of inhalation was available and was considered by the minority as inadequate for the evaluation due to lack of concurrent unexposed controls; and

- the available mechanistic data did not provide strong support for an upgrade of the overall evaluation.

References

ACGIH (2003). Silicon Carbide. Documentation of the threshold limit values and biological exposure indices. 7th ed. Cincinnati (OH), USA: American Conference of Governmental Industrial Hygienists (ACGIH); 9 pp.

Adachi S, Kawamura K, Takemoto K (2001). A trial on the quantitative risk assessment of man-made mineral fibres by the rat intraperitoneal administration assay using the JFM standard fibrous samples. *Ind Health*, 39(2):168–74. doi:10.2486/indhealth.39.168 PMID:11341547

Akiyama I, Ogami A, Oyabu T, Yamato H, Morimoto Y, Tanaka I (2003). Clearance of deposited silicon carbide whisker from rat lungs inhaled during a 4-week exposure. *J Occup Health*, 45(1):31–5. doi:10.1539/joh.45.31 PMID:14605426

Akiyama I, Ogami A, Oyabu T, Yamato H, Morimoto Y, Tanaka I (2007). Pulmonary effects and biopersistence of deposited silicon carbide whisker after 1-year inhalation in rats. *Inhal Toxicol*, 19(2):141–7. doi:10.1080/08958370601051784 PMID:17169861

Asgharian B, Yu CP (1989a). Deposition of fibers the rat lung. *J Aerosol Sci*, 20(3):355–66. doi:10.1016/0021-8502(89)90011-6

Asgharian B, Yu CP (1989b). A simplified model of interceptional deposition of fibers at airway bifurcations. *Aerosol Sci Technol*, 11(1):80–8. doi:10.1080/02786828908959301

ASTM (1998). Standard practice for handling silicon carbide whiskers. ASTM E1437–98 - Committee E-34 on Occupational Health and Safety (Subcommittee E34.70 on Single Crystal Ceramic Whiskers). West Conshohocken (PA), USA: The American Society for Testing and Materials.

ASTM (2011). Standard practice for determining concentration of airborne single-crystal ceramic whiskers in the workplace environment. ASTM D6058–96 - Committee D-22 on Sampling and Analysis of Atmospheres. West Conshohocken (PA), USA: The American Society for Testing and Materials.

Barillet S, Jugan ML, Laye M, Leconte Y, Herlin-Boime N, Reynaud C, et al. (2010a). In vitro evaluation of SiC nanoparticles impact on A549 pulmonary cells: cyto-, genotoxicity and oxidative stress. *Toxicol Lett*, 198(3):324–30. doi:10.1016/j.toxlet.2010.07.009 PMID:20655996

Barillet S, Simon-Deckers A, Herlin-Boime N, Mayne-L'Hermite M, Reynaud C, Cassio D, et al. (2010b). Toxicological consequences of TiO2, SiC nanoparticles and multi-walled carbon nanotubes exposure in several mammalian cell types: an in vitro study. *J Nanopart Res*, 12(1):61–73. doi:10.1007/s11051-009-9694-y

Barrett JC (1994). Cellular and molecular mechanisms of asbestos carcinogenicity: implications for biopersistence. *Environ Health Perspect*, 102(Suppl 5):19–23. doi:10.1289/ehp.94102s519 PMID:7882928

Batenburg JJ (1992). Surfactant phospholipids: synthesis and storage. *Am J Physiol*, 262(4 Pt 1):L367–85. PMID:1566854

Beaumont GP (1991). Reduction in airborne silicon carbide whiskers by process improvements. *Appl*

Occup Environ Hyg, 6(7):598–603. doi:10.1080/1047322X.1991.10387942

Bégin R, Dufresne A, Cantin A, Massé S, Sébastien P, Perrault G (1989). Carborundum pneumoconiosis. Fibers in the mineral activate macrophages to produce fibroblast growth factors and sustain the chronic inflammatory disease. *Chest*, 95(4):842–9. doi:10.1378/chest.95.4.842 PMID:2924613

Bégin R, Massé S, Rola-Pleszczynski M, Drapeau G, Dalle D (1985). Selective exposure and analysis of the sheep tracheal lobe as a model for toxicological studies of respirable particles. *Environ Res*, 36(2):389–404. doi:10.1016/0013-9351(85)90033-7 PMID:2983978

Bissonnette E, Rola-Pleszczynski M (1989). Pulmonary inflammation and fibrosis in a murine model of asbestosis and silicosis. *Inflammation*, 13(3):329–39. doi:10.1007/BF00914399 PMID:2753523

Boch P (2001). [Matériaux et processus céramiques.] Mécanique et Ingénierie des Matériaux. Série Alliages Métalliques. Paris, France: Paris Hermès Science Publications. [French]

Boudard D, Forest V, Pourchez J, Boumahdi N, Tomatis M, Fubini B, et al. (2014). In vitro cellular responses to silicon carbide particles manufactured through the Acheson process: impact of physico-chemical features on pro-inflammatory and pro-oxidative effects. *Toxicol In Vitro*, 28(5):856–65. doi:10.1016/j.tiv.2014.02.012 PMID:24603312

Boumahdi N (2009). [Approche pluridisciplinaire de l'étude de l'activité biologique de particules fines. Génie des procédés] [PhD Thesis]. Saint Etienne, France: Ecole Nationale Supérieure des Mines de Saint-Etienne. Available from: https://tel.archives-ouvertes.fr/tel-00419902/file/090114-N-Boumahdi.pdf. [French]

Brody AR, Overby LH (1989). Incorporation of tritiated thymidine by epithelial and interstitial cells in bronchiolar-alveolar regions of asbestos-exposed rats. *Am J Pathol*, 134(1):133–40. PMID:2913821

Brown DM, Beswick PH, Bell KS, Donaldson K (2000). Depletion of glutathione and ascorbate in lung lining fluid by respirable fibres. *Ann Occup Hyg*, 44(2):101–8. doi:10.1093/annhyg/44.2.101 PMID:10717261

Brown DM, Beswick PH, Donaldson K (1999). Induction of nuclear translocation of NF-kappaB in epithelial cells by respirable mineral fibres. *J Pathol*, 189(2):258–64. doi:10.1002/(SICI)1096-9896(199910)189:2<258::AID-PATH410>3.0.CO;2-E PMID:10547584

Brown DM, Fisher C, Donaldson K (1998). Free radical activity of synthetic vitreous fibers: iron chelation inhibits hydroxyl radical generation by refractory ceramic fiber. *J Toxicol Environ Health A*, 53(7):545–61. doi:10.1080/009841098159132 PMID:9561968

Bruch J, Rehn B, Duval-Arnould G, Efskind J, Röderer G, Sébastian P (2014). Toxicological investigations on the respirable fraction of silicon carbide grain products by

the in vitro vector model. *Inhal Toxicol*, 26(5):278–88. doi:10.3109/08958378.2014.885099 PMID:24669950

Bruch J, Rehn B, Song H, Gono E, Malkusch W (1993a). Toxicological investigations on silicon carbide. 1. Inhalation studies. *Br J Ind Med*, 50(9):797–806. PMID:8398873

Bruch J, Rehn B, Song W, Gono E, Malkusch W (1993b). Toxicological investigations on silicon carbide. 2. In vitro cell tests and long term injection tests. *Br J Ind Med*, 50(9):807–13. PMID:8398874

Bugge MD, Føreland S, Kjærheim K, Eduard W, Martinsen JI, Kjuus H (2011). Mortality from non-malignant respiratory diseases among workers in the Norwegian silicon carbide industry: associations with dust exposure. *Occup Environ Med*, 68(12):863–9. doi:10.1136/oem.2010.062836 PMID:21364203

Bugge MD, Kjærheim K, Føreland S, Eduard W, Kjuus H (2012). Lung cancer incidence among Norwegian silicon carbide industry workers: associations with particulate exposure factors. *Occup Environ Med*, 69(8):527–33. doi:10.1136/oemed-2011-100623 PMID:22611173

Bugge MD, Kjuus H, Martinsen JI, Kjaerheim K (2010). Cancer incidence among short- and long-term workers in the Norwegian silicon carbide industry. *Scand J Work Environ Health*, 36(1):71–9. doi:10.5271/sjweh.2875 PMID:19953212

Bye E, Eduard W, Gjønnes J, Sørbrøden E (1985). Occurrence of airborne silicon carbide fibers during industrial production of silicon carbide. *Scand J Work Environ Health*, 11(2):111–5. doi:10.5271/sjweh.2245 PMID:4001899

Bye E, Føreland S, Lundgren L, Kruse K, Rønning R (2009). Quantitative determination of airborne respirable non-fibrous α-silicon carbide by x-ray powder diffractometry. *Ann Occup Hyg*, 53(4):403–8. doi:10.1093/annhyg/mep022 PMID:19406909

CAMEO Chemicals (2014). Silicon carbide. Chemical datasheet. Office of Response and Restoration, National Ocean Service, National Oceanic and Atmospheric Administration. Available from: http://cameochemicals.noaa.gov/chemical/25062, accessed on 16 June 2014.

Case BW, Sebastien P (1987). Environmental and occupational exposures to chrysotile asbestos: a comparative microanalytic study. *Arch Environ Health*, 42(4):185–91. PMID:2821933

Chang L-Y, Overby LH, Brody AR, Crapo JD (1988). Progressive lung cell reactions and extracellular matrix production after a brief exposure to asbestos. *Am J Pathol*, 131(1):156–70. PMID:2833103

Chemical Book (2014). Silicon carbide (409-21-2). Available from: http://www.chemicalbook.com/ProductChemicalPropertiesCB2431905_EN.htm, accessed 24 June 2014.

Cheng TW, Hsu CW (2006). A study of silicon carbide synthesis from waste serpentine. *Chemosphere*,

64(3):510–4. doi:10.1016/j.chemosphere.2005.11.018 PMID:16405956

Cheng YS, Powell QH, Smith SM, Johnson NF (1995). Silicon carbide whiskers: characterization and aerodynamic behaviors. *Am Ind Hyg Assoc J*, 56(10):970–8. doi:10.1080/15428119591016395 PMID:7572614

Cook N (2006). A safe replacement. *The RoSPA Occupational Safety and Health Journal*, 36(8):22–4.

Cullen RT, Miller BG, Davis JMG, Brown DM, Donaldson K (1997). Short-term inhalation and in vitro tests as predictors of fibre pathogenicity. *Environ Health Perspect*, 105(Suppl 5):1235–40. doi:10.1289/ehp.97105s51235 PMID:9400730

Dakhama A, Kanehiro A, Mäkelä MJ, Loader JE, Larsen GL, Gelfand EW (2002). Regulation of airway hyperresponsiveness by calcitonin gene-related peptide in allergen sensitized and challenged mice. *Am J Respir Crit Care Med*, 165(8):1137–44. doi:10.1164/ajrccm.165.8.2109058 PMID:11956058

Dakhama A, Larsen GL, Gelfand EW (2004). Calcitonin gene-related peptide: role in airway homeostasis. *Curr Opin Pharmacol*, 4(3):215–20. doi:10.1016/j.coph.2004.01.006 PMID:15140411

Davis JMG, Brown DM, Cullen RT, Donaldson K, Jones AD, Miller BG, et al. (1996). A comparison of methods of determining and predicting the pathogenicity of mineral fibres. *Inhal Toxicol*, 8(8):747–70. doi:10.3109/08958379608995209

Davis JMG, Jones AD, Miller BG (1991). Experimental studies in rats on the effects of asbestos inhalation coupled with the inhalation of titanium dioxide or quartz. *Int J Exp Pathol*, 72(5):501–25. PMID:1742204

De Vuyst P, Vande Weyer R, De Coster A, Marchandise FX, Dumortier P, Ketelbant P, et al. (1986). Dental technician's pneumoconiosis. A report of two cases. *Am Rev Respir Dis*, 133(2):316–20. PMID:3946927

Deal BE, Grove AS (1965). General relationship for the thermal oxidation of silicon. *J Appl Phys*, 36(12):3770 doi:10.1063/1.1713945

Dion C, Dufresne A, Jacob M, Perrault G (2005). Assessment of exposure to quartz, cristobalite and silicon carbide fibres (whiskers) in a silicon carbide plant. *Ann Occup Hyg*, 49(4):335–43. doi:10.1093/annhyg/meh099 PMID:15650014

Donaldson K, Brown GM (1993). Bronchoalveolar lavage in the assessment of the cellular response to fiber exposure. In: Warheit D, editor. Fiber Toxicology, Chapter 6. San Diego (CA), USA: Academic Press; pp. 117–138.

Dufresne A, Lesage J, Perrault G (1987a). Evaluation of occupational exposure to mixed dusts and polycyclic aromatic hydrocarbons in silicon carbide plants. *Am Ind Hyg Assoc J*, 48(2):160–6. doi:10.1080/15298668791384562 PMID:3565270

Dufresne A, Loosereewanich P, Armstrong B, Infante-Rivard C, Perrault G, Dion C, et al. (1995). Pulmonary retention of ceramic fibers in silicon carbide

(SiC) workers. *Am Ind Hyg Assoc J*, 56(5):490–8. doi:10.1080/15428119591016917 PMID:7754979

Dufresne A, Loosereewanich P, Harrigan M, Sébastien P, Perrault G, Bégin R (1993). Pulmonary dust retention in a silicon carbide worker. *Am Ind Hyg Assoc J*, 54(6):327–30. doi:10.1080/15298669391354748 PMID:8328361

Dufresne A, Perrault G, Sébastien P, Adnot A, Baril M (1987b). Morphology and surface characteristics of particulates from silicon carbide industries. *Am Ind Hyg Assoc J*, 48(8):718–29. doi:10.1080/15298668791385471

Dufresne A, Sébastien P, Perrault G, Massé S, Bégin R (1992). Pulmonary clearance of fibrous and angular SiC particulates in the sheep model of pneumoconiosis. *Ann Occup Hyg*, 36(5):519–30. doi:10.1093/annhyg/36.5.519 PMID:1444071

Edling C, Järvholm B, Andersson L, Axelson O (1987). Mortality and cancer incidence among workers in an abrasive manufacturing industry. *Br J Ind Med*, 44(1):57–9. PMID:3814536

Elizegi E, Pino I, Vicent S, Blanco D, Saffiotti U, Montuenga LM (2001). Hyperplasia of alveolar neuroendocrine cells in rat lung carcinogenesis by silica with selective expression of proadrenomedullin-derived peptides and amidating enzymes. *Lab Invest*, 81(12):1627–38. doi:10.1038/labinvest.3780376 PMID:11742033

Encyclopaedia Britannica (2014). Silicon carbide. Available from: http://www.britannica.com/EBchecked/topic/544369/silicon-carbide, accessed 24 June 2014.

EPA (1988). Reference physiological parameters in pharmacokinetic modeling. EPA Report No. EPA/600/6-88/004. Washington (DC), USA: Office of Health and Environment Assessment, Exposure Assessment Group, United States Environmental Protection Agency.

EPA (2006). Approaches for the application of physiologically based pharmacokinetic (PBPK) models and supporting data in risk assessment. Washington (DC), USA: National Center for Environmental Assessment, Office of Research and Development, United States Environmental Protection Agency.

Fan J, Li H, Jiang J, So LK, Lam YW, Chu PK (2008). 3C-SiC nanocrystals as fluorescent biological labels. *Small*, 4(8):1058–62. doi:10.1002/smll.200800080 PMID:18618492

Føreland S (2012). Improved retrospective exposure assessment of dust and selected dust constituents in the Norwegian silicon carbide industry from 1913 to 2005. [PhD Thesis]. Oslo, Norway: University of Oslo, Department of Chemistry, Faculty of Mathematics and Natural Sciences. Available from: https://www.duo.uio.no/bitstream/handle/10852/34535/dravhandling-foreland.pdf?sequence=2.

Føreland S, Bakke B, Vermeulen R, Bye E, Eduard W (2013). Determinants of exposure to dust and dust constituents in the Norwegian silicon carbide industry.

Ann Occup Hyg, 57(4):417–31. doi:10.1093/annhyg/mes086 PMID:23204512

Føreland S, Bugge MD, Bakke B, Bye E, Eduard W (2012). A novel strategy for retrospective exposure assessment in the Norwegian silicon carbide industry. *J Occup Environ Hyg*, 9(4):230–41. doi:10.1080/15459624.2012.666189 PMID:22448628

Føreland S, Bye E, Bakke B, Eduard W (2008). Exposure to fibres, crystalline silica, silicon carbide and sulphur dioxide in the Norwegian silicon carbide industry. *Ann Occup Hyg*, 52(5):317–36. doi:10.1093/annhyg/men029 PMID:18550624

Fubini B, Fenoglio I, Elias Z, Poirot O (2001). Variability of biological responses to silicas: effect of origin, crystallinity, and state of surface on generation of reactive oxygen species and morphological transformation of mammalian cells. *J Environ Pathol Toxicol Oncol*, 20(Suppl 1):95–108. PMID:11570678

Funahashi A, Schlueter DP, Pintar K, Siegesmund KA, Mandel GS, Mandel NS (1984). Pneumoconiosis in workers exposed to silicon carbide. *Am Rev Respir Dis*, 129(4):635–40. PMID:6712005

Governa M, Valentino M, Amati M, Visonà I, Botta GC, Marcer G, et al. (1997). Biological effects of contaminated silicon carbide particles from a workstation in a plant producing abrasives. *Toxicol In Vitro*, 11(3):201–7. doi:10.1016/S0887-2333(97)00018-0 PMID:20654306

Gunnæs AE, Olsen A, Skogstad A, Bye E (2005). Morphology and structure of airborne-SiC fibres produced during the industrial production of non-fibrous silicon carbide. *J Mater Sci*, 40(22):6011–7. doi:10.1007/s10853-005-4591-y

Harmsen AG, Muggenburg BA, Snipes MB, Bice DE (1985). The role of macrophages in particle translocation from lungs to lymph nodes. *Science*, 230(4731):1277–80. doi:10.1126/science.4071052 PMID:4071052

Hawgood S, Clements JA (1990). Pulmonary surfactant and its apoproteins. *J Clin Invest*, 86(1):1–6. doi:10.1172/JCI114670 PMID:2195058

Hayashi H, Kajita A (1988). Silicon carbide in lung tissue of a worker in the abrasive industry. *Am J Ind Med*, 14(2):145–55. doi:10.1002/ajim.4700140205 PMID:3207100

Health Council of the Netherlands (2012). Silicon carbide. Evaluation of the carcinogenicity and genotoxicity. The Hague, The Netherlands: Health Council of the Netherlands; Publication No. 2012/29.

Holt PF (1950). The fate of siliceous dusts in the body; a comparison of the in vivo solubilities of cement, carborundum, quartz, and moulding sand. *Br J Ind Med*, 7(1):12–6. PMID:15403147

HSE (1988). Man-made mineral fibre. airborne number concentration by phase-contrast light microscopy. HSE Methods for the Determination of Hazardous Substances MDHS 59. London, United Kingdom:

Occupational Medicine and Hygiene Laboratory, Health and Safety Executive.

HSE (1995). Asbestos fibres in air. Sampling and evaluation by phase contrast microscopy (PCOM) under the control of asbestos at work regulation. HSE Methods for the Determination of Hazardous Substances MDHS 39/4. London, United Kingdom: Occupational Medicine and Hygiene Laboratory, Health and Safety Executive.

HSE (2011). EH/2005 Workplace exposure limits. Containing the list of workplace exposure limits for use with the Control of Substances Hazardous to Health Regulations (as amended). 2nd edition. London, United Kingdom: Health and Safety Executive.

Indian Institute of Science (2014). Silicon carbide manufacturing. Bangalore, India: Indian Institute of Science. Available from: http://materials.iisc.ernet.in/~govind/silicon_carbide_manufacture.htm, accessed 18 September 2014.

Infante-Rivard C, Dufresne A, Armstrong B, Bouchard P, Thériault G (1994). Cohort study of silicon carbide production workers. *Am J Epidemiol*, 140(11):1009–15. PMID:7985648

Jakobsson K, Mikoczy Z, Skerfving S (1997). Deaths and tumours among workers grinding stainless steel: a follow up. *Occup Environ Med*, 54(11):825–9. doi:10.1136/oem.54.11.825 PMID:9538356

Järvholm B, Thiringer G, Axelson O (1982). Cancer morbidity among polishers. *Br J Ind Med*, 39(2):196–7. PMID:7066237

Johnsen HL, Bugge MD, Føreland S, Kjuus H, Kongerud J, Søyseth V (2013). Dust exposure is associated with increased lung function loss among workers in the Norwegian silicon carbide industry. *Occup Environ Med*, 70(11):803–9. doi:10.1136/oemed-2012-101068 PMID:23852098

Johnson NF, Hahn FF (1996). Induction of mesothelioma after intrapleural inoculation of F344 rats with silicon carbide whiskers or continuous ceramic filaments. *Occup Environ Med*, 53(12):813–6. doi:10.1136/oem.53.12.813 PMID:8994400

Johnson NF, Hoover MD, Thomassen DG, Cheng YS, Dalley A, Brooks AL (1992). In vitro activity of silicon carbide whiskers in comparison to other industrial fibers using four cell culture systems. *Am J Ind Med*, 21(6):807–23. doi:10.1002/ajim.4700210604 PMID:1320327

Kawanami Y, Morimoto Y, Kim H, Nakamura T, Machida K, Kido T, et al. (2009). Calcitonin gene-related peptide stimulates proliferation of alveolar epithelial cells. *Respir Res*, 10(1):8. doi:10.1186/1465-9921-10-8 PMID:19192276

Kawase T, Okuda K, Wu CH, Yoshie H, Hara K, Burns DM (1999). Calcitonin gene-related peptide acts as a mitogen for human Gin-1 gingival fibroblasts by activating the MAP kinase signalling pathway. *J Periodontal Res*,

34(3):160–8. doi:10.1111/j.1600-0765.1999.tb02237.x PMID:10384404

Kohyama N, Tanaka I, Tomita M, Kudo M, Shinohara Y (1997). Preparation and characteristics of standard reference samples of fibrous minerals for biological experiments. *Ind Health*, 35(3):415–32. doi:10.2486/indhealth.35.415 PMID:9248227

Kordina O, Saddow SE (2006). Chapter 1: Silicon carbide overview. In: Saddow SE, Argawal A, editors. Semiconductor materials and devices series. Advances in silicon carbide processing and applications; pp. 1–27.

Kumar PV, Gupta GS (2002). Study of formation of silicon carbide in the Acheson Process. *Steel Res*, 73(2):31–8.

Lapin CA, Craig DK, Valerio MG, McCandless JB, Bogoroch R (1991). A subchronic inhalation toxicity study in rats exposed to silicon carbide whiskers. *Fundam Appl Toxicol*, 16(1):128–46. doi:10.1016/0272-0590(91)90142-Q PMID:2019338

Lippmann M (1993). Biophysical factors affecting fiber toxicity. In: Warheit DB, editor. Fiber toxicology. San Diego (CA), USA: Academic Press; pp. 259–303.

Lockey JE (1996). Man-made fibers and nonasbestos fibrous silicates. In: Harber P, Schenker MB, Balmes JR, editors. Occupational and environmental respiratory disease. St Louis (MO), USA: Mosby-Year book, Inc.; pp. 330–44.

Lozano O, Mejia J, Masereel B, Toussaint O, Lison D, Lucas S (2012). Development of a PIXE analysis method for the determination of the biopersistence of SiC and TiC nanoparticles in rat lungs. *Nanotoxicology*, 6(3):263–71. doi:10.3109/17435390.2011.572301 PMID:21504370

Malard S, Binet S (2012). État des connaissances sur les fibres monocristallines de carbure de silicium, d'octatitanate de potassium, d'oxyde de tungstène et de sulfate de magnésium et sur une fibre composite (Nicalon™).] *Documents pour le Médecin du Travail*, 129:19–25. [French]

Mango GW, Johnston CJ, Reynolds SD, Finkelstein JN, Plopper CG, Stripp BR (1998). Clara cell secretory protein deficiency increases oxidant stress response in conducting airways. *Am J Physiol*, 275(2 Pt 1):L348–56. PMID:9700096

Mantile G, Miele L, Cordella-Miele E, Singh G, Katyal SL, Mukherjee AB (1993). Human Clara cell 10-kDa protein is the counterpart of rabbit uteroglobin. *J Biol Chem*, 268(27):20343–51. PMID:8104186

Marcer G, Bernardi G, Bartolucci GB, Mastrangelo G, Belluco U, Camposampiero A, et al. (1992). Pulmonary impairment in workers exposed to silicon carbide. *Br J Ind Med*, 49(7):489–93. PMID:1637708

McCormack FX, King TE Jr, Bucher BL, Nielsen L, Mason RJ (1995). Surfactant protein A predicts survival in idiopathic pulmonary fibrosis. *Am J Respir Crit Care Med*, 152(2):751–9. doi:10.1164/ajrccm.152.2.7633738 PMID:7633738

McGavran PD, Brody AR (1989). Chrysotile asbestos inhalation induces tritiated thymidine incorporation by epithelial cells of distal bronchioles. *Am J Respir Cell Mol Biol*, 1(3):231–5. doi:10.1165/ajrcmb/1.3.231 PMID:2624762

Milewski JV, Gac FD, Petrovic JJ, Skaggs SR (1985). Growth of beta-silicon carbide whiskers by the VLS process. *J Mater Sci*, 20(4):1160–6. doi:10.1007/BF01026309

Miller BG, Searl A, Davis JM, Donaldson K, Cullen RT, Bolton RE, et al. (1999). Influence of fibre length, dissolution and biopersistence on the production of mesothelioma in the rat peritoneal cavity. *Ann Occup Hyg*, 43(3):155–66. doi:10.1093/annhyg/43.3.155 PMID:10366897

Morimoto Y, Ding L, Oyabu T, Hirohashi M, Kim H, Ogami A, et al. (2003b). Expression of Clara cell secretory protein in the lungs of rats exposed to silicon carbide whisker in vivo. *Toxicol Lett*, 145(3):273–9. doi:10.1016/S0378-4274(03)00308-4 PMID:14580898

Morimoto Y, Ding L, Oyabu T, Kim H, Ogami A, Hirohashi M, et al. (2003a). Gene expression of surfactant protein-A and thyroid transcription factor-1 in lungs of rats exposed to silicon-carbide whisker in vivo. *J Occup Health*, 45(5):307–12. doi:10.1539/joh.45.307 PMID:14646272

Morimoto Y, Ogami A, Nagatomo H, Hirohashi M, Oyabu T, Kuroda K, et al. (2007). Calcitonin gene-related peptide (CGRP) as hazard marker for lung injury induced by dusts. *Inhal Toxicol*, 19(3):283–9. doi:10.1080/08958370601069364 PMID:17365031

Morrow PE, Muhle H, Mermelstein R (1991). Chronic inhalation study findings as a basis for proposing a new occupational dust exposure limit. *J Am Coll Toxicol*, 10(2):279–90. doi:10.3109/10915819109078637

Mossman BT, Faux S, Janssen Y, Jimenez LA, Timblin C, Zanella C, et al. (1997). Cell signalling pathways elicited by asbestos. *Environ Health Perspect*, 105(Suppl 5): 1121–5. doi:10.1289/ehp.97105s51121 PMID:9400710

Murphy FA, Poland CA, Duffin R, Al-Jamal KT, Ali-Boucetta H, Nunes A, et al. (2011). Length-dependent retention of carbon nanotubes in the pleural space of mice initiates sustained inflammation and progressive fibrosis on the parietal pleura. *Am J Pathol*, 178(6):2587–600. doi:10.1016/j.ajpath.2011.02.040 PMID:21641383

NIOSH (1994a). NIOSH manual of analytical methods. Asbestos and other fibres by PCM. Cincinnati (OH), USA: National Institute for Occupational Safety and Health. 4th edition. Method No. 7400. Available from: http://www.cdc.gov/niosh/docs/2003-154/pdfs/7400.pdf.

NIOSH (1994b). NIOSH manual of analytical methods. Asbestos by TEM. Cincinnati (OH), USA: National Institute for Occupational Safety and Health. 4th edition. Method No. 7402:1-7. Available from: http://www.cdc.gov/niosh/docs/2003-154/.

NIOSH (1994c). NIOSH manual of analytical methods. Asbestos, chrysotile by XRD. Cincinnati (OH), USA: National Institute for Occupational Safety and Health. 4th edition. Method No. 9000. Available from: http://www.cdc.gov/niosh/docs/2003-154/pdfs/9000.pdf.

NIOSH (1998). Particulates not otherwise regulated, respirable, NIOSH method 0600. Cincinnati (OH), USA: National Institute for Occupational Safety and Health.

NIOSH (2003). Silica, crystalline, by XRD, NIOSH method 7500. Cincinnati (OH), USA: National Institute for Occupational Safety and Health.

NIOSH (2011). Silicon carbide. Cincinnati (OH), USA: National Institute for Occupational Safety and Health. Available from: http://www.cdc.gov/niosh/pel88/409-21.html.

NIOSH (2014). National Occupational Exposure Survey (NOES). Cincinnati (OH), USA: National Institute for Occupational Safety and Health. Available from: http://www.cdc.gov/noes/, accessed 4 July 2014.

Nixdorf RD (2008). Commercial process for silicon carbide fibrils. 22nd Annual Conference on Fossil Energy Materials, 10 July 2008. Work funded by United States Department of Energy, Fossil Energy Department, Advanced Research Materials Program.

Nordsletten L, Høgåsen AK, Konttinen YT, Santavirta S, Aspenberg P, Aasen AO (1996). Human monocytes stimulation by particles of hydroxyapatite, silicon carbide and diamond: in vitro studies of new prosthesis coatings. *Biomaterials*, 17(15):1521–7. doi:10.1016/0142-9612(96)89777-8 PMID:8853123

Nyberg B, Eklund L, Carlström E, Carlsson R (1995). Automated image analysis for morphology measurements and quantification of whisker and powder materials. In: Hansner H, Messing GL, Hirano S editors. Ceramic transactions: ceramic processing science and technology. Volume 51. Westerville (OH), USA: American Ceramic Society; pp. 133–7.

Oberdörster G (1994). Macrophage-associated responses to chrysotile. *Ann Occup Hyg*, 38(4):601–15, 421–2. doi:10.1093/annhyg/38.4.601 PMID:7978983

Oberdörster G (2000). Determinants of the pathogenicity of man-made vitreous fibers (MMVF). *Int Arch Occup Environ Health*, 73(S1):S60–8. doi:10.1007/PL00014628 PMID:10968563

Oberdörster G, Morrow PE, Spurny K (1988). Size dependent lymphatic clearance of amosite fibres in the lung. *Ann Occup Hyg*, 32(inhaled particles VI):149–56. doi:10.1093/annhyg/32.inhaled_particles_VI.149

Ogami A, Morimoto Y, Myojo T, Oyabu T, Murakami M, Nishi K, et al. (2007). Histopathological changes in rat lung following intratracheal instillation of silicon carbide whiskers and potassium octatitanate whiskers. *Inhal Toxicol*, 19(9):753–8. doi:10.1080/08958370701399869 PMID:17613083

Oliveros A, Guiseppi-Elie A, Saddow SE (2013). Silicon carbide: a versatile material for biosensor applications. *Biomed Microdevices*, 15(2):353–68. doi:10.1007/s10544-013-9742-3 PMID:23319268

OSHA (2015). OSHA Occupational Chemical Database. Washington (DC), USA: Occupational Safety and Health Administration. Available from: https://www.osha.gov/chemicaldata/chemResult.html?recNo=368.

Osterman JW, Greaves IA, Smith TJ, Hammond SK, Robins JM, Thériault G (1989). Respiratory symptoms associated with low level sulphur dioxide exposure in silicon carbide production workers. *Br J Ind Med*, 46(9):629–35. PMID:2789966

Peraud A, Riebe-Imre M (1994). Toxic and chromosome-damaging effects of natural and man-made fibers in epithelial lung cells in vitro. In: Dungworth DL, Mauderly JL, Oberdörster G, editors. Toxic and carcinogenic effects of solid particles in the respiratory tract. Washington (DC), USA: ILSI Press; pp. 569–74.

Plinke MA, Maus R, Leith D (1992). Experimental examination of factors that affect dust generation by using Heubach and MRI testers. *Am Ind Hyg Assoc J*, 53(5):325–30. doi:10.1080/15298669291359726 PMID:1609743

Pott F, Roller M, Rippe RM, et al. (1991). Tumors by the intraperitoneal and intrapleural routes and their significance for the classification of mineral fibres. In: Brown RC, Hoskins JA, Johnson NF, editors. Mechanisms in fibre carcinogenesis. New York (NY), USA: Plenum Press; pp. 547–65. doi:10.1007/978-1-4684-1363-2_48

Pourchez J, Forest V, Boumahdi N, Boudard D, Tomatis M, Fubini B, et al. (2012). In vitro cellular responses to silicon carbide nanoparticles: impact of physico-chemical features on pro-inflammatory and pro-oxidative effects. *J Nanopart Res*, 14(10):1143. doi:10.1007/s11051-012-1143-7

Revell G, Bard D (2005). An investigation into the potential health risks from commercial silicon carbide reinforced tools. Report HSL/2005/18. Harpur Hill, United Kingdom: Health and Safety Laboratory.

Rödelsperger K, Brückel B (2006). The carcinogenicity of WHO fibers of silicon carbide: SiC whiskers compared to cleavage fragments of granular SiC. *Inhal Toxicol*, 18(9):623–31. doi:10.1080/08958370600742987 PMID:16864553

Rodriguez-Lugo V, Rubio E, Gomez I, Torres-Martinez L, Castano VM (2002). Synthesis of silicon carbide from rice husk. *Int J Environ Pollut*, 18(4):378–87. doi:10.1504/IJEP.2002.003734

Rom WN, Travis WD, Brody AR (1991). Cellular and molecular basis of the asbestos-related diseases. *Am Rev Respir Dis*, 143(2):408–22. doi:10.1164/ajrccm/143.2.408 PMID:1990961

Romundstad P, Andersen A, Haldorsen T (2001). Cancer incidence among workers in the Norwegian silicon

carbide industry. *Am J Epidemiol*, 153(10):978–86. doi:10.1093/aje/153.10.978 PMID:11384954

Romundstad P, Andersen A, Haldorsen T (2002). Non-malignant mortality among Norwegian silicon carbide smelter workers. *Occup Environ Med*, 59(5):345–7. doi:10.1136/oem.59.5.345 PMID:11983851

Russwurm S, Stonans I, Stonane E, Wiederhold M, Luber A, Zipfel PF, et al. (2001). Procalcitonin and CGRP-1 mRNA expression in various human tissues. *Shock*, 16(2):109–12. doi:10.1097/00024382-200116020-00004 PMID:11508861

Saint-Gobain (2014). The art of silicon carbide. Courbevoie, France; Saint-Gobain. Available from: http://www.sic.saint-gobain.com/the-art-of-silicon-carbide.aspx, accessed 16 June 2014.

Scansetti G, Piolatto G, Botta GC (1992). Airborne fibrous and non-fibrous particles in a silicon carbide manufacturing plant. *Ann Occup Hyg*, 36(2):145–53. doi:10.1093/annhyg/36.2.145 PMID:1530231

SCOEL (2012). Recommendation from the Scientific Committee on Occupational Exposure Limits for man-made mineral fibres (MMMF) with no indication for carcinogenicity and not specified elsewhere. SCOEL/SUM/88, March 2012. Brussels, Belgium: Employment, Social Affairs & Inclusion, European Commission. Available from: http://ec.europa.eu/social/BlobServlet?docId=7722&langId=en.

Searl A, Buchanan D, Cullen RT, Jones AD, Miller BG, Soutar CA (1999). Biopersistence and durability of nine mineral fibre types in rat lungs over 12 months. *Ann Occup Hyg*, 43(3):143–53. doi:10.1093/annhyg/43.3.143 PMID:10366896

Shaffer PTB (1969). A review of the structure of silicon carbide. *Acta Crystallogr B*, 25(3):477–88. doi:10.1107/S0567740869002457

Sharma NK, Williams WS, Zangvil A (1984). Formation and structure of silicon carbide whiskers from rice hulls. *J Am Ceram Soc*, 67(11):715–20. doi:10.1111/j.1151-2916.1984.tb19507.x

Shibata K, Kudo Y, Tsunoda M, Hosokawa M, Sakai Y, Kotani M, et al. (2007). Magnetometric evaluation of the effects of man-made mineral fibers on the function of macrophages using the macrophage cell line RAW 264.7. *Ind Health*, 45(3):426–36. doi:10.2486/indhealth.45.426 PMID:17634692

Shvedova AA, Kisin E, Murray AR, Johnson VJ, Gorelik O, Arepalli S, et al. (2008). Inhalation vs. aspiration of single-walled carbon nanotubes in C57BL/6 mice: inflammation, fibrosis, oxidative stress, and mutagenesis. *Am J Physiol Lung Cell Mol Physiol*, 295(4):L552–65. doi:10.1152/ajplung.90287.2008 PMID:18658273

Skogstad A, Føreland S, Bye E, Eduard W (2006). Airborne fibres in the Norwegian silicon carbide industry. *Ann Occup Hyg*, 50(3):231–40. doi:10.1093/annhyg/mei081 PMID:16497830

Smith TJ, Hammond SK, Laidlaw F, Fine S (1984). Respiratory exposures associated with silicon carbide production: estimation of cumulative exposures for an epidemiological study. *Br J Ind Med*, 41(1):100–8. PMID:6691927

Sparks PJ, Wegman DH (1980). Cause of death among jewelry workers. *J Occup Med*, 22(11):733–6. PMID:7441392

Stanton MF, Layard M (1978). The carcinogenicity of fibrous material. In: Proceedings of the workshop on asbestos: Definitions and measurement methods; held at the National Bureau of Standards, Gaithersburg, MD, 1977. NBS Special Publication No. 506. Washington (DC), USA: National Bureau of Standards; pp. 143–51.

Stanton MF, Layard M, Tegeris A, Miller E, May M, Morgan E, et al. (1981). Relation of particle dimension to carcinogenicity in amphibole asbestoses and other fibrous minerals. *J Natl Cancer Inst*, 67(5):965–75. PMID:6946253

Stone KC, Mercer RR, Gehr P, Stockstill B, Crapo JD (1992). Allometric relationships of cell numbers and size in the mammalian lung. *Am J Respir Cell Mol Biol*, 6(2):235–43. doi:10.1165/ajrcmb/6.2.235 PMID:1540387

Svensson I, Artursson E, Leanderson P, Berglind R, Lindgren F (1997). Toxicity in vitro of some silicon carbides and silicon nitrides: whiskers and powders. *Am J Ind Med*, 31(3):335–43. doi:10.1002/(SICI)1097-0274(199703)31:3<335::AID-AJIM10>3.0.CO;2-1 PMID:9055957

Swedish Work Environment Authority (2011). The Swedish Work Environment Authority's Statute Book. AFS2011; December 2011. Available from: https://www.av.se/globalassets/filer/publikationer/foreskrifter/engelska/occupational-exposure-limit-values-provisions-afs2011-18.pdf.

Tomatis M, Prandi L, Bodoardo S, Fubini B (2002). Loss of surface reactivity upon heating amphibole asbestos. *Langmuir*, 18(11):4345–50. doi:10.1021/la011609w

Tran CL, Jones AD, Miller BG, Donaldson K (2003). Modeling the retention and clearance of manmade vitreous fibers in the rat lung. *Inhal Toxicol*, 15(6):553–87. doi:10.1080/08958370304469 PMID:12692731

Tran CL, Kuempel ED, Castranova V (2002). A rat lung model of exposure, dose, and response to inhaled silica. *Ann Occup Hyg*, 46(Suppl 1):14–7. doi:10.1093/annhyg/46.suppl_1.14

Turci F, Tomatis M, Lesci IG, Roveri N, Fubini B (2011). The iron-related molecular toxicity mechanism of synthetic asbestos nanofibres: a model study for high-aspect-ratio nanoparticles. *Chemistry*, 17(1):350–8. doi:10.1002/chem.201001893 PMID:21207631

USGS (2014). United States Geological Survey. Mineral Commodity Summaries 2014; pp. 14–15. Available from: http://minerals.usgs.gov/minerals/pubs/mcs/2014/mcs2014.pdf.

Vaughan GL, Jordan J, Karr S (1991a). The toxicity, in vitro, of silicon carbide whiskers. *Environ Res*, 56(1):57–67. doi:10.1016/S0013-9351(05)80109-4 PMID:1915190

Vaughan GL, Kennedy JR, Trently SA (1991b). The immediate effects of silicon carbide whiskers upon ciliated tracheal epithelium. *Environ Res*, 56(2):178–85. doi:10.1016/S0013-9351(05)80007-6 PMID:1769364

Vaughan GL, Trently SA, Wilson RB (1993). Pulmonary response, in vivo, to silicon carbide whiskers. *Environ Res*, 63(2):191–201. doi:10.1006/enrs.1993.1140 PMID:8243414

Wang QE, Han CH, Yang YP, Wang HB, Wu WD, Liu SJ, et al. (1999). Biological effects of man-made mineral fibers (II)–their genetic damages examined by in vitro assay. *Ind Health*, 37(3):342–7. doi:10.2486/indhealth.37.342 PMID:10441907

Warheit DB, Kellar KA, Hartsky MA (1992). Pulmonary cellular effects in rats following aerosol exposures to ultrafine Kevlar aramid fibrils: evidence for biodegradability of inhaled fibrils. *Toxicol Appl Pharmacol*, 116(2):225–39. doi:10.1016/0041-008X(92)90302-9 PMID:1412467

Watanabe M, Okada M, Aizawa Y, Sakai Y, Yamashina S, Kotani M (2000). Magnetometric evaluation for the effects of silicon carbide whiskers on alveolar macrophages. *Ind Health*, 38(2):239–45. doi:10.2486/indhealth.38.239 PMID:10812849

Wegman DH, Eisen EA (1981). Causes of death among employees of a synthetic abrasive product manufacturing company. *J Occup Med*, 23(11):748–54. doi:10.1097/00043764-198111000-00008 PMID:6275058

White SR, Hershenson MB, Sigrist KS, Zimmermann A, Solway J (1993). Proliferation of guinea pig tracheal epithelial cells induced by calcitonin gene-related peptide. *Am J Respir Cell Mol Biol*, 8(6):592–6. doi:10.1165/ajrcmb/8.6.592 PMID:8323744

WHO (1985). Reference methods for measuring airborne man-made mineral fibres. WHO/EURO MMMF reference scheme. Copenhagen, Denmark: World Health Organization.

WHO (1997). Determination of airborne fibre number concentrations. A recommended method, by phase-contrast optical microscopy (membrane filter method). Geneva, Switzerland: World Health Organization.

Wright NG (2006). Silicon carbide. In: Kirk-Othmer Encyclopedia of Chemical Technology. Hoboken (NJ), USA: John Wiley & Sons, Inc.; pp. 524–2546. doi:10.1002/0471238961.1909120904092201.a01.pub2

Yamato H, Morimoto Y, Tsuda T, Ohgami A, Kohyama N, Tanaka I (1998). Fiber numbers per unit weight of JFM standard reference samples determined with a scanning electron microscope. Japan Fibrous Material. *Ind Health*, 36(4):384–7. doi:10.2486/indhealth.36.384 PMID:9810155

Yamato H, Oyabu T, Ogami A, Morimoto Y, Higashi T, Tanaka I, et al. (2003). Pulmonary effects and clearance after long-term inhalation of potassium octatitanate whiskers in rats. *Inhal Toxicol*, 15(14):1421–34. doi:10.1080/08958370390248969 PMID:14648357

Zhang Z, Shen HM, Zhang QF, Ong CN (1999). Critical role of GSH in silica-induced oxidative stress, cytotoxicity, and genotoxicity in alveolar macrophages. *Am J Physiol*, 277(4 Pt 1):L743–8. PMID:10516215

LIST OF ABBREVIATIONS

AF-SWCNT	acid-functionalized single-walled carbon nanotubes
AP-1	activator protein 1
ApoE	apolipoprotein E
BALF	bronchoalveolar lavage fluid
BET	Brunauer–Emmett–Teller
BSI	British Standards Institution
bw	body weight
CCSP	Clara cell secretory protein
CGRP	calcitonin gene-related peptide
CI	confidence interval
CNF	carbon nanofibre
CNM	carbon-based nanomaterial
CNT	carbon nanotubes
COX-2	cyclooxygenase
CVD	chemical vapour deposition
dG	deoxyguanosine
DWCNT	double-walled carbon nanotubes
EC	elemental carbon
EC_{50}	concentration resulting in 50% survival
EDX	energy dispersive X-ray analyser
ENDOIII	endonuclease III
EPO	eosinophil peroxidase
ESR	electronic spin resonance
F-MWCNT	carboxylic acid-functionalized multiwalled carbon nanotubes
FPG	formamidopyrimidine glycosylase
GM	geometric mean
GPx	gluthathione peroxidase
GSD	geometric standard deviation
GSH	glutathione
HDM	house dust mites
HiPCO	high-pressure carbon monoxide
IFN	interferon
Ig	immunoglobulin
IL	interleukin

ISO	International Organization of Standardization
LDH	lactate dehydrogenase
LPS	lipopolysaccharide
MAPK	mitogen-activated protein kinase
MC	methylcholanthrene
MDA	malondialdehyde
MMAD	mass median aerodynamic diameter
MPO	myeloperoxidase
MPPD	multiple-path particle dosimetry
MWCNT	multiwalled carbon nanotubes
NAC	*N*-acetyl cysteine
NADPH	nicotinamide adenine dinucleotide phosphate
NF-κB	nuclear factor kappa B
NIOSH	National Institute for Occupational Safety and Health
O-MWCNT	original multiwalled carbon nanotubes
OEL	occupational exposure limit
OVA	ovalbumin
8-oxodG	8-oxodeoxyguanosine
P/B	process to background ratio
PBS	phosphate-buffered saline
PBZ	personal breathing zone
PCOM	phase-contrast optical microscope
PDGF	platelet-derived growth factor
PEG	polyethylene glycol
PGE2	prostaglandin
PLC	phospholipase C
P-MWCNT	purified multiwalled carbon nanotubes
PPARγ	peroxisome proliferator-activated receptor gamma
qRT-PCR	quantitative real-time polymerase chain reaction
ROS	reactive oxygen species
RT-PCR	reverse transcriptase-polymerase chain reaction
SD	standard deviation
SEM	scanning electron microscopy
SENTIERI	Epidemiological Study of Residents in National Priority Contaminated Sites
SIR	standardized incidence ratio
Smad	mothers against decapentaplegic homologue
SMR	standardized mortality ratio
SOD	superoxide dismutase
SP	surfactant protein
SWCNT	single-walled carbon nanotubes
TEM	transmission electron microscopy
TGF	transforming growth factor
Th	T helper
TNF	tumour necrosis factor
TTF	thyroid transcription factor
TWA	time-weighted average
VEGF	vascular endothelial growth factor

This volume of the *IARC Monographs* provides an assessment of the carcinogenicity of fluoro-edenite fibrous amphibole, silicon carbide fibres and whiskers, and carbon nanotubes, including single-walled and multiwalled types. None of these agents had been assessed previously by the *IARC Monographs* Working Group.

The Working Group relied mainly on epidemiological studies to evaluate the carcinogenic hazard to humans exposed to fluoro-edenite fibrous amphibole, an environmental contaminant that was reported to cause mesothelioma in the regional population of Biancavilla, Sicily, Italy.

Silicon carbide fibres are by-products of the manufacture of silicon carbide particles by the Acheson process; silicon carbide whiskers are produced by other processes. The evaluations of the fibres and of the occupational exposures associated with the Acheson process were mainly based on epidemiological studies, whereas the assessment of the whiskers – in the absence of epidemiological data – was based on carcinogenicity bioassays and consideration of their physical properties.

In view of the absence of epidemiological studies on carbon nanotubes and the limited information available from mechanistic data, the evaluations of single-walled and multiwalled carbon nanotubes relied essentially on carcinogenicity bioassays.

M IARC MONOGRAPHS